Tommaso Scarabino
Saverio Pollice
Editors

Imaging Gliomas After Treatment

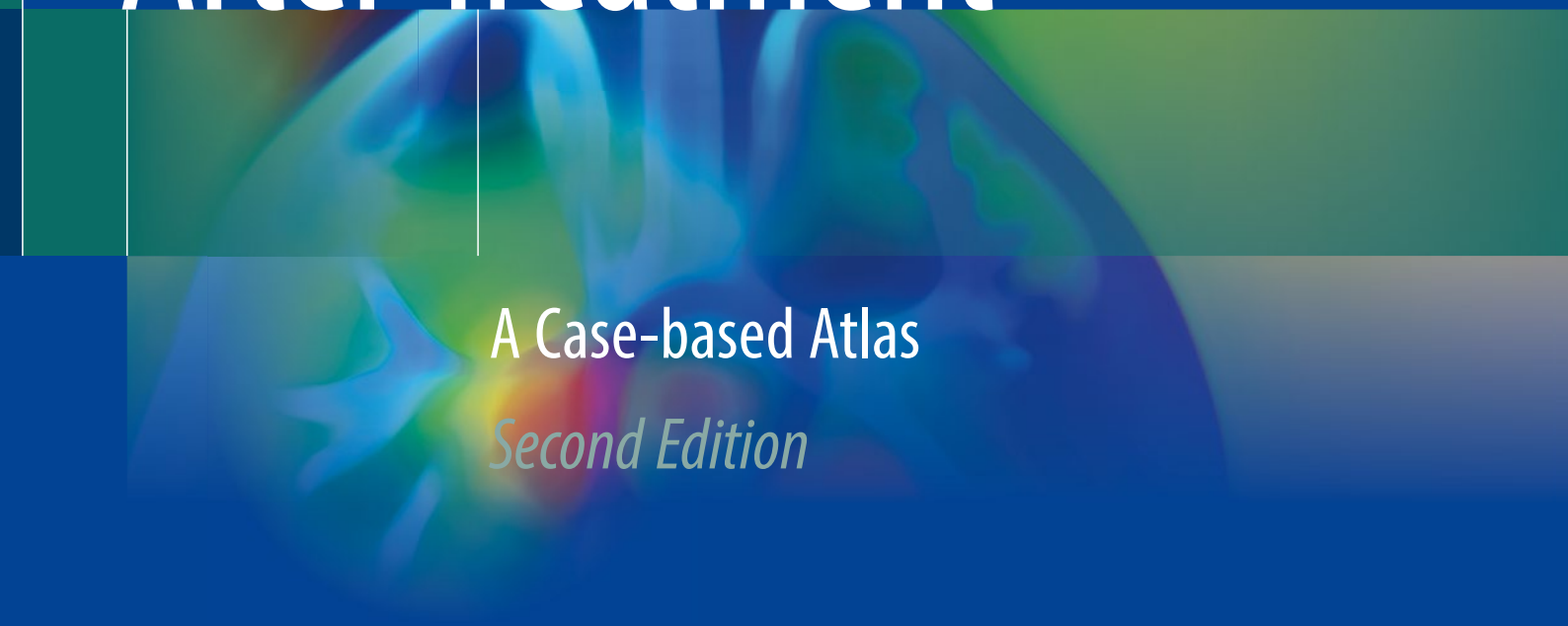

A Case-based Atlas

Second Edition

Springer

Imaging Gliomas After Treatment

Tommaso Scarabino • Saverio Pollice
Editors

Imaging Gliomas After Treatment

A Case-based Atlas

Second Edition

Springer

Editors
Tommaso Scarabino
Department of Radiology/ Neuroradiology
Ospedale 'L.Bonomo'
Andria
Italy

Saverio Pollice
Department of Radiology/ Neuroradiology
Ospedale 'L.Bonomo'
Andria
Italy

ISBN 978-3-030-31209-1 ISBN 978-3-030-31210-7 (eBook)
https://doi.org/10.1007/978-3-030-31210-7

This Springer imprint is published by the registered company Springer Nature Switzerland AG
The registered company address is: Gewerbestrasse 11, 6330 Cham, Switzerland

Preface

Seven years after the first edition, the authors decided to proceed with a revision of the editorial work, considering the progress made in the treatment of brain neoplasms with neurosurgery, radiotherapy, chemotherapy, and the technical-methodological advances in diagnosis in the field of neuroradiology and nuclear medicine.

The second edition of the book is therefore a decidedly renewed work in content, in step with the times, which nevertheless preserves the original approach: the first section consisting of the text (10 chapters) and the second section consisting of the atlas (55 cases).

We hope that this second edition, revised and expanded, can have the same editorial success as the previous one, as a testimony to the validity of the scientific initiative.

We take this opportunity to thank all the collaborators who with their expertise and experience have contributed to the realization of the work and in particular the radiologists of the operating unit I direct and the colleagues of our hospital with whom we interact daily: in particular Armando Rapanà (Director of Neurosurgery), Santa Bambace (Director of Radiotherapy), Gennaro Gadaleta (Director of Oncology), Samantha Cornacchia (Department of Health Physics).

We also owe a debt of gratitude to our Hospital's Strategic Management, always sensitive to the cultural and professional initiatives of the Diagnostics Department.

Andria, Italy — Tommaso Scarabino
Andria, Italy — Saverio Pollice

Contents

Part IV Clinical Cases

Part I

Introduction

Brain Tumors

1

Saverio Pollice, Angela Lorusso, and Tommaso Scarabino

1.1 General Findings

Primary brain tumors refer to a heterogeneous group of tumors arising from cells within the CNS. Meningiomas are the most common nonmalignant primary brain tumors, followed by pituitary and nerve sheath tumors. Gliomas represent 75% of malignant primary brain tumors in adults and of these, more than half are glioblastomas. Gliomas are tumors of neuroectodermal origin arising from glial or precursor cells [1].

Although CNS tumors are rare, they are a significant cause of cancer morbidity and mortality, especially in children and young adults where they respectively account for approximately 30% and 20% of cancer deaths. They are also a cause of excessive mortality relative to other cancers [2].

1.2 Classification

Classification of central nervous system (CNS) tumors has always been a critical component of the epidemiologic, clinical, and basic-level understanding of this type of neoplasms. Historically, brain tumor classification was exclusively carried out based on histomorphologic features, of tumors, an approach compatible within the capabilities of most clinical centers throughout the world and primarily dependent on light microscopic features in hematoxylin and eosin-stained sections.

Advances in the molecular understanding of brain tumors that have occurred since 2007 have driven the concept that incorporation of clinically relevant molecular markers can provide a biologic basis for classification, that, when integrated with morphologic features, may result in a classification that promotes increased accuracy and precision.

As a result, the recent 2016 update of the WHO Classification of Tumors of the Central Nervous System (2016 CNS WHO) represents a revolutionary shift from previous iterations by having, for the first time, tumor classes defined not only by their histomorphologic features, but also by key diagnostic molecular parameters.

The 2016 CNS WHO officially represents an update of the 2007 fourth Edition rather than a formal fifth Edition. The use of "integrated" phenotypic and genotypic parameters for CNS tumor classification adds a level of objectivity that has been missing from some aspects of the diagnostic process in the past. This new characterization has primarily involved gliomas that are further classified according to WHO grading [3, 4].

1.3 2016 World Health Organization Classification of Tumors of the Central Nervous System

Diffuse Astrocytic and Oligodendroglial Tumors

WHO grade II

Diffuse astrocytoma IDH-mutant—9400/3

– Gemistocytic astrocytoma IDH-mutant—9411/3

Diffuse astrocytoma IDH-wildtype—9400/3

Diffuse astrocytoma NOS—9400/3

Oligoastrocytoma NOS—9382/3

Oligodendroglioma IDH-mutant, 1p19q co-deleted—9450/3

Oligodendroglioma NOS

WHO grade III

Anaplastic astrocytoma IDH-mutant—9401/3

Anaplastic astrocytoma IDH-wildtype—9401/3

Anaplastic astrocytoma NOS 9401/3

Anaplastic oligoastrocytoma NOS—9382/3

Anaplastic oligodendroglioma IDH-mutant, 1p19q co-deleted—9451/3

Anaplastic oligodendroglioma NOS

WHO grade IV

Glioblastoma IDH wildtype—9440/3

S. Pollice (✉) · A. Lorusso · T. Scarabino
Department of Radiology, "L. Bonomo" Hospital, Andria, Italy

T. Scarabino, S. Pollice (eds.), *Imaging Gliomas After Treatment*, https://doi.org/10.1007/978-3-030-31210-7_1

– Giant cell glioblastoma—9441/3
– Gliosarcoma 9442/3
– *Epithelioid glioblastoma—9440/3*

Glioblastoma IDH-mutant—9440/3∗
Glioblastoma NOS—9440/3
Diffuse midline glioma, H3K27M-mutant—9385/3∗

Other Astrocytic Tumors
Pilocytic astrocytoma—9421/1

– Pilomixoid astrocytoma—9425/3

Subependymal giant cell astrocytoma—9384/1
Pleomorphic xanthoastrocytoma—9424/3
Anaplastic pleomorphic xanthoastrocytoma 9424/3

Ependymal Tumors
WHO grade I
Subependymoma—9383/1
Myxopapillary ependymoma—9394/1
WHO grade II
Ependymoma—9391/3

– Papillary ependymoma—9393/3
– Clear cell ependymoma—9391/3
– Tanycytic ependymoma—9391/3

Ependymoma RELA fusion-positive—9396/3 ∗
WHO grade III
Anaplastic ependymoma—9392/3

Other Gliomas
Angiocentric glioma—9431/1
Chordoid glioma of the third ventricle—9444/1
Astroblastoma—9430/3

Choroid Plexus Tumors
Choroid plexus papilloma—9390/0
Atypical choroid plexus papilloma—9390/1
Choroid plexus carcinoma—9390/3

Neuronal and Mixed Neuronal-Glial Tumors
Dysembryoplastic neuroepithelial tumor—9413/0
Gangliocytoma—9492/0
Ganglioglioma—9505/1
Anaplastic ganglioglioma—9505/3
Dysplastic gangliocytoma of the cerebellum—(Lhermitte-Duclos)—9493/0
Desmoplastic infantile astrocytoma and ganglioglioma—9412/1
Papillary glioneuronal tumor—9509/1
Rosette-forming glioneuronal tumor of the fourth ventricle—9509/1
Diffuse leptomeningeal glioneuronal tumor—no IDC-O code
Central neurocytoma—9506/1
Extraventricular neurocytoma—9506/1
Cerebellar liponeurocytoma—9506/1
Paraganglioma—8680/1

Tumors of the Pineal Region
Pineocytoma—9361/1
Pineal parenchymal tumor of intermediate differentiation—9362/3
Pineoblastoma—9362/3
Papillary tumor of the pineal region—9395/3

Embryonal Tumors
Medulloblastoma genetically defined

– WNT-activated—9475/3 ∗
– SHH-activated & TP53-mutant—9476/3
– SHH-activated & TP53-wildtype—9471/3
– *Group 3—9477/3*
– *Group 4—9477/3*

Medulloblastoma histologically defined

– Classic—9470/3
– Desmoplastic/nodular—9471/3
– Extensive nodularity—9471/3
– Large cell/anaplastic—9470/3.

Medulloblastoma NOS—9470/3
Embryonal tumors with multilayered rosettes C19MC altered—9478/3 ∗
Embryonal tumors with multilayered rosettes NOS 9478/3 ∗
Medulloepithelioma 9501/3
CNS neuroblastoma 9500/3
CNS ganglioneuroblastoma 9490/3
CNS embryonal tumor, NOS 9473/3
Atypical teratoid/rhabdoid tumor 9508/3
CNS embryonal tumor with rhabdoid features 9508/3

Tumors of Cranial and Paraspinal Nerves
Schwannoma (neurilemoma, neurinoma)—9560/0

– Cellular schwannoma—9560/0
– Plexiform schwannoma—9560/0
– Melanotic schwannoma—9560/1
– Neurofibroma—9540/0
– Atypical neurofibroma—9540/0
– Plexiform neurofibroma—9550/0

Perineurioma 9571/0
Malignant peripheral nerve sheath tumor (MPNST)—9540/3

– Epithelioid—9540/3
– With perineural differentiation 9540/3

Meningiomas
Meningioma—9530/0
Meningothelial meningioma—9531/0
Fibrous meningioma—9532/0
Transitional meningioma—9537/0
Psammomatous meningioma—9533/0
Angiomatous meningioma—9534/0
Microcystic meningioma—9530/0
Secretory meningioma—9530/0
Lymphoplasmacyte-rich meningioma—9530/0
Metaplastic meningioma—9530/0
Chordoid meningioma—9538/1
Clear cell meningioma—9538/1
Atypical meningioma—9539/1
Papillary meningioma—9538/3
Rhabdoid meningioma—9538/3
Anaplastic meningioma (malignant)—9530/3

Mesenchymal, Non-meningothelial Tumors
Solitary fibrous tumor of the dura/hemangiopericytoma

– Grade 1—8815/0
– Grade 2—8815/1
– Grade 3—8815/3

Hemangioblastoma—9161/1
Hemangioma—9120/0
Epithelioid hemangioendothelioma—9133/3
Angiosarcoma—9120/3
Kaposi sarcoma—9140/3
Ewing sarcoma / PNET—9364/3
Lipoma—8850/0
Angiolipoma—8861/0
Liposarcoma—8850/3
Desmoid-type fibromatosis—8821/1
Myofibroblastoma—8825/0
Inflammatory myofibroblastic tumor—8825/1
Benign fibrous histiocytoma—8830/0
Fibrosarcoma—8810/3
Undifferentiated pleomorphic sarcoma / malignant fibrous histiocytoma—8830/3
Leiomyoma—8890/0
Leiomyosarcoma—8890/3
Rhabdomyoma—8900/0
Rhabdomyosarcoma—8900/3
Chondroma—9220/0
Chondrosarcoma—9220/3
Osteoma 9180/0
Osteochondroma—9210/0
Osteosarcoma—9180/3

Melanocytic Tumors
Meningeal melanocytosis—8728/0
Meningeal melanocytoma—8728/1
Meningeal melanomatosis—8728/3
Meningeal melanoma—8720/3

Lymphomas
Diffuse large B-cell lymphoma of the CNS—9680/3
Immunodeficiency-associated CNS lymphomas

– AIDS-related diffuse large B-cell lymphoma
– EBV-positive diffuse large B-cell lymphoma, NOS
– lymphomatoid granulomatosis—9766/1

Intravascular large B-cell lymphoma—9712/3
Low-grade B-cell lymphomas of the CNS
T-cell and NK/T-cell lymphomas of the CNS
Anaplastic large cell lymphoma

– ALK-positive—9714/3
– ALK-negative—9702/3

MALT lymphoma of the dura—9699/3

Histiocytic Tumors
Langerhans cell histiocytosis—9751/3
Erdheim-Chester disease—9750/1
Rosai-Dorfman disease
Juvenile xanthogranuloma
Histiocytic sarcoma—9755/3

Germ Cell Tumors
Germinoma—9064/3
Embryonal carcinoma—9070/3
Yolk sac tumor—9071/3
Choriocarcinoma—9100/3
Teratoma

– Mature—9080/0
– Immature—9080/3
– With malignant transformation—9084/3
Mixed germ cell tumors—9085/3

Tumors of the Sellar Region

Craniopharyngioma—9350/1

- Adamantinomatous—9351/1
- Papillary—9352/1

Granular cell tumor of the sellar region—9582/0
Pituicytoma—9432/1
Spindle cell oncocytoma—8291/0

Metastatic Tumors

Notes: ***NOS****: not otherwise specified.is from the International Classification of Disease for Oncology (ICD-O).*

Four-digit code: *is from the International Classification of Disease for Oncology (ICD-O).*

/: the number after the slash (/) refers to biological behavior, not WHO Grade.

**: refers to a 'new' tumor in the classification.*

Italics*: refers to a provisional inclusion.*

CNS tumor diagnoses should consist of a histopathological name followed by the genetic features as adjectives, as *Diffuse astrocytoma IDH-mutant or Oligodendroglioma IDH-mutant and 1p/19q-codeleted.*

For a tumor lacking a genetic mutation, the term *wild-type* can be used if an official "wildtype" entity exists: ex. *Glioblastoma, IDH-wildtype*. However, it should be pointed out that in most such situations, a formal *wildtype* diagnosis is not available, and a tumor lacking a diagnostic mutation is given an NOS designation.

In other words, NOS does not define a specific entity; rather it designates a group of lesions that cannot be classified into any of the defined groups (insufficient information, not tested) [4]**.**

1.4 Molecular Markers

The most common markers used to characterize gliomas according to the new classification are listed below [1, 5].

IDH: Isocitrate dehydrogenase 1 and 2 (IDH1 and IDH2) mutations are thought to be an early event of gliomagenesis, and are more commonly found in lower-grade gliomas (>70% grades II–III astrocytomas; 100% oligodendrogliomas) than in glioblastomas, of which only 10% are referred to as secondary glioblastoma (defined when arising from a lower grade astrocytoma) or glioblastoma IDH-mutant (defined molecularly). Diffuse gliomas harboring IDH1/2 mutations are associated with a better prognosis than diffuse gliomas, IDH-wildtype.

1p/19q: Codeletion of chromosomes 1p and 19q results from a non-balanced centromeric translocation. This codeletion, combined with *IDH* mutation, is now required for the diagnosis of oligodendroglioma *IDH*-mutant and 1p/19q codeleted. 1p/19q codeletion confers a favorable prognosis among diffuse gliomas and is predictive of an increased response to alkylating chemotherapy.

H3 Lys27Met: Mutations in the genes encoding histone proteins H3.3 or H3.1 resulting in lysine to methionine substitution at amino acid 27 (Lys27Met or K27 M) molecularly defines the novel entity of diffuse midline glioma H3 Lys27Met-mutant, WHO grade IV.

H3 Lys27Met mutation is mutually exclusive with *IDH* mutation, and has been suggested to be an early event of gliomagenesis. Among all diffuse gliomas, and within diffuse midline gliomas in general, the H3 Lys27Met-mutant tumors portend the worst prognosis (2-year survival <10%). They are considered WHO grade IV even if their histology otherwise appears low-grade or anaplastic.

MGMT: O^6-methylguanine-DNA methyltransferase (MGMT) is a DNA repair protein involved in repairing the damage that has been induced by alkylating agents such as temozolomide. Methylation of the *MGMT* promoter (MGMTp) silences the *MGMT* gene and reduces the ability of tumor cells to repair such damage. MGMTp methylation predicts benefit from alkylating chemotherapies in glioblastoma patients, including elderly patients. MGMTp methylation also confers a favorable prognosis to both anaplastic astrocytomas and glioblastomas. MGMTp methylation is common in glioblastomas (30–50% of primary IDH-wildtype, glioblastoma) and in oligodendrogliomas (>90%), but less common in lower grade astrocytomas.

BRAF: B-raf is a protein kinase regulating the RAS-RAFMEK- ERK cellular signaling pathway. *BRAF* alterations, such as BRAF V600E mutation or KIAA1549-BRAF fusion, activate that pathway, and ultimately result in tumor growth and maintenance. BRAF V600E mutation is most commonly found in circumscribed gliomas, such as pleomorphic xanthoastrocytoma (60–80%), dysembryoplastic neuroepithelial tumors (30%), gangliogliomas (25%), and pilocytic astrocytomas (5–15%), but can also be found in about half of IDH-wildtype epithelioid glioblastomas. KIAA1549-BRAF fusion is almost exclusive to pilocytic astrocytomas, found in about 75% of those, and predict an indolent course.

C11orf95-RELA gene fusion: surrogate IHC (immunohistochemistry) marker to identify high-risk supratentorial RELA-fusion-positive ependymoma. No specific targeted therapy is related.

Additional markers although currently not required for diagnosis [5] may be helpful in supporting the morphological diagnosis and also provide prognostic and predictive information they can affect decision-making in the management of high-grade glioma. Moreover these markers include:

alpha-thalassemia/mental retardation syndrome Xlinked (ATRX) expression; *mutations in the tumor protein 53 (TP53) gene*; *mutations in the telomerase reverse transcriptase (TERT) promoter:* indicates poor prognosis and may guide more aggressive intervention; *combined chromosome 7gain*

and chromosome 10q loss (7þ10qe): indicate a more aggressive tumor paralleling a glioblastoma; *epidermal growth factor receptor (EGFR) amplification.*

1.5 Commentary

In the new 2016 classification, gliomas are separated into circumscribed gliomas (WHO grade I) and diffusely infiltrating gliomas (WHO grades II–IV; whether astrocytic or oligodendroglial) based on their pattern of growth and the presence or not of *IDH* mutation.

1.5.1 Circumscribed Gliomas

Circumscribed gliomas represent tumors mostly regarded as benign and curable by complete resection. Circumscribed gliomas do not have an *IDH* mutation and have frequent *BRAF* mutations and fusions (e.g., pilocytic astrocytoma and pleomorphic xanthoastrocytoma) [1].

1.5.2 Diffuse Infiltrating Gliomas

Diffuse gliomas are almost never cured by resection alone, are graded using histopathological criteria, and are now classified according to diagnostic molecular markers (presence or not of IDH mutation). In this new classification, the diffuse gliomas include the WHO grade II and III astrocytic tumors, the grade II and III oligodendrogliomas, and the grade IV glioblastomas.
Histologically, grade II (low grade) diffuse astrocytomas show nuclear atypia, grade III (anaplastic) display increased mitotic activity, and grade IV (glioblastomas) show additional microvascular proliferation, necrosis, or both [1].

1.5.3 Astrocytoma/Oligodendgroglioma

Gliomas wearing discriminating *IDH* gene alteration with *TP53* and *ATRX* mutations are called diffuse astrocytoma (WHO grade II) or anaplastic (WHO grade III) according to histological features and behavior; these tumors are thus distinguished from oligodendroglioma by the presence of intact 1p19q.

In grade II–III gliomas with *IDH*1 mutation but no *ATRX* mutation, 1p/19q codeletion status assessment in fact is required to distinguish astrocytomas from oligodendrogliomas [1].

Astrocytic tumors are classified as either IDH-mutant or IDH-wildtype, separating these tumors into two prognostic groups. Retrospective assessment of the IDH mutation status in patients from historical clinical trials confirms the marked separation of outcome between IDH-mutant and IDH-wildtype tumors with a median survival of 9.4 and 1.3 years in IDH-mutant and IDH-wildtype tumors, respectively [5], so the presence of IDH mutation is an index of better prognosis.

The diagnosis of oligodendroglioma hence requires the demonstration of IDH mutation and 1p/19q codeletion, as its correct definition including histological and molecular characteristics is: *diffusely infiltrating*, *slow-growing glioma with IDH1 or IDH2 mutation and codeletion of chromosomal arms 1p and 19q* in which microcalcifications and a delicate branching capillary network are typical, findings that however are highly characteristic of the entity, but not necessary for the diagnosis. These tumors are graded as oligodendroglioma (WHO grade II) or anaplastic oligodendroglioma (WHO grade III).

In the absence of molecular testing or in case of inconclusive genetic results, a histologically typical oligodendroglioma should be diagnosed as NOS.

In pediatric patients, tumors with classical morphological features of oligodendroglioma frequently lack IDH mutations and 1p19q co-deletion. After histological mimics are excluded, these tumors can be classified as oligodendroglioma lacking IDH mutation and 1p/19q co-deletion (pediatric-type oligodendroglioma).

Two diffuse astrocytoma variants have been deleted from the WHO classification: *protoplasmic astrocytoma* and *fibrillary astrocytoma.* Only *gemistocytic astrocytoma* remains as a distinct variant of diffuse astrocytoma, IDH-mutant.

Gliomatosis cerebri has also been deleted from the 2016 CNS WHO classification as a distinct entity, rather being considered a growth pattern found in many gliomas, including IDH-mutant astrocytic and oligodendroglial tumors as well as IDH-wildtype glioblastomas.

Currently, most diagnosis of oligoastrocytoma, using both genotype (IDH mutation and 1p/19q codeletion status) and phenotype features, results being compatible with either an astrocytoma or oligodendroglioma, remaining only rare reports of molecularly "true" oligoastrocytomas consisting of histologically and genetically distinct astrocytic (IDH-mutant, *ATRX*-mutant, 1p/19q-intact) and oligodendroglial (IDH-mutant, *ATRX*-wildtype and 1p/19q-codeleted) tumor populations coexisting in the same pathological tissue.

In the 2016 CNS WHO, therefore, the prior diagnoses of oligoastrocytoma and anaplastic oligoastrocytoma are now designated as NOS categories, since these diagnoses should be rendered only in the absence of diagnostic molecular testing or in the very rare instance of a dual-genotype oligoastrocytoma.

The diagnostic use of both histology and molecular genetic features also raises the possibility of discordant

results, e.g., a diffuse glioma that histologically appears astrocytic but proves to have IDH mutation and 1p/19q codeletion, or a tumor that resembles oligodendroglioma by light microscopy but has IDH, *ATRX,* and *TP53* mutations in the setting of intact 1p and 19q. Notably, in each of these situations, the genotype trumps the histological phenotype, necessitating a diagnosis of *oligodendroglioma, IDH-mutant* and *1p/19q-codeleted* in the first instance and *diffuse astrocytoma, IDH-mutant* in the second [4].

1.5.4 Glioblastoma

Glioblastomas are divided into *glioblastoma IDH-wildtype* (about 90% of cases), which corresponds most frequently with the clinically defined primary or de novo glioblastoma and predominates in patients over 55 years of age; *glioblastoma IDH-mutant* (about 10% of cases), which corresponds closely to so-called secondary glioblastoma with a history of prior lower grade diffuse glioma and preferentially arises in younger patients; *glioblastoma NOS*, a diagnosis that is reserved for those tumors for which full IDH evaluation cannot be performed.

IDH mutant gliomastomas have an improved median survival: 31 months for IDH-mutant versus 15 months for IDH-wildtype glioblastoma.

Diffuse Midline Glioma, H3 K27-mutant: this is a new addition to the WHO classification and is defined by the presence of a K27 M mutation in histone H3. In most cases, this mutation identifies clinically aggressive, contrast-enhancing WHO grade IV tumors in younger adults, usually within the thalamus or brainstem [4].

1.5.5 Ependymoma

The classification of ependymal tumors has remained essentially unchanged in the revised WHO classification. The 2016 WHO classification also includes a new genetically defined supratentorial ependymoma, predominantly, but not exclusively in children, characterized by a RELA fusion, usually to C11orf95. Compared with supratentorial ependymoma overall, this tumor has a worse prognosis, with the median progression-free survival reported as less than 24 months [5].

1.6 Incidence

Incidence rates of glioma vary significantly by histologic type, age at diagnosis, gender, race, and country. The lack of consistent definition of glioma and various glioma histologic types as well as differences in data collection techniques may cause difficulty in comparing incidence rates from different sources. Overall age-adjusted incidence rates (adjusted to the national population of each respective study) for all gliomas range from 4.67 to 5.73 per 100,000 persons. Age-adjusted incidence of glioblastoma, the most common and most deadly glioma subtype in adults, ranges from 0.59 to 3.69 per 100,000 persons. Anaplastic astrocytoma and glioblastoma increase in incidence with age, peaking in the 75–84 age group. Oligodendrogliomas and oligoastrocytomas are most common in the 35–44 age group. In general, gliomas are more common in men than women, with the exception of pilocytic astrocytoma, which occurs at similar rates in men and women. In the United States, gliomas are more common in non-Hispanic whites than in blacks, Asian/Pacific Islanders, and American Indians/Alaska Natives [6].

Brain cancer incidence is highest in Europe, where its annual age-standardized rate (ASR) is 5.5 per 100,000 persons, followed by North America (5.3 per 100,000 persons), Northern Africa (5.0 per 100,000 persons), Western Asia (5.2 per 100,000 persons), and Australia/New Zealand (5.3 per 100,000 persons). It is the lowest in sub-Saharan Africa (0.8 per 100,000 persons), South-Central Asia (1.8 per 100,000 persons), and Oceania beyond Australia and New Zealand (0.5 per 100,000 persons).

Although there was an apparent increase in brain tumor incidence in the decades between 1970 and 2000, this was deemed due to improvements in detection concomitant with the introduction of MRI in the 1980s. It is thought, therefore, that any change in incidence rates noted during that period is likely to be due to changing classifications of tumors, improved diagnostic accuracy, better reporting, and access to health care.

Many analyses have examined the incidence rates of glioma to assess whether rates are increasing. The results of these have generally shown the incidence of glioma overall and glioma subtypes to be fairly stable over the time periods assessed [2].

1.7 Risk Factors

Ionizing Radiation: can damage DNA by inducing both single and double-strand breaks, and this can induce genetic changes leading to cancer. Exposure to therapeutic doses or high-dose radiation is the most firmly established environmental risk factor for glioma development and genetic characteristics also influence the extent of this risk. Gliomas may present as early as 7–9 years after irradiation. Recently, a group of experts came to the consensus that the lowest dose of X-ray or gamma irradiation, for which there is a significant evidence of increased cancer risk, is about 10–50 mSv. It may be particularly relevant in children, whose brains are still in the process of developing at the time of irradiation [7].

The association between high-dose ionizing radiation and brain tumors is considered established in the brain tumor epidemiology literature, but it is not generally accepted in the radiation science literature. This may stem from several factors as brain is a highly differentiated organ with low mitotic activity, making it radioresistant and a series of limitations in studies currently available [6].

Nonionizing Radiation: Extremely Low-Frequency Magnetic Fields: although little is known about potential biological mechanisms through which ELF may play a role in the risk of glioma development, it is thought that it would likely act in cancer promotion/progression.

Cellular Phones: scientific evidence does not support a significant association between the use of cellular phones and the risk of glioma. Nevertheless, continuous surveillance on what may be the effects deriving from the use of these devices is desirable, especially because of the long exposure period and their use by children and adolescents.

Allergies and Atopic Disease: have been reported to be protective against multiple cancer types, including glioma. It has been suggested that this effect may be due to increased surveillance by the innate immune system in those with allergies, but this potential mechanism has not been definitively proven.

Heritable Genetic Risk Factors: several inherited, monogenic Mendelian cancer syndromes are associated with increased incidence of specific glioma subtypes: neurofibromatosis type 1 (astrocytoma and optic nerve glioma) and 2 (ependymoma), tuberous sclerosis (giant cell astrocytoma), Lynch syndrome (GBM and other gliomas), Li–Fraumeni syndrome (GBM and other gliomas), melanoma-neural system tumor syndrome (all gliomas), and Ollier disease/Maffucci syndrome (all gliomas). These monogenic disorders account for only a small proportion of glioma cases (<5% overall).

A small proportion (about 5–10%) of gliomas occur in familial clusters, where a patient has a family history of such tumor. First-degree relatives of patients with glioma have a twofold increased risk of developing a brain tumor, especially when the patient was diagnosed with the neoplasm at a younger age. Linkage studies within these familial glioma clusters have not definitely identified high-penetrance risk variants [7].

Occupational chemical exposure, pesticides, solvents: there are several studies in the literature that evaluate the correlation of other risk factors with the onset of gliomas, but they are not sufficient to clearly enumerate a substance among the established causes leading to this cancer type.

1.8 Prognostic Factors

Prognostic factors vary considerably by tumor type and grade across all glioma subtypes. Younger age, high performance status, lower tumor grade, and greater extent of resection are favorable prognostic factors for most adult primary brain tumors. Over the past decade, molecular genetic alterations have been recognized as more powerful prognostic and predictive markers than histological appearance alone [1].

1.9 Clinical Presentation

Patients with primary brain tumors can present with focal (i.e., related to a specific location in the brain) or generalized symptoms over days to weeks, or months to years, depending on the speed of growth and location of the tumor. Tumors can also be found by brain imaging that has been done for unrelated purposes. Tumors in some functional areas of the brain will cause more obvious focal neurological deficits than in other areas, and tend to be discovered sooner on imaging. Frontal lobe tumors might cause weakness or dysphasia; parietal lobe tumors might cause numbness, hemineglect, or spatial disorientation; tumors involving the optic radiations anywhere in the temporal, parietal, or occipital lobe might cause visual field defects. Conversely, tumors located in the prefrontal lobe, temporal lobe, or corpus callosum often result in subtler cognitive dysfunctions such as personality changes, mood disorders, and short-term memory deficits. Infratentorial tumors can cause a combination of cranial-nerve palsies, cerebellar dysfunction, and long-tract signs. Brain tumors can also present with generalized symptoms and signs, not specific to one anatomic location. For example, 50–80% of patients might present with seizures, about 30% with headaches, and 15% with symptoms of increased intracranial pressure, such as progressive headaches worse at night, morning nausea and vomiting, drowsiness, blurred vision from papilloedema, and horizontal diplopia from cranial nerve VI palsy [1].

1.10 Diagnostic Investigations

In a patient with a suspected brain tumor, MRI with gadolinium is the investigation of choice.

In many cases, this suspicion derives from pathological findings highlighted in the CT scan to which the patient has been subjected in the emergency room where he has addressed due to the onset of symptoms of variable severity.

Additionally, multimodal MRI such as diffusion-weighted imaging and diffusion tensor imaging, MR perfusion, and MR spectroscopy are used to better characterize the tumor cellularity, vascularity, and metabolism, respectively, and can help distinguish tumor from non-neoplastic processes, including treatment effect. CNS staging with craniospinal MRI is performed in selected cases. Whenever a brain metastasis is suspected, a systemic cancer screening with a careful clinical examination, and a chest-abdomen CT should be done [1].

1.11 Surgical Management

The initial treatment for most primary brain tumors is maximal safe resection, with goals of achieving an accurate histological diagnosis, establishing the tumor's molecular genotype, improving the quality of life, and increasing survival. Although there are no randomized controlled trials regarding the benefit of the extent of resection, the available evidence suggests that maximal safe resection improves functional status and reduces mortality in both low-grade and high-grade gliomas. The extent of resection is largely dependent on tumor location, surgeon experience, and use of preoperative and intraoperative techniques. In tumors adjacent to eloquent brain regions, extensive safe resection can be achieved with preoperative imaging techniques localizing functional cortical areas and their subcortical pathways via functional MRI and diffusion tensor imaging, respectively, although awake surgery with intraoperative cortical electrode mapping remains the gold standard. Generally, a contrast MRI should be done within 72 h post-surgery to determine the extent of resection and to differentiate the persistence of pathological tissue (postoperative enhancement) from post-surgical scar (late enhancement) [1].

1.12 Medical Management

Seizures are experienced by about two-thirds of glioma patients and require long-term treatment with antiepileptic drugs. For patients who have not had a seizure, routine antiepileptic drug prophylaxis is not recommended, but can be considered for a brief period perioperatively.

Almost all malignant brain tumor patients receive corticosteroids at some point, most commonly for symptomatic peritumoral vasogenic edema. Although there are no standardized guidelines for steroid dose, duration, and taper schedule, dexamethasone is often preferred due to its lack of mineralocorticoid activity and its long half-life (36–54 h). Usual dosing varies between 2 and 16 mg daily depending on symptoms severity, with similar bioavailability orally or intravenously.

Gliomas confer the highest risk for tumor-associated venous thromboembolism of all cancers. Up to 20% of high-grade glioma patients develop symptomatic venous thromboembolism during the perioperative period, and up to 30% at 1 year. Generally, postoperative venous thromboembolism prophylaxis with compression stocking and low-molecular-weight heparin within 12–24 h of surgery is recommended until ambulation, and does not confer increased risk of major bleeding. Prolonged venous thromboembolism prophylaxis over the perioperative period is, however, not advised due to increased intracranial hemorrhage (5% vs. 1%). Treatment of venous thromboembolism with low-molecular-weight heparin is recommended for at least 3–6 months in low-grade glioma, and lifelong in high-grade gliomas [1].

Acknowledgement The current chapter is a revision made by Saverio Pollice, Angela Lorusso, and Tommaso Scarabino of the original chapter written by Saverio Pollice, Gilda Morlino, Michela Capuano, and Tommaso Scarabino in the previous edition of the book.

References

1. Lapointe S, Perry A, Butowski NA. Primary brain tumours in adults. Lancet. 2018;392(10145):432–46. https://doi.org/10.1016/S0140-6736(18)30990-5.
2. McNeill KA. Epidemiology of brain tumors. Neurol Clin. 2016;34:981–98.
3. Diamandis P, Aldape K. World Health Organization 2016 classification of central nervous system tumors. Neurol Clin. 2018;36:439–47.
4. Louis DN, Perry A, Reifenberger G, et al. The 2016 World Health Organization classification of tumors of the central nervous system: a summary. Acta Neuropathol. 2016;131(6):803–20. https://doi.org/10.1007/s00401-016-1545-1.
5. Back M, Rodriguez M, Jayamanne D, et al. Understanding the revised fourth edition of the World Health Organization classification of tumours of the central nervous system (2016) for clinical decision-making: a guide for oncologists managing patients with glioma. Clin Oncol. 2018;30:1–7.
6. Ostrom QT, Bauchet L, Davis FG, et al. The epidemiology of glioma in adults: a "state of the science" review. Neuro-Oncology. 2014;16:1–18. https://doi.org/10.1093/neuonc/nou087.
7. Ostrom QT, Gittleman H, Stetson L, et al. Epidemiology of intracranial Gliomas. Intracranial Gliomas. Part I—surgery. Prog Neurol Surg. 2018;30:1–11. https://doi.org/10.1159/000464374.

Part II

Treatment of Gliomas

Surgery

2

Armando Rapanà, Maria Carmela Bruno, Pasquale Antonio Crudele, Claudia Pennisi, and Mariagrazia Dibenedetto

2.1 General Findings

A conclusive definition of the optimal treatment of brain tumors is probably still to be determined as it depends on several factors such as histology, location and extension of the disease, age and healthy status of the patient and, of course, specifical surgical expertise and technological availability.

Considering the great heterogeneity of the disease, a single treatment modality probably could not fit well to all primary cerebral neoplasms.

To the best of our knowledge, the most accepted and largely shared standard of care for infiltrating brain tumors is represented by a multistaged approach consisting of surgery, radiotherapy, and chemotherapy, often in combination and variously contributing to accomplish a strategy that also depends on both patient's health condition, tumor site, and histology [1].

Because of the continuous progress in diagnosis and surgical techniques, together with the advent of new image-guided surgical procedures, the surgical treatment for brain neoplasms is progressively improving in terms of outcome and complication rate thus becoming, very frequently, the first-line treatment.

Nevertheless, regardless of tumor characteristics and patient's individual considerations, surgery for cerebral tumors should obey to few universally accepted principles: removing the mass, confirming the histology of the lesion in order to address a proper adjuvant treatment, relieving from the intracranial hypertension syndrome without forgetting, of course, to minimize the neurological impact for the patient itself by maximally respecting the healthy tissue.

Summarizing, the leading concept of surgery for cerebral neoplasms should be the following: *maximal resection with minimal (if any…) morbidity*.

A. Rapanà (✉) · M. C. Bruno · P. A. Crudele · C. Pennisi
M. Dibenedetto
Department of Neurosurgery, "L. Bonomo" Hospital Andria, Andria, Italy

Consequently, recent technological advances that allow for real-time and quantitative visualization of cancer-infiltration and non-cancer parenchyma have been proposed [2]. Unfortunately, despite very promising aspects, a conclusive confirmation in order to determine if one or more of the described techniques should be recommended as standard care for brain tumors is still lacking [3].

While for benign tumors, the radical excision in most cases is the only and definitive therapy (curative surgery), for malignant tumors and/or in case of subtotal resection, a further treatment should be considered.

A radical resection is always advisable in order to improve the overall outcome in glioma surgery [4–7]; nevertheless, there could be cases for which a subtotal removal could represent an appropriate choice too (e.g., total resection not technically feasible, tumor in eloquent areas, etc). Possible benefits, also in case of incomplete resection, though not universally accepted, could also be the reduction of cancer mass; this would result in a better oxygenation of residual tumor and, consequently, a better response to radiotherapy also due to a significant reduction of clusters of necrotic cells possibly playing a role in chemoresistance development.

2.2 Surgical Treatment: Standard of Care and New Boundaries

To the best of actual knowledge, surgery is universally considered the first-line treatment for patients in good conditions affected by resectable brain tumors being the extent of resection the single factor more effectively influencing the final outcome of patients affected by infiltrating cerebral neoplasms [3–5, 7]. Consequently, a *Gross Total Resection* (GTR) should be pursued for both high-grade gliomas (HGG) and low-grade gliomas (LGG). Indeed, there are many evidences that, compared to a *SubTotal Resection* (STR), performing a GTR could improve the median survival rates for patients affected by HGG and LGG by 200% and 160% respectively [5, 8, 9].

T. Scarabino, S. Pollice (eds.), *Imaging Gliomas After Treatment*, https://doi.org/10.1007/978-3-030-31210-7_2

As a result, from its origins to today, neurosurgery of brain tumors, and particularly gliomas, has significantly evolved over the past 25 years with a wide variety of new operating instruments, new surgical approaches and, in addition, anesthetic and resuscitation techniques introduced in daylife activities.

Accordingly, criteria of operability are even changed, allowing an extension of surgical indications; patients that were previously considered inoperable could nowadays be eligible for surgery.

2.3 Preoperative Planning

Patient conditions (age, Karnofsky Performance Status, presence of comorbidities…), tumor extension and characteristics (e.g., vascularization, presence of cysts or necrotic areas, calcifications, etc) together with the perfect knowledge of its relationship with adjacent critical structures are fundamental aspects to be considered in order to plan a correct surgical approach.

The need for image guidance during neurosurgical operations has always been a concern for neurosurgeons and has continuously evolved through several steps over the last 60 years. Frame-based navigational system (also known as *stereotaxy*) is the most traditional guidance option offering the surgeon the possibility to calculate preoperatively the desired trajectory of the probe with the certainty of being able to reproduce it intraoperatively.

The subsequent development of neuronavigation represents a substantial improvement of image-guided neurosurgical technique. Neuronavigation, also known as frameless neuronavigational systems (as it does not require any frame-based devices), tracks the movements of surgical instruments within the surgical field and, mostly, their relationship with the lesion and any other anatomical structure graphically reproduced by an operative monitor into all the three different planes (axial, sagittal, and coronal) with an accuracy of 2–3 mm range using MR images. The preoperative planning consists of choosing the best trajectory (not necessarily the shorter one!) to deal with "that" specifical lesion avoiding any critical area accurately identified on preoperative MRI study.

Thus, given a target lesion and after that the desired entry point have been located, it is possible to identify preoperatively the best route to warrant the surgeon the maximal respect of critical areas and to pursue exactly the prefixed route at surgery with great accuracy.

2.4 Surgery

Patient positioning is critical for a successful procedure. The use of transcranial Mayfield head-holder is fundamental to warrant a stable head positioning and a good access to the involved area during the entire procedure. Usually, the target lesion should be at the highest point of the surgical field in order to allow the surgeon a comfortable access to the lesion together with an optimal control of crucial structures (vascular pedicle, dural sinuses…) in case of need.

The importance of ensuring a good venous outflow, in order to avoid any intraoperative brain swelling, should not be underestimated during the positioning of the patient. Neck should not be overturned and the head should be above the level of the heart.

All the possible pressure points should be adequately protected with silicon paddies and great care should also be paid in order to avoid nervous injuries in curarized patients.

Skin flap is carefully planned according to site and size of the lesion and, of course, to the need of exposing the lesion itself together with any other structure of interest. The description of the different approaches goes far behind the scope of this chapter but some essential rules must be underlined. Shaving of the hair is not mandatory as it does not affect the infective risk. Drawing the skin flap should obey to aesthetical principles but should also be taken into account the need to provide an adequate vascular supply to the wound. Regional arteries should be spared and coagulation limited at the minimum. Great attention should also be paid while reflecting the skin flap in order to avoid the occlusion of the vascular pedicle.

Bone flap and dural opening are also fundamental steps in managing cerebral neoplasms. The main concept is to create a bone flap that could be repositioned at the end of the operation with good aesthetic results trying to balance the need of an adequate exposition of the target with an acceptable bony demolition. Craniotomies for gliomas surgery usually are not technically demanding as those for skull base surgery but, when a basal exposure is required, a further bony demolition could be achieved in the same way.

After craniotomy, *dura mater* is firmed to the bone with tack-up silk sutures in order to avoid bleeding from epidural space; dural coagulation is limited to the very essential in order to avoid dural shrinkage. In case of sinus exposition, a great care should be paid not to damage it during the craniotomy and also not to traction or overturn the dura together with the sinus itself. Relaxant cuts could also be added at the corners of durotomy in order to further enhance the exposure and to relieve the pressure in case of swollen or congested brain. Dural opening should be done always keeping in mind that after the removal of the mass it must be closed again.

2.5 Tumor Resection: Approaching the Lesion

Superficial tumors could usually be approached directly by starting from the most visible point and, then, following the boundaries of the lesion under the microscope magnification,

the ideal purpose should be to remove completely the lesion or, alternatively, to remove as much of tumor as possible without sacrificing the healthy tissue.

When dealing with deep-seated lesions, in addition, the surgeon must face with two adjunctive problems: to find the lesion and to choose the best route to manage it.

Image-guided navigation systems (neuronavigation) offer the surgeon the possibility to plan preoperatively the most suitable approach and to replicate it during operation; for these and other reasons neuronavigation, nowadays, is considered mandatory for the management of deep-seated lesions and/or for lesions close to or within critical areas.

Regardless of the site and nature of the lesion, a transcortical approach is always the first step in many neurosurgical procedures. Cortical incision should be the smallest possible in order to reduce the risk of postoperative deficit while its location is mostly based on the lesion's features, the vascular architecture of the region and, of course, the functional relevance of that cortical area.

A transcortical route could be realized into two different ways: the trans-gyrus and the trans-sulcal approach.

The trans-gyrus path has been suggested for the management of subcortical mass lesions but some concerns have to be underlined. The risk of vascular damages, due to the presence of vascular structures encountered since from the pial layer underneath the central area of the gyrus, is not negligible; moreover, the prolonged manipulation or retraction of long association fibers underneath the gyral grey/white matter junction could be responsible for an inescapable vascular and white matter damage.

As an alternative, the trans-sulcal approach, as described by Yasargil [10], has traditionally been considered the safest and the shortest way to reach deep-seated lesions even if great care should be paid in order to minimize the risk of damaging the vessels that usually lies into the depth of cerebral sulci. After a sharp opening of the arachnoid along the longitudinal axis of the sulcus as much as it is possible, the vessels lying within the sulcus are dissected free [11]. Great care must be done not to sacrifice the sulcal vessels unless strictly necessary. A wide opening of the arachnoid allows the surgeon to spread the sulcal banks just using the bipolar tips. The routine use of self-retaining retractor could be replaced by using the bipolar and the suction tube that would provide an intermittent retraction thus avoiding an unnecessary prolonged compression and stretching over the nervous structures. While an extended opening of the sulcus is strongly advisable, the entry at the base of the sulcus should be minimal both in length and width and very careful in order to minimize the damage to neural structures. The sulcal areas present a lower density of associative fibers and, more importantly, a cortical incision running parallel to the sulcus main axis, reduces the fibers interruption to a minimal amount.

As a general rule, a sulcal approach could be considered when the target lesion lies into the depth of the sulcus or, alternatively, if it lies close to one of the banks of the sulcus itself. Thus, the trans-sulcal approach could be the best option for infiltrating mass lesions located in the subcortical space below a sulcus as it couples an easy access for resection with a minimal cortical disruption. Trans-gyrus approach, on the other hand, could be used for subcortical tumors that neither underlie an obvious sulcus nor involve eloquent cortical regions. Corticectomy should be performed in a linear fashion for small tumors while, for larger mass lesions, a circumferential corticectomy could be the best choice [12].

2.6 Removal of the Mass Lesions: Tips and Tricks

As a general rule, when dealing with superficial tumor, the first step would be to divide, under the magnification of the intraoperative microscope, the arachnoid that spans from the normal brain over the tumor by using microscissors and bipolar tips. The interface between the tumor and the normal tissue should be carefully identified and pursued all around the mass lesion doing the maximal efforts to preserve the regional vessels not going to the tumor. Once identified, the cleavage plane could be kept open with saline-soaked cottonoid strips. At this point the so-called internal decompression of the tumor, mostly in case of large mass lesions, could be a safe strategy as it offers the possibility to remove the remaining mass and then to go on by dividing it from the surrounding healthy white matter with less need for retraction of the normal brain. Very often it could be necessary to alternate between internal decompression and microscopic dissection around the tumor surface to achieve a complete resection of the mass leaving at the end of the procedure the part of the tumor possibly adjacent to major vascular structures, ventricle walls, or critical areas. The use of ultrasonic cavitating aspirator could be of great help in case of necrotic, softy, and relatively avascular lesions. The bed of the surgical field should be carefully inspected at the end of the procedure in search for residual tumor nodules and pathologic vessels that could result in a postoperative hematoma.

The surgical approach to tumors not surfacing the cerebral cortex does not differ significantly in case of tumors involving non-eloquent areas; in these cases, the possibility to be managed either by a trans-sulcal either by a trans-gyrus path according to the aforementioned considerations (see above for more details) should be carefully evaluated. The adoption of the image-guided navigation systems (see below for further details) is of great help for localizing deep-seated masses on the basis of the preoperative planning. Needless to say that intraoperative magnification is also fundamental.

Subcortical tumors growing into eloquent areas should be approached along the sulcus related to the most distended gyrus farthest away from the critical area and, of course, as close to the tumor as possible.

However, removing a brain neoplasm, also under magnification, may sometimes present further technical troubles as the tumoral tissue either could look like normal nervous substance or could be immediately close to the healthy and functional brain. New methods of identifying tumors during surgery have been developed to help surgeons to better differentiate pathologic tissue from normal brain.

2.7 Intraoperative Tools: Light and Shadows

Selective surgical excision and extent of resection are essential components for determining both tumor diagnosis and patient prognosis [3, 6, 7]; as both of them depend on the surgeon's capability to discriminate between cancer and normal tissues, incoming techniques that facilitate a well-demarcated differentiation between normal versus cancer-invaded parenchyma could, under this aspect, be of great help in order to achieve the maximal excision.

All the techniques and tools proposed during last years in order facilitate a radical and selective resection of infiltrating tumors can be essentially divided into two main groups: methods favoring the intraoperative visualization of tumors taking advantages from the different behavior of tumoral cells compared to normal ones under specific light excitation (*Fluorescence Guided System*) and methods driving the resection on the basis of preoperative neuroradiological imaging (mainly CT and MR) used as a map (*Image Guided Navigations Systems*).

2.8 Image-Guided Navigation Systems

Despite the wide applicability and many fascinating aspects of image-guided navigation systems, a major drawback of this technology became apparent right from the beginning of its implementation in neurosurgical operations: all neuronavigational systems use preoperative images (mainly from CT or MRI studies), which, of course, do not take into account for changes of brain anatomy due to intraoperative activities [13]**.** Therefore, neuronavigation could be considered a very reliable surgical tool for both preoperative planning and intraoperative lesion localization but its accuracy decreases progressively during surgery being it related to the so-called "*brain shift*" occurring after the opening of the dura mater and, to the unavoidable parenchymal deformation resulting either from surgical maneuvers either from ongoing tumor resection [13]**.**

In order to overcome the aforementioned critical issues, the use of intraoperative UltraSound (iUS) has also been suggested as it offers the surgeon the possibility to distinguish between the neoplastic tissue and the healthy one in a real-time way repeatable as many time as necessary. The major shortcomings of iUS are represented by the long learning curve as neurosurgeons are, usually, not specifically trained to evaluate US images and, mostly, the low quality of images and difficulties in anatomical orientation [14, 15]**.** Furthermore, it has also been reported that images resolution and their quality progressively deteriorates as resection proceeds because of surgical manipulation [15]**.** Intraoperative ultrasound (iUS), if used in combination with neuronavigation, could be able to potentially overcome the limitations of both techniques as it offers the possibility to bring up to date in a real-time modality the surgical anatomy and, more importantly, to delineate the residual mass of the tumor [15]**.**

Intraoperative MR (iMR) and CT (iCT) have also been proposed with the scope to update the imaging data during the ongoing surgery [16], but, apart from that both techniques are very expensive and quite time-consuming, they could not be considered pure real-time intraoperative imaging techniques as it is not possible to operate under their direct guidance. Nevertheless, a recent review provided level II evidence for the use of intraoperative MRI to improve extent of resection, quality of life, and also overall survival in glioma patients [17] but, despite encouraging promises, further data are expected in order to drive final conclusions.

2.9 Fluorescence-Guided Methods

Intraoperative visualization of tumors may not only allow a more radical resection and, consequently, decrease the need for second-look surgeries but may also improve safety of the procedure by avoiding unnecessary damage to normal tissue. In particular, because the margins of gliomas are usually diffuse, the boundaries of the lesion classically fixed by T1-weighted gadolinium-enhanced MRI (for high-grade gliomas), or T2-weighted hyperintensity (for low-grade gliomas) are, unfortunately, quite ambiguous and do not necessarily correspond precisely to real biological borders neither reflects the tumor-cell density [18]**.** In fact, since gadolinium contrast-enhancement relies on the disruption of the blood–brain barrier (BBB), infiltration of glioma cells at the tumor boundaries could be not discernable with MRI.

Following systemic administration, 5-ALA is metabolized in tumor cells into a photosensitizing porphyrin that under blue light excitation (400–410 nm) will appear brilliant red. Though the mechanism of accumulation in malignant glioma cells is not fully understood, ALA is highly specific (98%) in areas of infiltrating tumor; the tumoral tis-

sue will appear red, whereas normal tissue (including edematous areas) does not show fluorescence [19, 20].

As a proof, many studies have shown that 5-ALA-induced tumor fluorescence extends beyond the area of gadolinium contrast-enhancement found on preoperative MRI and, furthermore, a very high sensitivity, specificity, and positive predictive value (PPV) for tissue fluorescence and malignant glioma could be demonstrated. As a consequence, intraoperative fluorescence imaging could offer the potential to better define the true margins of the neoplastic lesion during the procedure thus improving the extent of resection together with its selectivity independent of neuronavigation and brain shift [21].

Furthermore, also in case of diffusely infiltrating gliomas with nonsignificant MRI contrast-enhancement, 5-ALA-induced tumor fluorescence could permit intraoperative identification of anaplastic foci and establishment of an accurate histopathological diagnosis for proper adjuvant treatment [21]. A phase-III study [22] reported very encouraging results demonstrating that the use of 5-ALA contrast resulted in higher rates of gross total removal (65% vs. 36%) and 6-month progression-free survival (41% vs. 21.1%) compared to traditional surgery.

Factors that correlate with fluorescence induced by 5-ALA are cellular density, tumor cell proliferative activity, neovascularization of the tumor, and BBB permeability [21]**.** As a consequence, unfortunately, visualization of 5- ALA-induced is very effective at revealing regions of bulk tumor (deep red), whereas, fluorescence intensities decay near the margins (lighter pink) and vanish almost entirely as the tumor cell density continues to decline despite the finding that glioma cells diffusion could be find also in the latter region [18, 21] whose cell concentration is too weak to be visualized directly with the microscope.

Another fluorophore is *fluorescein* sodium. Using a modified microscope with wavelength range of 560 nm the pathologic tissue will be clearly visible becoming more brilliant than normal tissue. The major disadvantage is that the fluorescence is not tumor-specific as it depends on blood–brain barrier integrity; thus, fluorescein is a marker of contrast enhancement rather than a real marker of neoplasm. Fluorescein concentration will be higher in all highly perfused tissues and vessels and, consequently, during surgery, an unspecific and progressive extravasation of fluorescein, that is related to the surgical trauma more than to tumor itself, could be expected [20] and should be kept into account. The FL-guided technique has the advantage that the illumination of the Y560 filter allows continuous dissection, resection, and coagulation without switching from one light source to the other, as necessary when using the 5-ALA technique.

Despite many promising aspects, it is, unfortunately, not clear yet whether any of these sometimes very expensive tools (or their combination) should be considered to be able to offer any real advantage in terms of extent of resection, overall survival and clinical benefits over standard surgery.

A recent review [3] analyzing results from four randomized controlled trials, using different intraoperative imaging technologies: iMRI (2 trials), fluorescence-guided surgery with 5-aminolevulinic acid (5-ALA) and neuronavigation demonstrated that intra-operative imaging technologies, specifically iMRI and 5-ALA, may be of some benefit in maximizing extent of resection in high-grade gliomas patients even though this is based on low to very low-quality evidence. Likewise, both short- and long-term neurological effects remain uncertain and also the impact on overall survival, progression-free survival, and quality of life are still unclear. Cost-analysis studies suggested that image-guided surgery has an uncertain effect on costs, compared with standard surgery use, while 5-aminolevulinic acid is more costly. No trials for ultrasound were found in literature thus justifying the need for further studies.

2.10 High-Grade Gliomas

Despite the advent of many emerging and very promising techniques and multidisciplinary protocols, patients affected by glioblastomas (grade IV according to WHO classification) [23] have, unfortunately, a poor prognosis with a median survival rates ranging from 12.2 to 18.2 months, whereas those affected by anaplastic astrocytomas (grade III according to WHO classification) can be expected to survive 41 months, on average.

Leaving out some biological markers, and preoperative Karnofsky Performance Status (KPS), the single factor mostly influencing survival of patients affected by GBM is the extent of resection [3, 4, 7, 8]. Indeed, a retrospective systematic meta-analysis study performed on over 41,000 newly diagnosed GBM patients demonstrated a clear benefit of gross-total removal (GTR) versus sub-total removal (STR) with a 61% increase in likelihood of a one-year survival and a 51% likelihood of a 12-month progression-free survival [9]**.**

Unfortunately, apart from the aforementioned difficulties in distinguishing between healthy tissue and infiltrated tissue, the infiltrative capacity of GBM cells over long distances makes a complete eradication of neoplastic cells almost impossible to achieve thus justifying a recurrence risk close to 100% [24]**.** Indeed, the infiltrative behavior of GBM is mainly due to the typical infiltrative pattern of glioma cells; their migratory capacity allows them to collect below the pial margins, surround the vasculature, and migrate through white matter tracts also crossing the corpus callosum where they could be found at least 3 cm away from their primary site [24]**.**

Although a radical excision is not always possible, it should be the widest possible (as long as it does not cause significant risks and/or additional neurological deficit). A great amount of scientific evidences supports the superiority of GTR over STR and biopsy. Therefore, GTR probably increases the likelihood of 1-year survival compared with STR by about 61% and increases the likelihood of 2-year survival by about 19%. Consequently, when clinically feasible, there is a general agreement encouraging a GTR in all patients with newly diagnosed GBM [9] even though the exact relationship existing between extent of resection, residual volume, and overall survival has not been established yet.

Many studies focused on the threshold of resection beyond which a significant survival benefit could be achieved [4, 8]. Though a 90% of resection without compromising functional pathways remains as the realistic desired goal for glioblastoma surgery, even an extent of resection of 70% has shown a statistically significant improvement in overall survival, progression-free survival and seizure control and for each 5% extent of resection increment, the risk of death decreases by ~5.2% and the risk of recurrence decreases by 3.2% [8].

Another important parameter that should be considered is the residual volume of the mass [8]. Indeed, it is easy to understand that patients with the same amount of resection (EOR) may have quite different residual volume, since while EOR is dependent on the preoperative tumor volume, the residual volume is, probably, more strictly related to the site of the tumor than to the volume of the mass itself. Furthermore, it should also be stressed that residual tumoral volume could influence prognosis also by affecting response to chemotherapy. In fact, larger residual volumes may have not only a larger number of tumor cells, but also a proportionally greater number of tumor stem cells, which may be responsible for the development of a condition of resistance to adjuvant therapies, including radiation and chemotherapy.

2.11 Low-Grade Gliomas

Although low-grade gliomas carry a better prognosis, in 45–86% of cases they could change their biological nature and evolve into high-grade gliomas with an average time of anaplastic transformation of about 7–8 years thus justifying the concept that an early surgical approach could be a successful therapeutical strategy.

As for high-grade gliomas, surgery remains a mainstay of therapy for low-grade gliomas too but, while for symptomatic patients the indication for surgery could be straightforward, the decision-making process can be more complex in case of incidentally discovered mass lesions and mostly for tumors located within or nearby eloquent cerebral areas.

Grade I tumors causing seizure disorders that are refractory to anticonvulsants usually can be removed with excellent control of the seizures and without significant risks. Patients with grade I tumors, also in case of subtotal resection, can mostly be considered cured and no further treatment is usually required.

Grade II lesions can also be resected to some degree but a complete removal can be obtained only in certain areas of the brain. Polar and superficial lesions are more readily excised than deeper and more extensive ones; lesions extending into the temporal, insular, or opercular regions represent a surgical challenge since perforating branches of the middle cerebral artery may transverse the tumor to supply quite important white matter tracts and, consequently, they must be respected in order to preserve neurological integrity of the patient.

One recent study compared the results of two different treatment modalities: biopsy with serial observation versus early surgical resection. Patients treated by early resection seem to have significantly longer overall survival, with an estimated 5-year survival of 74% compared with 60% for patients treated by biopsy and observation [25]**.** Apart from cytoreduction, it is also possible to speculate that there could be a significant benefit from a surgical debulking procedure compared with biopsy because needle biopsies, in case of heterogeneous tumors, could easily produce a misdiagnosis underestimating the real grade of the tumor.

Extension of removal could significantly affect prognosis even for slight differences. In particular, the possibility of a correlation between extent of resection and both recurrence rate and malignant transformation could be perceived just observing the finding that the 5-year overall survival rate of 97% for EOR >90% dramatically drops to a value as low as 76% when the extent of resection goes below the threshold of 90% [26]**.**

The impact of residual tumor volume on overall survival becomes significant when the residual volume is smaller than 10 cm^3; indeed, under this extent the weak amount of remaining cells theoretically decreases the risk of malignant cellular degeneration and, hence, potentially prolongs survival [27]**.**

Some concerns could significantly condition the possibility to obtain a radical resection in case of involvement of critical areas (see after for further details). In fact, the likelihood of complications increases with the proximity of the lesion to eloquent cortex. Even though in many cases the postoperative deficit will resolve over 1–3 months using awake craniotomy techniques [28], the risk of postoperative complications increases significantly in case of lesion located within 0.5–2 cm of functionally active areas [29]**.**

Therefore, it is advisable that patients with low-grade gliomas should undergo the greatest surgical resection that can be accomplished without exposing the patient to significant risk of a permanent deficit whose social impact has

greater significance if we consider the young age of these patients and the relatively long natural history of the disease.

Under this aspect the intraoperative identification of eloquent areas (motor, language, memory, visual…) by using the brain mapping technique and their respect is mandatory [29, 30]**.** By stopping the resection when language, motor, visuospatial, cortical, or subcortical eloquent areas are encountered, the risk of a permanent postoperative neurological deficits is very low. Furthermore, awake mapping technique for non-eloquent areas has a marked usefulness as it can allow the surgeon to safely pursue the target of a "supratotal" resection (extending the resection area far beyond the boundaries of the tumor visible on T2 or FLAIR images on MRI) with a significant positive impact on risk of future anaplastic transformation.

2.12 Surgery in Critical Areas

Indications for surgical resection for tumors in critical areas need to be carefully evaluated due to the high risk of neurological deterioration after surgery. Nowadays, the right management of tumor in critical areas cannot ignore a thorough preoperative assessment of "eloquent "cerebral areas completed and integrated by the brain mapping technique during surgery. These two steps are considered crucial in pursuing the main scope of neuro-oncological surgery: *maximal resection with minimal (if any…) morbidity*.

Talking about "eloquent cortex" we refer to cortical brain areas necessary for language, motor, and sensory functions. Specifically, we refer to the cortical regions of the inferior frontal lobe, superior temporal lobe, and angular gyrus of the dominant hemisphere for language function, the bilateral posterior frontal lobes for voluntary movement, the bilateral anterior parietal lobes for tactile sensation, and the bilateral medial occipital lobes for vision. An "eloquent brain area" is, on the other hand, a region of eloquent cortex together with its associated subcortical structures whose injury could result in loss of a specific function.

As a result, it becomes essential to distinguish functional brain (cortex and subcortical structures) from tumor to avoid neurological postoperative deficits. Under these aspects, many technologies able to prevent serious functional damages following surgery (navigation, image-guided surgery, awake surgery, functional mapping) have been proposed during the last decades.

Although routine structural MR images can accurately demonstrate brain tumors, they do not give precise information about the involvement or integrity of the white matter tracts in the immediate region surrounding the mass lesion due to the fact that the high-intensity signal often seen in the white matter adjacent to a tumor on T2-weighted or FLAIR images may represent either tumor extension either edema reaction in the surrounding normal white matter tracts.

Brain mapping will help to save as much as possible critical areas that may also improve functionality over time and reduce to the minimum the risk of a neurological deficit.

The intraoperative identification of a critical cortical area starts with a direct low-voltage electrical stimulation of the cortex overlying or adjacent to the tumor to be removed. Stimulation of the motor cortex produces a muscle contraction while language cortex stimulation would result in a speech arrest, inability to name objects shown to the awake patient, or inability to read numbers. If a stimulated cortical area appears to be functionally silent it is generally considered to be safe for resection. Once the underlying white matter is exposed, the white matter itself is similarly stimulated while neurological functions are closely monitored. If an eloquent cortical or subcortical area is identified, the tissue in this area, even if it contains gross tumor tissue, is generally left undisturbed to avoid the acquisition of permanent neurological deficits.

High-grade tumors in eloquent brain regions have traditionally been associated with limited resection and higher morbidity. As malignant glioma cannot be cured, extremely aggressive resection is not recommended if considered to be too hazardous. In order to avoid new postoperative neurological deficits, accurate localization of the sensorimotor cortex, corticospinal tracts, and language areas is advisable to enable a safe surgical resection. In these cases, overall worsening of neurological function following surgery can be estimated to be around 12% [31]**;** a gross total resection could be achieved in about one out of three patients and a subtotal resection (e.g., more than 90% of the tumor volumes removed) can be realized in about 20% of patients due to the necessity of sparing eloquent areas.

Surgical management of LGG, mostly when a clear involvement of critical areas is visible, is almost controversial. Due to their infiltrative pattern and possibility of malignant transformation, the mean 10-year survival is 30% when less than 90% of the tumor is resected [26]**.** The positive impact of residual tumor volume on overall survival becomes significant when the residual volume is smaller than 10 cm^3 with a possible benefit on overall survival [27]**.**

As a worse overall survival in patients with LGGs in eloquent locations compared to patients with similar tumors in other areas is demonstrated, surgical treatment of LGGs should obey to two conflicting requirements: maximizing the amount of tumor tissue excised and contemporary lowering the risk of poor functional outcome.

The common observation of absence of deficit despite a growing tumor in eloquent regions may be explained by the recruitment of compensatory areas and, also, by the persistence not only of eloquent neural networks, but also of functional astrocytes and intact neuron-glial interactions within

the tumor itself [28]. Furthermore, given the well-known concept of brain plasticity and functional compensation frequently seen after acute brain injuries (stroke, trauma, surgery…) it is possible to hypothesize a sort of functional compensation, related to recruitment of adjacent regions [28] able to reduce the incidence of neurological deficit.

Thus, in dealing with LGG presenting eloquent areas involvement, the crucial question would be to know if neurological functions will be compensated after the removal of "functioning brain" tissue together with the tumor. Repetitive intraoperative electric stimulation can reveal the existence of several brain regions able to perform the same function confirming the concept of "functional redundancy" within the primary sensorimotor area. The resection of functional glioneuronal structures comprised within the tumor might induce a functional reshaping by generating changes in neuronosynaptic networks as observed using transcranial magnetic stimulations [28] able to compensate the loss of a functionally relevant brain area.

However, despite brain plasticity, mechanisms of compensation are not unlimited. If a damaged area is compensated by a different region, a lesion of this recruited area will induce a permanent deficit. Consequently, surgical resection should avoid the involvement of an eloquent structure if its compensatory area is not perfectly functional (notably if infiltrated by tumor or also removed) [28].

The EOR is a strong independent factor associated with improved survival, as well as with delay of progression and malignant transformation. A surgical strategy comprising the use of modern technology such as 3D ultrasound, intraoperative MRI, and/or brain mapping techniques may probably outweigh the risks of neurological deficits even in eloquent locations being the major limitation in achieving a complete resection of the infiltrative growing pattern of these lesions, particularly at the subcortical level [27].

Further refinement of tools and techniques should be encouraged to safely enhance tumor removal in critical areas.

2.13 Recurrent Gliomas

Despite continuous improvements in both medical and surgical management of patients with glioblastoma, the risk of recurrence, unfortunately, should be considered unavoidable with a median survival of 12–15 months.

Notwithstanding the progression of the disease, many patients have, however, at the time of tumor recurrence, a good quality of life thus justifying the need for a further treatment.

At present, there is no standard treatment strategy for patients with recurrent glioblastoma. Indeed, while for newly diagnosed glioblastomas standard treatment consists of microsurgical resection followed by concomitant chemotherapy and radiation therapy, our understanding of the morbidity profile and survival benefit of re-resection remains incomplete.

Several recent studies [4, 32] have suggested the potential benefit of a re-resection for recurrent glioblastoma with an acceptable complication rate but their bias, due to small sample sizes, categorical measurements of the EOR, and heterogeneity in adjuvant treatment regimens, do not allow us to draw definitive conclusions.

At the same time, retrospective papers [4, 32, 33] showed a progressively increasing overall survival benefit for more extended resection of recurrent *de-novo* glioblastomas thus emphasizing the importance of identifying patients potentially suitable for re-resection and, of course, a minimum EOR threshold.

According to previous studies, a significant survival advantage could be appreciated for EOR as little as 80% whose median survival reaches the limit of 19 months while an EOR of 97% could produce a further survival benefit consisting of 30-month median survival [32]. Furthermore, a stepwise improvement in overall survival has also been reported for population with a 95%–100% EOR range depending on age (progressively worse overall survival with increasing age) and tumor volume (higher risk for tumors greater than 12 cm^3).

Survival analyses considering only the EOR without taking into account the possible neurological morbidity are likely to provide an incomplete assessment of the intervention. Intuitively, cytoreduction could have some neurological cost to the patient. In fact, significant differences in neurological morbidity could be observed for more extensive resection. Neurological deficit is mostly limited to the early postoperative period while a significant risk of a permanent deficit should be evaluated in case of a more extended resection. Furthermore, patients with preexisting neurological symptoms and/or tumors in eloquent areas are at particular risk for neurological deterioration after repeated surgery and the possibility of a second surgery should be considered very cautiously.

Overall, the perioperative complication rate is reported to be 33%, while a neurological deterioration is possible to occur in about 18% of patients and perioperative death in 2.2% of cases [34].

In conclusion, despite conclusive proofs are still to come, there is a common opinion that the role of second surgery in the treatment of recurrent GBM could be carefully considered for a selected subset of patients for which it might add a survival advantage of about 8–9 months [35]. Young patients (50 years or under) with a good Karnofsky performance status (higher than 60 to 70) are best candidates to second surgery. An EOR beyond the value of 80%, as well as preserving functional pathways to maximize quality of life, should be of critical concern to the neurosurgeon treating patients with recurrent glioblastoma.

Acknowledgments The current chapter is a revision made by Armando Rapanà, Maria Carmela Bruno, Pasquale Antonio Crudele, Claudia Pennisi, and Maria Grazia Dibenedetto of the original chapter written by Vincenzo D'Angelo, Raniero Mignini, and Tommaso Scarabino in the previous edition of the book.

References

1. Rampling R, James A, Papanastassiou V. The present and future management of malignant brain tumours: surgery, radiotherapy, chemotherapy. J Neurol Neurosurg Psychiatry. 2004;75:24–30.
2. Lara-Velazquez M, Al-Kharboosh R, Jeanneret S, et al. Advances in brain tumor surgery for glioblastoma in adults. Brain Sci. 2017;7:166.
3. Jenkinson MD, Barone DG, Bryant A, et al. Intraoperative imaging technology to maximise extent of resection for glioma. Cochrane Database Syst Rev. 2018;22:1.
4. Bloch O, Han SJ, Cha S, et al. Impact of extent of resection for recurrent glioblastoma on overall survival: clinical article. J Neurosurg. 2012;117:1032–8.
5. Lacroix M, Abi-Said D, Fourney D, et al. A multivariate analysis of 416 patients with glioblastoma multiforme: prognosis, extent of resection, and survival. J Neurosurg. 2001;95(2):190–8.
6. Pilchmeier U, Bink A, Schackert G, et al. Resection and survival in glioblastoma multiforme: an RTOG recursive analysis of ALA study patients. Neurol Oncol. 2008;10:1025–34.
7. Sanai N, Polley MY, McDermott MW, Parsa AT, et al. An extent of resection threshold for newly diagnosed glioblastomas. J Neurosurg. 2011;115:3–8.
8. Chaichana KL, Jusue-Torres I, Navarro-Ramirez R, et al. Establishing percent resection and residual volume thresholds affecting survival and recurrence for patients with newly diagnosed intracranial glioblastoma. Neuro Oncol. 2014;16:113–22.
9. Brown TJ, Brennan MC, Li M, et al. Association of the extent of resection with survival in glioblastoma: a systematic review and meta-analysis. JAMA Oncol. 2016;2:1460–9.
10. Yasargil MG. Microneurosurgery vol IIIA: AVM of the brain, history, embryology, pathological considerations, hemodynamics, diagnostic studies, microsurgical anatomy. New York: Thieme Medical; 1987.
11. Latini F, Hjortberg M, Aldskogius H, et al. The use of a cerebral perfusion and immersion-fixation process for subsequent white matter dissection. J Neurosci Methods. 2015;253:161–9.
12. Chaichana KL, Rincon-Torroella J, Acharya SY, et al. Transsulcal versus transcortical resection of subcortical metastases. In: Quiñones Hinojosa A, editor. Video atlas of neurosurgery contemporary tumor and skull base surgery. Oxford: Elsevier; 2017. p. 17–21.
13. Stieglitz LH, Fichtner J, Andres R, et al. The silent loss of neuronavigation accuracy: a systematic retrospective analysis of factors influencing the mismatch of frameless stereotactic systems in cranial neurosurgery. Neurosurgery. 2013;72(5):796–807.
14. Prada F, Del Bene M, Mattei L, et al. Fusion imaging for intraoperative ultrasound-based navigation in neurosurgery. J Ultrasound. 2014;17:243–51.
15. Moiyadi AV, Shetty P. Direct navigated 3D ultrasound for resection of brain tumors: a useful tool for intraoperative image guidance. Neurosurg Focus. 2016;40:1–8.
16. Black PM, Moriarty T, Alexander E 3rd, et al. Development and implementation of intraoperative magnetic resonance imaging and its neurosurgical applications. Neurosurgery. 1997;72(5):831–42.
17. Kubben PL, ter Meulen KJ, Schijns O, et al. Intraoperative MRI-guided resection of glioblastoma multiforme: a systematic review. Lancet Oncol. 2011;12(11):1062–70.
18. Liu JTC, Daphne Meza BS, Sanai N. Trends in fluorescence image-guided surgery for gliomas. Neurosurgery. 2014;75(1):61–71.
19. Esteves S, Alves M, Castel-Branco M, et al. A pilot cost-effectiveness analysis of treatments in newly diagnosed high-grade gliomas: the example of 5-aminolevulinic acid compared with white-light surgery. Neurosurgery. 2015;76(5):552–62; discussion 62
20. Stummer W. Factors confounding fluorescein-guided malignant glioma resections: edema bulk flow, dose, timing, and now: imaging hardware? Acta Neurochir. 2016;158(2):327–8.
21. Hadjipanayis CG, Georg Widhalm G, Stummer W. What is the surgical benefit of utilizing 5-ALA for fluorescence-guided surgery of malignant gliomas? Neurosurgery. 2015;77(5):663–73.
22. Stummer W, Pichlmeier U, Meinel T, et al. Fluorescence-guided surgery with 5-aminolevulinic acid for resection of malignant glioma: a randomised controlled multicentre phase III trial. Lancet Oncol. 2006;7:392–401.
23. Louis DN, Perry A, Reifenberger G, et al. The 2016 World Health Organization classification of tumors of the central nervous system: a summary. Acta Neuropathol. 2016;131(6):803–20.
24. Tilghman J, Wu H, Sang Y, et al. HMMR maintains the stemness and tumorigenicity of glioblastoma stem-like cells. Cancer Res. 2014;74:3168–79.
25. Jakola AS, Myrmel KS, Kloster R. Comparison of strategy favoring early surgical resection vs a strategy favoring watchful waiting in low-grade gliomas. JAMA. 2012;308(18):1881–8.
26. Smith JS, Chang EF, Lamborn KR, et al. Role of extent of resection in the longterm outcome of low-grade hemispheric gliomas. J Clin Oncol. 2008;26:1338–45.
27. Ius T, Isola M, Budai R, et al. Low-grade glioma surgery in eloquent areas: volumetric analysis of extent of resection and its impact on overall survival. A single-institution experience in 190 patients. J Neurosurg. 2012;117:1039–52.
28. Duffau H, Capelle L, Denvil D, et al. Functional recovery after surgical resection of low grade gliomas in eloquent brain: hypothesis of brain compensation. J Neurol Neurosurg Psychiatry. 2003;74:901–7.
29. Roux FE, Boulanouar K, Ranjeva JP, et al. Usefulness of motor functional MRI correlated to cortical mapping in Rolandic low-grade astrocytomas. Acta Neurochir. 1999;141(1):71–9.
30. Bertani G, Fava E, Casaceli E, et al. Intraoperative mapping and monitoring of brain functions for the resection of low-grade gliomas: technical considerations. Neurosurg Focus. 2009;27(4):E4.
31. Gulati S, Berntsen EM, Solheim O, et al. Surgical resection of high-grade gliomas in eloquent regions guided by blood oxygenation level dependent functional magnetic resonance imaging, diffusion tensor tractography, and intraoperative navigated 3D ultrasound. Minim Invas Neurosurg. 2009;52:17–24.
32. Oppenlander ME, Wolf AB, Snyder LA, et al. An extent of resection threshold for recurrent glioblastoma and its risk for neurological morbidity. J Neurosurg. 2014;120:846–53.
33. McGirt MJ, Chaichana KL, Gathinji M, et al. Independent association of extent of resection with survival in patients with malignant brain astrocytoma. J Neurosurg. 2009;110:156–62.
34. Chang SM, Parney IF, Mcdermott M, et al. Perioperative complications and neurological outcomes of first and second craniotomies among patients enrolled in the Glioma Outcome Project. J Neurosurg. 2003;98(6):1175–81.
35. Ryken TC, Kalkanis SN, Buatti JM, et al. The role of cytoreductive surgery in the management of progressive glioblastoma: a systematic review and evidence-based clinical practice guideline. J Neurooncol. 2014;118(3):479–88.

Radiation Therapy

3

Santa Bambace, Giuseppe Bove, Stefania Carbone, Samantha Cornacchia, Angelo Errico, Maria Cristina Frassanito, Giovanna Lovino, Anna Maria Grazia Pastore, and Girolamo Spagnoletti

3.1 General Findings

Radiotherapy has been the mainstay of treatment for gliomas since the 1980s when it was established that postoperative treatment improves survival [1, 2]. It remains the most effective nonsurgical treatment for the majority of patients, with or without chemotherapy [3].

3.2 Treatment Techniques

While 3D-CRT remains standard for the majority of high-grade gliomas, IMRT/VMAT is increasingly being used for some locations and for volumetrically or spatially challenging tumors. For smaller, spherical frontal and/or parietal tumors 3D-CRT is often sufficient, whereas IMRT/VMAT can provide superior solutions for tumors (e.g., temporal, insular) that are in close proximity to the brainstem or orbit, or which have irregular shapes [4, 5]. VMAT is more often used than IMRT due to its similar conformality and faster planning and delivery.

3.3 Preparation

To ensure accurate re-positioning, the patient's head should be immobilized using an individually adapted mask system. Thermoplastic systems are the most widely used and can be prepared at the same appointment as the planning CT scan. A flat position with the head in neutral is the most widely accepted practice as it is most comfortable for the patient. A CT scan should be obtained using 1–3 mm slice thickness from the vertex to the lower border of C3. As high-grade gliomas can grow rapidly, an up-to-date contrast-enhanced MRI scan should be fused with the planning CT to aid target delineation. If a recent MRI is not available, for example if MRI is contraindicated, then intravenous contrast should be administered during the planning CT scan to help identification of residual disease [6].

3.4 Treatment Planning

RT targets for gliomas are generated from gross tumor volume (GTV), clinical target volume (CTV), and planning target volume (PTV). GTV encompasses the visible inoperable tumor or any gross tumor remaining after maximal safe resection as well as the surgical cavity. Tumor volumes are defined using pre- and postoperative MRI imaging using enhanced T1 with/without T2/FLAIR sequences.

CTV is an expansion on GTV to account for subclinical disease. GTV is expanded 1–2 cm for grade II–III, and up to 2–2.5 cm for grade IV, adjusted to anatomical borders. Although trials in glioblastoma have historically used CTV expansion as indicated above, smaller CTV expansions are supported in the literature and can be appropriate [7, 8].

PTV is an expansion on CTV to account for daily setup errors and image registration. A margin of 5 mm is typically added to CTV. Daily image guidance is required if smaller PTV margins are used (3 mm or less). The definite margin should be based on the institutional fixation technique and quality assurance measurements [9, 10].

3.5 Organs at Risk

The OARs including the optic nerves, optic chiasm, eyes, lenses, brain, and brainstem should be contoured. Other potential OARs include the cochleas, lacrimal glands, pitu-

S. Bambace (✉) · S. Carbone · A. Errico · G. Lovino
Radiation Oncology Unit, Dimiccoli Hospital—ASL BT, Barletta, Italy

G. Bove · G. Spagnoletti
Foggia University Hospital, Foggia, Italy

S. Cornacchia
Medical Physics Unit, Dimiccoli Hospital—ASL BT, Barletta, Italy

M. C. Frassanito · A. M. G. Pastore
Mater Dei Hospital, C.B.H. Città di Bari Hospital, Bari, Italy

T. Scarabino, S. Pollice (eds.), *Imaging Gliomas After Treatment*, https://doi.org/10.1007/978-3-030-31210-7_3

itary gland, and hypothalamus, although these are considered "relative OARs" since few oncologists would compromise dose to PTV in order to reduce dose to these organs. Some radiation oncologists also contour the contralateral hippocampus when the tumor is in a location that will allow sparing without compromising dose to the target. Expansion of OARs to create a planning risk volume (PRV) for each OAR is frequently applied; the margin should reflect the accuracy of daily set-up [6].

3.5.1 Low-Grade Gliomas: Histomolecular Definition

Low-grade gliomas (LGG) are slow-growing World Health Organization (WHO) grade I or II primary brain tumors that predominantly affect young adults; they account for approximately 20% of primary brain tumors and typically present in the fourth decade of life [11]. LGG are composed of various distinct tumors based on histopathology: LGG WHO grade II are of two kinds: diffuse astrocytoma and oligodendroglioma. In 2002, EORTC 22844 and 22845 considered age ≥40 years, astrocytoma histology, diameter size ≥6 cm, tumor crossing midline and neurologic deficit before surgery as adverse features [12]. In 2016, the WHO reclassified LGG by combining classic histopathologic features with key molecular markers, including isocitrate dehydrogenase (IDH1-IDH2) mutation and 1p/19q codeletion status, ATRX and TERT promoters [13–17]. The presence of mutations in either IDH 1 or 2 is associated with significantly longer overall survival [18, 19]. Combined chromosomal 1p and 19q codeletion as well as 1;19 translocation are also associated with superior overall and progression-free survival in LGG [16].

The use of molecular biomarkers beyond IDH and 1p19q deletion status as potential predictive factors for RT sensitivity holds significant promise toward improving individualized treatment decision-making. Standard management gliomas involve observation, surgery, chemotherapy, and/or radiotherapy. Treatment decisions are based on many factors including prognostic molecular markers, potential benefits of increased progression-free survival, and potential long-term treatment complications.

3.6 Role of Radiotherapy (RT)

The goals of RT for LGG are to improve tumor control and survival while preventing/delaying malignant transformation and limiting the acute and late effects of treatment that may degrade quality of life. Multiple randomized, clinical trials have been published examining the role of dose for RT in LGG. Neither randomized trial showed an overall or progression-free survival benefit from dose escalation. In the United States, it is generally accepted that a reasonable RT dose for LGG is 50–54 Gy to balance efficacy and toxicity [18–21]. Regardless to the timing of treatment, the trials concluded that early RT improves progression-free survival and control of seizures, but not overall survival [22]. The lack of overall survival benefit has been used by some to justify deferring RT until disease progression for patients LGG with highly favorable prognostic features and minimal known disease (e.g., those younger than 40 years of age, with MRI confirmed gross totally resected, IDH mutated, WHO grade II oligodendroglioma), provided they are observed carefully [11].

Three factors predict significantly poorer progression-free survival: [11] preoperative tumor diameter of 4 cm or greater, [12] astrocytoma/oligoastrocytoma histologic type, and [13] residual tumor 1 cm or greater according to postoperative MRI [11].

The recent publication of the mature results of the treatment arms for higher risk patients with LGG enrolled in the RTOG 9802 trial showed that patients with LGG selected for postoperative RT should also receive adjuvant chemotherapy. This study evaluated 251 patients with LGG randomized to postoperative RT with or without 6 cycles of adjuvant PCV. The median PFS was 4.0 years in the RT arm versus 10.4 years in the CRT arm ($P < 0.001$). The median OS was also significantly improved for the CRT arm versus RT arm (13.3 years vs. 7.8 years, respectively). The added survival benefit from PCV was observed in all LGG histologies, with the greatest effect size in oligodendroglioma patients. Of note, there were significantly more grade III and IV hematologic toxicities in the CRT arm, although there were no treatment-related deaths [18].

It is, therefore, our contention that the current standard of care should be RT plus PCV until it is bested. Regardless comparison between RT alone and chemotherapy with TMZ in patients with at least one risk factor, the randomized trial EORTC 22033-26033 noted that median PFS was significantly higher in RT arm alone in IDH mutation and non-codeletion 1p-19q vs. TMZ alone [23]. OS and quality of life results are still pending. The more question is whether the sequential use of TMZ followed by delayed RT is superior to CRT.

Although PCV chemotherapy represents the standard care, it remains unclear whether TMZ, which is easier to administer and commonly used for high-grade gliomas, is just as efficacious as PCV. There have been no randomized trials for LGG directly comparing TMZ with PCV. Additional long-term data will be required to assess long-term efficacy of TMZ and RT for LGG.

3.7 Radiation Techniques

Because patients with LGG may live for many years, it is important not only to improve survival outcomes, but also to minimize RT-related late effects. The techniques most used

are 3D and intensity-modulated RT (IMRT/IMAT); therapy with protons and carbon ions is going on.

Intensity-modulated RT techniques have dosimetric advantages over three-dimensional conformal radiotherapy on health tissue sparing [24], although increase their low doses. In particular relating to lens dose, different IMRT techniques have been implemented in order to reduce maximum dose value [25]; in order to maintain neurocognitive skill, it is also crucial to maintain doses as low as possible to the hippocampal region [26].

Therapy with protons may provide neurocognitive advantages over photons but may not confer overall or progression-free survival advantages [27]. Ongoing trials randomizing patients with low-grade glioma to protons versus photons will help us to understand whether protons may provide improved neurocognitive preservation.

Recent studies have broadened our understanding of both the diagnosis and treatment of LGG. Molecular biomarkers play an important role in the prognostication of LGG. Treatment options for LGG include surgery, observation (in highly selected subsets), radiotherapy, and/or chemotherapy. The preponderance of data suggests that, for those needing either RT or chemotherapy, the combination is the superior approach. Treatment decisions including RT must consider all prognostic factors including molecular biomarkers and weight both the long-term benefits and risks of RT. Patients with high-risk LGG should be considered for early adjuvant RT. Long-term results and additional studies are needed to address the role of adjuvant TMZ combined with RT and the benefits of advanced RT technologies, such as protons and carbon ion therapy.

3.7.1 Radiation Therapy in High-Grade Gliomas

Strategies for CTV definition vary with respect to the inclusion of edema in an initial target volume. When edema is assessed by T2/FLAIR and included in an initial phase of treatment, fields are usually reduced for the last phase of treatment (boost). The boost target volume typically encompasses only the gross residual tumor and the resection cavity.

Sufficient radiation doses are required to maximize survival benefit. However, radiation dose escalation alone above 60 Gy has not been shown to be beneficial [28]. The recommended dose for high-grade astrocytomas is 60 Gy in 2.0 Gy fractions (or 59.4 Gy in 1.8 Gy fractions). If a boost volume is used, the initial phase of the RT plan will receive 46 Gy in 2 Gy fractions (or 45–50.4 Gy in 1.8 Gy fractions), followed by a boost plan of 14 Gy in 2 Gy fractions (or 9–14.4 Gy in 1.8 Gy fractions). Both strategies appear to produce similar outcomes [29]. The recommendation of the European Organization for Research and Treatment of Cancer (EORTC) is to deliver RT in a single phase while the Radiotherapy and Oncology Group (RTOG) recommends two phases. Therefore, in Europe single-phase treatment is advocated, which results in a smaller volume of irradiated brain and is also more convenient as only one planning phase is necessary [6].

A slightly lower dose, such as 54–55.8 Gy in 1.8 Gy or 57 Gy in 1.9 Gy fractions, can be applied when the tumor volume is very large (gliomatosis), there is brainstem/spinal cord involvement, or for grade III astrocytoma.

Also anaplastic oligodendrogliomas are generally treated with lower doses per fraction (1.8 Gy/fraction vs. 2.0 Gy/fraction) to theoretically decrease the risk of late side effects, given the improved prognosis in these patients. As per recent trials such as RTOG 9813 [30], these gliomas are treated to 50.4 Gy in 1.8 Gy fractions for 28 fractions followed by a five-fraction boost of 1.8 Gy/fraction to a total of 59.4 Gy [31].

Special attention has been given to determine the optimal therapy in older adults, given their especially poor prognosis and limited functional status. Overall, the approach in these patients has been to reduce treatment time while attempting to maintain treatment efficacy. In poorly performing patients (KPS < 70) or elderly patients (>70 years), a hypofractionated course should be considered with the goal of completing the treatment in 2–4 weeks [32]. Typical fractionation schedules are 34 Gy/10 fractions [33], 40.05 Gy/15 fractions, or 50 Gy/20 fractions [34]. Moreover, a shorter fractionation schedule of 25 Gy/5 fx days may be considered for elderly and/or frail patients with smaller tumors for whom a longer course of treatment would not be tolerable [35]. Alternatively, 30 Gy in 5/6 Gy per fraction delivered on alternate days is frequently used in the UK and other European countries [6].

3.7.2 Reirradiation in High-Grade Glioma

Local recurrence represents the main pattern of failure in the treatment of high-grade glioma (HGG), after a standard treatment approach which includes surgical resection, adjuvant chemotherapy, and radiotherapy. In case of recurrence, only a selected number of patients are healthy enough to sustain another surgical intervention, and, in the majority of the clinical cases, the most appropriate salvage treatment consists in a combined chemo-radiation therapy.

Multiple treatment modalities are available for retreatment. 3D-conventional radiotherapy using coregistered MRI has improved target definition and allows the dose to normal structures to be reduced. Further developments such as IMRT/VMAT can improve conformality at the target using modulated beams [36]. Conventionally fractionated reirradiation may theoretically allow more generous target volumes. Variable doses have been used with conventional fractionation and 18 doses of 2 Gy have been proposed [37].

A moderate hypofractionation (35 Gy in 10 days) is another option for recurrent gliomas [29]. Currently, Radiation Therapy Oncology Group (RTOG) 1205 [38] is examining the role of reirradiation for recurrent HGG with a randomized phase II trial consisting in: hypofractionated radiotherapy (35Gy in 10 fractions) with concurrent bevacizumab (BEV) for 2 weeks versus bevacizumab alone for 2 weeks as control arm. BEV works as a vascular endothelial growth factor inhibitor and has recently shown promising result in the treatment of recurrent HGG, replacing temozolomide as the standard of care [39–42].

The recent development of radiotherapy techniques, able to deliver high dose of radiation in small volumes sparing the surrounding organ at risk, has opened the possibility to reirradiate recurrent tumors in a high hypofractionated regime while minimizing the risk of radiation-induced side effects.

Fractionated stereotactic radiotherapy (fSRT) delivers radiation in few fractions (2–5) while stereotactic radiosurgery (SRS) employs a single fraction to hit the target: both techniques have stood out as powerful therapeutic modalities for recurrent brain tumors due to their ability to deliver a highly conformal dose with precision.

The technology available to perform fSRT or SRS includes linear accelerator (LINAC)-based systems using X-ray beams, with an image-guided delivery of radiation to the target and a stereotactic frame to immobilize the patient.

The Cyberknife (Accuray, Inc., Sunnyvale, CA, USA) [43, 44] is a system in which the linear accelerator is mounted on a robotic arm and can deliver hundreds of beams in any direction and angle. The beams hit the lesion with a submillimetric precision while sparing the surrounding normal tissue. The immobilization system is not invasive and consists in a thermoplastic mask which is comfortably adapted to the patient head. The geometric accuracy of this system and the possibility to deliver single or multifraction treatment, according to the characteristics of the lesion (mainly tumor volume and location), make Cyberknife one of the most suited technologies in the case of reirradiation [45].

The Cyberknife treatment planning is developed on a computed tomography (CT) image with 1 mm thickness which is fused with a T1-weighted magnetic resonance image (MRI) with gadolinium in order to better delineate target volumes and critical structures. Gross tumor volume (GTV) includes the entirety of the contrast-enhanced lesion representing the tumor or the surgical cavity for postoperative treatment. Clinical target volume (CTV) coincides with GTV, while planning target volume (PTV) corresponds to the CTV plus 1–2 mm margin.

Patient alignment is performed with the "skull tracking" procedure that uses cranial bones as a spatial reference to localize the target. During treatment, digitally reconstructed radiographs (DRR) derived from CT Images are compared with patient live radiograph acquired every of 1–2 min and the robot executes the extracted spatial corrections in order to deliver dose to the target with sub-millimetric precision [46].

The dose prescribed varies from 18 Gy to 35 Gy, to the 78–80%, in one to five fraction depending on the size and localization of the target [43, 47–50]. Radiosurgery can be used only with PTVs up to 3 cm in the maximum dimension. The biologically equivalent dose (BED) is 50–60 Gy, considering an alpha/beta ratio of 10 for brain tumors.

Acute side effects of therapy include nausea, vomiting, and headache; vertigo and seizures are less frequent. These symptoms are transient and generally respond to medication with steroids. Late toxicity is correlated to the high risk of tissue complications deriving from brain reirradiation.

The cumulative total dose tolerated by the brain is 100Gy (normalized to 2Gy/fraction, alpha/beta ratio 2) [51, 52]; exceeding this limit could lead to the development of radiation necrosis, cranial nerve neuropathies, vascular injuries (including carotid artery stenosis) and severe edema [53, 54].

Favorable prognostic factors for fSRT or SRS in recurrent glioma are small tumor volume (<10 cc), patient age younger than 70 years, Karnofsky performance score >60 [55]. Other criteria that may affect a better outcome include unifocal tumors and tumors located in hemispheric and supratentorial cortical sites [56].

Follow-up consists in periodical oncological visits for monitoring clinical, cognitive-psychological and radiological aspects. In particular, MRI with gadolinium is performed every 2–3 months for the first 2 years to evaluate tumor response, recurrence, or radionecrosis by examining DWI and T2/flair sequences.

References

1. Walker MD, Strike TA, Sheline GE. An analysis of dose–effect relationship in the radiotherapy of malignant gliomas. Int J Radiat Oncol Biol Phys. 1979;5:1725–31.
2. Kristiansen K, Hagen S, Kollevold T, et al. Combined modality therapy of operated astrocytomas grade III and IV. Confirmation of the value of postoperative irradiation and lack of potentiation of bleomycin on survival time: a prospective multicenter trial of the Scandinavian Glioblastoma Study Group. Cancer. 1981;47:649–52.
3. Laperriere N, Zuraw L, Cairncross G. Radiotherapy for newly diagnosed malignant glioma in adults: a systematic review. Radiother Oncol. 2002;64:259–73.
4. Amelio D, Lorentini S, Schwarz M, et al. Intensity-modulated radiation therapy in newly diagnosed glioblastoma: a systematic review on clinical and technical issues. Radiother Oncol. 2010;97:361–9.
5. Lorentini S, Amelio D, Giri MG, et al. IMRT or 3D-CRT in glioblastoma? A dosimetric criterion for patient selection. Technol Cancer Res Treat. 2013;12:411–20.
6. Niyazi M, Brada M, Chalmers AJ, et al. ESTRO-ACROP guideline "target delineation of glioblastomas". Radiother Oncol. 2016;118:35–42.

7. Aydin H, Sillenberg I, von Lieven H. Patterns of failure following CT-based 3-D irradiation for malignant glioma. Strahlenther Onkol. 2001;177:424–31.
8. Chang EL, Akyurek S, Avalos T, et al. Evaluation of peritumoral edema in the delineation of radiotherapy clinical target volumes for glioblastoma. Int J Radiat Oncol Biol Phys. 2007;68:144–50.
9. Boda-Heggemann J, Walter C, Rahn A, et al. Repositioning accuracy of two different mask systems-3D revisited: comparison using true 3D/3D matching with cone-beam CT. Int J Radiat Oncol Biol Phys. 2006;66:1568–75.
10. Rosenfelder NA, Corsini L, McNair H, et al. Comparison of setup accuracy and intrafraction motion using stereotactic frame versus 3-point thermoplastic mask-based immobilization for fractionated cranial image guided radiation therapy. Pract Radiat Oncol. 2013;3:171–9.
11. Youland RS, Schomas DA, Brown PD, et al. Changes in presentation, treatment, and outcomes of adult low-grade gliomas over the past fifty years. Neuro-Oncology. 2013;15(8):1102–10.
12. Pignatti F, van den Bent M, Curran D, et al. Prognostic factors for survival in adult patients with cerebral low-grade glioma. J Clin Oncol. 2002;20(8):2076–84.
13. Louis DN, Perry A, Reifenberger G, et al. The 2016 World Health Organization Classification of Tumors of the Central Nervous System: a summary. Acta Neuropathol. 2016;131(6):803–20.
14. Cancer Genome Atlas Research Network, Brat DJ, Verhaak RG, et al. Comprehensive, integrative genomic analysis of diffuse lower-grade gliomas. N Engl J Med. 2015;372(26):2481–98.
15. Eckel-Passow JE, Lachance DH, Molinaro AM, et al. Glioma groups based on 1p/19q, IDH, and TERT promoter mutations in tumors. N Engl J Med. 2015;372(26):2499–508.
16. Jenkins RB, Blair H, Ballman KV, et al. A t(1;19)(q10;p10) mediates the combined deletions of 1p and19q and predicts a better prognosis of patients with oligodendroglioma. Cancer Res. 2006;66(20):9852–61.
17. Reuss DE, Kratz A, Sahm F, et al. Adult IDH wild type astrocytomas biologically and clinically resolve into other tumor entities. Acta Neuropathol. 2015;130(3):407–17.
18. Buckner JC, Shaw EG, Pugh SL, et al. Radiation plus procarbazine, CCNU, and vincristine in low grade glioma. N Engl J Med. 2016;374(14):1344–55.
19. Sun H, Yin L, Li S, et al. Prognostic significance of IDH mutation in adult low-grade gliomas: a metaanalysis. J Neuro-Oncol. 2013;113(2):277–84.
20. Shaw E, Arusell R, Scheithauer B, et al. Prospective randomized trial of low- versus high-dose radiation therapy in adults with supratentorial low-grade glioma: initial report of a North Central Cancer Treatment Group/Radiation Therapy Oncology Group/Eastern Cooperative Oncology Group study. J Clin Oncol. 2002;20(9):2267–76.
21. Karim AB, Maat B, Hatlevoll R, et al. A randomized trial on dose-response in radiation therapy of low grade cerebral glioma: European Organization for Research and Treatment of Cancer (EORTC) Study 22844. Int J Radiat Oncol Biol Phys. 1996;36(3):549–56.
22. Van den Bent MJ, Afra D, de Witte O, et al. Long term efficacy of early versus delayed radiotherapy for low-grade astrocytoma and oligodendroglioma in adults: the EORTC 22845 randomised trial. Lancet. 2205;366(9490):985–90.
23. Baumert BG, Hegi ME, van den Bent MJ, et al. Temozolomide chemotherapy versus radiotherapy in high-risk low-grade glioma (EORTC 22033-26033): a randomised, open-label, phase 3 intergroup study. Lancet Oncol. 2016;17(11):1521–3.
24. Navarria P, Pessina F, et al. Can advanced new radiation therapy technologies improve outcome of high grade glioma (HGG) patients? Analysis of 3D-conformal radiotherapy (3DCRT) versus volumetric-modulated arc therapy (VMAT) in patients treated with surgery, concomitant and adjuvant chemo-radiotherapy. BMC Cancer. 2016;16:362.
25. Cornacchia S, Caivano R, Califano G, et al. Rapid arc versus a new sectorial sliding window IMRT template in radiotherapy brain treatments: Lens sparing. Phys Med. 2018;52:167–8.
26. Brown PD, Buckner JC, et al. Effects of radiotherapy on cognitive function in patients with low-grade glioma measured by the Folstein mini-mental state examination. J Clinical Oncol. 2003;21(13):2519–24.
27. Shi HA, Sherman JC, et al. Proton therapy for low-grade gliomas: results from a prospective trial. Cancer. 2015;121(10):1712–9.
28. Tsien C, Moughan J, Michalski JM, et al. Phase I three-dimensional conformal radiation dose escalation study in newly diagnosed glioblastoma: radiation therapy oncology group trial 98-03. Int J Radiat Oncol Biol Phys. 2009;73(3):699–708.
29. Cabrera AR, Kirkpatrick JP, Fiveash JB, et al. Radiation therapy for glioblastoma: executive summary of an American Society for Radiation Oncology evidence-based clinical practice guideline. Pract Radiat Oncol. 2016;6:217–25.
30. Chang S, Zhang P, Cairncross JG, et al. Phase III randomized study of radiation and temozolomide versus radiation and nitrosourea therapy for anaplastic astrocytoma: results of NRG Oncology RTOG 9813. Neuro-Oncology. 2017;19:252–8.
31. National Comprehensive Cancer Network. NCCN Guidelines-Central Nervous System Cancers, version 1; (2019). http://www.nccn.org.
32. Stupp R, Brada M, van den Bent MJ, et al. High-grade glioma: ESMO Clinical Practice Guidelines for diagnosis, treatment and follow-up. Ann Oncol. 2014;25(suppl 3):93–101.
33. Malmström A, Grønberg BH, Marosi C, et al. Temozolomide versus standard 6-week radiotherapy versus hypofractionated radiotherapy in patients older than 60 years with glioblastoma: the Nordic randomised, phase 3 trial. Lancet Oncol. 2012;13:916–20.
34. Roa W, Brasher PM, Bauman G, et al. Abbreviated course of radiation therapy in older patients with glioblastoma multiforme: a prospective randomized clinical trial. J Clin Oncol. 2004;22:1583–8.
35. Roa W, Kepka L, Kumar N, et al. International Atomic Energy Agency randomized phase III study of radiation therapy in elderly and/or frail patients with newly diagnosed glioblastoma multiforme. J Clin Oncol. 2015;33:4145–50.
36. Nieder C, Langendijk J. Re-irradiation: new frontiers. 2nd ed. Berlin: Springer; 2017. p. 127–42.
37. Weller M, van den Bent M, Hopkins K, et al. EANO guideline for diagnosis and treatment of anaplastic gliomas and glioblastoma. Lancet Oncol. 2014;15:395–403.
38. RTOG 1205: Randomized Phase II trial of concurrent Bevacizumab and re-irradiation versus Bevacizumab alone as treatment of recurrent Glioblastoma; (2016).
39. Chamberlain MC. Bevacizumab plus irinotecan in recurrent glioblastoma. J Clin Oncol. 2008;26:1012–3.
40. Kreisl TN, Kim L, Moore K, et al. Phase II trial of single-agent bevacizumab followed by bevacizumab plus irinotecan at tumor progression in recurrent glioblastoma. J Clin Oncol. 2008;27:740–5.
41. Raizer JJ, Abrey LE, Lassman AB, et al. A phase II trial of erlotinib in patients with recurrent malignant gliomas and nonprogressive glioblastoma multiforme postradiation therapy. Neuro-Oncology. 2010;12:95–103.
42. Vredenburgh J, Desjardins A, Herndon JE, et al. Bevacizumab plus irinotecan in recurrent glioblastoma multiforme. J Clin Oncol. 2007;25:4722–9.
43. Adler JR, Murphy MJ, Chang SD, et al. Image-guided robotic radiosurgery. Neurosurgery. 1999;44:1299–307.
44. Antypas C, Pantelis E. Performance evaluation of a CyberKnife G4 image-guided robotic stereotactic radiosurgery system. Phys Med Biol. 2008;53:4697–718.

45. Romanelli P, Conti A, Pontoriero A, et al. Role of stereotactic radiosurgery and fractionated stereotactic radiotherapy for the treatment of recurrent glioblastoma multiforme. Neurosurg Focus. 2009;27:E8.
46. Murphy MJ, Chang SD, Gibbs IC, et al. Patterns of patient movement during frameless image-guided radiosurgery. Int J Radiat Oncol Biol Phys. 2003;55(5):1400–8.
47. Hasan S, Chen E, Lanciano R, et al. Salvage fractionated stereotactic radiotherapy with or without chemotherapy and immunotherapy for recurrent glioblastoma multiforme: a single institution experience. Front Oncol. 2015;5:106.
48. King K, Blumenfeld P, Shin JY, et al. Fractionated stereotactic radiotherapy and stereotactic radiosurgery as salvage treatment for recurrent malignant high-grade gliomas. J Radiat Oncol Res. 2018;2(1):1003.
49. Yazici G, Cengiz M, Ozyigit G, et al. Hypofractionated stereotactic reirradiation for recurrent glioblastoma. J Neuro Oncol. 2014;120:117.
50. Martínez-Carrillo M, Tovar-Martín I, Zurita-Herrera M, et al. Salvage radiosurgery for selected patients with recurrent malignant gliomas. Biomed Res Int. 2014;2014:657953.
51. Mayer R, Sminia P. Reirradiation tolerance of the human brain. Int J Radiat Oncol Biol Phys. 2008;70(5):1350–60.
52. Lawrence YR, Li XA, el Naqua I, et al. Radiation dose volume effects in the brain. Int J Radiat Oncol Biol Phys. 2010;76(3 Suppl):S20–7.
53. DiBiase SJ, Kwok Y, Yovino S, et al. Factors predicting local tumor control after gamma knife stereotactic radiosurgery for benign intracranial meningiomas. Int J Radiat Oncol Biol Phys. 2004;60:1515–9.
54. Kondziolka D, Levy EI, Niranjan A, et al. Long-term outcomes after meningioma radiosurgery: physician and patient perspectives. J Neurosurg. 1999;91:44–50.
55. Shrieve DC, Alexander E III, Black PM, et al. Treatment of patients with primary glioblastoma multiforme with standard postoperative radiotherapy and radiosurgical boost: prognostic factors and long-term outcome. J Neurosurg. 1999;90:72–7.
56. Larson DA, Gutin PH, McDermott M, et al. Gamma knife for glioma: selection factors and survival. Int J Radiat Oncol Biol Phys. 1996;36:1045–53.

Chemotherapy and Future Developments

4

Ileana De Roma, Lucia Lombardi, and Gennaro Gadaleta-Caldarola

4.1 General Findings

The incidence of primary malignant brain tumors has been increasing over the past 30 years, and it is estimated that in the year 2010, approximately 22,020 cases were diagnosed in the USA alone, with 13,140 deaths [1, 2]. Gliomas account for 32% of all primary brain tumors, but within the malignant subset, they account for 80% of tumors. Histological classification of tumors of the nervous system was initiated by the WHO in 1979, as a means of predicting the biological behavior of a neoplasm, and thereby determining the choice of therapies. The 2016 World Health Organization Classification of Tumors of the Central Nervous System (CNS) is both a conceptual and practical advance over its 2007 predecessor (Table 4.1). For the first time, the WHO classification of CNS tumors uses molecular parameters in addition to histology to define many tumor entities, thus formulating a concept for how CNS tumor diagnoses should be structured in the molecular era. As such, the 2016 CNS WHO presents major restructuring of the diffuse gliomas, medulloblastomas, and other embryonal tumors, and incorporates new entities that are defined by both histology and molecular features, including glioblastoma, IDH-wild-type and, IDH-mutant glioblastoma; diffuse midline glioma, H3 K27 M-mutant; RELA fusion-positive ependymoma; medulloblastoma, WNT-activated and medulloblastoma, SHH-activated; and embryonal tumor with multilayered rosettes, C19MC-altered. The 2016 edition has added newly recognized neoplasms, and has deleted some entities, variants, and patterns that no longer have diagnostic and/or biological relevance. Other notable changes include the addition of brain invasion as a criterion for atypical meningioma and the introduction of a soft tissue-type grading system for the now combined entity of solitary fibrous tumor/hemangiopericytoma a departure from the manner by which other CNS tumors are graded. Overall, it is hoped that the 2016 CNS WHO will facilitate clinical, experimental, and epidemiological studies that will lead to improvements in the lives of patients with brain tumors [3].

Table 4.1 The ongoing Phase III clinical trials of targeted therapy or combination treatment in glioblastoma

NCT number	Title
NCT02573324	A study of ABT-414 in subjects with newly diagnosed GBM with EGRF amplification
NCT02761070	Bevacizumab alone versus dose-dense temozolamide followed by bevacizumab for recurrent GBM, phase III
NCT02152982	Temozolamide with or without veliparib in treating patients with newly diagnosed GBM multiforme
NCT02667587	An investigational immunotherapy study of TMZ plus radiation therapy with nivolumab or placebo, for newly diagnosed patients with GBM
NCT02617589	An investigational immunotherapy study of nivolumab compared to TMZ, each given with radiation therapy, for newly diagnosed patients with GBM

GBM glioblastoma, *EGFR* Epidermal growth factor receptor, *TMZ* temozolamide

4.2 Molecular Biology of Gliomas

Low-grade glioma represents a spectrum of tumor types with diverse histologic features; however, recently molecular analysis of tumors has become a critical part of tumor classification and prognostication. In 2016, the WHO updated its classification of primary brain tumors to include molecular characterization, now defining tumors both on phenotype and genotype. Oligodendrogliomas on traditional hematoxylin and eosin staining have round nuclei and fine delicate branching vessels but are now also defined as having both an isocitrate dehydrogenase (IDH) gene family mutation and combined whole-arm losses of 1p and 19q (1p/19q codeletion) [4–7]. Astrocytomas are characterized by prominent glial fibrillary acidic protein processes, typically also have muta-

The original version of this chapter was revised. The correction to this chapter can be found at https://doi.org/10.1007/978-3-030-31210-7_66

I. De Roma · L. Lombardi · G. Gadaleta-Caldarola (✉)
Medical Oncology Unit, "Mons. R. Dimiccoli" Hospital, Barletta, Italy
e-mail: deromaileana@libero.it; gergad@libero.it

T. Scarabino, S. Pollice (eds.), *Imaging Gliomas After Treatment*, https://doi.org/10.1007/978-3-030-31210-7_4

tions in IDH, but have intact 1p and 19q chromosomes as well as loss of ATRX. Mutations in either IDH1 or IDH2 occur in up to 80% of grade 2 and 3 diffuse gliomas and carry a more favorable prognosis compared with IDH wild-type tumors [7].

High-grade gliomas (HGG), including glioblastoma (GBM), anaplastic astrocytoma (AA), and anaplastic oligodendroglioma (AO), originate from the supporting neuroglial cells of the CNS. GBM, the most common and most aggressive of the primary brain tumors, typically presents in late adulthood. AA and AO affect a younger age group and generally have a more protracted clinical course. High-grade gliomas can be debilitating, owing to physical disability, cognitive impairment, personality change, depression and seizure disorder, and require complex multidisciplinary care. Histologically, tumors showing anaplasia and mitotic activity are classified as grade III, while the sine qua non of grade IV tumors is microvascular proliferation and/or necrosis. Historically, all HGG have been treated in the same manner, but the treatment modality for grade III tumors is currently being investigated separate of grade IV tumors through ongoing clinical trials. The average survival time of approximately 1 year for patients with glioblastoma (GBM) has minimally improved despite decades of basic and clinical research. However, in recent years a significant survival benefit has been achieved with the addition of concurrent temozolomide (TMZ) to adjuvant RT.

There have been substantial advances in our understanding of the molecular aberrations found in malignant gliomas. Key discoveries include the isocitrate dehydrogenase (IDH) mutation, codeletion of the short arm of chromosome 1, and long arm of chromosome 19 (1p19q) and O^6-methylguanine-DNA methyltransferase (MGMT) gene promoter methylation. These have emerged as being important determinants of treatment response and survival. Consequently, they are now routinely tested and have become fundamental to glioma classification.

IDH catalyzes the oxidative decarboxylation of isocitrate to α-ketoglutarate, and subsequently to the oncometabolite 2-hydroxyglutarate [8]. In turn, 2-hydroxyglutarate acts via a family of dioxygenases to impair epigenetic regulation and increase hypoxia-inducible factor 1-α. The prevalent *IDH1* R132H mutation is detectable with immunohistochemistry in over 90% of cases [9]. IDH mutations can also be identified by sequencing *IDH1* codon 132 and *IDH2* codon 172. These mutations are common in low-grade gliomas and secondary GBMs, and confer significantly improved prognosis [10].

The 1p19q codeletion is an unbalanced reciprocal translocation that is a characteristic of oligodendrogliomas. Multiple studies have demonstrated the favorable prognostic and predictive utility of the 1p/19q codeletion, although the biologic basis remains unclear. Specifically, in randomized Phase III trials evaluating chemoradiotherapy with PCV for AO, patients harboring the 1p19q codeletion derived greater benefit from PCV and lived substantially longer [11, 12]. In contrast, partial 1p or 19q loss did not confer this significance.

MGMT gene promoter methylation causes epigenetic silencing of MGMT, which is necessary for DNA repair. Notably, based on the review of randomized Phase III trials evaluating temozolomide in patients with GBM, those containing the MGMT gene promoter methylation obtained meaningful survival benefit from temozolomide, whereas those without the methylation did not [13]. Initially, MGMT status was assessed with immunohistochemistry and MGMT methylation-specific PCR; however, widespread clinical use was limited by numerous technical issues including poor reliability, reproducibility, and the labor-intensive work [14, 15]. Newer methods include bisulfite sequencing, pyrosequencing, high-resolution melt analysis, and infinium methylation BeadChip, which have improved standardization and accuracy of MGMT testing [16, 17].

As mentioned above, in 2016 the WHO published the Fifth Edition Classification of Tumors of the Central Nervous System [3]. This represents a seminal update, with the introduction of integrated diagnoses combining histology and molecular parameters for many entities. This incorporates the recently established prognostic and predictive information from IDH and 1p19q.

GBM is now subdivided into IDH wild-type (predominantly primary GBM, patients over 55 years of age, poor prognosis) and IDH-mutant entities (predominantly secondary GBM, younger patients, favorable prognosis). The diagnosis of AO requires IDH-mutant and 1p19q-codeleted status, whereas AA requires IDH-mutant and non-codeleted status. Importantly, both entities are IDH mutant; a glioma that is IDH wild-type with or without 1p19q codeletion instead represents a genomically unstable GBM. In addition, 1p19q codeletion is mutually exclusive with TP53 mutation and ATRX inactivation [18]. Accordingly, a glioma that is IDH-mutant, TP53-mutant, and ATRX-inactivated is considered AA. Finally, the use of molecular parameters handles the problematic and indeterminate entity called anaplastic oligoastrocytoma, which was previously defined by a mixed histological pattern and was subject to poor interobserver agreement [19, 20]. The combination of histology and molecular parameters effectively differentiates nearly all cases as either AO or AA. To facilitate clinical decision making, the current standard is to incorporate all the tissue-based information (histology, grade, molecular findings) into an integrated diagnosis, which is then reported to clinicians.

Molecular markers have significantly contributed to diagnostic precision in high-grade glioma, and yield important therapeutic implications. The next steps will be to improve understanding of clinical and molecular heterogeneity within glioma subtypes. Ongoing efforts include assessment of additional molecular markers, methylation profiling, and a coordinated approach to histologic–molecular correlation as part of clinical trials.

4.3 Standard of Care for Malignant Low-Grade Glioma

The precise optimal management of patients with low-grade glioma after surgical resection remains to be determined. The risk–benefit ratio of treatment with radiation and chemotherapy must be weighed for each individual patient. Prior studies stratified patients into high- and low-risk low-grade glioma on the basis of clinical features of age (older or younger than 40 years) and the extent of resection. A large prospective study of observation of patients with low-risk low-grade glioma younger than 40 years who had gross total resections reported 52% of patients had recurrence within 5 years of surgery. On the basis of these data, in patients who are considered low risk, defined as age younger than 40 years with a gross total resection, it is an attractive option to forgo further treatment with radiation and chemotherapy at the time of diagnosis and instead undergo regular magnetic resonance imaging (MRI) surveillance [21]. The choice of chemotherapy is also under active investigation. PCV was originally used in early trials for low-grade glioma on the basis of efficacy in higher-grade tumors [11]. It has been largely replaced by temozolomide in later trials because of an improved adverse effect/toxicity profile and the expectation that both alkylating therapies would have similar efficacies, but a direct comparison of the two agents has yet to be completed [22].

There is no known curative therapy for low-grade gliomas. When low-grade gliomas recur, they may either be the original tumor/grade or they may also undergo malignant transformation into high-grade tumors. Oligodendrogliomas can malignantly transform into anaplastic oligodendrogliomas, and astrocytomas can transform into anaplastic astrocytomas or glioblastomas. Treatment options at the time of recurrence can include further surgery, radiation therapy and/or chemotherapy, or clinical trials. If surgical resection can safely be performed, it is again recommended. If a patient did not receive radiation at initial diagnosis or has had significant time pass before recurrence, radiation therapy may also be an option. Treatment with chemotherapy is also usually a possibility. Choices can include the original chemotherapy, if safe from a toxicity perspective, versus an alternative chemotherapeutic agent. At this time, there are few data to direct treatment decisions at recurrence, but reports do suggest that there may be at least some benefit for treatment with chemotherapy with either temozolomide or PCV [23]. Treatments after failure of alkylator-based chemotherapy vary widely, and there is no consensus opinion on the basis of current National Comprehensive Cancer Network and European Association of Neuro-Oncology guidelines [24, 25].

4.4 Standard of Care for Malignant High-Grade Glioma

Historically, glioblastoma has been treated with postoperative radiotherapy to kill remaining tumor cells. Addition of radiotherapy extends survival from 3–4 months to about 12 months [26, 27]. In the 1990s, the DNA alkylating agent temozolomide was tested and approved by the FDA as a chemotherapeutic agent for the treatment of malignant glioma [28]. Addition of temozolomide to surgical resection and radiotherapy extends median survival to 14.6 months and the 2-year survival rate to 27% compared to 10% [22]. Additional studies have shown that patients with DNA methylation in the promoter region of the DNA repair enzyme O6-methylguanine-DNA methyltransferase (MGMT) are more likely to respond to temozolomide therapy [29]. The current standard of care for glioblastoma is GTR with concomitant temozolomide and radiotherapy followed by adjuvant temozolomide.

Carmustine is the only other FDA-approved first-line chemotherapeutic agent approved for glioblastoma. Like temozolomide, carmustine is a DNA-alkylating agent. BCNU (carmustine)-polymer wafers are positioned in the tumor bed after tumor resection. A Phase III clinical trial showed evidence of survival benefit [30]. However, the efficacy of carmustine has never been directly compared to that of temozolomide.

Nearly all patients with malignant glioma will recur [31]. Despite maximal initial resection and multimodality therapy, about 70% of GBM patients will experience disease progression within 1 year of diagnosis [32] with less than 5% of patients surviving 5 years after diagnosis [33]. Re-resection is an option for some patients, and surgical debulking can alleviate mass effect and symptoms, such as seizures, speech, and motor deficits, frequently seen at recurrence. Repeat surgery may be required to confirm a diagnosis of tumor recurrence versus pseudoprogression or radiation necrosis and may also provide tissue for molecular testing to identify potential new targeted agents [34]. Opinion varies as to whether repeat surgery enhances OS. Some evidence exists that a greater extent of resection at recurrence is associated with improved survival [35]; however, other studies have not found an absolute benefit in terms of survival [36, 37].

Additional radiation may be possible for some patients, but tolerance of healthy brain tissue to radiation is limited because of the increased risk of radiation necrosis. A wide variety of radiation techniques, including brachytherapy, gamma knife, and stereotactic radiosurgery, may be used for the treatment of recurrent disease [38].

Upon recurrence of GBM, chemotherapy and corticosteroids may be used to palliate symptoms and improve qual-

ity of life, but objective response rates are dismal, and time to progression for standard cytotoxic agents is only 3–6 months [39]. Rechallenging with TMZ may be an option, and other agents, such as carboplatin (Paraplatin®), etoposide (Toposar®), irinotecan (Camptosar®), and nitrosourea-based chemotherapy, may be tried as single agents or in regimens.

The options for the treatment of GBM are limited due to the presence of the blood–brain barrier (BBB), which prevents molecules >500 Da [40] from entering the brain. The BBB is a selective physical barrier, as the tight junctions between the adjacent endothelial cells do not allow for the normal, paracellular transport, but force molecules into a transcellular transport. Small molecules, such as O_2, CO_2, and ethanol may diffuse freely through the membrane [41]. The presence of specific transport systems on the membrane surface enables nutrients to enter the brain, but prevents potentially toxic substances from harming the CNS. Large molecules, such as peptides and proteins, are not able to enter the brain, unless there is a strictly regulated receptor-mediated or adsorption-mediated transcytosis [42]. The BBB has a protective role: it mediates the efflux of waste products, maintains the ionic concentrations, which may change significantly following a meal and cause a disruption of normal brain function, and it separates the pools of the neurotransmitters that act centrally and peripherally. Overall, the BBB maintains the homeostasis of the CNS. Considering the limited penetration in the brain, alternative drug-delivery strategies are required for the more effective treatment of gliomas.

4.5 Chemotherapy and More

The current standard of care for malignant glioma has limited efficacy. One limitation of radiotherapy and temozolomide chemotherapy is that the therapy is nonspecific. The therapy does not exploit specific weakness of individual tumors. As we enter a time of greater understanding of the genetic landscape and gene expression of malignant gliomas, we will have a better idea of the targets to attack [43]. The Cancer Genome Atlas (TCGA) is a project sponsored by the National Institutes of Health (NIH) to better elucidate the genetics and gene expression of multiple cancer types, including glioblastoma. The TCGA has analyzed over 500 untreated glioblastoma samples for DNA sequence and epigenetic modification, gene expression, and microRNA expression [44]. This project has led to a deeper understanding of glioblastoma enabling high-throughput pathway analysis and massive data synthesis. One of the major findings of the project was that glioblastoma is divided into four distinct subtypes: mesenchymal, proneural, classical, and neuronal [45]. Each subtype has novel mutations and expression patterns. Some of these novel pathways and targets will hopefully prove to be exploitable for effective treatments in the future.

Utilizing TCGA data and other genome-wide studies, new molecular targets for malignant gliomas have been detected. Molecular targets are common in pathways central to malignant glioma survival such as proliferation, evasion of apoptosis, invasiveness, and angiogenesis [46]. Aberrant growth factor signaling drives proliferation in many malignant gliomas. Epidermal growth factor (EGFR), platelet-derived growth factor (PDGF), insulin-like growth factor (IGF), and fibroblast growth factor (FGF) are either highly upregulated or mutated in a large percentage of malignant gliomas [47]. Several clinical trials have tried to capitalize on blocking these pathways. EGFR is the most widely studied growth factor in malignant glioma. Several small molecular inhibitors (gefitinib, erlotinib, lapatinib, and cetuximab) have been evaluated in Phase II clinical trials for use in therapy of malignant gliomas. Unfortunately, these drugs have only shown modest efficacy for treating malignant glioma.

Personalized medicine will play a better role in identifying certain exploitable pathways or targets in an individual tumor [48, 49] . In the near future, genetic tests will determine if a patient will respond to temozolomide. Deep sequencing of tumor DNA and gene expression analysis of fresh tumor samples will eventually direct therapy for patients suffering from malignant glioma. By synthesizing ascertainable data from the tumor, therapy can be tailored and combined to select the appropriate combination of therapies to best target the tumor. As technology evolves to make medicine more personalized, new methods will be utilized to choose the proper combinatorial therapy to treat each malignant glioma.

4.6 Role of Bevacizumab

GBM is a highly vascular neoplasm, with abnormal vasculature characterized by tortuous blood vessels, vascular permeability and resulting hypoxia leading to the histological finding of pseudopalisading necrosis [50]. Tumor growth and invasion are intrinsically linked to hypoxia, which results in upregulation of hypoxia-inducible factor 1-α, and downstream upregulation of VEGF, which is associated with glioma cell stemness, mesenchymal phenotype, and an immunosuppressive cellular milieu [51]. Thus, there is a strong biologic rationale for the use of antiangiogenic agents in GBM, and these drugs have thus been extensively studied as therapeutic targets in both newly diagnosed and recurrent GBM.

Bevacizumab, a humanized monoclonal antibody which binds VEGF-A, is the most extensively studied of the antiangiogenic agents for GBM. Bevacizumab was

approved by the US FDA for use in recurrent GBM in 2009 [52]. The "Bevacizumab Alone and in Combination with Irinotecan in Recurrent GBM" (BRAIN) study [53] was a randomized Phase II trial that assigned 167 patients with recurrent GBM to receive bevacizumab 10 mg/kg with or without irinotecan. This trial demonstrated objective response rates of 38 and 28% in patients treated with bevacizumab with and without irinotecan, respectively. Progression-free survival at 6 months (PFS-6) was 42% in patients treated with bevacizumab alone and 50% in the combination arm. In a single-arm study, 48 patients with recurrent GBM were treated with bevacizumab 10 mg/kg with irinotecan added upon disease progression, demonstrating an objective response rate of 35% and PFS-6 of 29% [54]. While these findings led to FDA approval for recurrent GBM in the USA, its use has not been approved in Europe due to concerns regarding the lack of a bevacizumab-free control arm, the modest improvement in OS, and difficulties with interpreting MRI-based disease progression in patients treated with bevacizumab [55].

In the USA, the widespread use of bevacizumab for recurrent GBM has limited the opportunity for further evaluation in this setting. In Europe, the randomized Phase II "Single-Agent Bevacizumab or Lomustine Versus a Combination of Bevacizumab Plus Lomustine in Patients with Recurrent GBM" (BELOB) trial [56] showed promising results for the combination of bevacizumab and lomustine versus either agent alone. Unfortunately, these findings were not borne out in the subsequent Phase III trial which compared the combination of lomustine and bevacizumab with lomustine alone [57]. This trial showed no difference in OS, although there was a significant increase in PFS from 1.5 to 4.2 months in the combination arm. Several other Phase II trials have evaluated the combination of bevacizumab with a variety of other cytotoxic and targeted agents, including temozolomide, temsirolimus, and erlotinib, but none have shown significant activity [58].

Similarly, bevacizumab has been tested in the setting of newly diagnosed GBM, with a series of Phase II trials using bevacizumab in combination with radiotherapy and temozolomide [59, 60]. As seen in the recurrent setting, PFS was prolonged in comparison to historical controls (13–14 months), while the effect on OS was modest (10–21 months). Subsequently, two randomized Phase III trials were conducted, "A Study of Avastin in Combination With Temozolomide and Radiotherapy in Patients With Newly Diagnosed GBM" (AVAGlio) [61] and RTOG-0825 [62]. These studies showed longer PFS in patients treated with bevacizumab, but failed to show OS benefit. Thus, despite encouraging preclinical results with in vivo activity and reduction of vasogenic edema, there is abundant high-quality evidence that bevacizumab is not indicated in unselected patients with newly diagnosed GBM.

4.7 Future Directions

4.7.1 Growth Factor Receptor Inhibitors

EGFRvIII, the most common variant of EGFR, is only found in GBM and other tumor cell surface without expression in normal tissue cells [63].

Biological targeted therapy targets the pathway of the EGF/EGFR ligand and involves the use of mAb against EGFR, such as cetuximab and nimotuzumab, and tyrosine kinase inhibitors (TKIs), including gefitinib, erlotinib, afatinib, canertinib, and lapatinib. A current retrospective study carried out based on clinical trials found that both gefitinib and erlotinib had good therapeutic responses in GBM patients with co-expression of EGFRvIII and PTEN [64].

Cetuximab has been used in Phase I and Phase II clinical trials and have demonstrated effective improvement in the treatment for patients with GBM.

Radiotherapy followed adjuvant therapy with the combination of ABT-414 (anti-EGFR antibody) and TMZ has shown promising results in OS among patients with newly diagnosed GBM with EGFR amplification.

4.7.2 Tumor-Treating Electric Fields for Glioblastoma

Tumor-Treating Fields (TTFields) have considered the "fourth cancer treatment modality," after surgery, RT, and pharmacotherapy; is a locoregionally antimitotic treatment that delivers low-intensity, intermediate-frequency (200 kHz), alternating electric fields, through four transducer arrays, consisting of nine insulated electrodes applied to the shaved scalp and connected to a portable device. In vitro TTFields arrest cell division and kill tumor cells through multiple mechanisms [65].

In 2011 TTFields were approved from FDA as a therapeutic option for use in rGBM. In the EF-14 trial, an open-label Phase III study, 695 patients were treated with TTFields in combination with TMZ maintenance treatment, after chemoradiation therapy for patients with nGBM. The trial showed a significant improvement in PFS and OS. The percentage of patients alive at 2 years was 43% in the TTFields/TMZ group and 29% in the TMZ alone group (P = 0.006). In October 2015, the FDA approved TTFields for use in newly diagnosed GBM patient [66] and National Comprehensive Cancer Network has further incorporated TTFields in their updated guidelines.

4.8 Vaccine Therapy

These vaccines work by activating T cells (CD4 and CD8) against specific tumor antigens and by inducing an antitumoral cellular response by using dendritic cells (DC) and heat shock proteins [67].

4.8.1 DC Therapy

Current preparation of DC vaccines involves exposing the lysate of a patient's tumor to the patient's autologous DCs, which are then treated with a differentiation factor such as GM-CSF. The primed APCs are then injected back into the patient with hopes of generating a T-cell response against the tumor. The primed APCs (antigen-presenting cells) are then injected back into the patient with hopes of generating a T-cell response against the tumor.

DC vaccines have demonstrated some efficacy in improving outcomes for glioblastoma. Bregy et al. in a systematic review demonstrated that autologous DC vaccination improved median OS in patients with newly diagnosed and recurrent GBM compared to historical trends [68]. Parney and Gustafson explored the benefits of adding DC therapy with concurrent temozolomide in patients with resected newly diagnosed glioblastoma. DCs were generated from the patient's CD14+ monocytes, pulsed with allogeneic tumor lysate from two patient-derived GBM cell cultures, and given to patients during their temozolomide therapy. After vaccination, increased circulating tumor-associated antigen-specific CD8 T cells were identified, demonstrating that allogenic tumor lysate vaccines are feasible and may generate a tumor antigen-specific immune response.

4.8.2 Heat Shock Protein (HSP) Vaccines

The HSPs intracellularly have the function to assemble and transport nascent proteins. HSPs also have a very critical role in the stress response to cellular insult and function by stabilizing proteins and preventing them from aggregating.

Tumor-derived HSPs and other proteins can be complexed together and serve as an antitumor vaccine in patients with glioblastoma. The advantage of these vaccines, respect to others, is that HSPs are not targeted to a specific predefined antigen but instead to varying types of antigenic proteins upon vaccination, which serves to broadly target the intratumoral heterogeneity that is normally seen in GBM [69].

Bloch et al. [70] reported a median overall survival of 42.6 weeks after HSP peptide complex-96 vaccination in patients with recurrent glioblastoma. Of note, 66% of patients in this study were lymphopenic prior to therapy, which is believed to have significantly impacted the antitumor immune response.

These studies demonstrate that the HSPPC-96 vaccination may be safe and deserve additional investigation.

4.9 Checkpoint Inhibitors

Immune checkpoints are very important in the balance of self-tolerance and immunogenicity. Failed immune checkpoints impede immune responses in refractory cancers that are prone to T-cell anergy and toleragenicity. Programmed cell death protein and ligand (PD-1, PDL-1), metabolic enzymes (e.g., Arginase), and inhibitory immune pathways CTLA4 (Cytotoxic T-Lymphocyte-Associated Antigen 4) have been hypothesized to play a role in immune tolerance. CTLA4, expressed on T cells, regulates the extent of the T-cell immune response by impeding the CD28 T-cell stimulatory pathway. In the clinical setting, CTLA4 blockade, through the use of monoclonal antibodies, increases CD4 T-cell activity, and inhibits regulatory T-cell immunosuppression. In glioma mouse models, systemic blockade of PD-L1 demonstrated long-term survival with concurrent inhibition of regulatory T-cell activity. In animal models, activation of co-stimulatory receptors such as OX40 and blockade of co-inhibitory receptors such as PD1 and CTLA4 induced tumor regression and increased long-term survival. Currently, several clinical trials are ongoing for assessment of monoclonal antibody checkpoint inhibitors (anti-PD-L1 and CTLA-4) for glioblastoma [71, 72].

An increasing number of clinical trials are ongoing since 2011 to evaluate the potential therapeutic efficacy of PD-1/PD-L1 inhibitors, including nivolumab, pembrolizumab, pidilizumab (anti-PD-1), and MEDI4736, MPDL3280A (anti-PD-L1) as monotherapies and combination therapies for GBMs. There are still two ongoing clinical trials to investigate the nivolumab, TMZ, and radiation therapy or their combination for newly diagnosed patients with GBM (Table 4.1). The combination of ipilimumab (anti-CTLA-4) and nivolumab was tested in a Phase III randomized trial in recurrent GBM.

4.10 Chimeric T-Cell Receptors (TCR)

Chimeric antigen receptors (CARs) are a diverse class of receptors that have been created by combining the variable region of an antibody with a T-cell-signaling molecule such as CD3. These newly created receptors are advantageous compared to the TCR-transduced T cells. CARs have the ability to mimic endogenous TCR-mediated activation without the disadvantages of classical MCH restriction as the antigen recognition site is derived from an antibody.

Brown et al. examined the bioactivity and safety of IL13Ralpha2 redirected chimeric antigen receptor CD8 T cells in the resection cavity of three patients, and noted transient immune-mediated antitumor responses in 2/3 patients

with recurrent glioblastoma. Other case reports of similar IL13Ralpha2-directed CAR conducted demonstrated tumor regression and immune responses after intrathecal therapy in patients with multifocal recurrent GBM [73, 74].

4.11 Viroimmunotherapy

The use of viruses to mediate gene immunotherapy in the treatment of tumors is a promising approach and has a wide variety of applications. Treatments can include transferring genes for inflammatory proteins to tumor cells, inhibition of immunosuppressing tumor genes, or transferring proinflammatory and tumor antigen genes to professional antigen-presenting cells. Previous clinical trials have focused on conditional cytotoxicity and oncolytic viruses, which may induce a secondary immune response by generating foreign antigens and producing a proinflammatory immune beacon in tumor cells.

Several clinical trials using adenovirus, herpes simplex virus, and replicating retroviruses have been conducted with preliminary results demonstrating survival benefit [75, 76]. In a Phase I/IIa trial (ParvOryx01) the oncolytic H-1 parvovirus (H-1PV) induced markers of immune activation in patients with recurrent glioblastoma; nine patients (age 29 to 69 years) with primary ($n = 2$) or recurrent ($n = 7$) glioblastoma were treated in a compassionate use (CU) program with a combination of H-1PV followed by bevacizumab and PD-1 blockade. Seven of the patients received both intratumoral and intravenous injection of H-1PV and two patients only intravenous virus treatment. Objective tumor response was observed in seven of nine patients (78%). Two patients showed complete responses (22%), five patients had partial remissions (56%) with tumor reduction between 49% and 94%, and two patients progressive disease (22%). H-1PV-based viroimmunotherapy leads to ORR in 78% of glioblastoma patients and this is a much higher response rate than reported for treatment with either bevacizumab or checkpoint blockade.

4.12 Conclusions

The recent research in vaccine therapy, checkpoint inhibitors, chimeric antigen T-cell receptors, and viroimmunotherapy has provided an opportunity to supplement the current treatment of glioblastoma potentially, improving prognosis and overall survival for these patients. Although there are several barriers to an effective safe treatment, future larger prospective studies may help elucidate the role of immunotherapy in these patients.

Acknowledgement The current chapter is a revision made by Ileana De Roma, Lucia Lombardi, and Gennaro Gadaleta-Caldarola of the original chapter written by Evaristo Maiello, Lucia Lombardi, Mario Brandi, and Tommaso Scarabino in the previous edition of the book.

References

1. Thakkar JP, Dolecek TA, Horbinski C, et al. Epidemiologic and molecular prognostic review of glioblastoma. Cancer Epidemiol Biomarkers Prev. 2014;23:1985–96.
2. Ostrom QT, Gittleman H, Liao P, et al. CBTRUS statistical report: primary brain and central nervous system tumors diagnosed in the United States in 2007–2011. Neuro-Oncology. 2014;16(Suppl. 4):ivl–63.
3. Louis DN, Perry A, Reifenberger G, et al. The 2016 World Health Organization classification of tumors of the central nervous system: a summary. Acta Neuropathol. 2016;131(6):803–20.
4. Cairncross JG, Ueki K, Zlatescu MC, et al. Specific genetic predictors of che- motherapeutic response and survival in patients with anaplastic oligodendrogliomas. J Natl Cancer Inst. 1998;90:1473–9.
5. Jenkins RB, Blair H, Ballman KV, et al. A t(1;19)(q10;p10) mediates the combined deletions of 1p and 19q and predicts a better prognosis of patients with oligodendroglioma. Cancer Res. 2006;66:9852–61.
6. Griffin CA, Burger P, Morsberger L, et al. Identification of der(1;19)(q10;p10) in five oligodendrogliomas suggests mechanism of concurrent 1p and 19q loss. J Neuropathol Exp Neurol. 2006;65:988–94.
7. Houillier C, Wang X, Kaloshi G, et al. IDH1 or IDH2 mutations predict longer survival and response to temozolomide in low-grade gliomas. Neurology. 2010;75:1560–6.
8. Dang L, White DW, Gross S, et al. Cancer-associated IDH1 mutations produce 2-hydroxyglutarate. Nature. 2009;462(7274):739–44.
9. Preusser M, Wohrer A, Stary S, et al. Value and limitations of immunohistochemistry and gene sequencing for detection of the IDH1-R132H mutation in diffuse glioma biopsy specimens. J Neuropathol Exp Neurol. 2011;70(8):715–23.
10. Parsons DW, Jones S, Zhang X, et al. An integrated genomic analysis of human glioblastoma multiforme. Science. 2008;321(5897):1807–12.
11. Cairncross G, Wang M, Shaw E, et al. Phase III trial of chemoradiotherapy for anaplastic oligodendroglioma: long-term results of RTOG 9402. J Clin Oncol. 2013;31(3):337–43.
12. Van Den Bent MJ, Brandes AA, Taphoorn MJ, et al. Adjuvant procarbazine, lomustine, and vincristine chemotherapy in newly diagnosed anaplastic oligodendroglioma: long-term follow-up of EORTC brain tumor group study 26951. J Clin Oncol. 2013;31(3):344–50.
13. Hegi ME, Diserens AC, Gorlia T, et al. MGMT gene silencing and benefit from temozolomide in glioblastoma. N Engl J Med. 2005;52(10):997–1003.
14. Preusser M, Elezi L, Hainfellner JA. Reliability and reproducibility of PCR-based testing of O6-methylguanine-DNA methyltransferase gene (MGMT) promoter methylation status in formalin-fixed and paraffin-embedded neurosurgical biopsy specimens. Clin Neuropathol. 2008;27(6):388–90.
15. Lalezari S, Chou AP, Tran A, et al. Combined analysis of O6-methylguanine-DNA methyltransferase protein expression and promoter methylation provides optimized prognostication of glioblastoma outcome. Neuro-Oncology. 2013;15(3):370–81.
16. Switzeny OJ, Christmann M, Renovanz M, et al. MGMT promoter methylation determined by HRM in comparison to MSP and pyrosequencing for predicting high-grade glioma response. Clin Epigenetics. 2016;8:49.

17. Bady P, Sciuscio D, Diserens AC, et al. MGMT methylation analysis of glioblastoma on the Infinium methylation BeadChip identifies two distinct CpG regions associated with gene silencing and outcome, yielding a prediction model for comparisons across datasets, tumor grades, and CIMP-status. Acta Neuropathol. 2012;124(4):547–60.
18. Sahm F, Reuss D, Koelsche C, et al. Farewell to oligoastrocytoma: in situ molecular genetics favor classification as either oligodendroglioma or astrocytoma. Acta Neuropathol. 2014;128(4):551–9.
19. Coons SW, Johnson PC, Scheithauer BW, et al. Improving diagnostic accuracy and interobserver concordance in the classification and grading of primary gliomas. Cancer. 1997;79(7):1381–93.
20. Kros JM, Gorlia T, Kouwenhoven MC, et al. Panel review of anaplastic oligodendroglioma from European Organization for Research and Treatment of Cancer Trial 26951: assessment of consensus in diagnosis, influence of 1p/19q loss, and correlations with outcome. J Neuropathol Exp Neurol. 2007;66(6):545–51.
21. Shaw EG, Berkey B, Coons SW, et al. Recurrence following neurosurgeon- determined gross-total resection of adult supratentorial low-grade glioma: results of a prospective clinical trial. J Neurosurg. 2008;109:835–41.
22. Stupp R, Mason WP, van den Bent MJ, et al. Radiotherapy plus concomitant and adjuvant temozolomide for glioblastoma. N Engl J Med. 2005;352:987–96.
23. Nahed BV, Redjal N, Brat DJ, et al. Management of patients with recurrence of diffuse low grade glioma: a systematic review and evidence-based clinical practice guideline. J Neuro-Oncol. 2015;125:609–30.
24. Nabors LB, Portnow J, Ammirati M, et al. Central nervous system cancers, version 2.2014. Featured updates to the NCCN guidelines. J Natl Compr Cancer Netw. 2014;12:1517–23.
25. Soffietti R, Baumert BG, Bello L, et al. Guidelines on management of low-grade gliomas: report of an EFNS-EANO Task Force. Eur J Neurol. 2010;17:1124–33.
26. Walker MD, Alexander E, Hunt WE, et al. Evaluation of BCNU and/or radiotherapy in the treatment of anaplastic gliomas. Acooperative clinical trial. J Neurosurg. 1978;49(3):333–43.
27. Walker MD, Green SB, Byar DP, et al. Randomized comparisons of radiotherapy and nitrosoureas for the treatment of malignant glioma after surgery. N Engl J Med. 1980;303(23):1323–9.
28. Newlands ES, Stevens MF, Wedge SR, et al. Temozolomide: a review of its discovery, chemical properties, pre-clinical development and clinical trials. Cancer Treat Rev. 1997;23(1):35–61.
29. Hegi ME, Diserens A-C, Gorlia T, et al. MGMT gene silencing and benefit from temozolomide in glioblastoma. N Engl J Med. 2005;352(10):997–1003.
30. Westphal M, Hilt DC, Bortey E, et al. A phase 3 trial of local chemotherapy with biodegradable carmustine (BCNU) wafers (Gliadel wafers) in patients with primary malignant glioma. Neuro Oncol. 2003;5(2):79–88.
31. Bloch O, Han SJ, Cha S, et al. Impact of extent of resection for recurrent glioblastoma on overall survival: clinical article. J Neurosur. 2012;117(6):1032–8.
32. Stupp R, Hegi ME, Mason WP, et al. Effects of radiotherapy with concomitant and adjuvant temozolomide versus radiotherapy alone on survival in glioblastoma in a randomised phase III study: 5-year analysis of the EORTCNCIC trial. Lancet Oncol. 2009;10:459–66.
33. Ostrom QT, Bauchet L, Davis FG, et al. The epidemiology of glioma in adults: a “state of the science” review. Neuro Oncol. 2014;16:896–913.
34. Brandes AA, Bartolotti M, Francheschi E. Second surgery for recurrent glioblastoma: advantages and pitfalls. Expert Rev Anticancer Ther. 2013;13:583–7.
35. Bloch O, Han SJ, Cha S, et al. Impact of extent of resection for recurrent glioblastoma on overall survival. J Neurosurg. 2012;117:1032–8.
36. Brandes AA, Bartolotti M, Francheschi E. Second surgery for recurrent glioblastoma: advantages and pitfalls. Expert Rev Anticancer Ther. 2013;13:583–7.
37. Franceschi E, Bartolotti M, Tosoni A, et al. The effect of reoperation on survival in patients with recurrent glioblastoma. Anticancer Res. 2015;35:1743–8.
38. Davis ME, Stoiber AM. Glioblastoma multiforme: enhancing survival and quality of life. Clin J Oncol Nurs. 2011;15:291–7.
39. Franceschi E, Tosoni A, Bartolini S, et al. Treatment options for recurrent glioblastoma: pitfalls and future trends. Expert Rev Anticancer Ther. 2009;9:613–9.
40. Pardridge WM. Blood-brain barrier drug targeting: the future of brain drug development. Mol Interv. 2003;3:90–105.
41. Abbott NJ. Evidence for bulk flow of brain interstitial fluid: significance for physiology and pathology. Neurochem Int. 2004;45:545–52.
42. Cserr HF, Bundgaard M. Blood-brain interfaces in vertebrates: a comparative approach. Am J Phys. 1984;246:R277–88.
43. Brennan CW, Verhaak RGW, McKenna A, et al. The somatic genomic landscape of glioblastoma. Cell. 2013;155(2):462–77.
44. Network TCGA. Comprehensive genomic characterization defines human glioblastoma genes and core pathways. Nature. 2008;455(7216):1061–8.
45. Verhaak RG, Hoadley KA, Purdom E, et al. Integrated genomic analysis identifies clinically relevant subtypes of glioblastoma characterized by abnormalities in PDGFRA, IDH1, EGFR, and NF1. Cancer Cell. 2010;17(1):98–110.
46. Wang Y, Jiang T. Understanding high grade glioma: molecular mechanism, therapy and comprehensive management. Cancer Lett. 2013;331(2):139–46.
47. Squatrito M, Holland EC. DNA damage response and growth factor signaling pathways in gliomagenesis and therapeutic resistance. Cancer Res. 2011;71(18):5945–9.
48. Zhu J-J, Wong ET. Personalized medicine for glioblastoma: current challenges and future opportunities. Curr Mol Med. 2013;13(3):358–67.
49. Weller M, Stupp R, Hegi M, et al. Individualized targeted therapy for glioblastoma: fact or fiction? Cancer J. 2012;18(1):40–4.
50. Wang N, Jain RK, Batchelor TT. New directions in anti-angiogenic therapy for glioblastoma. Neurotherapeutics. 2017;14(2):321–32.
51. Lu-Emerson C, Duda DG, Emblem KE, et al. Lessons from anti-vascular endothelial growth factor and anti-vascular endothelial growth factor receptor trials in patients with glioblastoma. J Clin Oncol. 2015;33(10):1197–213.
52. Cohen MH, Shen YL, Keegan P, et al. FDA drug approval summary: bevacizumab (Avastin) as treatment of recurrent glioblastoma multiforme. Oncologist. 2009;14(11):1131–8.
53. Friedman HS, Prados MD, Wen PY, et al. Bevacizumab alone and in combination with irinotecan in recurrent glioblastoma. J Clin Oncol. 2009;27(28):4733–40.
54. Kreisl TN, Kim L, Moore K, et al. Phase II trial of single-agent bevacizumab followed by bevacizumab plus irinotecan at tumor progression in recurrent glioblastoma. J Clin Oncol. 2009;27(5):740–5.
55. Wick W, Weller M, Van Den Bent M, et al. Bevacizumab and recurrent malignant gliomas: a European perspective. J Clin Oncol. 2010;28(12):e188–9.
56. Taal W, Oosterkamp HM, Walenkamp AM, et al. Single-agent bevacizumab or lomustine versus a combination of bevacizumab plus lomustine in patients with recurrent glioblastoma (BELOB trial): a randomised controlled phase 2 trial. Lancet Oncol. 2014;15(9):943–53.
57. Wick W, Brandes AA, Gorlia T, et al. EORTC 26101 phase III trial exploring the combination of bevacizumab and lomustine in patients with first progression of a glioblastoma. J Clin Oncol. 2016;34(15 Suppl):2001–10.

58. Lai A, Tran A, Nghiemphu PL, et al. Phase II study of bevacizumab plus temozolomide during and after radiation therapy for patients with newly diagnosed glioblastoma multiforme. J Clin Oncol. 2011;29(2):142–8.
59. Vredenburgh JJ, Desjardins A, Kirkpatrick JP, et al. Addition of bevacizumab to standard radiation therapy and daily temozolomide is associated with minimal toxicity in newly diagnosed glioblastoma multiforme. Int J Radiat Oncol Biol Phys. 2012;82(1):58–66.
60. Vredenburgh JJ, Desjardins A, Reardon DA, et al. The addition of bevacizumab to standard radiation therapy and temozolomide followed by bevacizumab, temozolomide, and irinotecan for newly diagnosed glioblastoma. Clin Cancer Res. 2011;17(12):4119–24.
61. Chinot OL, Wick W, Mason W, et al. Bevacizumab plus radiotherapy-temozolomide for newly diagnosed glioblastoma. N Engl J Med. 2014;370(8):709–22.
62. Gilbert MR, Dignam JJ, Armstrong TS, et al. A randomized trial of bevacizumab for newly diagnosed glioblastoma. N Engl J Med. 2014;370(8):699–708.
63. Johansson M, Oudin A, Tiemann K, et al. The soluble form of the tumor suppressor Lrig1 potently inhibits in vivo glioma growth irrespective of EGF receptor status. Neuro Oncol. 2013;15(9):1200–11.
64. Gallego O, Cuatrecasas M, Benavides M, et al. Efficacy of erlotinib in patients with relapsed gliobastoma multiforme who expressed EGFRVIII and PTEN determined by immunohistochemistry. J Neurooncol. 2014;116(2):413–9.
65. Hottinger AF, Pacheco P, Stupp R. Tumor treating fields: a novel treatment modality and its use in brain tumors. Neuro Oncol. 2016;18(10):1338–49.
66. Stupp R, Taillibert S, Kanner AA. Maintenance therapy with tumor-treating fields plus temozolomide vs temozolomide alone for glioblastoma: a randomized clinical trial. JAMA. 2015;314(23):2535–43.
67. Guo C, Manjili MH, Subjeck JR. Therapeutic cancer vaccines: past, present, and future. Adv Cancer Res. 2013;119:421–75.
68. Bregy A, Wong TM, Shah AH, et al. Active immunotherapy using dendritic cells in the treatment of glioblastoma multiforme. Cancer Treat Rev. 2013;39(8):891–0.
69. Winograd EK, Ciesielski MJ, Fenstermaker RA. Novel vaccines for glioblastoma: clinical update and perspective. Immunotherapy. 2016;8(11):1293–308.
70. Bloch O, Crane CA, Fuks Y, et al. Heat-shock protein peptide complex-96 vaccination for recurrent glioblastoma: a phase II, single-arm trial. Neuro Oncol. 2014;16:274–9.
71. Wainwright DA, Chang AL, Dey M, et al. Durable therapeutic efficacy utilizing combinatorial blockade against IDO, CTLA-4, and PD-L1 in mice with brain tumors. Clin Cancer Res. 2014;20:5290–301.
72. Berghoff AS, Kiesel B, Widhalm G, et al. Programmed death ligand 1 expression and tumor-infiltrating lymphocytes in glioblastoma. Neuro Oncol. 2015;17:1064–75.
73. Brown CE, Badie B, Barish ME, et al. Bioactivity and safety of IL13Ralpha2-redirected chimeric antigen receptor CD8+ T cells in patients with recurrent glioblastoma. Clin Cancer Res. 2015;21:4062–72.
74. O'Rourke DM, Nasrallah M, Morrissette JJ, et al. Pilot study of T cells redirected to EGFRvIII with a chimeric antigen receptor in patients with EGFRvIII+ glioblastoma. J Clin Oncol. 2016;17:110–1.
75. Markert JM, Medlock MD, Rabkin SD, et al. Conditionally replicating herpes simplex virus mutant, G207 for the treatment of malignant glioma: results of a phase I trial. Gene Ther. 2000;7:867–74.
76. Geletneky K, Huesing J, Rommelaere J, et al. Phase I/IIa study of intratumoral/intracerebral or intravenous/intracerebral administration of parvovirus H-1 (ParvOryx) in patients with progressive primary or recurrent glioblastoma multiforme: ParvOryx01 protocol. BMC Cancer. 2012;12:99.

Part III

Post Treatment Neuroradiologic Imaging

Magnetic Resonance Technique

5

Saverio Pollice, Michela Capuano,
and Tommaso Scarabino

5.1 Morphological MRI

Conventional morphological magnetic resonance imaging (MRI) represents the standard imaging method for neuro-oncologic assessment; its primary roles consist of initial brain tumor evaluation.

Conversely, after diagnosis, each treatment alters anatomy and structural framework evaluated at baseline imaging, so interpretation of images has to be supported from a set of knowledge that include physiology of the tissue response to any type of treatment: chemotherapy, surgical, radiation therapy, and new immunological treatments.

Standardized brain tumor MRI protocol should include the following sequences: TSE T1, TSE T2, fluid-attenuated inversion recovery (FLAIR), diffusion-weighted imaging (DWI), and 3-D gadolinium contrast-enhanced FFE T1, performed on a minimum 1.5 T MR system. T2∗-weighted imaging, such as susceptibility-weighted imaging (SWI), is usually performed as part of the routine brain MRI examination. If 3-D sequences cannot be performed due to time constraints or technical limitations, 2-D sequences can be substituted.

These sequences provide exquisite anatomic detail, and the use of a gadolinium-based contrast agent in this protocol allows for the detection of areas where the blood–brain barrier is compromised.

In general, gliomas are hypointense on T1W images and hyperintense on T2W images. Contrast enhancement, necrosis, hemorrhage, infiltration of surrounding brain and abundant peritumoral edema are commonly considered imaging characteristics of aggressive lesions and raise the possibility of a high-grade glial neoplasm.

Specific presurgical sequences such as high-resolution isovolumetric 3D T2-weighted and postcontrast 3D T1 spoiled gradient echo imaging can be obtained for intraoperative navigation or with a head frame for stereotactic radiosurgical planning.

MRI after treatment imaging includes the same sequences of a standard evaluation [1, 2].

5.2 Susceptibility-Weighted Imaging

High-resolution 3D T2∗ gradient echo sequences such as SWI are highly sensitive to magnetic susceptibility effects from blood products or mineralization. This technique is useful to depict internal vascular architecture and hemorrhage in tumors, which can be used to suggest grade, as well as calcification to narrow the differential diagnosis. Both blood products and mineralization appear dark on magnitude images and can be differentiated on filtered phase images in which paramagnetic blood products appear dark and diamagnetic calcium appears bright. Minimum intensity projection images can also be reviewed to more clearly visualize normal venous structures, tumoral vascularity, and parenchymal foci of susceptibility.

SWI is also used in noninvasive grading of primary brain neoplasms by assessment and counting, of intratumoral susceptibility signals (ITSS) that refers to linear dot-like or small mass-like areas of low signal within or along the edges of the tumor on non-CE SWI. SWI is sensitive to hemorrhage, calcification, deoxiHb, and all show low signal on SWI.

The morphological pattern of ITSS has been shown to correlate with neoangiogenesis (linear), calcifications or necrosis (dot like and conglomerated). The number of ITSS can reflect the WHO histological grading, so ITSS enables estimating of tumor grade as well as imaging surveillance of tumor progression or more malignant transformation.

The additional ITSS observed on CE-SWI when compared with the unenhanced/conventional SWI image comes from the CIPS effect: contrast-induced phase shift, that are T2∗ effects more frequently observed at the border zone of high-grade glioma.

S. Pollice (✉) · M. Capuano · T. Scarabino
Department of Radiology, "L. Bonomo" Hospital—ASL BT, Andria, Italy

T. Scarabino, S. Pollice (eds.), *Imaging Gliomas After Treatment*, https://doi.org/10.1007/978-3-030-31210-7_5

Postcontrast SW images can show bright enhancement along the tumor that suggested leakage of contrast material due to breakdown of the blood–brain barrier. All the features described about SWI imaging make this sequence essential in the assessment of gliomas especially in posttreatment imaging and follow-up [3, 4, 5].

5.3 Diffusion-Weighted Imaging

DWI is a technique with a multitude of applications within neuroimaging as well as in other areas of radiology. The technique employs MRI sequences sensitized to the movement of water molecules. Pulse sequences are generated so that water molecules that do not move between pulse applications are refocused, and thus are able to generate signal, whereas those that do move lose their ability to generate signal in the reconstructed image. Thus areas of restricted diffusion are bright on DWI, whereas areas of free water motion are dark.

DWI offers significant value in the evaluation of brain tumors, allowing for the assessment of tumor cellularity, peritumoral edema, regions of tumor hypoxia, integrity of white matter tracts, and postoperative injury. Corresponding apparent diffusion coefficient (ADC) values, reflecting the magnitude of diffusivity, are derived for each voxel and displayed as a calculated ADC map.

DWI best serves to characterize tumor cellularity on the premise that water diffusivity within the extracellular compartment is inversely correlated to the volume of the intracellular space.

Low ADC values, representing decreased water diffusivity, can be used to suggest highly cellular tumors. Additionally, low ADC values can be used as a surrogate for increasing tumor grade or as an independent biomarker signifying poor outcomes both in glioma and lymphoma. ADC values have also been used to better localize tumor infiltrated foci among regions of vasogenic edema to better direct tissue sampling and therapy [2].

5.4 MR Perfusion Imaging

It is now established that tumors produce factors which initiate the development of new blood vessels, a process known as neoangiogenesis; perfusion-weighted imaging (PWI) is the MR imaging technique able in assessing the neoangiogenic properties of proliferating gliomas.

Several MR perfusion techniques are currently employed: dynamic susceptibility contrast (DSC), dynamic contrast-enhanced (DCE), and arterial spin labeling (ASL). Of these, DSC perfusion is the most studied and widely applied, while ASL, which does not require intravenous contrast, has been the subject of increasing investigation and clinical implementation.

DSC is based on the detection of susceptibility induced signal loss on T2∗-weighted sequences after the administration of an intravenous gadolinium contrast agent. A signal intensity time curve is generated from which relative cerebral blood volume (rCBV) and other perfusion metrics are derived. rCBV is elevated in tumor, where it is seen as a marker of angiogenesis.

rCBV has been positively correlated to glioma grade, although some lower-grade gliomas such as oligodendrogliomas may have elevated rCBV; rCBV has been noted to be increased in infiltrative edema of gliomas compared to acellular vasogenic edema; rCBV may also predict areas of progression in glioma prior to changes on contrast-enhanced MRI.

The new underlying principle behind DCE is that disordered tumor vasculature permits intravascular contrast diffusion into the interstitial compartment which is then quantifiable over a dynamic MR acquisition. A modified version of the Tofts pharmacokinetic model is the most commonly used analytic approach in DCE, producing three main imaging biomarkers: estimates of the vascular fraction (vp), extravascular extracellular space fraction (ve), and the transfer contrast coefficient (Ktrans). The volume transfer constant or ktrans, a measure of capillary permeability, is the primary metric derived from DCE perfusion; ktrans can be used to grade tumors, particularly gliomas, as gliomas with increased capillary permeability are more likely to be higher grade than lower grade. Another metric quantified by DCE is ve, an estimate of fractional extracellular extravascular space, which has been shown to be related to tumor cellularity.

ASL is a noninvasive perfusion imaging technique which quantitatively measures cerebral blood flow. It uses an inversion pulse to label inflowing blood proximal to the area of imaging with subsequent subtraction of these labeled spins from control static images. ASL is of particular clinical interest due to its noncontrast technique, relative speed, ability to image the whole brain, and minimal postprocessing.

Several studies have shown a promising role for ASL differentiating high- from low-grade gliomas based on a degree of microvascular proliferation [2, 10].

5.5 MR Spectroscopy

Proton MRI is dependent on signal generated from free protons, which are most abundant in water. In addition to free protons, the MRI signal is also affected to a much lesser degree by protons bound to macromolecules, which are found in low relative concentrations in biologic tissues. Despite their scarcity, these bound protons have specific

frequency variations, which are expressed in parts per millions (ppm) in relation to a known reference frequency. Acquiring data which allows separation of these small frequency peaks, each representing a specific macromolecular component, is known as MR spectroscopy (MRS).

Proton (1H) MRS can be performed with long (288 or 144 ms) and short (35 ms) echo times. MRS can be obtained using a single-voxel technique to a targeted region of interest or a multivoxel technique to cover a broader area and better evaluate regional biochemical differences. The most recognizable metabolite peaks on long echo 1H MRS include N-acetylaspartate (NAA) at 2.0 parts per million (ppm), creatine (Cr) at 3.0 ppm, choline (Cho) at 3.2 ppm, and myo-inositol (MI) at 3.5 ppm. NAA is a marker of neuronal viability, Cr reflects normal cellular metabolism, Cho is a marker of cell membrane turnover, and MI reflects astrocyte integrity. Lipid and lactate, which have a broad peak at 1.3 ppm, are not seen in normal tissue and considered markers of necrosis and hypoxia, respectively.

Brain tumor spectra reflect cellular turnover and loss of normal neuronal metabolites, typically as elevated Cho and decreased NAA.

Generally, absolute heights of metabolite peaks are not used, and rather the peaks are analyzed as ratios such as Cho/NAA and Cho/Cr.

MRS has been shown to differentiate gliomas by grade on the basis of a positive correlation between Cho/NAA and Cho/Cr ratios and grade. Additionally, lower-grade gliomas have been associated with elevated MI/Cr ratio.

Within regions of nonenhancing signal abnormality, elevated Cho/NAA and Cho/Cr ratios have been observed in infiltrative edema compared to vasogenic edema reflecting the increased cellularity underlying the signal abnormality. In this way, MRS can be used to differentiate glioma from noninfiltrative tumor such as metastasis or for biopsy targeting and treatment planning.

Widespread adoption of MRS is limited by technical issues such as variability in acquisition techniques, differences in metabolite ratio calculations, and volume averaging due to lesion location or voxel size [1, 2, 10].

5.6 Chemical Exchange Saturation Transfer (CEST): AMID Amide Proton Transfer Imaging

CEST creates imaging contrast based on sensitivity to chemical exchange of protons on functional metabolic groups rather than exogenously administered contrast. The CEST technique which has primarily been applied to brain tumor imaging is the exchange of amide protons of endogenous tissue proteins and peptides, known as amide proton transfer (APT). Early studies have shown a potential use of APT in the differentiation of tumor from edema and true progression versus pseudoprogression, although these techniques have yet to be widely applied clinically.

Quantitative APT parameters have been proposed as prognostic indicators of brain gliomas by reflecting the cellular proliferation levels that correlated with Ki-67 and as a sensitive biomarker of treatment responses [1, 10].

5.7 Diffusion Tensor Imaging

An advanced application of diffusion imaging is DTI, which interrogates the 3D shape of diffusion using both diffusivity (eigenvalues) and direction (eigenvectors). The principle metrics obtained from DTI include mean diffusivity (MD) and fractional anisotropy (FA). In presurgical planning, DTI-based tractography is used to guide surgical resection by analyzing the integrity of white matter fiber trajectory in order to determine whether there is tumor invasion or tumor displacement of the adjacent white matter tracts.

FA represents the degree of directionality of water diffusion and in the normal brain reflects the presence of intact myelinated white matter tracts. In brain tumors, disrupted cellular architecture results in altered FA that correlates to cellularity. Longer progression-free survival and overall survival were seen in glioblastoma patients in whom more DTI abnormality was resected. Additionally, FA has been reported to be increased in the infiltrative peritumoral edema surrounding high-grade gliomas as compared to the vasogenic edema surrounding metastases.

Often, tumor boundaries are not clearly delineated by conventional imaging, and DTI tractography may improve border characterization leading to greater resection and improved outcomes. The identification and preservation of white matter tracts is also important in preserving the neurological functional integrity of patients undergoing resection of lesions near eloquent cortex [2].

5.7.1 Diffusion Kurtosis Imaging

With free diffusion, the distribution of diffusion-driven molecular displacements obeys the Gaussian law. In biologic tissue, the complex microstructures in biological tissue result in hindered and restricted diffusion of water molecules, and which leads to a non-Gaussian distribution. The non-Gaussianity of water diffusion is thought to depend on cell membranes, organelles, and water compartments which represent the microstructure of the tissue. DKI has been used to measure non-Gaussian diffusion which has the potential to characterize both normal and pathologic tissue better than diffusion tensor imaging.

Compared to the DTI which describes the unrestricted but hindered anisotropic diffusion of water protons, DKI reflects unrestricted diffusion determined by the cytoarchitectonic complexity and can measure the degree of tissue organization. The mean kurtosis (MK), which is one of the principle DKI parameters, is thought to be an index of microstructural complexity. Increased values of the kurtosis parameters in high-grade gliomas may reflect a higher degree of tissue complexity resulting from tumor invasion, increased tumor cellularity, necrosis, hemorrhage, and endothelial proliferation. Whereas low-grade gliomas usually have relatively homogeneous areas of tumor cells with sparse tumor-cell density, and thus resulting in lower kurtosis parameter values [6].

5.8 Functional MRI

fMRI indirectly measures neuronal activity using the ratio of deoxyhemoglobin to oxyhemoglobin as a contrast mechanism, known as blood oxygen level-dependent (BOLD) signal. fMRI can be used for sensory motor, language, and memory mapping, all of which have important implications for presurgical planning and intraoperative navigation.

In task-based fMRI, the patient alternates between a passive resting state and task performance, usually motor or language function, while relative changes in BOLD signal are measured and used to infer areas of cortical activation. Anatomic areas localized with task-based fMRI have been validated to approximate functional sites identified with cortical stimulation mapping. Apart from localizing eloquent cortex, task-based fMRI can be used to characterize tumors. Decreased BOLD signal is noted in cortex involved by tumor and differences are also seen between high- and low-grade tumor suggesting alterations in cerebral blood volume of the tumor affected area.

Recently, there has been increased interest in resting-state functional MRI (rs-fMRI), which does not require patient cooperation with task paradigms and can be performed under anesthesia. rs-fMRI detects spontaneous low-frequency fluctuations in the BOLD signal between regions that are spatially distinct to identify functional networks, so-called resting-state networks (RSNs).

The most fundamental RSN is the default mode network (DMN) and evidence regarding other RSNs including somatosensory, visual, auditory, language, attention, and cognitive control networks is evolving. Compared with task-based fMRI, rs-fMRI has the ability to identify many networks simultaneously, thereby providing more comprehensive information on the functional architecture of the brain while reducing imaging time [2, 10].

5.9. MRI Molecular Characterization

The 2016 WHO classification of central nervous system tumors represented a substantial change in comparison to the 2007 predecessor for defining and categorizing intracranial malignancies. The 2016 guidelines, for the first time, specified the importance of molecular findings, in addition to histology, for the identification of tumor types.

Most clinically relevant molecular markers are the following [1, 6–9].

5.9.1 Codeletion of 1p/19q

The 1p/19q co-deletion in oligodendroglioma is a prognostic factor for better chemoradiotherapy response and longer survival. An indistinct tumor border on T1W and T2W images and heterogeneous signal intensity on T2W images are some of the conventional MR features that have been correlated with 1p/19q co-deletion status. 1p/19q co-deleted tumors also appear to have higher rCBV than their non-deleted counterparts [1].

5.9.2 Isocitrate Dehydrogenase Mutation

Mutations of the IDH gene are associated with improved survival irrespective of tumor grade. They are found in secondary but only rarely in primary GBM.

Several studies have suggested that IDH1 mutant gliomas have a predilection for the frontal lobe and have larger volumes of nonenhancing tumor. Low-grade wildtype IDH1 glioma may be more infiltrative than IDH1 mutant tumors. rCBV is higher in IDH1 wildtype GBM than in IDH1 mutants.

IDH1 mutations cause the production of 2-hydroxyglutarate (2-HG), an oncometabolite that can be detected with MR spectroscopy.

The presence of 2-HG is highly specific for IDH1 mutant tumors. In a recent study, MRS was used to measure 2-HG in patients with IDH mutant gliomas before and after radiochemotherapy. 2-HG levels declined significantly on posttreatment scans raising the possibility that measurements of 2-HG levels could be a biomarker of drug response [1].

5.9.3 MGMT Promoter Methylation

Methylation of the MGMT repair protein promoter inhibits transcription of MGMT, increases sensitivity to TMZ, and positively impacts patient prognosis. Tumor features derived from standard and advanced MRI have been investigated as

a way of noninvasively identifying MGMT promoter methylation status. For instance, ring enhancement is associated with nonmethylated MGMT promoter.

A study of 43 GBM patients using DCE-MRI found that MGMT methylated tumors had increased permeability (higher Ktrans) compared to unmethylated tumors.

A recent study combined both structural and physiologic MR imaging found that MGMT promoter methylation was associated with increased ADC and decreased rCBF (from ASL imaging) [1].

5.10 Imaging of Treatment Response

Assessing brain tumor treatment response by MRI presents considerable challenges such as differentiating progression from treatment-related changes.

Therapies can either mimic or mask disease progression, serial imaging is often the most helpful and reliable noninvasive method to assess disease activity.

Brain tumor follow-up after treatment imaging reflects both treatment effect and natural evolution of tumor [1, 2, 10].

5.10.1 Pseudoprogression

Pseudoprogression consist of inflammatory response marked by a transient increase in contrast enhancement and edema upon completion of chemoradiotherapy, which is observed in up to 30% of high-grade glioma patients and can also be seen in the setting of low-grade glioma. It occurs within the first 3 months following therapy and more frequently in tumors harboring O6-methylguanine DNA methyltransferase (MGMT) promoter methylation.

Since both pseudoprogression and true tumor progression share pathophysiology characterized by an underlying disruption of the BBB, it is difficult to differentiate using conventional imaging.

5.10.2 Pseudoresponse

Pseudoresponse represents a marked decrease in contrast enhancement on MRI related to diminished leakiness of the BBB following treatment with antiangiogenic agents, most commonly bevacizumab, in patients with recurrent glioblastoma. The marked decrease in contrast enhancement, and often in peritumoral edema, can be observed as early as 1 day after initiation of antiangiogenic therapy and does not necessarily reflect biological antitumor effect of therapy.

Antiangiogenic agents may select for a hypoxic and invasive tumor phenotype that is capable of co-opting existing vasculature and therefore growing as nonenhancing infiltrative tumor before manifesting as progressive enhancing disease.

Decreased enhancement should persist for greater than 4 weeks to be considered a true response.

5.10.3 Long-Term Complications of Therapy

Several other chronic changes attributable to brain tumor therapy are well cataloged. Symmetric white matter signal abnormality representing gradual demyelination, gliosis, and vascular injury following chemotherapy, radiotherapy, or both is associated with progressive neurocognitive decline and disordered white matter diffusion. In extreme cases, a diffuse necrotizing leukoencephalopathy can develop following intrathecal chemotherapy without or with radiotherapy.

Rarely, patients with a remote history of intracranial irradiation present with headaches and neurological deficits and are found to have abnormal cortical enhancement.

Acknowledgments The current chapter is a revision made by Saverio Pollice, Michela Capuano, and Tommaso Scarabino of the original chapter written by Saverio Pollice, Teresa Popolizio, and Tommaso Scarabino in the previous edition of the book.

References

1. Pope WB, Brandal G. Conventional and advanced magnetic resonance imaging in patients with high-grade glioma. Q J Nucl Med Mol Imaging. 2018;62(3):239–53.
2. Villanueva-Meyer JE, Mabray MC, Cha S. Current clinical brain tumor imaging. Neurosurgery. 2017;81(3):397–415.
3. Fahrendorf D, Schwindt W, Wölfer J, et al. Benefits of contrast-enhanced SWI in patients with glioblastoma multiforme. Eur Radiol. 2013;23(10):2868–79.
4. Hsu CC, Watkins TW, Kwan GN, et al. Susceptibility weighted imaging of glioma: update on current imaging statusand future directions. J Neuroimaging. 2016;26(4):383–90.
5. Hori M, Ishigame K, Kabasawa H, et al. Precontrast and postcontrast susceptibility-weighted imaging in the assessment of intracranial brain neoplasms at 1.5 T. Jpn J Radiol. 2010;28(4):299–304.
6. Kim M, Kim HS. Emerging techniques in brain tumor imaging: what radiologists need to know. Korean J Radiol. 2016;17(5):598–619.
7. Patel SH, Poisson LM, Brat DJ, et al. T2-FLAIR mismatch, an imaging biomarker for IDH and 1p/19q status in lower-grade gliomas: a TCGA/TCIA project. Clin Cancer Res. 2017;23(20):6078–85.
8. Batchala PP, TJE M, Donahue JH, et al. Neuroimaging-based classification algorithm for predicting 1p/19q-codeletion status in IDH-mutant lower grade gliomas. AJNR Am J Neuroradiol. 2019;40(3):426–32.
9. Delfanti RL, Piccioni DE, Handwerker J, et al. Imaging correlates for the 2016 update on WHO classification of grade II/III gliomas: implications for IDH, 1p/19q and ATRX status. J Neurooncol. 2017;135(3):601–9.
10. Hyare H, Thust S, Rees J. Advanced MRI techniques in the monitoring of treatment of gliomas. Curr Treat Options Neurol. 2017;19(3):11.

Post-surgical MR Morfologic Imaging

6

Alessandro Stecco, Eleonora Soligo, Alessio Paschè, and Alessandro Carriero

6.1 General Findings

After glioma resection, the neuroradiological evaluation performed with MRI could be an authentic challenge. The knowledge of changes of brain tissue during time and other normal consequences related to craniectomy and surgical trauma is helpful and allows to choose correct treatment in case of complications.

Imaging follow-up should be properly performed not only to find early or later complication but also to recognize possible residual disease, progression or recurrence.

Actually, surgery represents the best way to increase overall survival of low- and high-grade glioma and analysis of imaging could not be performed without a precise knowledge of surgical approach and procedures and their complications [1].

6.2 Surgical Approach

If maximum resection of glioma is considered the best way to increase overall survival, a compromise between tumour removal and neurological risk could be found. Surgical approaches are different: craniotomy, with a bone flap to replace the hole; craniectomy, without a bone flap, burr hole or key hole, a smaller hole related to a minimally invasive procedure.

Burr hole is a small hole created with a drill on the bone calvaria, used for stereotactic biopsies, and provides a way to cut the dura mater envelope. On imaging it appears like a well-rounded hole, with often fluid or fluid-air level inside, sometimes extended in deep dural spaces, with impregnation of margins or fully filled of contrast. In addition to common neurosurgical complications (e.g. bone fracture, bleeding), a specific consequence is the plunge of the drill through the dura mater with the possibility of intracranial haemorrhage (frequently intracerebral hematoma): on T2-weighted imaging, high signal of brain deep to the hole could be seen ("mushroom sign").

Craniotomy is an exposure of intra-cranial content after removal of a bone flap that replaces the hole after the procedure. Normally, in the early post-surgery period, the scalp should be swollen, for the filling of haemorrhage, CSF, air, but it disappears in few weeks and the margin of bone flap became progressively less evident for the reabsorption. A small fluid collection, heterogeneous for different product of haemoglobin, could be seen inner or outer dura mater, hypointense. After surgery, enhancement on T1 image after contrast bolus could be seen in the facial muscles, around the bone flap for granulation tissue. Dura mater progressively acquires impregnation that disappears after a month. Complications of this approach are: tensive pneumoencephalus, deep venous thrombosis, meningitis, extradural abscess, subdural empyema, brain abscess (imaging should evaluate the extension of the process), and osteomyelitis of bone flap that could appear early, after 1–2 weeks, or later, after a month. In this infectious process, bone appears hyperintense in T2-weighted image and presents enhancement. Other insidious complication is CSF leakage, an abnormal drainage of liquor in paranasal sinus, ear or nose, through skull foramen. Haemorrhagic events are not uncommon: hematomas intraparenchymal, extradural, subdural and mixed.

Craniectomy is an exposure of intra-cranial content without the positioning of bone flap. Normally, this procedure is connected to reduce high pressure in bone skull, in condition like intra-cranial hypertension, refractory to medical therapy or subarachnoid bleeding. If bone flap is not replaced, dura mater is closed or a duraplasty were done. Normal sequelae are pseudomeningocele, herniation of sub-arachnoid space through the defect, or meningogaleal complex, a layer composed of dura mater, connective tissue and galea. The most

A. Stecco (✉)
Neuroradiology Unit, AOU "Maggiore della Carità", DIMET, Università del Piemonte Orientale, Novara, Italy
e-mail: alessandro.stecco@uniupo.it

E. Soligo · A. Paschè · A. Carriero
Department of Radiology, AOU "Maggiore della Carità", DIMET, Università del Piemonte Orientale, Novara, Italy

T. Scarabino, S. Pollice (eds.), *Imaging Gliomas After Treatment*, https://doi.org/10.1007/978-3-030-31210-7_6

common complication is extracranial herniation of brain, followed by: subdural or sub-galeal hygroma, a fluid collection that could be placed on the same side of craniectomy or, less frequently, in the opposite side, that disappear after months; external brain tamponade, a sub-galeal fluid collection that compresses brain, a clinical and surgical emergence; "trephine syndrome", a sunken skin flap with a depressed meningogaleal complex or skin flap that depressed the brain; paradoxical herniation, is rare, but due to the defect of passage of CSF.

Surgical approaches for glioma resection are different: total resection, subtotal resection (with residue less than 10% of the original mass) and partial resection (with residue more than 10%) and the knowledge of MRI post-operative changes are important to recognize [2, 3].

6.3 Neuroimaging

MRI of the brain is the key to find a common and dangerous complication: the brain ischemia. Ischemia contributes to reduce survival and degrade quality of life of patients treated for low- and high-grade glioma.

After surgery, on DWI sequence it is possible to see a hyperintensity around the operative cavity. This hyperintensity is not always related to low adc value, and it is due to a different kind of causes.

A new restriction of diffusivity, in the setting of cellular injury, that disappears in following images and hesitates in an encephalomalacia is probably due to a new ischemia. Sometimes this area presents transitory impregnations on contrast image, as found in sub-acute phase of vascular ischemia. Post-operative ischemia reflected the cellular injuries due to direct surgical trauma, devascularization of the tumour and vascular injuries. In all cases, cells develop intracellular oedema with related reduction of extracellular space: these mechanisms reflected restricted diffusion on DWI image. Imagings are often associated with neurological findings, that reduce or disappear in few days [4, 5].

In accordance with recent literature, the cellularity of the glioma reflected the different grade of extracellular diffusivity of water and lower value of adc. Diffusion and the related adc value reflected the grade of glioma: before surgery knowing the cellularity and the probable grade of this tumour is very important. In fact, on post-operative images a new or persistent area of restriction could be suspicious for residual disease and, after time, or recurrence or progression [6].

On post-operative imaging, the residual disease represents an insidious trap. For lower grade of glioma, that not present enhancement, residual cancer could be defined with the comparison of morphologic and signal characteristic between pre- and post-surgery. For glioma with a strong baseline enhancement, that reflected medium and high grade and the anarchic vascularization, recognizing residual cancer after surgery could be not easy. In fact, impregnation around surgical margins could be "reactive", linear and benign, or "residual", nodular, irregular and malign. Linear impregnation is considered as a stripe lining the cavity board reactive to the surgery due to the damage of BEE, inflammation, granulation tissue, "reactive" to the surgery. This develops, according to the more and more recent literature, not only after 72 hours from surgery, but sometimes before, in the first temporal window from 24 to 48 hours. It is fundamental, to plan correct therapy, the recognition of "reactive" impregnation from nodular impregnation, "residual" evaluated as a larger, inhomogeneous, solid micronodular masses around the cavity, due to persistence of neoplasia. "Residual" appears in the first 24 hours, and the correct and appropriate time windows to perform post-operative MRI could be helpful to discriminate it from the other "reactive". This last one could disappear in 6 months or, later, after years: the key to make a correct differential diagnosis is the stability in following images of reactive enhancement against the increasing of residual-nodular, as tumour progression [7–12].

New and functional technique could be helpful to diagnose residual disease, particularly perfusion image, or demonstrate damage on brain matter with tractography that allows to visualize the integrity of the nerve fibers.

References

1. Kessler AT, et al. Brain tumour post-treatment imaging and treatment-related complications. Insights Imaging. 2018;9(6):1057–75.
2. Sinclair AG, et al. Imaging of the post-operative cranium. Radiographics. 2010;30(2):461–82.
3. Sato N, et al. Postoperative changes in the brain: MR imaging findings in patients without neoplasms. Radiology. 1997;204:839–46.
4. Thiepold AL, Luger S, et al. Perioperative cerebral ischemia promote infiltrative recurrence in glioblastoma. Oncotarget. 2015;6(16):14537–44.
5. Bette S, et al. Patterns and time dependence of unspecific enhancement in postoperative magnetic resonance imaging after glioblastoma resection. World Neurosurg. 2016;90:440–7.
6. Smith JS, et al. Serial diffusion-weighted magnetic resonance imaging in cases of glioma: distinguishing tumor recurrence from postresection injury. J Neurosurg. 2005;103:428–38.
7. Matthew M, Grabowski BS, et al. Residual tumor volume versus extent of resection: predictors of survival after surgery for glioblastoma. J Neurosurg. 2014;121:1115–23.
8. LeScher S, et al. Time window for postoperative reactive enhancement after resection of brain tumors: less than 72 hours. Neurosurg Focus. 2014;37(6):E3.
9. Albert FK, et al. Early postoperative magnetic resonance imaging after resection of malignant glioma: objective evaluation of residual tumor and its influence of regrowth and prognosis. Neurosurgery. 1994;34:45–61.
10. Stummer W, et al. Extent of resection and survival in glioblastoma multiforme: identification of and adjustment for bias. Neurosurgery. 2008;62:564–76.
11. Xing Y, et al. Which parameter is more important for the prognosis of new-onset adult glioblastoma: residual tumor volume or extent of resection? World Neurosurg. 2018;116:444–551.
12. Carles M, et al. Early post-operative magnetic resonance imaging in glioblastoma: correlation among radiological findings and overall survival in 60 patients. Eur Radiol. 2015;26:1048–55.

Postradiation Changes in Morphologic MRI

7

Alessandro Stecco, Alessio Paschè, Laura Masini, Marco Krengli, and Alessandro Carriero

7.1 General Findings

The role of radiotherapy (RT) in the treatment of different brain tumors is now widely consolidated. Standard treatment of patients with glioblastoma consists of surgery and postoperative radiotherapy with temozolomide followed by adjuvant temozolomide.

Three-dimensional conformal radiotherapy, Intensity Modulated Radiation Therapy (IMRT) and Volumetric Arc Therapy (VMAT), allows delivery of a high dose of radiation to a target while sparing surrounding organs at risk. Hypofractionated stereotactic radiotherapy might be an option for elderly patients and for recurrence.

Intracranial and regional radiation to the brain often produces a number of significant changes that complicate the assessment of posttreatment outcomes: during follow-up, RT may produce new lesions that can mimic tumor progression or recurrence on imaging.

RT effects can continue in the targeted organ for many months after therapy, at least 3–12 months and in some cases years after the end of treatment; moreover, post-RT alterations are almost always associated with post-chemotherapy and post-surgical changes which strengthen the harmful effect.

Therefore, it is imperative that radiologists have a thorough understanding of the advanced imaging techniques available to view these tumors as well as the possible common treatment-related complications: a wrong interpretation can change the patient's management.

A. Stecco (✉)
Neuroradiology Unit, AOU "Maggiore della Carità", DIMET, Università del Piemonte Orientale, Novara, Italy
e-mail: alessandro.stecco@uniupo.it

A. Paschè · A. Carriero
Department of Radiology, AOU "Maggiore della Carità", DIMET, Università del Piemonte Orientale, Novara, Italy

L. Masini · M. Krengli
Department of Radiation Oncology, AOU "Maggiore della Carità", DIMET, Università del Piemonte Orientale, Novara, Italy

During post-RT follow-up, the development in contrast enhancement or an increase in size of volume of the initial lesion therefore raises the question of whether the disease has progressed despite treatment, or whether temporary irradiation-induced necrosis has developed.

The difficult role of the radiological expert is to attempt to make this differential diagnosis in order to adapt the subsequent treatment plan or to program the radiological monitoring.

7.2 Neuroradiologic Imaging

Regular follow-up treatment is extremely important after RT for a brain tumor. Besides regular physical and neurological exams, the diagnostic option available include as the first option morphologic and functional MR (spectroscopy, perfusion or diffusion) and also computed tomography (CT) and positron emission tomography (PET), which are rarely used in patients with brain tumors, although they may be used to monitor extracranial (outside of the brain) disease.

These studies should first be performed within 24–36 h after surgery to obtain early information useful to minimize doubts in subsequent patient evaluation.

For the study and follow-up of brain tumors, various MR sequences are used, among which the most common present in everyday clinical practice can be cited.

In primary brain neoplasms T2 fluid-attenuated inversion recovery (FLAIR) sequence is often the first choice as it clearly delineates abnormal signal from normal brain parenchyma. In fact, low-grade gliomas rarely exhibit vasogenic edema, and therefore T2 FLAIR imaging can be particularly accurate in delineating tumor extent. T2 FLAIR imaging with high-grade gliomas has its limitations in that it cannot reliably differentiate infiltrating tumor from vasogenic edema as both are hyperintense on T2 FLAIR sequences.

Another important sequence to remember is the T1-weighted contrast-enhanced sequence, because it is easy to perform and accurately depict the margins of most brain metastasis and dural-

T. Scarabino, S. Pollice (eds.), *Imaging Gliomas After Treatment*, https://doi.org/10.1007/978-3-030-31210-7_7

based lesions. T1-weighted contrast-enhanced sequence should be used within the 2 days after surgery in order to assess extent of resection and no later than 72 h after operation. Moreover, increased contrast enhancement detected by MR imaging just after or during treatment can be produced by several causes such as postoperative or postradiotherapy changes, micro-ischemic lesions, and treatment-associated inflammation.

However, in primary brain neoplasms, particularly gliomas, it is not the first choice because these tumors often demonstrate non-enhancing or infiltrative components.

Therefore, advanced imaging techniques are often used to differentiate residual/recurrent tumor from posttreatment changes. The most common advanced imaging techniques are diffusion-weighted imaging (DWI), perfusion-weighted imaging (PWI), and MR spectroscopy.

It is important to remember that by itself none of these techniques has been revealed very specific; however, a thoughtful synthesis using all of them can usually allow the radiologist to correctly separate tumor from posttreatment changes [1, 4].

7.3 Radiation-Related Treatment Effects and MR

Radiation therapy is usually administered 5 days a week (conventional fractionation schedule is 1.8–2 Gy per day) for up to 6–7 weeks until the prescribed dose is reached. In case of stereotactic treatment, 1–5 large fraction doses are delivered to the target. The radiation targets dividing cells directly and indirectly leading to vasodilation, disruption of the blood–brain barrier, and edema. This leads to vascular damage, glial and white matter damage, endocrine disturbance, neural structural fibrosis, effects on fibrinolytic enzyme system and immune mechanism.

The pathophysiology of CNS injury after RT is not unique because there can be multiple variables in its development, including total dose, fraction size, time between fractions, treatment volume, age of the patient, concurrent chemotherapy, and duration of survival.

Three distinct types of radiation injury are recognized and can be identified on the basis of the time of presentation:

- *Acute* (during or shortly after radiation): acute radiation effects can occur during or immediately after the course of radiation. Clinically, acute encephalopathy often manifests as signs of increased intracranial pressure with headache, nausea/vomiting and/or mental status changes. Symptoms are often transient and reversible and can usually be alleviated with corticosteroids. Acute toxicity is thought to be secondary to radiation-induced cytokine release and vasodilation resulting in increased edema and disruption of the blood–brain barrier.

  MR findings in acute radiation injury are usually negative but occasionally can demonstrate peripheral edema to the lesion or diffuse brain swelling (small hyperintense signal changes in T2-weighted imaging and FLAIR sequences in the white matter of both hemispheres).
- *Subacute* (or early-delayed; often within the first 12 weeks after radiation): subacute reaction is due to cell death of myelin producing-oligodendrocytes that follows remyelinization of the brain tissue. It can appear from a few weeks to a few months after radiotherapy and it is defined as treatment-related changes that can often stabilize or diminish over time. It can present as somnolence, fatigue, or worsening of pre-existing neurological focal deficits (such as dysphagia, dysarthria, and intracranial hypertension), although patients may remain asymptomatic. Corticosteroids are sometimes needed to control symptoms. Improvement usually occurs within a few weeks or months, sometimes spontaneously. A specific entity, known as Somnolence Syndrome may also occur in the subacute period and is characterized by fatigue and lethargy, and may or may not be associated with imaging changes. Somnolence Syndrome is thought to be secondary to demyelination and is more frequent in children, particularly when concurrent methotrexate is administered with whole brain radiation.

  MR findings can vary from non-enhancing hyperintensities on T2-weighted imaging and FLAIR sequences of the white matter, representing edema, to new enhancing lesions or enlargement of pre-existing lesions described at first postradiotherapy MR. These findings can mimic recurrence or progression and may have an impact on management, resulting in premature discontinuation of effective adjuvant therapy and inappropriate patient selection for clinical trials on recurrent gliomas.

  It may be appropriate to warn patients that development or recurrence of symptoms in the months after radiation treatment may very well be related to the treatment rather than progression of disease, especially for conditions where radiotherapy is highly successful.
- *Late* (months to years after completion of radiation): late radiation effects are often progressive and irreversible. CNS toxicity is relatively common and after RT for gliomas, white matter changes can occur in up to 50% of patients. This mechanism is probably secondary to cerebral edema, diffuse changes due to wall thickening of the vascular structures, decreasing number of glial-supporting cells, and diffuse demyelinization; these changes may be confused with tumor progression, so that a high-grade glioma may appear similar to radiation white matter changes on MR.

This category includes several entities: vascular lesions (lacunar infarcts, large-vessel occlusion, Moyamoya-like

syndrome, telangiectasias), parenchymal calcifications (mineralizing microangiopathy), radiation-induced tumors (the most common being meningioma), cranial neuropathy (relatively rare, most often related to necrosis of the optic nerve system), leukoencephalopathy syndrome, and radionecrosis.

Moreover, radiation can cause cerebral hemorrhage resulting in the formation of cerebral microbleeds; they contain perivascular hemosiderin that persist for years. Hemosiderin contains iron and therefore MR can show small, round, hypointense lesions on T2∗-weighted images, obtained using gradient echo or susceptibility-weighted sequences.

In case of slowly progressive changes in the radiation field, it may be considered appropriate a conservative follow-up, especially without progressive symptoms or evidence of mass effect. These white matter changes are more often associated with symptoms like amnesic deficit, disorientation, cognitive decline, but can also be asymptomatic.

MR findings in late radiation injury can show extensive confluent T2 and FLAIR hyperintense areas in the periventricular white matter of both hemispheres and cerebral atrophy [2–4].

7.4 Changes After RT

Enhancement on MR can also be caused by many factors from tumor reoccurrence to inflammation (treatment-related), postsurgical changes, ischemia, and postradiation effects.

The major findings that can be observed after radiation are:

- *Pseudoprogression*: when RT is finished, with or without concomitant chemotherapy, patients with brain tumors can present with new lesions or with an increase in contrast-enhancing previous lesions and perilesional edema. Pseudoprogression has been reported to occur predominantly (in almost 60% of cases) in the first 3 months after completing treatment. This phase is reported in 20 to 30% of all cases and is followed by a secondary improvement or stabilization without additional treatment. Patients with methylation of the gene coding for a repair enzyme for chemotherapy-induced lesions (O-6-methylguanine-DNA-methyltransferase, MGMT) develop this reaction more commonly. The reaction is subacute and asymptomatic in most patients (70%). These features (increase or development of contrast enhancement occurring early and decreasing over time) are also seen in radiotherapy without temozolomide while is more common and occurs earlier when temozolomide is used in association. It can constitute an overresponse to effective therapy and is associated with damage to the endothelium, BBB (blood–brain barrier) disruption, and oligodendroglial injury.

  Usually the patient is asymptomatic and this condition manifests itself in MR as a hyperintense image in the FLAIR sequences and as a post-contrastographic impregnation in the T1-weighted sequences. In PWI there is relatively low mean cerebral blood volume compared with true tumor progression, while in DWI and MR spectroscopy there is not a clear indication of a possible tumor progression.
- *Pseudoresponse*: in recent years, anti-VEGF agents have entered the use of clinical practice for high-grade glioma treatment in several trials. This drug can produce in a short time (sometimes hours) a "normalization" of the BBB. On imaging, it can view a reduction in the degree of enhancement by the tumor and a decrease of the surrounding edema on fluid-attenuated inversion recovery sequences (FLAIR). This effect is called "pseudoresponse" because this is due to alterations in vascular permeability instead of tumor response to treatment. So, this radiologic response should be interpreted with caution. It is important to remember that sometimes there may be a rebound later effect with the presence of enhancement and edema.
- *Radionecrosis:* this event has an incidence of 3–24% and often develops 3–12 months after treatment, but can also present up to years later. The radiation, in combination with chemotherapy, increases the risk. Overall, 70% of radionecrosis is stable or improved after time while 30% of radionecrosis is variable on follow-up and can reappear, progress (with re-radiation), or have new distant lesions. It is characterized histopathologically by fibrinoid necrosis of blood vessel walls, with adjacent perivascular parenchymal coagulative necrosis. Collections of abnormally dilated and thin-walled telangiectasias can be also observed. Hyalinization caused vessel wall thickening and is a late finding. Focal and diffuse demyelination constitutes the white matter changes observed.

  Radionecrosis appears as a ring-enhancing lesion with characteristic stellate margins and surrounding vasogenic edema. It usually occurs at the site of maximum RT dose in and around the tumor bed and within the margins of the irradiation high-dose volume. The pattern of enhancement has been described as "Swiss cheese" or "soap bubble" appearance.

  The "soap bubble" pattern results from diffuse necrosis affecting the white matter and adjacent cortex, while the "Swiss cheese" pattern is typically more diffuse and larger in area.

  Perfusion, MR spectroscopy, diffusion, and diffusion tensor imaging are used to distinguish radiation necrosis from recurrence. Unlike tumor, the ring-enhancing lesions of radiation necrosis are hypoperfused with presence of

lipid–lactate complexes and decrease in other metabolites including choline on MR spectroscopy. Apparent diffusion coefficient (ADC) and fractional anisotropy (FA) values in radiation necrosis are higher, as compared to tumor recurrence. The role of advanced MRI techniques in differentiating tumor from treatment necrosis is very important. However, often, recurrent tumor and radiation necrosis co-exist.

It can be challenging to differentiate between radiation necrosis versus re-occurrence of the tumor. Similarities include: contrast enhancement, mass effect, and vasogenic edema. However, tumor, not radiation necrosis, has increased relative cerebral blood volume (rCBV). Advanced imaging of radionecrosis demonstrates low rCBV, no restricted diffusion, and low choline peak on MR spectroscopy. Radionecrosis tends to be stable or improve over time. Also, if enhancing lesions develop at a distance away from the primary tumor, radiation necrosis should first be suspected. Additionally, combination of corpus callosum involvement and multiple enhancing lesions crossing the midline and sub-ependymal spread favors tumor progression.

Clinically, symptoms are those produced by an expansive lesion. In addition, it may lead to focal neurologic deficits and intracranial hypertension. Treatment involves steroid therapy or surgical resection.

- *Leukoencephalopathy*: this condition often occurs months to years after treatment. The reported prevalence ranges between 38 and 100% of patients receiving RT. It is strongly related to the volume of brain irradiated, the radiation dose, the interval between irradiation and imaging, concomitant medical diseases predisposing to vascular injury, age and concurrent chemotherapy.

This can be accompanied by chronic mental status impairment with progressive cognitive decline (memory disturbance, mental slowing), personality changes.

MR findings in FLAIR and T2-weighted imaging include diffuse, symmetric hyperintense foci in the periventricular white matter near the frontal or occipital horns, which can lead to a confluent pattern extending from the ventricles to the corticomedullary junction, with no enhancement or significant mass effect (undifferentiable from the deep white matter changes seen in normal older people and patients with risk factors for cerebral vascular disease).

Additionally, cerebral atrophy with hydrocephalus may be seen.

In some cases, extensive diffuse white matter injury can lead to a disseminated necrotizing form of leukoencephalopathy, due to the combined effects of chemotherapy and RT.

MR finding is similar to leukoencephalopathy, with petechial or ring-shaped hemorrhages and calcification deposits along with areas of contrast enhancement in the white matter at variable distances from the primary tumor (with a predilection for periventricular and, less commonly, cortical involvement). Enhancement patterns can be nodular, linear or curvilinear in varying sizes and can be single or multiple, mimicking tumor progression.

Leukoencephalopathy and disseminated necrotizing leukoencephalopathy may occur together; alternatively, one may follow the other. These lesions do not warrant biopsy if they remain stable or regress in size. However, progression to RN should be suspected if the lesions increase in size or are accompanied by edema and mass effect. For some authors, follow-up should also be recommended if a peripheral restriction of water diffusion is found on DWI, as it may be indicative of a trend toward RN.

Other possible findings can be vascular changes, such as capillary telangiectasia and cavernous malformation, or radio-induced tumor.

- Capillary telangiectasias are thin-walled capillaries with intervening normal brain parenchyma and occur 3–9 months after irradiation.
- Cavernous malformations develop years later RT and not contain the intervening brain parenchyma. On MR imaging, there may be core heterogeneous signal intensity with dark peripheral hemosiderin rim and minimal surrounding edema (“popcorn” or “berry” appearance).
- Meningioma is the most common central nervous system neoplasm caused by ionizing radiation, usually after 5–10 years follow-up. The risk of radiation-induced secondary cancer after radiotherapy is estimated of less than 1%. Risk increases with increasing doses but also low doses can increase the risk of inducing meningioma. Higher proportions of multiple meningiomas and atypical or anaplastic meningiomas are observed in patients who have received RT compared to those patients who have not [2–4].

7.5 Conclusion

In conclusion, radiation injuries to the central nervous system can occur in few weeks but often have additional delayed effects months to years later, including radionecrosis, leukoencephalopathy, cerebral atrophy, induction of neoplasm, and vasculopathy.

By understanding the typical posttreatment responses seen in MR imaging, appropriate clinical decisions can be made.

References

1. Kessler A, Alok AB. Brain tumour post-treatment imaging and treatment-related complications. Insights Imaging. 2018;9:1057–75.
2. Zikou A, Sioka C, et al. Radiation necrosis, pseudoprogression, pseudoresponse, and tumor recurrence: imaging challenges for the evaluation of treated gliomas. Contrast Media Mol Imaging. 2018;2018:6828396.
3. Raimbault A, Cazals X, et al. Radionecrosis of malignant glioma and cerebral metastasis: a diagnostic challenge in MRI. Diagn Interv Imaging. 2014;95:985–1000.
4. Shukla G, Alexander SG, et al. Advanced magnetic resonance imaging in glioblastoma: a review. Chin Clin Oncol. 2017;6(4):40.

8 Postchemotherapy Morphological MR Imaging

Teresa Popolizio, Roberto Izzo,
Rosario Francesco Balzano, and Anna Maria Pennelli

8.1 General Findings

Neurotoxicity of drugs is a pathological entity in growth for the wider use of specific antiblastic therapies and also for better clinical and neuroradiological performance that allow early and specific diagnosis.

Chemotherapy often carried with combined drugs may be neurotoxic especially if associated with RT that therefore should be used only after chemotherapy. It has been shown that radio-induced endothelium effects can promote BBB alteration and allow passage and retention of potentially damaging molecules to brain structures. Polychemotherapy treatment in combination with RT results in toxicity, and it is very difficult, impossible in many cases, to establish accurately the damage being exercised by each treatment, radiologically similar in most cases. There are, however, typical radio and/or chemo-induced effect which must be recognized not only for evaluating the effectiveness of treatment but also to apply an effective and timely treatment.

8.2 Neuroradiologic Imaging

While radiotherapy and neurosurgical procedures modify morphologically target tissue, drug treatments act "at a distance" and can cause organ damage and toxicity also in tissues not directly targeted by treatment.

Therefore, in patients undergoing CT, brain MRI should be included in follow-up. Morphological MRI should be performed before the beginning of neurotoxic therapy, to represent for neuro-radiologist a reference for follow-up and to define and clarify doubts and problems on findings observed. Exact knowledge of pre-drug treatment imaging is even more important in follow-up of the neoplastic brain primarily surgically treated. In these cases, MRI with gadolinium performed within 2–3 days after surgery is the neuroradiological reference.

Combined treatment of Temozolomide (TMZ) and RT in patients with glioblastoma must be carefully evaluated. In these cases, combination therapy may allow appearance in MRI imaging, of progressive evolving lesions with CE areoles immediately after the end of treatment (usually at 30 days after treatment) which persist up to 3 months and sometimes longer. This entity, known as "pseudo-progressive", is almost indistinguishable from the real progression of disease and has an incidence of approximately 22–31% of cases [1–3]. Therefore, caution is recommended in the assessment of neuroradiological examinations carried within a month after the end of combination therapy.

Pseudo-progression is caused by the consumption of many tumor and endothelial cells, resulting in necrosis of neoplastic lesion and BBB damage increase. This finding is more frequent and early with combination treatment compared to RT alone. These lesions decrease in size over time or become stable without additional treatments. Often they remain clinically asymptomatic and sometimes can explain clinical deterioration following completion of chemotherapy. Simple MRI follow-up may easily allow to differentiate pseudo-progression from a real progression through real-time dynamics evaluation. Moreover, hypothesis of a pseudo-progression rather than a true progression, clinically asymptomatic, especially in the first 3 months after the end of chemotherapy, should recommend to continue adjuvant therapy with Temozolomide.

This phenomenon, presumably related to radio-necrosis, is related with methylation of MGMT gene coding for DNA 06-methylguanine methyltransferase enzyme. This enzyme is able to repair the alkylating induced damage thus protecting tumor cell. Conversely, if MGTM is methylated (inactive), chemotherapy appears to be effective.

On current scientific knowledge, determination of MGMT gene methylation status should be performed in all clinical trials on malignant gliomas involving the use of

T. Popolizio (✉) · R. Izzo · A. M. Pennelli
Department of Neuroradiology, Fondazione IRCCS "Casa Sollievo della Sofferenza", San Giovanni Rotondo, FG, Italy

R. F. Balzano
Department of Radiology, University of Foggia, Foggia, FG, Italy

T. Scarabino, S. Pollice (eds.), *Imaging Gliomas After Treatment*, https://doi.org/10.1007/978-3-030-31210-7_8

alkylating drugs. Outside clinical trials, in daily practice, state of methylation of MGMT gene is not currently validated as a decision parameter in the choice of diagnostic and treatment [4, 5].

Assessment of chemotherapy response should consider radiological findings and clinical condition, type of treatment and any use of steroids [6, 7].

Based on a careful clinical, anamnestic and neuroradiological analysis, four assumptions may be expressed:

- Complete remission: characterized by CE disappearance in the tumor on consecutive CT scans or MRI performed after at least 4 weeks in absence of steroid therapy and clinically stable or improved.
- Partial remission: reduction of at least 50% of CE tumor area measured by the product of the two largest perpendicular diameters, in presence of stable or reduced steroid therapy and clinically stable or improved.
- Progression of disease: increase of 25% of CE tumor area or appearance of new tumor in presence of stable or increased steroid therapy and clinical deteriorated.
- Stable disease: characterized by the stability of neuroradiological status compared to reference examination performed at least after 2 months after starting treatment.

Moreover, not always there is direct correspondence between MRI findings and clinical condition and in some cases it is not possible to discriminate tumor recurrence and radio-induced damage. Therefore, it is very important to correlate neuroimaging data with clinical condition, time between the treatment and characteristics of therapy.

Morphological MRI and functional studies (spectroscopy, DWI and PWI) are taking a leading role in the evaluation of neuroradiological findings such as pseudo-progression and in the assessment of response of anti-angiogenic therapy which reduces the amount of CE. In this regard, spectroscopy is considered useful to measure the true extension of neoplastic tissue, to evaluate response to chemotherapy, for the early detection of recurrence and in differential diagnosis between radio-necrosis and progression\recurrence.

Neurotoxic effects caused by drugs used in extracranial neoplastic diseases or in lymphoproliferative, hematologic and not tumoral disorders constitute a different chapter.

In this regard are important methotrexate, used in the treatment of leukemia, L-Asparagine used in acute lymphocytic leukemia, 5-fluoro-uracil, cyclosporin A, vincristine, capecitabine, cytarabine, cisplatin, steroids and other drugs like morphine and amphetamines.

Combination of several drugs can strengthen toxic effects of each, such as combination of methotrexate and cisplatin. Neurotoxic effect is further amplified by superselective intra-arterial or intrathecal administration (e.g., methotrexate in chemical meningitis) of some drugs, used in the treatment of primary brain tumors or lymphoproliferative disorders. Neurotoxic effect is also favored by other predisposing factors such as cerebrovascular disease, advanced age; in these cases neurotoxicity can be expressed with ischemic stroke, hemorrhage or acute edema often reversible. Alterations of peripheral blood counts (patients with leukemia or lymphoma) can promote a synergistic negative effect and induce intracranial hemorrhage. Neurotoxic drug effects (isolated or associated with radiotherapy) according to a temporal classification are distinguished in:

1. Acute during treatment or within a maximum of 50 days from the end of therapy,
2. Sub-acute or delayed after treatment and within 3 months after the end of therapy,
3. Late that arise even after several years.

Acute and sub-acute forms may be reversible while later remaining in scar.

Acute effects include:

- Stroke-like forms. Methotrexate is the more involved drug. Probably, cause of brain damage is homocysteine blood concentration increase that induces direct detrimental action to cerebrovascular endothelium. Symptoms are related to cerebral ictus and prognosis depends from the timeliness of treatment.
- Acute thrombosis of dural sinuses. L-asparaginase is the more involved drug. Etiology depends from a direct action on coagulation. Symptoms are headache, convulsions, and coma. Prognosis is related to the timeliness of treatment.
- PRES (Posterior Reversible Encephalopathy Syndrome). This syndrome, first recognized in association with eclampsia, with cyclosporine therapy after transplantation and severe hypertension, is a complex drug-induced neurotoxicity, with well-defined clinical and neuroradiological findings. It also can promote myocardial ischemia and hemorrhage. Most important feature of the syndrome is represented by bilateral and symmetrical edema that involves mainly parietal and occipital lobes, followed by frontal lobes, temporo-occipital junction, and inferior cerebellum. There are two pathogenetic mechanism describing this syndrome: both supporting vasogenic hypothesis of edema: the first, most reliable, consider hypoperfusion the cause of disease, determined by alternation of vasospasm and vasodilatation, as documented by MR angiography in eclampsia. The second theory supports the etiopathogenetic role of hyperperfusion secondary to dysregulation of blood pressure and capillary vasodilatation resulting in malfunction of the BBB and extravasation in interstitium of macromolecules and fluid.

Vasogenic edema, related to endothelial dysregulation, was also evidenced as a result of immunosuppressive treatment and drug-induced hypomagnesemia. MR imaging typically shows focal regions of bilateral and symmetrical edema with signal hyperintensity in long TR sequences. These findings have no correspondence in DWI imaging, except in untreated cases in which hyperintensity signal areas appear for the evolution in cytotoxic edema, sometimes irreversible. In this sense, DWI can be considered as a means for prognostic evaluation.

Sub-acute effects include the DLEPs (Leuco-encephalopathy Delayed Presentation with stroke-like syndrome.

This is a rare pathological entity caused by methotrexate with intra-thecal administration. Etiology is based on direct endothelial damage. Symptoms mimic a stroke, may be fluctuating with alternating involvement of both hemispheres. Prognosis is related to the timeliness of treatment. MRI imaging is characterized by a T2-weighted focal hyperintensity signal available especially in peri-ventricular areas (semi-oval center, corona radiata, internal capsule) that do not show a clear correspondence in DWI imaging, while they are markedly hypointense on ADC map, with rapid normalization of the same. Increased signal in T2-weighted without correspondence in DWI could be due to accumulation of water between myelin strips, a condition readily reversible if treated promptly. There is no CE.

Late effects include leukoencephalopathy. It is usually persistent (may be transient in children), and is drug- and dose-dependent. It is characterized by axonal and myelin loss, pallor, rarefaction, spongiosis, and gliosis of white matter probably secondary to chronic ischemia caused by an extended radio-endothelial damage. Preferred site is periventricular white matter and semi-oval centers, even if compromise of all the deep and subcortical white matter is not rare. Axonal loss would be responsible for serious and irreversible clinical aspects, characterized by progressive deterioration and worsening of executive functions that may result in dementia.

Initial symptoms are often misunderstood or overlooked, especially because it affect patients clinically very compromised by the underlying disease. Generally, confusion and short-term memory loss can be seen initially; more late, urinary incontinence, dysphasia, aphasia, and visual disturbances may be associated. In the most severe forms, dementia for associative pathways dysfunction can be established.

On T2-FLAIR images, signal hyperintensity appears in subcortical white matter and especially in deep periventricular and retrotrigonal areas. These findings are not evident on DWI. Generally there is no CE, except in rare cases of pointly impregnation, usually reversible.

References

1. Brandes AA, Franceschi E, Tosoni A, et al. MGMT promoter methylation status can predict the incidence and out come of pseudoprogression after concomitant radiochemiotherapy in newly diagnosed glioblastoma patients. J Clin Oncol. 2008;26(13):2192–7.
2. Brandsma D, Stalpers L, Taal, et al. Clinical features, mechanisms, and management of pseudoprogression in malignant gliomas. Lancet Oncol. 2008;9(5):453–61.
3. Sanghera P, Perry J, Sahgal A, et al. Pseudoprogression following chemoradiotherapy for glioblastoma multiforme. Can J Neurol Sci. 2010;37:36–42.
4. Stupp R, Hegi M. Methylguanine methyltransferase testing in glioblastoma: when and how ? J Clin Oncol. 2007;25:1459–60.
5. Forster VJ, McDonnell A, Theobald R, et al. Effect of methotrexate/vitamin B12 on DNA methylation as a potential factor in leukemia treatment-related neurotoxicity. Epigenomics. 2017;9(9):1205–18.
6. Macdonald DR, Cascino TL, Schold SC, et al. Response criteria for phase II studies of supratentorial malignant glioma. J Clin Oncol. 1990;8:1277–80.
7. Magge RS, DeAngelis LM. The double-edged sword: neurotoxicity of chemotherapy. Blood Rev. 2015;29(2):93–100.

PET Imaging

9

Pasquale Di Fazio

9.1 General Findings

The diagnostic capabilities are explained both by methods using gamma emitters radiopharmaceuticals (SPET-TC) and by methods using positronic radiopharmaceuticals (PET-CT and PET-NMR). However, the role of standard in the diagnosis of gliomas remains a specific prerogative of radiological diagnostic techniques (CT and MRI).

9.2 Diagnostics with Gamma Emitters Radiopharmaceuticals

9.2.1 Brain SPET with 201tallio and 99mTc Sestamibi

This is a simple method that can be performed in any nuclear medicine center and has played an important role in the diagnosis of brain tumors in the historical phase prior to the development and spread of the PET-TC method.

The 201talium SPET is performed early after radionuclide administration (within 20') due to the rapid washout of the 201talium from the brain neoplasm.

In the absence of brain neoplastic lesions, the radionuclide does not show focal accumulation lesions to the tomographic investigation since it is not able to cross the blood–brain barrier if it is intact.

The intra-cerebral accumulation of the 201 thallium is allowed by the non-integrity of the blood–brain barrier and the uptake of the radionuclide by the neoplastic cells of the gliomas is favored by the sodium-potassium pump (ATPase dependent) exalted in vital tumor cells. There is a correlation between the intensity of radionuclide accumulation and the degree of malignancy of the lesion, although benign lesions such as meningiomas and pituitary adenomas may present a significant accumulation of the radiotracer [1].

In the diagnosis phase, the qualitative visualization of the hyper-accumulation in the presumed neoplastic site is also associated with a semi-quantitative analysis linked to the counting ratio between the accumulation detected and normal brain tissue. For values of this ratio higher than 2.5 the presence of a malignant neoplastic lesion is assumed, while for values below 1.5 it is hypothesized that the lesion is not malignant.

These numerical indicators present good levels of diagnostic accuracy for newly diagnosed untreated lesions, but are not reliable when evaluating the treated tumors even if a numerical value of the ratio that is sufficiently higher than 2.5 indicates the presence of tumor recurrence.

A similar diagnostic contribution can be obtained using the 99mTc-SESTAMIBI and its intracellular accumulation in the mitochondrial area is an indicator of the viability of the neoplastic cell. The numerical indexes of 99mTc-SESTAMIBI uptake as for the 201Tallium are correlated to the degree of malignancy of the brain neoplastic cell.

The 99mTc-SESTAMIBI is a good indicator of the response to radiation treatment and chemotherapy, certifying the damage of the oxidative capacity of neoplastic cells in the event of a decrease in the radiopharmaceutical uptake intensity.

9.3 Diagnostics with Positronic Radiopharmaceuticals

9.3.1 Brain PET/TC with 18F-FDG

The radiopharmaceutical mainly used for PET diagnosis of neoplasms is 18F-FDG.

In general, neoplastic cells capture 18F-FDG thanks to: increase metabolism, aerobic and anaerobic glucose metabolism, number of glycolytic enzymes, and cellular glucose transport. The uptake of the positronic radiopharmaceutical is proportional to the degree of non-differentiation of the neoplasm.

P. Di Fazio (✉)
Department of Nuclear Medicine, "Dimiccoli" Hospital—ASL BT, Barletta, Italy

T. Scarabino, S. Pollice (eds.), *Imaging Gliomas After Treatment*, https://doi.org/10.1007/978-3-030-31210-7_9

Despite these generic characteristics of the metabolic function of neoplasms, 18F-FDG is not an ideal radiopharmaceutical in the diagnosis of brain tumors especially if they are small or with a low degree of malignancy. The intensity of uptake of this type of neoplasms of the CNS does not show a significant difference compared to the intensity of uptake of the gray matter which physiologically possesses a high uptake [2].

The glucose loading appears to improve PET detection of lesions thanks to a more significant suppression of FDG uptake in normal brain tissue compared to neoplastic lesions linked to the lack of normal physiological control of glucose metabolism in neoplastic lesions.

A further aid to favor the FDG uptake by neoplastic cells is found in delaying the time of the pet scan compared to the administration of the radiopharmaceutical allowing a greater visibility of the lesion.

The coregistration with MR or CT images appears to be of great help in detecting brain neoplastic lesions.

Despite the limitations described, there are low-grade cerebral neoplasms such as pilocystic astrocytoma, ganglioglioma, choroid plexus papilloma, pleomorphic xanthoastrocytoma, and pituitary adenoma which often show a high 18F-FDG uptake.

Meningiomas show a variable intensity of 18F-FDG uptake linked to the likelihood of relapse whereas brain metastases can generally show lower accumulation intensity than normal cortex.

FDG imaging has a role in prognosis, since the lower or greater intensity of uptake compared to the physiological background correlates respectively with greater survival (75% at 1 year) or lesser survival (25% at 1 year).

Increased uptake of 18F-FDG in lesions with high metabolism makes it useful as a guide for stereotactic biopsy. Furthermore, PET imaging provides additional information useful for the planning of radiotherapy treatment of brain neoplastic lesion [2].

9.3.2 Other Positronic Radiopharmaceuticals Used for CNS Neoplasms Imaging

In addition to the 18F-FDG, there are other positronic radiopharmaceuticals that allow diagnostic imaging of CNS neoplasms with greater accuracy.

These include positronic radionuclide-labeled amino acids that have a better sensitivity than the 18F-FDG in the diagnosis of primary brain tumors thanks to the low uptake in normal brain tissue and the better uptake difference between the tumor and the adjacent normal parenchyma.

Amino acids are transported into cells thanks to processes mediated by increased active transfer in tumor cells at all stages of the cell cycle [2].

The uptake of amino acids by gliomas is independent of the rupture of the blood–brain barrier, and these types of tracers are useful in monitoring chemotherapy especially in the early stages with 80% higher sensitivity when they are coregistrated with MR images.

9.4 11C-Methylmethionine (11C-MET)

The uptake of 11C-methylmethionine (11C-MET) correlates with protein synthesis and cell proliferation, and is increased in 80–90% of malignant brain tumors thanks to the physiological need to increase the external requirement of methionine.

The uptake of the tracer appears to correlate with the histological grade of the tumor, with greater activity in higher-grade lesions (grade III and IV), compared to a low intensity of uptake in grade II tumors.

Since the cerebral amino acid metabolism is physiologically low in the brain, intralesional accumulation is characterized by a significant increase in the lesion/background ratio.

The sensitivity for high-grade lesions is 97% and the pet with methionine has sensitivity values of 76% and specificity of 87% in differentiating neoplastic from non-neoplastic lesions.

The pet with methionine has prognostic significance: the increase in the intensity of uptake of the neoplastic lesion over time certifies the progression of neoplastic aggression since the persistence or representation of new areas of methionine-labeled uptake after radiotherapy appears useful in differentiating recurrences from radionecrosis, with a sensitivity of 78–79% and specificity between 75% and 100% (higher accuracy than the 18F-FDG) [3].

False positivity can be found in case of brain abscesses and in areas of inflammation, while a serious impediment to the use of the method is due to the low half-life of the positronic radionuclide (11C): the methionine pet can be performed in pet centers with a cyclotron on site (limit not present when using the 18F-FDG).

9.5 18F-Fluorothymidine (18F-FLT)

18F-FLT (fluorothymidine) measures the activity of thymidine kinase-1 metabolic indicator of tumor cell proliferation and uptake by neoplastic cells is related to the proliferative marker Ki-67 [3].

The 18F-FLT uptake is not present in normal brain cells since it does not cross the blood–brain barrier, while the rupture of the blood–brain barrier can lead to an increase in activity in the absence of cell proliferation.

Uptake in CNS neoplasms is rapid with peak activity at 5–10 min after injection with activity that remains stable up to 75 min allowing PET imaging.

As for the 18F-FDG the uptake of 18F-FLT correlates with the degree of malignancy of the tumor, with high uptake in grade III and IV lesions compared to the lower detectable uptake in lower grade lesions and the MAX SUV correlates with the prognosis of neoplastic disease also in terms of survival.

Compared to 11C-methylmethionine, 18F-FLT has lower sensitivity values (78 vs. 91%).

Interesting is the ability of imaging with 18F-FLT to identify patients with greater possibility of response to bevacizumab therapy and in this sense a variation of the SUV of at least 25% indicates a response to therapy.

9.6 18F-Fluoroethyl-L-Thyrosin (18F-FET)

18F-fluoroethyl-L-tyrosine (18F-FET) is an artificial amino acid metabolic indicator of protein synthesis of neoplastic cells and its uptake is independent of the permeability of the blood–brain barrier. The uptake is possible thanks to the L-type amino acid transporter, but it is not incorporated into the proteins (unlike the natural amino acids such as 11C-methyl methionine) [4].

This positronic radiopharmaceutical is able to identify both low- and high-grade gliomas. However, other authors indicate that radiopharmaceutical uptake is higher in high-grade lesions. Dynamic analysis using activity/time curves helps to differentiate low-grade and high-grade tumors and also has prognostic implications. A faster time to peak activity (within the first 12.5–20 min) followed by a decrease over time is associated with high-grade glioma with a worse prognosis. Activity/time curves that increase without an identifiable peak are typical of low-grade gliomas.

In a meta-analysis, for the diagnosis of primary brain tumor, PET with 18F-FET has a sensitivity of 82% and a specificity of 76%.

In low-grade gliomas (grade II), between 66% and 82% of patients will demonstrate an increase in tracer uptake compared to normal brain tissue. However, about 30% of low-grade gliomas and 5% of high-grade gliomas do not demonstrate an increase in the absorption of 18F-FETs and 65% of these lesions will become positive, suggesting that gliomas change their metabolism in time.

Pre-treatment baseline 18F-FET imaging may be useful for tumor diagnosis, indicating the anatomical site where the guided biopsy is to be performed and contributing to radiotherapy planning. Furthermore, the method is useful for evaluating the tumor response to radiotherapy or chemotherapy.

The uptake of this radiopharmaceutical correlates with the prognosis.

The most favorable prognosis is associated with the low uptake of 18F-FET.

However, other authors suggest that the low uptake of the radiopharmaceutical in astrocytomas with a low degree of malignancy in the diagnosis phase does not definitively indicate an indolent course of disease.

Other studies have shown that 18F-FET uptake after therapy is more predictive of survival than MRI results.

9.7 18F-FDOPA

18F-FDOPA is an agent normally used for imaging neuroendocrine tumors, however, CNS neoplasms also show uptake. The uptake mechanism is not known, but it is probably mediated by a specific amino acid transport system, in the absence of rupture of the blood–brain barrier.

Radiopharmaceutical uptake appears to be similar for both low-grade and high-grade CNS lesions while tracer wash out is faster in high-grade tumors than low-grade lesions.

The sensitivity is 96%, the specificity 43%, with an accuracy of 83%.

An advantage of this radiopharmaceutical is the early time of peak uptake by the lesion within 10–30 min after injection, with early image acquisition.

In patients with suspected tumor recurrence, the results of the 18F-FDOPA exam can lead to changes in patient management in 41% of cases [5].

9.8 18F-Fluoromisonidazole (18F-FMISO)

18F-fluoromisonidazole (18F-FMISO) is trapped exclusively in hypoxic but viable neoplastic cells and is consequently used for the evaluation of tissue hypoxia which, if present, characterizes lesions more resistant to radiotherapy and chemotherapy.

18F-FMISO crosses the blood–brain barrier and is rapidly distributed in the tissues independently of the perfusion and with a capture ratio higher than 1.2 there is the identification of hypoxic tissue.

Increased uptake of 18F-FMISO is generally observed in high-grade gliomas compared to low-grade lesions, and increased uptake of this positronic radiopharmaceutical is associated with a decrease in response to therapy and a worse prognosis [6].

9.9 Recurrent Brain Tumor Versus Radionecrosis

Generally, brain tumor therapy is surgical resection of the neoplastic lesion, followed by radiotherapy treatment with or without chemotherapy.

Local radiotherapy or stereotactic radiosurgery is used for the treatment of solitary lesions, while multiple or metastatic lesions are treated with external radiant treatment.

Radiological imaging does not help in the differential diagnosis between disease recurrence and radionecrotic outcomes that are usually observed 2–32 months after radiotherapy.

PET studies with 18F-FDG showed that neoplastic recurrence is evidenced by the representation of areas with increased metabolism (accumulation), while necrotic outcomes do not show detectable metabolic activity.

False negatives with 18F-FDG can occur when the neoplastic lesion is small (partial volume effect) or in recurrences of low-grade tumors (well-differentiated) due to their intrinsically lower metabolic activity.

False-positive scans can be caused by radiation injury, which by activating the repair mechanisms can induce an increase in glucose metabolism.

Post-radiation treatment PET imaging should not be performed until 6 weeks after radiotherapy and no earlier than 3 months after surgery.

PET with 18F-FDG has a sensitivity of 73–86% and a specificity of 40–94% in recurrent tumor differentiation from a brain radiation injury and is clearly superior to 99mTc-SESTAMIBI for the differentiation of recurrent neoplasia from radionecrosis.

18F-FET is a useful positronic radiopharmaceutical to distinguish radionecrosis from tumor recurrence since macrophages commonly present in post-therapy reactions do not take the tracer.

18F-FDOPA is useful for differentiating tumor recurrence from radionecrosis with a sensitivity of 81%, a specificity of 84%, and a diagnostic accuracy of 83%. The uptake of 18F-FDOPA correlates with tumor progression and certifies a worse prognosis. The lesion with low uptake of fluorodopa has a mean time to progression that is 4.6 times longer than those with high uptake [7].

9.10 Metabolic Radiotherapy of GLIOMI

Conventional radiotherapy for the treatment of malignant brain tumors has the undesirable effect of excessive radiation damage to normal CNS tissues.

The medical-nuclear therapeutic applications tend to produce a targeted therapy based on the principle that the radionuclide, which must ideally irradiate neoplastic cells in the most specific way, is transported by a molecular carrier which, thanks to the metabolic or immunological characteristics, guarantees this specificity with respect to brain neoplasia, trying to save healthy brain tissue as much as possible.

In this sense the ideal radionuclide for this selective metabolic radiotherapy must have the ability to have the maximum radiant capacity using low path radioactive emissions.

The two most commonly used radionuclides in metabolic radiotherapy of brain tumors are 131 Iodine and 90 Yttrium, beta particle emitters capable of depositing 95% of their energy in a space between 0.922 and 5.94 mm, respectively.

The use of these radionuclides and alpha emitters allows the targeted irradiation of brain tissue portions adjacent to the resection cavity of the brain tumor, where the presence of morphologically undetectable malignant cellularity can be the cause of glioma recurrence.

In particular, alpha emitters massively affect neoplastic cells present in the minimal residual disease, sparing the normal tissues of the CNS.

The radionuclide-carrying molecule for this type of targeted radiotherapy is almost exclusively a monoclonal antibody specific for the epidermal growth factor receptor and for the neuronal cell adhesion molecule (NCAM).

The vast majority of research studies for the targeted treatment of brain tumors have used radiolabelled antibodies reactive with the tenacine molecule.

The direct link between antibody and radionuclide is limited in its real therapeutic efficacy, due to the large macromolecular dimensions that involve a slow diffusion through the tissues, breaking down the radiating power on neoplastic cells distant from the injection site.

To overcome this limitation, the pretargeting method is used by first administering the antibody, followed after an appropriate time interval by the injection of a low molecular weight radiolabelled transporter.

This radiotherapy model plans to exploit the extraordinarily high affinity of avidin for biotin.

Proceed with a 3-phase therapeutic treatment:

- Phase 1: administration of biotinylated complex (biotin).

  After 24 hours

- Phase 2: administration of avidin.

  After 18 hours
- Phase 3: biotin labeled with 90Ittrio.

In the study by Paganelli (2001) on the 3-step scheme, the administration of the substances involves the use of a catheter inserted in the surgical resection cavity. Sixteen patients with glioblastoma and 8 with anaplastic astrocytoma treated with two cycles of metabolic radiotherapy administered at a distance of 8–10 weeks were studied. Median survival was 19 months for glioblastoma and 11.5 months for patients with anaplastic astrocytoma.

Later, Grana studied newly diagnosed patients, 17 grade III and 20 gliomas with glioblastoma, after surgery and external radiation treatment.

Nineteen of the 37 patients received the three reagents in the sequence described above, while the remaining 18 patients played the role of control audience. Unlike Paganelli's clinical study, all the reagents were administered

intravenously rather than directly into the surgical resection cavity. Estimated survival for patients with grade IV glioma was 8 months in the control group ($n = 12$) and 33.5 months in the treated group ($n = 8$).

The results obtained with this pretargeting protocol are highly encouraging, because a significant prolongation of survival could be obtained even when the radiopharmaceutical is administered intravenously [8].

References

1. Abdel-Dayem HM, et al. Role of Tl-201 chloride and Tc-99m-sestamibi in tumor imaging. Nucl Med Annual. 1994:181–234.
2. Chen W. Clinical applications of PET in brain tumors. J Nucl Med. 2007;48:1468–81.
3. Singhal T, et al. ^{11}C-methionine PET for grading and prognostication in gliomas: a comparison study with ^{18}F-FDG PET and contrast enhanced MRI. Nucl Med. 2012;53:1709–15.
4. Unet V, et al. Peformance of ^{18}F-fluoro-ethyl-tyrosine (^{18}F-FET) PET for the differential diagnosis of primary brain tumor: a systematic review and metaanalysis. J Nucl Med. 2012;53:207–14.
5. Walter F, et al. Impact of 3,4-Dihydroxy-6-18F-Fluoro-L-phenylalanine PET/CT on managing patients with brain tumors: the referring Physician's perspective. J Nucl Med. 2012;53:393–8.
6. Cher LM, et al. Correlation of hypoxic cell fraction and angiogenesis with glucose metabolic rate in gliomas using ^{18}F-fluoromisonidazole, ^{18}F-FDG PET, and immunohistochemical studies. J Nucl Med. 2006;47:410–8.
7. Langleben DD, Segall GM. PET in differentiation of recurrent brain tumor from radiation injury. J Nucl Med. 2001;41:1861–7.
8. Paganelli G, et al. Antibody-guided three-step therapy for high grade glioma with yttrium-90 biotin. Eur J Nucl Med. 1999;26(4):348–35.

Advanced MR Imaging

10

Teresa Popolizio, Roberto Izzo,
Rosario Francesco Balzano, and Daniela Grasso

10.1 General Findings

MRI basal study, consisting in acquisition of morphological sequences without and with contrast agent, can be completed with new advanced MRI techniques (spectroscopy, diffusion, and perfusion), useful especially in cases of diagnostic doubt. These techniques are usually not used in the evaluation of normal and pathological sequelae after treatment, well documented with MR morphological imaging, but are essential, especially when combined, in treatment response assessment. Their use is often essential in differential diagnosis between scar vs. residual, stability versus progression/recurrence, recurrence vs. radionecrosis.

10.2 Role of Spectroscopy

MR spectroscopy has higher sensitivity compared to conventional MRI in detecting changes of common metabolites in absence of radiologically visible morphological changes [1].

In literature there is extensive documentation on its usefulness in diagnosis and post-treatment follow-up in a wide variety of CNS tumor.

10.2.1 Response to Treatment

Surgery and/or RT treatment tumor response usually consist in initial reduction of NAA, which may be evident before Cho and Cr changes. Then Cho, Cr, NAA reduce (NAA may also be absent) with the possible occurrence of the peak of Lac/Lip, result of radiation necrosis [2].

T. Popolizio (✉) · R. Izzo · D. Grasso
Department of Neuroradiology, IRCCS "Casa Sollievo della Sofferenza", San Giovanni Rotondo, FG, Italy

R. F. Balzano
Department of Radiology, University of Foggia, Foggia, FG, Italy

10.2.2 Stability vs. Progression/Recurrence

Spectroscopy puts in evidence progression of disease, showing spectral anomalies at the resection borders or outside the surgical bed, even in absence of CE and before an increase of it [3, 4]. Changes in Cho signal and Cho/Cr and Cho/NAA ratio are predictive of tumor progression. Cho increase over 45% respect to opposite healthy hemisphere is indicative of disease progression, whereas a value equal to or less than 35% is indicative of stability [5]. For the other ratio, differentiation between progression and stability has a sensitivity of 93.8% and a specificity of 85.7% [6]. Lip signal increase can be an early marker of malignant transformation [7].

In post-surgery [8] and post-radiosurgery [3] follow-up, areas with Cho/NAA and Cho/Cr high ratio, usually undergo contrast-medium impregnation. Tissue volume with abnormal spectrum correlates inversely with the time of appearance of new impregnation.

In post-chemotherapy, Cho/Cr and Lac/Cr ratio are the most useful marker for follow-up of low-grade gliomas. In CE areas, Lac/Cr increase during treatment has a significant association with progression/survival reduction, whereas a low NAA/Cr in normal-appearing brain tissue adjacent to tumor without CE is associated with reduced progression-survival. Moreover, Cho/Cr and Lac/Cr ratio increase in normal-appearing brain tissue adjacent to tumor may become evident a few months before disease progression in morphological MRI [9].

10.2.3 Recurrence vs. Radionecrosis

Spectroscopy can detect a characteristic metabolic pattern. In presence of radio-necrosis, peak of Lac/Lip appear in absence of other metabolic signal with persistence for several months [3, 10] contrary to what happens in case of recurrence instead characterized by Cho increase. Distinction between recurrence and radiation injury can be made using

T. Scarabino, S. Pollice (eds.), *Imaging Gliomas After Treatment*, https://doi.org/10.1007/978-3-030-31210-7_10

Cho/NAA, Cho/Cr, and NAA/Cr ratio: the first two are the main discriminant for differential diagnosis. They are in fact significantly higher in recurrence than in radiation injury and even higher than the apparently healthy white matter. NAA/Cr ratio has instead an opposite trend [11–13].

Really, in co-existence of necrosis and recurrence, however, (frequently situation in clinical practice) spectroscopy is not always clarifying as well as it is not always possible to distinguish radionecrosis from tumor necrosis because of frequent coexistence and overlapping of events. In this case, metabolic changes may be more informative of data collected at time distance from therapy.

10.3 Role of Diffusion

DWI can be used not only to characterize and define tumor grade, basing on cellularity, but also to assess how cellularity changes with treatment.

10.3.1 Treatment Response

In immediate post-surgery period, ADC is more useful than CE in defining persistence or absence of disease thanks to a reduction of ADC due to acute brain injury [14].

Later, during initial post-treatment period, cellular changes within the tumor (cell swelling, cell lysis, cell necrosis, apoptosis) may influence DWI and thus ADC map. In fact, when cell is not responsive there is no change in ADC, whereas the cell swelling, ADC decreases his value. Eventual cell lysis for hypoxic-ischemic events leads to increased diffusivity that occurs even when apoptosis directly occurs.

In early stage, DWI can document presence of ischemic changes surrounding surgical bed [15]. Tractography moreover can also highlight preservation of white matter tracts, such as motor fibers, in order to obtain prognostic information about functional recovery of neurological conditions.

10.3.2 Stability vs. Progression/Recurrence

Functional diffusion mapping (FDM) has been recently proposed as noninvasive method to assess quantitative response to therapy of the disease, comparing diffusion maps before and after treatment [16, 17]. FDM, 3 weeks after treatment can already predict whether the tumor is responsive or not in relation to early abnormalities in diffusion tumor values. Then it is not necessary to wait classical 10 weeks that are used to evaluate treatment response. Comparison between FDM after 3 weeks and changes after 10 weeks is therefore an early quantitative biomarker to predict response to treatment, its effectiveness, progression time, and median survival. Association between FDM and neuroradiological findings provides a more accurate prediction of survival respect to only quantitative parameter [18]. Clinical implications are then very useful to optimize management of patient, to avoid expensive and toxic therapies and other kinds of treatment.

10.3.3 Recurrence vs. Radionecrosis

In follow-up of treated high-grade glioma, radio-induced injuries may present with a variety of DWI patterns, usually hypointense with high ADC, but sometimes hyperintense with low ADC, for example due to the presence of bleeding, viscous mucinous components, coagulation necrosis [19].

ADC can be used to differentiate RT effects from tumor recurrence being significantly higher in radionecrosis respect to recurrence (for the high cellularity) even if there can be some overlap as a result of various factors such as cellularity, viscosity, and permeability [20]. In fact, it is possible to differentiate tumor from necrosis, but ADC do not always get more information respect to spectroscopy in discriminating tumor and necrosis mixed with tumor or necrosis alone [21–23].

Diffusion tensor imaging (DTI) provides more accurate data, showing lower ADC ratio and higher FA in recurrence in contrast to what happens in necrosis [24].

In CE lesions evaluation, cellularity is not the only factor that can influence ADC after therapy. Contribution of other components (necrosis, gliosis, scarring, granulation tissue) may alter ADC values, hence the need to study only the average absolute value of ADC in order to minimize influence of all these components. Use of ADC ratio certainly improves differentiation between the two entities, reducing overlapping of data [20].

ADC quantitative study in theory would then be able to distinguish between radionecrosis and recurrence, but structural complexity and heterogeneity of lesion, dynamic evolving, often involves abnormal values (i.e., ADC increase in presence of increased cellularity and thus recurrence). This state depend from inclusion or not of vascular structures and necrosis in peri-tumoral district. These findings consequently could cause confusion as the measure of ADC is often made in CE areas, which have low specificity in distinguishing the two entities.

In this regard, recently, imaging based on magnetic susceptibility was used to better visualize heterogeneous pattern of tumor tissue. With the same sequence, using contrast medium, allow to evaluate clinically useful information such as tumor microvasculature, degree of intratumoral necrosis, and presence of small alterations of the BBB in surrounding tissue. Ability of CE-SWI (Susceptibility-Weighted Imaging Contrast Enhancement) to distinguish these pathological

findings thus provides a new mechanism to evaluate ADC within the parenchymal tissue with abnormal BBB, often location of tumor recurrence. CE-SWI, used as a guide in ADC quantitative diffusion study, especially in CE areas, can therefore distinguish districts anatomically related to vascular, blood, and/or necrosis components. Therefore, in recurrence, respect to stable disease, a correlation between increased CE in CE-SWI maps and low ADC in CE areas has been found [25].

Moreover, in the CE lesion, ADC was significantly higher in peri-lesional edema and in radiation injury respect to recurrence [26].

10.4 Role of Perfusion

PWI is useful in post-treatment monitoring of gliomas, especially in lesions with extensive neovascularization and microvessel density. Increase of angiogenesis, typical feature of the most aggressive gliomas, is an essential histological criteria for determining biological behavior of gliomas, which is shown with cerebral blood volume (CBV) increase, considered one of the strongest predictors of tumor aggressiveness and survival in glioma [27, 28].

10.4.1 Treatment Response

Initial tumor response to surgery and/or to RT is usually the reduction of CBV. This feature is further supported in relation to the size of necrotic contextual component [29].

10.4.2 Stability vs. Progression/Recurrence

PWI assumes a prominent role especially in presence of diffuse CE lesions, sometimes due to overlapping of multiple-surgical treatments. In cases of residual or progressive tumor, PWI shows rCBV values higher than the normal white matter. These findings are also confirmed with morphological MRI controls.

10.4.3 Recurrence vs. Radionecrosis

CBV, being correlated with angiogenesis, is significantly higher in recurrence respect to radio-necrosis, although there is some overlap of findings in relation to non-high spatial resolution, to tissue heterogeneity and to frequent coexistence of vascularized recurrence and radio-necrosis with iperplastic and enlarged vessels [30].

Presence of petechial hemorrhages in recurrence can cause susceptibility artifacts and reduce CBV. An inaccurate estimation of CBV may also be due to severe damage or absence of BBB [31].

Some authors, in addition to CBV, use other hemodynamic variables such as RPH (peak height) and rPSR (percentage of signal intensity recovery).

RPH is a quantifiable measure of tumor vascularity, highly correlated with CBV and then with tumor vascular density and histopathological grade. For this reason, it is suggested that it may reflect total vascular volume within the ROI and is therefore high, such as CBV, in CE recurrence, contrary to what happens in radionecrosis.

RPSR is significantly different in the two states. In particular it is lower in tumor recurrence in relation to alteration of BBB that then is more permeable to macromolecular contrast agents. This parameter is more useful than Ktrans value, that measure capillaries permeability in relation to T1 relaxation changes (T1 DSC) that occur during the infusion of contrast media or during washout of the CE lesion [32].

Perfusion may be useful to distinguish pseudo-progression from a real progression [33].

Using parametric response map (PRM), an innovative voxel-by-voxel method of image analysis in patients with progressive disease, a significantly reduced CBV was noted after 3 weeks respect to the patients with pseudo-progression [33].

10.5 Multimodal MR Imaging

Use of morphological or advanced MR examination alone in the diagnosis of gliomas is not enough for defining histological grading, for optimal treatment planning and correct post-treatment follow-up. Therefore, the use of combined studies is necessary to increase MR diagnostic accuracy, as a function of recent development and of new and more effective anticancer treatments that require a complete morphofunctional MRI study. By these techniques, it is possible to obtain noninvasively "neuropathological in vivo" interpretation of typical biological heterogeneity of these tumors.

These advanced techniques should be used for a qualitative and quantitative assessment. Quantitative data, especially when combined, can provide real biomarker findings, very important for tumor tissue characterization, also can allow multicenter studies, clinical trials, and longitudinal studies. Only by combining data from various imaging techniques, that are often quite different, essential information with an effective clinical influence can be found.

In a personal experience [34], we conducted a multimodal study by combining MR imaging with spectroscopy, diffusion, and perfusion in order to minimize low specificity of each methods and especially to provide surgeon oncologist, more accurate and comprehensive information in order to plan a more accurate treatment.

This study involved 31 patients with cerebral gliomas of different degrees. All parameters used, with the exception of ADC, have helped to differentiate low-grade gliomas from high-grade. In particular, metabolic information provided by levels of Lac/Lip and CBV were sufficient for a correct classification of 100% of the tumors. In addition, we studied spatial changes of metabolic structural and hemodynamic findings, in gliomas and surrounding tissues. Combining these information, we sought to identify true tumor edges margins whose exact definition is essential for accurate treatment planning and for prognosis.

Quin Shi-Zeng et al. [35] found a significant difference in Cho/Cr, Cho/NAA, and ADC ratio. Cho/Cr, Cho/NAA, and ADC ratios were found to be the key to distinguish recurrence from radio-necrosis. ADC ratio, in addition to spectroscopy, further improves spectroscopy differentiation ability. Accuracy of differential diagnosis with spectroscopy and ADC ratio is higher respect to spectroscopy alone.

Bobek-Billewicz et al. [36] documented the role of perfusion compared to diffusion and spectroscopy in the differential diagnosis between recurrence and radiation injury. In particular, the mean value of CBV was more discriminating respect to CBV maximum value, while spectroscopy and diffusion do not seem to differentiate the two entities in a significant way, despite lower ADC values in recurrence compared to radiation injury.

Voglein et al. [37] show more efficacy of perfusion imaging compared to spectroscopy in identifying disease progression and predicting response to treatment.

Kim et al. [38] and Prat et al. [39], comparing effectiveness of PET and perfusion in the differential diagnosis between recurrence and radionecrosis, documented superiority of MRI respect to PET (using FDG methionine as drug).

References

1. Howe FA, Barton SJ, Cudlip SA, et al. Metabolic profiles of human brain tumors using quantitative in vivo 1H magnetic resonance spectroscopy. Magn Reson Med. 2003;49:223–32.
2. Howe FA, Opstad KS. 1H MR spectroscopy of brain tumours and masses. NMR Biomed. 2003;16:123–31.
3. Möller-Hartmann W, Herminghaus S, Krings T, et al. Clinical application of proton magnetic resonance spectroscopy in the diagnosis of intracranial mass lesions. Neuroradiology. 2002;44:371–81.
4. Graves EE, Nelson SJ, Vigneron DB, et al. Serial proton MR spectroscopic imaging of recurrent malignat gliomas after gamma knife radiosurgery. AJNR Am J Neuroradiol. 2001;22(4):613–24.
5. Ricard D, Soussain C, Psimaras D. Neurotoxicity of the CNS: diagnosis, treatment and prevention. Rev Neurol. 2011;167(10):737–45.
6. Tedeschi G, Lundbom N, Raman R, et al. Increased choline signal coinciding with malignant degeneration of cerebral gliomas: a serial proton magnetic resonance spectroscopy imaging study. J Neurosurg. 1997;87:516–24.
7. Lichy MP, Bachert P, Hamprecht F, et al. Application of 1H-MRS spectroscopic imaging in radiation oncology: choline a marker for determining the relatove probability of tumor progression after radiation of glial brain tumors. Rofo. 2006;178(6):627–339.
8. Murphy PS, Rowland IJ, Viviers L, et al. Could assessment of glioma methylene lipid resonance by in vivo 1H-MRS be of clinical value? Br J Radiol. 2003;76:459–63.
9. Pirzkall A, Mcknight TR, Graves EE, et al. MR-spectroscopy guided target delineation for high-grade gliomas. Int J Radiat Oncol Biol Phys. 2001;50:915–28.
10. Balmaceda C, Critchell D, Mao X, et al. Multisection 1H magnetic resonance spectroscopic imaging assessment of glioma response to chemiotherapy. J Neuro-Oncol. 2006;76(2):185–91.
11. Weybright P, Sundgren PC, Maly, et al. Differentiation between brain tumor recurrence and radiation injury using MR spectroscopy. Am J Roentgenol. 2005;185(6):1471–6.
12. Zeng QS, Li CF, Liu H, et al. Distinction between recurrent glioma and radiation injury using magnetic resonance spectroscopy in combination with diffusion-weigthed imaging. Int J Radiat Oncol Biol Phys. 2007;68(1):151–8.
13. Chuang MT, Liu YS, Tsai YS, et al. Differentiating radiation-induced necrosis from recurrent brain tumor using MR perfusion and spectroscopy: a meta-analysis. PLoS One. 2016;11(1):e0141438.
14. Smith JS, Cha S, Mayo MC, et al. Serial diffusion-weighted magnetic resonance imaging in cases of glioma: distinguishing tumor recurrence from postresection injury. J Neurosurg. 2005;103(3):428–38.
15. Ulmer S, Braga TA, Barker FG, et al. Clinical and radiographics features of peritumoral infarction following resection of glioblastoma. Neurology. 2006;67:1668–70.
16. Moffat BA, Chenevert TL, Lawrence TS, et al. Functional diffusion map: a non invasive MRI biomarker for early stratification of clinical brain tumor response. Proc Natl Acad Sci U S A. 2005;102(5):5524–9.
17. Moffat BA, Chenevert TL, al MCR. The functional diffusion map: an imaging biomarker for the early prediction of cancer treatment outcome. Neoplasia. 2006;8(4):259–67.
18. Hamstra DA, Galban CJ, Meyer CR, et al. Functional diffusion map as an early imaging biomarker for high-grade glioma: correlation with conventional radiologic response and overall survival. J Clin Oncol. 2008;26(10):3387–94.
19. Asao CH, Korogi Y, Kitajima M, et al. Diffusion weighted imaging of radiation-induced brain injury for differentiation from tumor recurrence. AJNR. 2005;26:1455–60.
20. Hein PA, Eskey CJ, Dunn JF, et al. Diffusion-wighted imaging in the follow-up of treated high-grade gliomas: tumor recurrence versus radiation injury. AJNR Am J Neuroradiol. 2004;25:201–9.
21. Rock JP, Scarpace L, Hearshen D, et al. Associations among magnetic resonance spectroscy, apparent diffusion coefficients, and image-guided histopatology with special attention to radiotion necrosis. Neurosurgery. 2004;54(5):1111–7.
22. Zeng QS, Li CF, Zhang K, et al. Multivoxel 3D proton MR spectroscopy in the distinction of recurrent glioma from radiation injury. J Neuro-Oncol. 2007;84(1):63–9.
23. Verma N, Cowperthwaite MC, Burnett MG, et al. Differentiating tumor recurrence from treatment necrosis: a review of neuro-oncologic imaging strategies. Neuro-Oncology. 2013;15(5):515–34.
24. Xu JL, Li L, Lian JM, et al. Distinction between postoperative recurrent glioma and radiation injury using MR diffusion tensor imaging. Neuroradiology. 2010;52:1193–9.
25. Al Sayyari A, Buckley R, McHenery C, et al. Distinguishing recurrent primary brain tumor from radiation injury: a preliminary study using a susceptibility-weighted MR imaging-guided apparent diffusion coefficient analysis strategy. AJNR Am J Neuroradiol. 2011;31(6):1049–54.
26. Sudgren PC, Fan X, Weibright P, et al. Differentiation of recurrent brain tumor versus radiation injury using diffusion tensor imaging in patients with new contrast-enhancing lesions. Magn Reson Imaging. 2006;24(9):1131–42.

27. Leon SP, Folkerth RD, Black PM. Microvessel density is a prognostic indicator for patients with astroglial brain tumors. Cancer. 1996;77:362–72.
28. Covarrubias DJ, Rosen BR, Lev MH. Dynamic magnetic resonance perfusion imaging of brain tumors. Oncologist. 2004;9:528–37.
29. Chaskis C, Stadnik T, Michotte A, et al. Prognostic value of perfusion-weighted imaging in brain glioma: a prospective study. Acta Neurochir. 2006;148(3):277–85.
30. Sugahara T, Korogi Y, Tomiguchi S, et al. Posttherapeutic intraaxial brain tumor: the value of perfusion-sensitive contrast-enhanced MR imaging for differentiating tumor recurrence fron non neoplastic contrast-enhancing tissue. AJNR Am J Neuroradiol. 2000;21(5):901.909.
31. Prazincola L, Steno J, Srbecky M, et al. Mr imaging of late radiation therapy- and chemiotherapy-induced injured: a pictorial essay. Eur Radiol. 2009;19:2716–27.
32. Barajas RF, Chang JS, Segal MS, et al. Differentiation of recurrent glioblastoma multiforme from radiation necrosis after external beam radiation therapy with dynamic susceptibility-weighted contrast-enhanced perfusion MR imaging. Radiology. 2009;253(2):486–96.
33. Tsien C, Galban CJ, Chenevert TL, et al. Parametric response map as an imaging biomarker to distinguish progression from pseudoprogressi on in high-grade glioma. J Clin Oncol. 2010;28(13):2293–9.
34. Di Costanzo A, Scarabino T, Trojsi F, et al. Multiparametric 3T MR approach to the assessment of cerebral gliomas: tumor extent and malignancy. Neuroradiology. 2006;48(9):622–31.
35. Zeng Q-S, Li C-F, Liu H, et al. Distinction between recurrent glioma and radiation injury using magnetic resonance spectroscopy in combination with diffusion-weighted imaging. Int J Radiat Oncol Biol Phys. 2007;68(1):151–8.
36. Bobek-Billewicz B, Stasik-Pres G, Majchrzak H, et al. Differentiation between brain tumor recurrence and radiation injury using perfusion, diffusion-weighted imaging and MR spectroscopy. Folia Neuropathol. 2010;48(2):81–92.
37. Voglein J, Tuttenberg J, Weimer M, et al. Treatment monitoring in gliomas: comparisons of dynamic susceptibility-weighted contrast-enhanced and spectroscopic MRI techniques for identifying treatment failure. Investig Radiol. 2011;46(6):390–400.
38. Kim JH, Chang KN, Na DG, et al. 3 T ^{1}H-MRS spectroscopy in grading of cerebral gliomas: comparison of short and intermediate echo time sequences. AJNR Am J Neuroradiol. 2006;27(7):1412–8.
39. Prat R, Galeano I, Lucas A, et al. Relative value of magnetic resonance spectroscopy, magnetic resonance perfusion, and 2-(18F) fluoro-2-deoxy-D-glucose positron emission tomography for detection of recurrence or grade increase in gliomas. J Clin Neurosci. 2010;17(1):50–3.

Part IV

Clinical Cases

Pre- and Postoperative MR Scan in Low-Grade Astrocytoma

Case 1

Alessandro Stecco, Eleonora Soligo, Alessio Paschè, and Alessandro Carriero

- 36-year-old patient arrived in the emergency room after an epilectic attack; he was treated with surgery for a low-grade astrocytoma localized in the right fronto-temporo-insular area.
- Postoperative follow-up MR scan was performed late (12 months) with morphologic sequences.

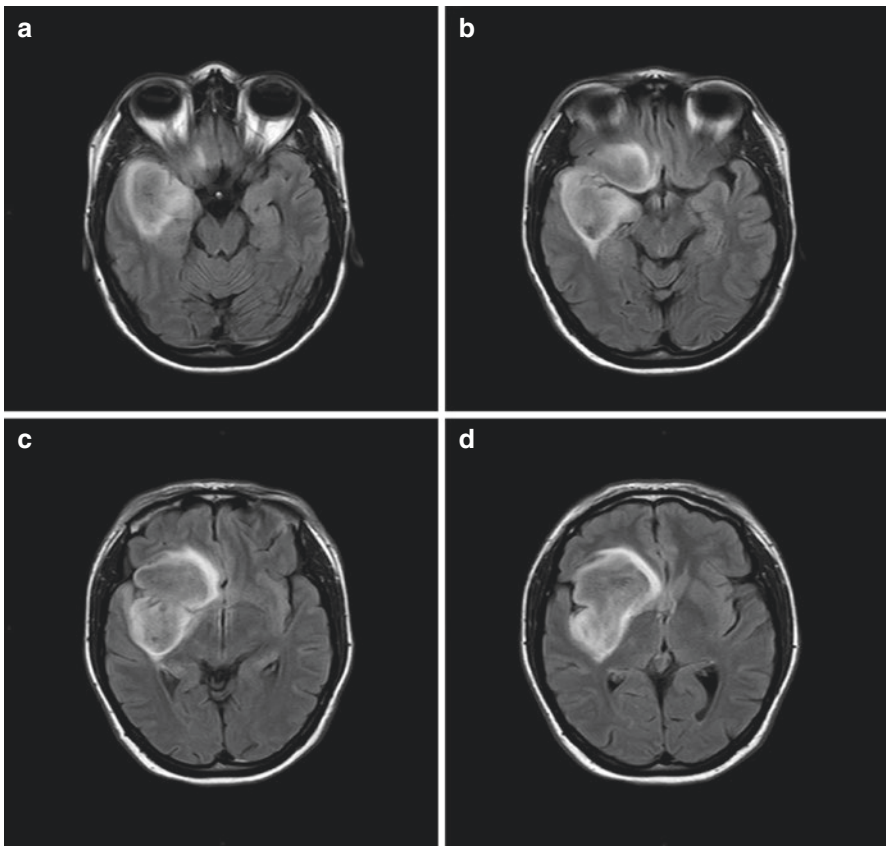

Fig. 1.1 (**a**–**d**) Preoperative imaging *MR FLAIR-weighted sequences*. A lesion with indefinite morphology but defined margins, in the right fronto-temporo-insular area, with marked perilesional edema, which determines shifts in the structures of the midline

A. Stecco (✉)
Neuroradiology Unit, AOU "Maggiore della Carità", DIMET, Università del Piemonte Orientale, Novara, Italy
e-mail: alessandro.stecco@uniupo.it

E. Soligo · A. Paschè · A. Carriero
Department of Radiology, AOU "Maggiore della Carità", DIMET, Università del Piemonte Orientale, Novara, Italy

T. Scarabino, S. Pollice (eds.), *Imaging Gliomas After Treatment*, https://doi.org/10.1007/978-3-030-31210-7_11

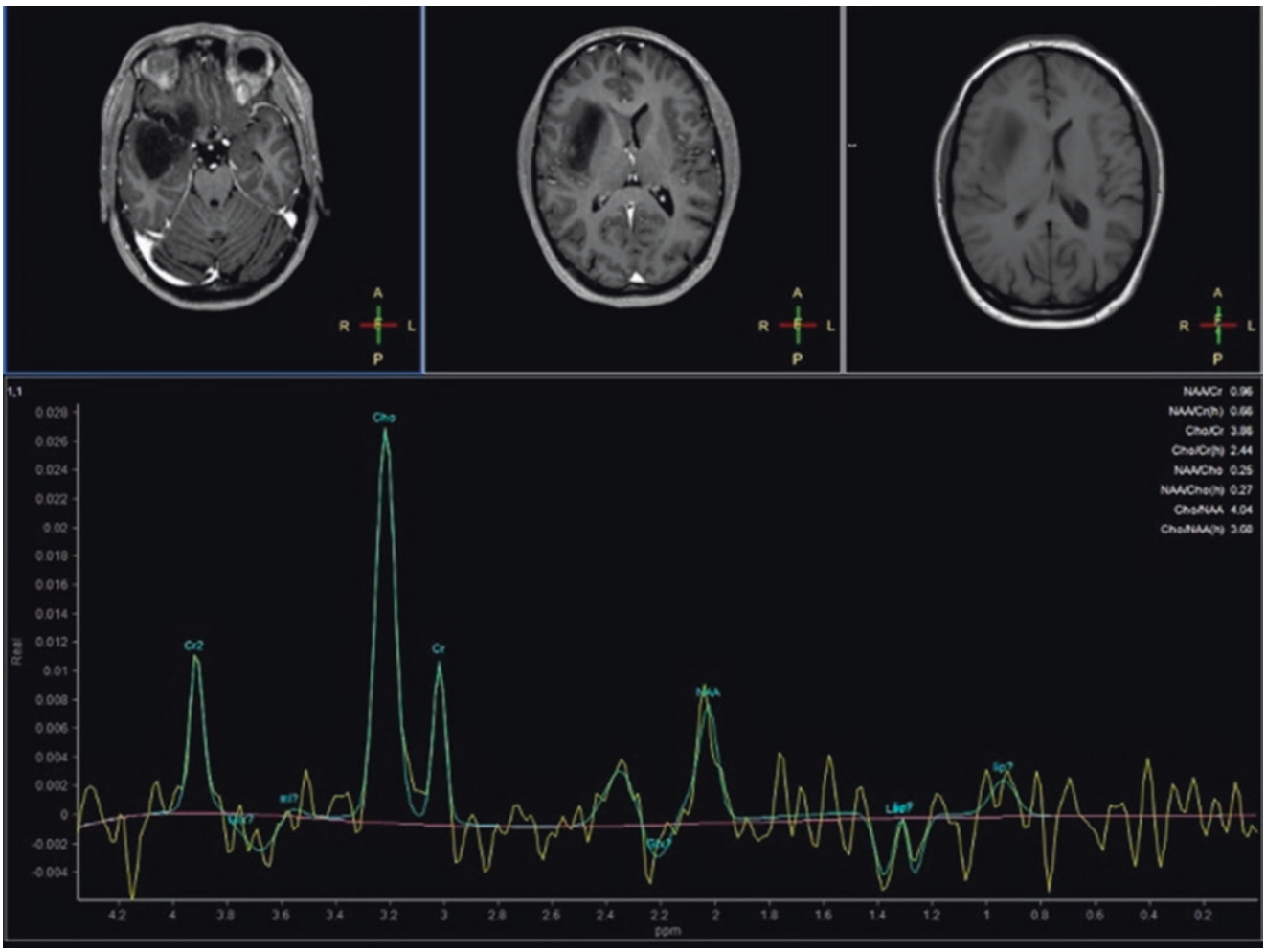

Fig. 1.2 The spectroscopic study shows an increase in the choline peak and a decrease in the NAA peak

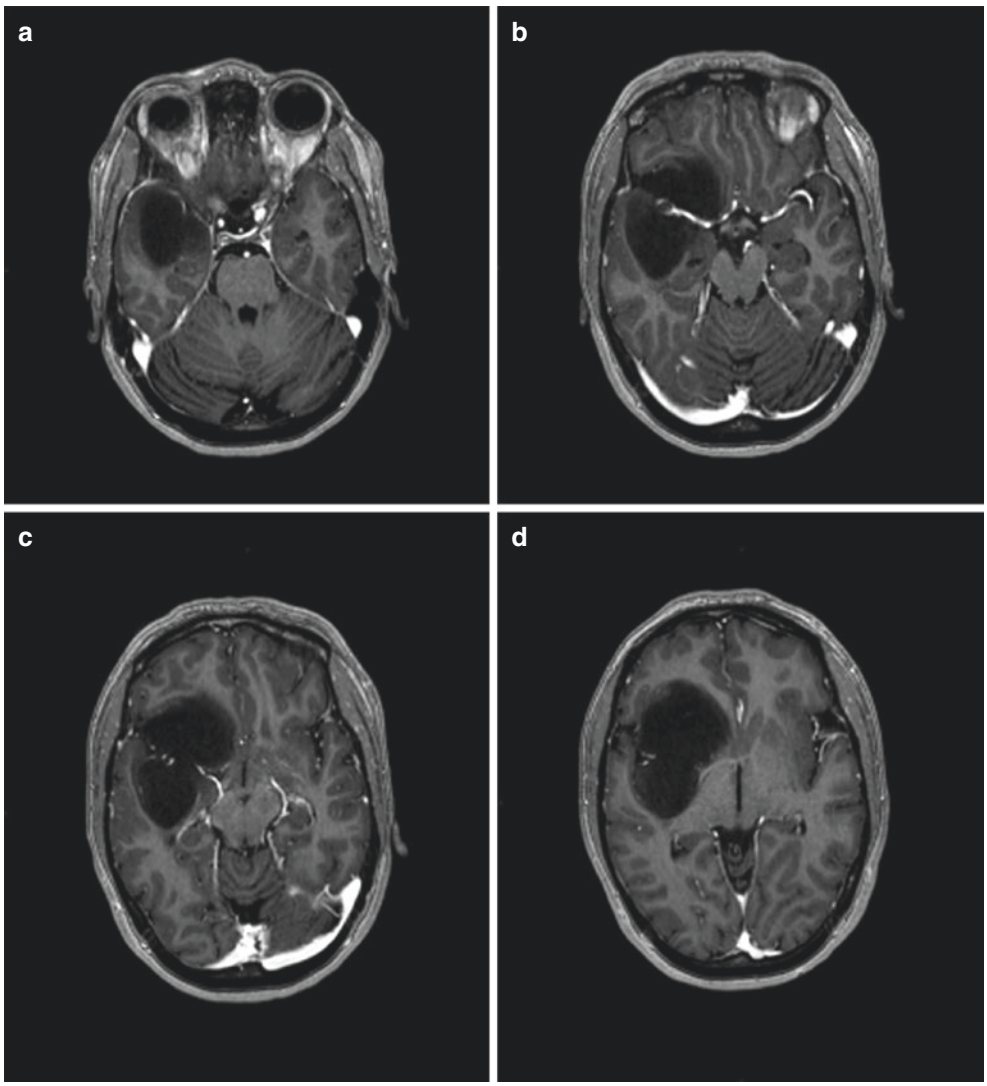

Fig. 1.3 (**a**–**d**) *Contrast-enhanced MR SE T1-weighted images.* The lesion does not show significant impregnation after intravenous contrast. Margins are well defined

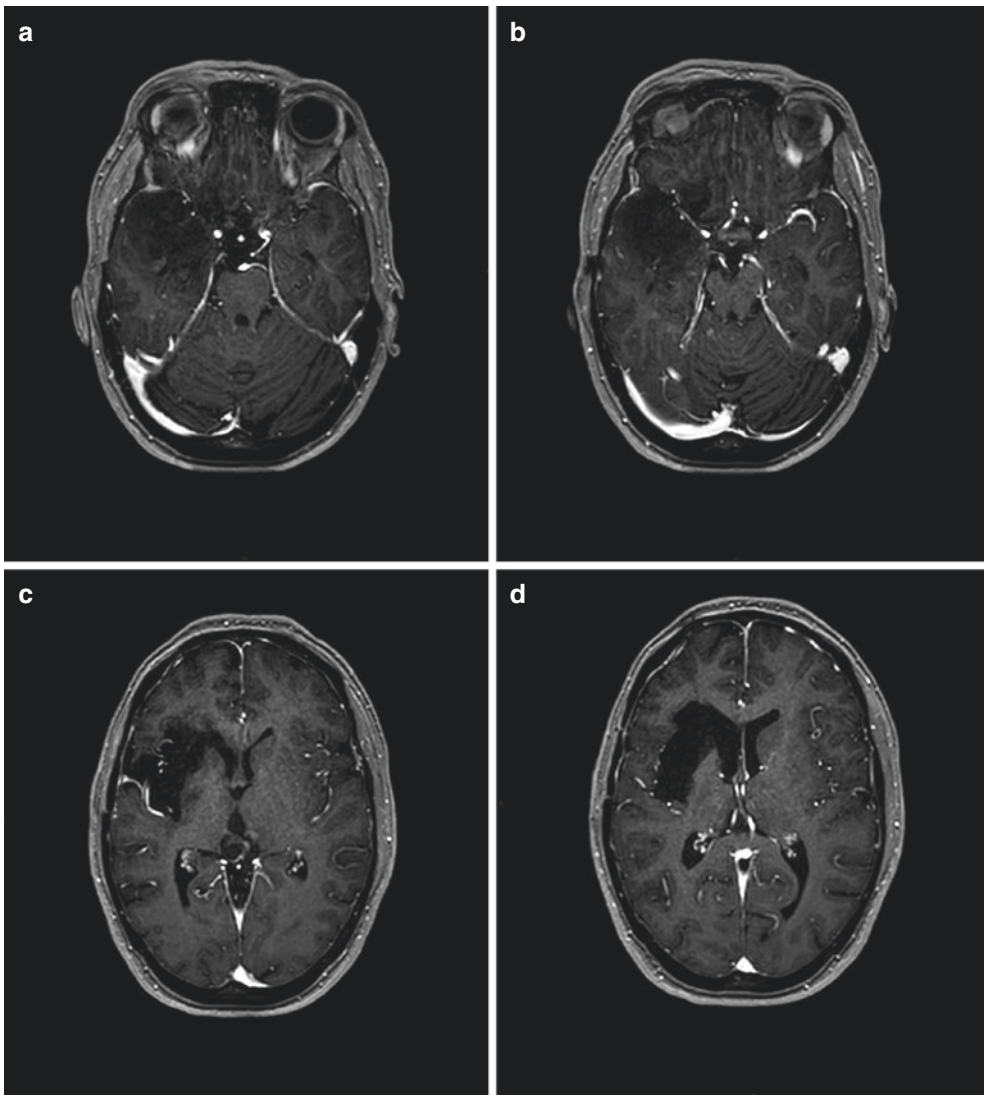

Fig. 1.4 (**a**–**d**) Postoperative follow-up at 12 month *contrast-enhanced MR SE T1-weighted images.* A large fronto-temporo-insular poro-encephalic cavity with associated gliotic outcomes is detected, in the results of surgical intervention. There are no pathological focal impregnations and an ex-vacual consensual enlargement of the right lateral ventricle

Pre- and Postoperative MR Scan in Glioblastoma Multiforme

Case 2

Alessandro Stecco, Eleonora Soligo, Alessio Paschè, and Alessandro Carriero

- 19-year-old patient came to the emergency room with headache and intracranial hypertension and he was treated with surgery for a GBM localized in the left temporal lobe.
- Postoperative MR scan was performed within 24–48 h.

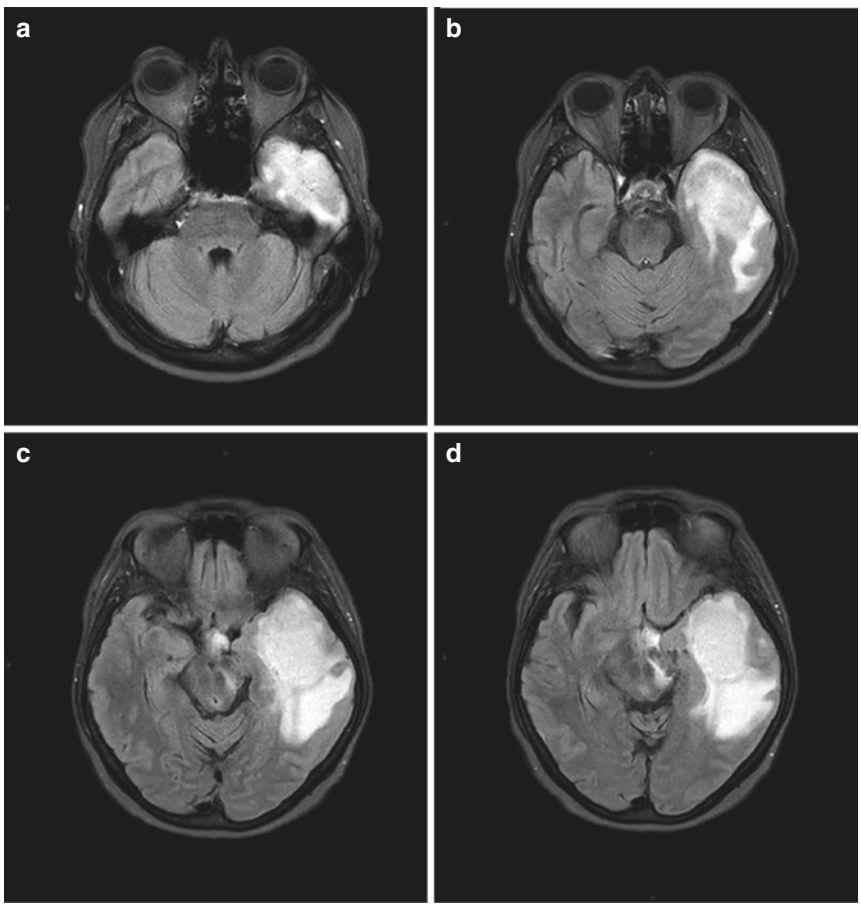

Fig. 2.1 (**a**–**d**) Preoperative imaging *MR FLAIR-weighted sequences.* A roughly oval-shaped lesion at the left temporal lobe can be seen with poorly defined margins and uneven structure, surrounded by a halo of edema

A. Stecco (✉)
Neuroradiology Unit, "AOU Maggiore della Carità", DIMET, Università del Piemonte Orientale, Novara, Italy
e-mail: alessandro.stecco@uniupo.it

E. Soligo · A. Paschè · A. Carriero
Department of Radiology, AOU Maggiore della Carità", DIMET, Università del Piemonte Orientale, Novara, Italy

T. Scarabino, S. Pollice (eds.), *Imaging Gliomas After Treatment*, https://doi.org/10.1007/978-3-030-31210-7_12

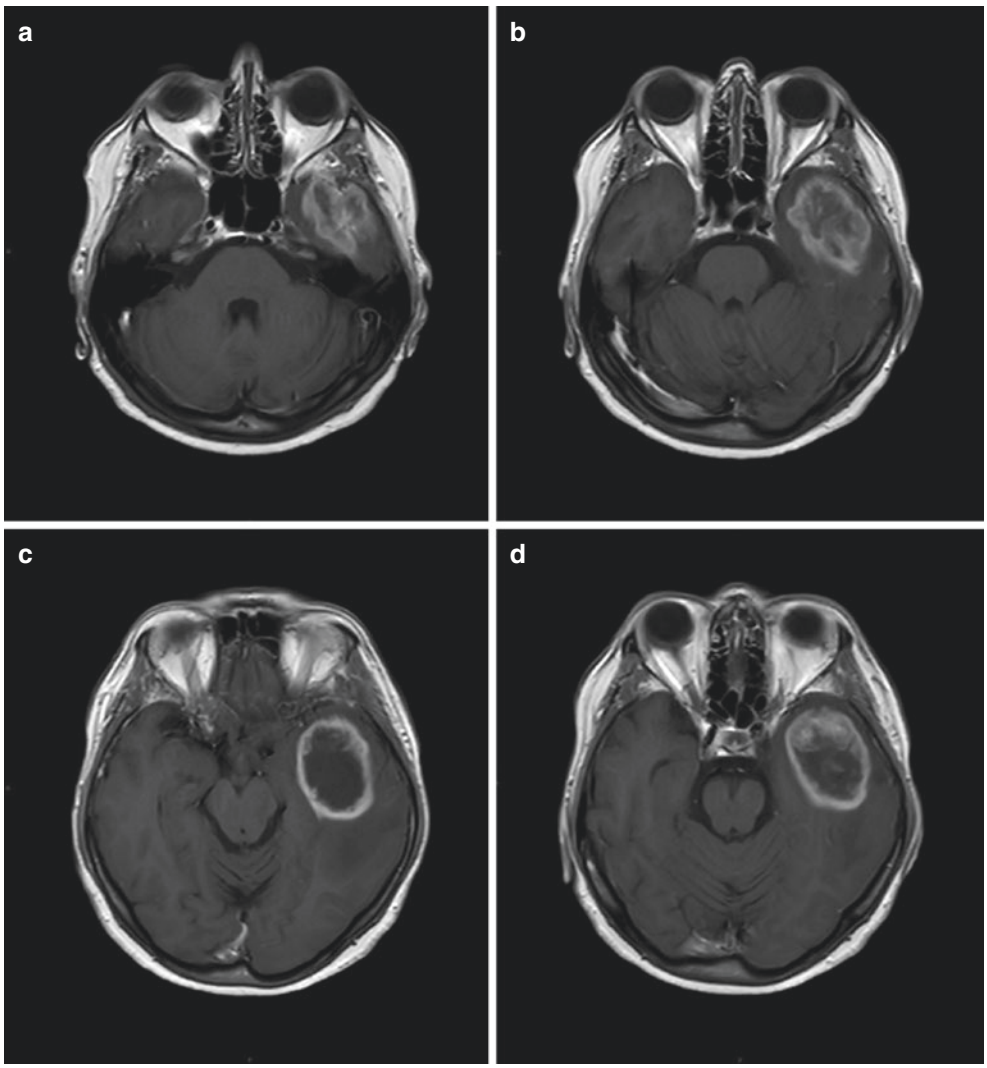

Fig. 2.2 (**a**–**d**) *Contrast-enhanced MR SE T1-weighted images.* Ring enhancement can be appreciated due to the presence of a large necrotic component within the lesion

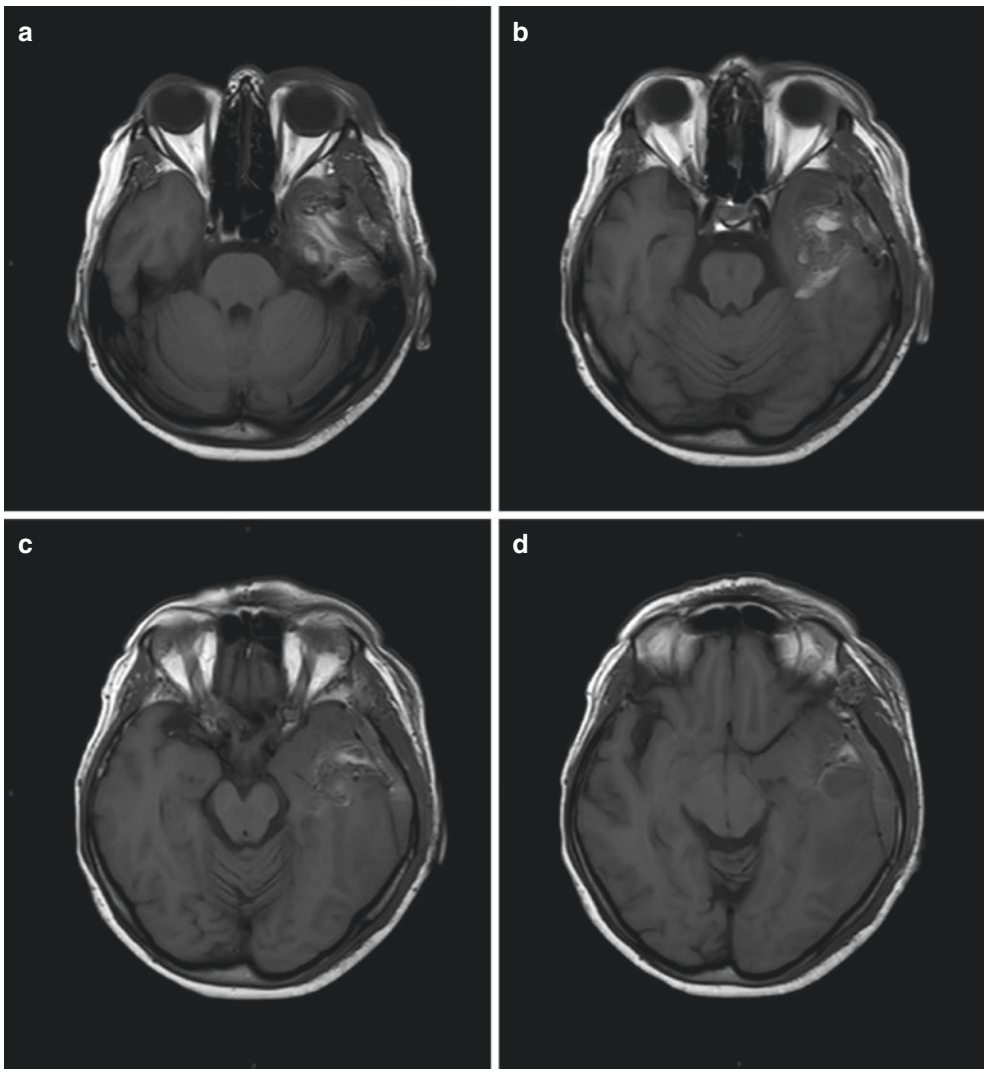

Fig. 2.3 (**a**–**d**) Postoperative follow-up at 24 hours *contrast-enhanced MR SE T1-weighted images.* Phlogistic hemorrhagic outcomes of exeresis of GBM are observed in the left temporo-frontal area. The surgical site shows inhomogeneous signal: peripheral to the small cavity there is an intense and irregular enhancement, indicative of the residual tissue (at this stage there are no changes in the blood–brain barrier)

Early Sequelae: Postoperative CT Scan in Glioblastoma Multiforme

Case 3

Ferdinando Caranci, Andrea Elefante, and Arturo Brunetti

- Patient with surgically treated right frontal glioblastoma multiforme.
- Postoperative CT scan performed within 24 h.

Preoperative Imaging

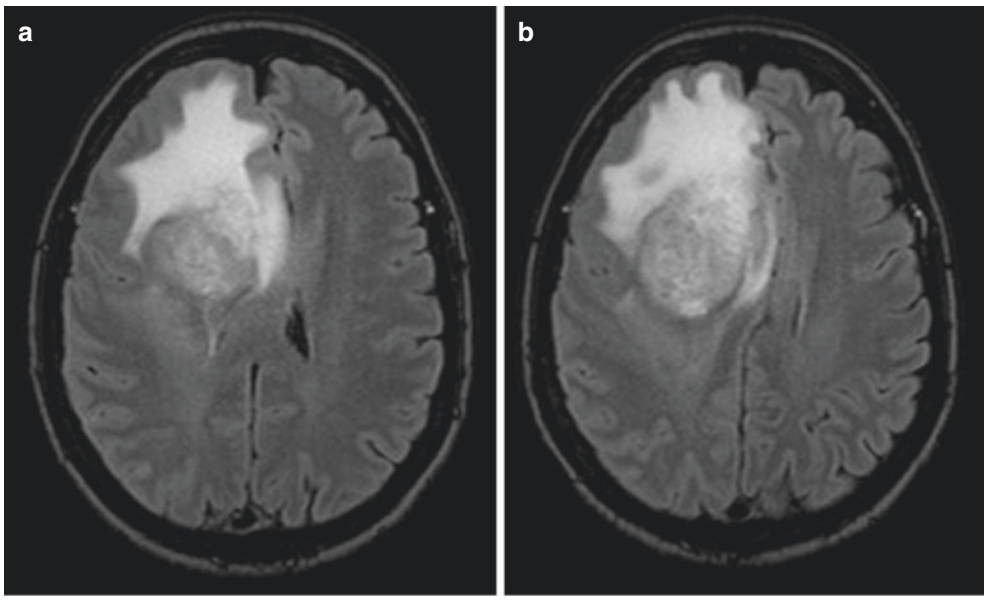

Fig. 3.1 (**a-d**) MR FLAIR sequences. A roughly oval-shaped lesion at the right frontal convexity can be seen with irregular margins and inhomogeneous structure, surrounded by a halo of edema

F. Caranci (✉) · A. Elefante · A. Brunetti
Department of Precision Medicine, School of Medicine, University of Campania "Luigi Vanvitelli", Naples, Italy

T. Scarabino, S. Pollice (eds.), *Imaging Gliomas After Treatment*, https://doi.org/10.1007/978-3-030-31210-7_13

Fig. 3.1 (continued)

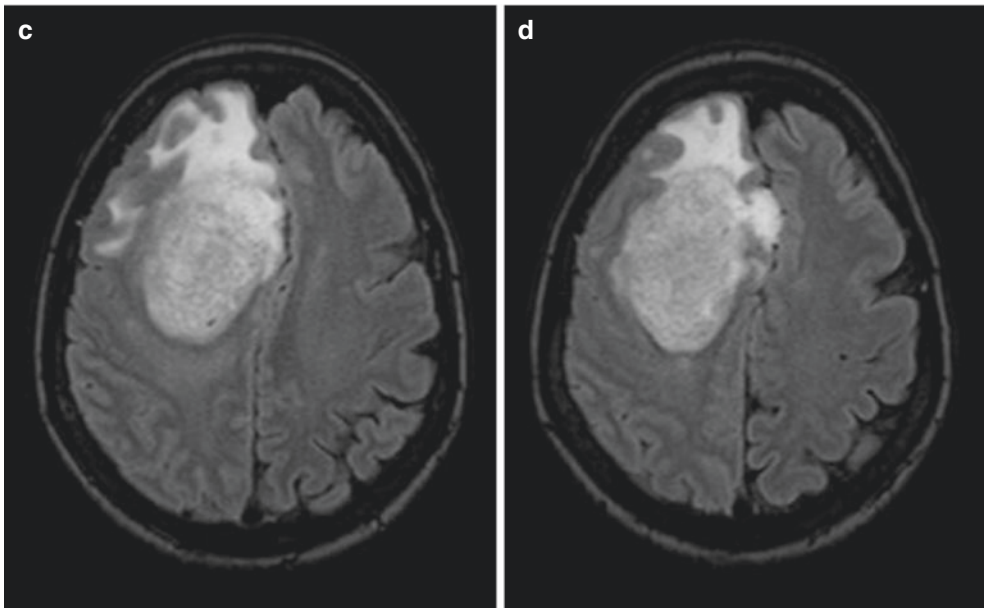

Fig. 3.2 (**a-d**) Contrast-enhanced MR SE T1-weighted images. Ring enhancement can be appreciated due to the presence of a large necrotic component within the lesion

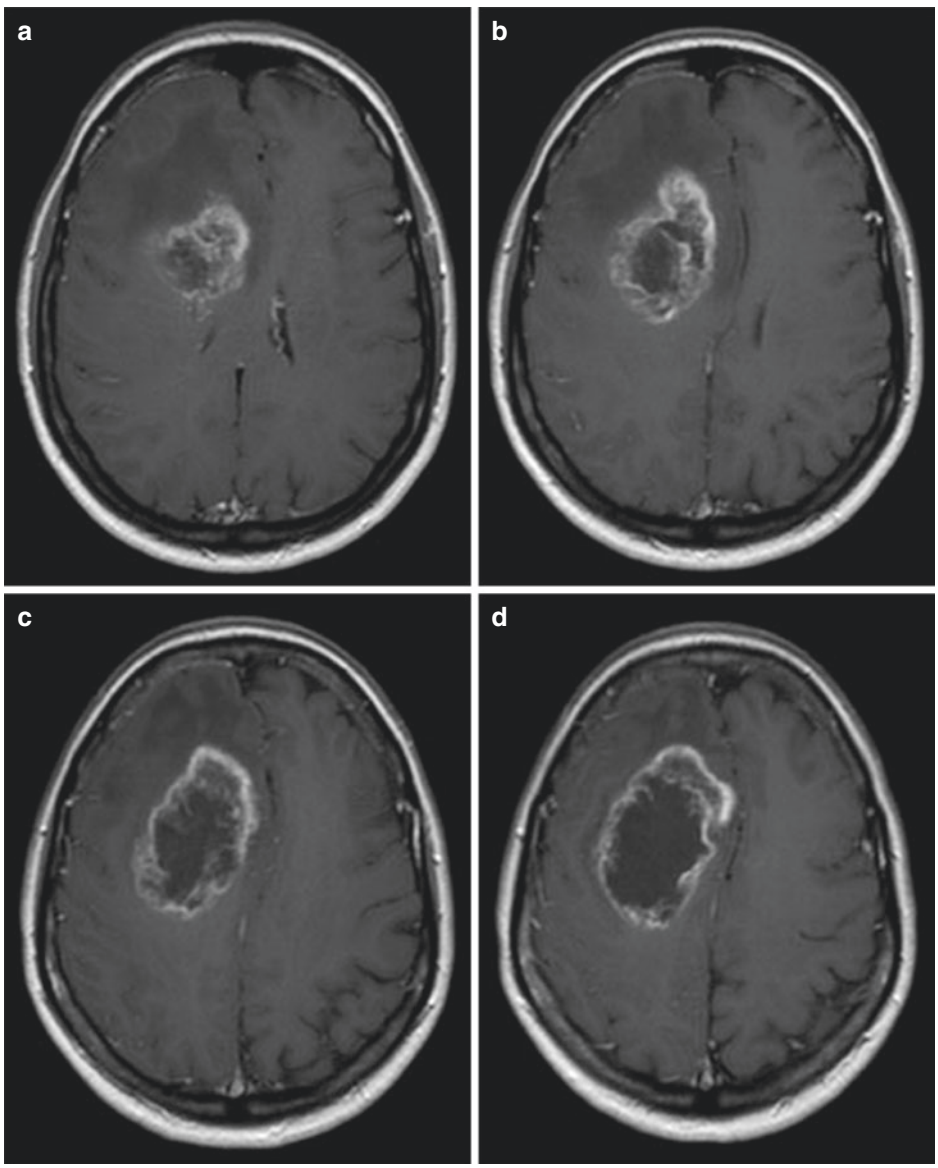

Early Postoperative Follow-Up (Within 24 h)

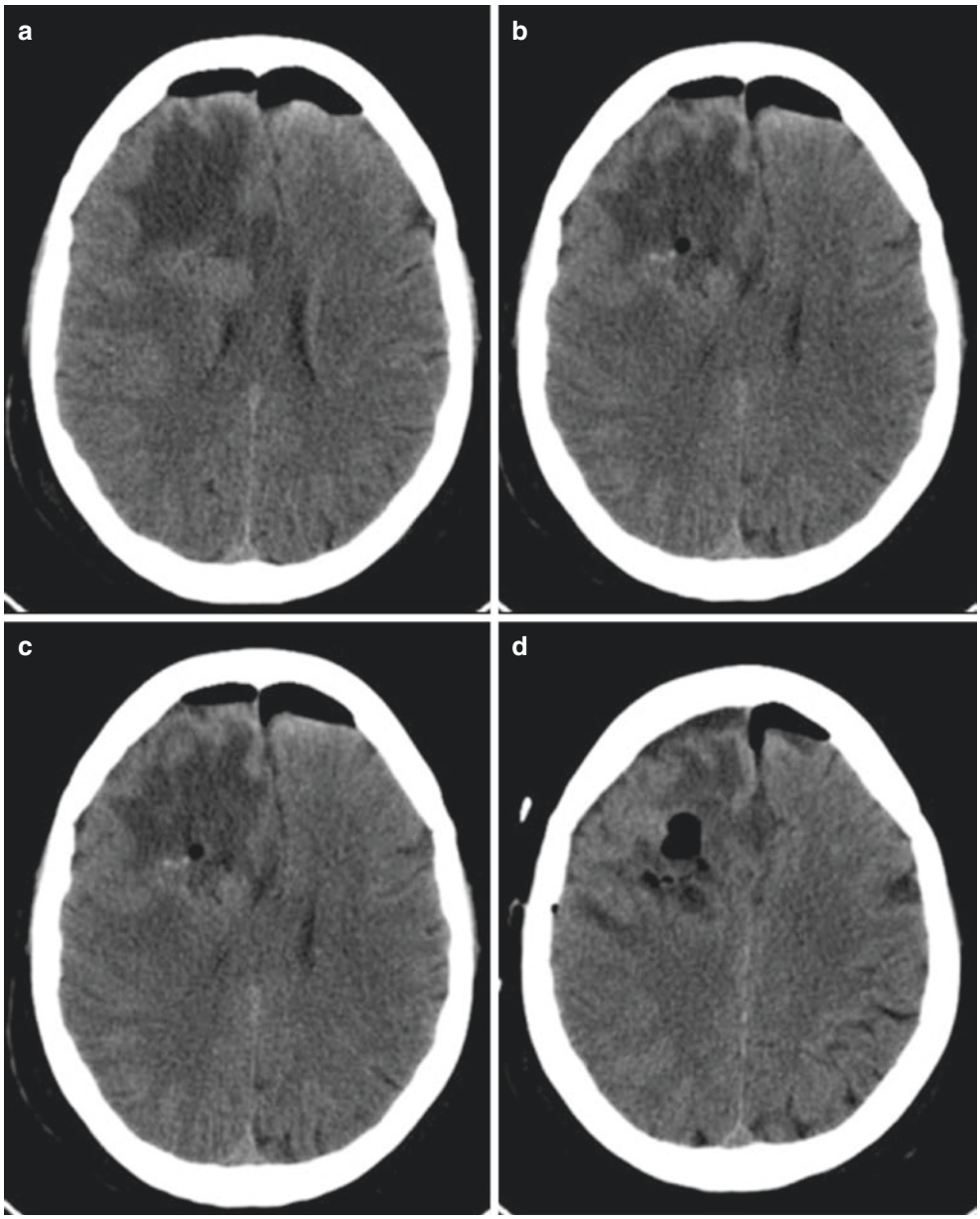

Fig. 3.3 (**a-d**) CT scan. Good repositioning of the bone flap is shown, with a small amount of extracerebral air at the surgical access site. The surgical bed in the right frontal lobe appears inhomogeneously hypodense due to the coexistence of edema, moderate blood effusion, and small air bubbles. Superiorly to the ventricular roof a small amount of relatively hyperdense tissue can be appreciated, attributable to residual lesion

Early and Late Sequelae: Evolution of Postsurgical Area—Postoperative MR Follow-Up in Glioblastoma Multiforme

Case 4

Ferdinando Caranci, Francesco Briganti, and Arturo Brunetti

- Patient with surgically treated right temporo-occipital glioblastoma multiforme.
- Postoperative MR follow-up performed early (3 days) and late (3, 6, and 10 months).

Postoperative Follow-Up at 3 Days

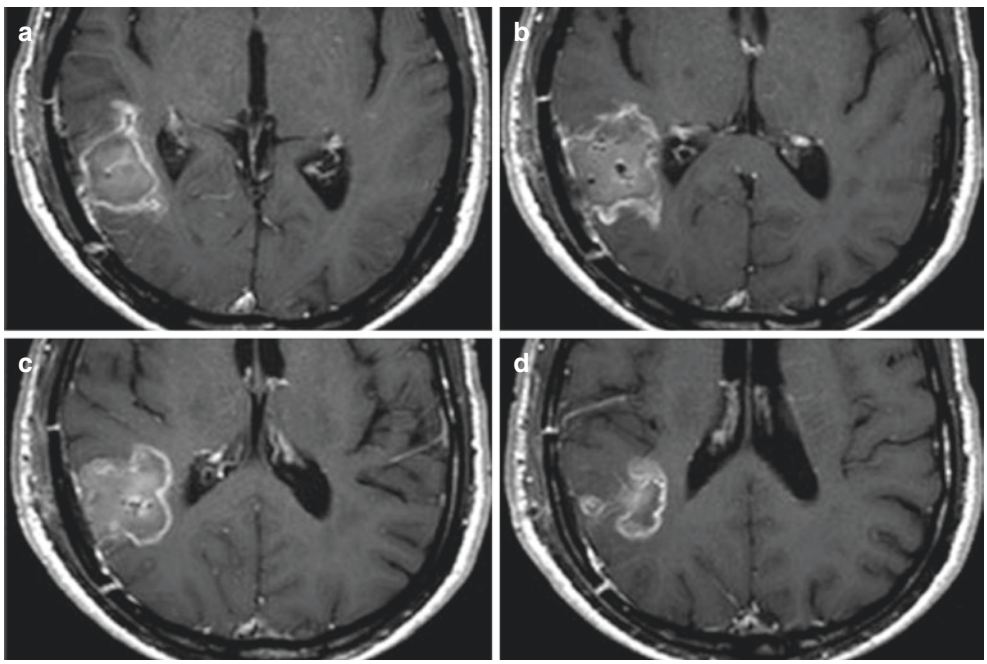

Fig. 4.1 (**a**–**d**) Contrast-enhanced MR SE T1-weighted images. The postoperative right temporo-occipital cavity signal is extremely inhomogeneous due to the mixture of blood–fluid components (hyperintense signal) and air. Peripheral enhancement is associated with irregular margins and a linear morphology, produced by blood–brain barrier injury, with enhancing dura adjacent to the bone flap. The ventricular trigone appears mildly compressed

F. Caranci (✉) · F. Briganti · A. Brunetti
Department of Precision Medicine, School of Medicine, University of Campania "Luigi Vanvitelli", Naples, Italy

T. Scarabino, S. Pollice (eds.), *Imaging Gliomas After Treatment*, https://doi.org/10.1007/978-3-030-31210-7_14

Postoperative Follow-Up at 3 Months

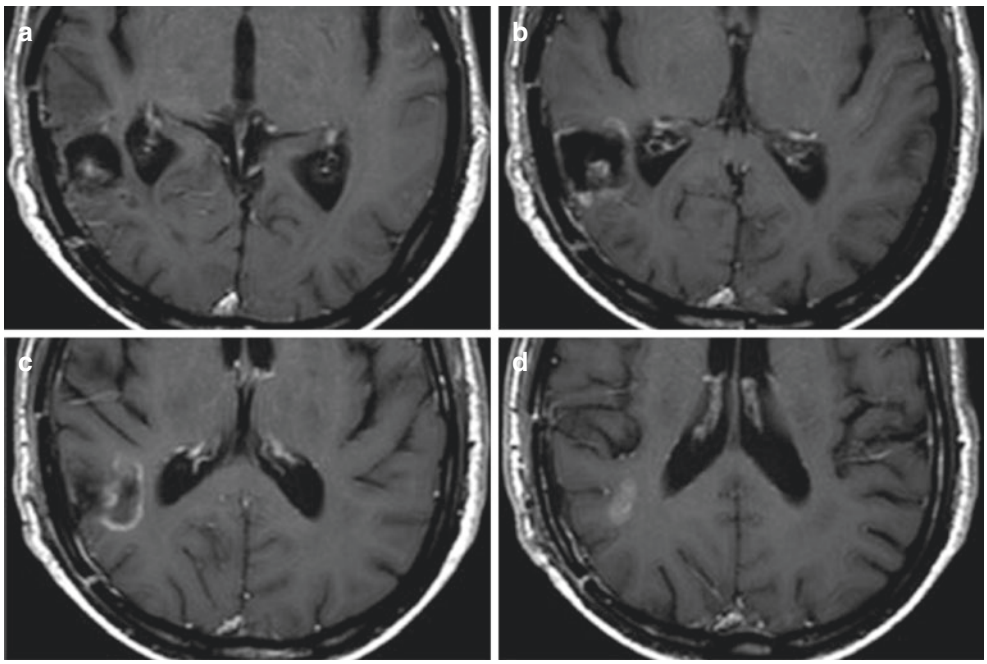

Fig. 4.2 (**a**–**d**) Contrast-enhanced MR SE T1-weighted images. A reduction in the size of the surgical foci is evident, with reexpansion of the ipsilateral ventricular trigone. There is evident resorption of the intralesional blood component and disappearance of the air. The lesion shows a CSF-like signal, with the presence of several internal blood clots. The peripheral enhancement produced by the blood–brain barrier injury is also still present, although reduced. The enhancing dura is also markedly reduced

Postoperative Follow-Up at 6 Months

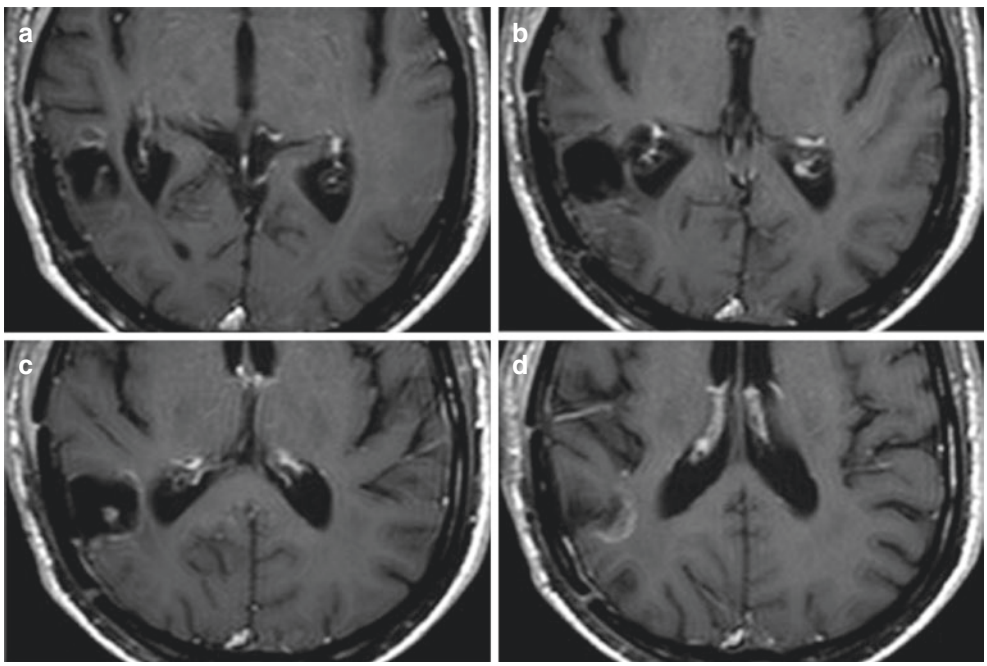

Fig. 4.3 (**a**–**d**) Contrast-enhanced MR SE T1-weighted images. Both the internal blood clots and the peripheral enhancement of the dura appear further reduced

Postoperative Follow-Up at 10 Months

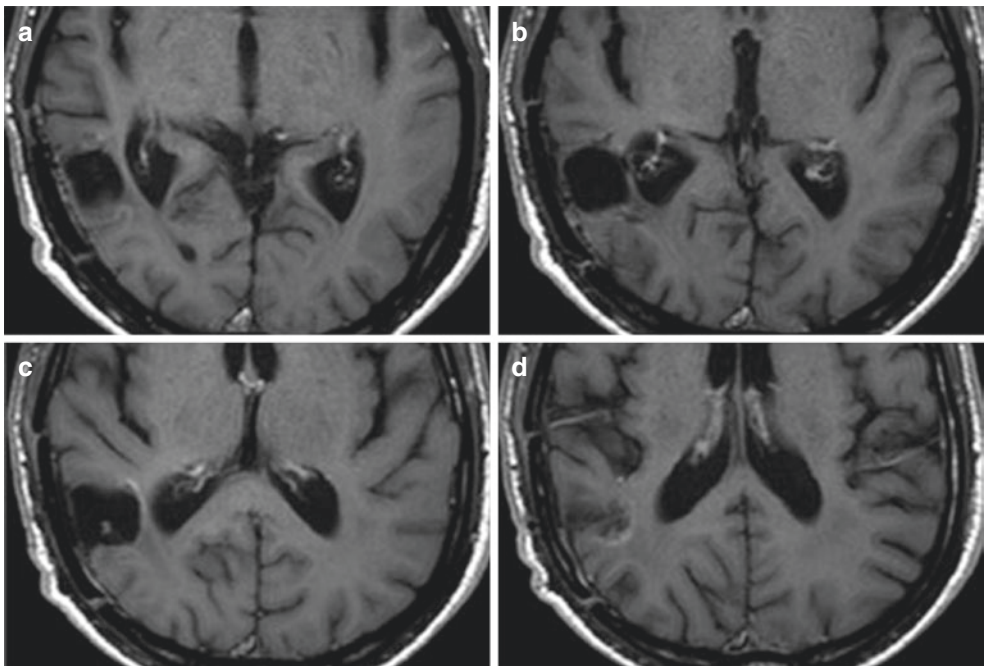

Fig. 4.4 (**a**–**d**) Contrast-enhanced MR SE T1-weighted images. Further progression of the phenomena described above is evident, with the formation of a cavity with a prevalent CSF content

Late Sequelae: Gliotic Scar Formation—Postoperative MR Follow-Up in Grade II Oligoastrocytoma

Case 5

Bianca Cusati, Ferdinando Caranci, and Alfonso Ragozzino

- Patient with surgically treated right temporo-fronto-insular grade II oligoastrocytoma.
- Postoperative follow-up performed late (at 6 months) with MR morphologic sequences and spectroscopy.

Preoperative Imaging

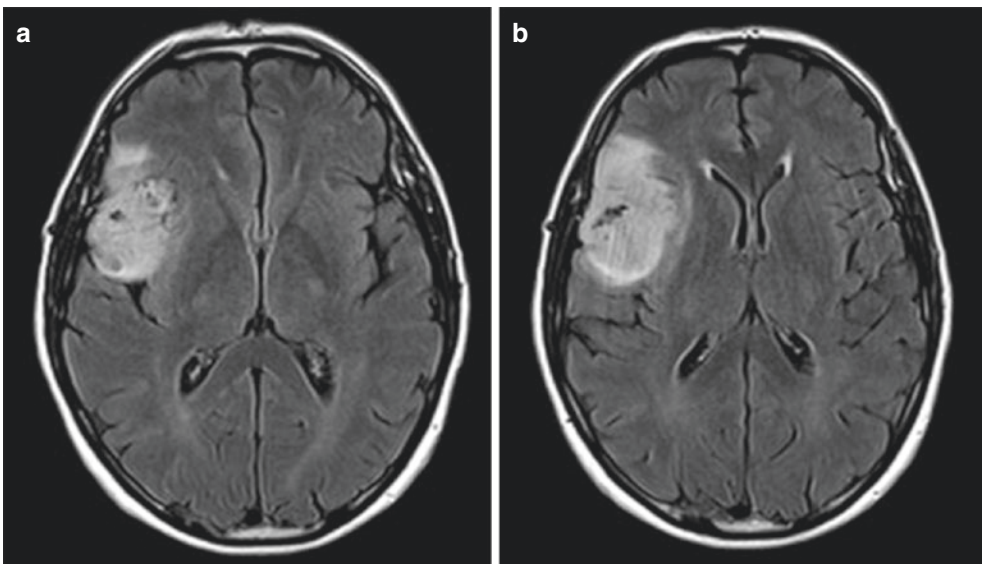

Fig. 5.1 (**a**–**d**) MR FLAIR sequence. An intra-axial right temporo-fronto-insular lesion can be appreciated infiltrating the cortex and extending into the white matter, with irregular margins and heterogeneous structure due to the presence of initial internal necrosis

B. Cusati · F. Caranci (✉) · A. Ragozzino
Department of Precision Medicine, School of Medicine, University of Campania "Luigi Vanvitelli", Naples, Italy

T. Scarabino, S. Pollice (eds.), *Imaging Gliomas After Treatment*, https://doi.org/10.1007/978-3-030-31210-7_15

Fig. 5.1 (continued)

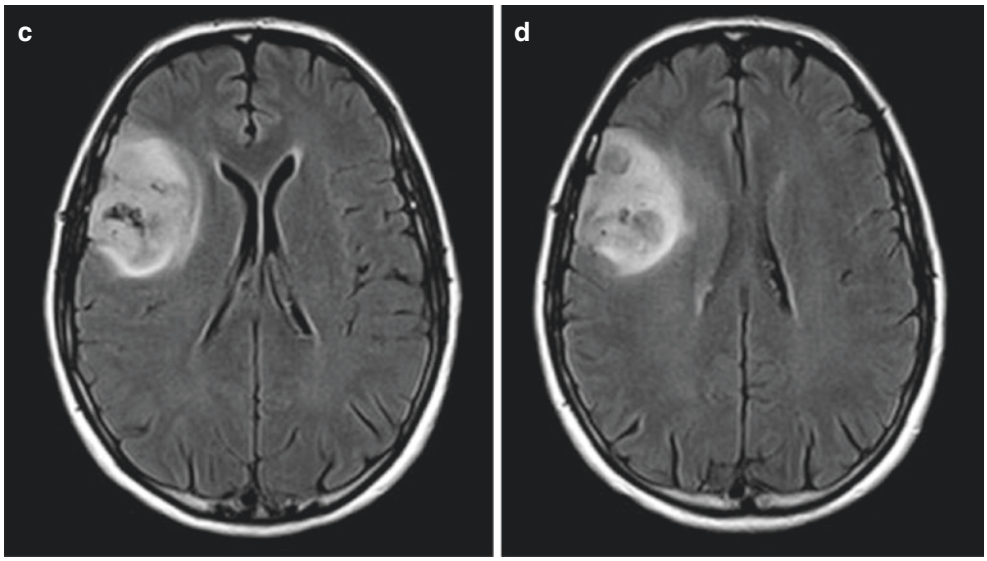

Fig. 5.2 (**a**–**d**) Contrast-enhanced MR SE T1-weighted images. No focal areas of pathologic enhancement can be seen within the lesion

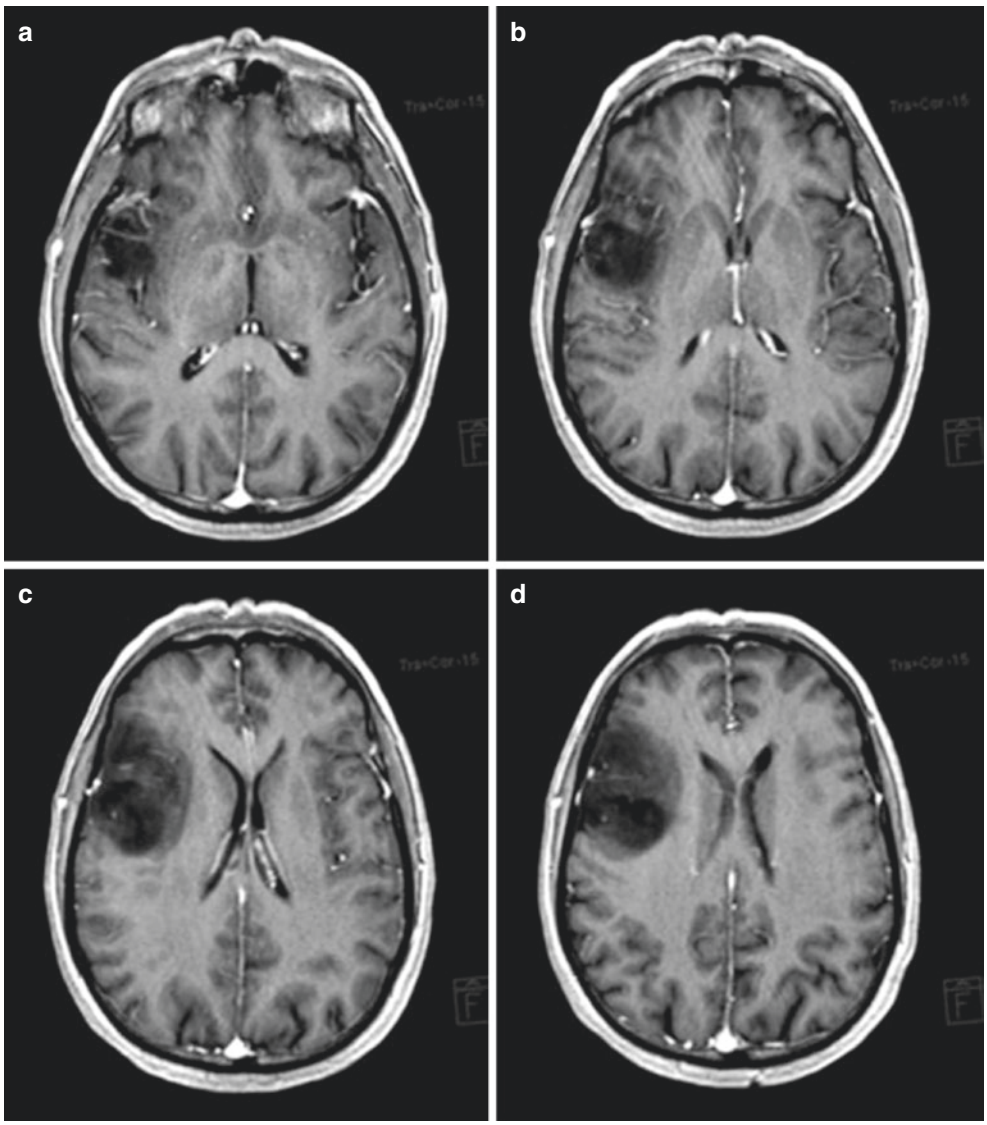

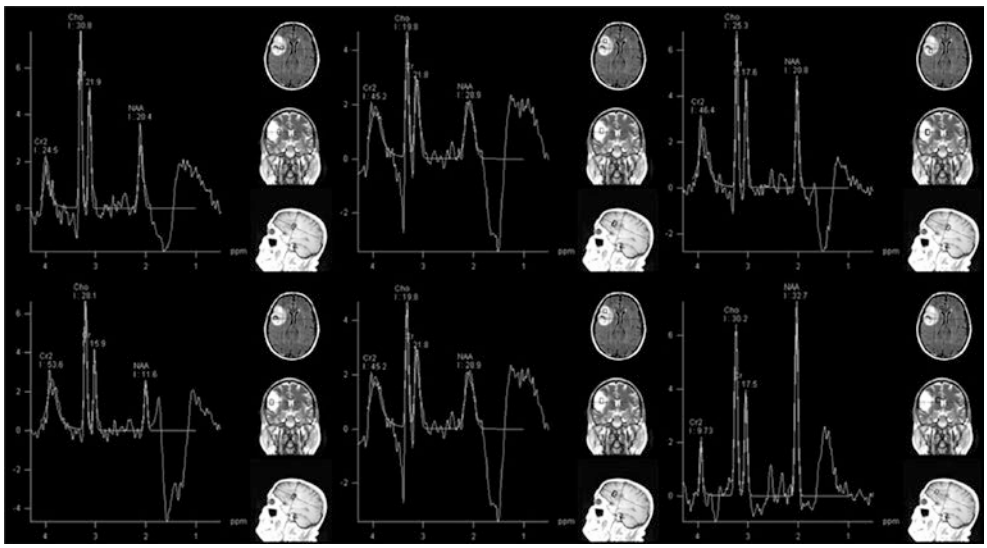

Fig. 5.3 Multi-voxel MR spectroscopy. Constant elevation in the concentration of choline can be appreciated, with reversal of the ratio with creatine

Postoperative Follow-Up at 6 Months

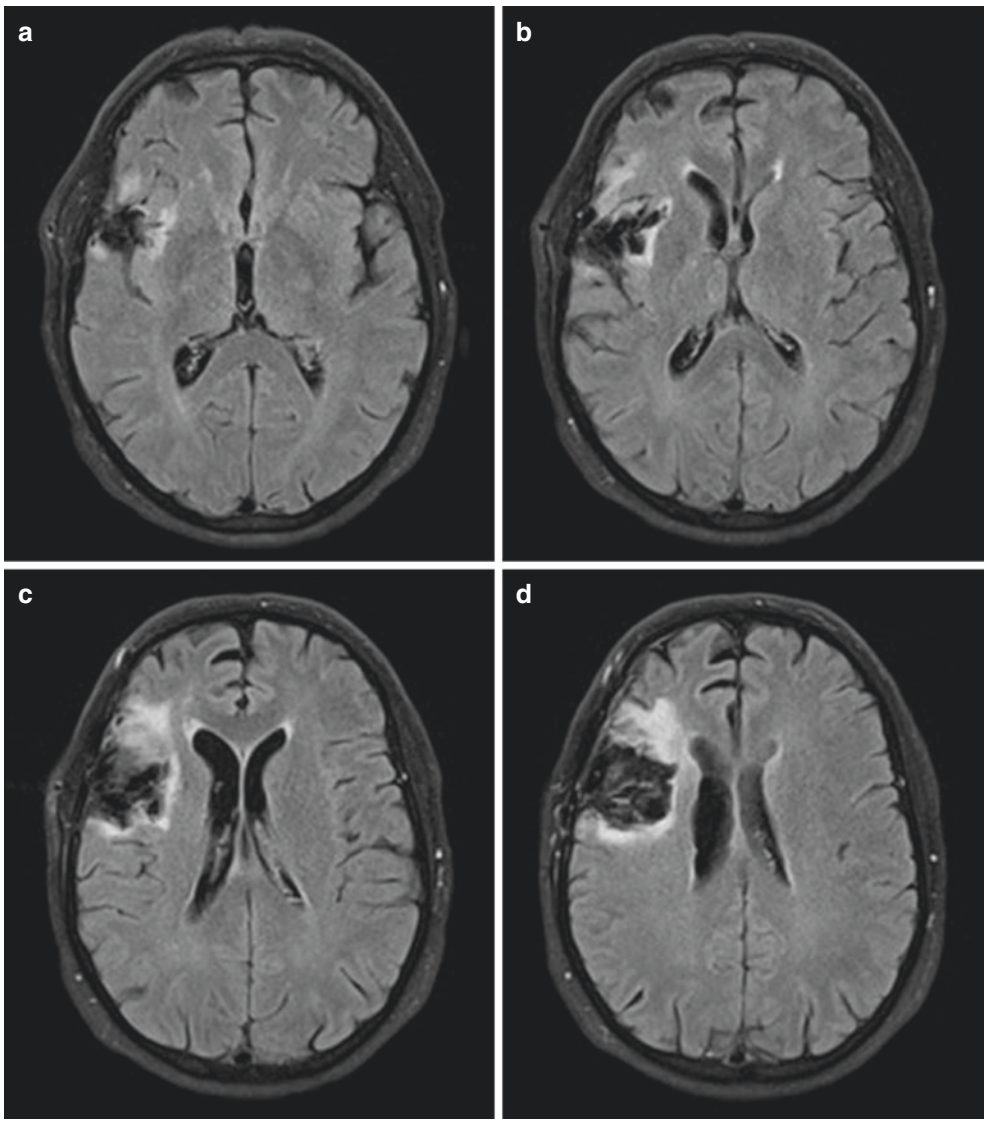

Fig. 5.4 (**a**–**d**) MR FLAIR sequence. The images clearly show the postsurgical cavity. A peripheral halo of high signal is associated, which does not exceed the margins of the original lesion. This may be likely due to postsurgical gliotic modifications and should be the basis for subsequent follow-up

Early and Late Squeal: Early Complications—Intralesional Hemorrhage After Biopsy

Case 6

Domenico Cicala, Ferdinando Caranci, Carmela Russo, Anna Nastro, Federica Mazio, and Sossio Cirillo

- 7-year-old patient with surgically treated right frontal high-grade glial tumor.
- Evolution of postsurgical area.
- MR follow-up after surgery and radiation therapy.

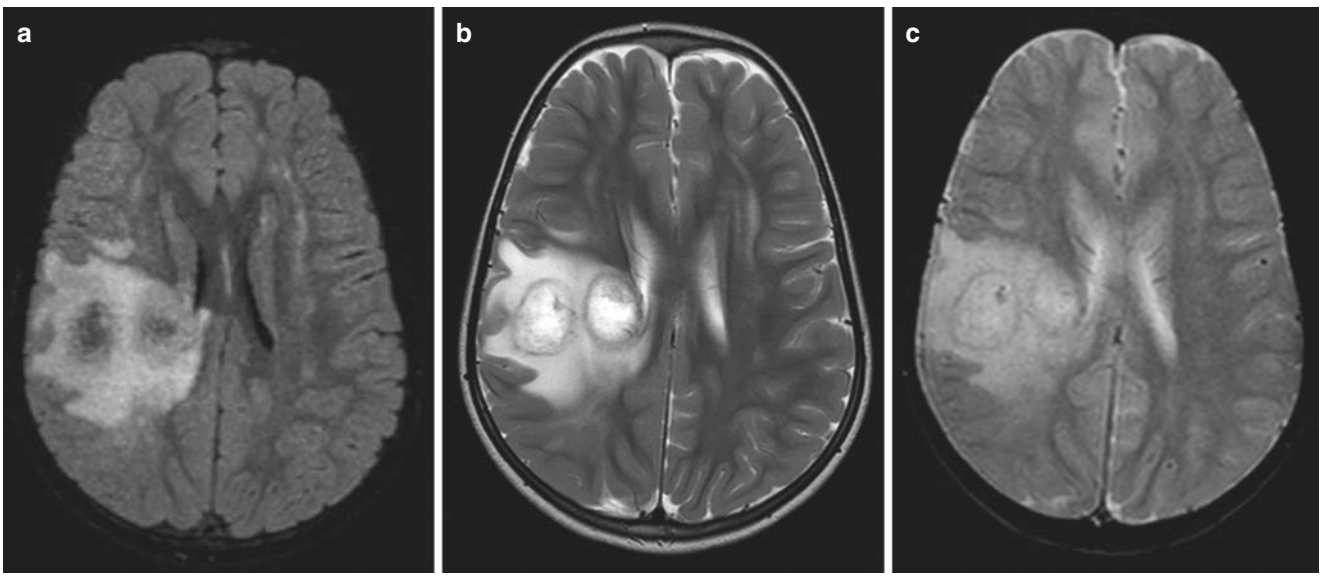

Fig. 6.1 Preoperative imaging. *Axial FLAIR* (**a**), *T2-weighted* (**b**), *T2*-weighted* (**c**), *DWI-b1000* (**d**), *ADC map* (**e**), *contrast-enhanced SE T1-weighted* (**f**) *sequences*. MR images show an expansive lesion infiltrating the right frontal rolandic cortical–subcortical region, with extensive halo of edema that extends to the deep white matter, causing compression of the ipsilateral ventricle and reduction of CSF spaces. Two large cystic components are observed within the lesional area with inhomogeneous structure, showing high intralesional diffusion coefficient suggestive of necrotic-cystic nature, irregular margins, and intense rim enhancement on contrast-enhanced SE T1 sequence. A smaller nodular enhancement is observed anterior to the components described above

D. Cicala · C. Russo · A. Nastro · F. Mazio
Department of Neurosciences, "Santobono-Pausilipon" Pediatric Hospital, Naples, Italy

F. Caranci (✉)
Department of Precision Medicine, School of Medicine, University of Campania "Luigi Vanvitelli", Naples, Italy

S. Cirillo
Department of Medicine and Health Sciences "V. Tiberio", University of Molise, Campobasso, Italy

T. Scarabino, S. Pollice (eds.), *Imaging Gliomas After Treatment*, https://doi.org/10.1007/978-3-030-31210-7_16

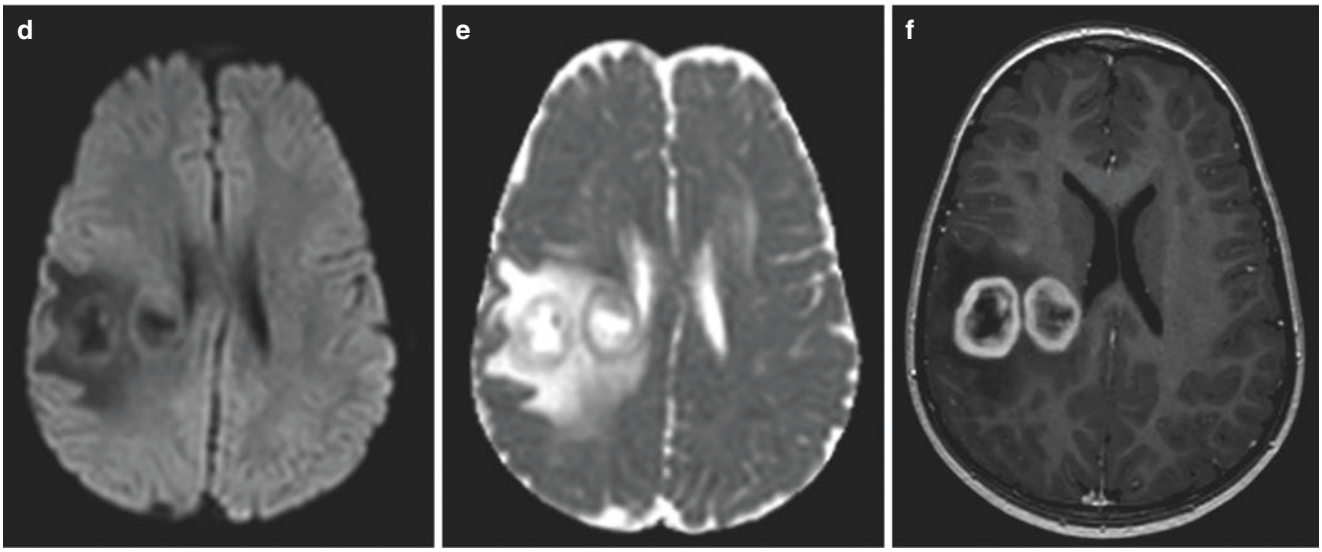

Fig. 6.1 (continued)

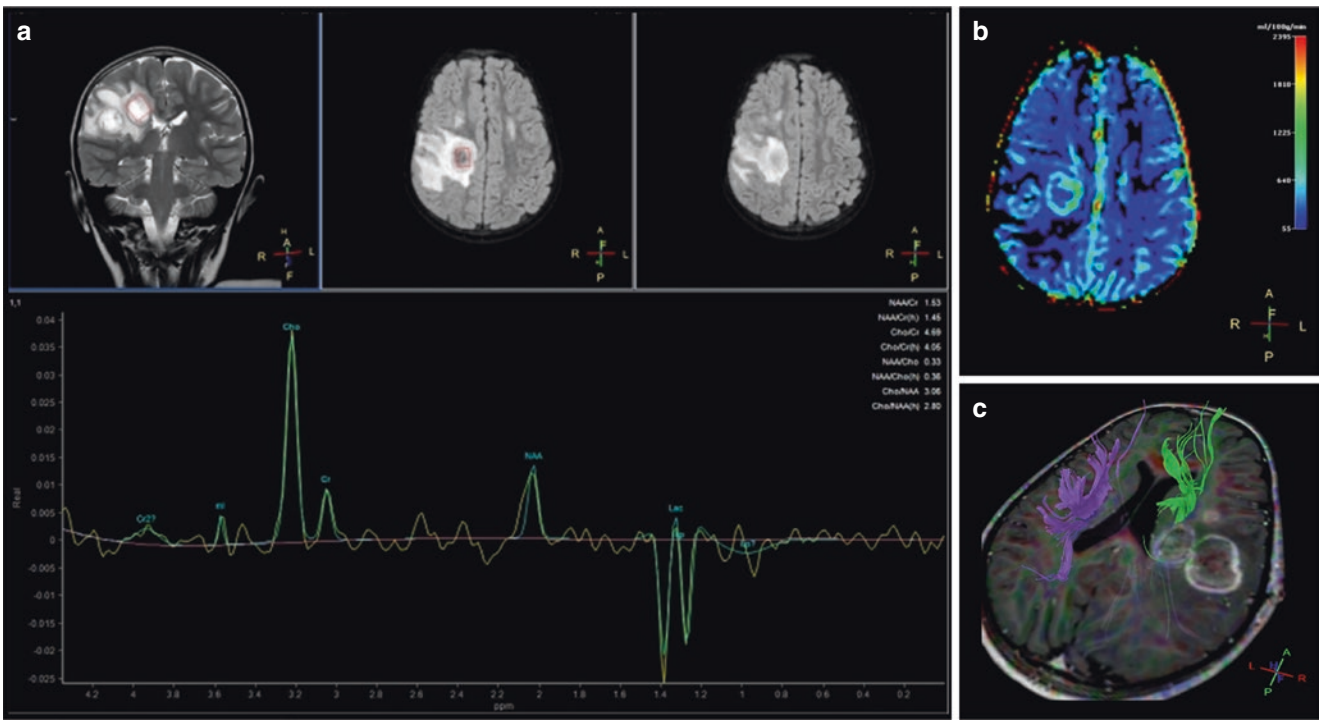

Fig. 6.2 Preoperative imaging *single-voxel MR spectroscopy* (**a**). The ROI placed on the enhancing lesion shows marked elevation of the Cho peak and reduced NAA with metabolic ratios consistent with a high-grade lesion. Increased Lac-Lip peak is observed, indicative of necrotic-colliquative phenomena. *MR perfusion study with relative CBV map* (**b**) shows an increase in perfusion at the margins of cystic components. *DTI MR tractography* (**c**) shows the impairment of the corticospinal fibers

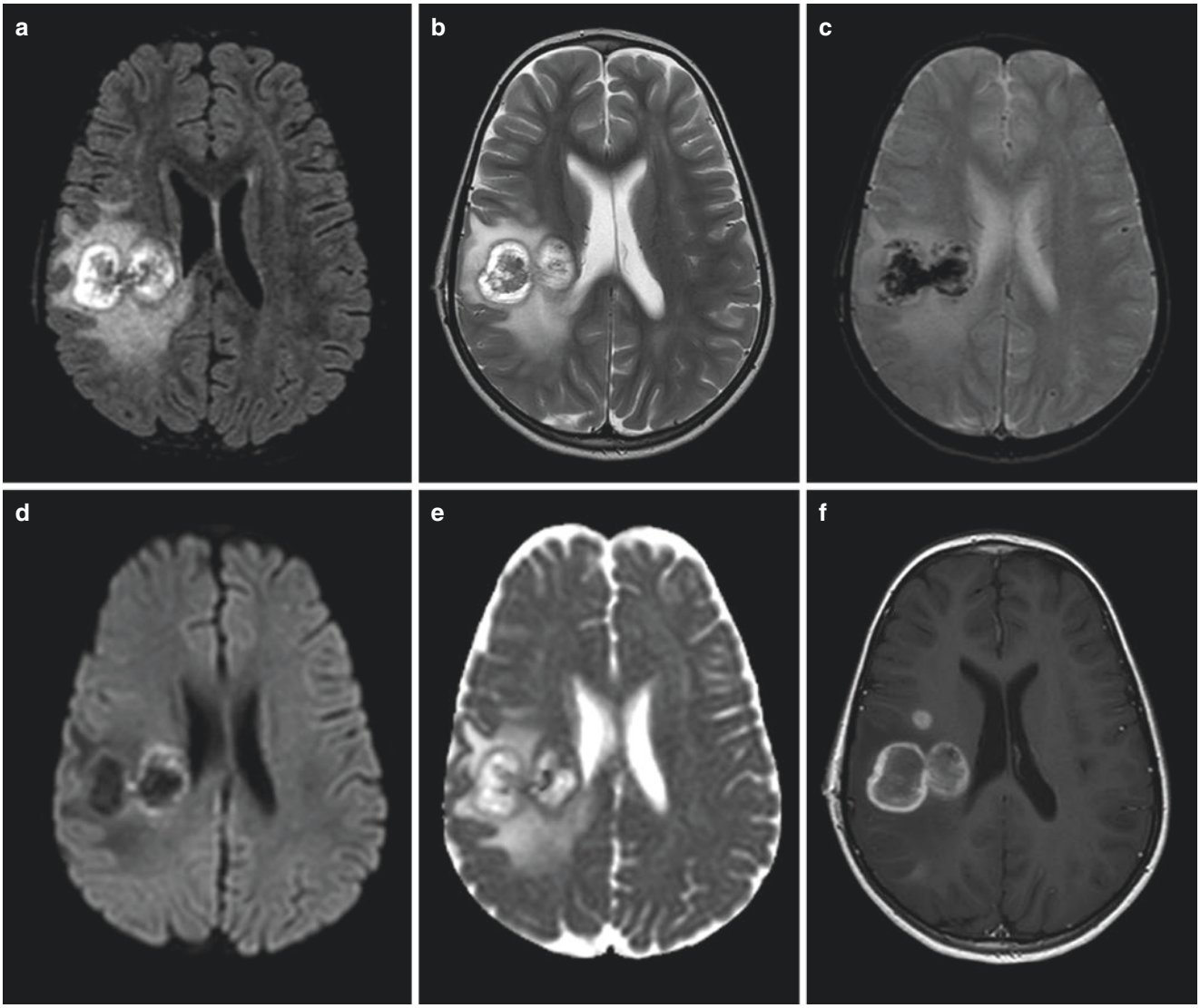

Fig. 6.3 Early postoperative follow-up. *Axial FLAIR* (**a**), *T2-weighted* (**b**), *T2∗-weighted* (**c**), *DWI-b1000* (**d**), *ADC map* (**e**), *contrast-enhanced MR SE T1-weighted* (**f**) *sequences.* Few days after needle biopsy, worsening of clinical status is observed. Signs of bleeding can be seen along the path of the biopsy, with blood–fluid collections in the cystic areas of lesion

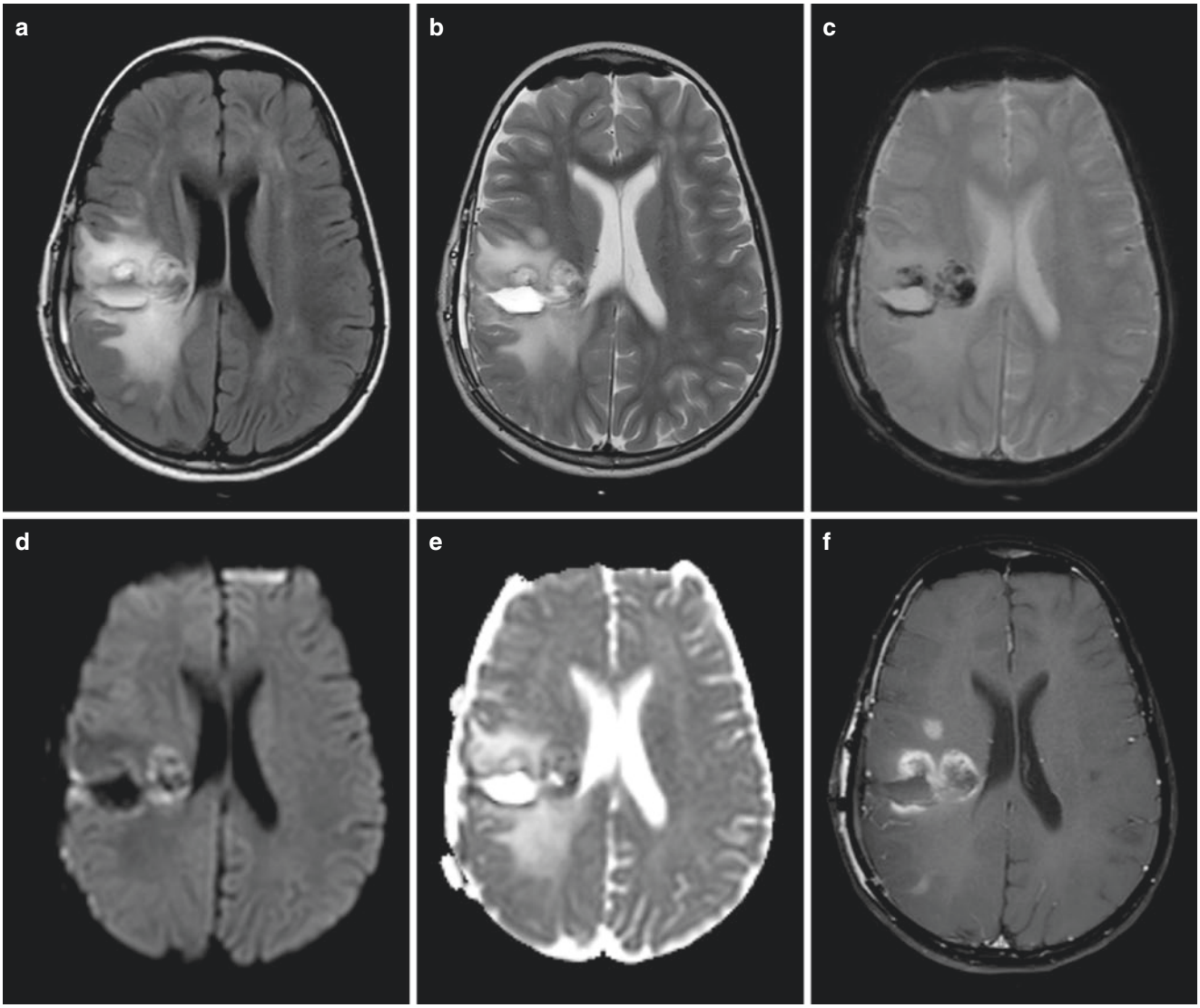

Fig. 6.4 Early postoperative follow-up. *Axial FLAIR* (**a**), *T2-weighted* (**b**), *T2∗-weighted* (**c**), *DWI-b1000* (**d**), *ADC map* (**e**), *contrast-enhanced SE T1-weighted* (**f**) *sequences.* On postoperative MR study, performed the day after the partial evacuation of the hematoma, the surgical cavity appears inhomogeneous containing mixture of blood–fluid components with residual hemorrhagic signal at the tissutal rim. There is a small amount of extracerebral air in frontal pole. A thin layer of blood–fluid collection is observed below the bone flap of craniotomy, well repositionated. Subgaleal drainage above the bone flap is also shown

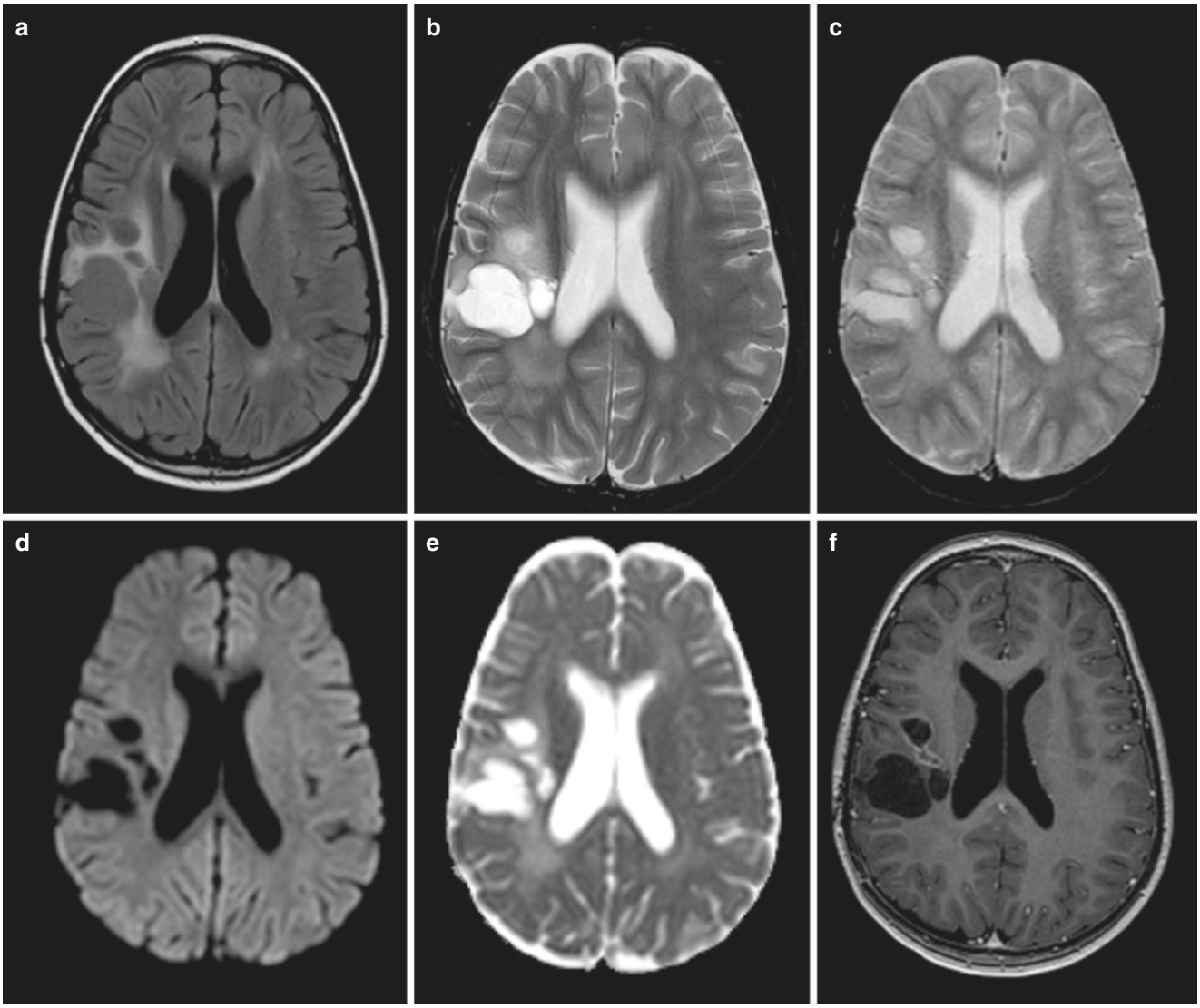

Fig. 6.5 Follow-up at 4 months after surgery, radiation therapy. *Axial FLAIR* (**a**), *T2-weighted* (**b**), *T2∗-weighted* (**c**), *DWI-b1000* (**d**), *ADC map* (**e**), *contrast-enhanced SE T1-weighted* (**f**) *sequences*. Evident resorption of the intralesional blood collections and disappearance of the solid margins of the necrotic-cystic components; slight residual inhomogeneous signal is observed in the surgical cavity. Cystic transformation of the anterior nodule and neighboring white matter is observed, due to loss of solid tissue; slight peripheral rim enhancement is present, produced by the blood–brain barrier injury. FLAIR images show a small amount of residual perilesional edema, coexisting with confluent hyperintensity within the deep white substance due to radiotherapy, as well as a slight enlargement of the ventricles

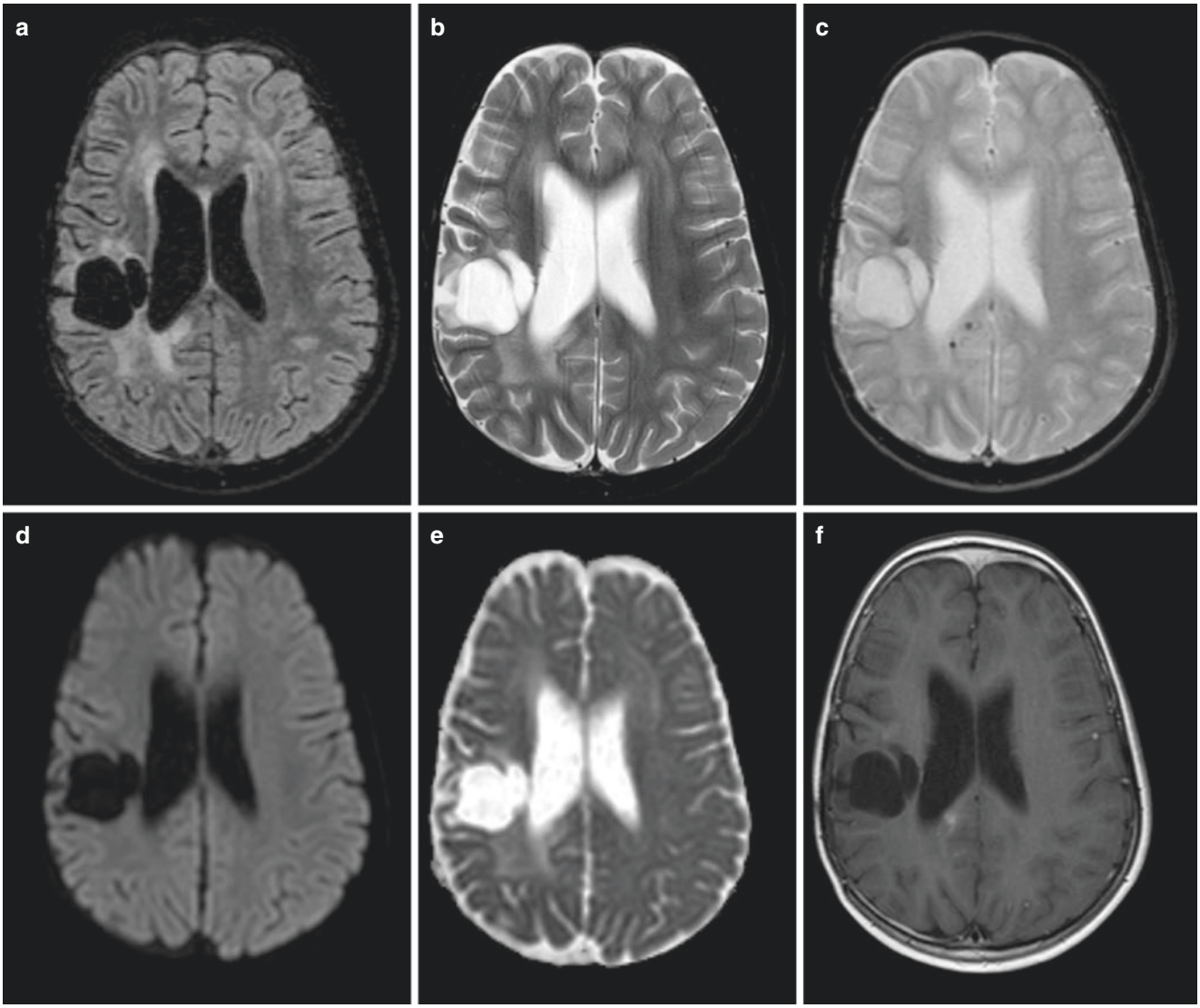

Fig. 6.6 Follow-up at 7 months after surgery, radiation therapy. *Axial FLAIR* (**a**), *T2-weighted* (**b**), *T2∗-weighted* (**c**), *DWI-b1000* (**d**), *ADC map* (**e**), *contrast-enhanced SE T1-weighted* (**f**) *sequences*. Slight further enlargement of the cavity in response to therapy is observed, with a prevalent CSF content. No areas of pathologic enhancement can be seen within the lesion. Further progression of the radiation-induced phenomena is evident at the deep white matter extending to the corpus callosum, where small foci of hypointensity on T2∗ images and patchy enhancement are observed, due to related microangiopathy

Early Complications: Perilesional Ischemia—Postoperative MR Follow-Up in Glioblastoma Multiforme

Case 7

Ferdinando Caranci, Enrico Tedeschi, and Arturo Brunetti

- Patient with surgically treated right temporal glioblastoma multiforme.
- Postoperative MR follow-up performed early (5 days) with morphologic sequences and diffusion-weighted imaging.

Preoperative Imaging

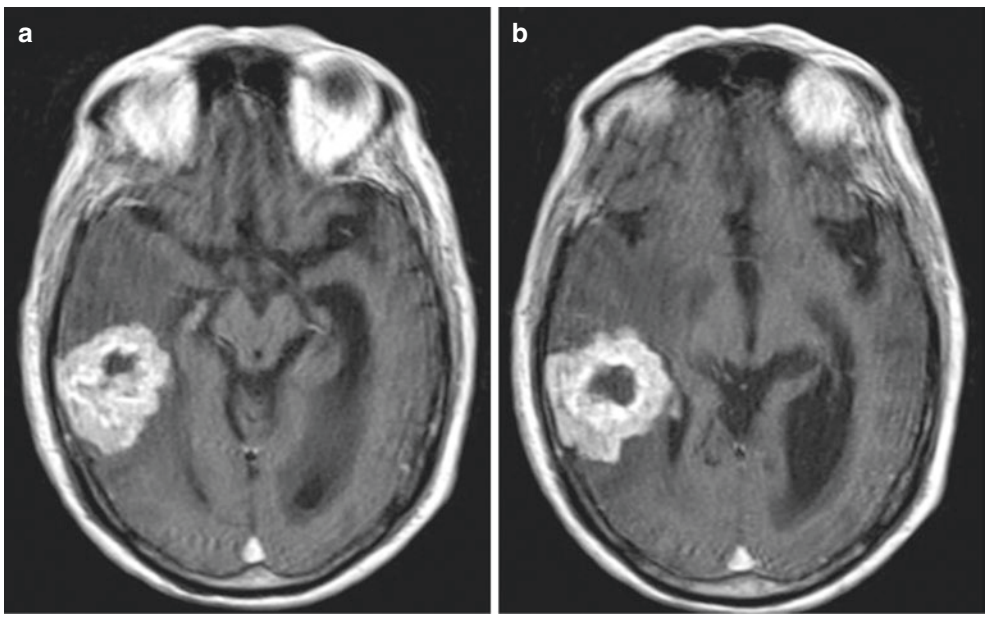

Fig. 7.1 (**a**–**d**) Contrast-enhanced MR SE T1-weighted images. Despite the presence of motion artifacts, an intra-axial lesion with irregular margins and heterogeneous structure due to the coexistence of a necrotic component can be appreciated in the right posterior temporal region

F. Caranci (✉) · E. Tedeschi · A. Brunetti
Department of Precision Medicine, School of Medicine, University of Campania "Luigi Vanvitelli", Naples, Italy

T. Scarabino, S. Pollice (eds.), *Imaging Gliomas After Treatment*, https://doi.org/10.1007/978-3-030-31210-7_17

Fig. 7.1 (continued)

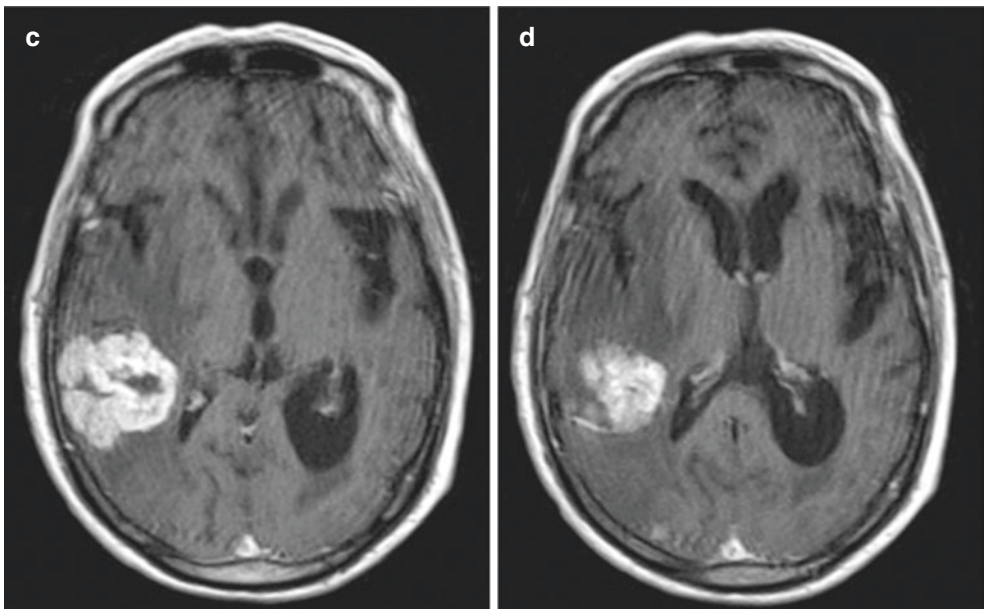

Early Postoperative Follow-Up (at 5 Days)

Fig. 7.2 (**a**–**d**) MR FLAIR sequence. The postoperative cavity filled with CSF is clearly shown, peripheral to which a diffuse signal alteration due to edema can be seen, with focal areas of partial blood effusion

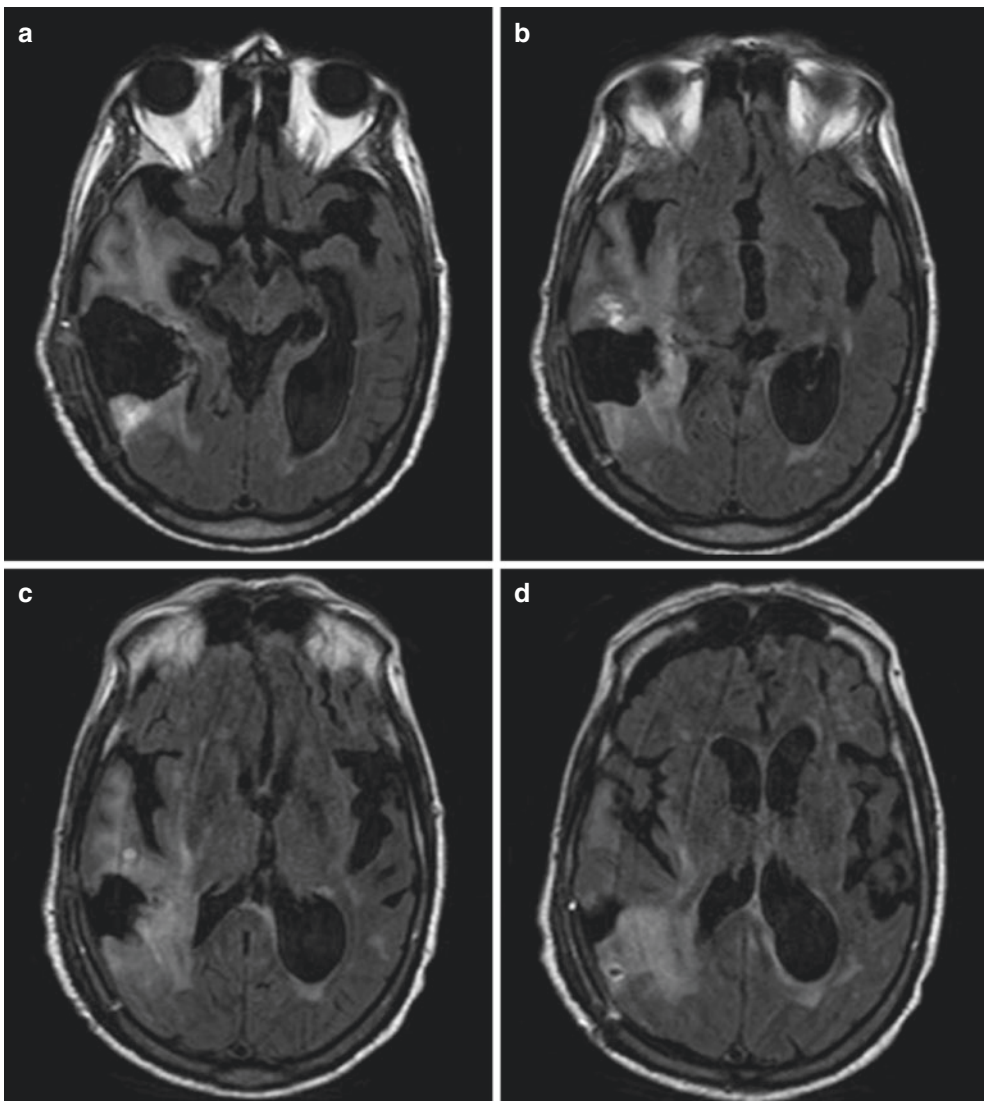

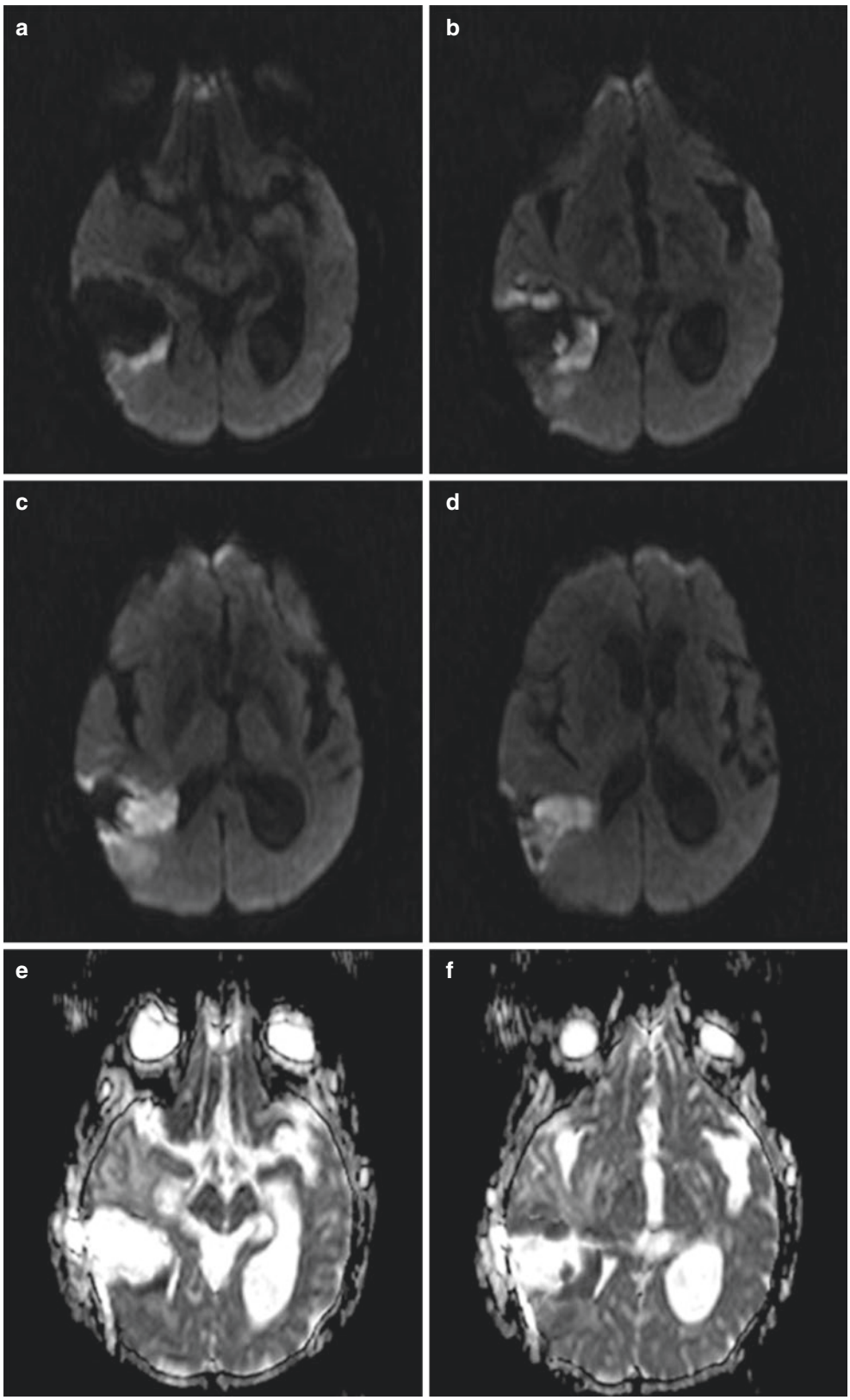

Fig. 7.3 (**a**–**h**) DWI with ADC maps. The postoperative cavity filled with CSF is surrounded by tissue with restricted diffusion, suggestive of ischemic changes

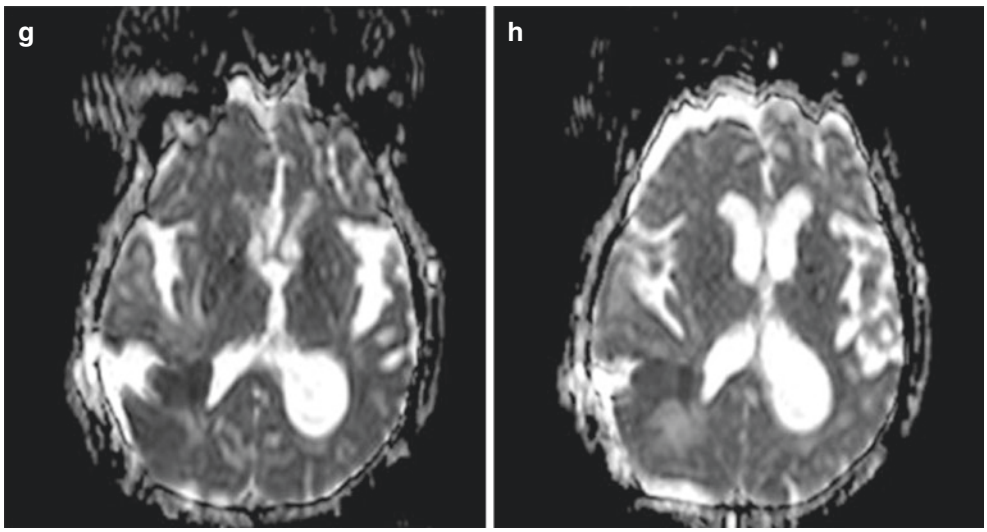

Fig. 7.3 (continued)

Late Complications: Subdural Empyema — CT/MR Follow-Up in Glioblastoma Multiforme

Case 8

Alessandro Stecco, Francesco Fabbiano, Mariangela Lombardi, Sara Zizzari, Gerardo Di Nardo, Andrea Pietro Sponghini, Lucrezia Emanuela Guerra, and Alessandro Carriero

- 30-year-old patient with right frontal glioblastoma multiforme treated with surgery and combined radiation therapy–chemotherapy.
- Morphologic CT/MR studies performed at 5 months (following diastasis of the craniotomy bone flap with underlying purulent collection and subsequent acrylic resin cranioplasty) and at 12 months after resection.

Postoperative Follow-Up at 5 Months

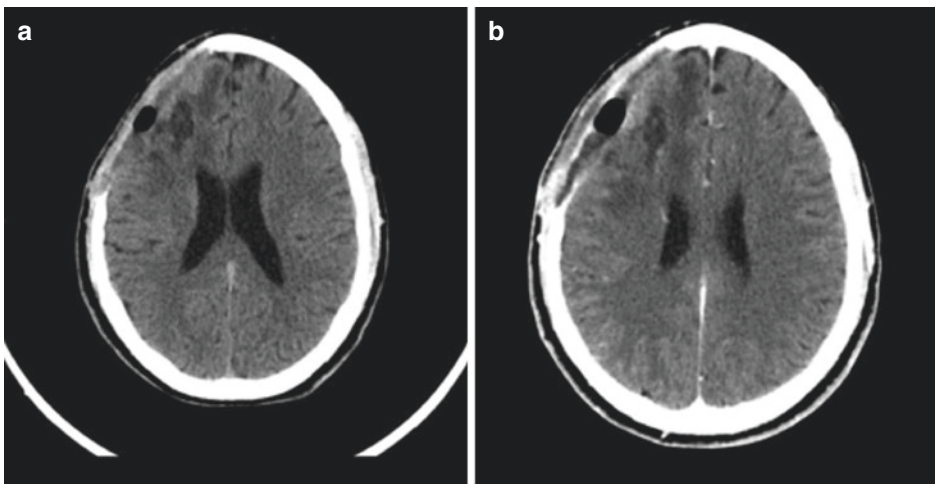

Fig. 8.1 (**a**, **b**) Contrast-enhanced CT scan shows craniotomy with removal of bone and the right frontal subdural postsurgical empyema

A. Stecco (✉)
Neuroradiology Unit, AOU "Maggiore della Carità", DIMET, Università del Piemonte Orientale, Novara, Italy
e-mail: alessandro.stecco@uniupo.it

F. Fabbiano
Department of Neuroradiology, I.R.C.C.S. INM Neuromed, Pozzilli, Isernia, Italy

Department of Diagnostic Imaging, Valmontone Hospital, Rome, Italy

Department of Radiology and Neuroradiology, Villa Benedetta, Rome, Italy

M. Lombardi
Department of Radiology, Cesena Hospital—AUSL Romagna, Cesena, Italy

S. Zizzari
Department of Radiology, Hospital "Sacred Heart of Jesus", ASL LECCE, Gallipoli, Italy

G. D. Nardo · A. Carriero
Department of Radiology, AOU Maggiore della Carità", DIMET, Università del Piemonte Orientale, Novara, Italy

A. P. Sponghini
Department of Oncology, AOU Maggiore della Carità, DIMET, Università del Piemonte Orientale, Novara, Italy

L. E. Guerra
Department of Radiology, Hospital "Carlo Poma", ASST Mantova, Mantova, Italy

T. Scarabino, S. Pollice (eds.), *Imaging Gliomas After Treatment*, https://doi.org/10.1007/978-3-030-31210-7_18

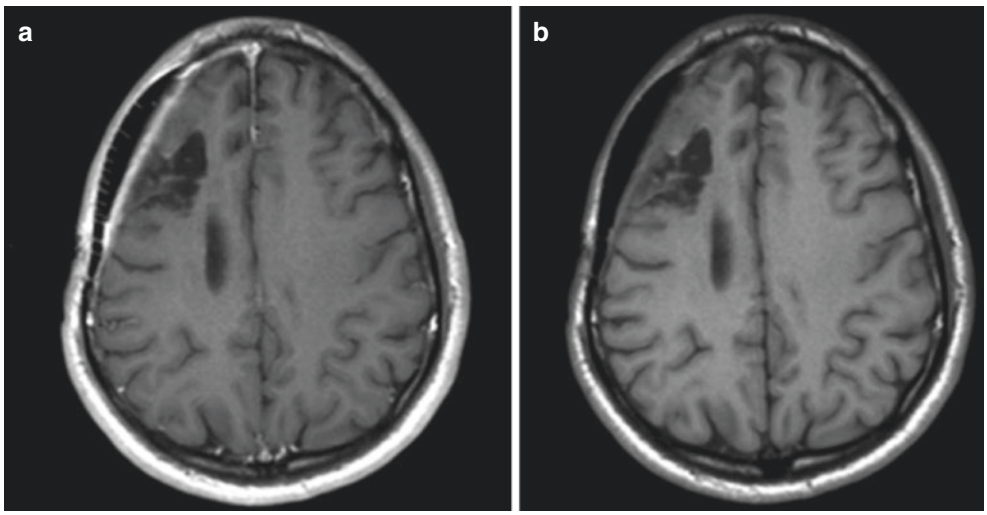

Fig. 8.2 (**a**, **b**) Contrast-enhanced MR SE T1-weighted sequences show the presence of pathologic epidural enhancement and more evidence of the gaseous component which compresses the soft tissue overlying the subdural empyema

Late Complications: Abscess—Postoperative MR Follow-Up in Glioblastoma Multiforme

Case 9

Ferdinando Caranci, Alessandra D'Amico, and Sossio Cirillo

- Patient with surgically treated right fronto-parieto-temporal glioblastoma multiforme.
- Late postoperative MR imaging with morphologic sequences and diffusion-weighted imaging.

Late Postoperative Follow-Up

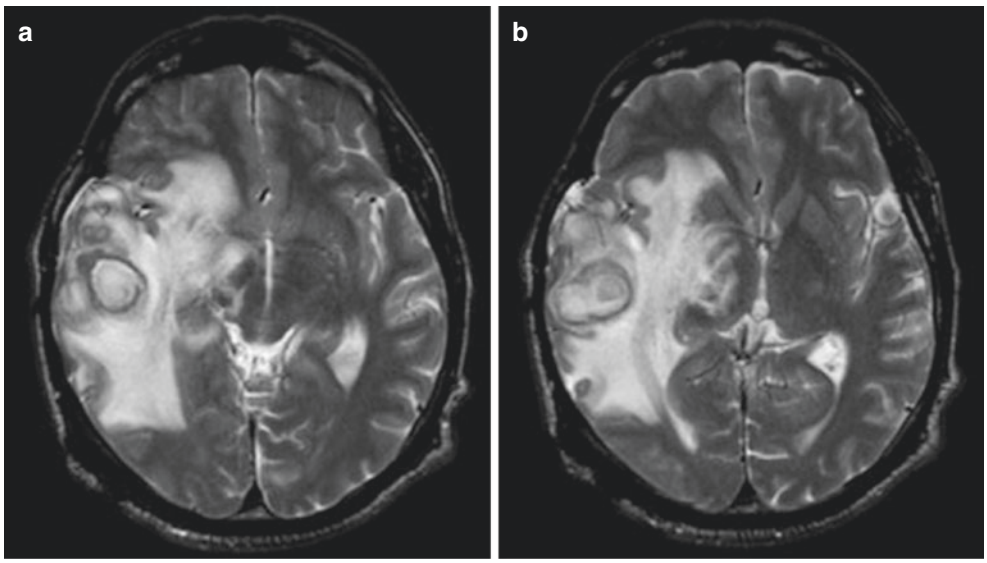

Fig. 9.1 (**a**-**d**) MR FSE T2-weighted sequence. The images show evidence of the previous right fronto-parieto-temporal craniotomy performed for the surgical excision of glioblastoma multiforme. Below the bone flap a lobulated structure can be appreciated, with inhomogeneously hyperintense fluid-type signal and a hypointense peripheral capsule, surrounded by a broad halo of edema

F. Caranci (✉) · A. D'Amico
Department of Precision Medicine, School of Medicine, University of Campania "Luigi Vanvitelli", Naples, Italy

S. Cirillo
Department of Medicine and Health Sciences "V. Tiberio", University of Molise, Campobasso, Italy

T. Scarabino, S. Pollice (eds.), *Imaging Gliomas After Treatment*, https://doi.org/10.1007/978-3-030-31210-7_19

Fig. 9.1 (continued)

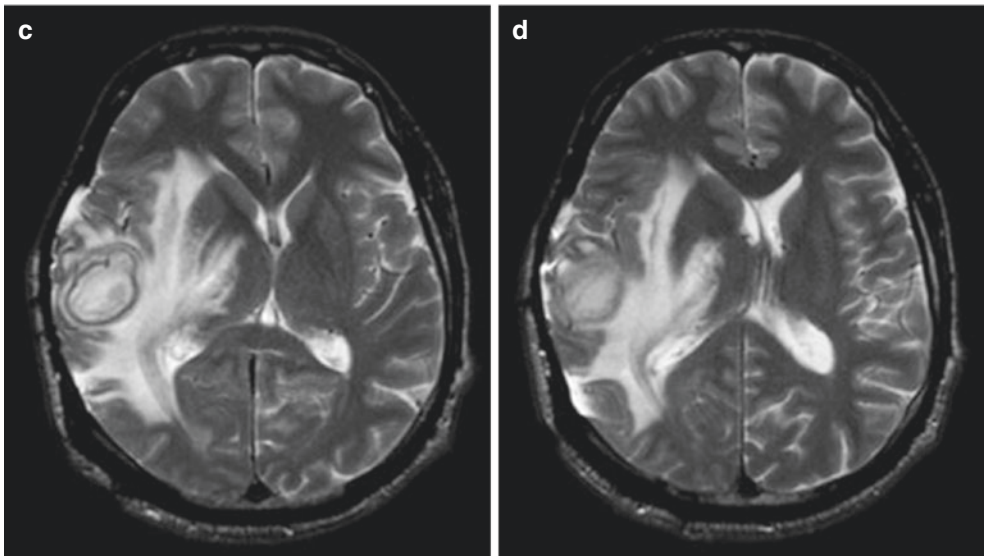

Fig. 9.2 (**a**-**d**) Contrast-enhanced MR SE T1-weighted images. The images show intense enhancement of the peripheral capsule

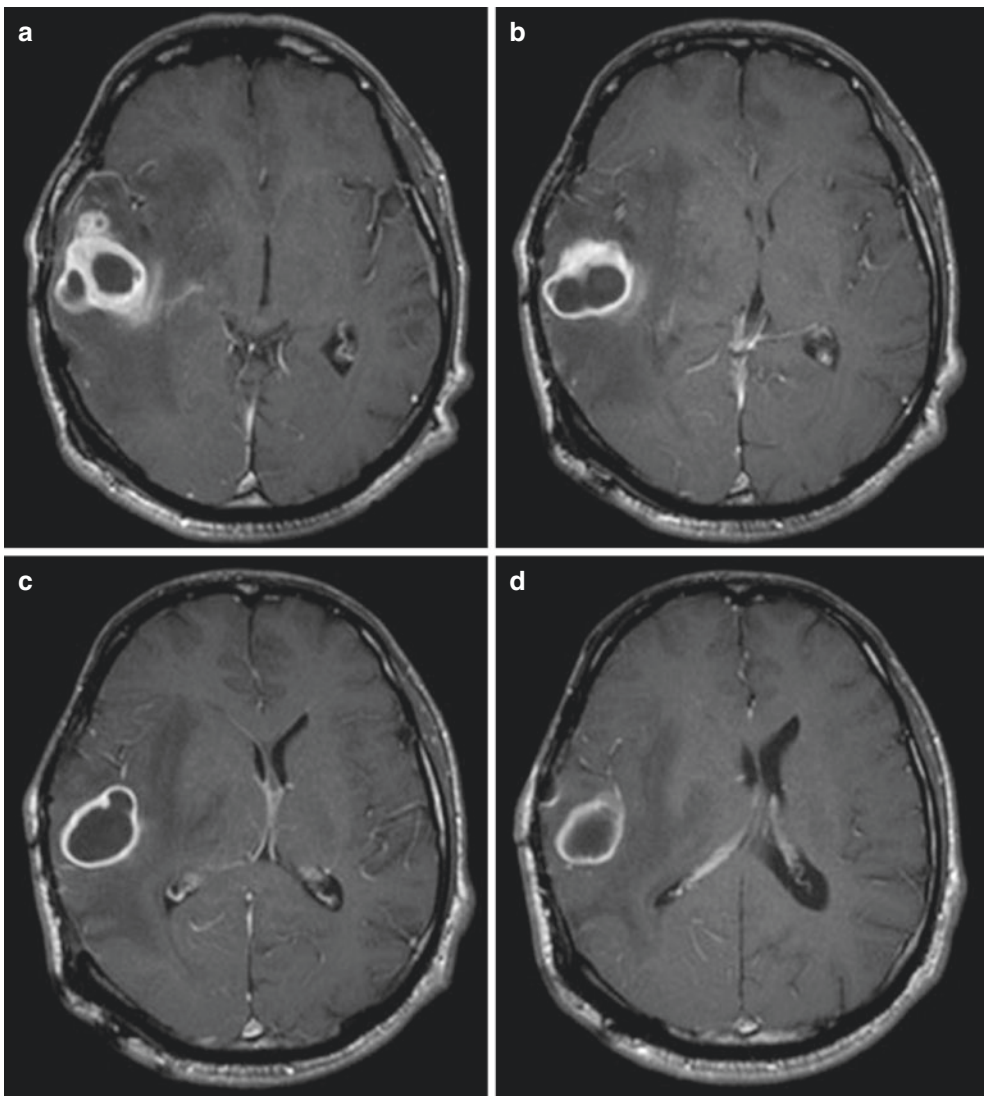

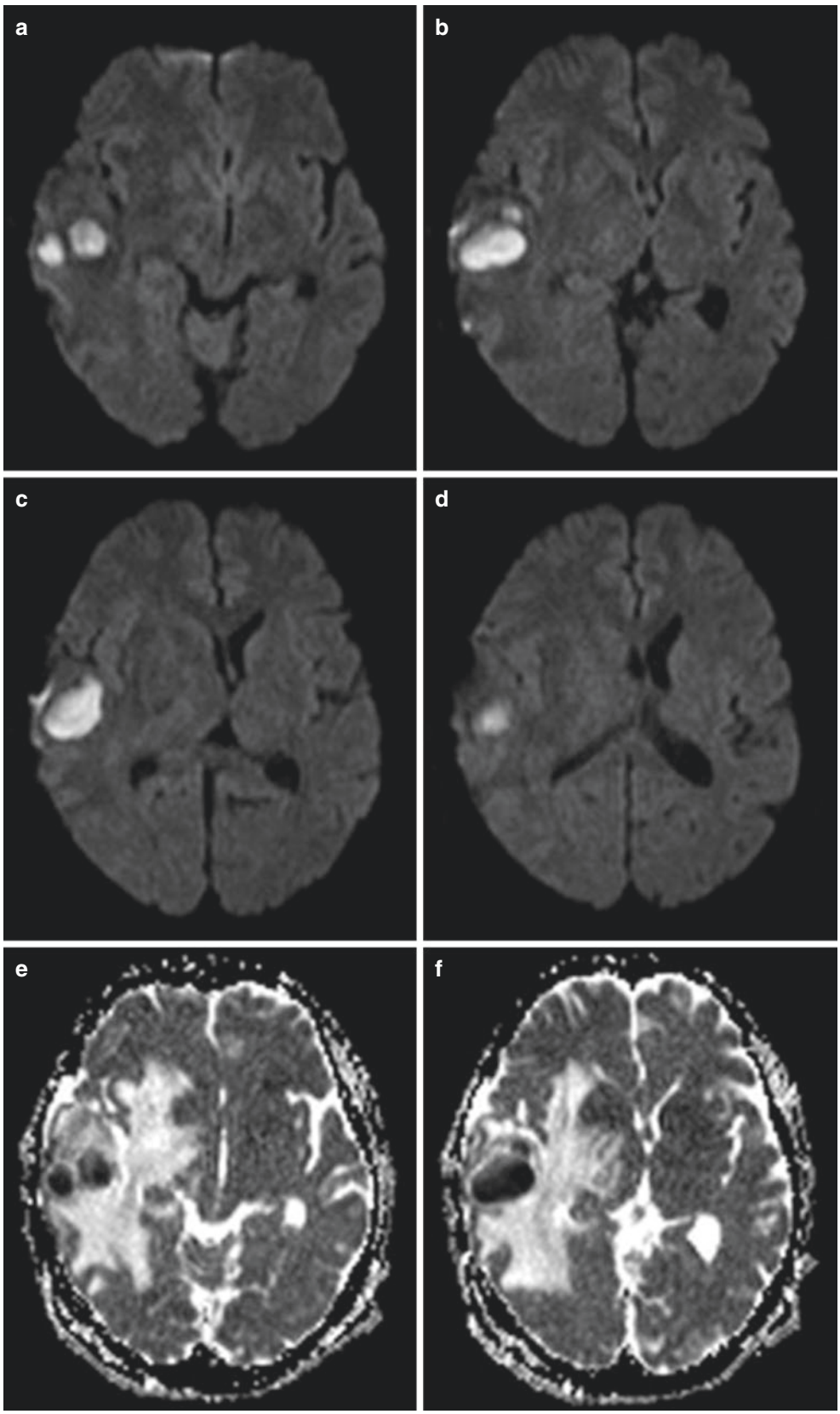

Fig. 9.3 (**a**-**h**) MR diffusion-weighted imaging and ADC map. The fluid content within the lesion has greatly restricted diffusion coefficients due to its high viscosity

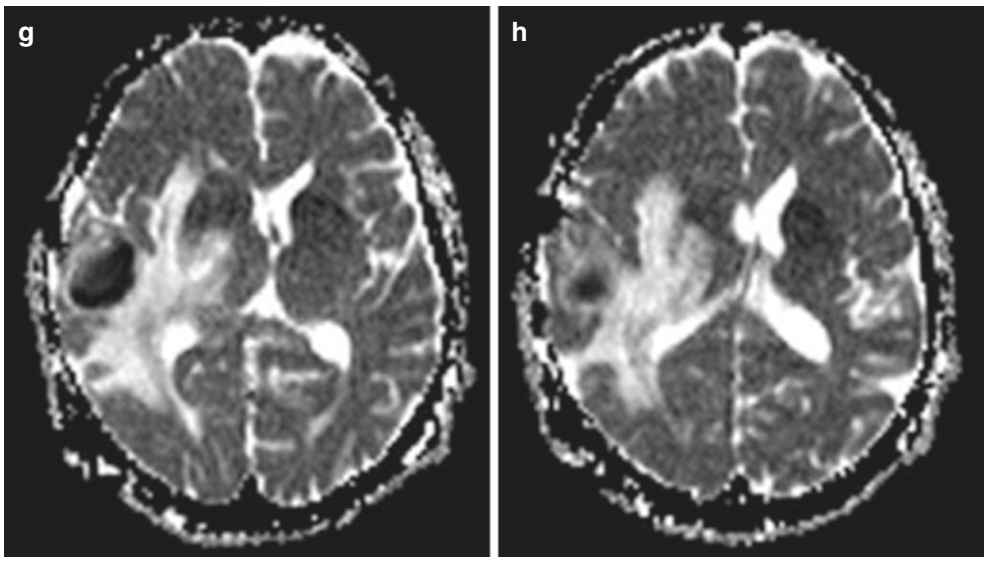

Fig. 9.3 (continued)

Early Residual Tumor: Postoperative MR Follow-Up in Glioblastoma Multiforme

Case 10

Luigi Cirillo, Antonella Bacci, Raffaele Agati, and Marco Leonardi

- Patient with surgically treated right temporo-occipito-parietal glioblastoma multiforme.
- Postoperative follow-up performed early (24 hours and 2 weeks) with MR morphologic sequences.

Preoperative Imaging

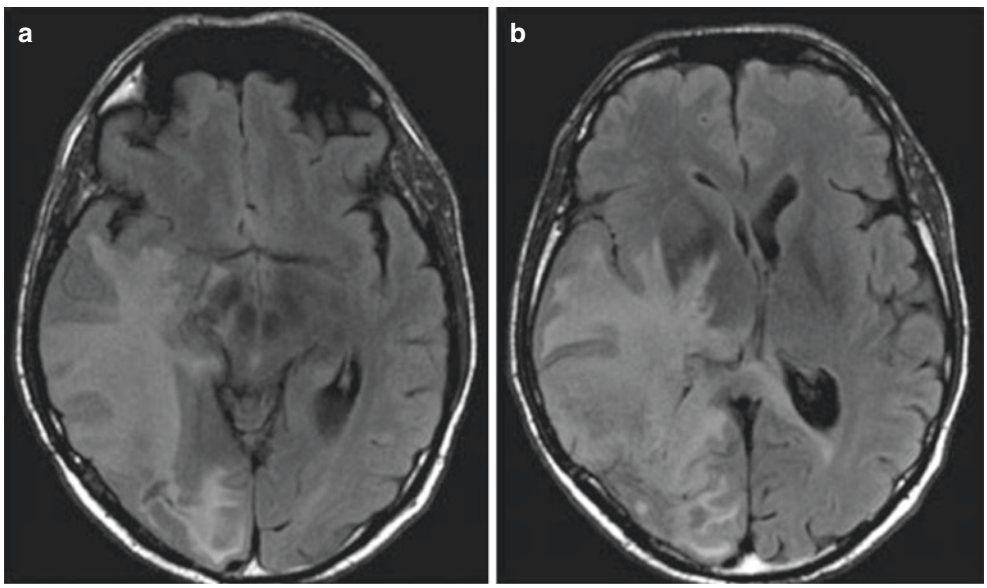

Fig. 10.1 (**a**–**d**) MR FLAIR sequence. A large area of high signal in the right temporo-occipito-parietal region is appreciable, with the characteristics of vasogenic edema extending contralaterally through the splenium of the corpus callosum. A relatively poorly defined hypointense tissue with infiltrating features is visualized

L. Cirillo (✉) · A. Bacci · R. Agati · M. Leonardi
Department of Neurological Sciences, Alma Mater University of Bologna, Bologna, Italy
e-mail: luigi.cirillo2@unibo.it

T. Scarabino, S. Pollice (eds.), *Imaging Gliomas After Treatment*, https://doi.org/10.1007/978-3-030-31210-7_20

Fig. 10.1 (continued)

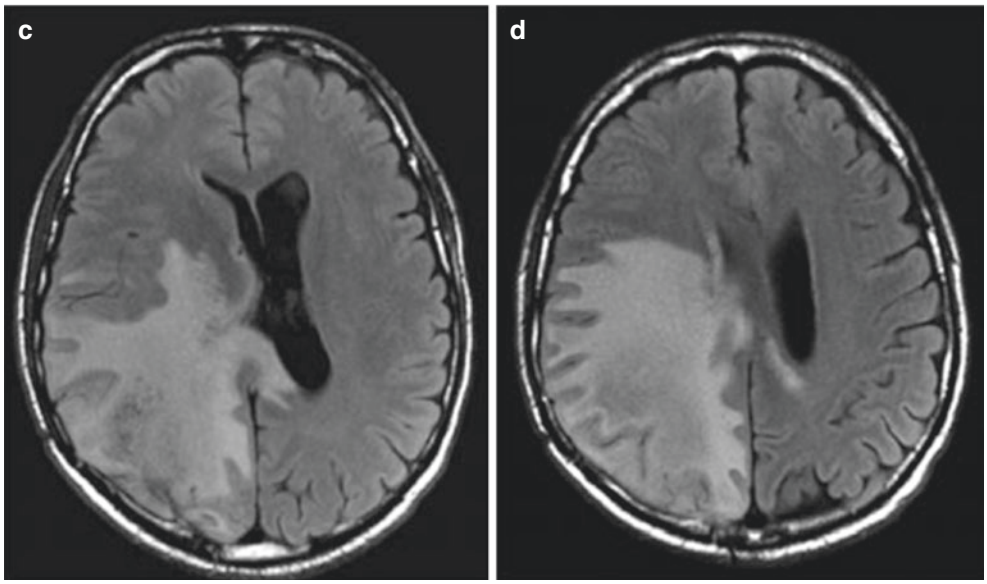

Fig. 10.2 (**a**–**d**) Contrast-enhanced MR SE T1-weighted images. Evidence of tissue with irregular margins, intense enhancement, and an internal necrotic component

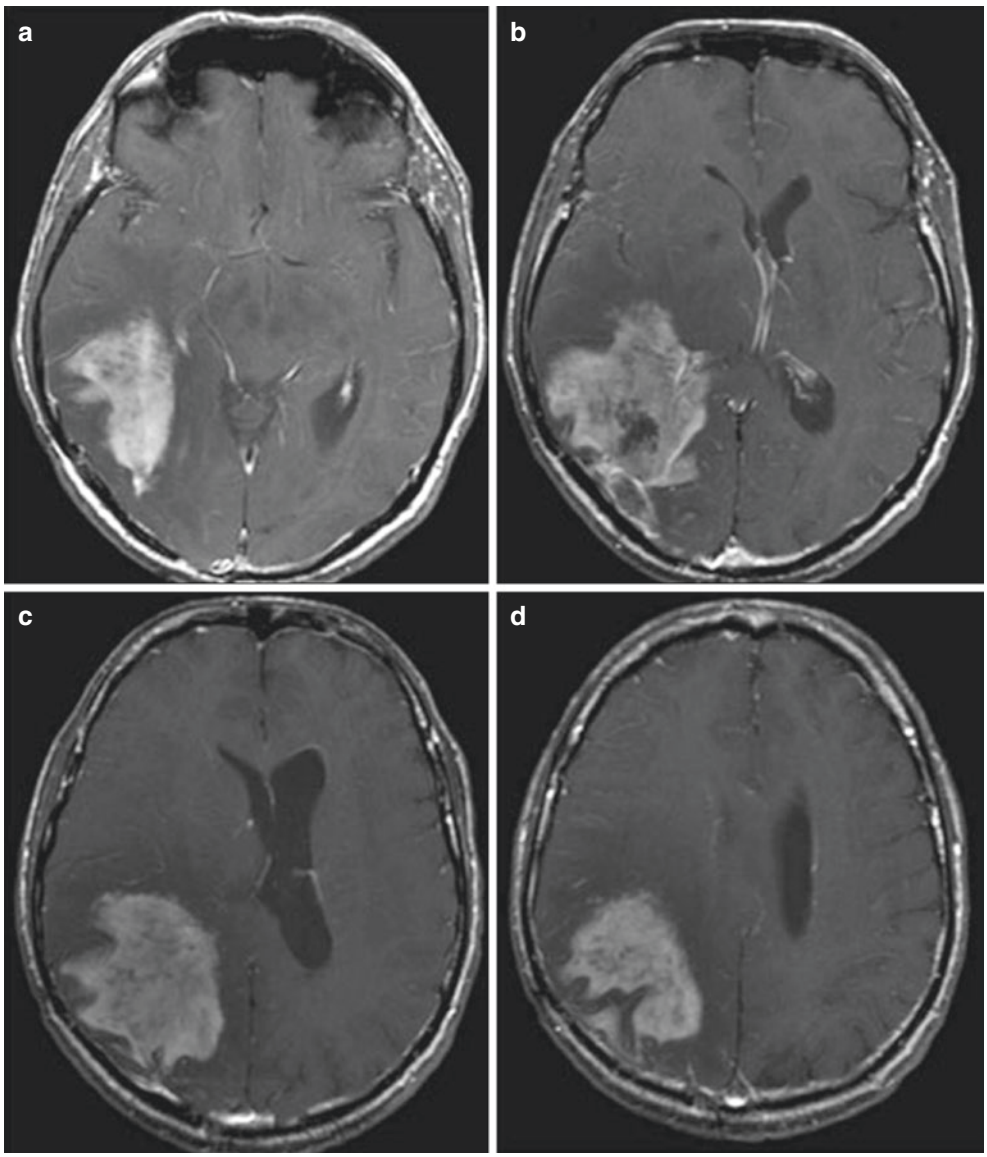

Postoperative Follow-Up at 24 h

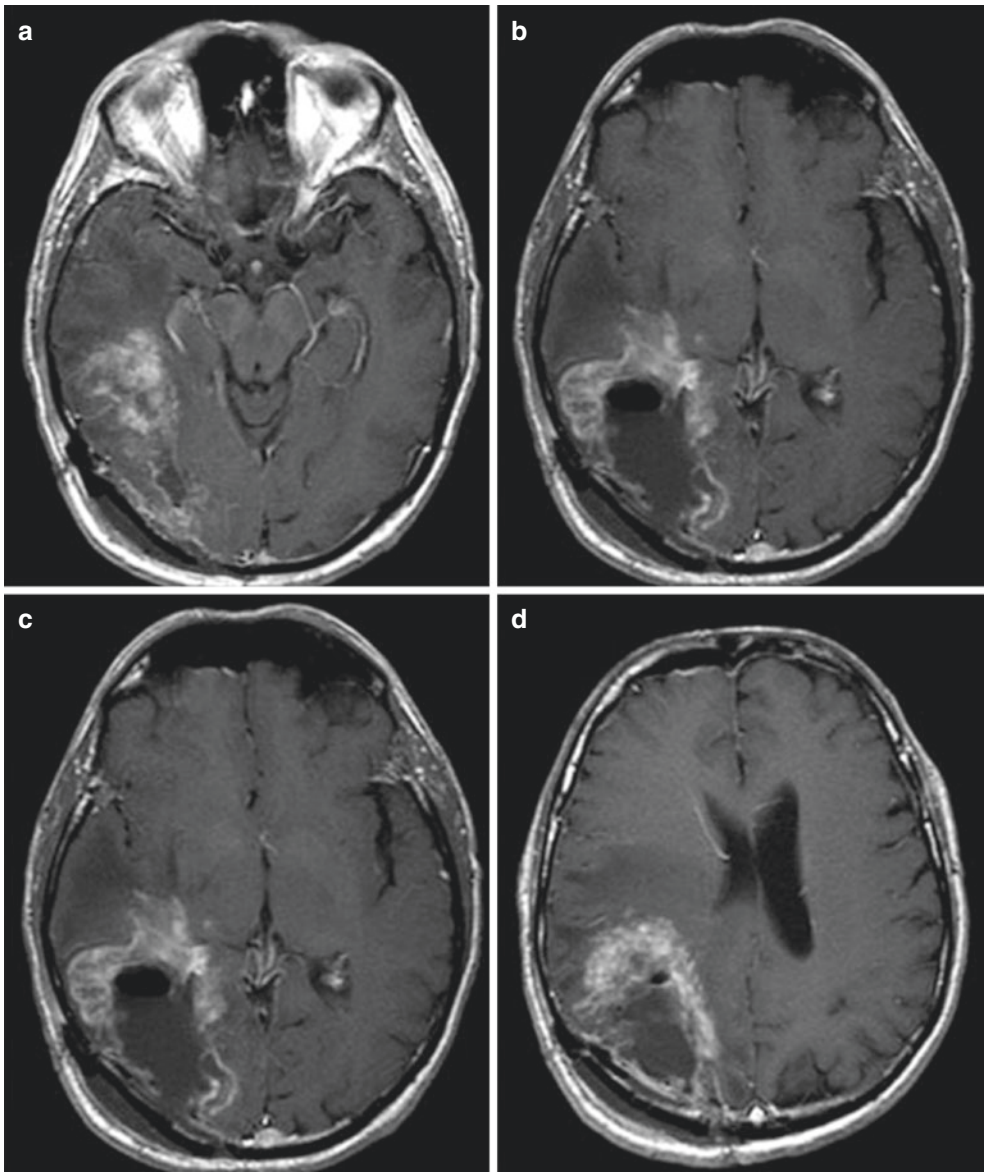

Fig. 10.3 (**a**–**d**) Contrast-enhanced MR SE T1-weighted images. The postsurgical cavity shows inhomogeneous fluid-like signal with air component. Peripheral to the cavity, there is an intense and irregular enhancement, indicative of the residual heteroplastic tissue (at this stage there are no changes in the blood–brain barrier)

Postoperative Follow-Up at 2 Weeks

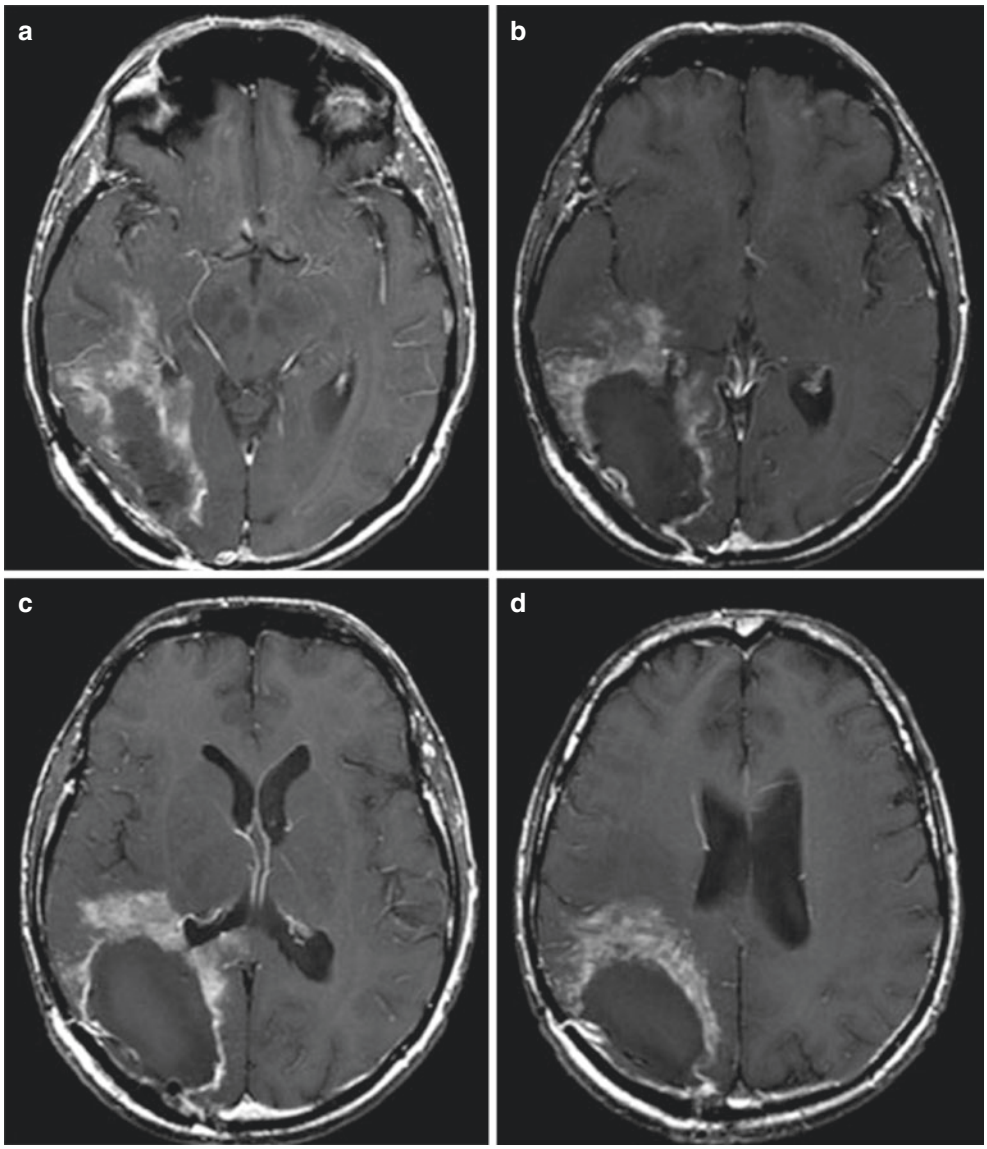

Fig. 10.4 (**a**–**d**) Contrast-enhanced MR SE T1-weighted images. The air component in the surgical cavity has been reabsorbed. The images confirm the presence of the peripheral heteroplastic tissue extending toward the splenium of the corpus callosum

Late Residual Tumor: Postoperative MR Follow-Up in Low-Grade Astrocytoma

Case 11

Ferdinando Caranci, Francesco Briganti, and Arturo Brunetti

- Patient with surgically treated right temporal grade II astrocytoma.
- Postoperative MR follow-up performed late (4 months) with MR morphologic sequences, spectroscopy, and PET.

Preoperative Imaging

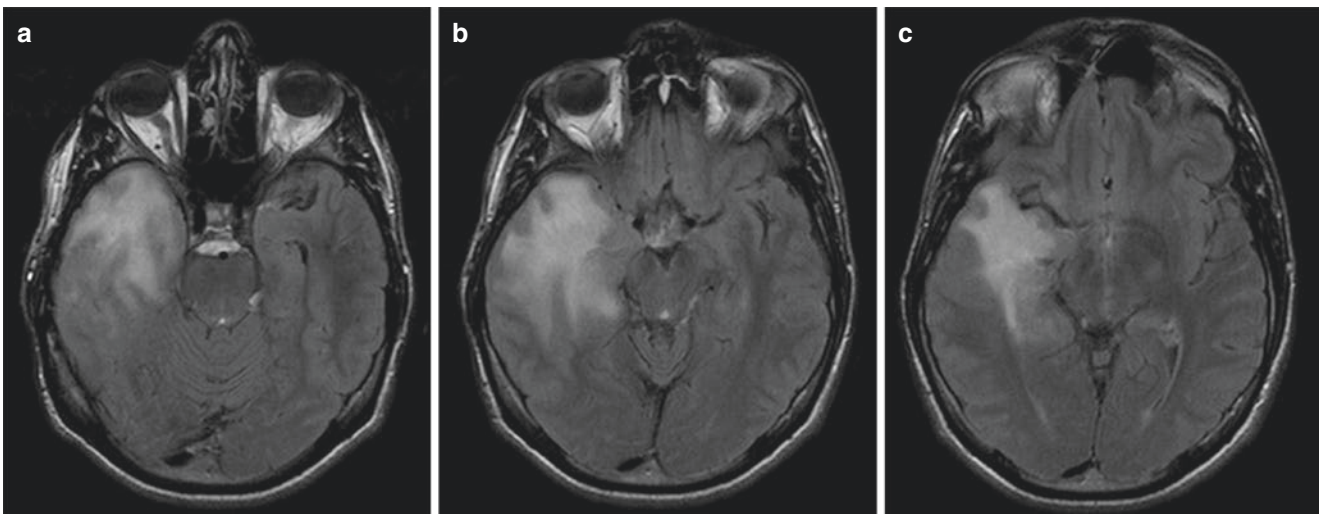

Fig. 11.1 (**a**–**c**) MR FLAIR sequence. Infiltrating tissue with high signal intensity can be appreciated in the right temporal region, indistinguishable from the associated edema, extending medially to the parahippocampal–hippocampal region

F. Caranci (✉) · F. Briganti · A. Brunetti
Department of Precision Medicine, School of Medicine, University of Campania "Luigi Vanvitelli", Naples, Italy

T. Scarabino, S. Pollice (eds.), *Imaging Gliomas After Treatment*, https://doi.org/10.1007/978-3-030-31210-7_21

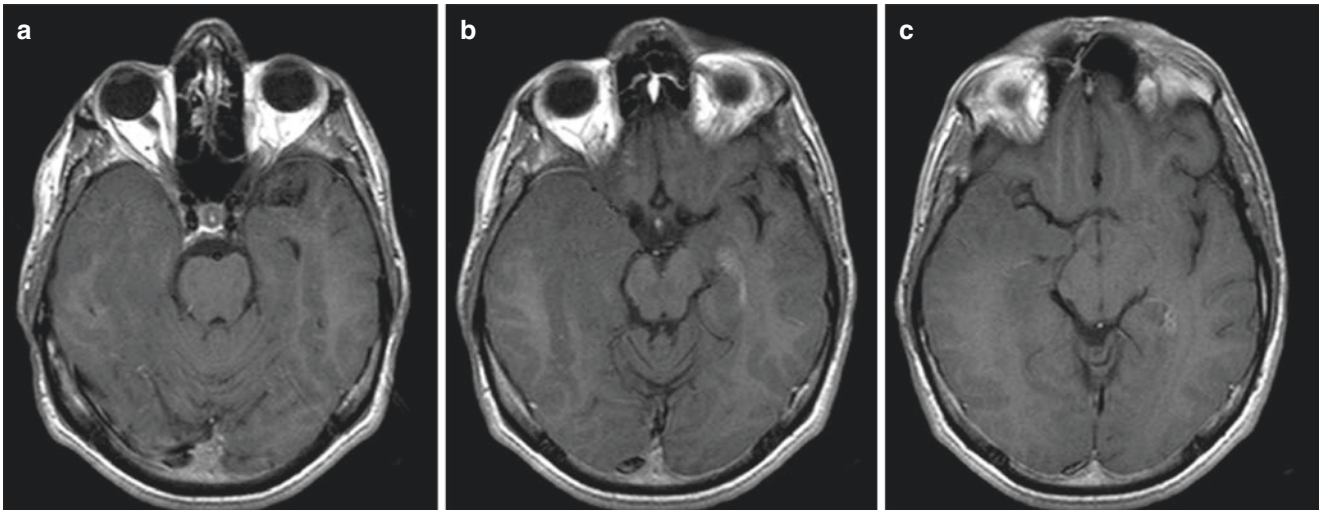

Fig. 11.2 (**a**–**c**) Contrast-enhanced MR SE T1-weighted images. No enhancement is appreciable after the administration of contrast medium

Postoperative Follow-Up at 4 Months

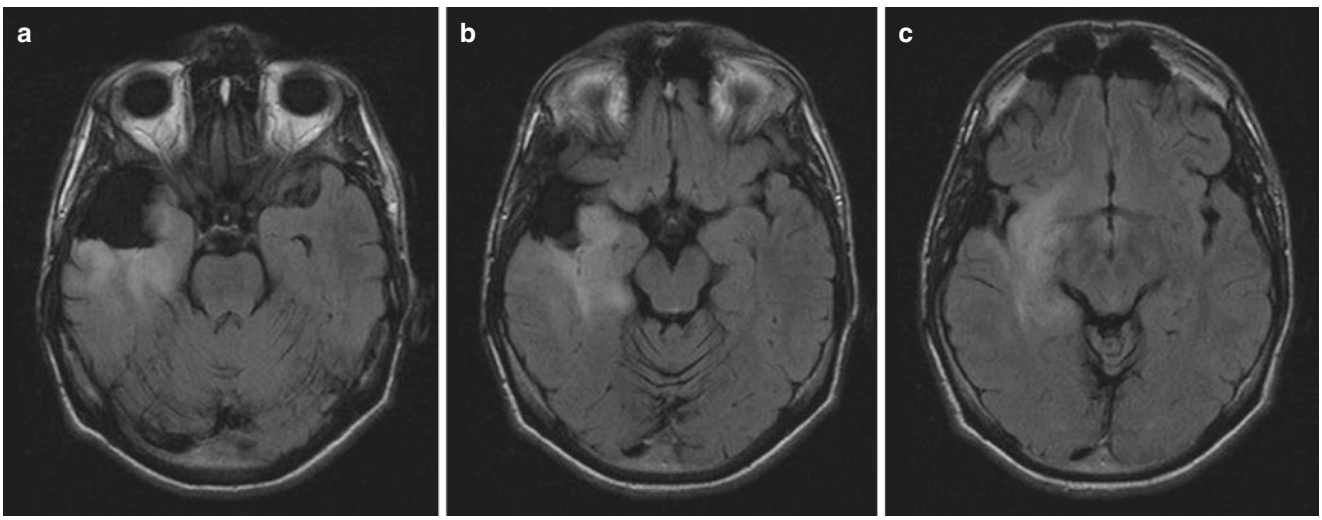

Fig. 11.3 (**a**–**c**) MR FLAIR sequence. Hyperintense signal indicative of residual neoplastic tissue can be appreciated peripheral to the area of CSF-like signal produced by the postsurgical cavity

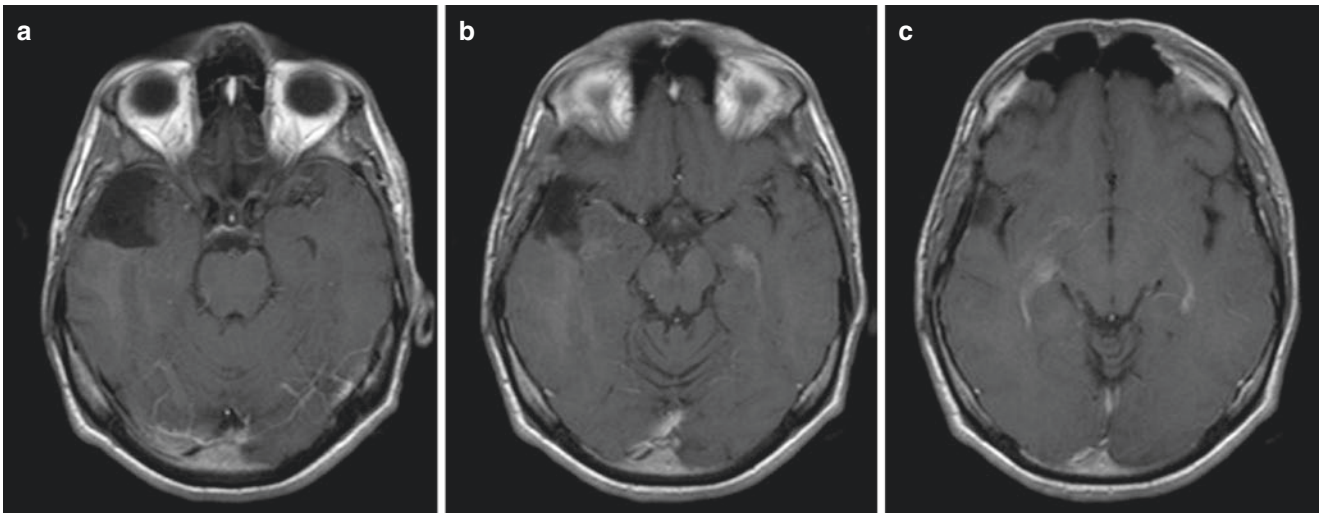

Fig. 11.4 (**a**–**c**) Contrast-enhanced MR SE T1-weighted images. The study confirms the absence of contrast enhancement of the residual tumor

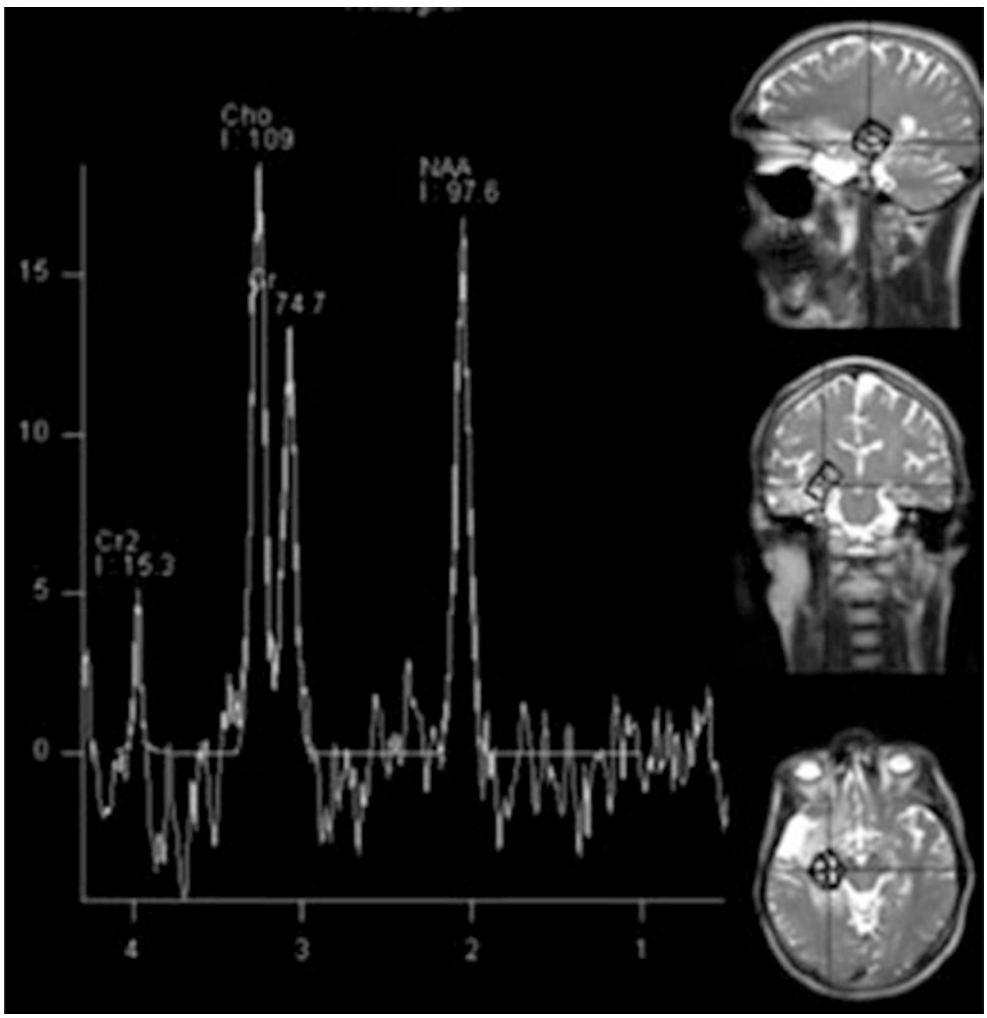

Fig. 11.5 Single-voxel MR spectroscopy. Inversion of the choline–creatine peak level in the residual tumor can be appreciated

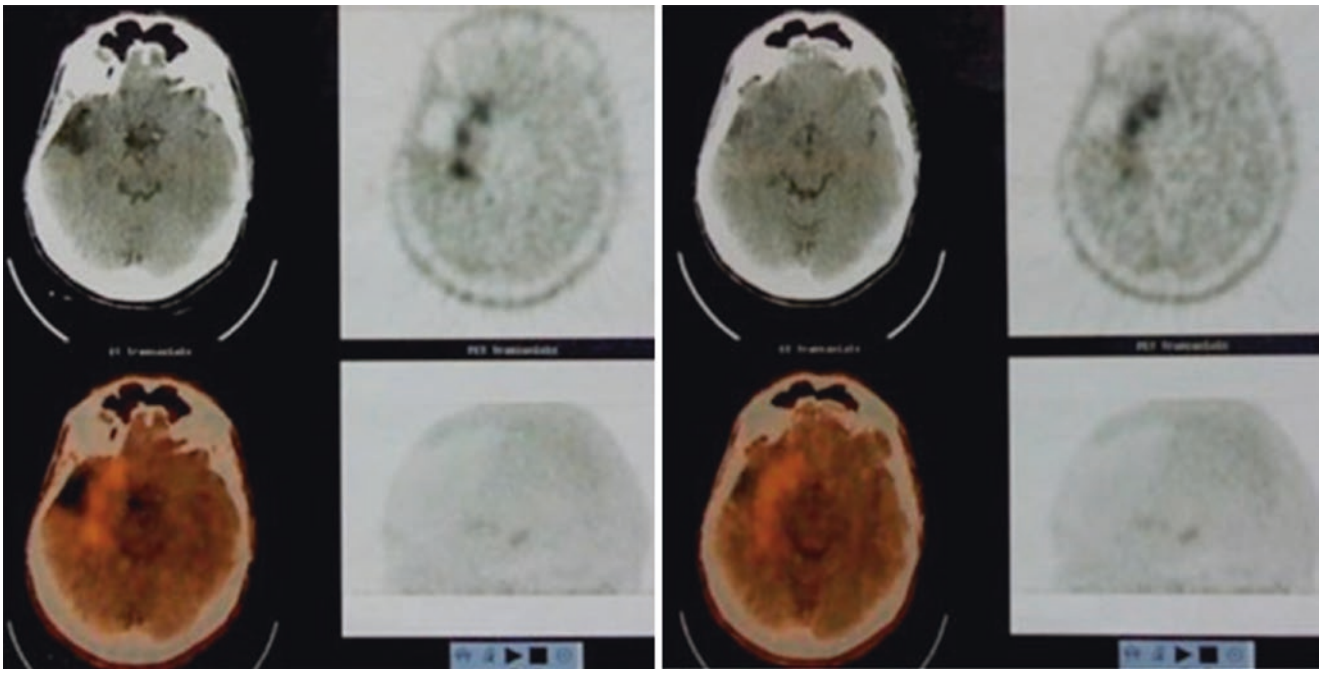

Fig. 11.6 Methionine PET study. The residual tissue shows high metabolic activity

Postoperative Follow-Up at 4 Years

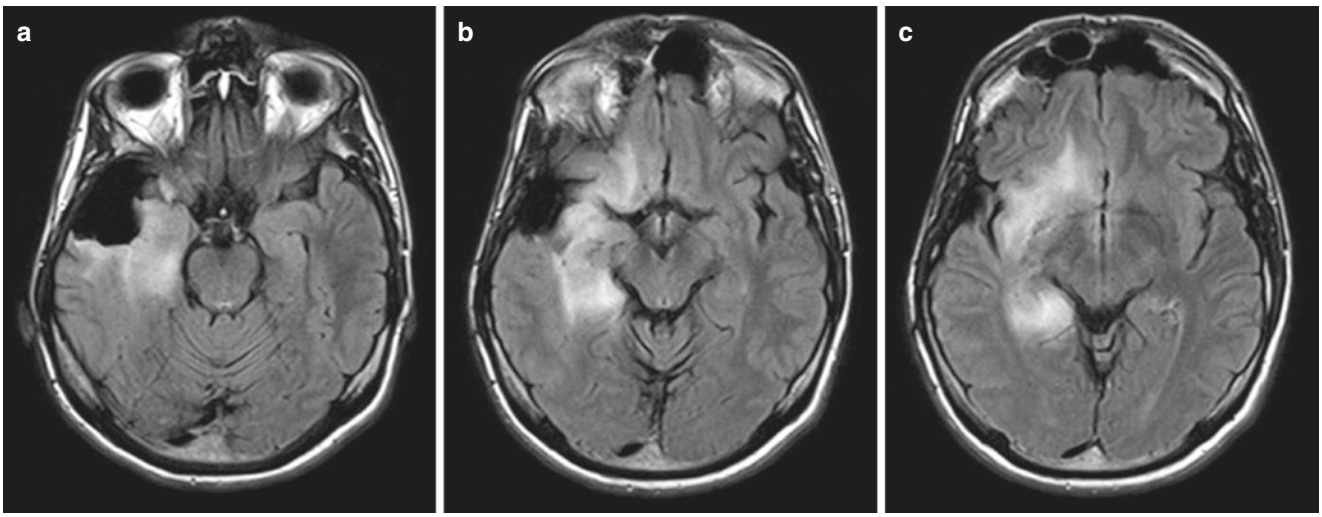

Fig. 11.7 (**a**–**c**) MR FLAIR sequence. The images show an increase of the infiltrating tissue, which extends to the temporal-mesial and frontal-basal regions

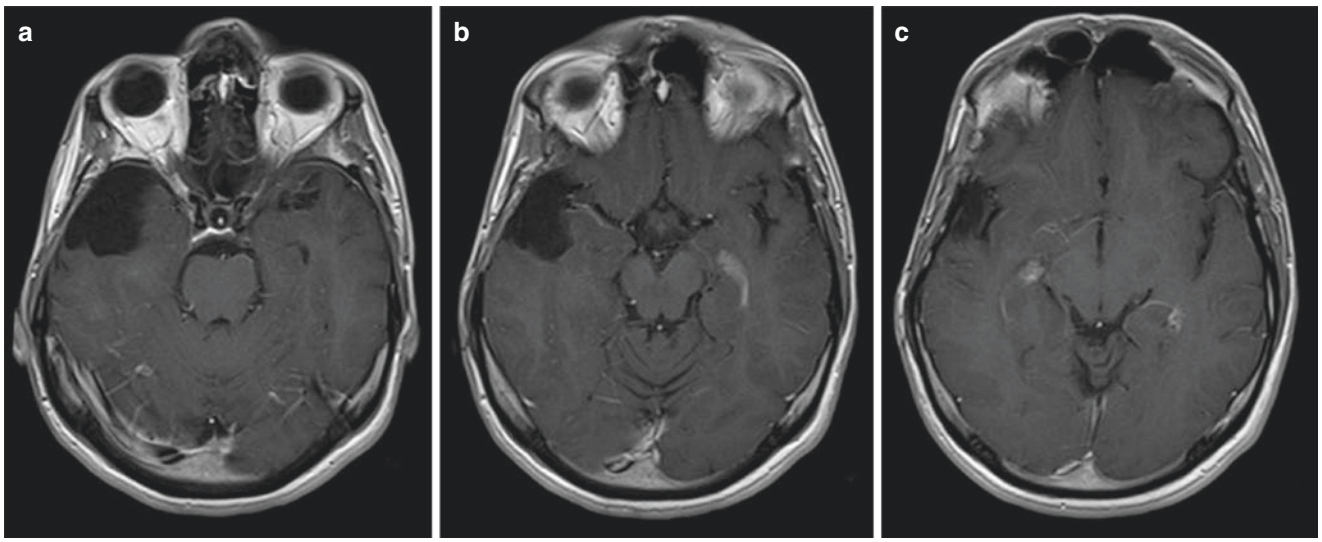

Fig. 11.8 (**a**–**c**) Contrast-enhanced MR SE T1-weighted images. The study confirms the absence of contrast enhancement of the residual tumor

Low-Grade Residual Tumor: Morphofunctional MR Follow-Up in Anaplastic Oligoastrocytoma

Case 12

Alessandro Stecco, Francesco Fabbiano, Sara Zizzari, Gerardo Di Nardo, Mariangela Lombardi, Andrea Pietro Sponghini, Alessandro Carriero, and Lucrezia Emanuela Guerra

- 45-year-old patient with bilateral frontal anaplastic oligoastrocytoma treated with subtotal resection and subsequent combined radiation therapy–chemotherapy.
- Morphofunctional MR follow-up performed with morphologic study, perfusion, and spectroscopy preoperatively and at 3 months after surgery and radiation therapy–chemotherapy.

A. Stecco (✉)
Neuroradiology Unit, AOU "Maggiore della Carità", DIMET, Università del Piemonte Orientale, Novara, Italy
e-mail: alessandro.stecco@uniupo.it

F. Fabbiano
Department of Neuroradiology, I.R.C.C.S. INM Neuromed, Pozzilli, Isernia, Italy

Department of Diagnostic Imaging, Valmontone Hospital, Rome, Italy

Department of Radiology and Neuroradiology, Villa Benedetta, Rome, Italy

S. Zizzari
Department of Radiology, Hospital "Sacred Heart of Jesus", ASL LECCE, Gallipoli, Italy

G. D. Nardo · A. Carriero
Department of Radiology, AOU "Maggiore della Carità", DIMET, Università del Piemonte Orientale, Novara, Italy

M. Lombardi
Department of Radiology, Cesena Hospital—AUSL Romagna, Cesena, Italy

A. P. Sponghini
Department of Oncology, AOU Maggiore della Carità, DIMET, Università del Piemonte Orientale, Novara, Italy

L. E. Guerra
Department of Radiology, Hospital "Carlo Poma", Mantova, Italy

T. Scarabino, S. Pollice (eds.), *Imaging Gliomas After Treatment*, https://doi.org/10.1007/978-3-030-31210-7_22

Preoperative Imaging

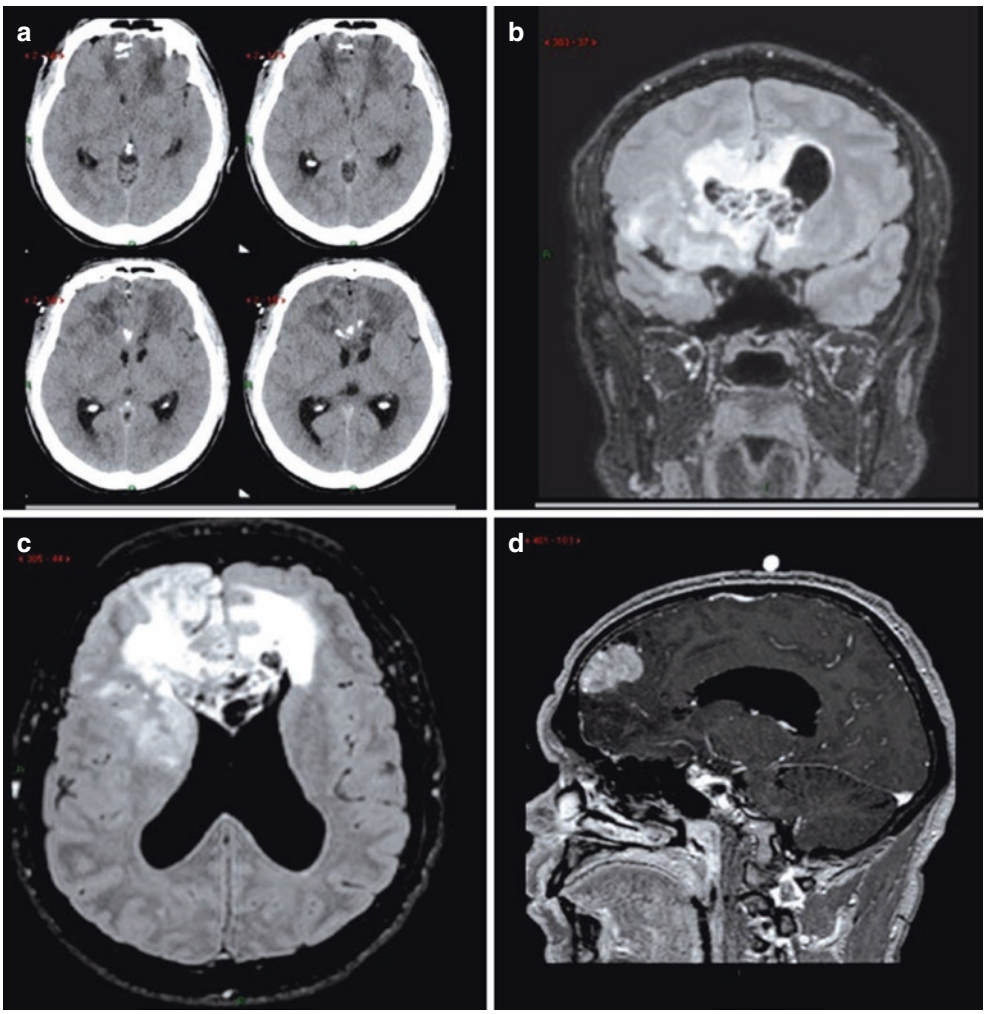

Fig. 12.1 (**a**) Baseline CT scan. A bilateral frontal lesion can be seen spanning the anterior genu of the corpus callosum with macrocalcifications in the frontal polar (right paramedian) region and at the level of the corpus callosum. (**b**) MR fluid-attenuated inversion recovery with fat saturation (FLAIR FS) sequences show the hyperintense lesion extending across the corpus callosum and midline area. The presence of areas of altered signal compatible with microcalcifications in the anterior genu of the corpus callosum and diffuse perilesional hyperintensity can also be appreciated. (**c**) MR fluid-attenuated inversion recovery with fat saturation (FLAIR FS) sequences show the hyperintense lesion extending across the corpus callosum and midline area. The presence of areas of altered signal compatible with microcalcifications in the anterior genu of the corpus callosum and diffuse perilesional hyperintensity can also be appreciated. (**c**) MR fluid-attenuated inversion recovery with fat saturation (FLAIR FS) sequences show the hyperintense lesion extending across the corpus callosum and midline area. The presence of areas of altered signal compatible with microcalcifications in the anterior genu of the corpus callosum and diffuse perilesional hyperintensity can also be appreciated. (**d**) Contrast-enhanced MR SE T1-weighted sequence depicts intense pathologic enhancement of the polar component of the frontal lesion

Follow-Up at 3 Months After Surgery and Radiation Therapy

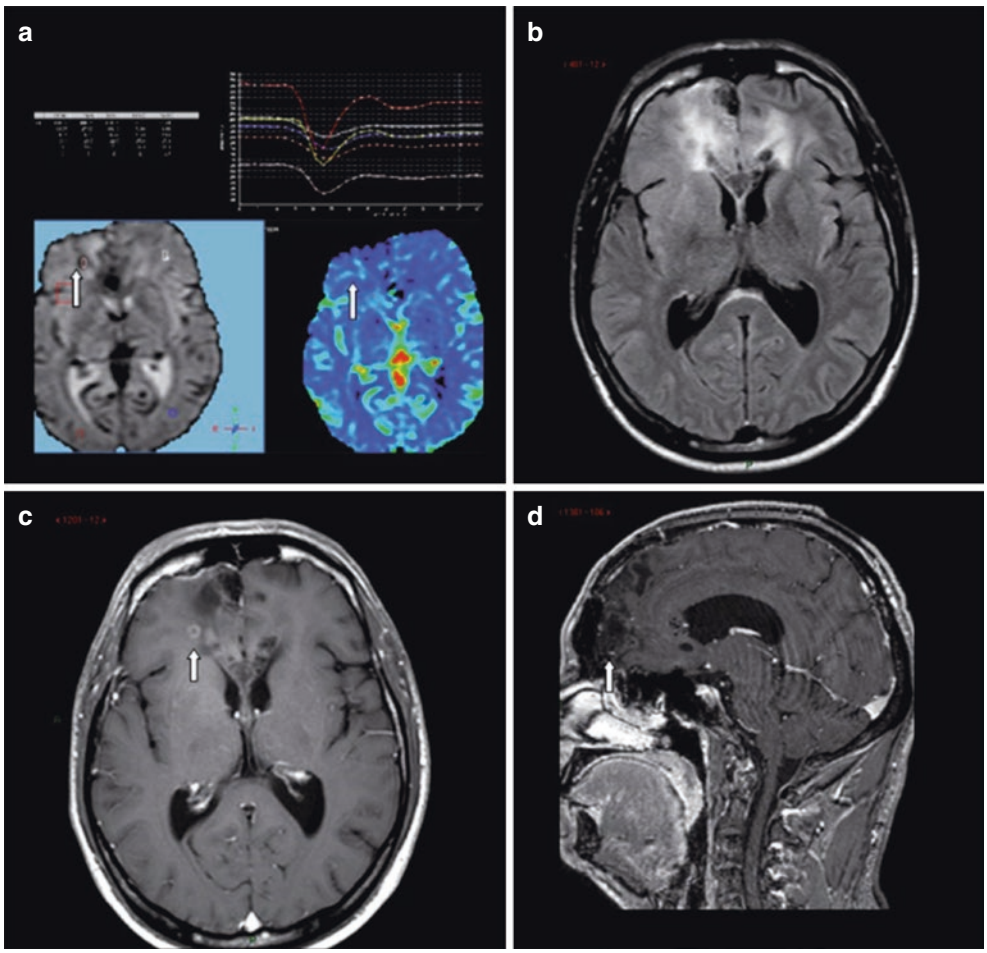

Fig. 12.2 (**a**) MR perfusion study with relative CBV map. An ROI (*white arrow*) is placed on a hypoperfused nodule on the CBV map (*white circle*). (**b**) MR FLAIR sequence shows residual alteration in the deep frontal white matter and in the anterior genu of the corpus callosum, which appears smaller than in Fig. 10.1 c, in partial response to therapy. (**c**, **d**) Contrast-enhanced MR SE T1-weighted sequences show a small nodule of rim enhancement in the context of hypointense area, partly attributable to postsurgical cavitation and in part to residual low-grade tissue

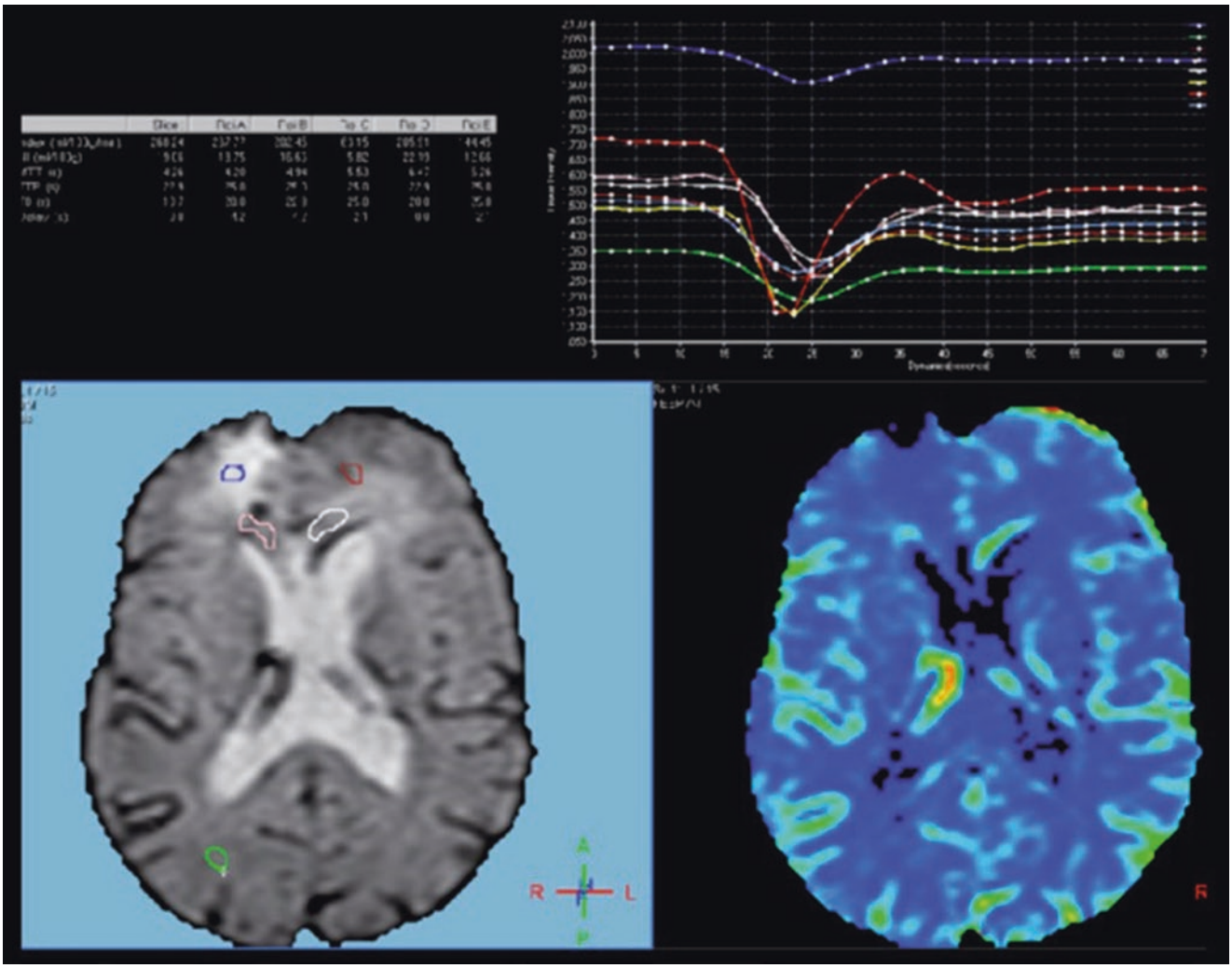

Fig. 12.3 MR perfusion study with relative CBV map. Measurement of CBV perfusion in the bilateral anterior paracallosal area (*pink and white freehand ROIs*) compared with ROIs placed in the bilateral frontal polar subcortical white matter (*blue and red freehand ROIs*) and as a reference in apparently healthy right parietal white matter (*green freehand ROI*) shows evidence of increased CBV in the anterior paracallosal area

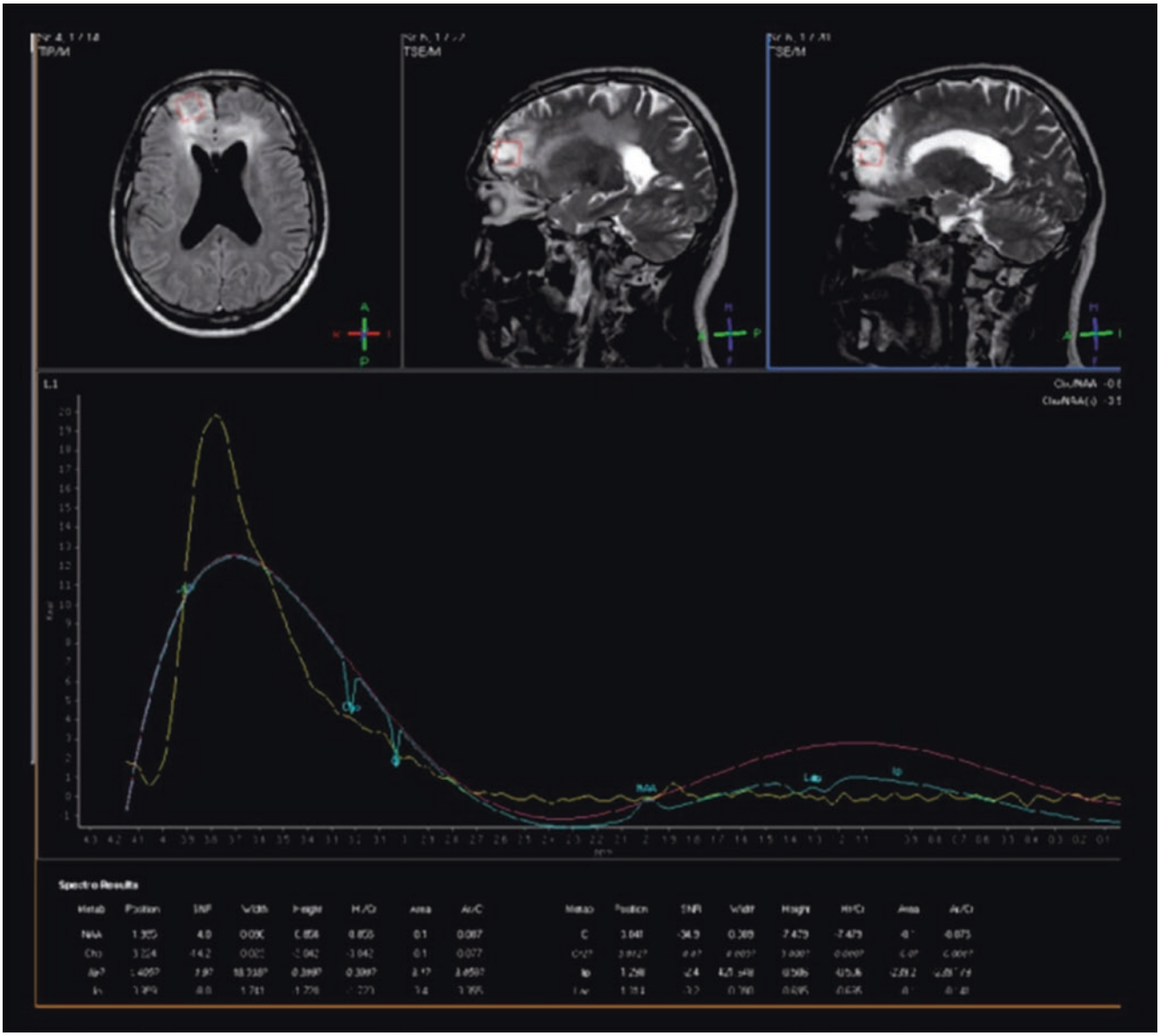

Fig. 12.4 Single-voxel MR spectroscopy. The sampling area has prevailing lesion characteristics of gliosis, cavitation, and absence of neuronal metabolites

Medium–Low Grade Residual Tumor: Morphofunctional MR Follow-Up in Astrocytoma

Case 13

Alessandro Stecco, Sara Zizzari, Francesco Fabbiano, Gerardo Di Nardo, Mariangela Lombardi, Emanuele Malatesta, and Alessandro Carriero

- 45-year-old patient with a low-grade astrocytoma of the right temporal lobe treated with subtotal excision and subsequent chemotherapy.
- Morphofunctional MR follow-up performed with morphologic study, perfusion, and spectroscopy at 36 months after surgery and combined chemotherapy.

Follow-Up at 36 Months After Surgery and Combined Chemotherapy

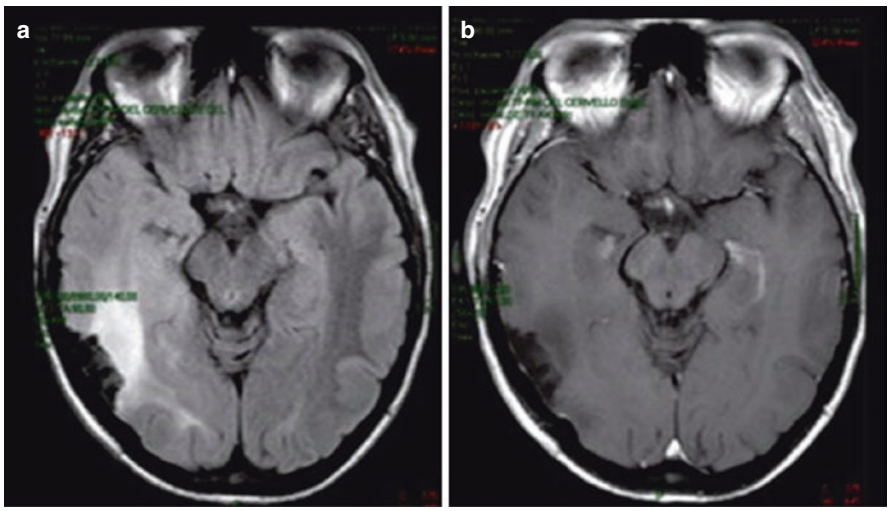

Fig. 13.1 (**a**–**d**) MR FLAIR and contrast-enhanced SE T1-weighted sequences on two contiguous sections. A cavitary cystic area can be seen accompanied by a solid residual portion appearing hyperintense in FLAIR and hypointense in T1 without pathologic enhancement, located in the deep white matter of the right temporal lobe

A. Stecco (✉)
Neuroradiology Unit, AOU "Maggiore della Carità", DIMET, Università del Piemonte Orientale, Novara, Italy
e-mail: alessandro.stecco@uniupo.it

S. Zizzari
Department of Radiology, Hospital "Sacred Heart of Jesus", ASL LECCE, Gallipoli, Italy

F. Fabbiano
Department of Neuroradiology, I.R.C.C.S. INM Neuromed, Pozzilli, Isernia, Italy

Department of Diagnostic Imaging, Valmontone Hospital, Rome, Italy

Department of Radiology and Neuroradiology, Villa Benedetta, Rome, Italy

G. D. Nardo · A. Carriero
Department of Radiology, AOU "Maggiore della Carità", DIMET, Università del Piemonte Orientale, Novara, Italy

M. Lombardi · E. Malatesta
Department of Radiology, Cesena Hospital—AUSL Romagna, Cesena, Italy

T. Scarabino, S. Pollice (eds.), *Imaging Gliomas After Treatment*, https://doi.org/10.1007/978-3-030-31210-7_23

Fig. 13.1 (continued)

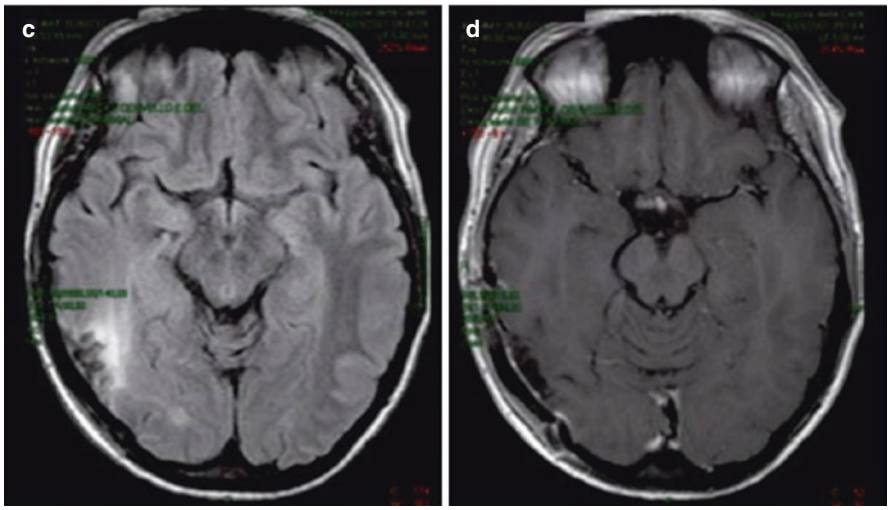

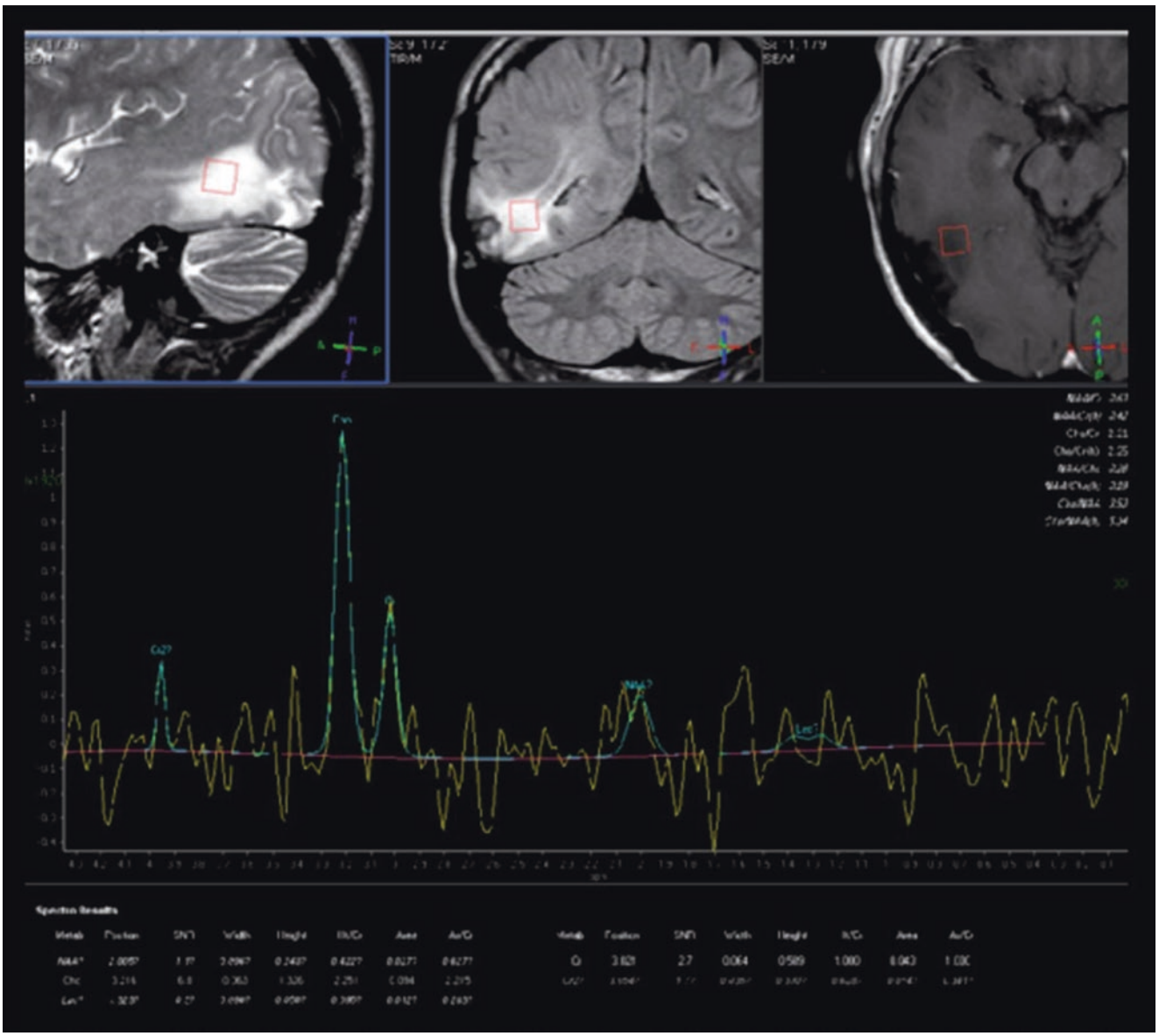

Fig. 13.2 Single-voxel MR spectroscopy. The ROI placed in the residual solid tissue in the temporal lobe shows a reduction in NAA and an increase in Cho with metabolic ratios compatible with medium-low-grade residual disease, in the context of the perilesional hyperintense area in FLAIR

Medium–Low Grade Residual Tumor: Morphofunctional MR Follow-Up in Fibrillar Astrocytoma

Case 14

Alessandro Stecco, Sara Zizzari, Francesco Fabbiano, Gerardo Di Nardo, Mariangela Lombardi, Giuseppe Fiscer, and Alessandro Carriero

- 58-year-old patient with low-grade astrocytoma of the left frontal lobe treated with surgery and first-line chemotherapy.
- Morphofunctional MR follow-up performed with morphologic study, perfusion, and spectroscopy preoperatively and at 5 and 10 months after surgery and combined chemotherapy.

A. Stecco (✉)
Neuroradiology Unit, AOU "Maggiore della Carità", DIMET, Università del Piemonte Orientale, Novara, Italy
e-mail: alessandro.stecco@uniupo.it

S. Zizzari
Department of Radiology, Hospital "Sacred Heart of Jesus", ASL LECCE, Gallipoli, Italy

F. Fabbiano
Department of Neuroradiology, I.R.C.C.S. INM Neuromed, Pozzilli, Isernia, Italy

Department of Diagnostic Imaging, Valmontone Hospital, Rome, Italy

Department of Radiology and Neuroradiology, Villa Benedetta, Rome, Italy

G. D. Nardo · A. Carriero
Department of Radiology, AOU "Maggiore della Carità", DIMET, Università del Piemonte Orientale, Novara, Italy

M. Lombardi
Department of Radiology, Cesena Hospital—AUSL Romagna, Cesena, Italy

G. Fiscer
"Studio Radiologico" Hospital, Reggio Calabria, Italy

T. Scarabino, S. Pollice (eds.), *Imaging Gliomas After Treatment*, https://doi.org/10.1007/978-3-030-31210-7_24

Preoperative Imaging

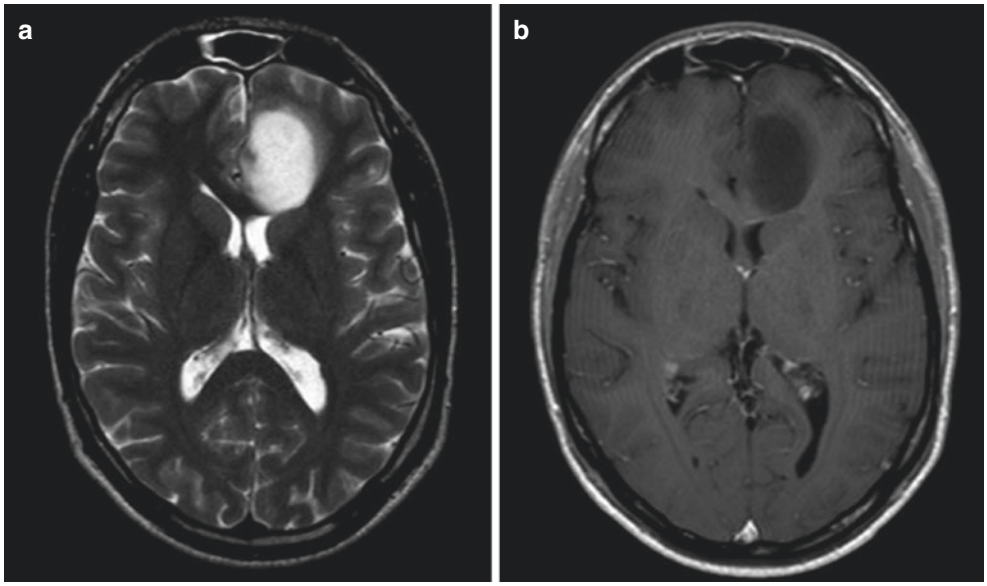

Fig. 14.1 (**a**) MR FSE T2-weighted sequence shows intra-axial deep left frontal lesion with involvement of the rostrum of the corpus callosum and mass effect on neighboring structures. (**b**) Contrast-enhanced MR SE T1-weighted sequence. No pathologic enhancement is evident at the lesion site

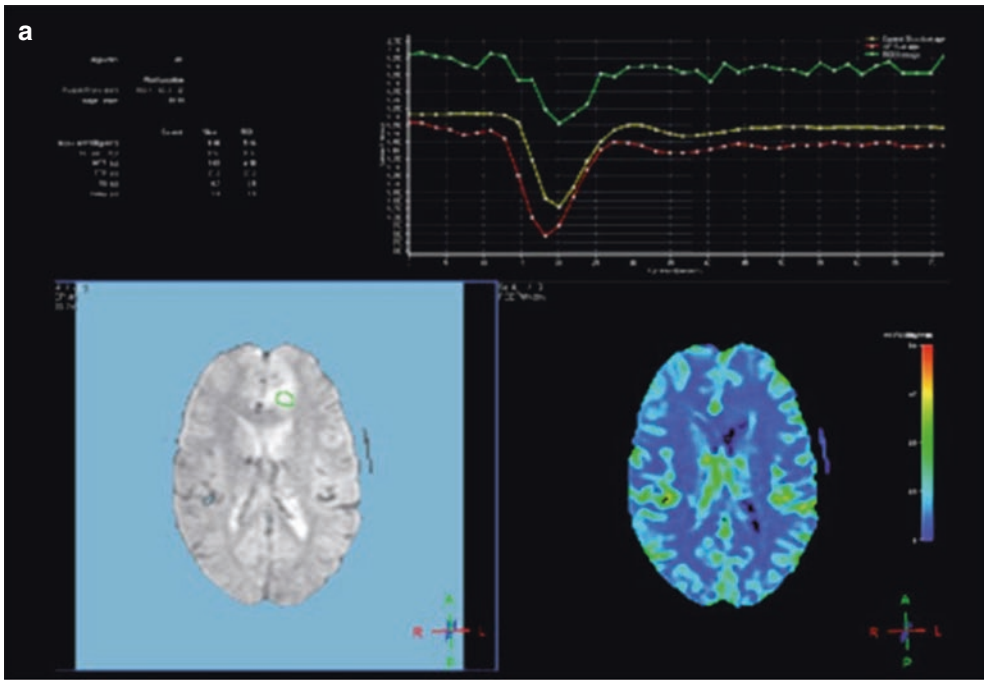

Fig. 14.2 MR perfusion study with relative CBV map showing an ROI placed on the lesion (**a**) and on an apparently healthy contralateral area. (**b**) The comparison shows the lower CBV in the lesion area than in the healthy contralateral tissue, thus indicating weak neovascularization

Fig. 14.2 (continued)

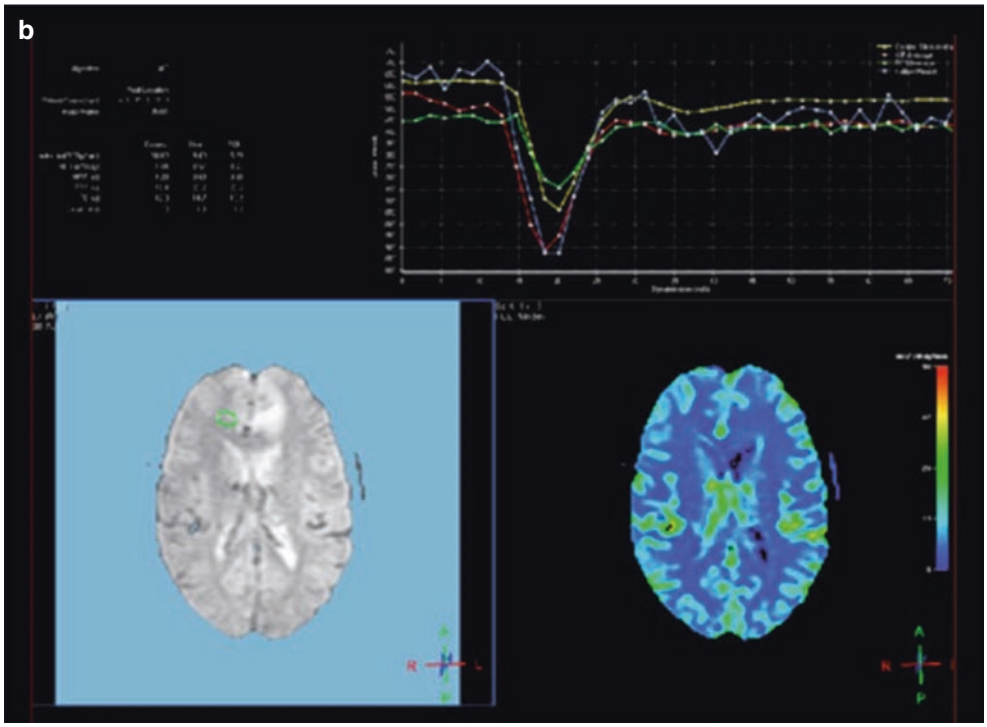

Follow-Up at 5 Months After Surgery

Fig. 14.3 (**a**–**c**) Contrast-enhanced MR SE T1-weighted and FSE T2-weighted sequences show postsurgical findings of partial resection at 1 month with residual disease. (**d**) Single-voxel MR spectroscopy. Sampling of the residual lesion shows a metabolic pattern consistent with medium-low grade lesion

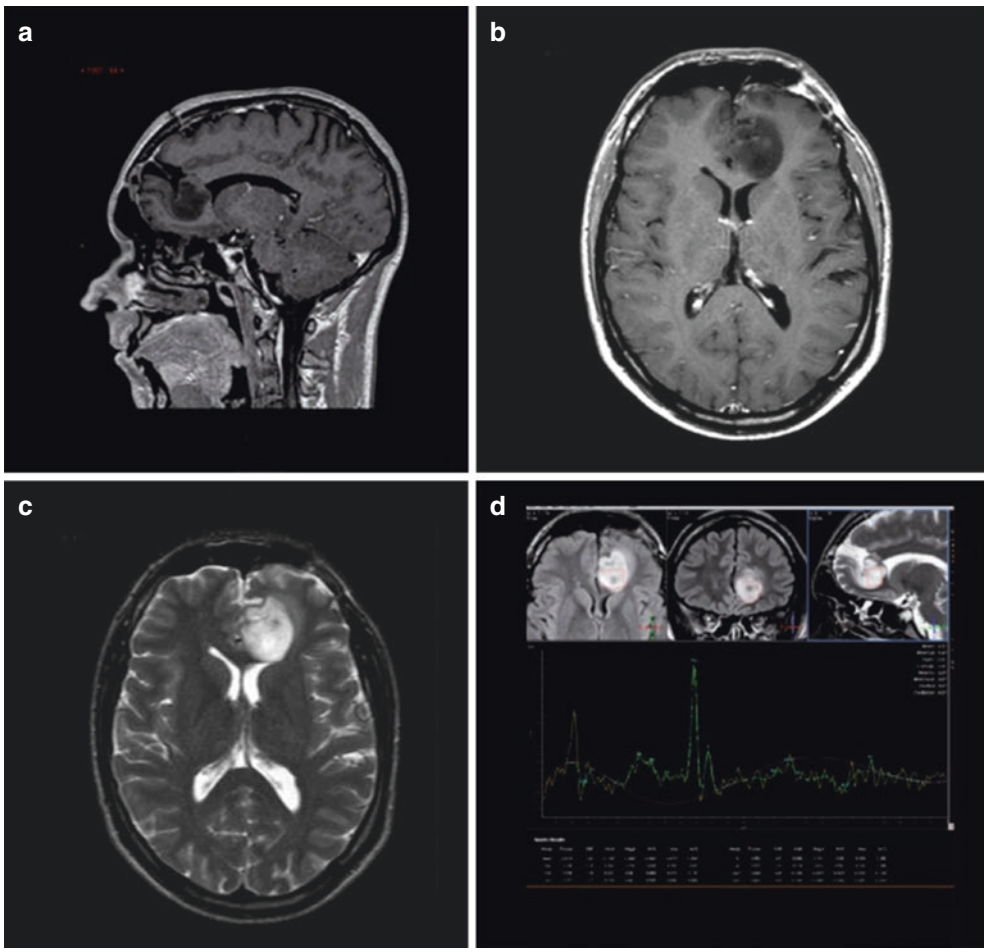

Follow-Up at 10 Months

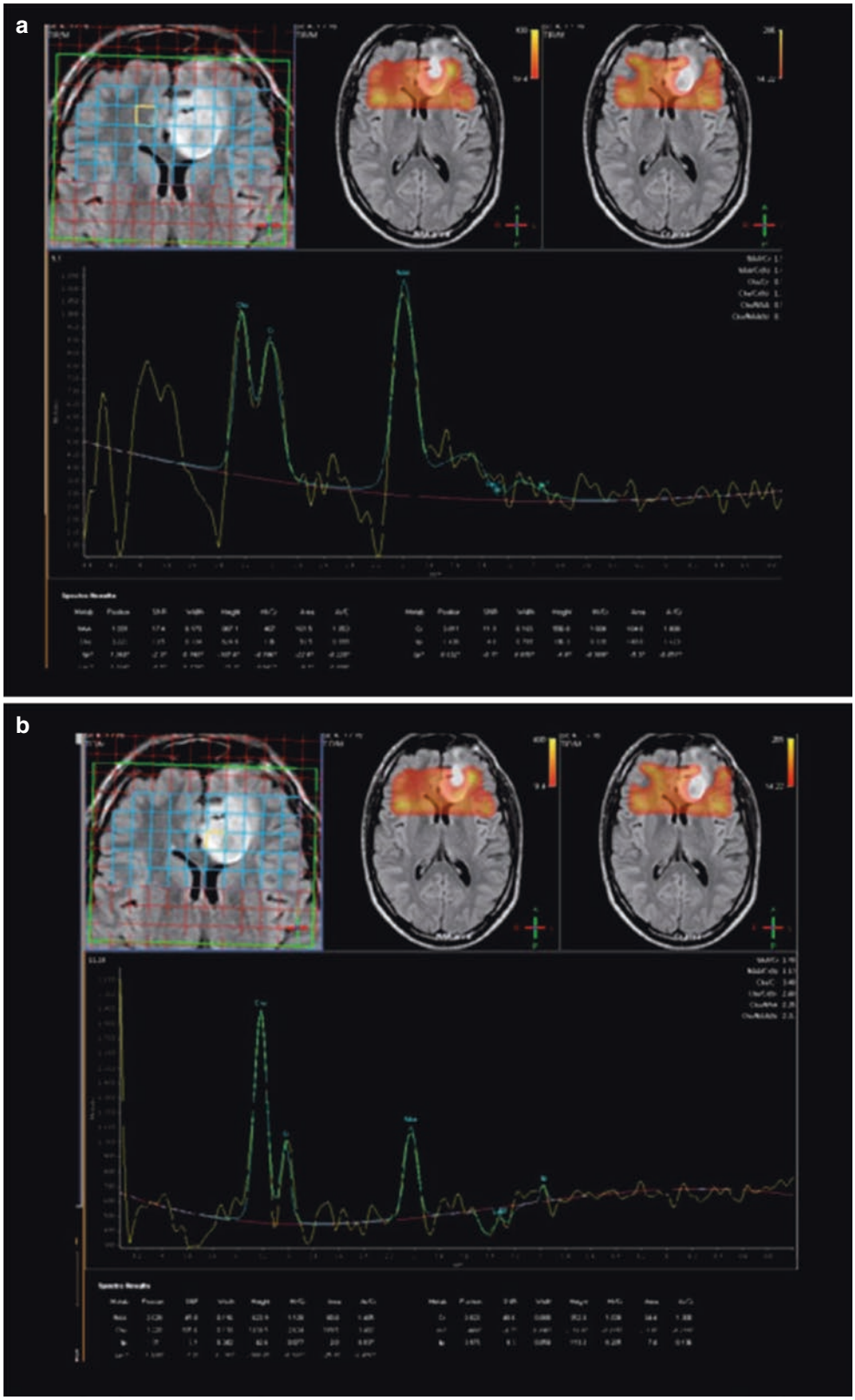

Fig. 14.4 Multivoxel MR spectroscopy. The apparently healthy sampling area (**a**) and pathologic tissue (**b**) show at that level a pattern of metabolites consistent with the presence of medium-low grade residual cancer

Medium–Low Grade Residual Tumor: Morphofunctional MR Follow-Up in Anaplastic Oligodendroglioma

Case 15

Alessandro Stecco, Francesco Fabbiano, Sara Zizzari, Gerardo Di Nardo, Mariangela Lombardi, Lorenzo Fortunelli, and Alessandro Carriero

- 58-year-old patient with right frontal-temporal-parietal-insular anaplastic oligodendroglioma treated with surgery and subsequent combined radiation therapy–chemotherapy and second-line chemotherapy.
- Morphofunctional MR follow-up performed with morphologic study, perfusion, and spectroscopy preoperatively and at 10, 15, and 19 months after surgery and combined chemotherapy.

A. Stecco (✉)
Neuroradiology Unit, AOU "Maggiore della Carità", DIMET, Università del Piemonte Orientale, Novara, Italy
e-mail: alessandro.stecco@uniupo.it

F. Fabbiano
Department of Neuroradiology, I.R.C.C.S. INM Neuromed, Pozzilli, Isernia, Italy

Department of Diagnostic Imaging, Valmontone Hospital, Rome, Italy

Department of Radiology and Neuroradiology, Villa Benedetta, Rome, Italy

S. Zizzari
Department of Radiology, Hospital "Sacred Heart of Jesus", ASL LECCE, Gallipoli, Italy

G. D. Nardo · A. Carriero
Department of Radiology, AOU "Maggiore della Carità", DIMET, Università del Piemonte Orientale, Novara, Italy

M. Lombardi
Department of Radiology, Cesena Hospital—AUSL Romagna, Cesena, Italy

L. Fortunelli
Department of Radiology, CDC, Novara, Italy

T. Scarabino, S. Pollice (eds.), *Imaging Gliomas After Treatment*, https://doi.org/10.1007/978-3-030-31210-7_25

Preoperative Imaging

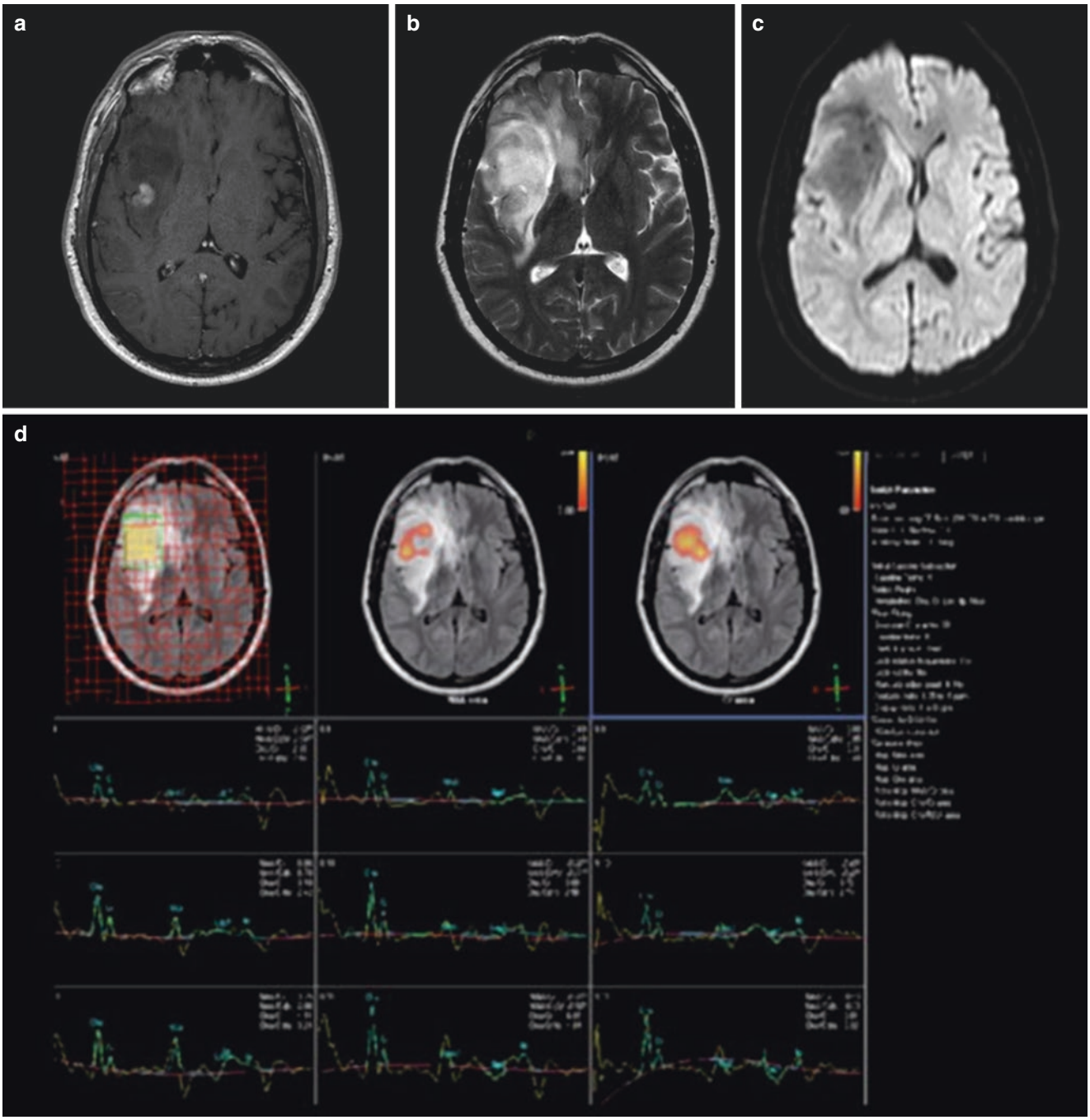

Fig. 15.1 Contrast-enhanced MR SE T1-weighted (**a**), FSE T2-weighted (**b**), and diffusion-weighted (**c**) sequences. A primary intra-axial neoplasm can be appreciated in the right frontal-insular lobe with diffuse perilesional signal alterations at the level of the white matter and in the frontal basal ganglia, with associated mass effect on neighboring structures. After contrast medium administration, a pseudonodular enhancement can be appreciated in the subcortical right insular region. (**d**) Multi-voxel MR spectroscopy shows a Cho peak within the lesion

Follow-Up at 10 Months After Surgery, Radiation Therapy, and Chemotherapy

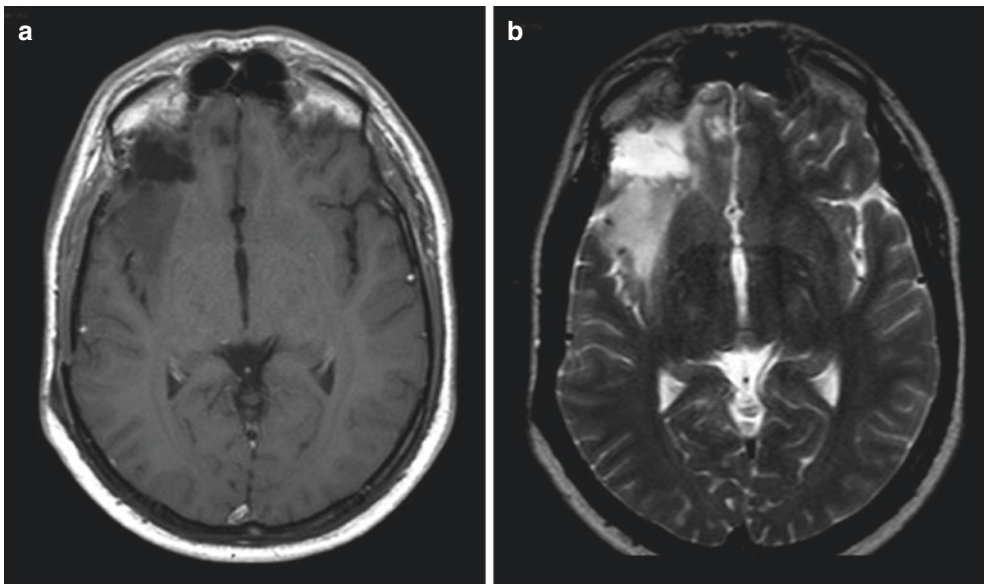

Fig. 15.2 (**a**) Contrast-enhanced MR SE T1-weighted sequence shows nonenhancing residual tumor in inferior frontal location and postsurgical cavity in anteroinferior location at the level of the upper right orbital gyrus. (**b**) Contrast-enhanced MR SE T1-weighted sequence. The residual signal alteration appears to extend to the insula and external capsule

Follow-Up at 15 Months

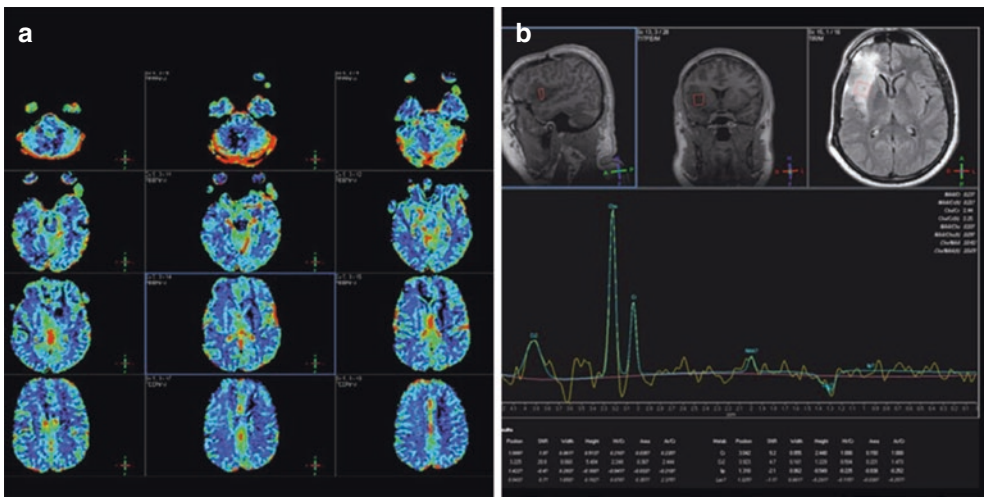

Fig. 15.3 (**a**) MR perfusion study with relative CBV map shows no significant increase in perfusion in the lesion. (**b**) Single-voxel MR spectroscopy confirms the findings of residual cancer without disease progression

Follow-Up at 19 Months

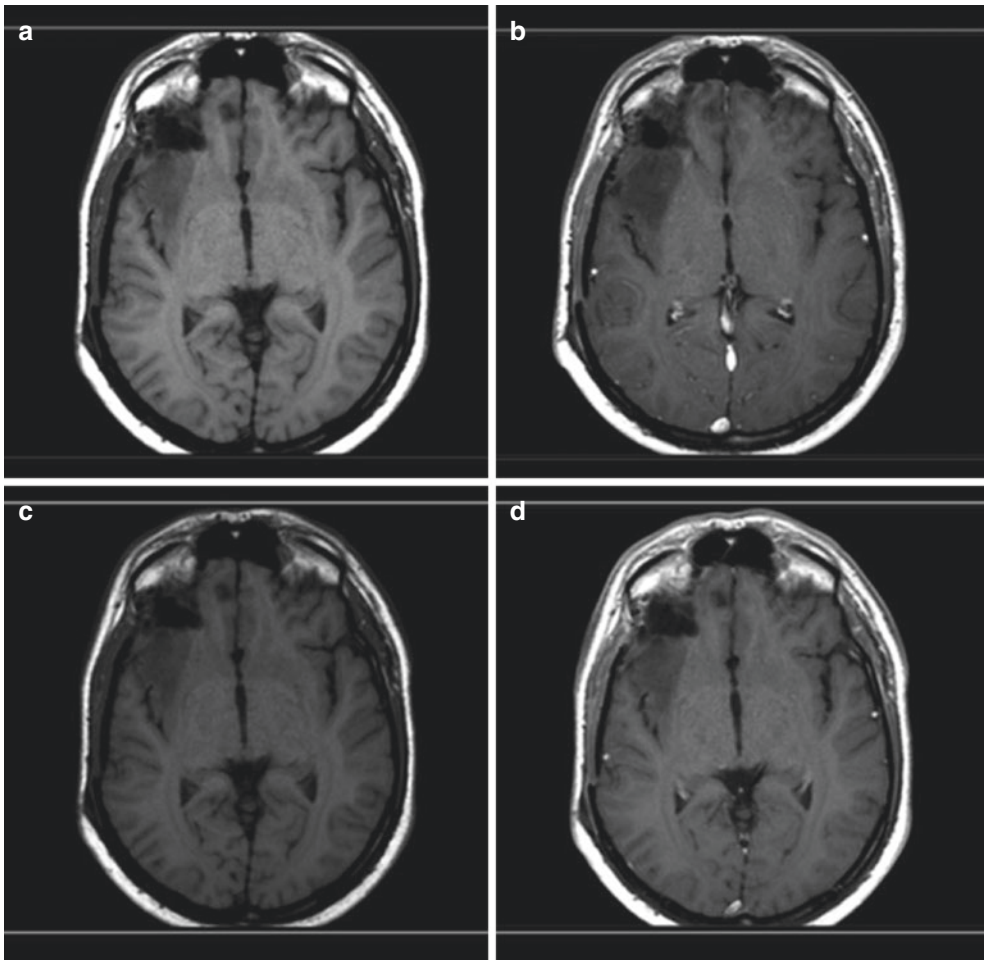

Fig. 15.4 Comparison between contrast-enhanced MR SE T1-weighted sequences at 5 months after surgery and prior to chemotherapy and radiation therapy (**a**, **b**) and post-chemotherapy images at 19 months postoperatively (**c**, **d**). The post-chemotherapy images show less hypointensity at the level of residual tissue with increasing amplitude of the cavitary cyst in response to therapy

High-Grade Residual Tumor: Morphofunctional MR Follow-Up in Gemistocytic Astrocytoma

Case 16

Francesco Fabbiano, Alessandro Stecco, Sara Zizzari, Gerardo Di Nardo, Anthony Azubuike Obaze, Mariangela Lombardi, and Alessandro Carriero

- 71-year-old patient affected by right parietal gemistocytic astrocytoma treated with subtotal resection and subsequent combined radiation therapy–chemotherapy.
- Morphofunctional MR follow-up performed with morphologic study, perfusion, and spectroscopy preoperatively and at 3 months after surgery and radiation therapy–chemotherapy.

F. Fabbiano (✉)
Department of Neuroradiology, I.R.C.C.S. INM Neuromed, Pozzilli, Isernia, Italy

Department of Diagnostic Imaging, Valmontone Hospital, Rome, Italy

Department of Radiology and Neuroradiology, Villa Benedetta, Rome, Italy

A. Stecco · S. Zizzari · G. D. Nardo · A. A. Obaze · M. Lombardi
Department of Neuroradiology, "Maggiore della Carità" University Hospital, Novara, Italy

A. Carriero
Department of Radiology, AOU "Maggiore della Carità", DIMET, Università del Piemonte Orientale, Novara, Italy

T. Scarabino, S. Pollice (eds.), *Imaging Gliomas After Treatment*, https://doi.org/10.1007/978-3-030-31210-7_26

Preoperative Imaging

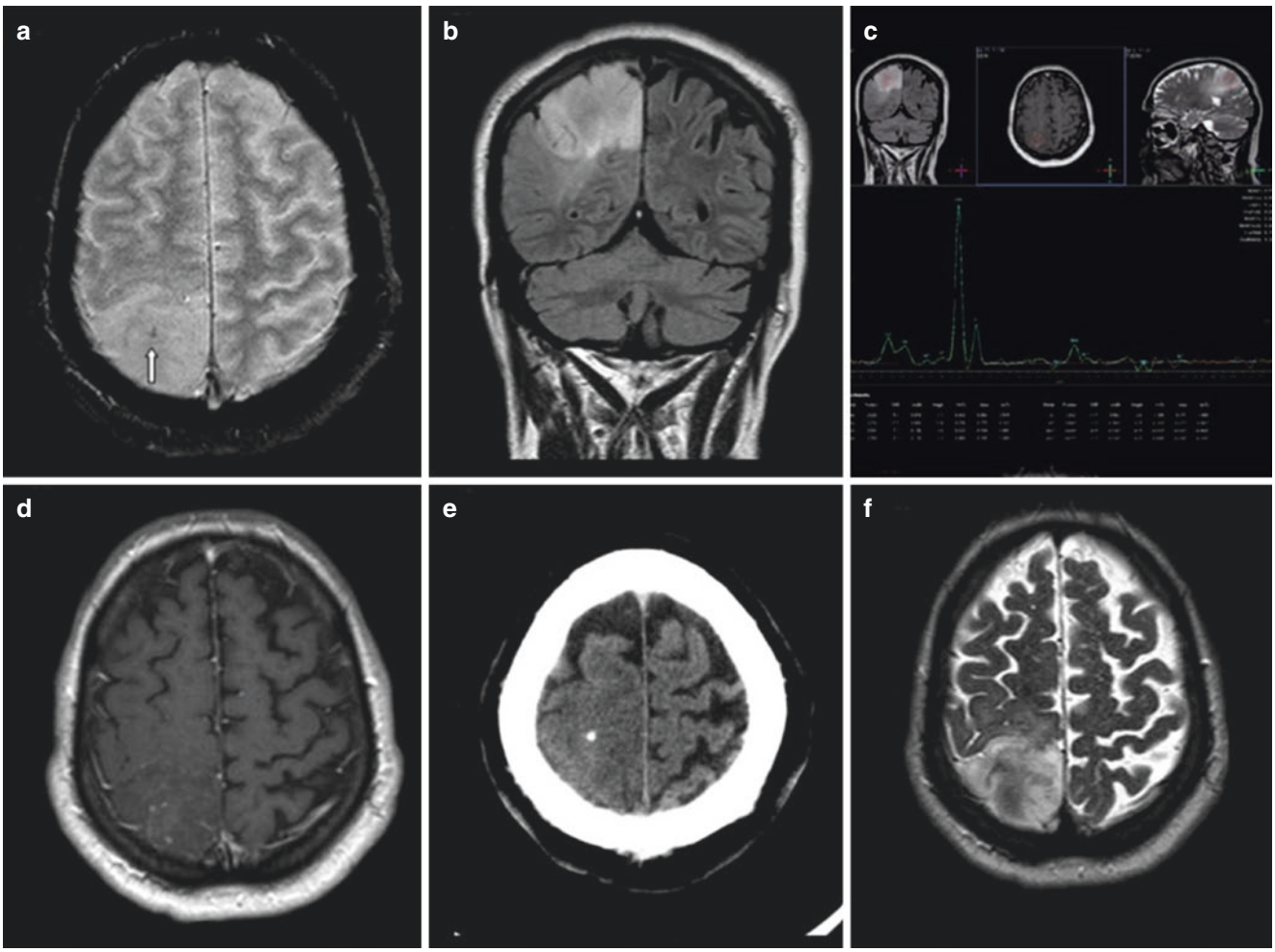

Fig. 16.1 (**a**) MR FFE T2∗-weighted sequence shows small focal inhomogeneities induced by microcalcification (*white arrow*) within the lesion in the right parietal lobe. (**b**) Morphologic MR FLAIR images show right parietal cortical–subcortical pathologic tissue and perilesional signal alteration. (**c**) Single-voxel MR spectroscopy. The metabolic ratios are consistent with the presence of a high-grade glial lesion. (**d**) Contrast-enhanced MR SE T1-weighted sequence shows a slight pathologic enhancement in the right parietal cortical–subcortical lobe. (**e**) Baseline CT scan shows microcalcification in the lesion in the right parietal lobe. (**f**) MR FSE T2-weighted sequence. The right parietal cortical–subcortical pathologic tissue is visible with low signal in T2 accompanied by perilesional changes

Follow-Up at 3 Months After Subtotal Resection and Radiation Therapy–Chemotherapy

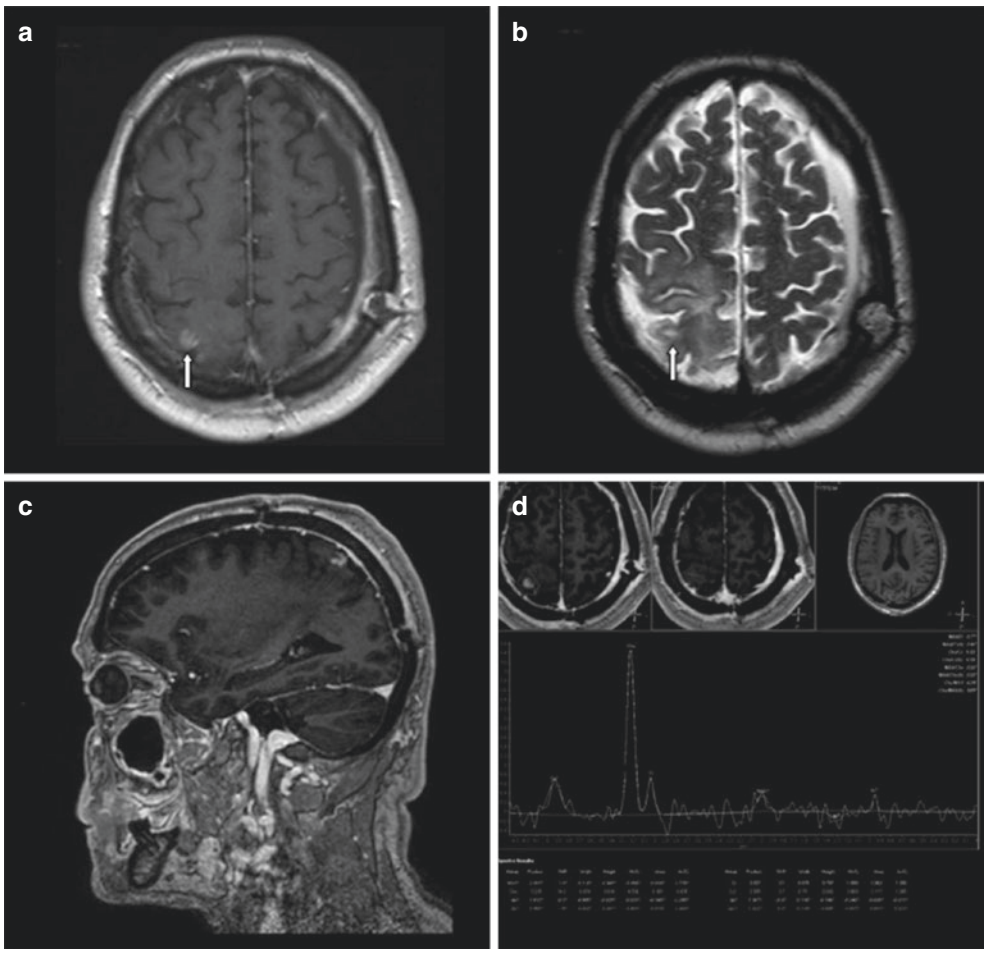

Fig. 16.2 (**a**) Contrast-enhanced MR SE T1-weighted sequence shows slight pathologic enhancement with the presence of a more notable enhancing nodule in the cortical–subcortical area (*white arrow*). (**b**) MR FSE T2-weighted sequence visualizes the area of pathologic enhancement corresponding to tissue with low signal in T2 (*white arrow*). (**c**) Contrast-enhanced MR SE T1-weighted sequence shows the residual tumor with enhancement in the right parietal cortical–subcortical lobe. (**d**) Single-voxel MR spectroscopy. Sampling on the enhancing lesion shows marked elevation of the Cho peak and reduced NAA with metabolic ratios consistent with a high-grade lesion

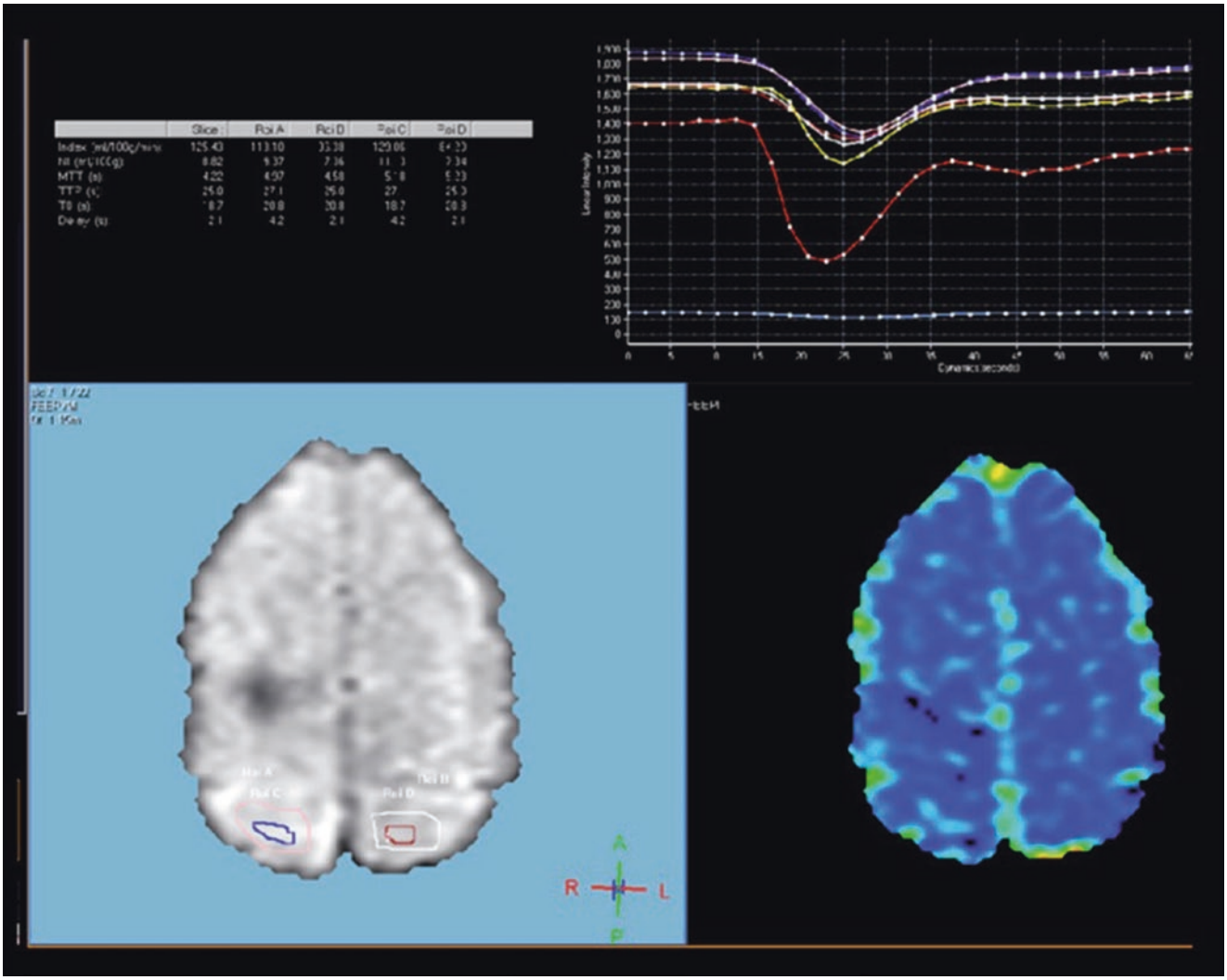

Fig. 16.3 MR perfusion study with relative CBV map shows a blue ROI placed on the residual tumor and a red ROI on apparently normal contralateral area. The elevated CBV is compatible with high-grade residual tumor

High-Grade Residual Tumor: Morphofunctional MR Follow-Up in Low-Grade Oligoastrocytoma and Following Anaplastic Transformation

Case 17

Alessandro Stecco, Sara Zizzari, Francesco Fabbiano, Gerardo Di Nardo, Mariangela Lombardi, Ignazio Divenuto, and Alessandro Carriero

- Patient with right frontal low-grade oligoastrocytoma treated with partial excision surgery and subsequent combined radiation therapy–chemotherapy following anaplastic transformation.
- Morphofunctional MR follow-up performed with morphologic study, perfusion, and spectroscopy at 24 months after surgery and combined chemotherapy.

A. Stecco (✉)
Neuroradiology Unit, AOU "Maggiore della Carità", DIMET, Università del Piemonte Orientale, Novara, Italy
e-mail: alessandro.stecco@uniupo.it

S. Zizzari
Department of Radiology, Hospital "Sacred Heart of Jesus", ASL LECCE, Gallipoli, Italy

F. Fabbiano
Department of Neuroradiology, I.R.C.C.S. INM Neuromed, Pozzilli, Isernia, Italy

Department of Diagnostic Imaging, Valmontone Hospital, Rome, Italy

Department of Radiology and Neuroradiology, Villa Benedetta, Rome, Italy

G. D. Nardo · A. Carriero
Department of Radiology, AOU "Maggiore della Carità", DIMET, Università del Piemonte Orientale, Novara, Italy

M. Lombardi
Department of Radiology, Cesena Hospital—AUSL Romagna, Cesena, Italy

I. Divenuto
Department of Diagnostic Imaging, Humanitas Hospital, Rozzano, Italy

T. Scarabino, S. Pollice (eds.), *Imaging Gliomas After Treatment*, https://doi.org/10.1007/978-3-030-31210-7_27

Follow-Up at 24 Months After Surgery and Radiation Therapy–Chemotherapy

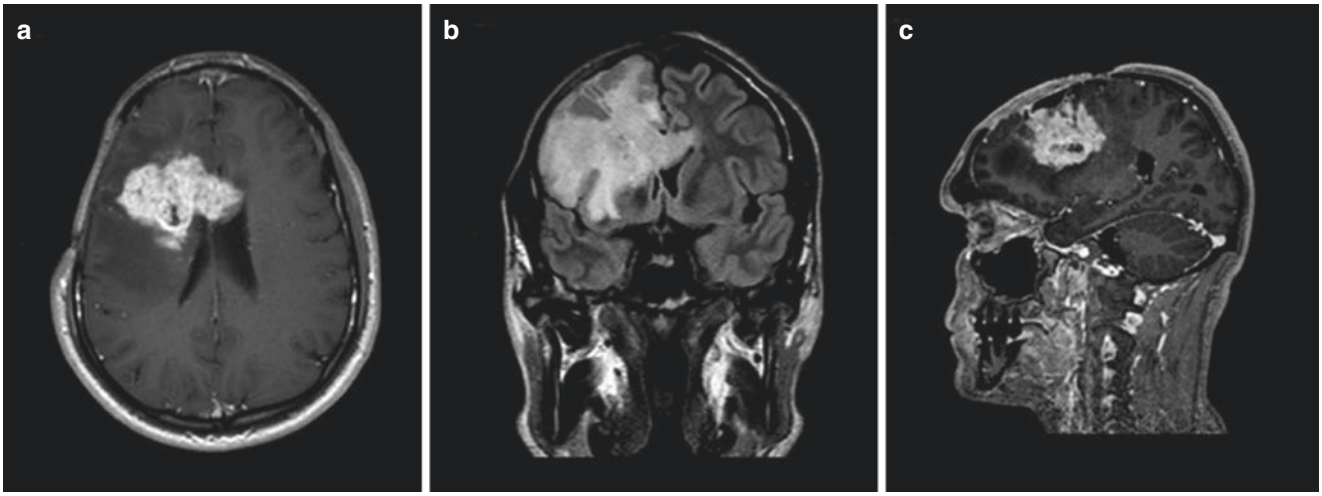

Fig. 17.1 (**a**–**c**) Contrast-enhanced MR SE T1-weighted and FLAIR sequences show massive recurrence of disease in the right deep frontal region involving the basal ganglia, the corpus callosum, and extending across the midsagittal line. The FLAIR sequence shows the extension of pathologic tissue in the midline and contralateral area

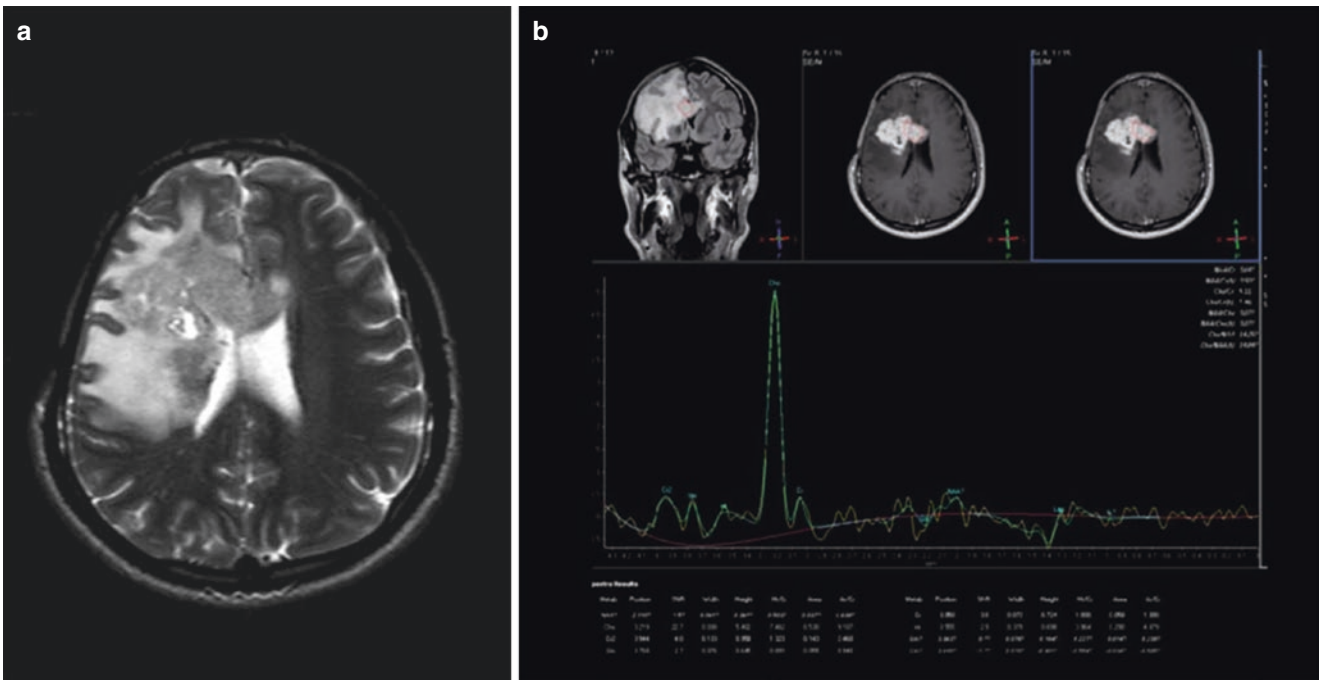

Fig. 17.2 (**a**) MR FSE T2-weighted sequence shows pathologic tissue with low signal on T2 indicating a high ratio of nucleus–cytoplasm. (**b**) Single-voxel MR spectroscopy. NAA is almost completely absent, and there is a marked elevation of Cho with metabolic ratios compatible with the presence of residual high-grade cancer. The presence of small Lac peak indicates necrosis

Stable Disease: Multimodal CT/MR Follow-Up in Glioblastoma Multiforme

Case 18

Alessandro Stecco, Sara Zizzari, Mariangela Lombardi, Gerardo Di Nardo, Francesco Fabbiano, Andrea Pietro Sponghini, and Alessandro Carriero

- 45-year-old patient with left parietal-occipital glioblastoma multiforme treated with surgery and combined radiation therapy–chemotherapy and subsequent second-line adjuvant chemotherapy.
- Multimodal CT (morphologic and perfusion) and morphologic MR follow-up at 3, 5, and 8 months after surgery and combined radiation therapy–chemotherapy.

A. Stecco (✉) · G. D. Nardo
Neuroradiology Unit, AOU "Maggiore della Carità", DIMET, Università del Piemonte Orientale, Novara, Italy
e-mail: alessandro.stecco@uniupo.it

S. Zizzari
Department of Radiology, Hospital "Sacred Heart of Jesus", ASL LECCE, Gallipoli, Italy

M. Lombardi
Department of Radiology, Cesena Hospital—AUSL Romagna, Cesena, Italy

F. Fabbiano
Department of Neuroradiology, I.R.C.C.S. INM Neuromed, Pozzilli, Isernia, Italy

Department of Diagnostic Imaging, Valmontone Hospital, Rome, Italy

Department of Radiology and Neuroradiology, Villa Benedetta, Rome, Italy

A. P. Sponghini
Department of Oncology, AOU Maggiore della Carità, DIMET, Università del Piemonte Orientale, Novara, Italy

A. Carriero
Department of Radiology, AOU "Maggiore della Carità", DIMET, Università del Piemonte Orientale, Novara, Italy

T. Scarabino, S. Pollice (eds.), *Imaging Gliomas After Treatment*, https://doi.org/10.1007/978-3-030-31210-7_28

Follow-Up at 3 Months After Surgery

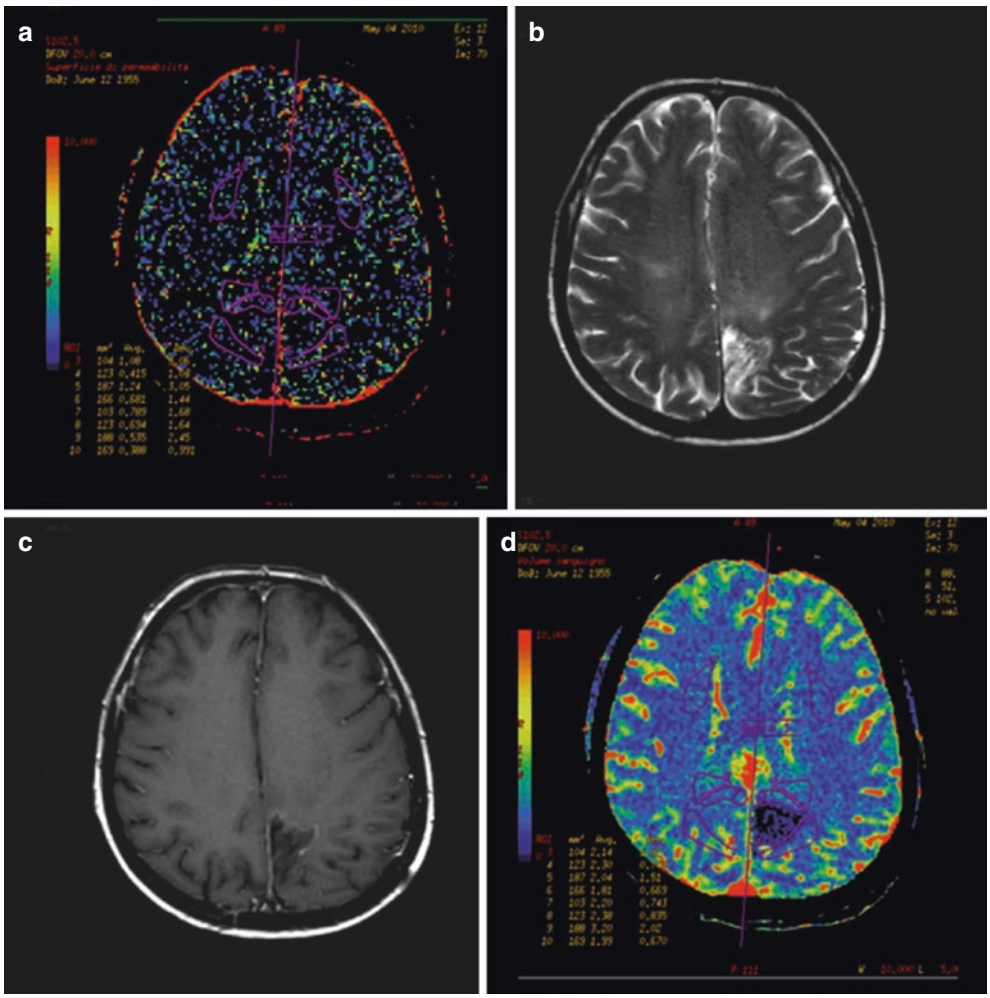

Fig. 18.1 (**a**) CT perfusion map of permeability surface (PS) shows an absence of significant residual tumor around the surgical cavity. (**b**) MR FSE T2-weighted sequence depicting the postsurgical cavity. (**c**) Contrast-enhanced MR SE T1-weighted image. Postsurgical cavitation with non-neoplastic fine rim enhancement visualized shortly after the surgical procedure. (**d**) CT perfusion study with relative CBV map shows an absence of elevated tissue parameters

Follow-Up at 5 Months After Surgery and Subsequent Radiation Therapy–Chemotherapy

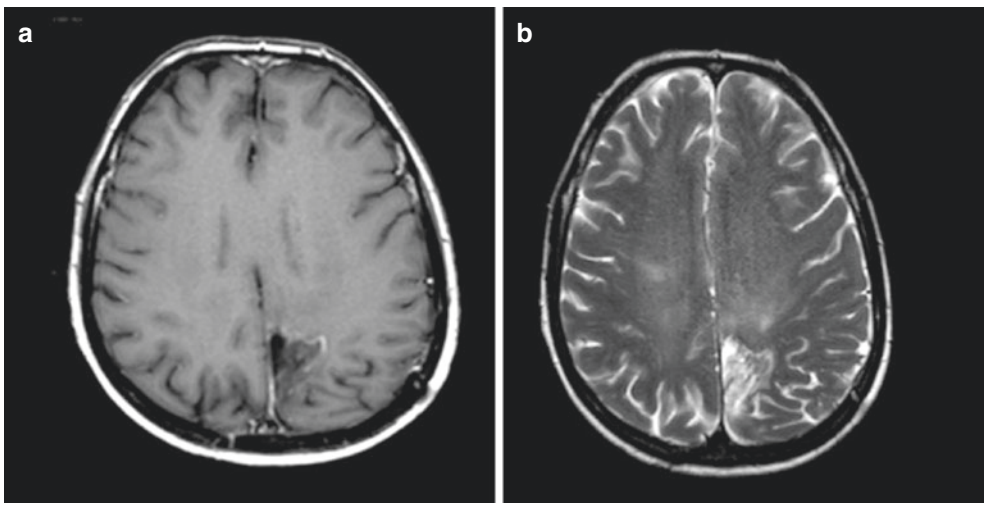

Fig. 18.2 Contrast-enhanced MR SE T1-weighted (**a**) and FSE T2-weighted (**b**) sequences depict an absence of disease progression and reduction in the solid tissue component at the surgical site in response to treatment with associated enlargement of the cavity compared to Case 6 Fig. 6.1c

Follow-Up at 8 Months

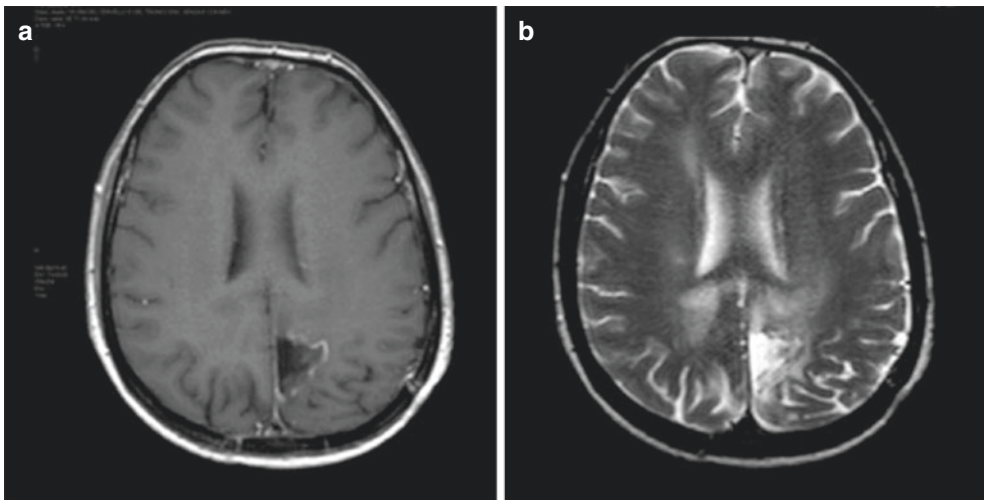

Fig. 18.3 Contrast-enhanced MR SE T1-weighted (**a**) and FSE T2-weighted (**b**) sequences show further enlargement of the cavity in response to therapy

Stable Disease: Morphofunctional MR Follow-Up in Glioblastoma Multiforme

Case 19

Gabriele Polonara, Lorenzo Alvaro, and Nathalie Herber

- 66-year-old patient with (methylated MGMT gene promoter) temporal-insular glioblastoma multiforme treated with surgery and subsequent radiotherapy and concomitant adjuvant chemotherapy.
- Morphofunctional MR follow-up performed with morphologic study, diffusion-weighted imaging, perfusion, and spectroscopy preoperatively, at 48 hours, 4, 7, 9, and 12 months after surgery.

Preoperative Imaging

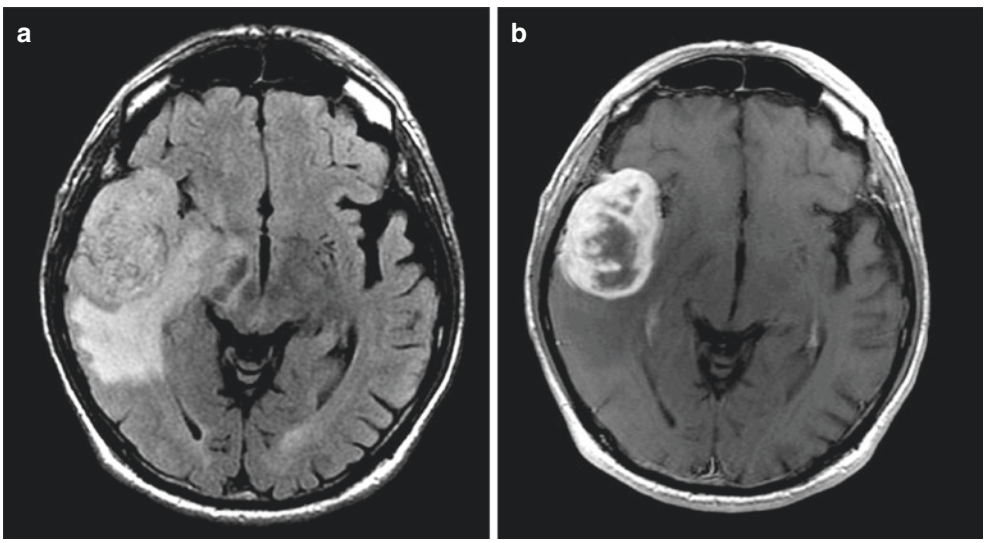

Fig. 19.1 (**a**) MR FLAIR sequence shows massive intra-axial right temporal-insular lesion, with maximum antero-posterior diameter of 5.5 cm and heterogeneous signal. The lesion is associated with white matter signal hyperintensity in the temporal lobe and right capsular-insular region with signs of compression on the right lateral ventricle. A slight midline shift to the left can also be seen. (**b**) Contrast-enhancement MR SE T1-weighted sequence displays an intensely enhancing nodule with ill-defined margins and central necrosis

G. Polonara (✉) · L. Alvaro · N. Herber
Department of Radiology, University Hospital "Ospedali Riuniti", Ancona, Italy

T. Scarabino, S. Pollice (eds.), *Imaging Gliomas After Treatment*, https://doi.org/10.1007/978-3-030-31210-7_29

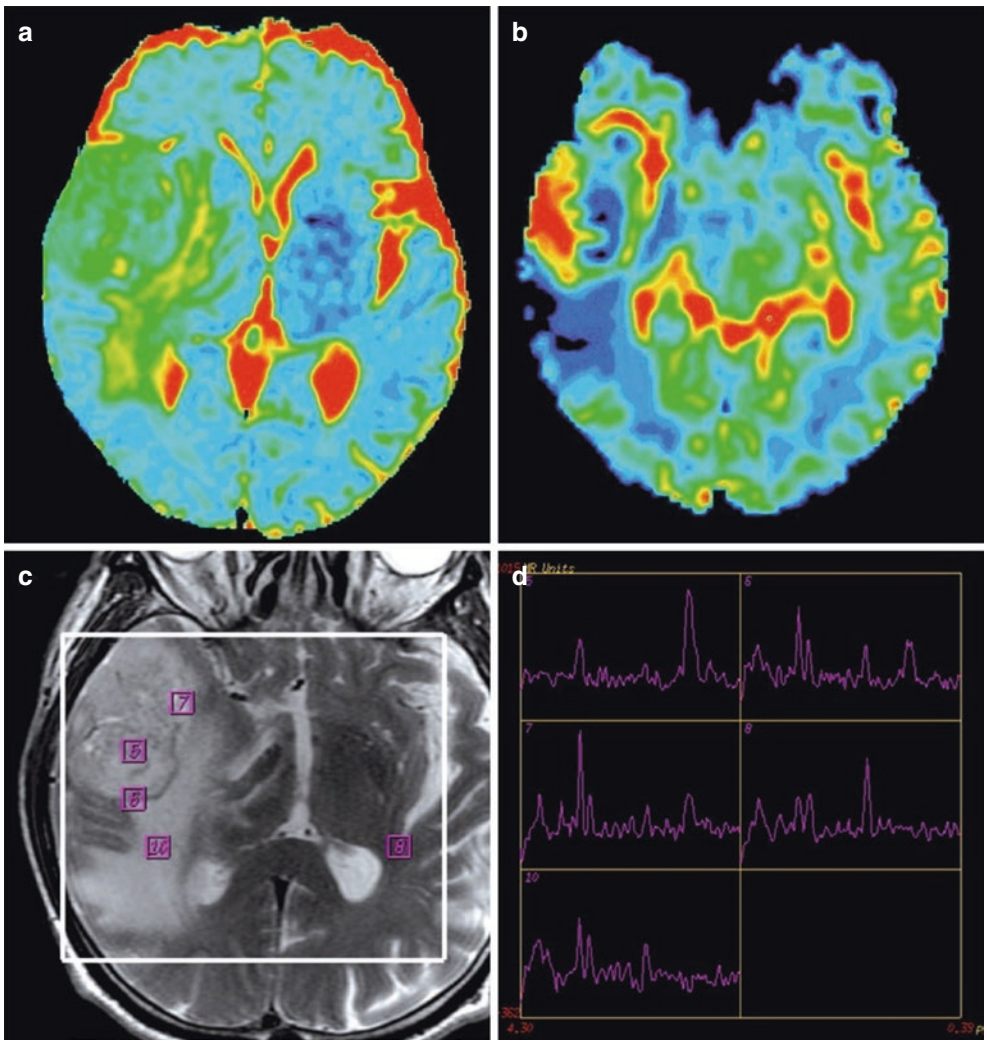

Fig. 19.2 (**a**) MR diffusion-weighted image shows an increase in the apparent diffusion coefficient at the infiltrative-expansive mass with perilesional signal alteration. (**b**) MR perfusion study shows an increase in perfusion more evident at the margins, in the right inferolateral region. (**c**, **d**) MR spectroscopy. In the center of the lesion there is an increase in the lipid peak (necrosis) and choline peak (cell proliferation), whereas choline is high and lipids are low at the margins. The choline is still high and NAA is low at about 1 cm from the macronodular lesion, a finding suggestive of neoplastic infiltration in the peripheral area

Early Postoperative Follow-Up (at 48 h)

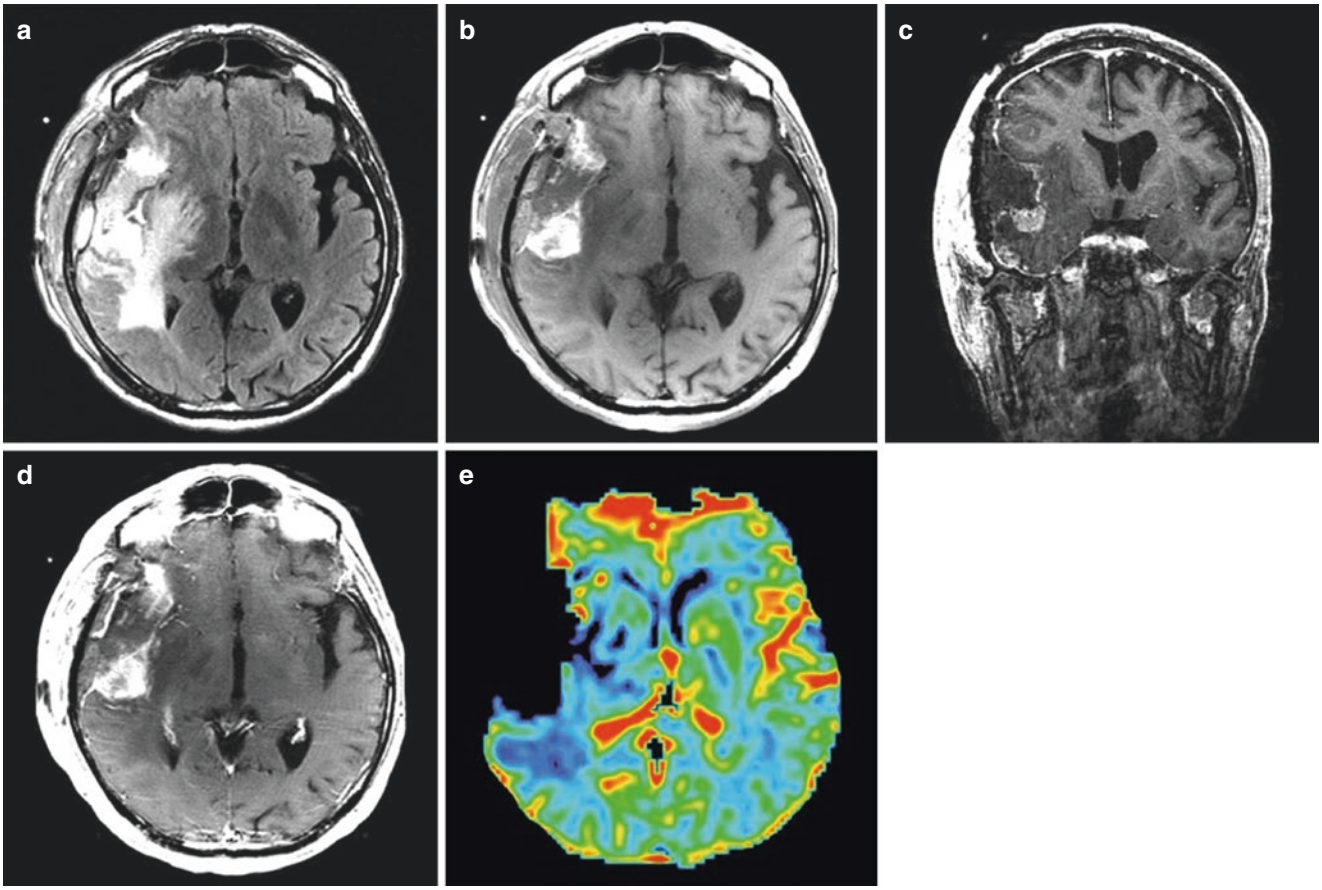

Fig. 19.3 (**a**) MR FLAIR sequence shows evidence of the frontal-parietal craniotomy and surgical removal of the right temporal-insular lesion. Signs of bleeding can be seen in the surgical cavity, as well as re-expansion of the frontal horn right ventricle and a reduction in the compression on the right lateral ventricle and the left lateral shift of the midline structures. A thin layer of fluid can be appreciated below the bone flap. (**b**) MR SE T1-weighted sequence shows hyperintense tissue at the margins of the surgical cavity suggestive of blood and tamponade material. (**c**, **d**) Contrast-enhanced MR SE T1-weighted sequences show enhancing tissue in the temporal lobe at the anterior-inferior-medial margin of the surgical cavity possibly compatible with a small residual of the resected lesion. (**e**) MR perfusion study shows no sign of increased perfusion at the margins of the surgical cavity

Follow-Up Performed at 4 Months After Surgery, Radiotherapy, and Concomitant Adjuvant Chemotherapy

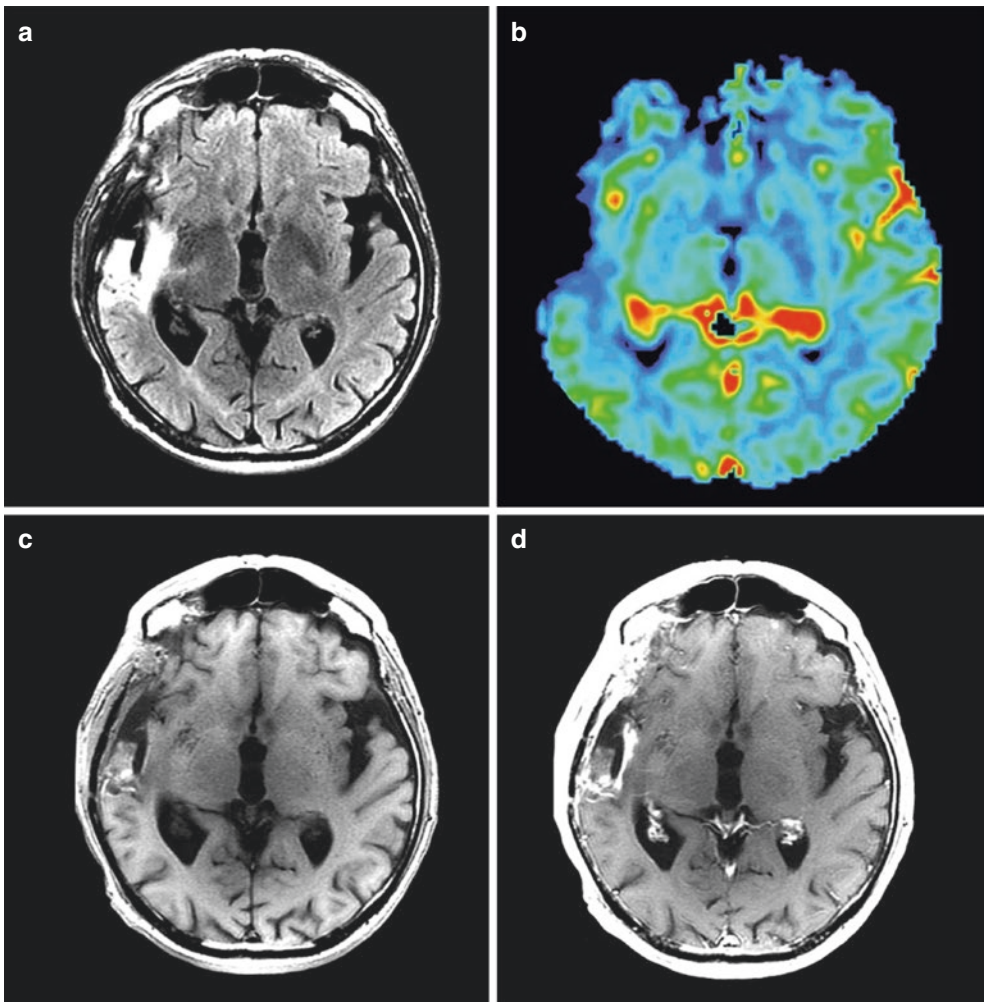

Fig. 19.4 (**a**) MR FLAIR sequence shows a reduction in the signs of bleeding within the right temporal-insular surgical cavity, the perilesional edema and the size of the surgical cavity, with dilation of the temporal horn and right ventricular trigone. The thin fluid layer beneath the bone flap is no longer appreciable and the midline structures appear completely realigned. (**b**) MR perfusion study shows no sign of increased perfusion at the margins of the surgical cavity. MR SE T1-weighted sequences before (**c**) and after contrast media injection (**d**) show a marked reduction in the signs of altered BBB at the surgical margins, which remained more pronounced posteriorly

Follow-Up Performed at 7 Months

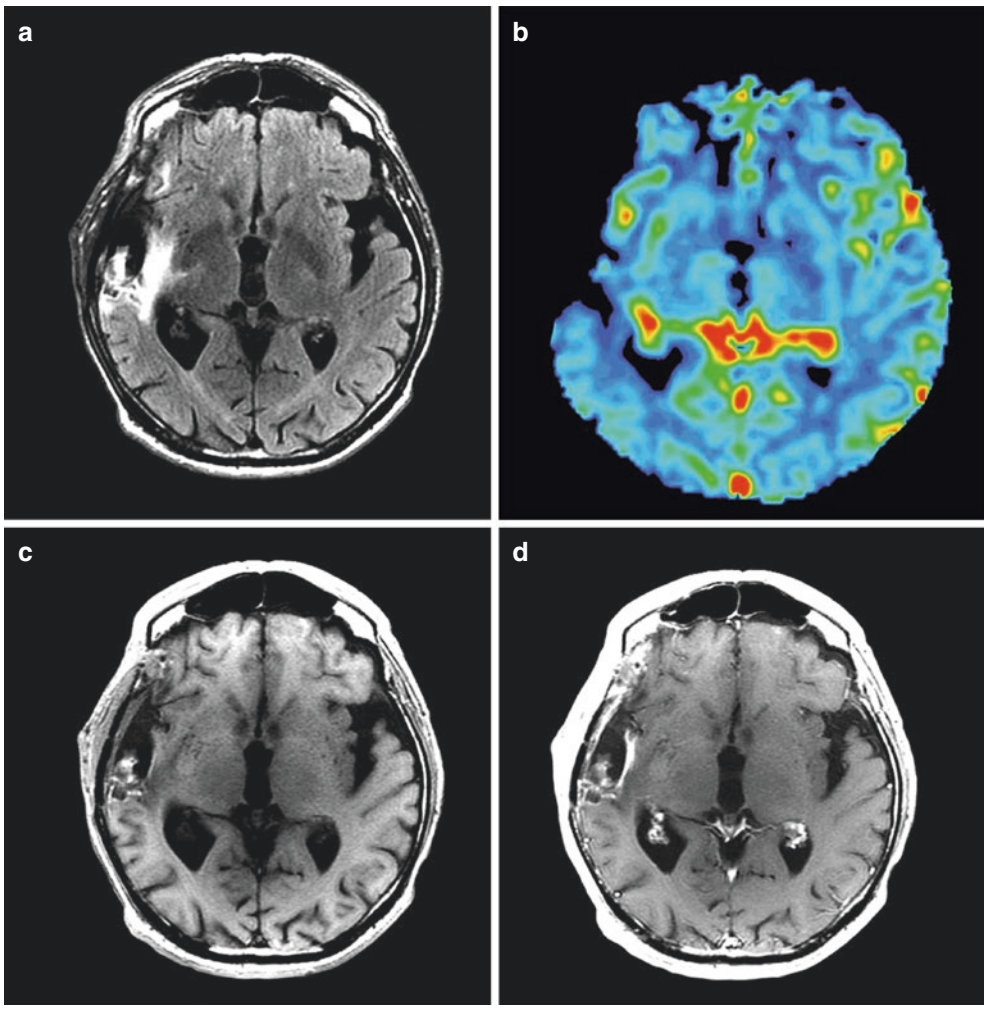

Fig. 19.5 MR FLAIR sequence (**a**), perfusion study (**b**), and SE T1-weighted sequences before (**c**) and after gadolinium-based contrast agent injection (**d**) show a reduction in T1 signal enhancement after contrast medium administration at the level of the dura and the margins of the surgical cavity correlated with the findings of the previous surgery. No other appreciable changes compared to the previous study can be seen

Follow-Up Performed at 9 Months After Surgery and Further Adjuvant Chemotherapy

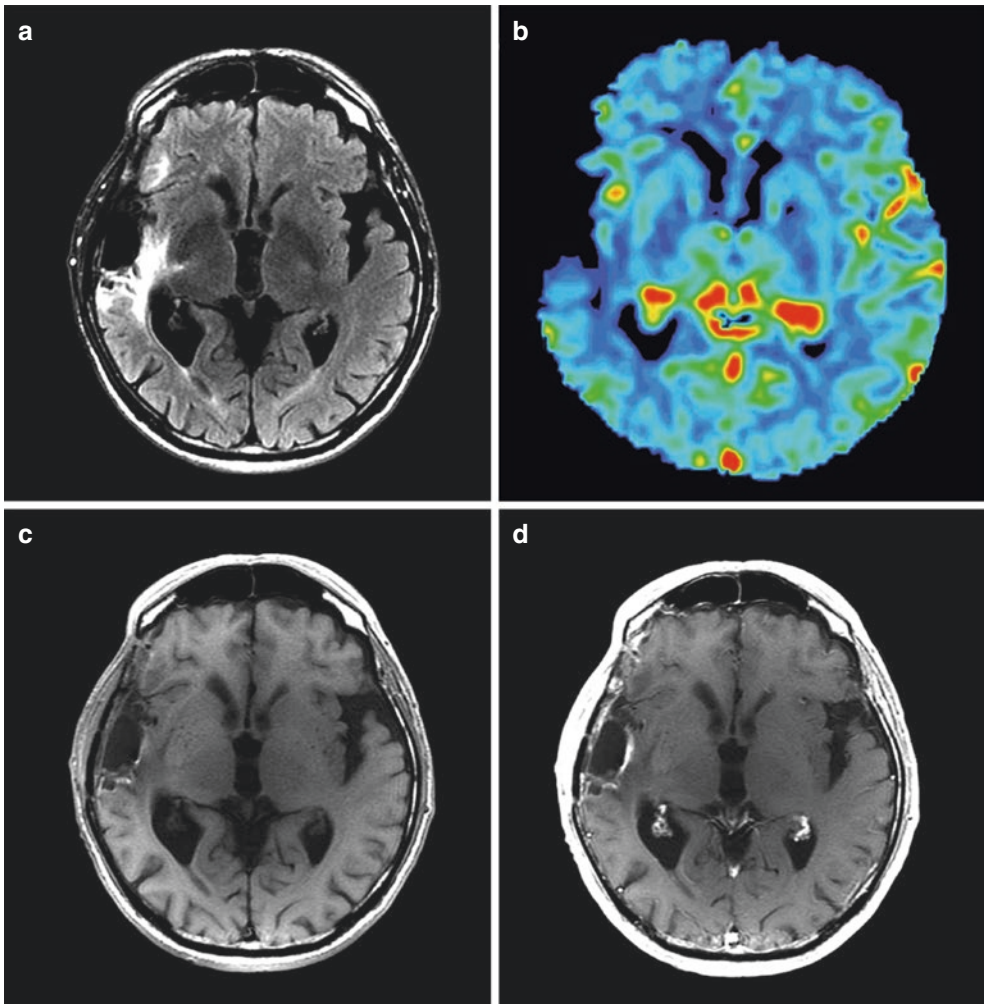

Fig. 19.6 MR FLAIR sequence (**a**), perfusion study (**b**), and SE T1-weighted sequences before (**c**) and after gadolinium-based contrast agent injection (**d**) show a reduction in T1 signal enhancement after contrast medium administration at the level of the dura and the margins of the surgical cavity correlated with the findings of the previous surgery. No other appreciable changes compared to the previous study can be seen

Follow-Up Performed at 12 Months

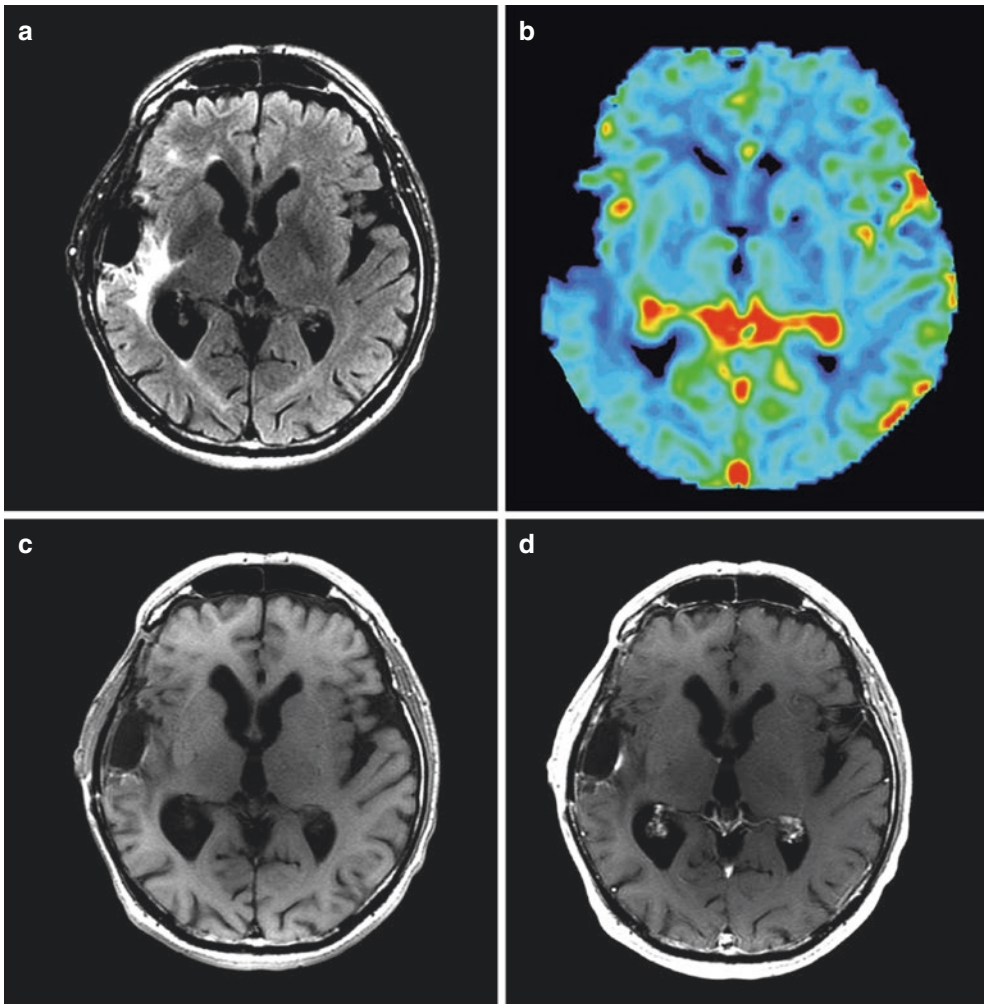

Fig. 19.7 MR FLAIR sequence (**a**), perfusion study (**b**), and SE T1-weighted sequences before (**c**) and after gadolinium-based contrast agent injection (**d**) show a reduction in T1 signal enhancement after contrast medium administration at the level of the dura and the margins of the surgical cavity correlated with the findings of the previous surgery. No other appreciable changes compared to the previous study can be seen

Stable Disease: 3T Multimodal MR Follow-Up in Glioblastoma Multiforme

Case 20

Tommaso Scarabino, Teresa Popolizio, Saverio Pollice, Vincenzo D'Angelo, and Alfonso Di Costanzo

- 45-year-old patient with left frontal-insular glioblastoma multiforme treated with subtotal resection and combined radiation therapy–chemotherapy.
- 3T multimodal MR follow-up performed with morphologic imaging, diffusion, perfusion, and spectroscopy preoperatively and at 6 and 12 months after surgery and combined radiation therapy–chemotherapy.

T. Scarabino (✉) · S. Pollice
Department of Radiology, "L. Bonomo" Hospital, Andria, BT, Italy

T. Popolizio · V. D'Angelo
Department of Neuroradiology, IRCCS "Casa Sollievo della Sofferenza", San Giovanni Rotondo, FG, Italy

A. Di Costanzo
Department of Neurology, University of Molise, Campobasso, Italy

T. Scarabino, S. Pollice (eds.), *Imaging Gliomas After Treatment*, https://doi.org/10.1007/978-3-030-31210-7_30

Preoperative Imaging

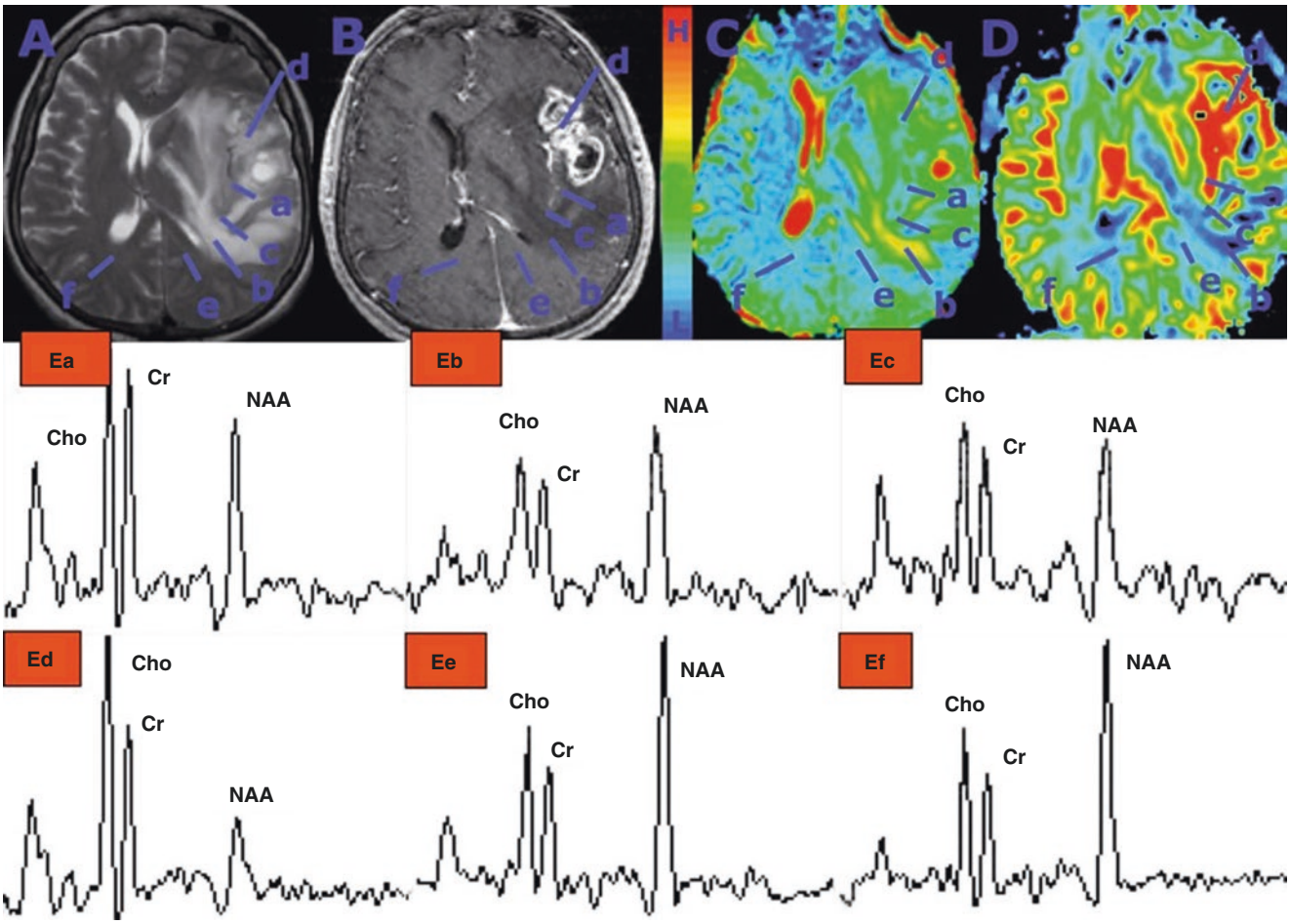

Fig. 20.1 MR FSE T2-weighted (**a**) and contrast-enhanced SE T1-weighted (**b**) sequences show a large mass with heterogeneous signal and enhancement due to the presence of large components of central necrosis, with abundant edema and moderate mass effect on the midline structures which appear shifted laterally. The MR multimodal study with diffusion-weighted imaging and ADC map (**c**), perfusion study with CBV map (**d**), and single-voxel spectroscopy with multiple ROIs (**e**) show spectra relative to the areas with enhancing tumor and immediately behind the lesion with the typical pattern of high Cho and inversion of the Cho/NAA ratio. In these ROIs, the ADC is decreased and the CBV is increased; the opposite happens in the necrotic-colliquative area. The spectra in the apparently edematous area beyond the enhancing margins have overall reduced levels of all metabolites but with spectroscopic patterns indicating tumor-infiltrated edema. In these locations, ADC is reduced while CBV is high. Moving away from the lesion the metabolic pattern along with ADC and CBV values return to normal as in the contralateral hemisphere

Follow-Up Performed at 6 Months After Surgery and Combined Radiation Therapy–Chemotherapy

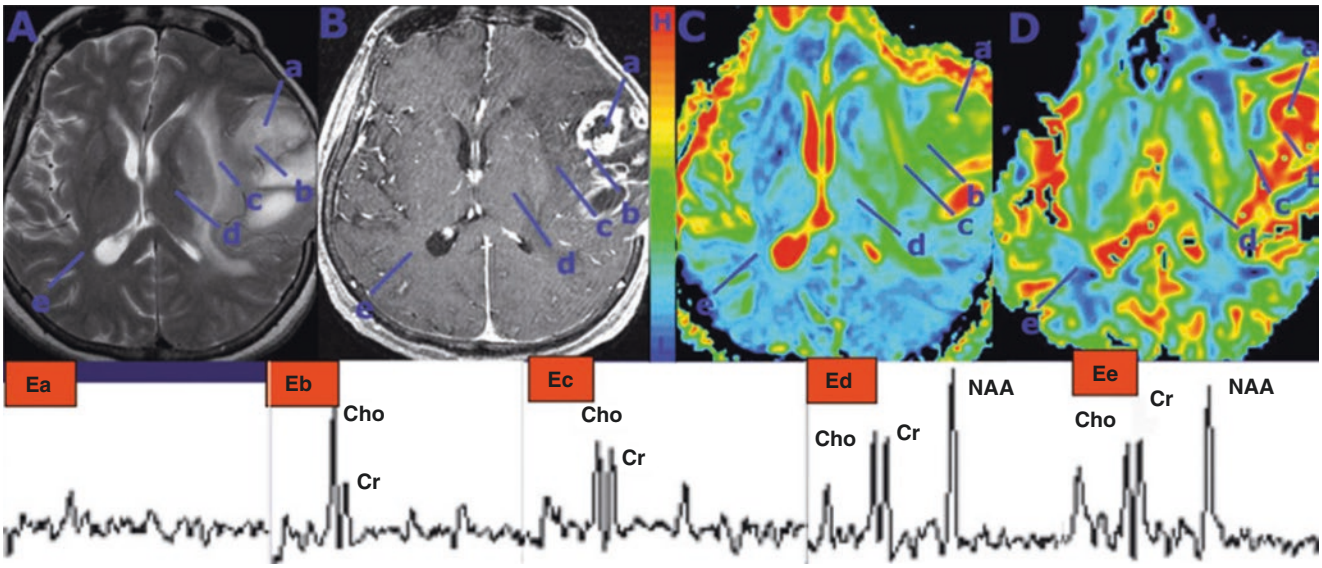

Fig. 20.2 Morphofunctional MR with FSE T2-weighted (**a**) and contrast-enhanced SE T1-weighted (**b**) sequences, diffusion-weighted imaging with ADC map (**c**), perfusion study with CBV map (**d**), and multivoxel spectroscopy with multiple ROIs (**e**). The imaging findings following treatment show an increase in the necrotic component, characterized by a reduction in the spectral levels of all metabolites, increased ADC, and decreased CBV. These indices instead retain the tumor pattern in the enhancing areas and those immediately adjacent to the lesion

Follow-Up Performed at 12 Months

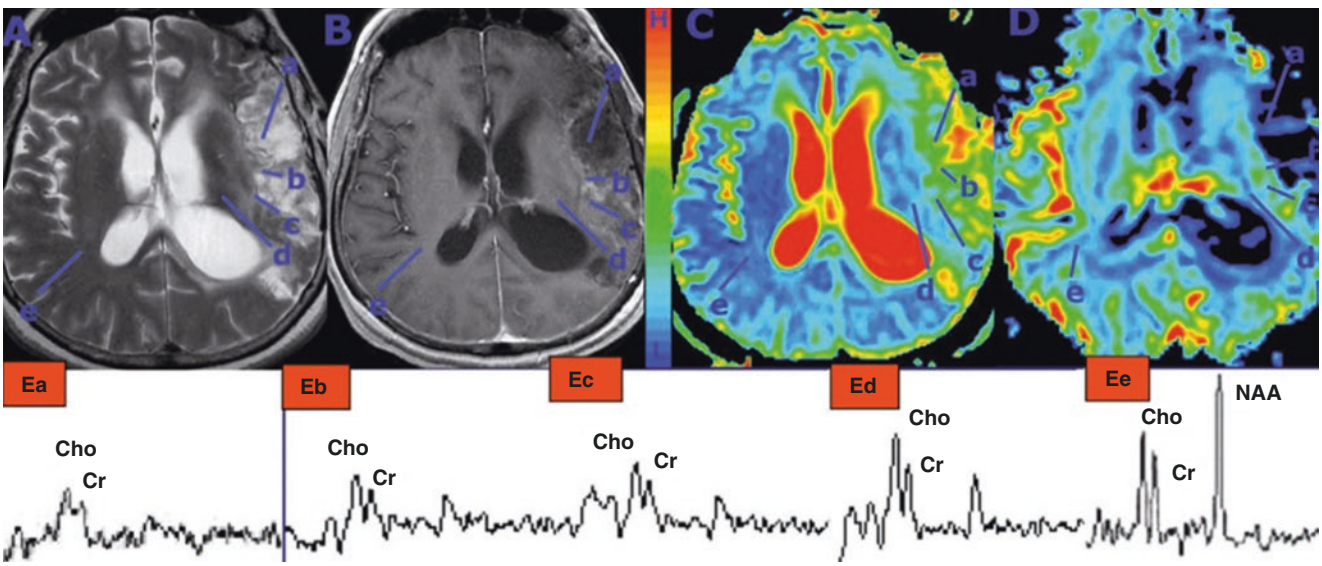

Fig. 20.3 Multimodal MR with FSE T2-weighted (**a**) and contrast-enhanced SE T1-weighted (**b**) sequences, diffusion-weighted imaging with ADC map (**c**), perfusion study with CBV map (**d**), and multivoxel spectroscopy with multiple ROIs (**e**). The results obtained by radiation therapy and chemotherapy show an almost complete necrotic transformation of the lesion with no sign of significant enhancement and with associated retraction dilatation of the adjacent lateral ventricle. There is a concomitant reduction in the spectra of all metabolites, an increase in ADC, and a decrease in CBV. These indices can also be appreciated in the surrounding tissue

3T Morphofunctional MR Follow-Up in High-Grade Oligodendroglioma

Case 21

Massimo Caulo, Chiara Briganti, Valentina Panara, Simone Salice, Domenico Tortora, and Armando Tartaro

- 54-year-old patient with right parietal high-grade oligodendroglioma treated with subtotal surgery and combined radiation therapy–chemotherapy.
- 3T morphofunctional MR follow-up performed with morphologic sequence and spectroscopy at 2 years after surgery and combined radiation therapy–chemotherapy.

Follow-Up Performed at 2 Years After Surgery and Combined Radiation Therapy–Chemotherapy

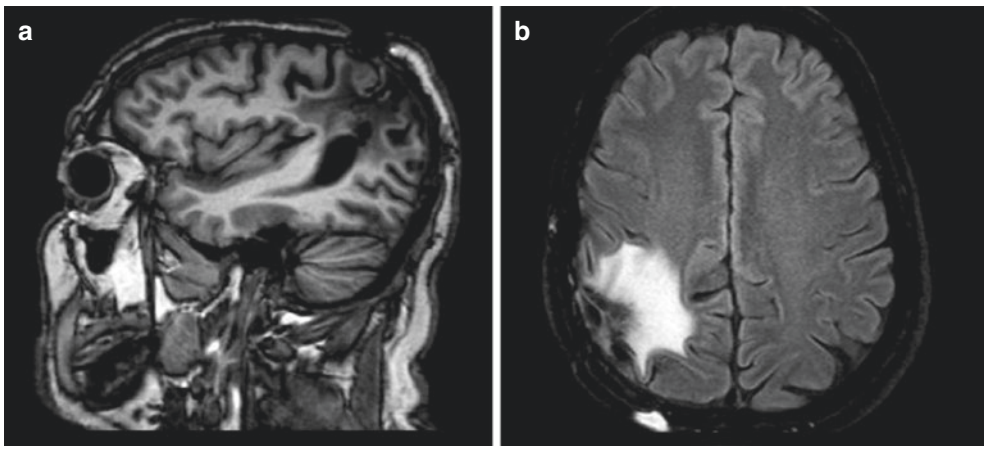

Fig. 21.1 Contrast-enhanced MR SE T1-weighted (**a**) and FLAIR (**b**) sequences show the surgical site in the right parietal region characterized by cavitation surrounded by diffuse signal alteration of the white matter

M. Caulo · C. Briganti · V. Panara · S. Salice · D. Tortora
A. Tartaro (✉)
Department of Neurosciences and Imaging, Institute of Advanced Biomedical Technologies, "G. d'Annunzio" University, Chieti-Pescara, Italy
e-mail: tartaro@unich.it

T. Scarabino, S. Pollice (eds.), *Imaging Gliomas After Treatment*, https://doi.org/10.1007/978-3-030-31210-7_31

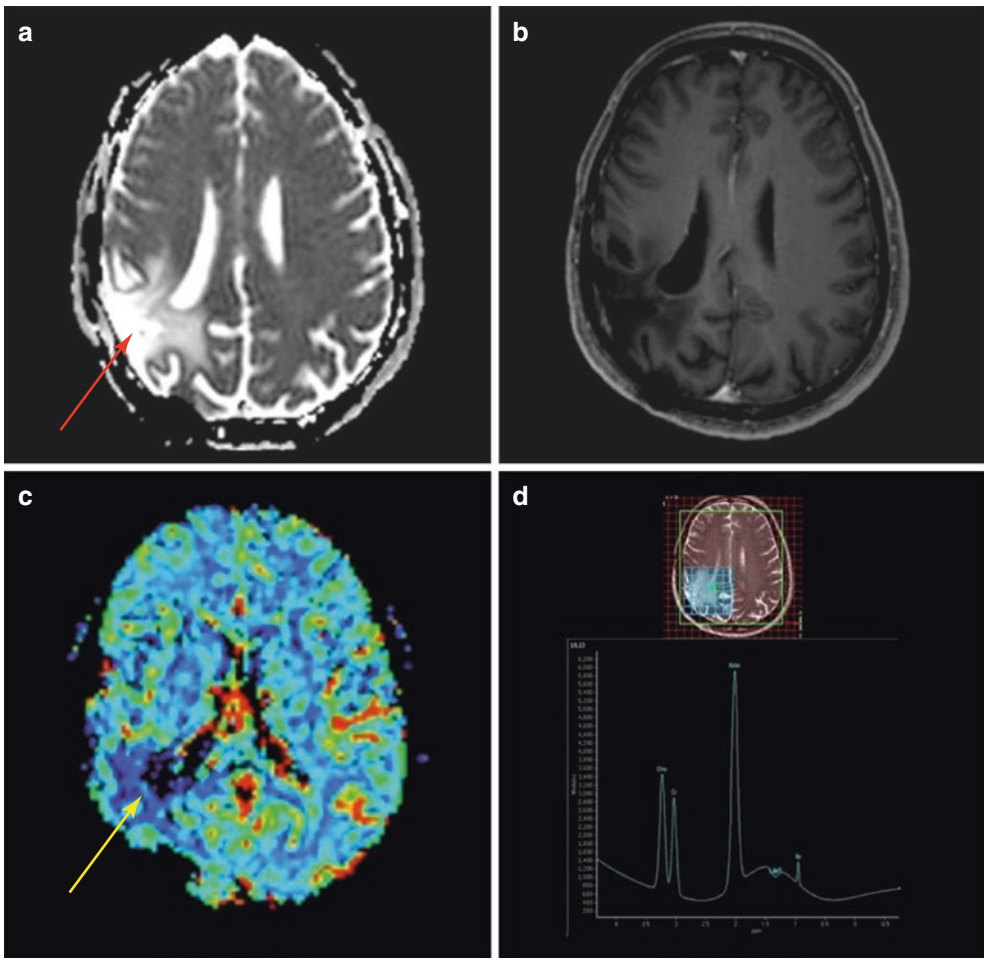

Fig. 21.2 (**a**) MR diffusion-weighted imaging with ADC map shows increased ADC values (1.832 ± 0.832 mm^2/s) at the surgical cavity (*red arrow*). (**b**) Contrast-enhanced MR SE T1-weighted sequence. Contrast enhancement is absent. (**c**) MR perfusion study with CBV map. The value of rCBV (CBV lesions/contralateral white matter CBV) is 0.78 close to the surgical cavity (*yellow arrow*). (**d**) Multi/single-voxel spectroscopy shows no increase in the concentration of Cho, which indicates low cell turnover and thus the absence of disease progression

Tumor Recurrence: Postoperative MR Follow-Up in Grade III Oligodendroglioma

Case 22

Ferdinando Caranci, Alessandra D'Amico, and Sossio Cirillo

- Patient with surgically treated grade III left fronto-parietal oligodendroglioma.
- Postoperative follow-up performed late (9 months) with MR morphologic sequences.

Preoperative Imaging

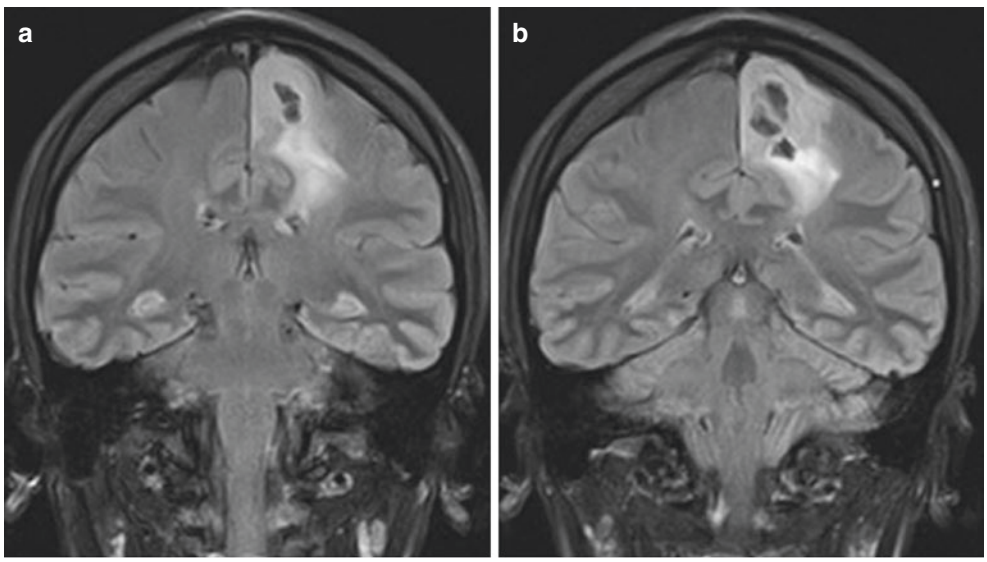

Fig. 22.1 (**a**–**d**) MR FLAIR sequence. Images show an infiltrating lesion at the left parasagittal fronto-parietal convexity, extending from the cortical profile to the deep white matter, with inhomogeneous structure due to internal areas of necrosis

F. Caranci (✉) · A. D'Amico
Department of Precision Medicine, School of Medicine, University of Campania "Luigi Vanvitelli", Naples, Italy

S. Cirillo
Department of Medicine and Health Sciences "V. Tiberio", University of Molise, Campobasso, Italy

T. Scarabino, S. Pollice (eds.), *Imaging Gliomas After Treatment*, https://doi.org/10.1007/978-3-030-31210-7_32

Fig. 22.1 (continued)

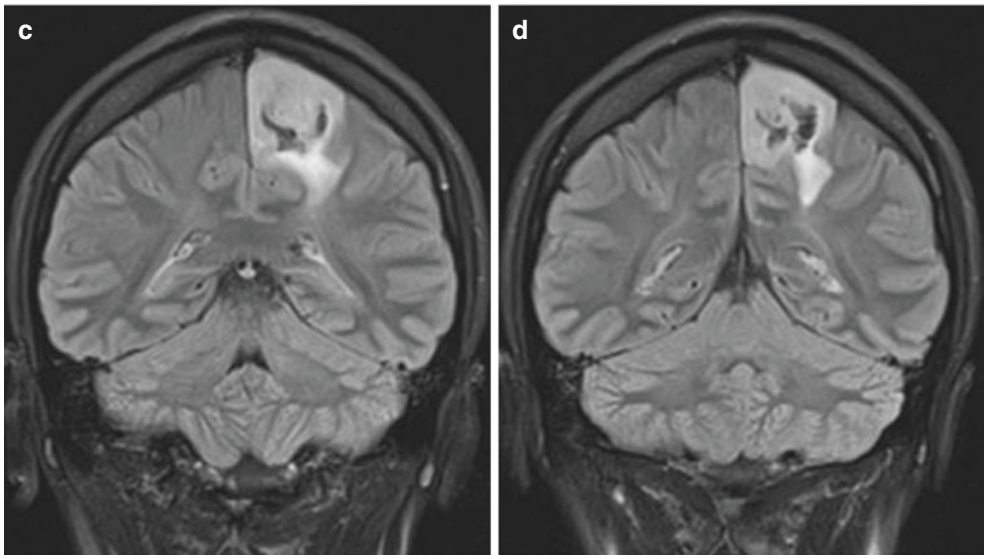

Fig. 22.2 (**a**–**d**) Contrast-enhanced MR SE T1-weighted images. Thin linear streaks of enhancement can be appreciated in the posterior portion of the lesion

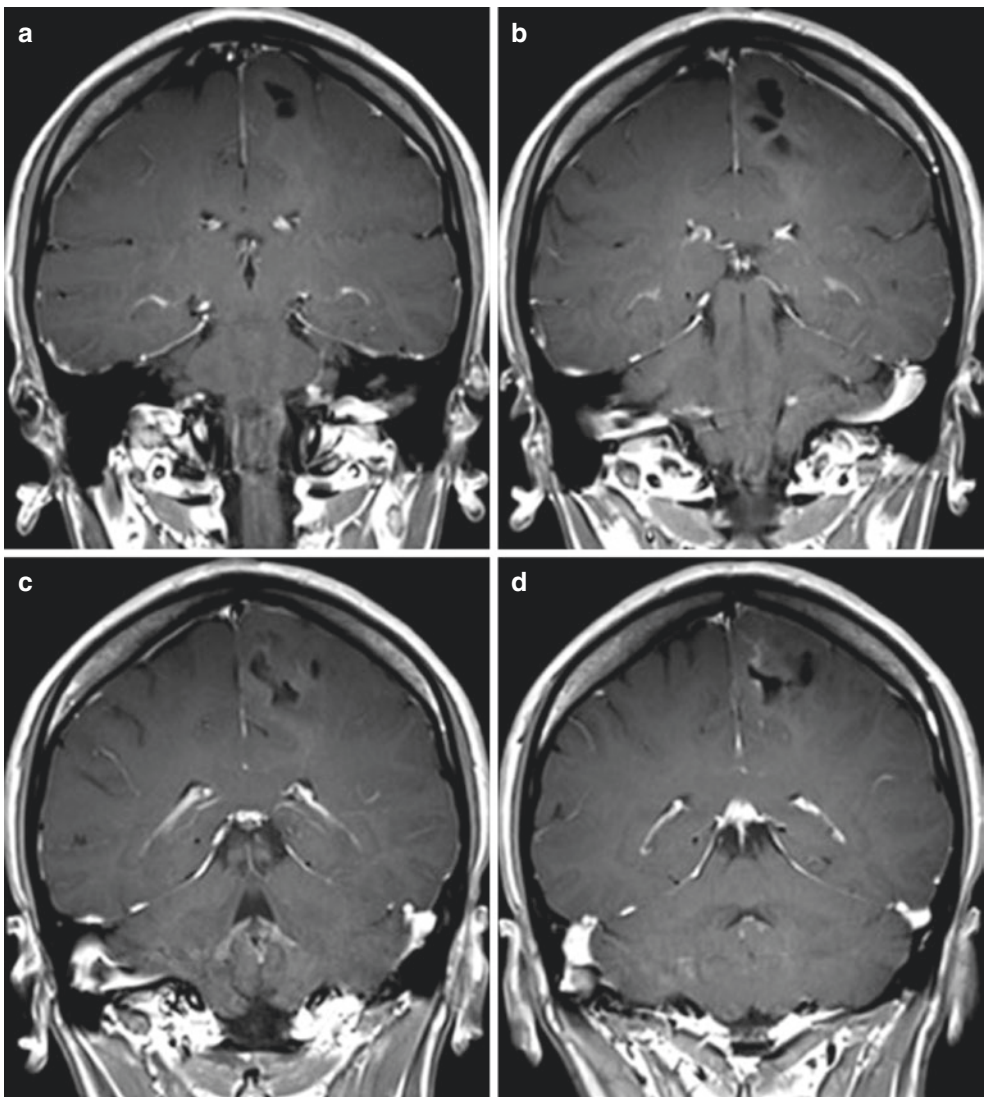

Postoperative Follow-Up at 9 Months

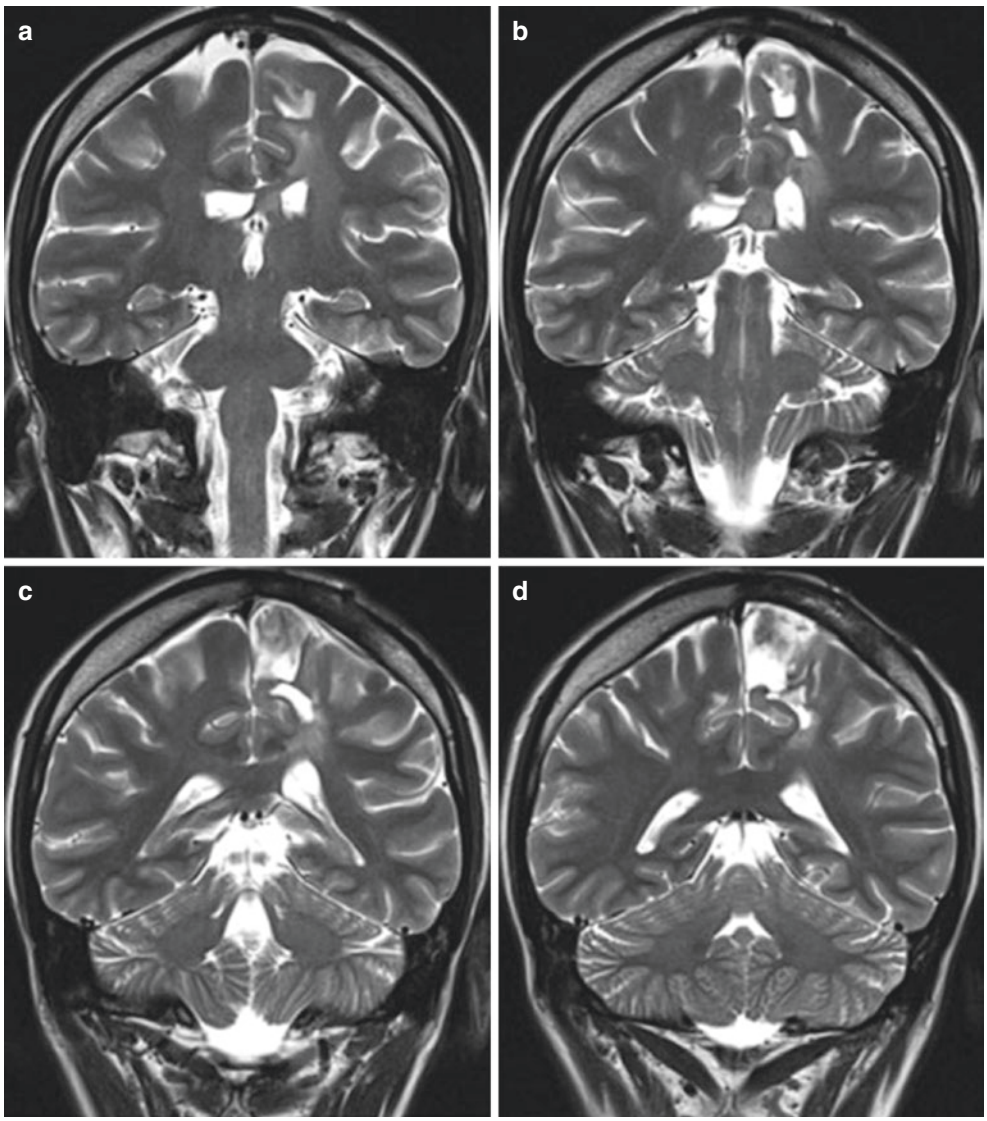

Fig. 22.3 (**a**–**d**) MR FSE T2-weighted sequence. The inhomogeneous appearance of the surgical cavity resulting from partial resection of the lesion is associated with evident heteroplastic pseudonodular thickening of the ipsilateral fornix

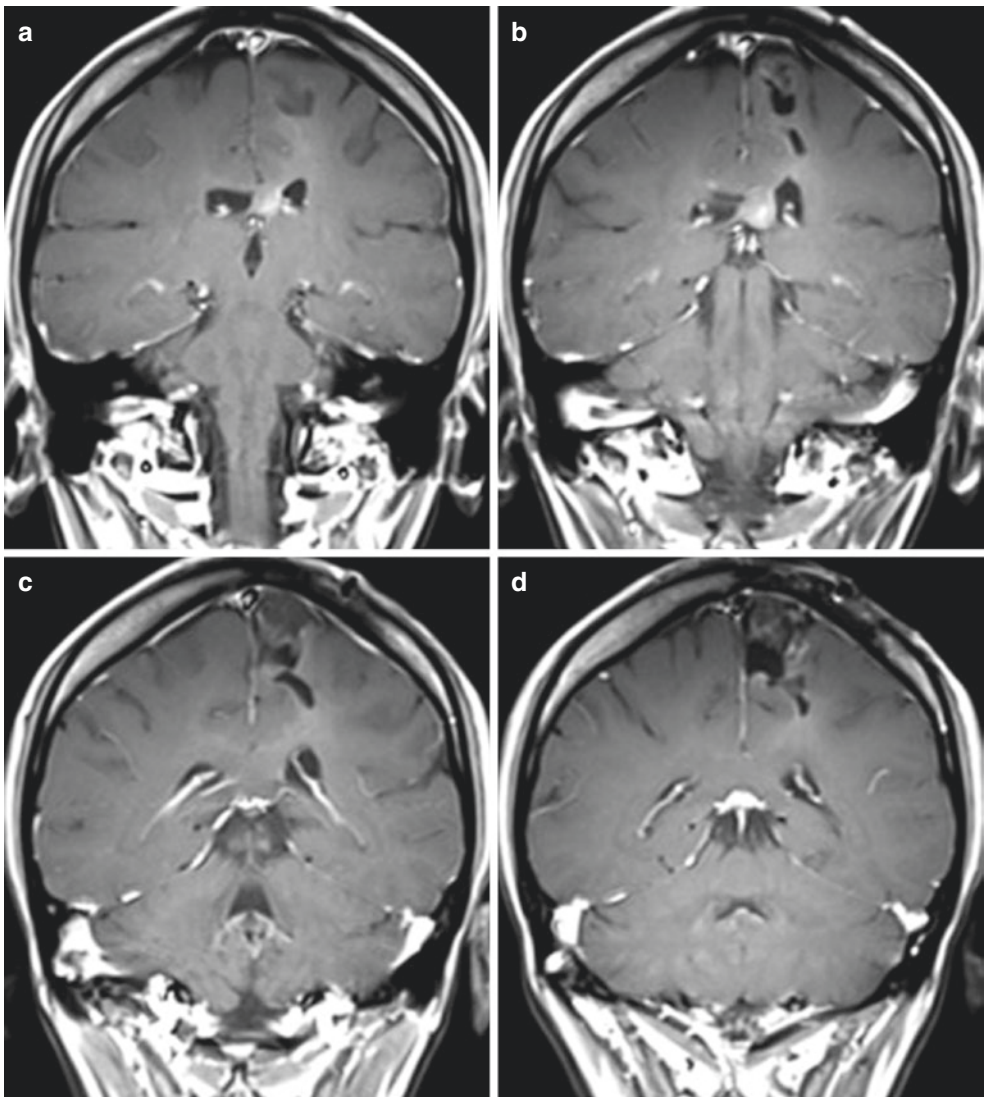

Fig. 22.4 (**a**–**d**) Contrast-enhanced MR SE T1-weighted images. Peripheral linear enhancement of the surgical cavity is appreciable, in part caused by blood–brain barrier injury. Enhancement of the tumor component at the fornix is also evident

Tumor Recurrence: Postoperative MR Follow-Up in Gliosarcoma

Case 23

Ferdinando Caranci, Antonio Volpe, and Arturo Brunetti

- Patient with surgically treated left temporo-occipital gliosarcoma.
- Postoperative follow-up performed late (6 and 9 months) with MR morphologic sequences.

Preoperative Imaging

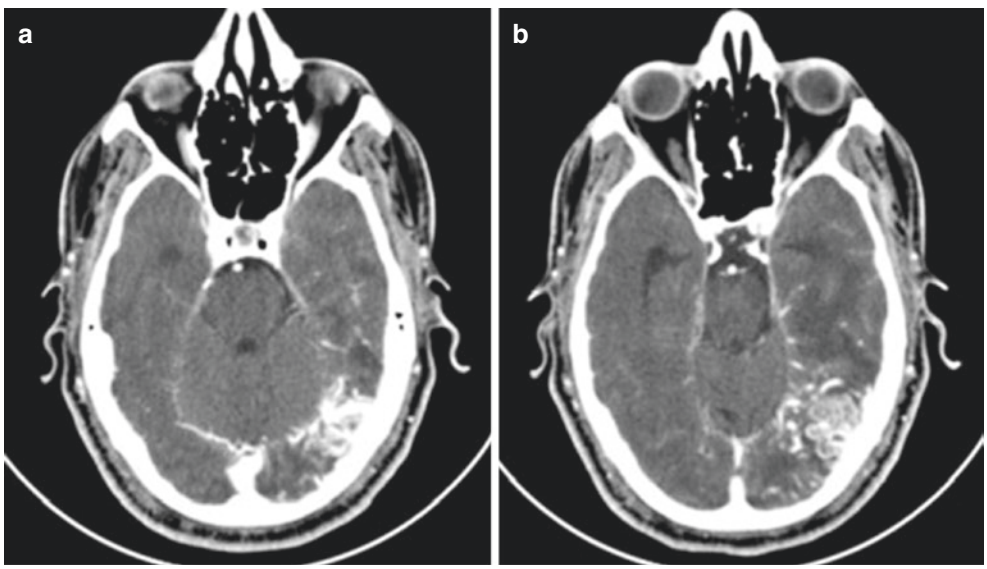

Fig. 23.1 (**a**–**d**) Contrast-enhanced CT scan. Left temporo-occipital lesion characterized by intense enhancement associated with high vascularity

F. Caranci (✉) · A. Volpe · A. Brunetti
Department of Precision Medicine, School of Medicine, University of Campania "Luigi Vanvitelli", Naples, Italy

T. Scarabino, S. Pollice (eds.), *Imaging Gliomas After Treatment*, https://doi.org/10.1007/978-3-030-31210-7_33

Fig. 23.1 (continued)

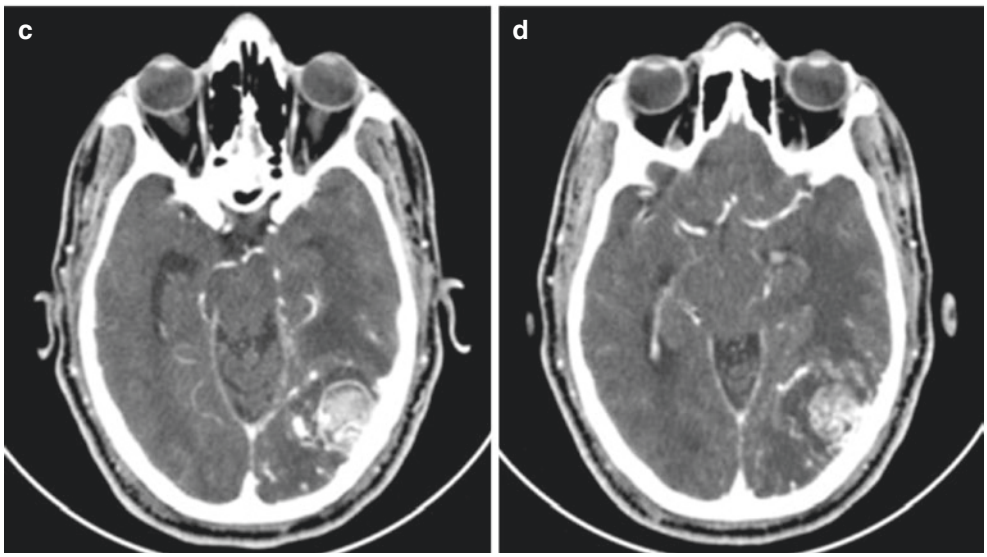

Postoperative Follow-Up at 6 Months

Fig. 23.2 (**a**–**d**) Contrast-enhanced MR SE T1-weighted images. A nodular pattern of enhancement is appreciable at the site of the previously removed lesion indicating tumor recurrence

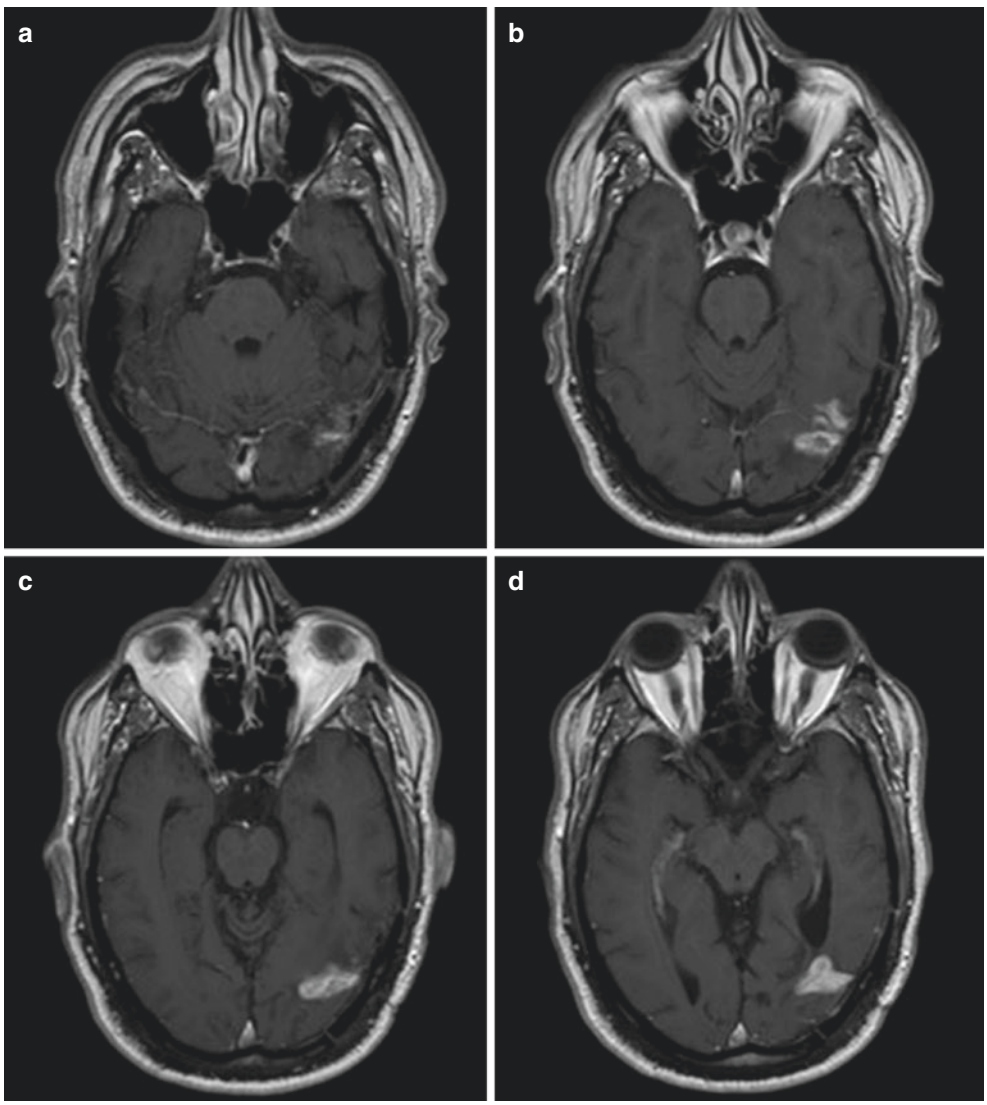

Postoperative Follow-Up at 9 Months

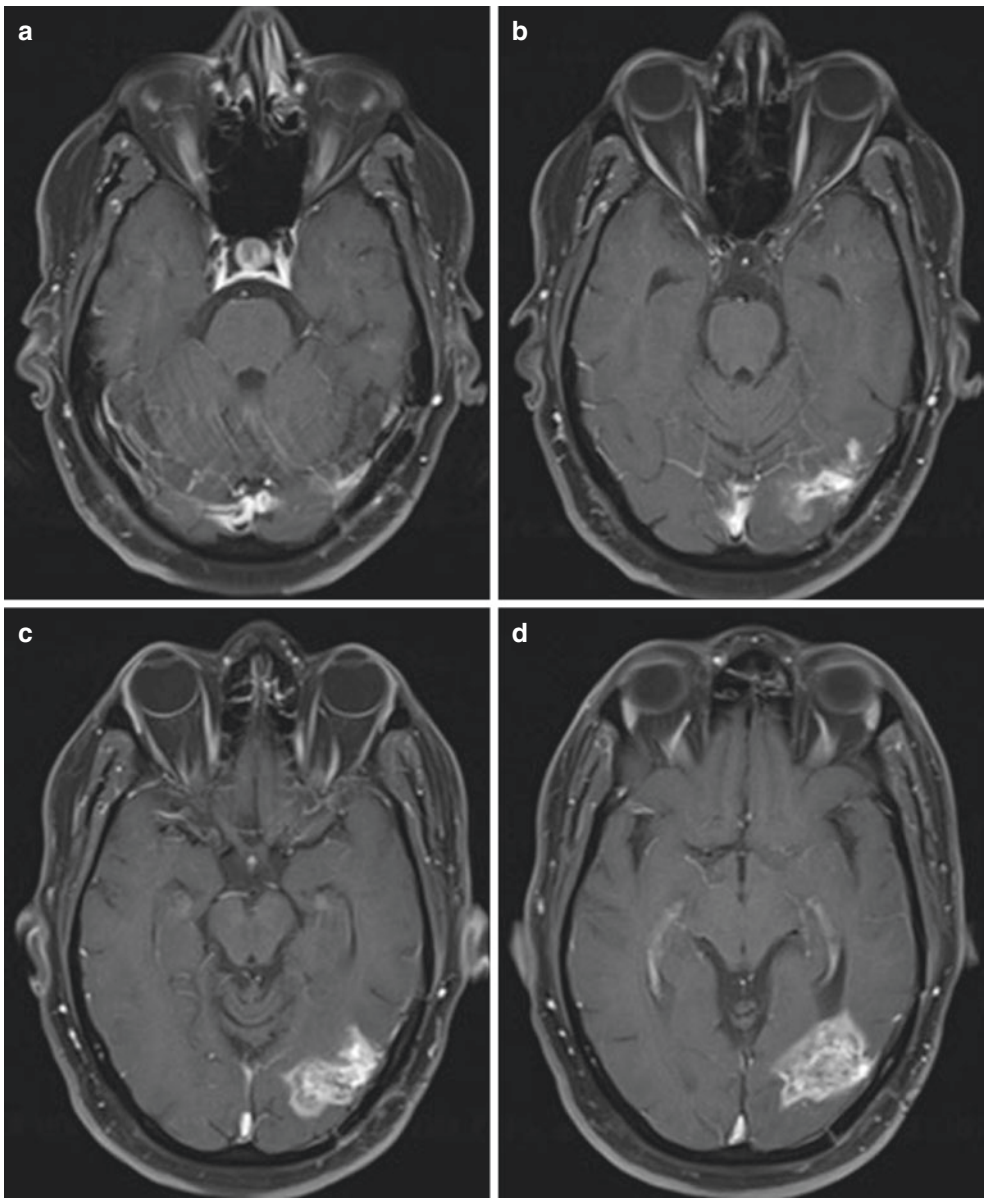

Fig. 23.3 (**a**–**d**) Contrast-enhanced MR SE T1-weighted images. Further expansion of tumor recurrence

Tumor Recurrence: Postoperative MR Follow-Up in Low-Grade Astrocytoma

Case 24

Ferdinando Caranci, Antonio Volpe, and Arturo Brunetti

- Patient with surgically treated grade II left frontal astrocytoma.
- Postoperative follow-up performed late (at 9 and 24 months) with MR morphologic sequences.

Postoperative Follow-Up at 9 Months

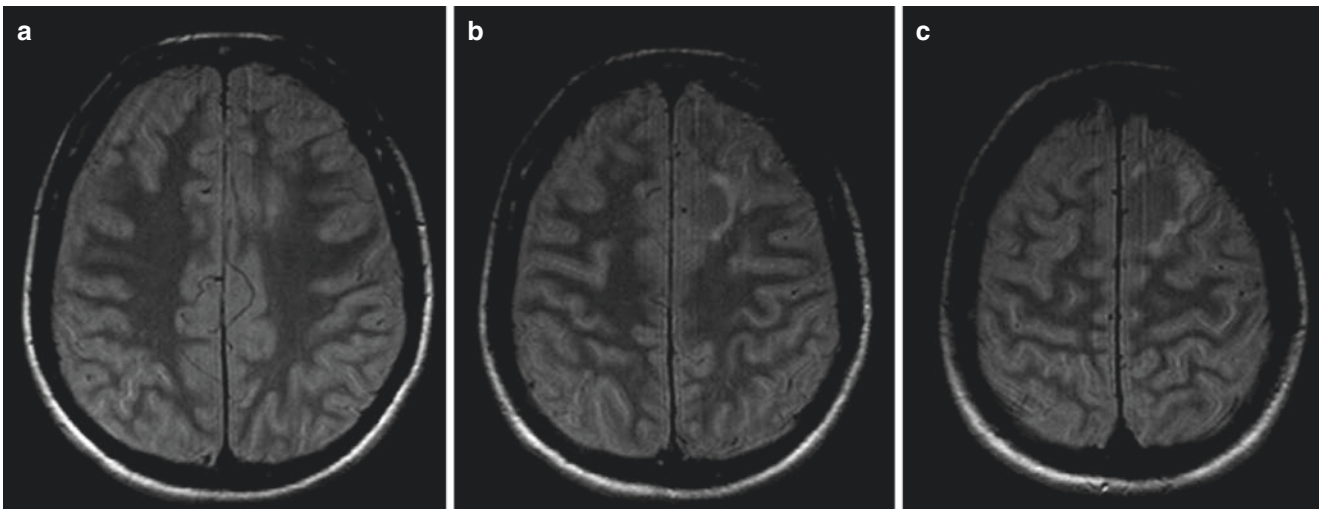

Fig. 24.1 (**a**–**c**) MR DP sequence. A CSF-like area indicating the postsurgical cavity can be appreciated in the white matter of the left frontal convexity surrounded by a halo of high signal

F. Caranci (✉) · A. Volpe · A. Brunetti
Department of Precision Medicine, School of Medicine, University of Campania "Luigi Vanvitelli", Naples, Italy

T. Scarabino, S. Pollice (eds.), *Imaging Gliomas After Treatment*, https://doi.org/10.1007/978-3-030-31210-7_34

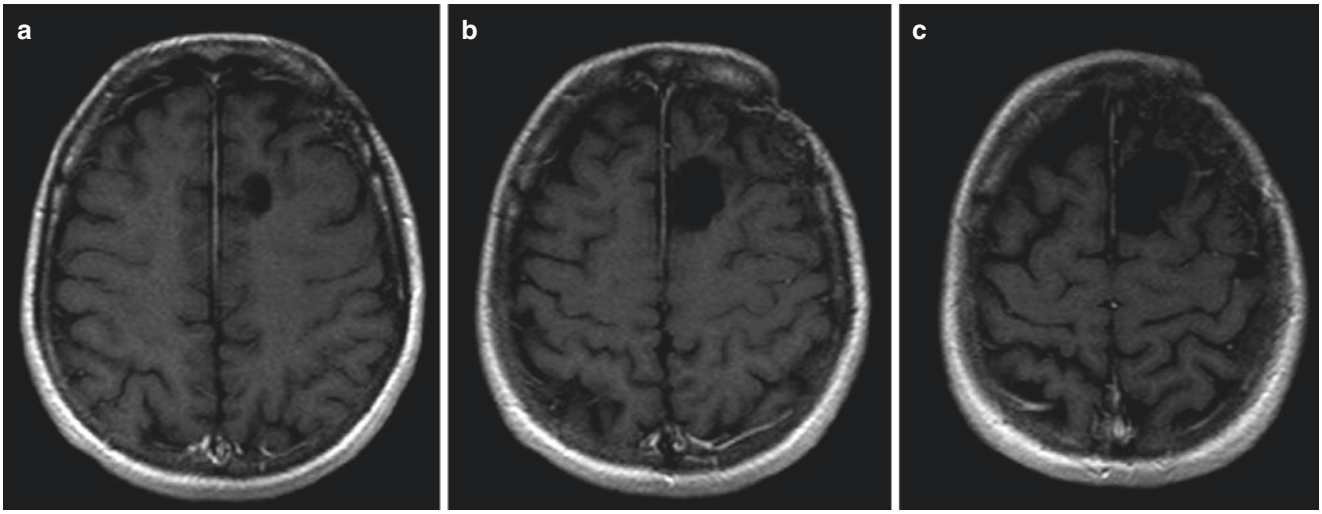

Fig. 24.2 (**a**–**c**) Contrast-enhanced MR SE T1-weighted images. No areas of pathologic enhancement can be appreciated

Postoperative Follow-Up at 24 Months

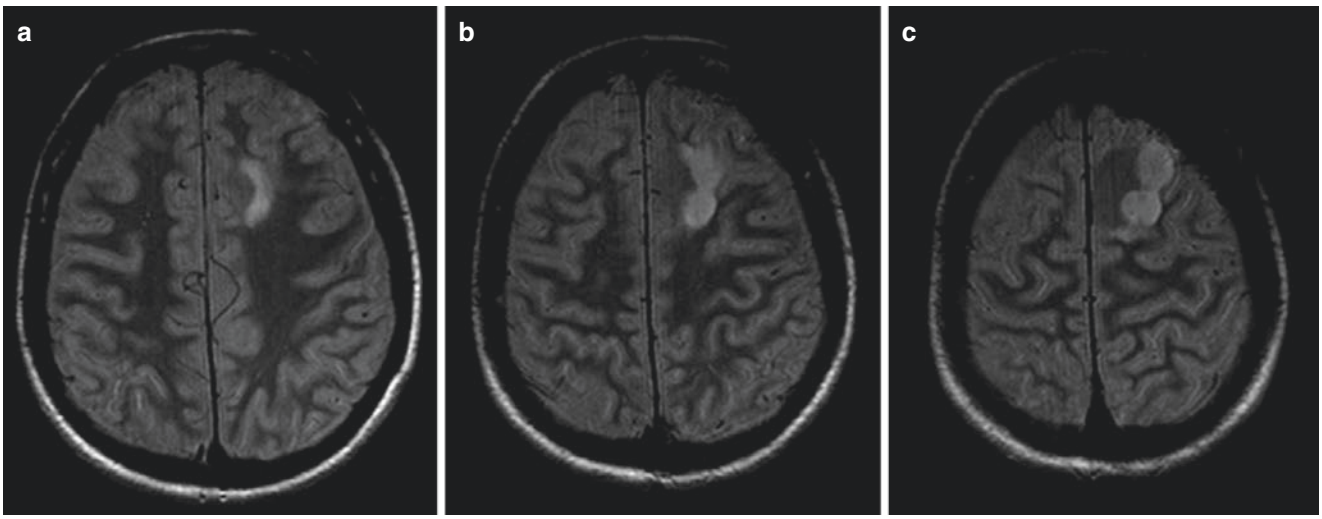

Fig. 24.3 (**a**–**c**) MR DP sequence. The images show an increase of the tissue with pseudonodular characteristics at the lateral margins of the postsurgical cavity (tumor recurrence)

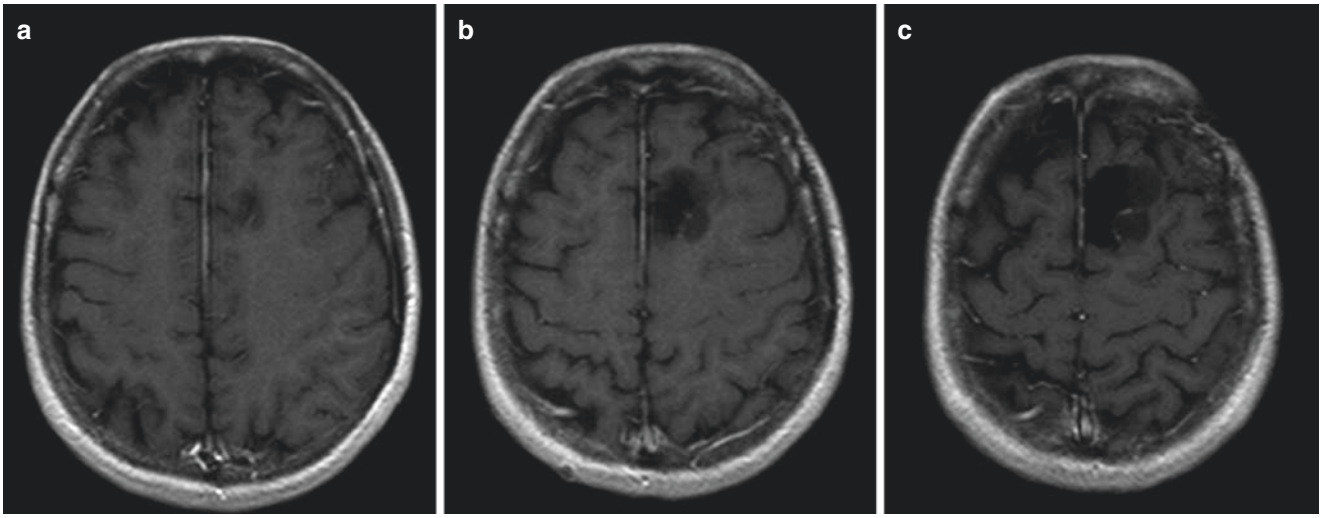

Fig. 24.4 (**a**–**c**) Contrast-enhanced MR SE T1-weighted images. The appearance of slight enhancement corresponding to the recurrence can be seen

Tumor Recurrence: Postoperative MR Follow-Up in Anaplastic Oligoastrocytoma

Case 25

Ferdinando Caranci and Sossio Cirillo

- Patient with posterior left temporal anaplastic oligoastrocytoma treated with surgery and subsequent radiation.
- Postoperative and postradiation therapy follow-up performed late (6, 15, and 24 months) with MR morphologic and perfusion sequences.

Postoperative Follow-Up at 6 Months

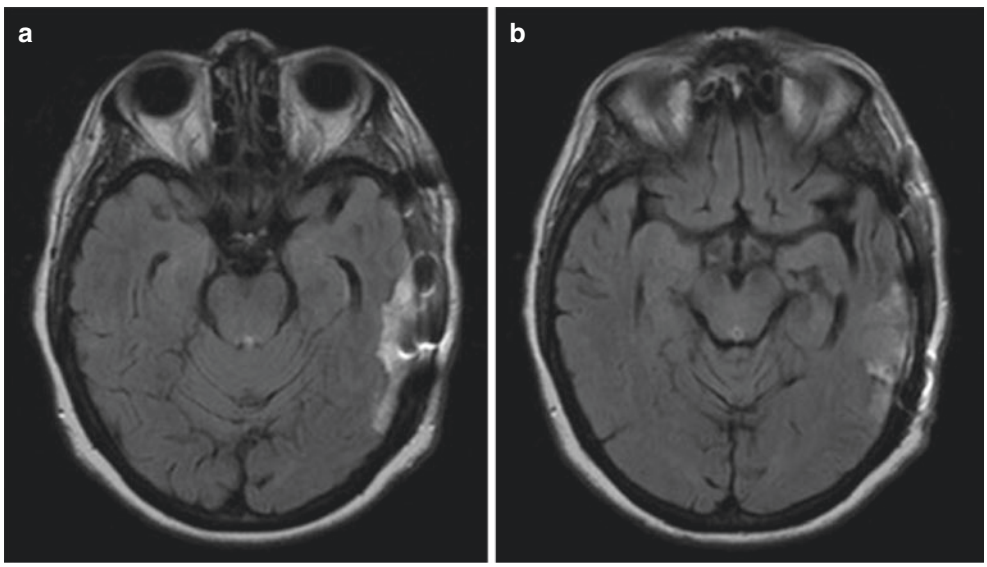

Fig. 25.1 (**a**–**d**) MR FLAIR sequence. Nodular neoplastic residual is visualized in the left posterior temporal region (**c**) and associated with a cortical blood effusion (**a**, **b**)

F. Caranci (✉)
Department of Precision Medicine, School of Medicine, University of Campania "Luigi Vanvitelli", Naples, Italy

S. Cirillo
Department of Medicine and Health Sciences "V. Tiberio", University of Molise, Campobasso, Italy

T. Scarabino, S. Pollice (eds.), *Imaging Gliomas After Treatment*, https://doi.org/10.1007/978-3-030-31210-7_35

Fig. 25.1 (continued)

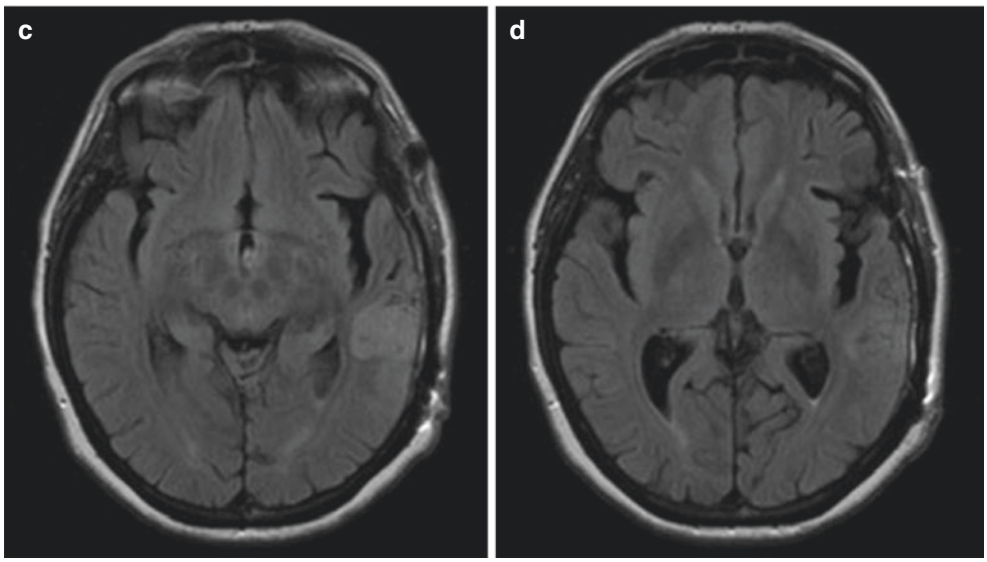

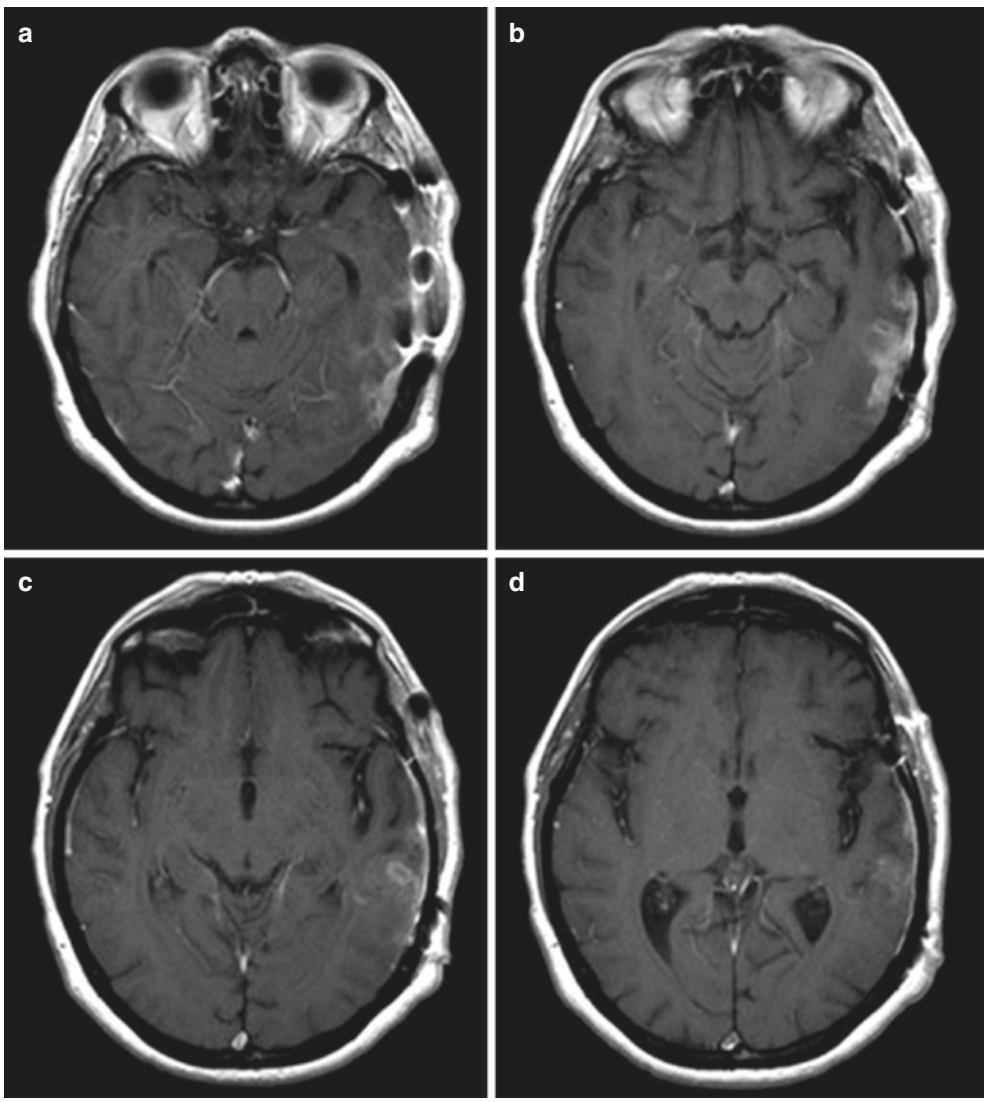

Fig. 25.2 (**a**–**d**) Contrast-enhanced MR SE T1-weighted images. Cortical-subcortical enhancement can be appreciated in the left posterior temporal region, in part caused by blood–brain barrier injury, with reactive enhancing dura adjacent to the bone flap

Postoperative Follow-Up (Postradiation) at 15 Months

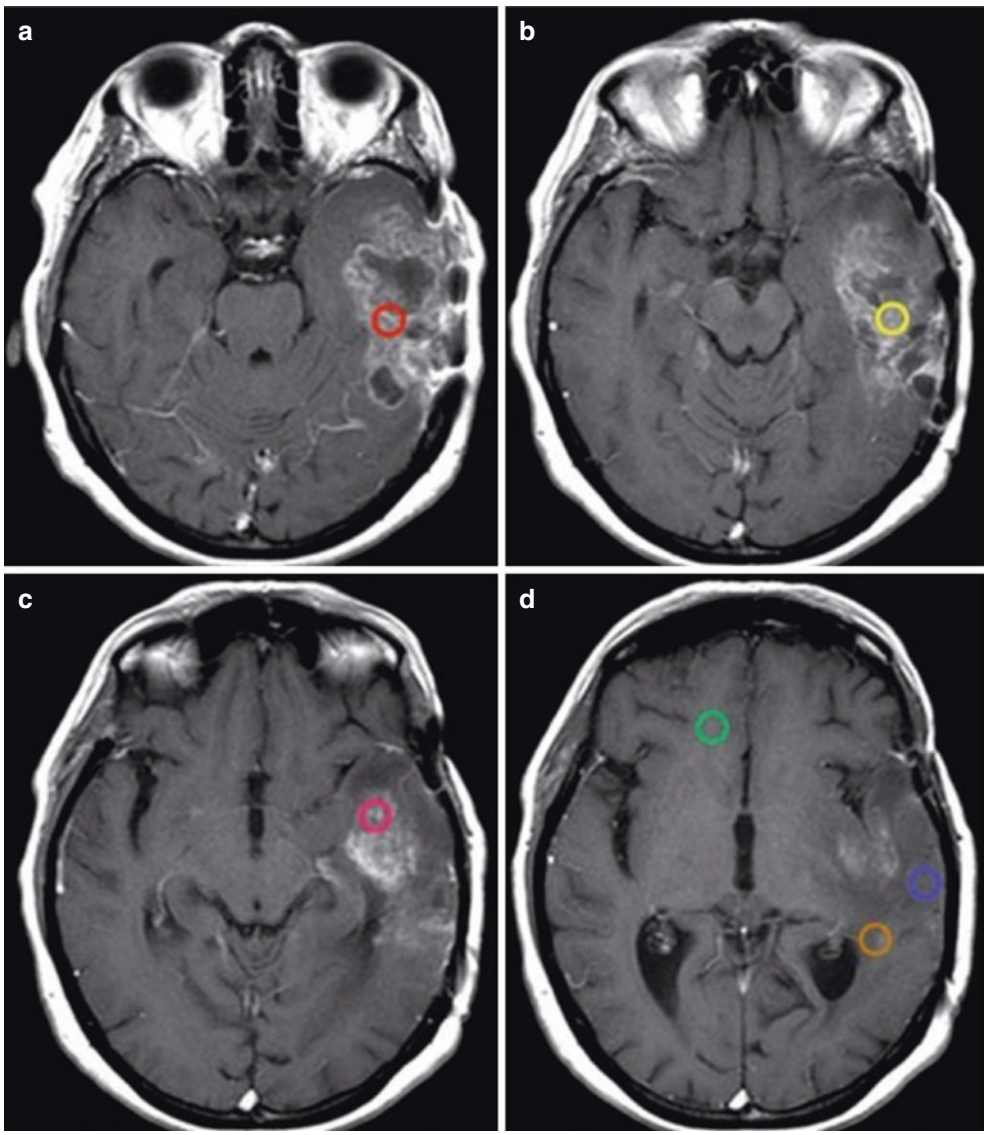

Fig. 25.3 (**a**–**d**) Contrast-enhanced MR SE T1-weighted images. The area of pathologic enhancement in the left temporal region appears increased, with irregular margins and internal necrotic components. The colored rings denote several regions of interest in the context of the lesion

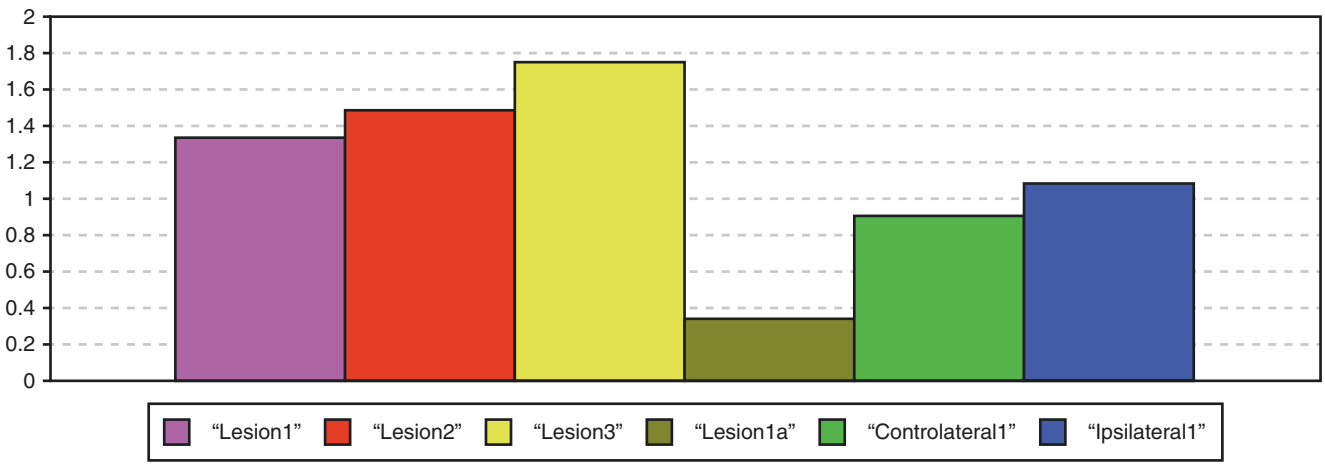

Fig. 25.4 MR perfusion study with CBV values. Compared to white matter (*green*) which is taken as a reference value, the graph shows multiple areas of increased CBV (*yellow, red, pink*, and *blue*) which indicate heteroplastic tissue. Reduced CBV (*brown*) in the left paratrigonal region indicates an area free from neoplastic infiltration

Postoperative Follow-Up at 24 Months

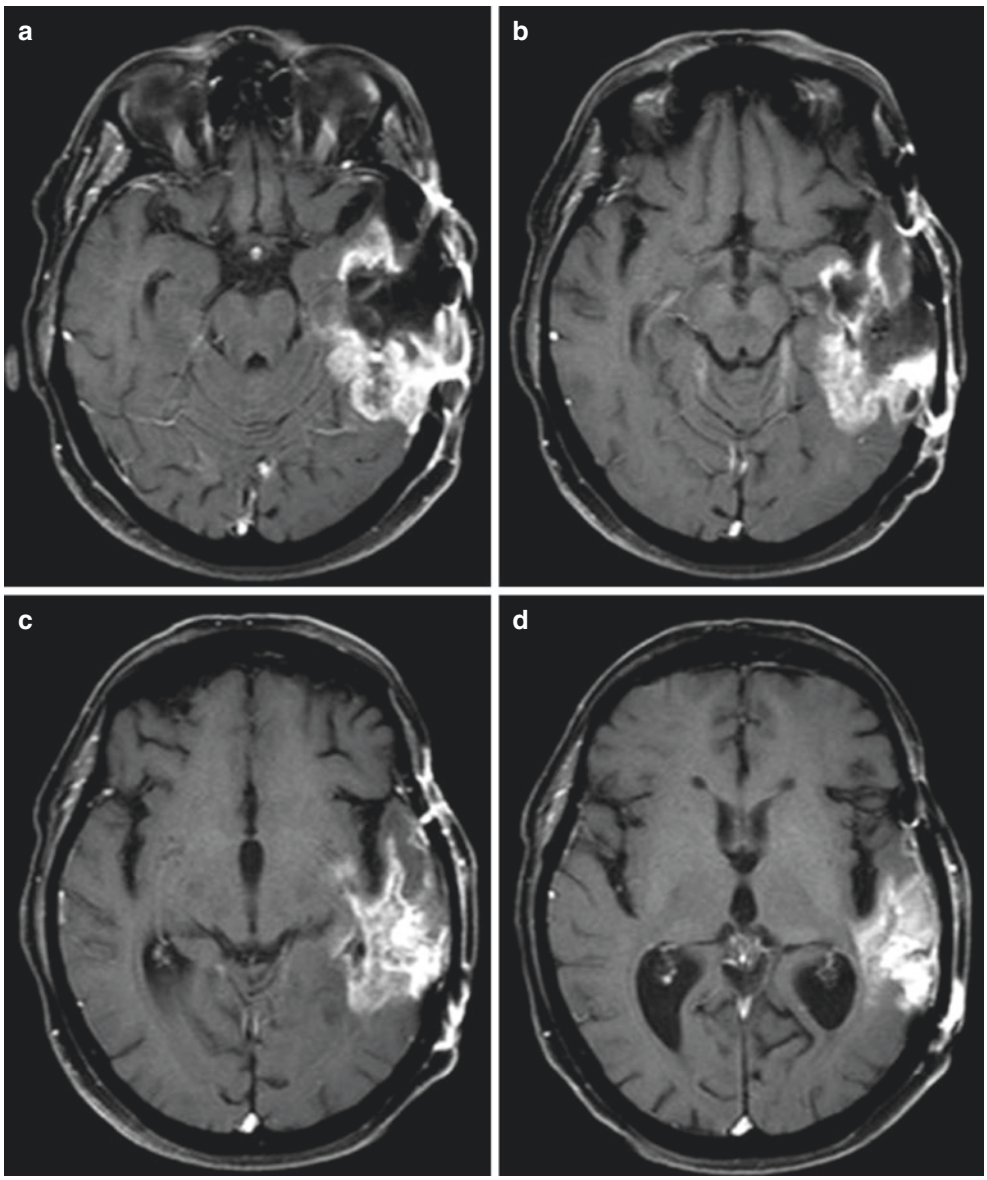

Fig. 25.5 (**a**–**d**) Contrast-enhanced MR SE T1-weighted images. An increase in the tissue with pathologic enhancement is evident

Low-Grade Glioma: High-Grade Tumor Recurrence

Case 26

Francesco Fabbiano, Jacopo Scaggiante, Andrea Wlderk, Gualtiero Innocenzi, Sergio Paolini, Nicola Modugno, Claudio Colonnese, and Marcello Bartolo

- 32-year-old man.
- Generalized tonic-clonic seizure while in complete well-being. The EEG test did not show any electrical activity related to the seizure.

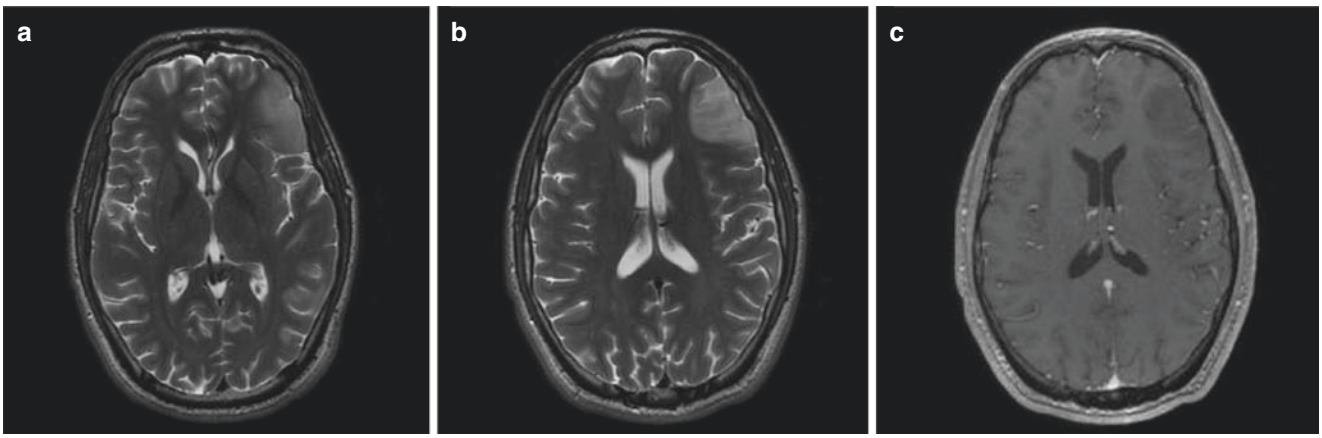

Fig. 26.1 (**a**–**c**) Presurgical imaging. Imaging shows an area of weak hyperintensity on T2-weighted FLAIR MRI with parenchymal swelling and junctional blurring in the left frontal cortical–subcortical lobe, with no enhancement

F. Fabbiano (✉)
Department of Neuroradiology, I.R.C.C.S. INM Neuromed, Pozzilli, Isernia, Italy

Department of Diagnostic Imaging, Valmontone Hospital, Rome, Italy

Department of Radiology and Neuroradiology, Villa Benedetta, Rome, Italy

J. Scaggiante
Department of Diagnostic and Interventional Radiology, University of Rome Tor Vergata, Rome, Italy

A. Wlderk
Department of Radiology and Neuroradiology, Villa Benedetta, Rome, Italy

Department of Diagnostic and Interventional Radiology, University of Rome Tor Vergata, Rome, Italy

G. Innocenzi
Department of Neurosurgery, I.R.C.C.S. INM Neuromed, Pozzilli, Isernia, Italy

S. Paolini
Department of Neurosurgery, I.R.C.C.S. INM Neuromed, Pozzilli, Isernia, Italy

Department of Sciences and Medical Biotechnologies, University La Sapienza, Rome, Italy

N. Modugno
Parkinson and Movement Disorders Center, I.R.C.C.S. INM Neuromed, Pozzilli, Isernia, Italy

C. Colonnese
Department of Diagnostic and Therapeutic Neuroradiology, I.R.C.C.S. INM Neuromed, Pozzilli, Isernia, Italy

Department of Human Neurological Sciences, University La Sapienza, Rome, Italy

M. Bartolo
Department of Diagnostic and Therapeutic Neuroradiology, I.R.C.C.S. INM Neuromed, Pozzilli, Isernia, Italy

T. Scarabino, S. Pollice (eds.), *Imaging Gliomas After Treatment*, https://doi.org/10.1007/978-3-030-31210-7_36

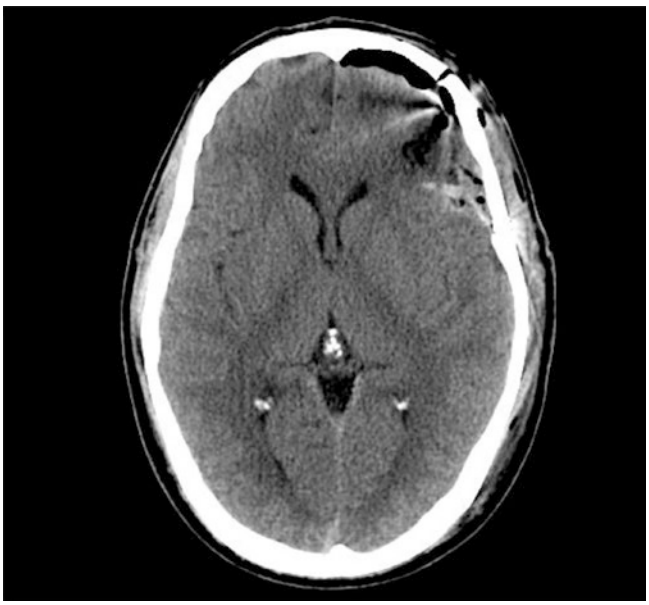

Fig. 26.2 First postoperative CT scan. Brain CT shows a small intracranial hemorrhage close to the surgical cavity. There is pneumocephalus in the left frontal anterior region

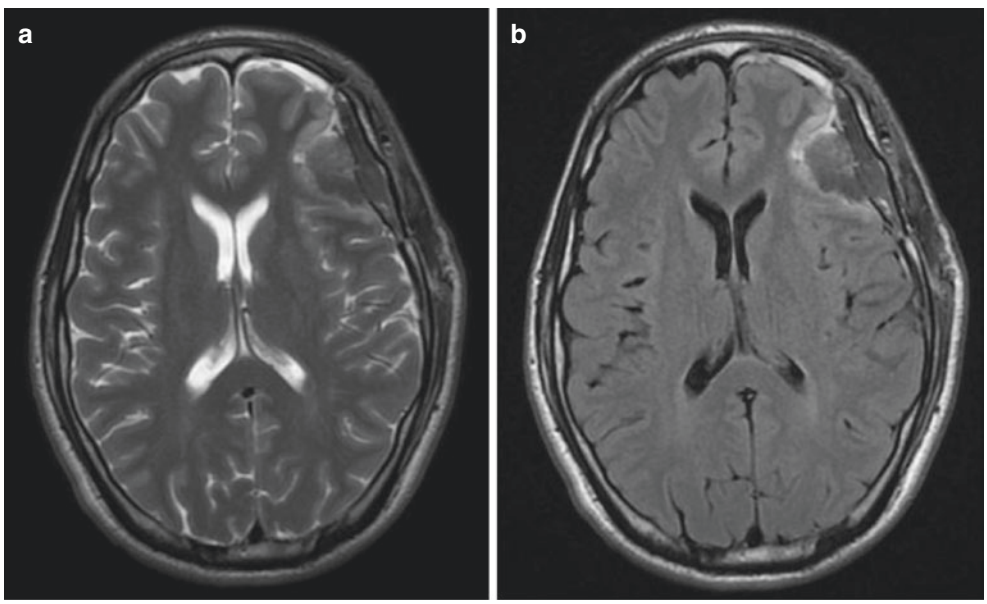

Fig. 26.3 (**a**–**d**) Early postoperative MRI. Imaging reports a thin T2 FLAIR hyperintensity close to the surgical cavity, with no enhancement

Fig. 26.3 (continued)

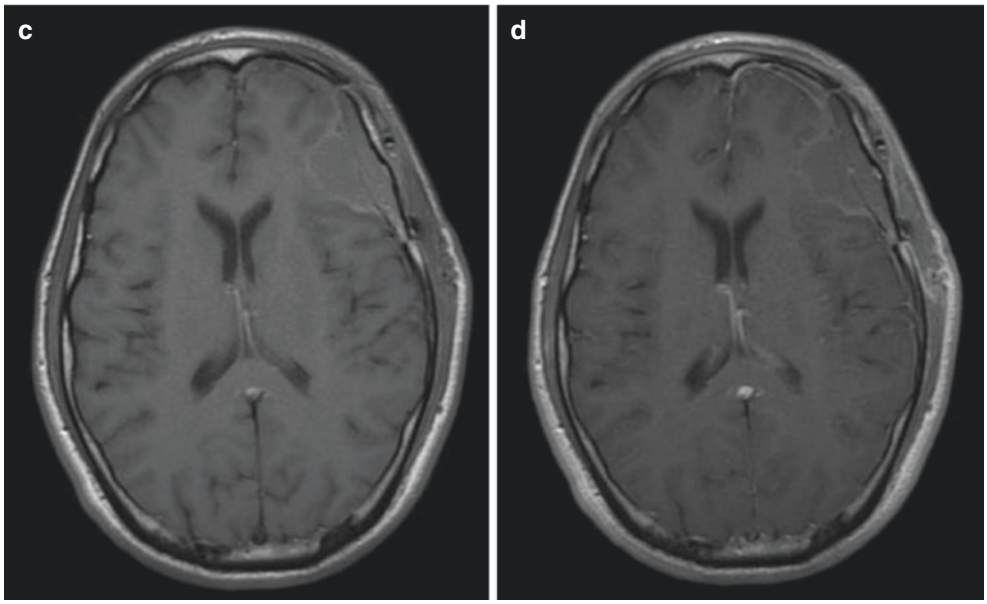

Fig. 26.4 (**a**–**d**) 1-year follow-up. Brain MRI shows a T2 FLAIR hyperintensity on the upper side of the surgical cavity with junctional blurring suspicious for low-grade tumor recurrence. On the postero-inferior side of the surgical cavity, there is a non-specific T2 FLAIR hyperintensity. There is no pathologic contrast enhancement

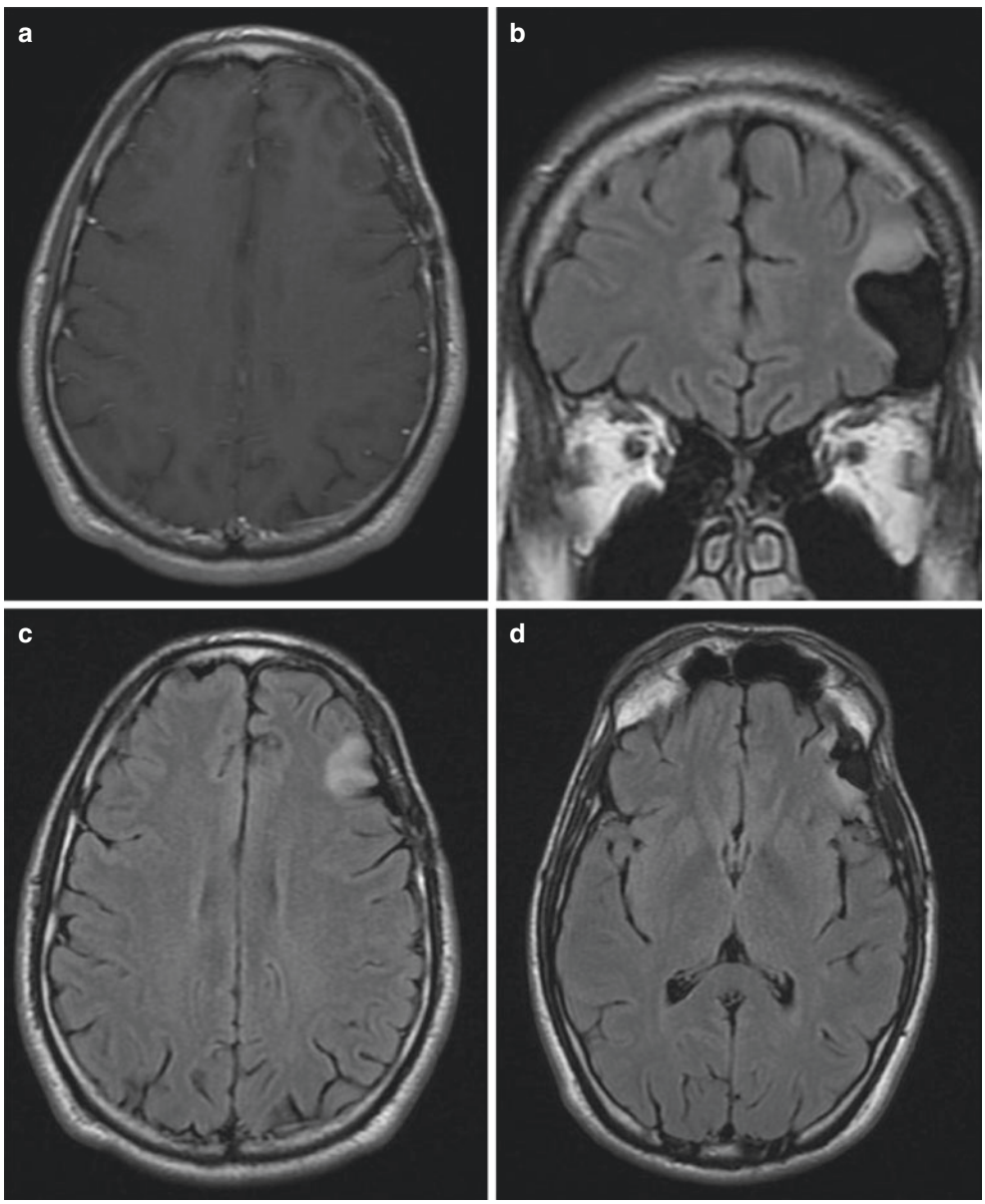

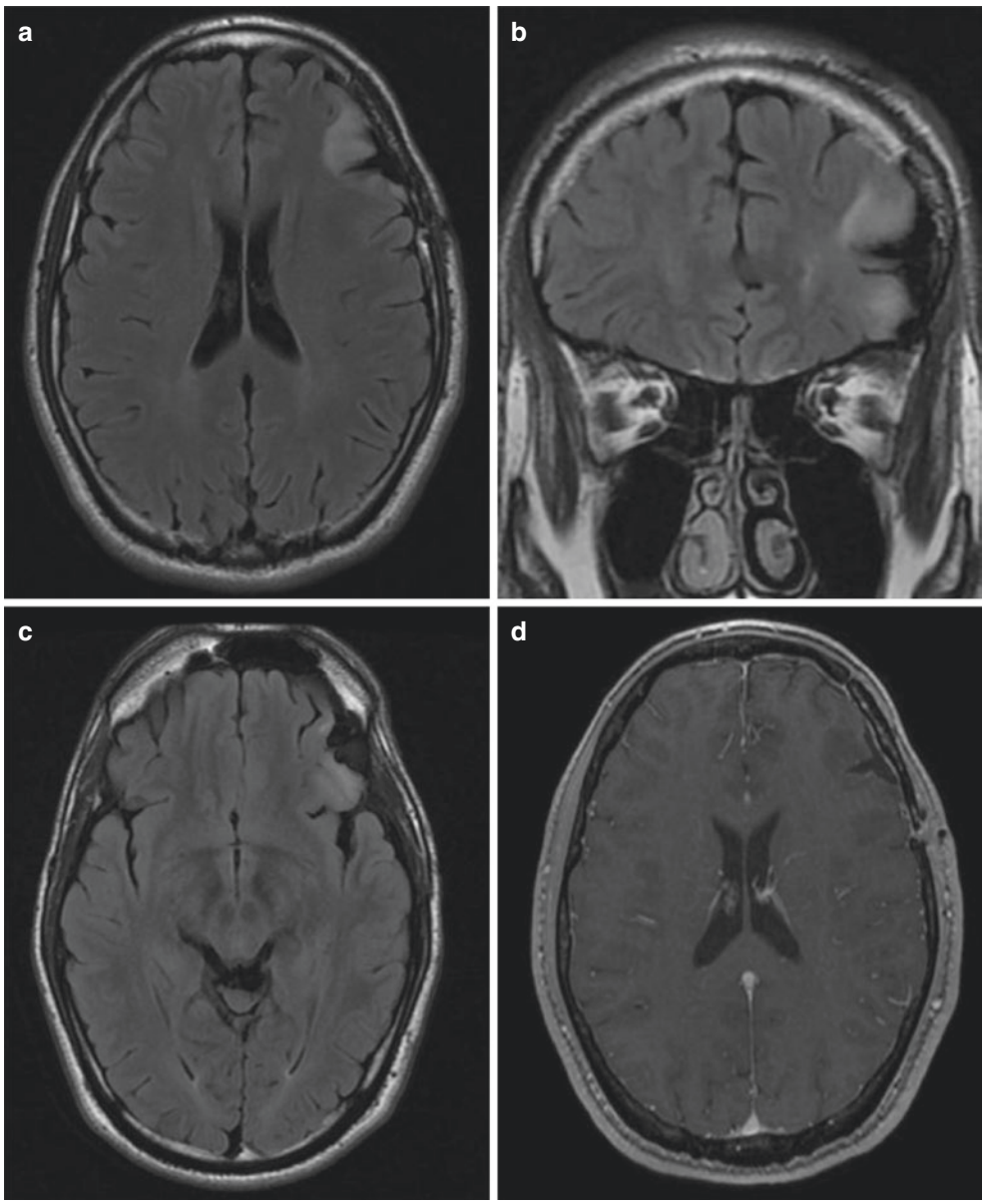

Fig. 26.5 **(a–d)** 18-month follow-up. Imaging does not show any change in the low-grade tumor recurrence on the upper side of the surgical cavity. There is an increased hyperintensity on T2-weighted FLAIR on the postero-inferior side of the surgical cavity with junctional blurring related with a further low-grade tumor recurrence

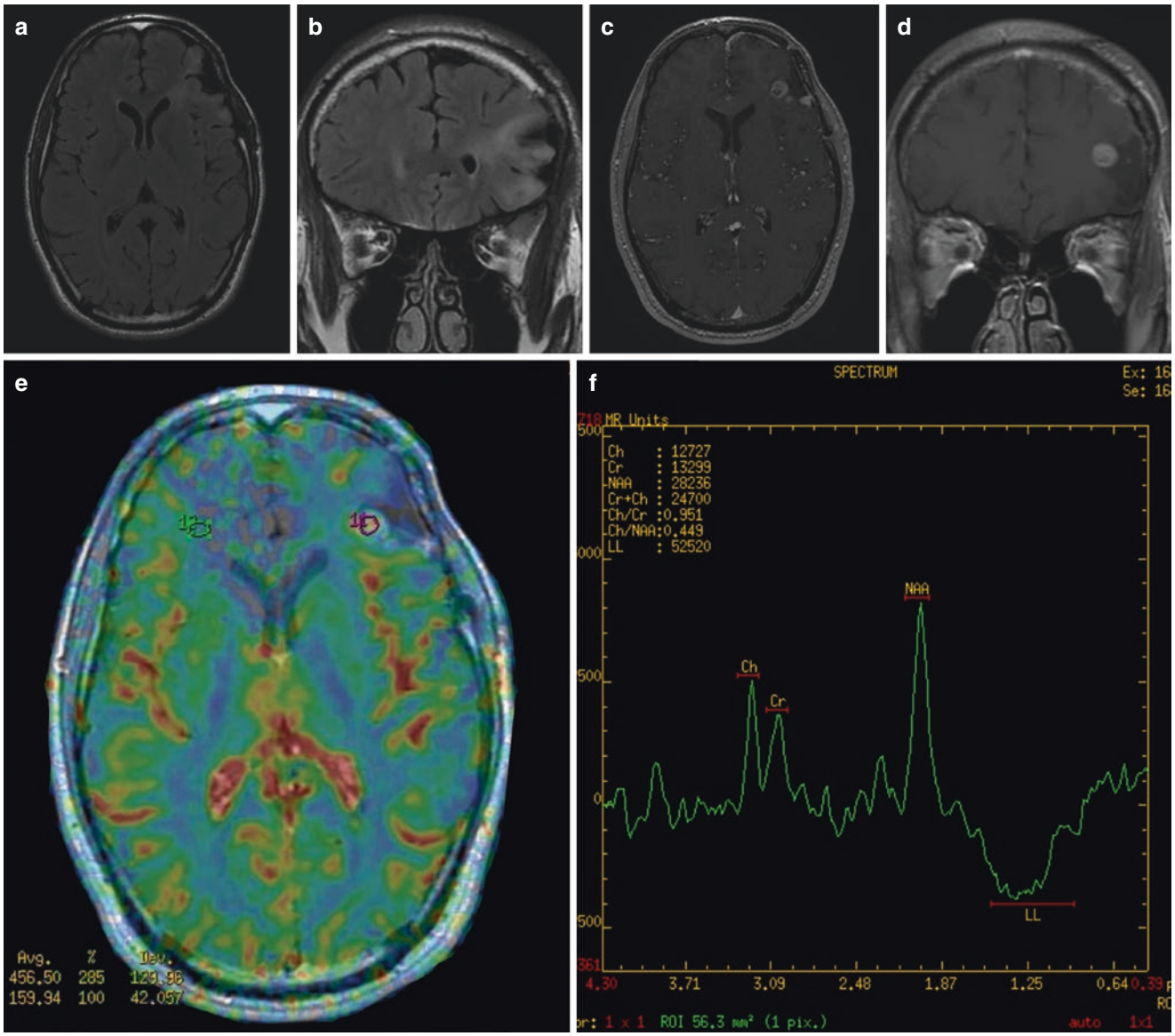

Fig. 26.6 (**a**–**f**) 21-month follow-up. Imaging shows three enhancing nodules close to the surgical cavity, the biggest with an axial diameter of 1cm, colliquative necrosis appearance and Cerebral Blood Volume ratio (rCBV) of 2.8:1 as compared with the contralateral side. Multivoxel long TE MR spectroscopy shows increased ratio of choline to creatine (Ch/Cr) and choline to N-acetylaspartate (Cho/NAA). The neuroradiological findings are suggestive of high-grade tumor recurrence

Tumor Progression/Recurrence: Multimodal CT/MR Follow-Up in Glioblastoma Multiforme

Case 27

Alessandro Stecco, Sara Zizzari, Francesco Fabbiano, Gerardo Di Nardo, Andrea Pietro Sponghini, Mariangela Lombardi, and Alessandro Carriero

- 58-year-old patient with left temporal glioblastoma multiforme treated with subtotal surgery, combined radiation therapy–chemotherapy and second-line adjuvant chemotherapy.
- Multimodal CT (morphologic and perfusion study) follow-up performed at 5 and 9 months after surgery and combined radiation therapy–chemotherapy.

Follow-Up at 5 Months After Surgery and Combined Radiation Therapy–Chemotherapy

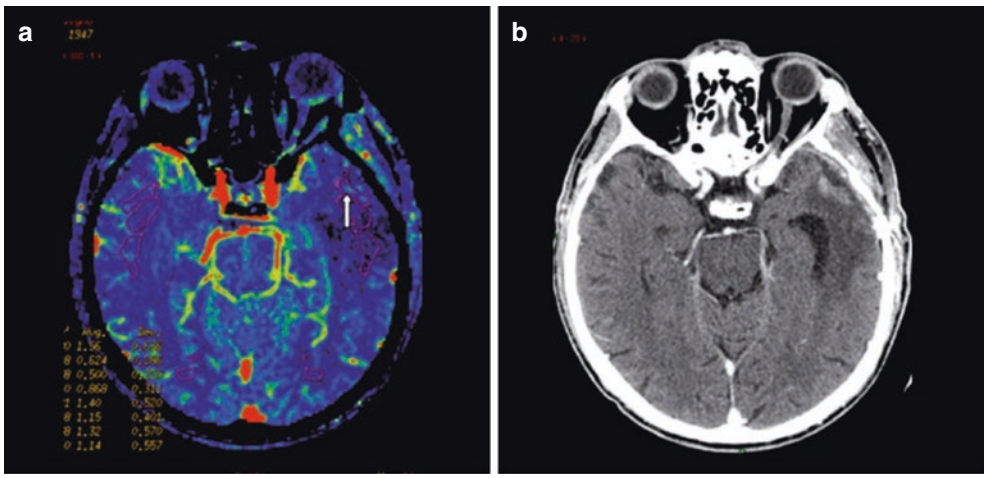

Fig. 27.1 (**a**) CT perfusion study with relative CBV map shows a small nodular area with the highest levels of CBV (*white arrow*). (**b**) Contrast-enhanced CT scan. An enhancing area is visible corresponding to the area of elevated CBV. (**c**) CT permeability surface (PS) perfusion map confirms the findings reported in the CBV map. (**d**) MR FSE T2-weighted sequence shows evidence of residual tissue with low signal in T2 (*white arrow*) accompanied by widespread perilesional alteration

A. Stecco (✉)
Neuroradiology Unit, AOU "Maggiore della Carità", DIMET, Università del Piemonte Orientale, Novara, Italy
e-mail: alessandro.stecco@uniupo.it

S. Zizzari
Department of Radiology, Hospital "Sacred Heart of Jesus", ASL LECCE, Gallipoli, Italy

F. Fabbiano
Department of Neuroradiology, I.R.C.C.S. INM Neuromed, Pozzilli, Isernia, Italy

Department of Diagnostic Imaging, Valmontone Hospital, Rome, Italy

Department of Radiology and Neuroradiology, Villa Benedetta, Rome, Italy

G. D. Nardo · A. Carriero
Department of Radiology, AOU "Maggiore della Carità", DIMET, Università del Piemonte Orientale, Novara, Italy

A. P. Sponghini
Department of Oncology, AOU Maggiore della Carità, DIMET, Università del Piemonte Orientale, Novara, Italy

M. Lombardi
Department of Radiology, Cesena Hospital—AUSL Romagna, Cesena, Italy

T. Scarabino, S. Pollice (eds.), *Imaging Gliomas After Treatment*, https://doi.org/10.1007/978-3-030-31210-7_37

Fig. 27.1 (continued)

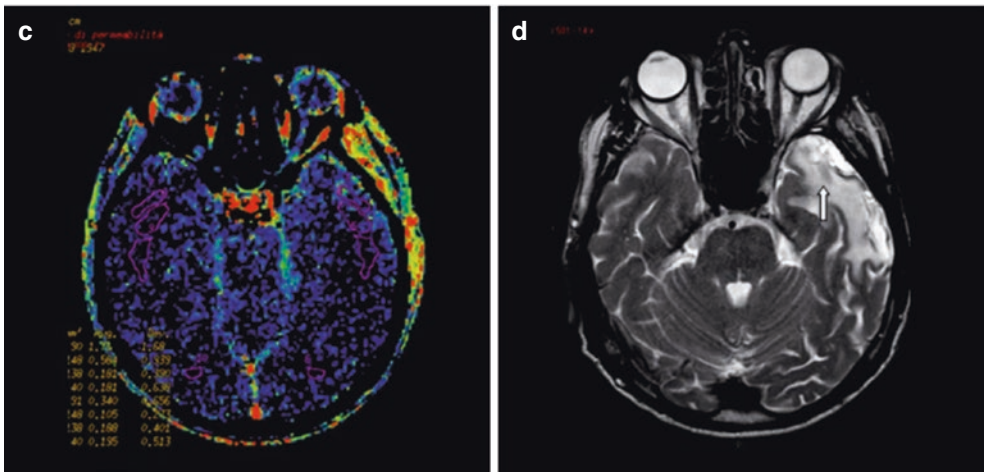

Follow-Up at 9 Months

Fig. 27.2 (**a**) Contrast-enhanced MR SE T1-weighted sequence shows increased size and enhancement of the pathologic tissue. (**b**) CT perfusion study with relative CBV map. Higher CBV values can be appreciated at the site of the lesion than in the surrounding and contralateral parenchyma

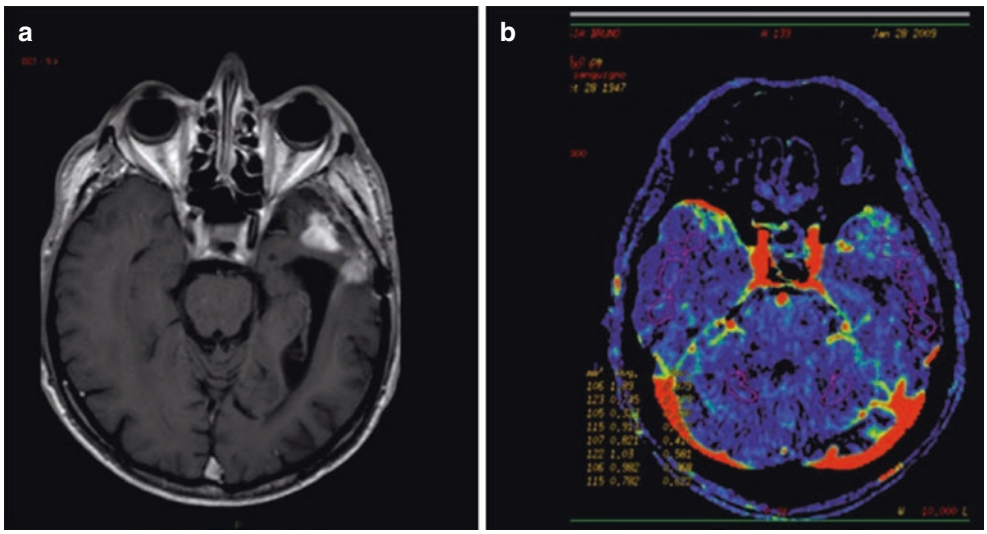

Tumor Progression/Recurrence: Multimodal CT/MR Follow-Up in Anaplastic Astrocytoma

Case 28

Alessandro Stecco, Francesco Fabbiano, Sara Zizzari, Gerardo Di Nardo, Mariangela Lombardi, Ignazio Divenuto, Alessandro Carriero, and Andrea Pietro Sponghini

- 58-year-old patient with left frontal anaplastic astrocytoma treated with surgery and subsequent combined radiation therapy–chemotherapy.
- Multimodal CT/MR (morphologic and perfusion study) follow-up performed in the early and late postoperative phase at 1, 9, and 12 months after surgery and combined radiation therapy–chemotherapy.

Early Postoperative Imaging in Patient Candidate for Radiation Therapy and Chemotherapy

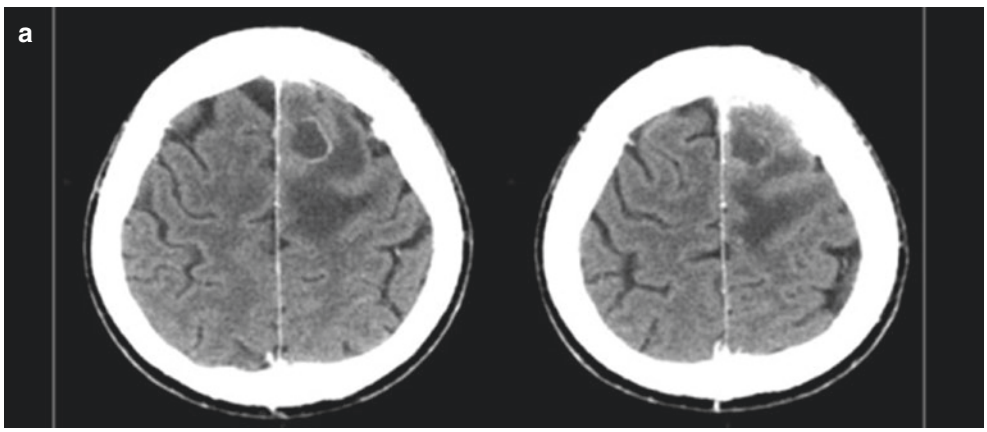

Fig. 28.1 (**a**) Contrast-enhanced CT scan shows a left parafalcal enhancing ring lesion accompanied by perilesional hypodensity of white matter. (**b**) Postoperative CT perfusion study with permeability surface (PS) map. The fusion image shows high PS values along the lesion margins (*white arrow*)

A. Stecco (✉)
Neuroradiology Unit, AOU "Maggiore della Carità", DIMET, Università del Piemonte Orientale, Novara, Italy
e-mail: alessandro.stecco@uniupo.it

F. Fabbiano
Department of Neuroradiology, I.R.C.C.S. INM Neuromed, Pozzilli, Isernia, Italy

Department of Diagnostic Imaging, Valmontone Hospital, Rome, Italy

Department of Radiology and Neuroradiology, Villa Benedetta, Rome, Italy

S. Zizzari
Department of Radiology, Hospital "Sacred Heart of Jesus", ASL LECCE, Gallipoli, Italy

G. D. Nardo · A. Carriero
Department of Radiology, AOU "Maggiore della Carità", DIMET, Università del Piemonte Orientale, Novara, Italy

M. Lombardi
Department of Radiology, Cesena Hospital—AUSL Romagna, Cesena, Italy

I. Divenuto
Depatment of Radiology, Humanitas Hospital, Rozzano, Italy

A. P. Sponghini
Department of Oncology, AOU Maggiore della Carità, DIMET, Università del Piemonte Orientale, Novara, Italy

T. Scarabino, S. Pollice (eds.), *Imaging Gliomas After Treatment*, https://doi.org/10.1007/978-3-030-31210-7_38

Fig. 28.1 (continued)

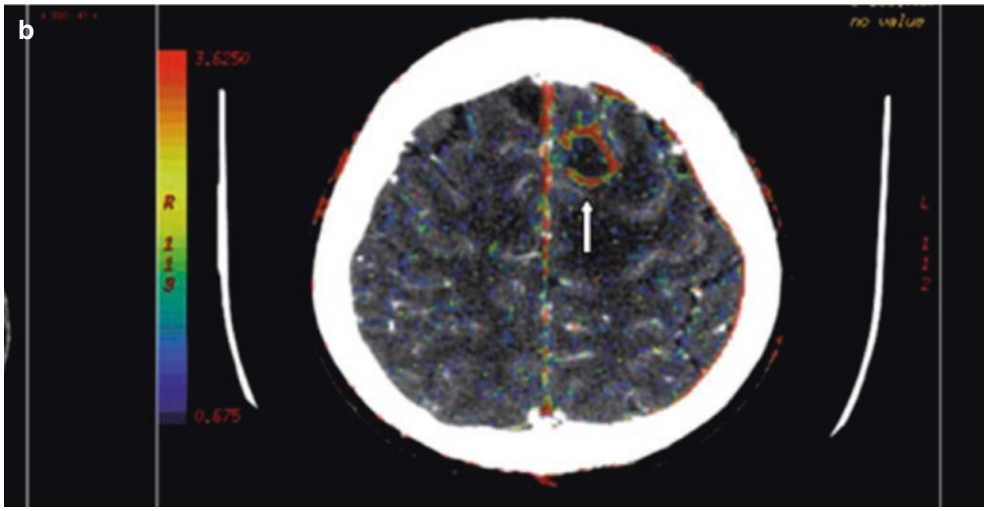

Follow-Up at 1 Month After Surgery During Radiation Therapy

Fig. 28.2 (**a**) MR perfusion study with relative CBV map. The highest values of CBV are seen along the peripheral margins of the lesion (*white arrows*). (**b**) Contrast-enhanced MR SE T1-weighted sequence shows peripheral enhancement of the lesion (*white arrow*)

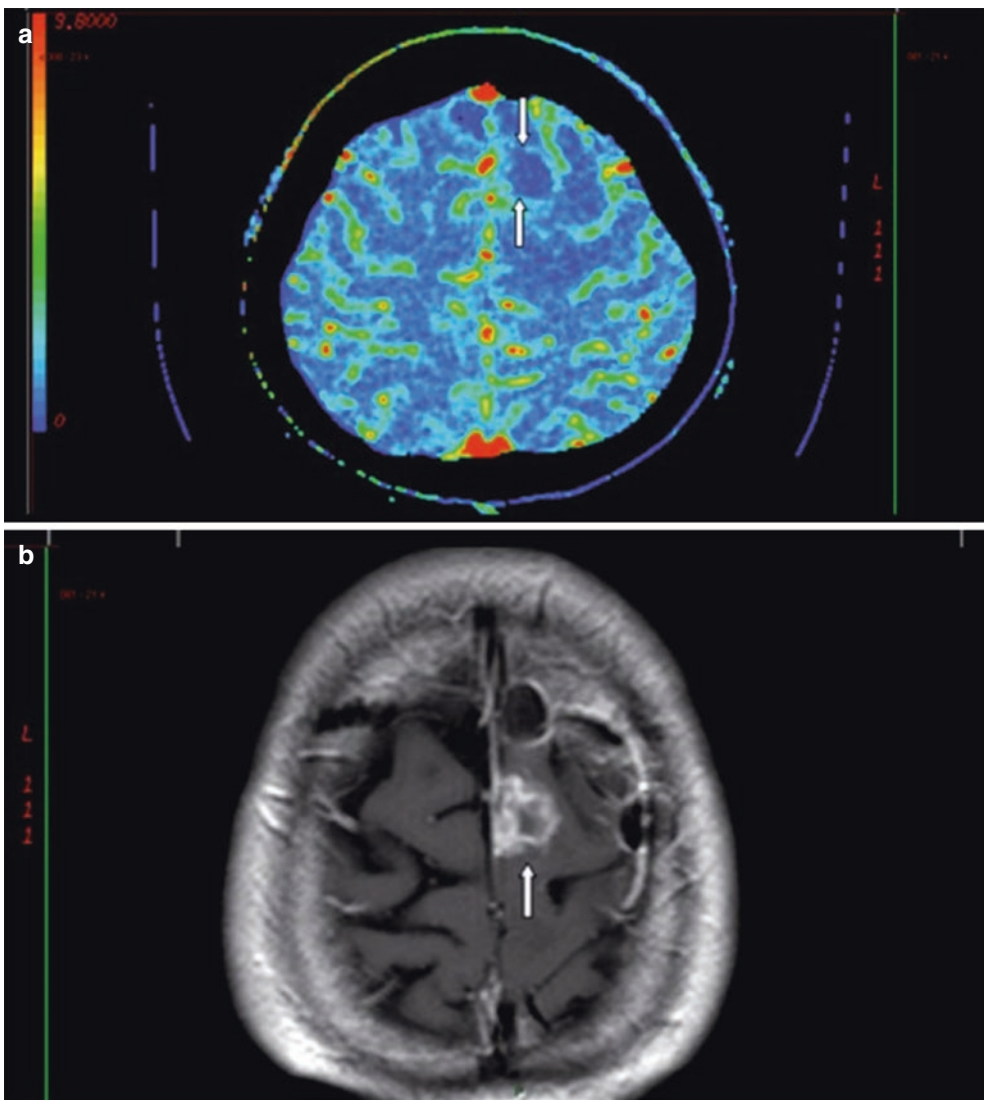

Follow-Up at 9 Months After Surgery Following Combined Radiation Therapy–Chemotherapy

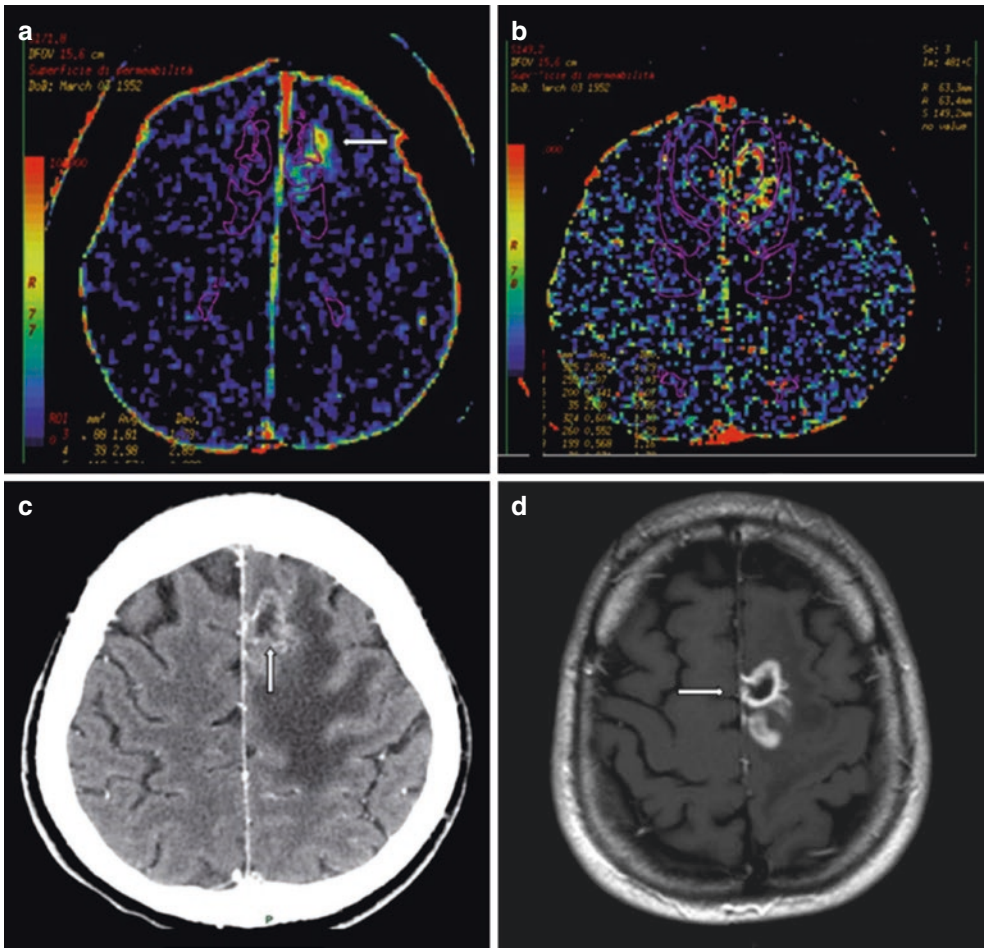

Fig. 28.3 (**a**) CT perfusion study shows focal elevation of PS in the lateral portion of the neurosurgical cavity, resulting from resection (*white arrow*). (**b**) Greater extension of the pathologic increase in PS than in the previous examination (Fig. 8.1 b), with rim appearance along the margins of the surgical resection. (**c**) Contrast-enhanced CT scan depicts evidence of recurrence with irregular enhancement of surgical margins with less extent than the corresponding PS map in (**b**) (*white arrow*). (**d**) Contrast-enhanced MR SE T1-weighted sequence confirms the CT morphologic and perfusion findings (*white arrow*)

Follow-Up at 12 Months

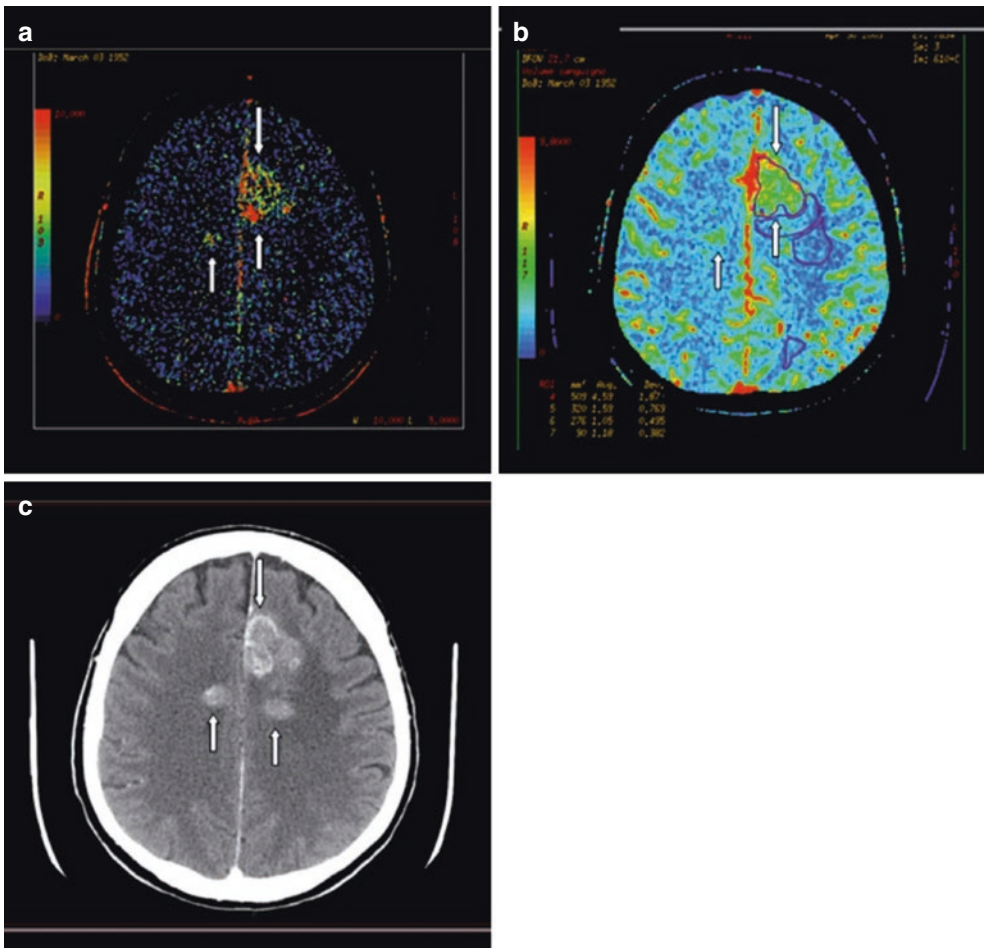

Fig. 28.4 (**a**) CT perfusion study shows disease progression with the involvement of the previous surgical site and complete revascularization of the neurosurgical cavity and the bilateral paracallosal area (*white arrows*). (**b**) CT perfusion study with CBV map shows the same findings in (**a**) with evidence of increased CBV values (*white arrows*). (**c**) Contrast-enhanced CT shows pathologic enhancement in the area of disease progression (*white arrows*)

Tumor Progression/Recurrence: Multimodal CT/MR Follow-Up in Glioblastoma Multiforme

Case 29

Alessandro Stecco, Mariangela Lombardi, Francesco Fabbiano, Gerardo Di Nardo, Sara Zizzari, Andrea Pietro Sponghini, and Alessandro Carriero

- 53-year-old patient affected by right temporal glioblastoma multiforme treated with subtotal surgery, combined radiation therapy–chemotherapy, and second- and third-line adjuvant chemotherapy.
- Multimodal CT/MR follow-up with morphologic and perfusion studies performed preoperatively and at 1, 4, and 8 months after surgery and combined radiation therapy–chemotherapy.

Preoperative Imaging

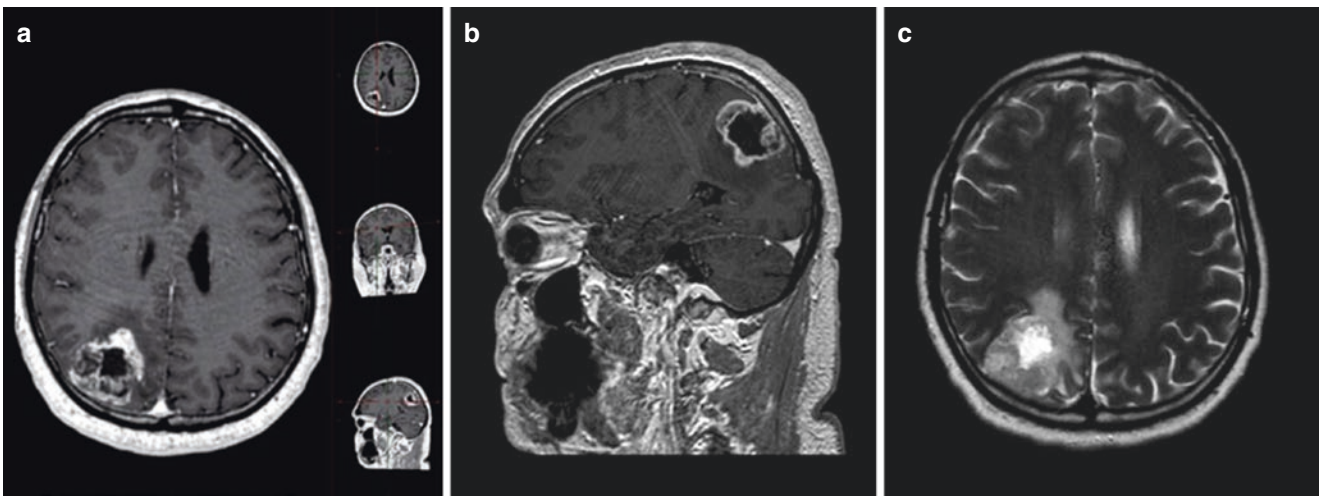

Fig. 29.1 Contrast-enhanced MR SE T1-weighted (**a**), FSE T2-weighted (**b**), and FLAIR (**c**) sequences show a right parietal lesion with irregular peripheral enhancement and central necrosis, findings consistent with high-grade lesion

A. Stecco (✉)
Neuroradiology Unit, AOU "Maggiore della Carità", DIMET, Università del Piemonte Orientale, Novara, Italy
e-mail: alessandro.stecco@uniupo.it

M. Lombardi
Department of Radiology, Cesena Hospital—AUSL Romagna, Cesena, Italy

F. Fabbiano
Department of Neuroradiology, I.R.C.C.S. INM Neuromed, Pozzilli, Isernia, Italy

Department of Diagnostic Imaging, Valmontone Hospital, Rome, Italy

Department of Radiology and Neuroradiology, Villa Benedetta, Rome, Italy

G. D. Nardo · A. Carriero
Department of Radiology, AOU "Maggiore della Carità", DIMET, Università del Piemonte Orientale, Novara, Italy

S. Zizzari
Department of Radiology, Hospital "Sacred Heart of Jesus", ASL LECCE, Gallipoli, Italy

A. P. Sponghini
Department of Oncology, AOU Maggiore della Carità, DIMET, Università del Piemonte Orientale, Novara, Italy

T. Scarabino, S. Pollice (eds.), *Imaging Gliomas After Treatment*, https://doi.org/10.1007/978-3-030-31210-7_39

Follow-Up at 1 Month After Surgery

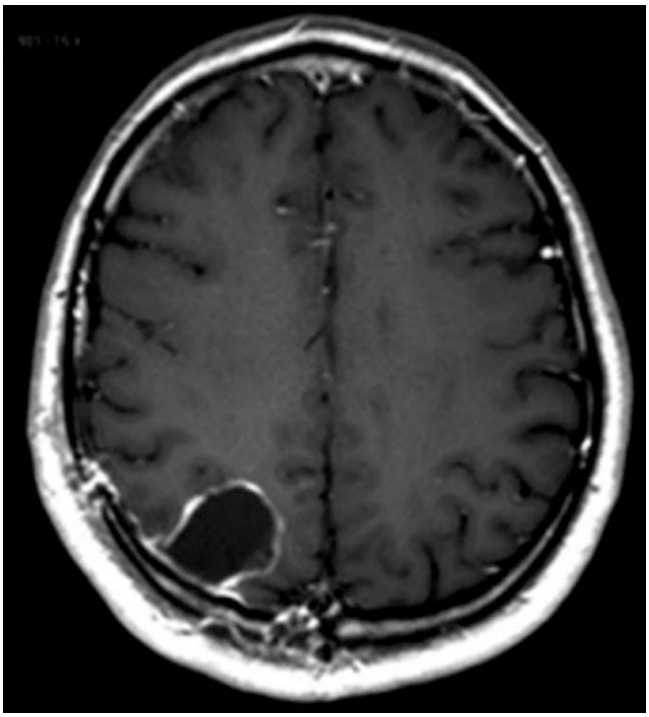

Fig. 29.2 Contrast-enhanced MR SE T1-weighted sequence shows wide surgical cavity with enhancing surgical margins

Follow-Up at 4 Months After Surgery and Radiation Therapy

Fig. 29.3 (**a**) Contrast-enhanced CT scan. A millimetric nodular rim enhancement can be seen on the posterior edge of the surgical cavity (*white arrow*). (**b**) MR perfusion study with relative CBV map shows elevated CBV nodule at the site of nodular enhancement shown on CT (*white arrow*)

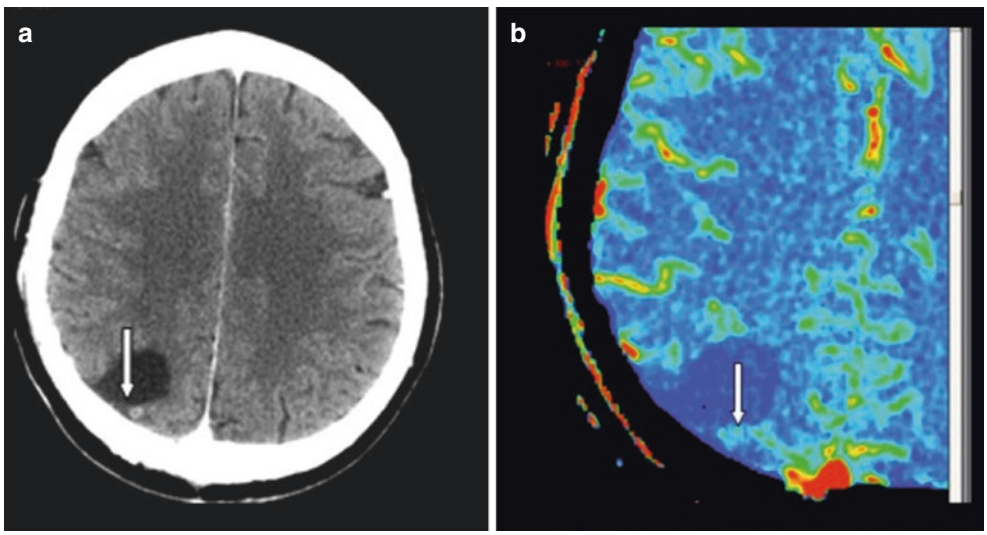

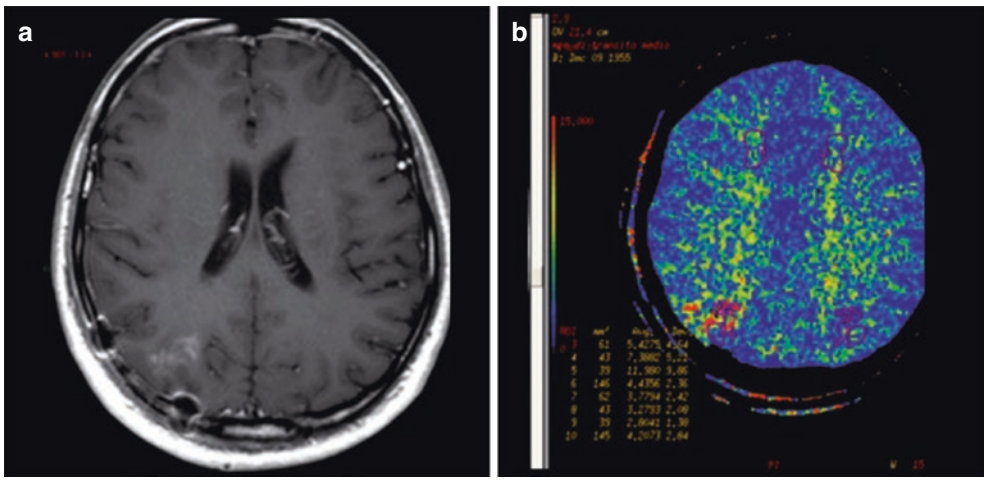

Fig. 29.4 (**a**) Contrast-enhanced MR SE T1-weighted image. This lower section shows revascularization of the cavity by newly formed tissue with inhomogeneous pattern of enhancement. (**b**) CT perfusion map of permeability surface (PS). This lower section shows marked elevation of the PS coefficient at the surgical site

Follow-Up at 8 Months After Surgery and Radiation Therapy–Chemotherapy

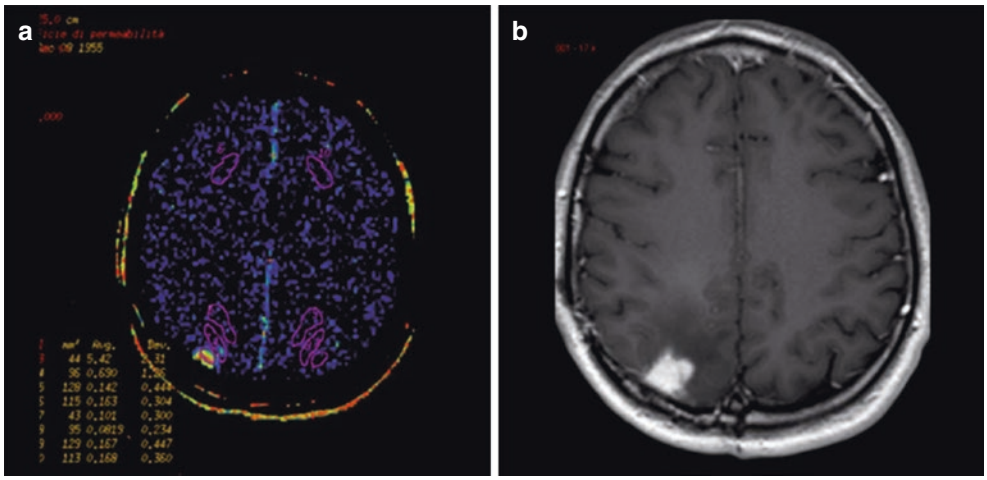

Fig. 29.5 (**a**) CT perfusion study. This higher section shows another area of disease recurrence with marked elevation of the permeability coefficient. (**b**) Contrast-enhanced MR SE T1-weighted sequence shows marked enhancement at the site of recurrence

Local and Distant Recurrence: 3T Multimodal MR Follow-Up in Glioblastoma Multiforme

Case 30

Tommaso Scarabino, Teresa Popolizio, Saverio Pollice, Vincenzo D'Angelo, and Alfonso Di Costanzo

- 46-year-old patient with right frontal-insular glioblastoma multiforme treated with subtotal excision and combined radiation therapy–chemotherapy and subsequent second-level adjuvant chemotherapy.
- 3T multimodal MR follow-up performed with morphologic imaging, diffusion, perfusion, and spectroscopy preoperatively and at 6, 9, and 12 months after surgery and combined radiation therapy–chemotherapy.

T. Scarabino (✉) · S. Pollice
Department of Radiology, "L. Bonomo" Hospital, Andria, BT, Italy

T. Popolizio · V. D'Angelo
Department of Neuroradiology, IRCCS "Casa Sollievo della Sofferenza", San Giovanni Rotondo, FG, Italy

A. Di Costanzo
Department of Neurology, University of Molise, Campobasso, Italy

T. Scarabino, S. Pollice (eds.), *Imaging Gliomas After Treatment*, https://doi.org/10.1007/978-3-030-31210-7_40

Preoperative Imaging

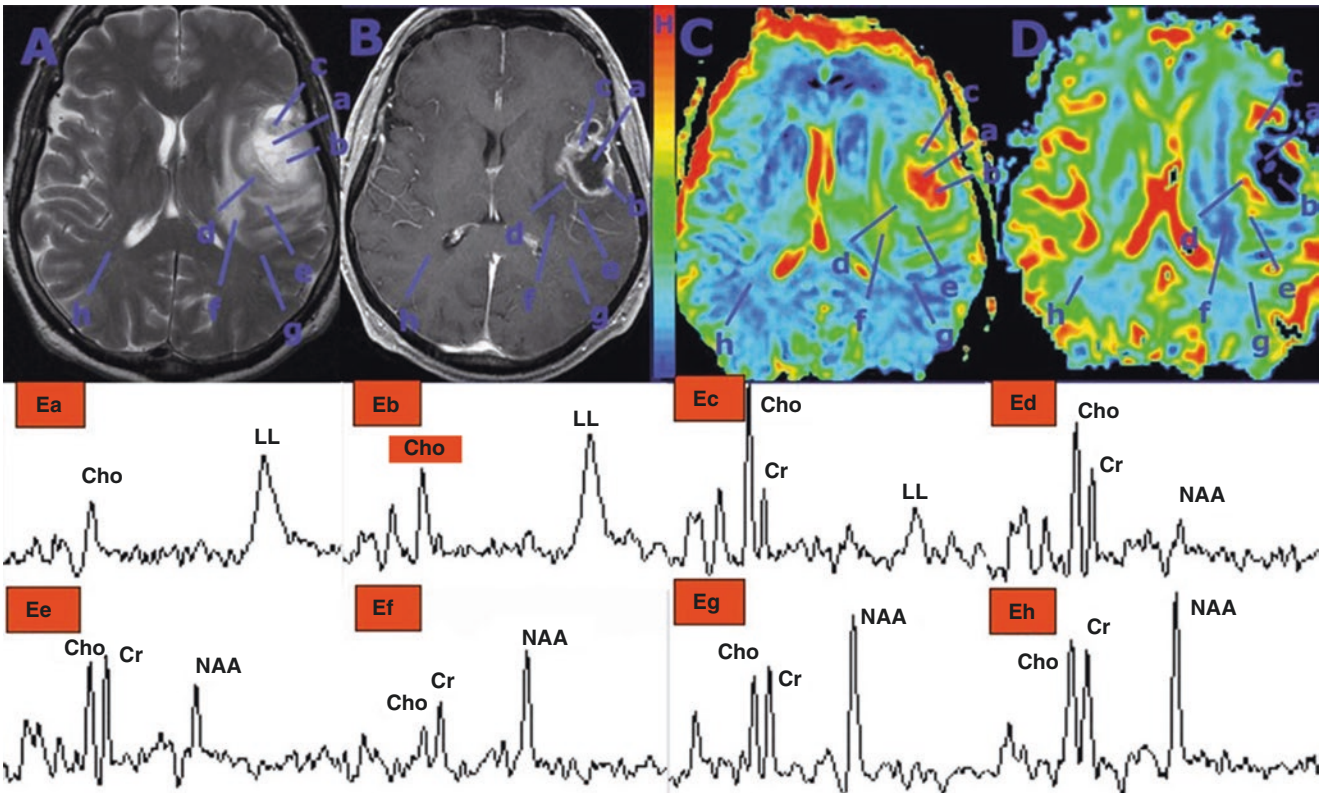

Fig. 30.1 FSE T2-weighted (**a**) and contrast-enhanced SE T1-weighted (**b**) sequences show a large mass with significant central necrotic component, moderate edema with mild mass effect on midline structures which appear shifted contralaterally. The MR multimodal study with diffusion-weighted imaging and ADC map (**c**), perfusion study with CBV map (**d**), and single-voxel spectroscopy with multiple ROIs (**e**) show spectra relative to the enhancing areas and those immediately adjacent to the lesion with the typical biological behavior of an aggressive tumor, characterized by high Cho, inversion of the Cho/NAA ratio, and the presence of Lac/Lip (LL). In these ROIs, ADC is decreased and CBV is increased. In the large necrotic-colliquative area, there is a reduction in the spectral levels of all metabolites with a minimum Cho peak, the presence of LL, an increase in ADC, and a decrease in CBV. The spectra associated with apparently edematous areas outside the enhancement have reduced levels of all metabolites, but different patterns, i.e., normal Cho/NAA in the non-infiltrated vasogenic edema and tumor pattern (high Cho/NAA) in the infiltrated edema. ADC and CBV in these locations have the opposite behavior, with the former being elevated and the latter reduced in the area of pure edema and vice versa in the infiltrated edema. Moving away from the lesion the metabolic pattern along with the ADC and CBV values returns to normal as in the contralateral hemisphere

Follow-Up Performed at 6 Months After Surgery and Combined Radiation Therapy–Chemotherapy

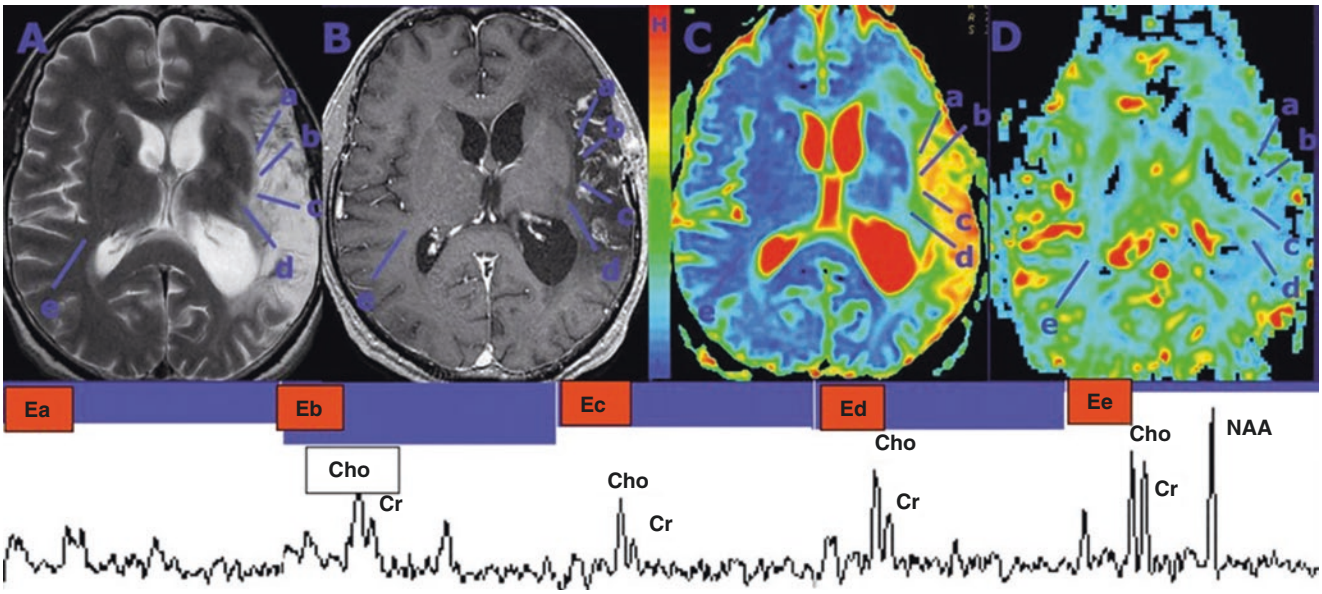

Fig. 30.2 Morphofunctional MR with FSE T2-weighted (**a**) and contrast-enhanced SE T1-weighted (**b**) sequences, diffusion-weighted imaging with ADC map (**c**), perfusion study with CBV map (**d**), and multivoxel spectroscopy with multiple ROIs (**e**). The imaging findings after treatment show an almost complete necrotic transformation of the lesion free from significant pathologic enhancement with associated retraction dilatation of the adjacent lateral ventricle. At that level there is a spectral reduction in the levels of all metabolites, an increase in ADC and a decrease in CBV. These indicators are also appreciable in the surrounding tissue with the exception of a small area of high CBV lesion located posterior to the tumor (distant recurrence)

Follow-Up Performed at 9 Months

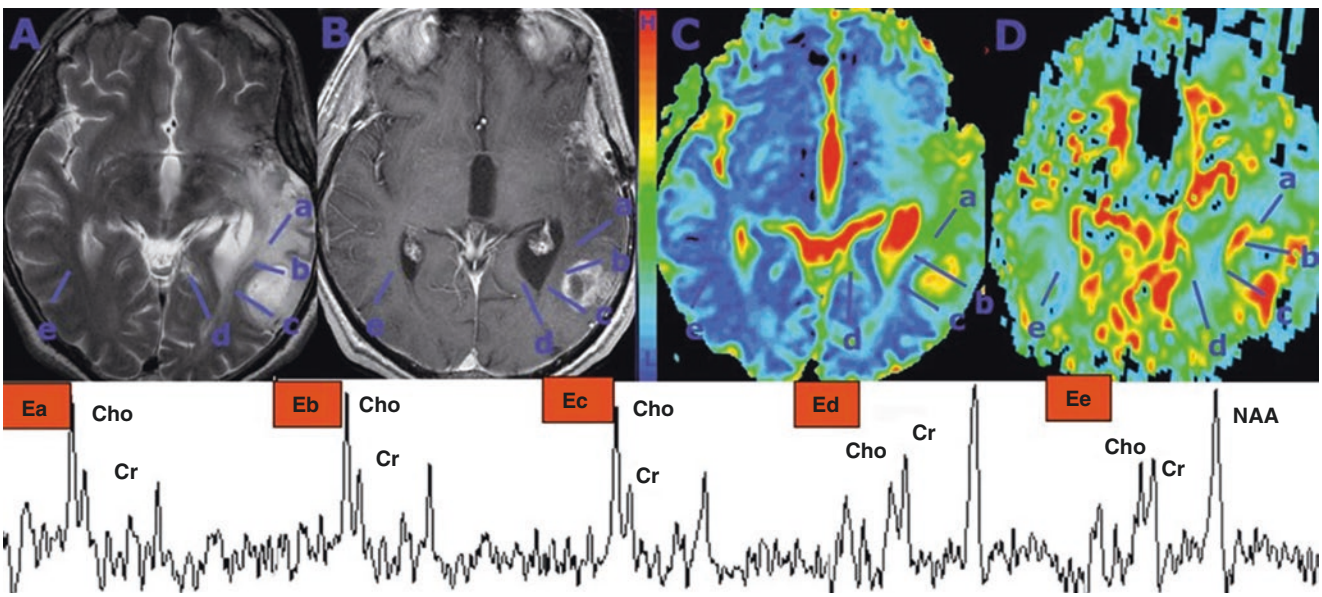

Fig. 30.3 MR with FSE T2-weighted (**a**) and contrast-enhanced SE T1-weighted (**b**) sequences. The images show distant recurrence posterior to the main surgical site which appears free from persistence/recurrence with the exception of mild peripheral thickening with pathologic enhancement. Multimodal MR with diffusion-weighted imaging and ADC map (**c**), perfusion study with CBV map (**d**), and multivoxel spectroscopy with multiple ROIs (**e**). The recurrence has morphofunctional characteristics similar to the original lesion with a large component of central tumor necrosis and typical pattern of the spectra in the areas with enhancing tumor immediately behind the lesion (high Cho and inversion of the Cho/NAA ratio), of ADC (decreased) and CBV (increased); the opposite can be seen in the necrotic-colliquative area

Follow-Up Performed at 12 Months

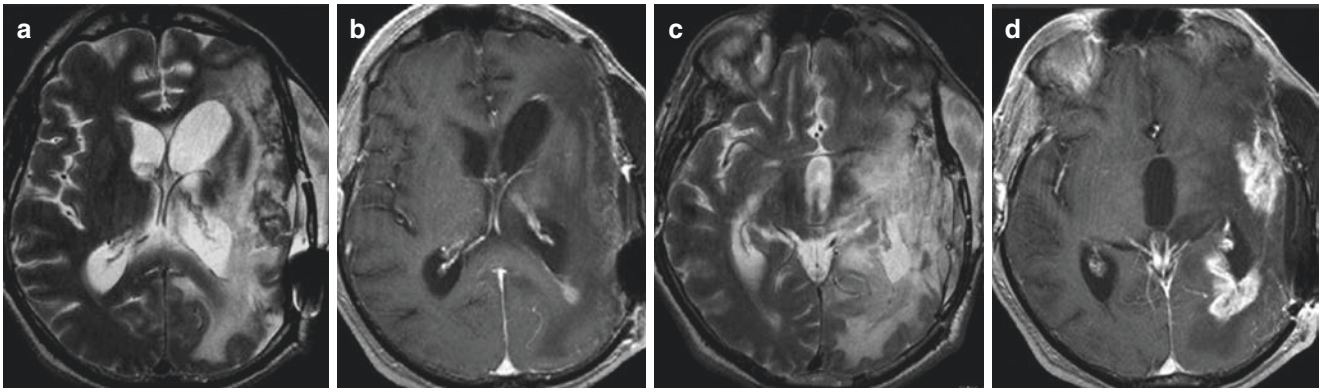

Fig. 30.4 MR FSE T2-weighted (**a**, **c**) and contrast-enhanced SE T1-weighted (**b**, **d**) sequences show not only the distant recurrence but also the recurrence of the lesion in the original sites. In both cases, apart from the extensive surrounding edema, there is the presence of a solid lesion with irregular margins

Tumor Recurrence: 3T Morphofunctional MR Follow-Up in Low-Grade Astrocytoma with Anaplastic Appearance

Case 31

Massimo Caulo, Chiara Briganti, Valentina Panara, Simone Salice, Domenico Tortora, and Armando Tartaro

- 46-year-old patient with right frontal low-grade astrocytoma treated with subtotal surgery and combined radiation therapy–chemotherapy.
- 3T morphofunctional MR follow-up performed with morphologic imaging, diffusion, perfusion, and spectroscopy at 4 years after surgery and combined radiation therapy–chemotherapy.

Follow-Up Performed at 4 Years After Surgery and Combined Radiation Therapy–Chemotherapy

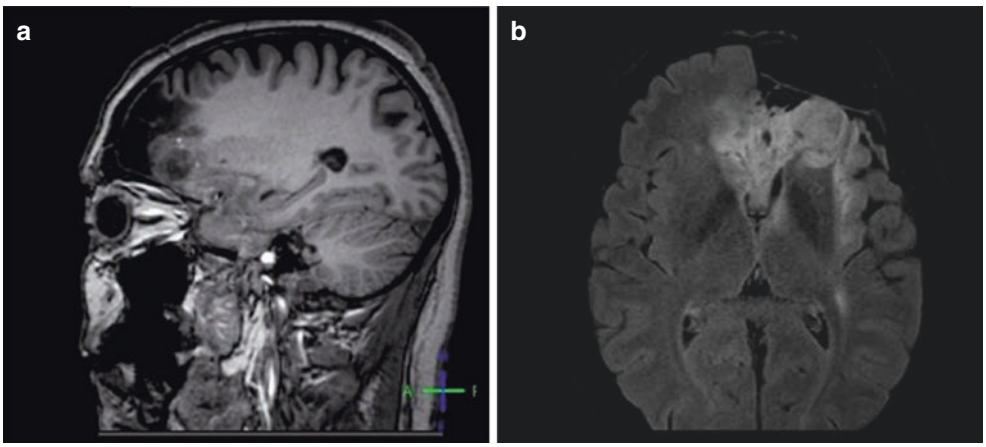

Fig. 31.1 (**a**) Contrast-enhanced MR SE T1-weighted sequence shows a nodular lesion with thick and irregular walls and necrotic-hemorrhagic content. (**b**) MR FLAIR sequence visualizes the tumor almost completely infiltrating the polar and basal portions of the frontal lobes, the genu of the corpus callosum, and the left temporal lobe

M. Caulo · C. Briganti · V. Panara · S. Salice · D. Tortora
A. Tartaro (✉)
Department of Neurosciences and Imaging, Institute of Advanced Biomedical Technologies, "G. d'Annunzio" University, Chieti-Pescara, Italy
e-mail: tartaro@unich.it

T. Scarabino, S. Pollice (eds.), *Imaging Gliomas After Treatment*, https://doi.org/10.1007/978-3-030-31210-7_41

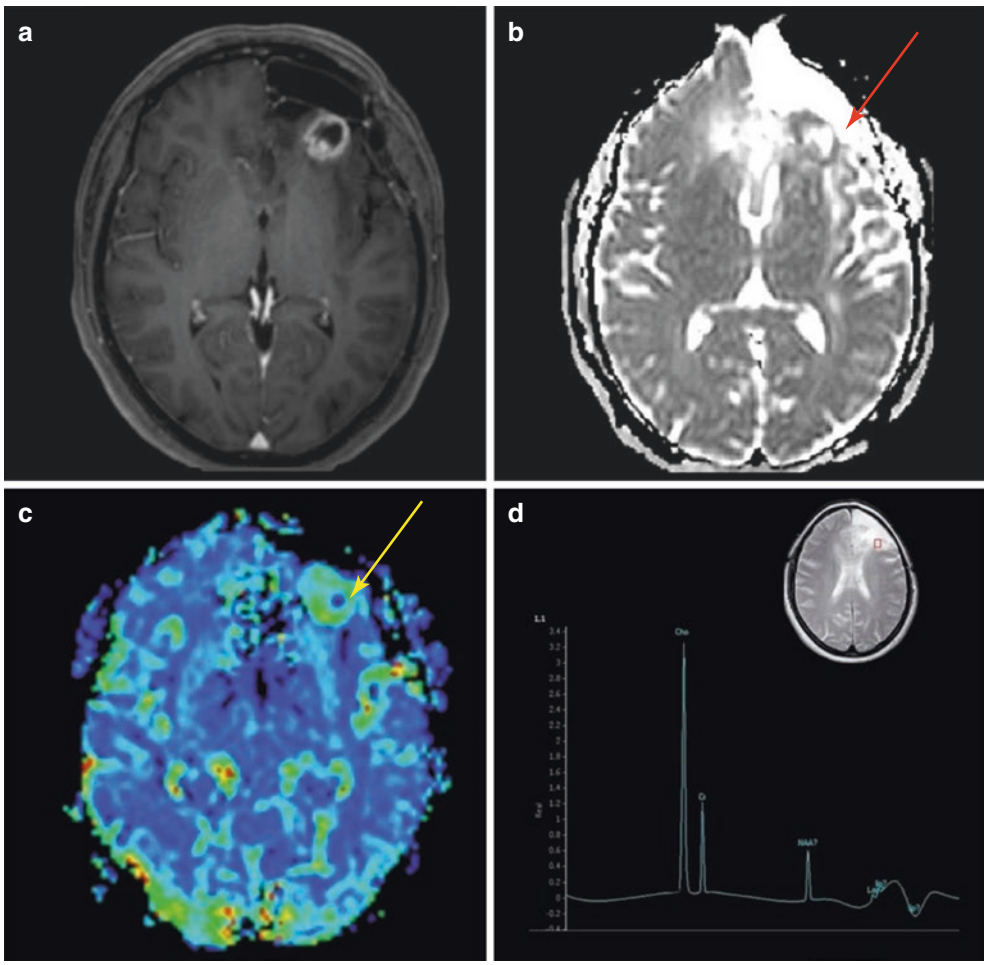

Fig. 31.2 (**a**) Contrast-enhanced MR SE T1-weighted sequence shows nodular contrast enhancement of the surgical cavity indicative of disease progression. (**b**) MR diffusion-weighted imaging with ADC map is characterized by a low ADC mean value of 0.672 ± 0.122 mm^2/s in the nodule (*arrow*). (**c**) MR perfusion study with CBV map. The high value of the rCBV of 4.1 [CBV lesion/contralateral white matter CBV sound] corresponds to the areas of enhancement adjacent to the surgical cavity (*yellow arrow*). (**d**) MR single/multivoxel spectroscopy shows a reversal of the Cho/Cr (3.1) and Cho/NAA (4.2) ratios corresponding to the areas of tumor recurrence, indicative of recurrence with anaplastic appearance

Glioblastoma Multiforme: Tumor Recurrence

Case 32

Francesco Fabbiano, Jacopo Scaggiante, Andrea Wlderk, Alessandro D'Elia, Vincenzo Esposito, Claudio Colonnese, and Marcello Bartolo

- Subtle hemiparesis of the left upper limb with fingers paresthesia. Ideational/conceptual apraxia.

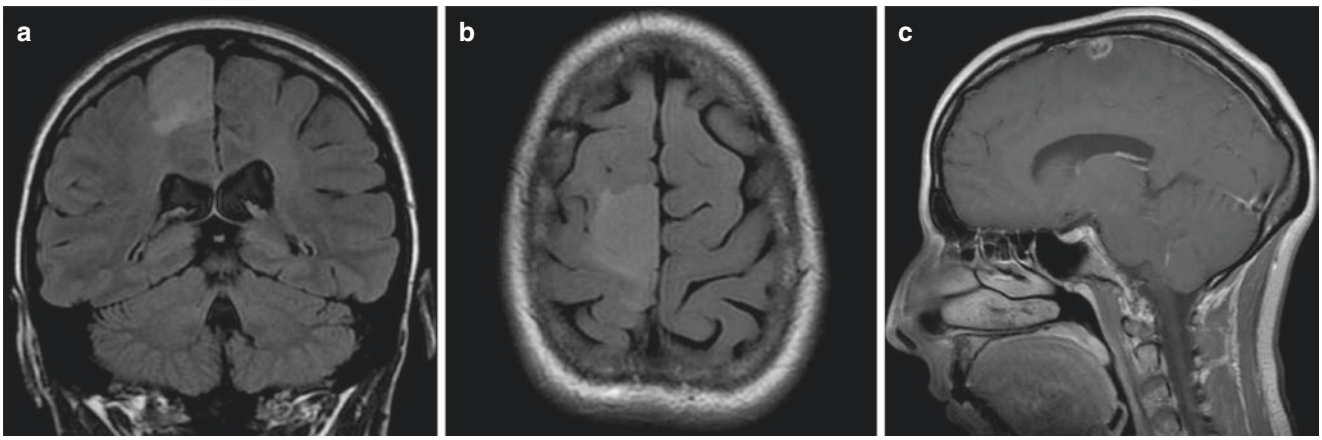

Fig. 32.1 (**a**–**c**) Presurgical imaging. Right frontal parasagittal area of altered signal intensity, with involvement of the precentral convolution characterized by parenchymal swelling and junctional blurring. Contrast-enhanced T1-weighted MRI shows an heterogeneous ring-enhancing mass in its context (longest diameter: 9 mm)

F. Fabbiano (✉)
Department of Neuroradiology, I.R.C.C.S. INM Neuromed, Pozzilli, Isernia, Italy

Department of Diagnostic Imaging, Valmontone Hospital, Rome, Italy

Department of Radiology and Neuroradiology, Villa Benedetta, Rome, Italy

J. Scaggiante
Department of Diagnostic and Interventional Radiology, University of Rome Tor Vergata, Rome, Italy

A. Wlderk
Department of Radiology and Neuroradiology, Villa Benedetta, Rome, Italy

Department of Diagnostic and Interventional Radiology, University of Rome Tor Vergata, Rome, Italy

A. D'Elia
Department of Neurosurgery, I.R.C.C.S. INM Neuromed, Pozzilli, Isernia, Italy

V. Esposito
Department of Neurosurgery, I.R.C.C.S. INM Neuromed, Pozzilli, Isernia, Italy

Department of Neurology and Psichiatry, University La Sapienza, Rome, Italy

C. Colonnese
Department of Diagnostic and Therapeutic Neuroradiology, I.R.C.C.S. INM Neuromed, Pozzilli, Isernia, Italy

Department of Human Neurological Sciences, University La Sapienza, Rome, Italy

M. Bartolo
Department of Diagnostic and Therapeutic Neuroradiology, I.R.C.C.S. INM Neuromed, Pozzilli, Isernia, Italy

T. Scarabino, S. Pollice (eds.), *Imaging Gliomas After Treatment*, https://doi.org/10.1007/978-3-030-31210-7_42

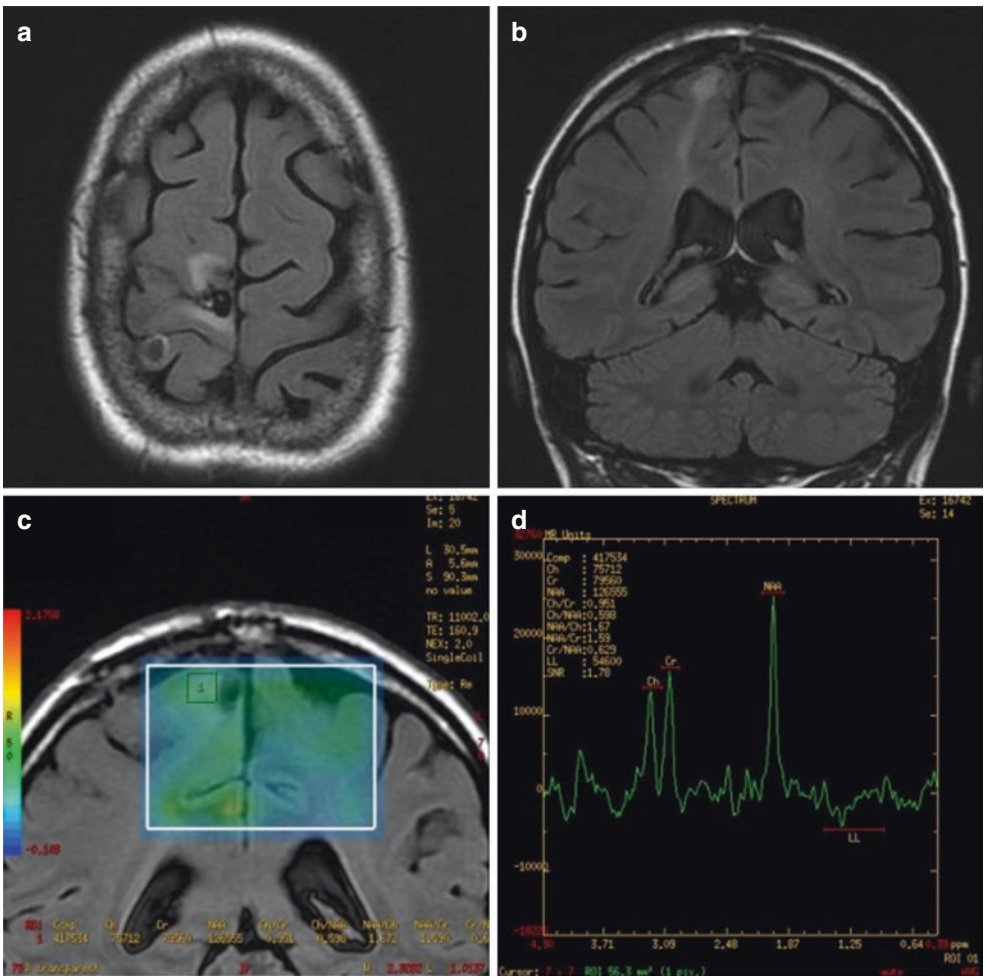

Fig. 32.2 (**a**–**d**) First postoperative follow-up. (**a**, **b**) Imaging shows an area of weak hyperintensity on T2-weighted FLAIR MRI, nonenhancing and without increased values of CBV in perfusion MRI. (**c**, **d**) Multivoxel long TE MR spectroscopy with normal ratio of choline to creatine (Ch/Cr) and choline to N-acetylaspartate (Cho/NAA)

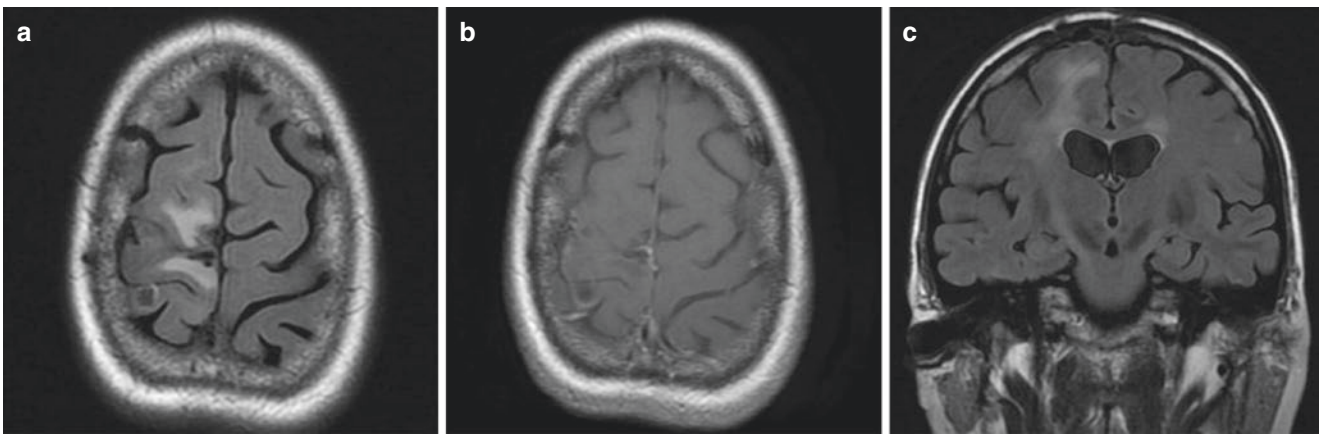

Fig. 32.3 (**a**–**c**) Second postoperative follow-up. Imaging reports increased T2 FLAIR signal intensity close to the surgical cavity (**a**), with no enhancement (**b**) or increased values of CBV in perfusion MRI. There is a contralateral periventricular white matter hyperintensity (**c**) related with brain radiotherapy

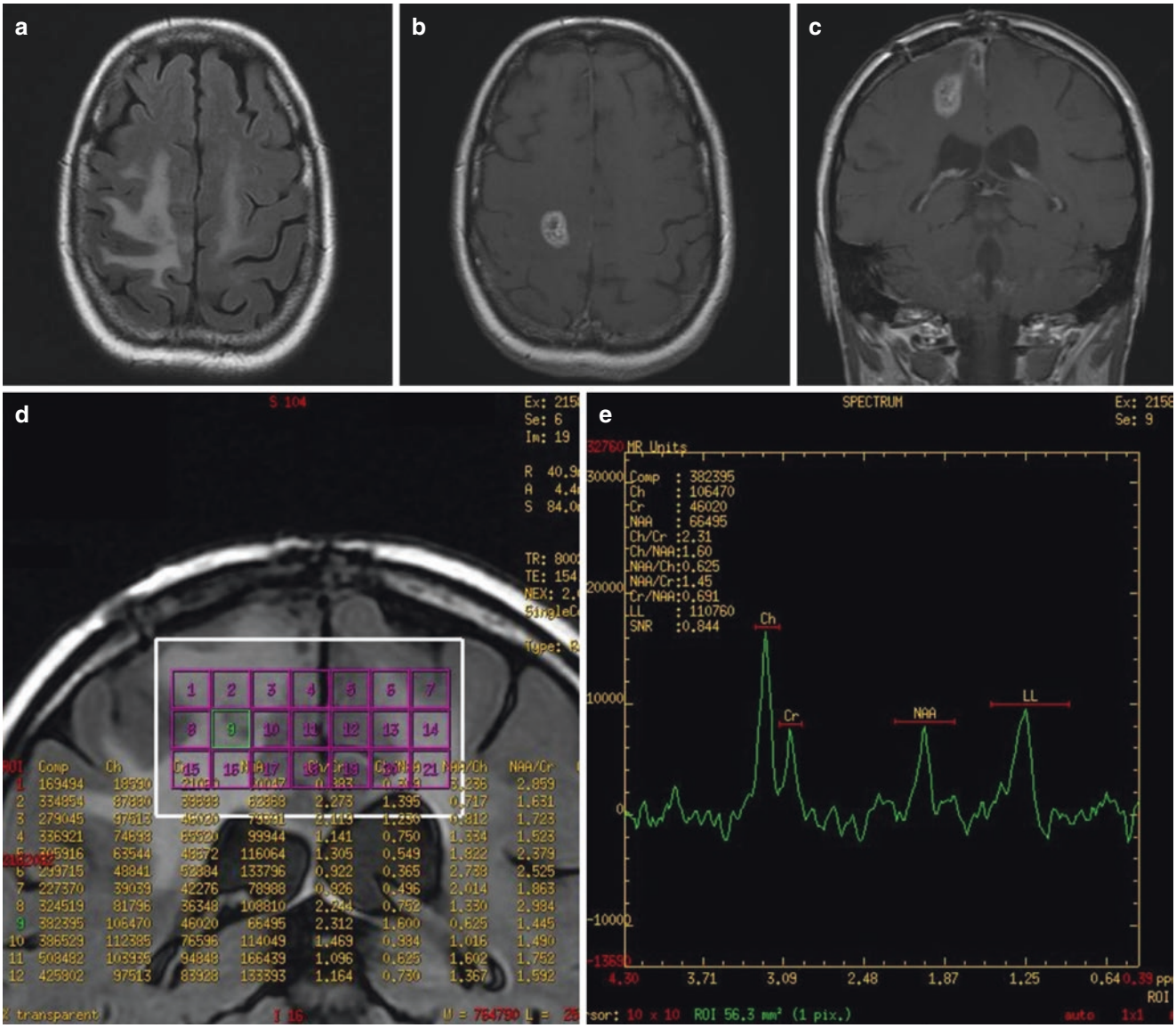

Fig. 32.4 (**a**–**e**) Tumor recurrence at 15-month follow-up. Multivoxel long TE MR spectroscopy shows increased ratio of choline to creatine (Ch/Cr) and inverted ratio of choline to N-acetylaspartate (Cho/NAA) due to neuronal depletion and increased turnover of the cell membranes. The peak in the lipid and lactate range is increased due to lesion conversion to anaerobic metabolism and necrosis

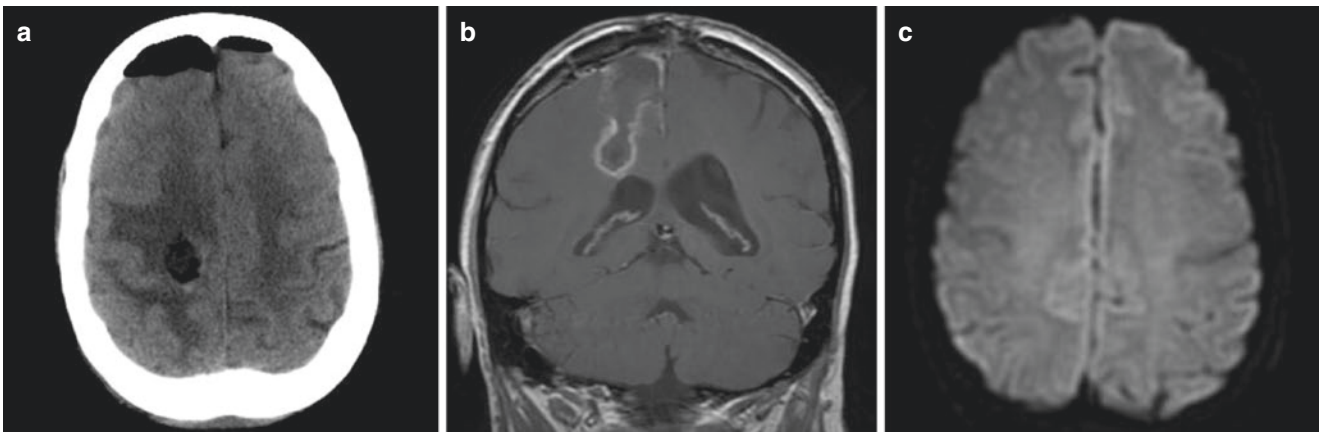

Fig. 32.5 (**a**–**c**) First postoperative follow-up after second surgery. (**a**) Brain CT shows pneumocephalus and without blood in the surgical cavity. (**b**, **c**) Brain MRI shows linear contrast enhancing close to the surgical cavity, partially related with damage of the blood–brain barrier

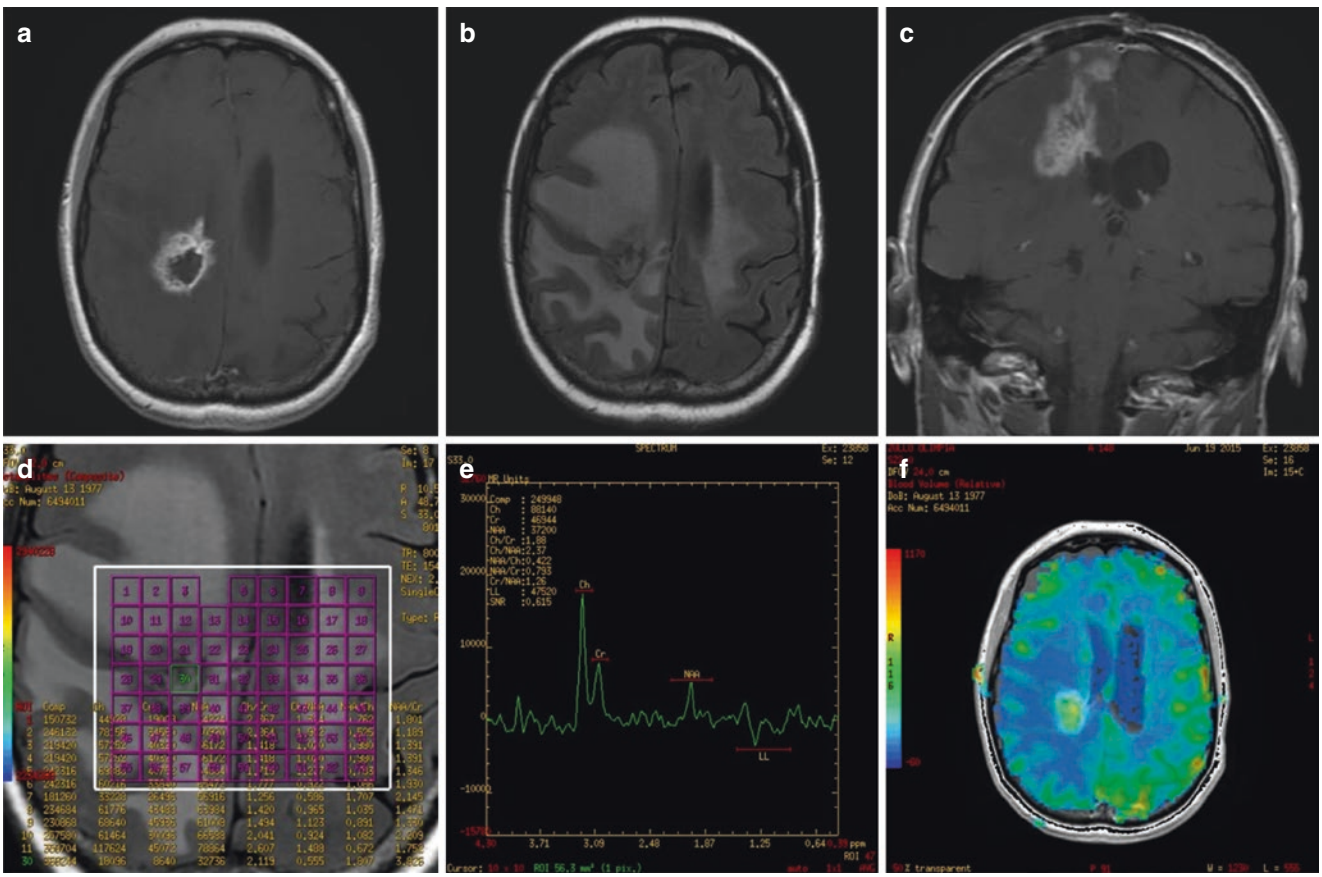

Fig. 32.6 (**a**–**f**) Second postoperative follow-up after second surgery. Perfusion-weighted imaging (PWI) reports a Cerebral Blood Volume ratio (rCBV) of 4:1 as compared with the contralateral side, suggesting neoangiogenesis related with a high-grade tumor recurrence. Contrast enhancement involves the thickened ventricular ependyma

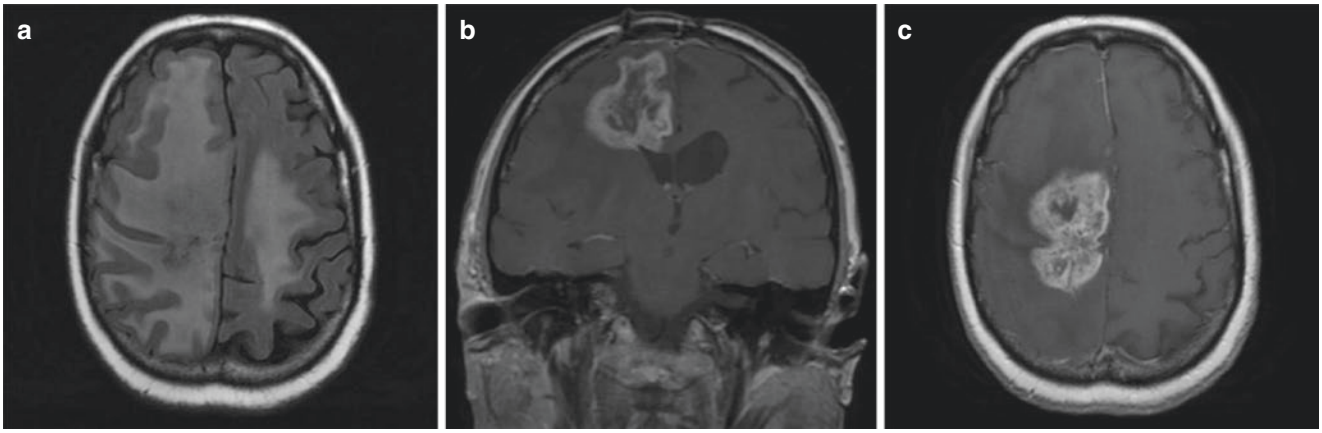

Fig. 32.7 (**a**–**c**) Follow-up after radiotherapy treatment of recurrence. Brain MRI shows volumetric increase in disease recurrence with extension to the periventricular white matter and splenium of the corpus callosum. T2 FLAIR MRI reports increased bihemispheric hyperintensity and ventricular enlargement. The neuroradiological findings are related with high-grade, aggressive, tumor recurrence

Tumor Progression: Morphofunctional MR Follow-Up in Glioblastoma Multiforme

Case 33

Mario Muto and Alessandra D'Amico

- 56-year-old patient with right frontal-temporal glioblastoma multiforme treated with surgical removal and combined radiation therapy–chemotherapy.
- Morphofunctional MR follow-up at 24 hours, 2, 6, 8, 13, and 15 months after surgery and combined radiation therapy–chemotherapy in glioblastoma multiforme.

Preoperative Imaging

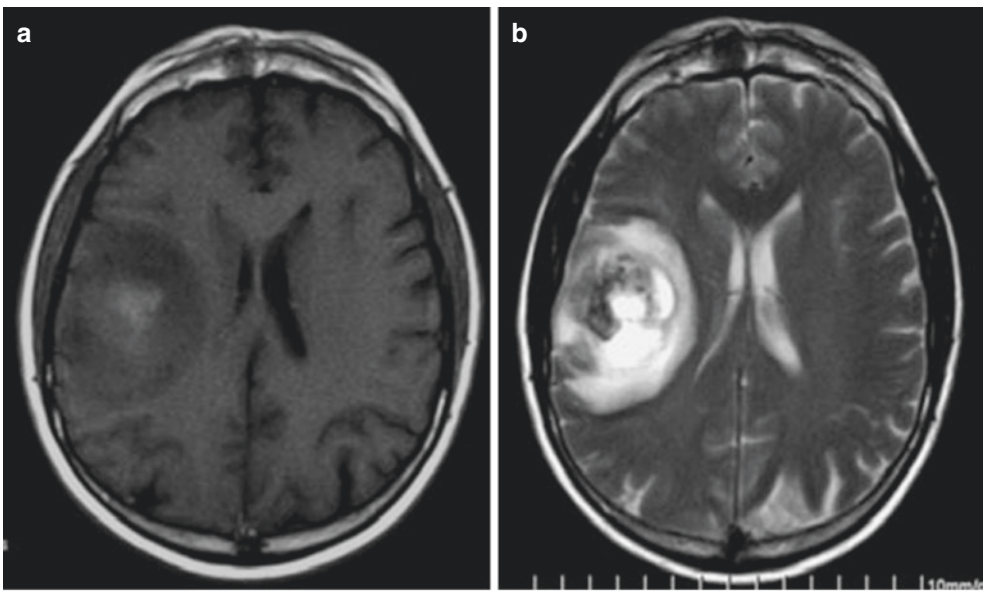

Fig. 33.1 MR morphofunctional study performed with SE T1-weighted (**a**), FSE T2-weighted (**b**), contrast-enhanced SE T1-weighted (**c**) sequences, and single-voxel spectroscopy (**d**). A right frontal-temporal lesion can be appreciated with edema and inhomogeneous signal due to the presence of central hemorrhagic areas, more peripheral cystic-necrotic areas and peripheral pathologic rim enhancement. Compression of the adjacent sulcuses and slight compression of the lateral ventricle below are also evident. Spectroscopic analysis shows a decrease in all metabolites and an increase in Lip/Lac peak, indicative of necrosis within the infiltrating lesion

M. Muto (✉) · A. D'Amico
Department of Neuroradiology, "Cardarelli" Hospital,
Naples, Italy

T. Scarabino, S. Pollice (eds.), *Imaging Gliomas After Treatment*, https://doi.org/10.1007/978-3-030-31210-7_43

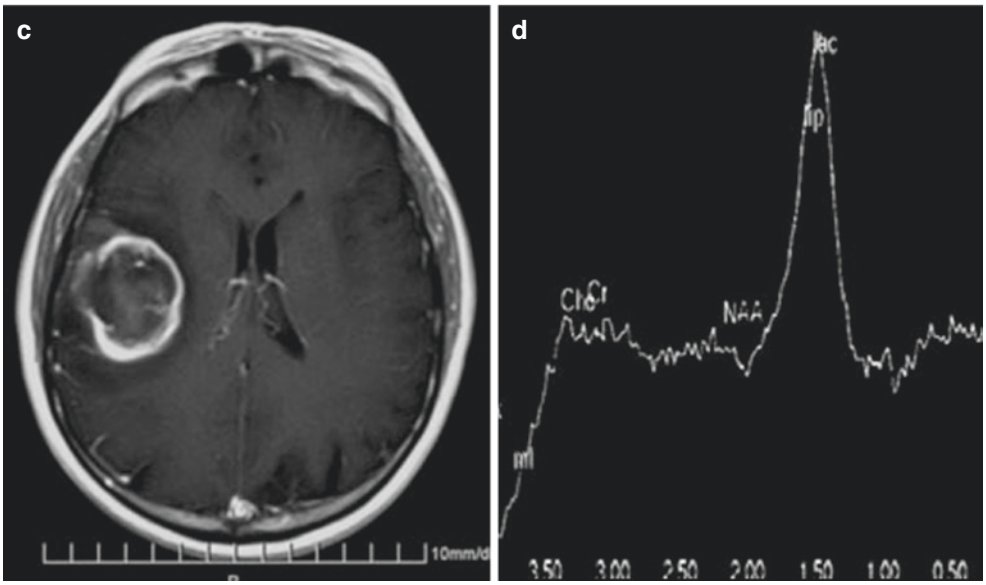

Fig. 33.1 (continued)

Early Postoperative Follow-Up (Within 24 Hours)

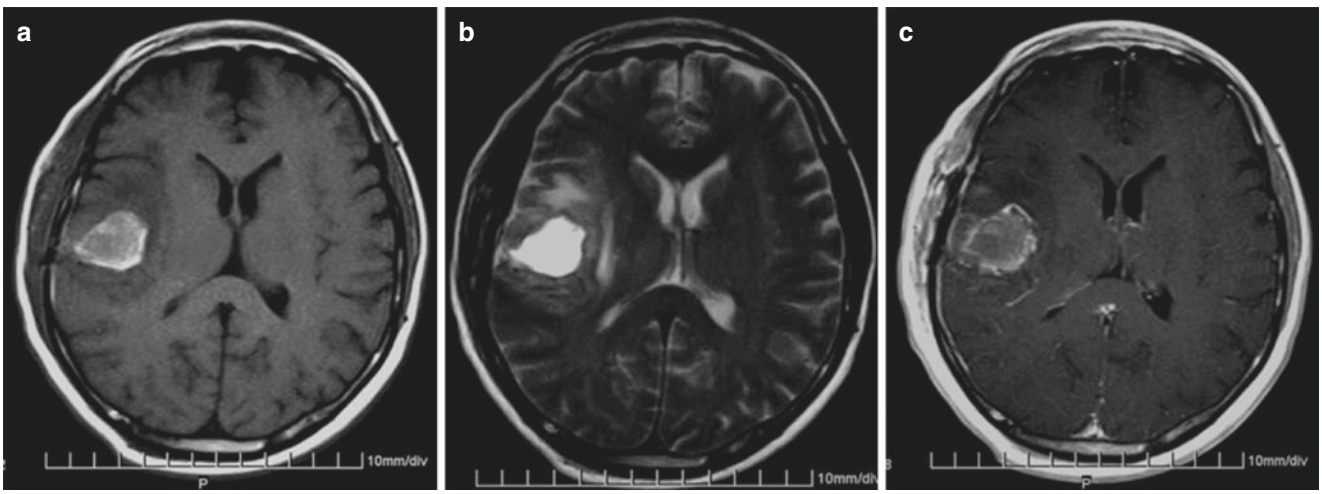

Fig. 33.2 MR SE T1-weighted (**a**), FSE T2-weighted (**b**), and contrast-enhanced SE T1-weighted (**c**) sequences. The right frontal-temporal craniotomy with well-positioned bone flap and the underlying surgical cavity with hyperintense blood signal are visualized. A reduction in perifocal edema can be seen and consequent slight residual compression on the underlying lateral ventricle. After contrast medium administration, faint marginal enhancement of the surgical cavity is visible, caused by blood–brain barrier injury (normal early postoperative finding)

Postoperative Follow-Up at 2 Months

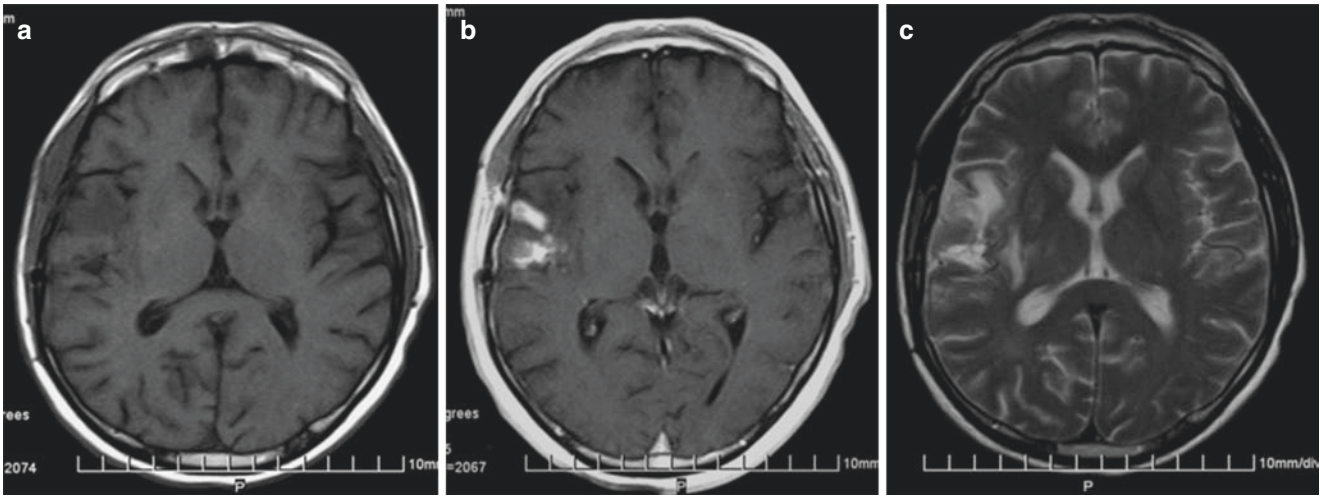

Fig. 33.3 MR SE T1-weighted (**a**), FSE T2-weighted (**b**), and contrast-enhanced SE T1-weighted (**c**) sequences. A slight signal alteration can be appreciated within the surgical cavity and the subcortical areas with re-expansion of the lateral ventricle of the same side. After contrast medium administration some marginal enhancement can be seen

Follow-Up at 6 Months After Surgery and Combined Radiation Therapy–Chemotherapy

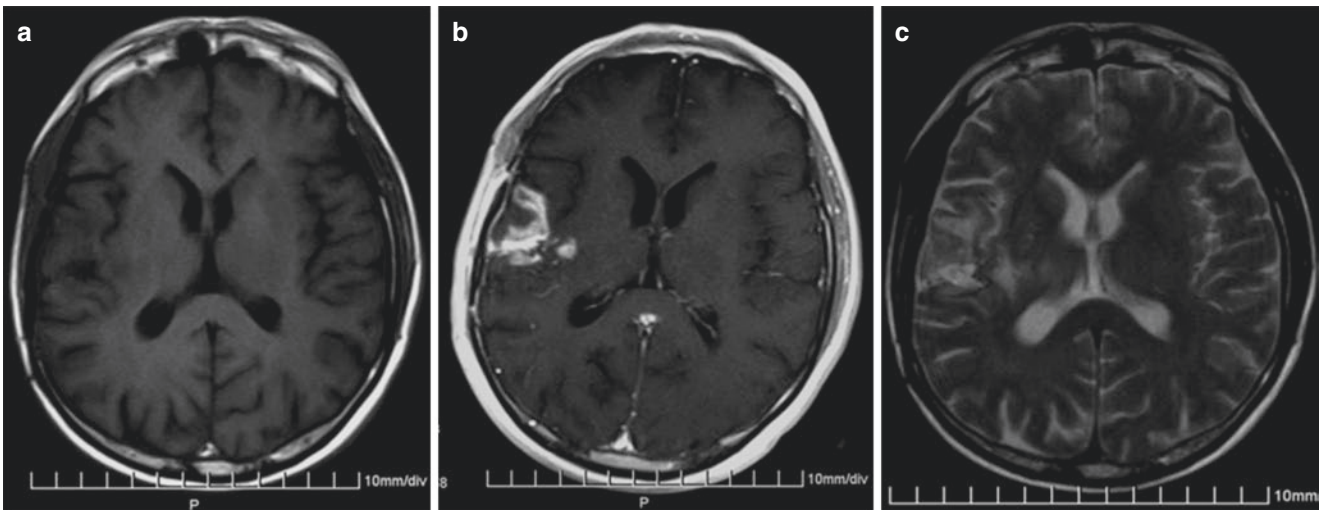

Fig. 33.4 MR SE T1-weighted (**a**), contrast-enhanced SE T1-weighted (**b**), and FFSE T2-weighted (**c**) sequences. The postsurgical gliotic findings are more pronounced than in the previous examination. After contrast medium administration, a slight increase in the size of the enhancing foci is appreciable

Follow-Up at 8 Months

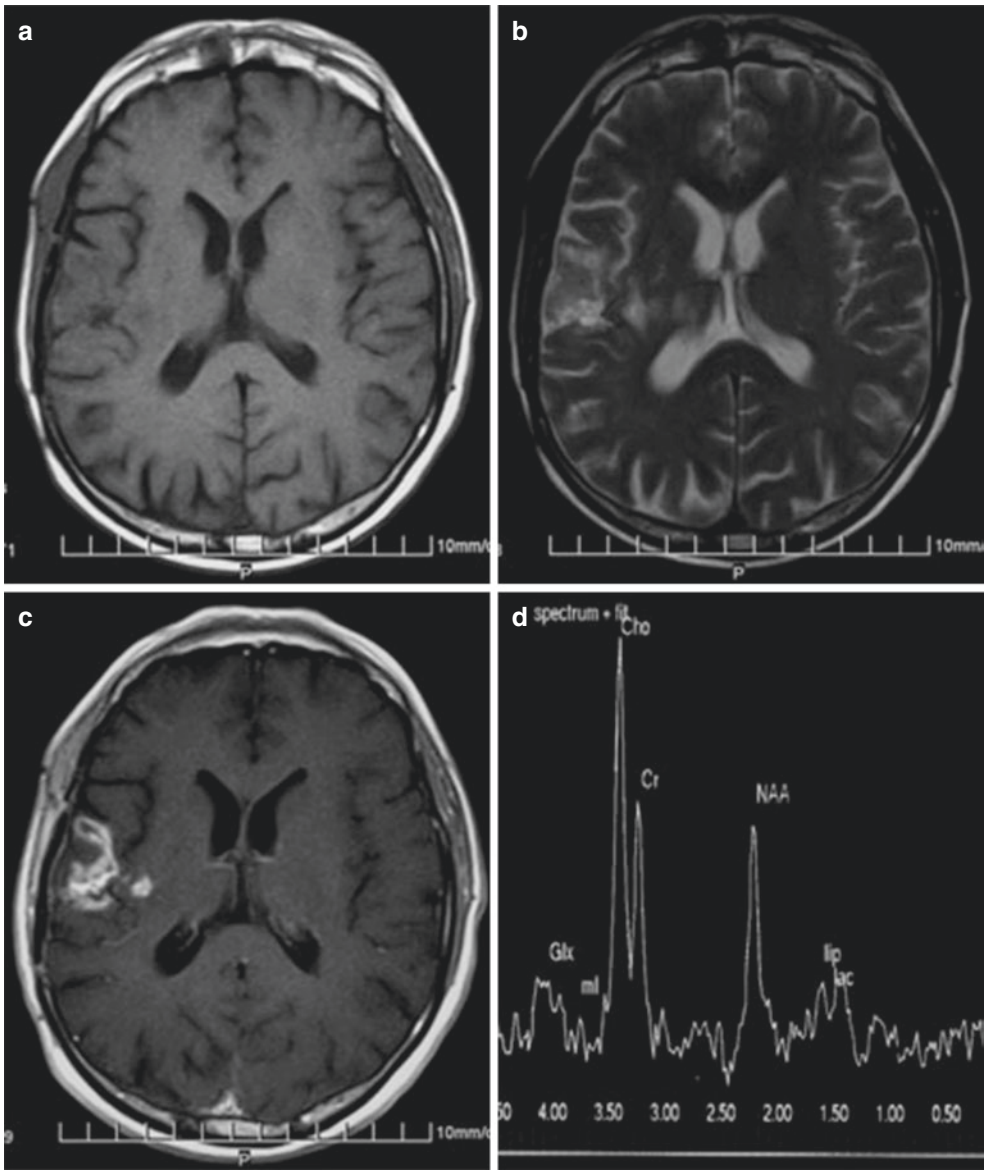

Fig. 33.5 MR morphofunctional study performed with SE T1-weighted (**a**), FSE T2-weighted (**b**), and contrast-enhanced SE T1-weighted (**c**) sequences, and single-voxel spectroscopy (**d**). There are no major changes to the findings already known, with enhancing foci substantially unchanged in size and signal characteristics. Spectroscopic analysis with a voxel placed in the previous surgical site shows a reversal of the Cho/NAA peak (indicating altered turnover of the cell membrane and neuronal loss) and a small Lip\Lac peak (initial index of necrotic changes)

Follow-Up at 13 Months

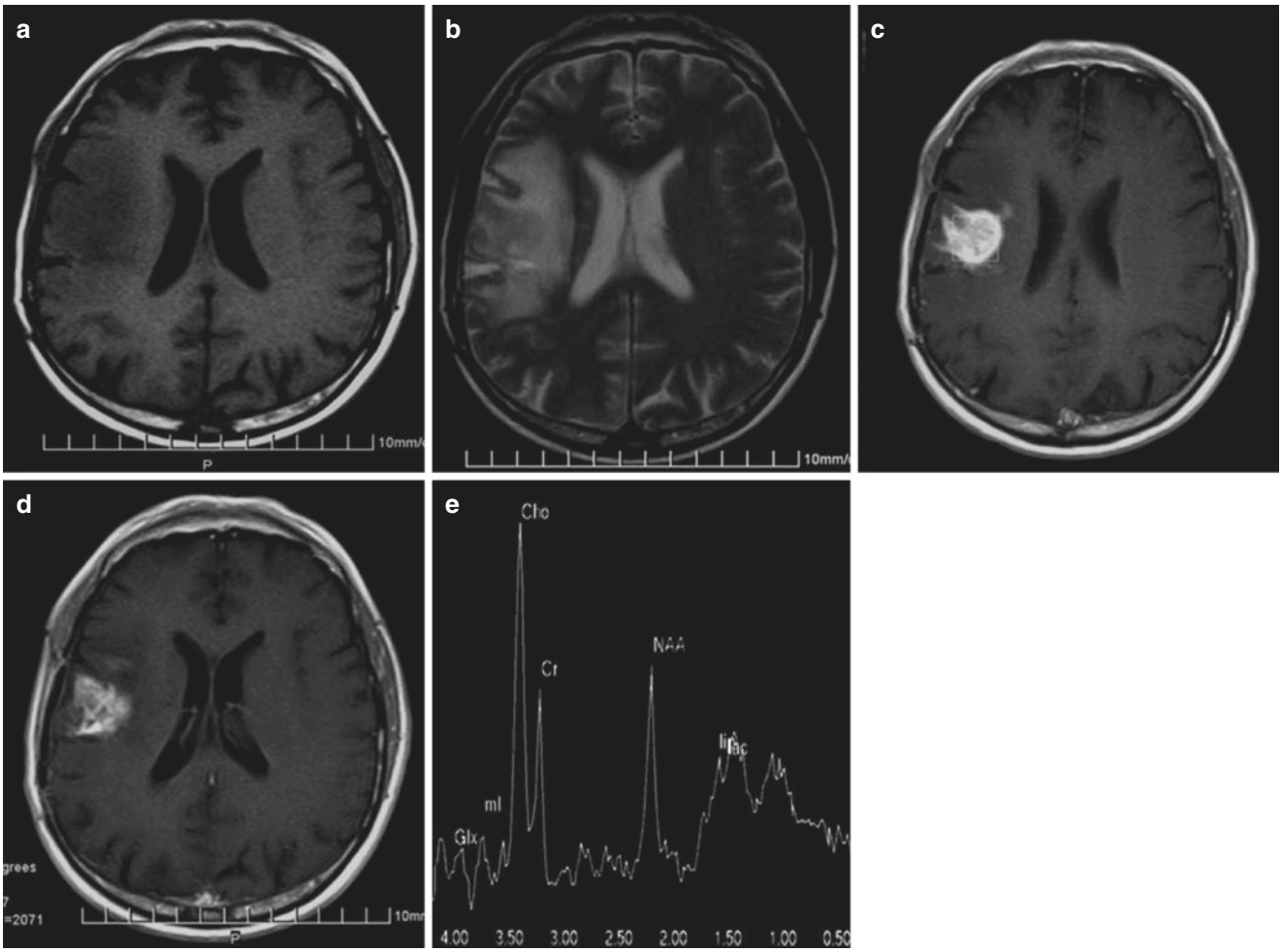

Fig. 33.6 MR morphofunctional study performed with SE T1-weighted (**a**), FSE T2-weighted (**b**) and contrast-enhanced SE T1-weighted (**c**, **d**) sequences, and single-voxel spectroscopy (**e**). The images show evidence of subcortical signal alteration in the right frontal-temporal region with obliteration of the opercular groove from edema. After contrast medium administration, a clearer, more extensive, and marked enhancement can be appreciated in the previous surgical cavity. Spectroscopic analysis indicates moderate inversion of the Cho/NAA ratio and increase in the Lip/Lac peak

Follow-Up at 15 Months

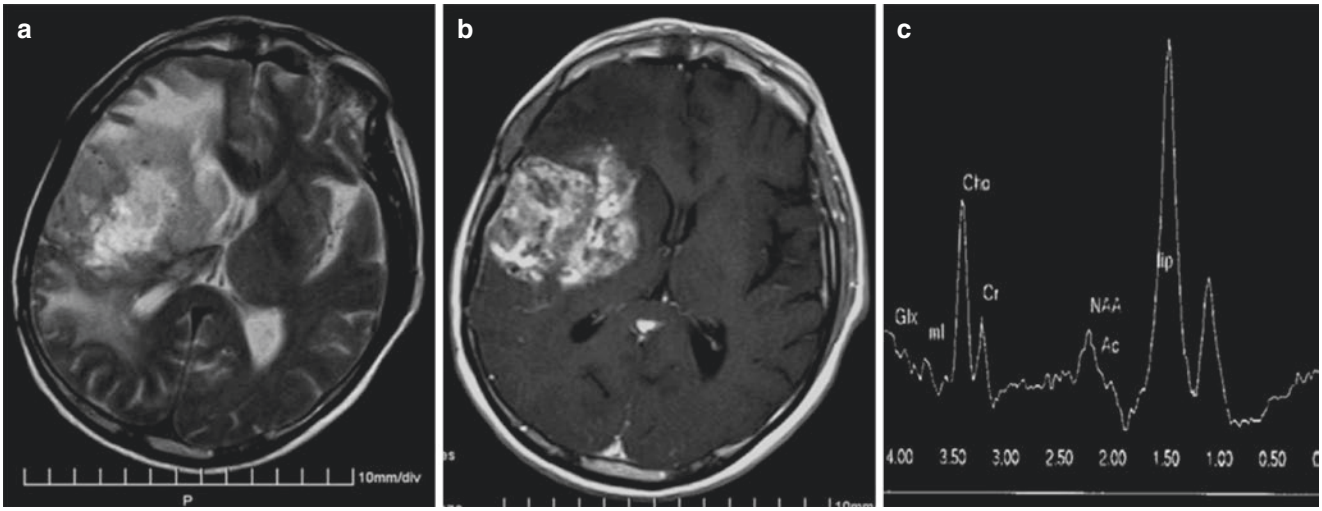

Fig. 33.7 MR morphofunctional study performed with SE T1-weighted (**a**), FSE T2-weighted (**b**) and contrast-enhanced SE T1-weighted (**c**) sequences, and single-voxel spectroscopy (**d**). The images document a worsening of the previous situation with a noticeable extension of signal abnormalities in the right frontal-temporal region, which appears inhomogeneous due to the presence of necrosis. Perilesional edema extends to the ipsilateral frontal-polar and peritrigonal regions, with mass effect on adjacent structures and the underlying contralateral lateral ventricle with a mild midline shift. After contrast medium administration, there is irregular enhancement of the surgical cavity extending to the frontal-temporal cortex and temporal-insular infiltration of the basal ganglia (lenticular nucleus and internal capsule). Spectroscopic analysis shows a further net inversion of the Cho/NAA ratio and a marked increase in the Lip/Lac peak

Tumor Progression: Morphofunctional MR Follow-Up in Glioblastoma Multiforme

Case 34

Gabriele Polonara, Lorenzo Alvaro, and Francesco Sessa

- 44-year-old patient with right frontal-parietal pararolandic anaplastic astrocytoma (WHO III) treated with surgery, radiotherapy, chemotherapy, and subsequent co-adjuvant level II chemotherapy
- Morphofunctional MR follow-up performed with morphologic imaging, diffusion, perfusion, and spectroscopy preoperatively and at 48 hours, 4 (contrast-enhanced CT scan), 7, 10, 12, and 14 months after surgery

Preoperative Imaging

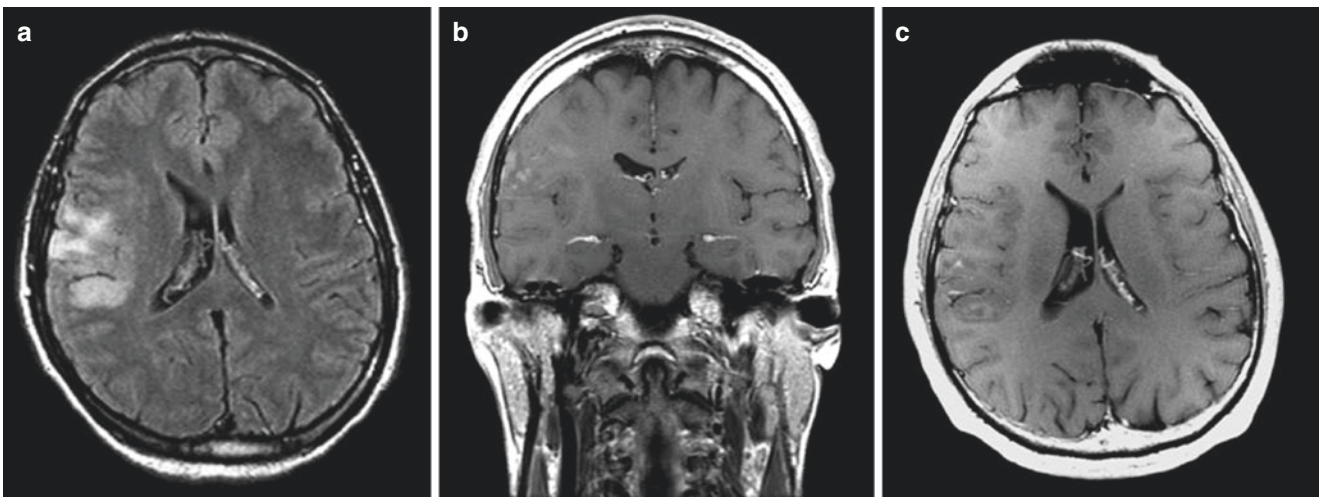

Fig. 34.1 (**a**) MR FLAIR sequence shows a cortical-subcortical area of altered signal with poor visualization of the corresponding cortical sulci in the right frontal-parietal pararolandic region, at the level of the frontal-parietal opercular area and the right insular region. (**b**, **c**) Contrast-enhanced MR SE T1-weighted sequences show minimal signs of altered BBB in the context of the lesion, mainly located in the cortical and immediately subcortical regions at the level of the parietal operculum and ascending parietal gyrus

G. Polonara (✉) · L. Alvaro · F. Sessa
Department of Radiology, University Hospital "Ospedali Riuniti", Ancona, Italy

T. Scarabino, S. Pollice (eds.), *Imaging Gliomas After Treatment*, https://doi.org/10.1007/978-3-030-31210-7_44

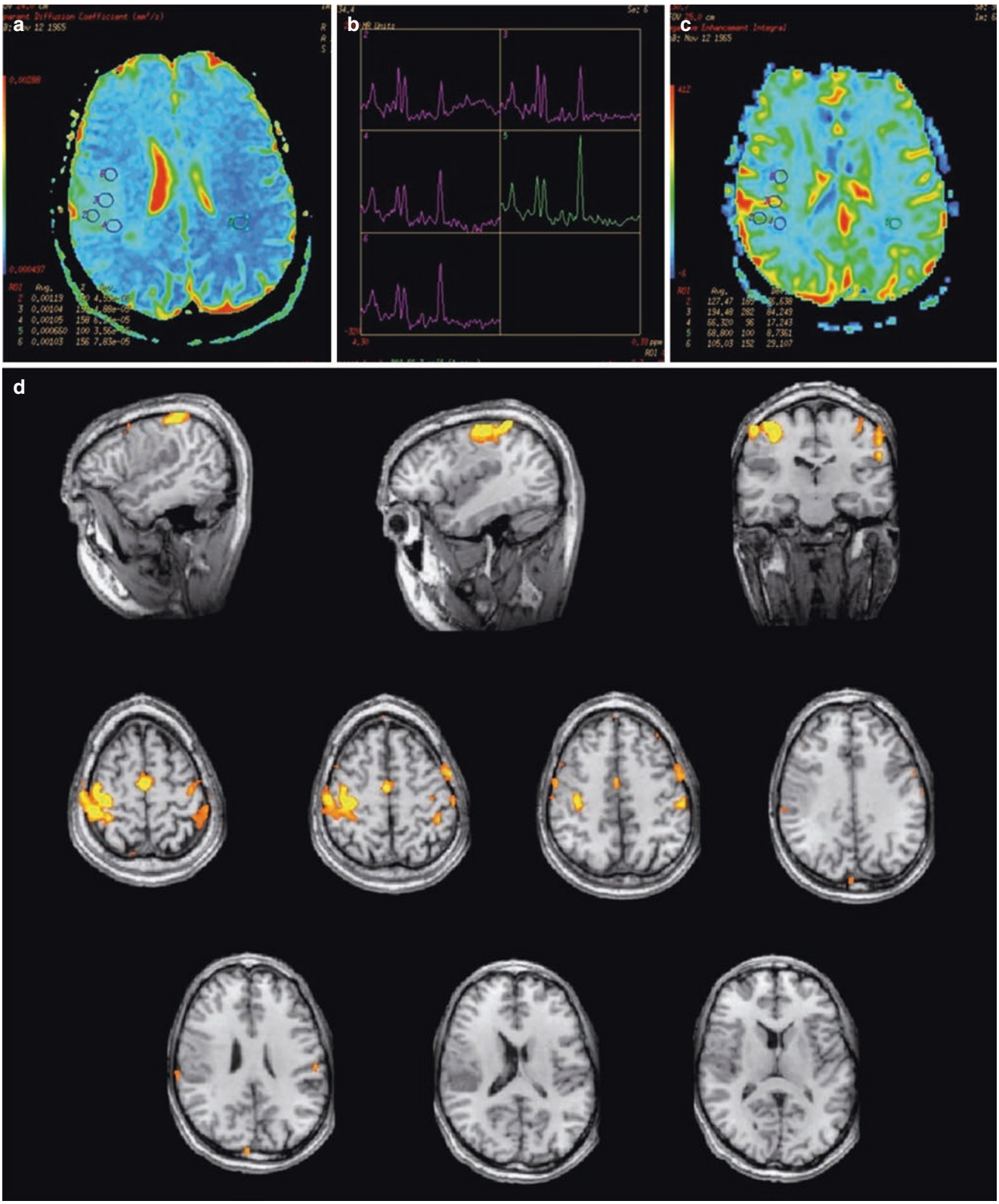

Fig. 34.2 (**a**) MR diffusion-weighted imaging shows moderate increase in the apparent diffusion coefficient in the right frontal-parietal lesion. (**b**) MR multivoxel and long TE spectroscopy. A decrease in the NAA/Cr ratio, a slight increase in the Cho/Cr and Cho/NAA ratios (indices of increased proliferative activity) are shown and an absence of lactic acid or lipid peaks. (**c**) MR perfusion study shows a moderate increase in perfusion of the lesion compared with the apparently healthy contralateral brain parenchyma. (**d**) MR study mapping functional areas shows areas that are activated during the opening and closing movements of the left hand

Early (48 h) Postoperative Follow-up

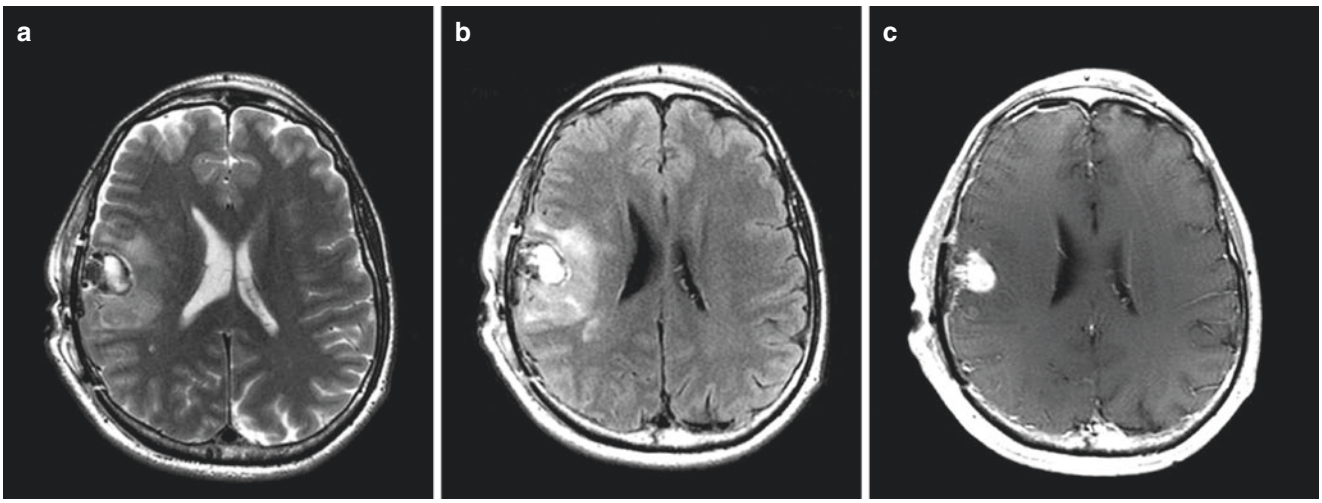

Fig. 34.3 MR FSE T2-weighted (**a**) and FLAIR (**b**) sequences display the right parietal-temporal craniotomy (with repositioned bone flap) and postsurgical evidence of partial removal of a right frontal-parietal lesion. In particular, a postsurgical area of loss of white matter can be appreciated at the level of the inferior portion of the right postcentral gyrus. A small amount of hyperintense perilesional edema and minimal signs of expansion can also be seen. (**c**) Contrast-enhanced MR SE T1-weighted sequence shows evidence in the right frontal-parietal lobe of a slight accentuation of the CSF spaces, a slight thickening of the dura and probably a residual lesion

Follow-Up Performed at 4 Months After Surgery, Radiotherapy, and Concomitant Chemotherapy

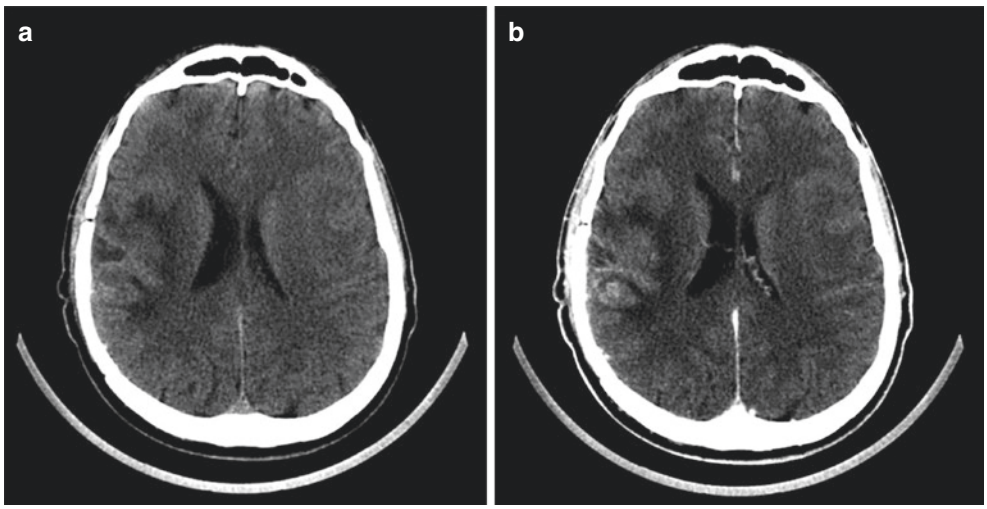

Fig. 34.4 CT scan without (**a**) and with (**b**) administration of contrast medium. Regrowth of the tumor can be seen in the right cortical-subcortical inferior parietal region, with associated peripheral hypodensity indicating infiltration/edema, and mild signs of locoregional expansion. After administration of contrast medium, there is an irregular enhancement of the tumor

Follow-Up Performed at 7 Months After Surgery and Three Cycles of Adjuvant Chemotherapy

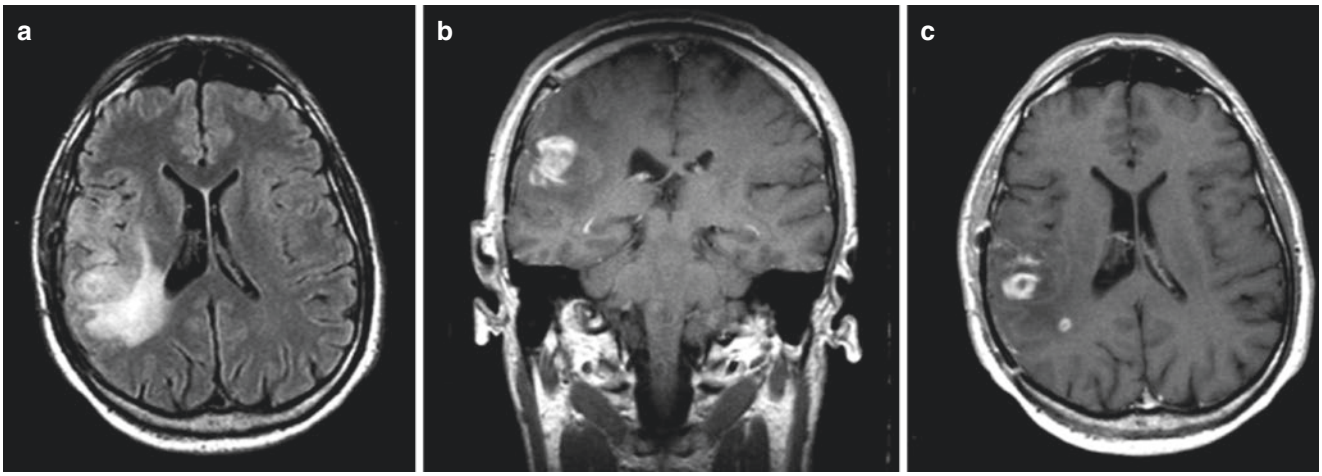

Fig. 34.5 (**a**) MR FLAIR sequence shows inhomogeneous increase in size of infiltrating lesion with ill-defined margins located in the right frontal-parietal pararolandic region, surrounded by slight perilesional edema extending in the right subependymal paratrigonal region. Increased signs of compression on the right frontal-parietal cortex and mild compression of the ipsilateral ventricular trigone can also be seen. (**b**, **c**) Contrast-enhanced MR SE T1-weighted sequences show considerable enhancement of the infiltrating lesion in the right frontal-parietal pararolandic region associated with micronodular lesions in the right subcortical parietal region adjacent to and above the trigone

Follow-Up Performed at 10 Months After Surgery, Two Conventional Cycles and Other Intensified Cycles of Chemotherapy

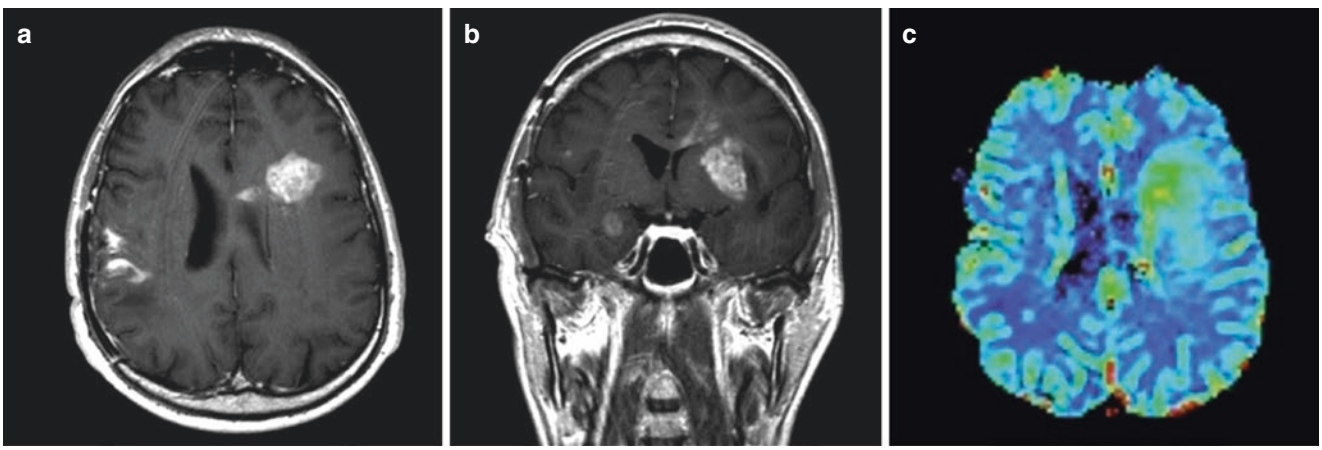

Fig. 34.6 (**a**, **b**) Contrast-enhanced MR SE T1-weighted sequence identifies the appearance of new expansive-infiltrative lesions in the left anterior frontal-insular region, with partial infiltration of the adjacent corpus callosum. Less evident changes can be seen in the contralateral residual lesion-recurrence at the site of previous surgery. On the left increased enhancement of the entire lesion is evident, whereas enhancement on the right appears more heterogeneous and appreciable mainly in the portion of right cortical-subcortical frontal-parietal region. Enhancement can also be seen in the right parauncal region which was absent in the previous study. MR study performed with perfusion imaging (**c**) and spectroscopy (**d**, **e**) seems to confirm a possible increased aggressiveness of the new-onset lesions on the left, which tend to appear hyperperfused (**c**), unlike the contralateral lesions. On the left there is also a marked increase in the Cho peak (**d**), associated with a marked reduction in the principal metabolites and appearance of a lactate peak, likely due to a poorly differentiated lesion with high cell turnover and initial necrosis. On the right the spectroscopic changes (**e**), despite a clearly pathologic appearance of infiltration-proliferation, appear less marked, with the exception of the right cortical-subcortical frontal-parietal portion immediately below the bone flap, which appears comparable to those on the left

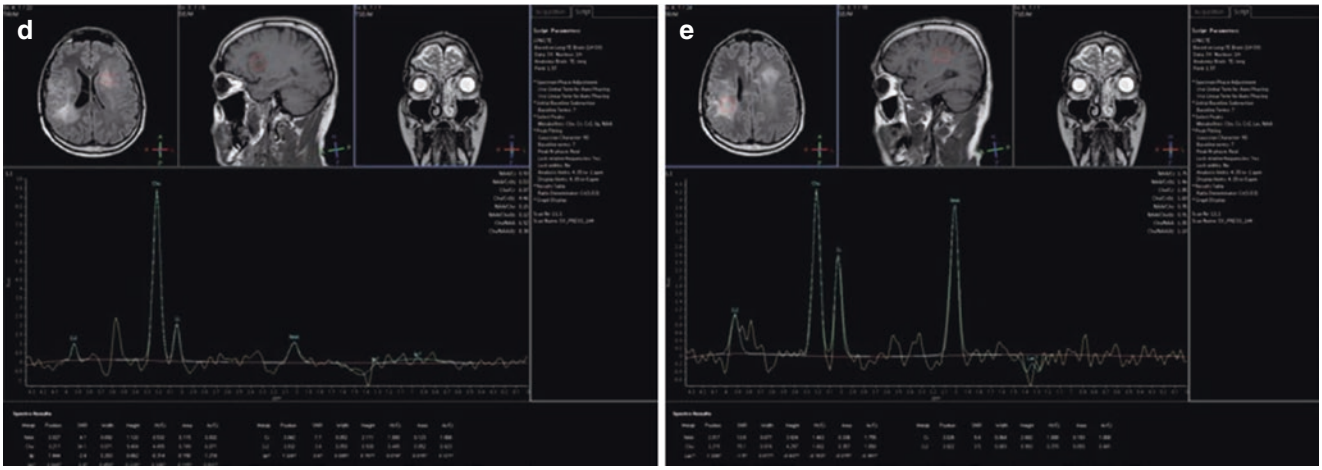

Fig. 34.6 (continued)

Follow-Up Performed at 12 Months After Surgery and After Starting Level II Chemotherapy

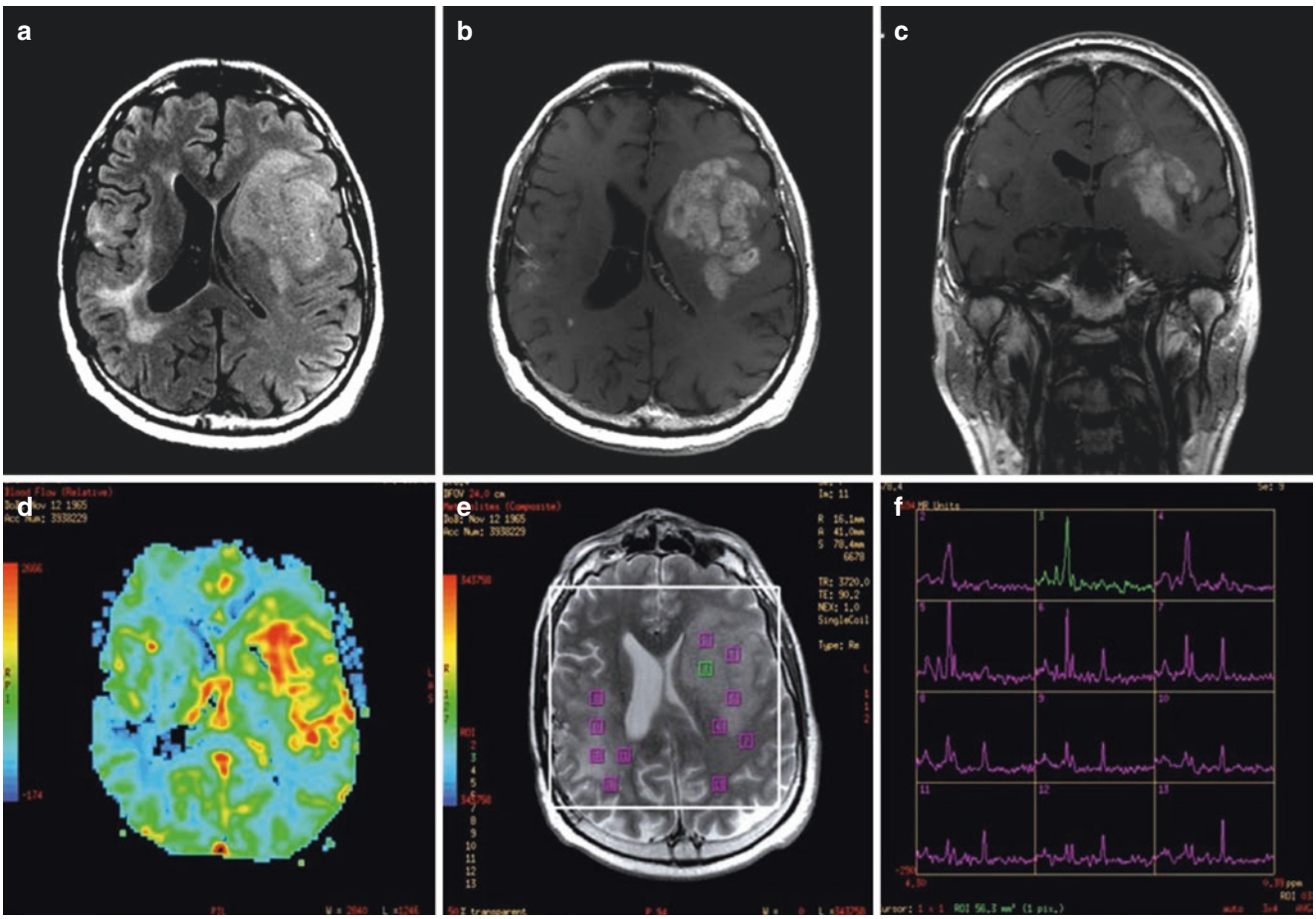

Fig. 34.7 (**a**) MR FLAIR sequence shows an overall extension of the expansive/infiltrating lesions. The increase is much more evident on the left with overall increase in the size of the known lesion. A concomitant increase in signs of expansion can also be seen characterized by increased compression of the ipsilateral ventricle and initial midline shift to the right. Contrast-enhanced MR SE T1-weighted sequences (**b**, **c**) and perfusion study (**d**). A slight reduction in the enhancement of the lesion on the right can be appreciated, while there is an extension of the hyperperfused area (**d**) and enhancement of the lesion on the left. (**e**, **f**) MR multivoxel spectroscopy with long TE shows a marked increase in the Cho/Cr and Cho/NAA ratios (indices of increased proliferation), while no lactic acid or lipid peaks are observed in relation to the lesions located in the left hemisphere. Only a slight increase in the Cho/Cr and Cho/NAA ratios can be seen on the right

Follow-Up Performed at 14 Months After Surgery and After Continuing Level II Chemotherapy

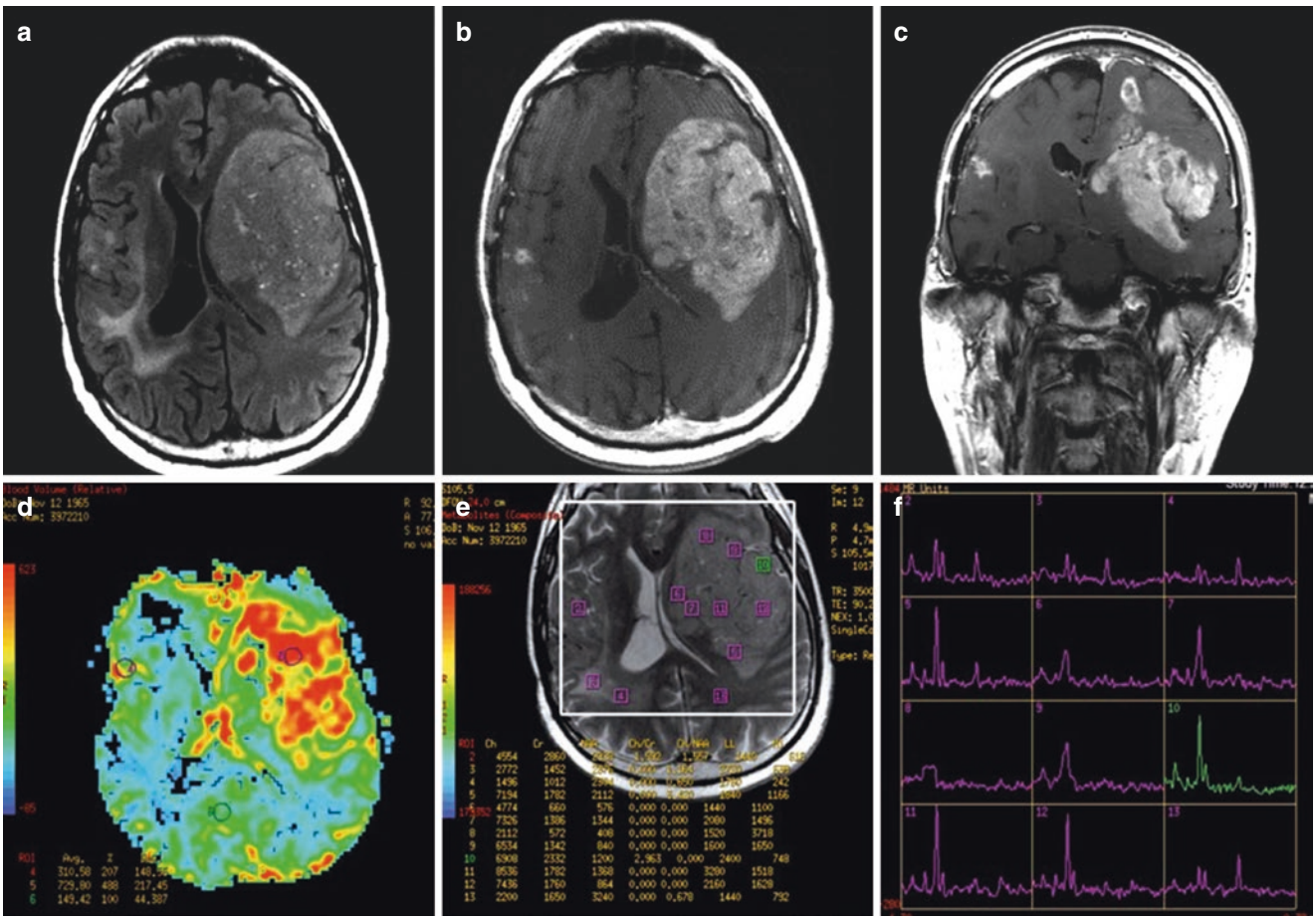

Fig. 34.8 MR FLAIR (**a**) and contrast-enhanced SE T1-weighted (**b**, **c**) sequences show further marked increase in the overall size of the left expansive/infiltrative lesion and the associated signs of expansion. The changes are characterized by the near complete disappearance of the frontal CSF spaces and compression/displacement of the supratentorial ventricular system and midline shift to the right. (**d**) MR perfusion study show high perfusion associated with the lesion in the left hemisphere. (**e**, **f**) MR spectroscopy shows a marked increase in the Cho/Cr and Cho/NAA ratios in the progressive neoplastic lesions in the left hemisphere

Tumor Progression: Morphofunctional MR Follow-Up in Glioblastoma Multiforme

Case 35

Gabriele Polonara, Lorenzo Alvaro, and Luana Regnicolo

- 66-year-old patient with (unmethylated MGMT gene promoter) left posterior temporal glioblastoma multiforme treated with surgery and subsequent radiotherapy and concomitant adjuvant chemotherapy.
- Morphofunctional MR follow-up performed with morphologic study, diffusion, perfusion, and spectroscopy preoperatively, at 48 hours, 4, 7, and 9 months after surgery.

Preoperative Imaging

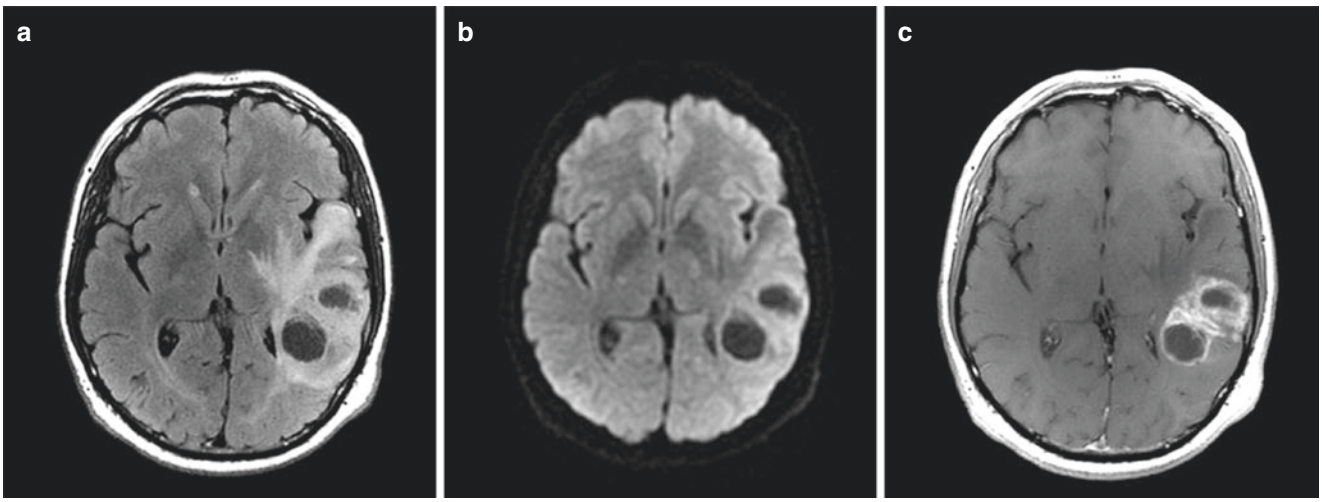

Fig. 35.1 (**a**) MR FLAIR sequence shows a partly cystic voluminous heterogeneous expansive lesion infiltrating the left temporal cortical-subcortical region, with extensive perilesional hyperintense signal indicating edema-infiltration that extends forward to the posterior arm of the internal capsule and the posterior portion of the external capsule. The lesion extends deep to the temporal horn, trigone, and occipital horn of the left ventricle ependyma. A reduction of CSF spaces, compression of the ipsilateral ventricle, and mild right-deviation of the midline can also be appreciated. (**b**) MR diffusion-weighted image confirms the presence of two large cysts with higher intralesional diffusion coefficient suggestive of necrotic-cystic nature. (**c**) Contrast-enhanced MR SE T1-sequence shows intense enhancement with the presence of two inhomogeneous areas of rim enhancement with cystic-like areas indicating necrosis

G. Polonara (✉) · L. Alvaro · L. Regnicolo
Department of Radiology, University Hospital "Ospedali Riuniti", Ancona, Italy

T. Scarabino, S. Pollice (eds.), *Imaging Gliomas After Treatment*, https://doi.org/10.1007/978-3-030-31210-7_45

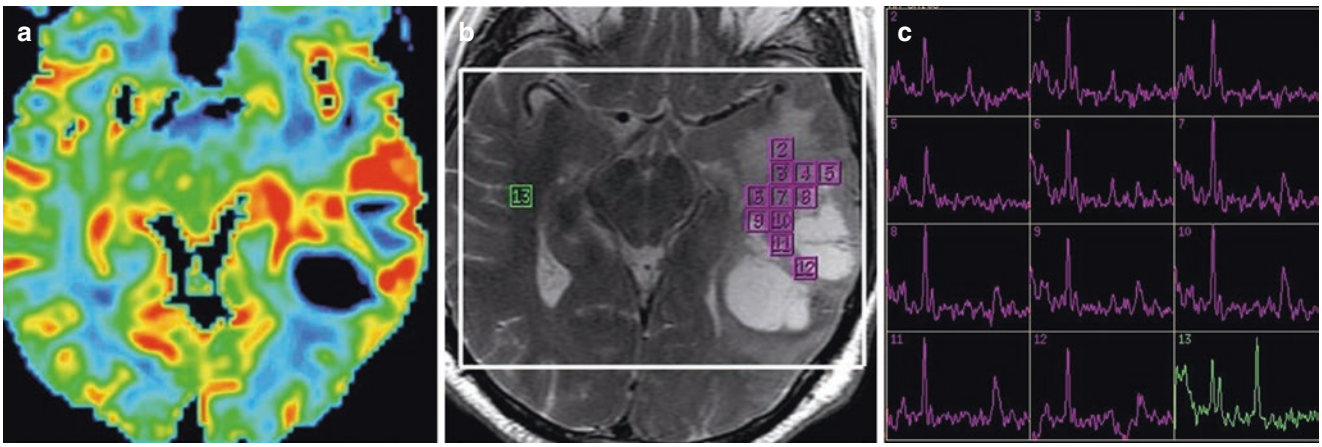

Fig. 35.2 (**a**) MR perfusion study shows inhomogeneous increase in perfusion with hypoperfused areas in the context of the expansive/infiltrative lesion. (**b**, **c**) Multi-voxel MR spectroscopy with long echo times shows an increase in the Cho/Cr and Cho/NAA ratios (indices of increased proliferative activity), with a high lipid peak compatible with the presence of necrosis

Early (48 h) Postoperative Follow-Up

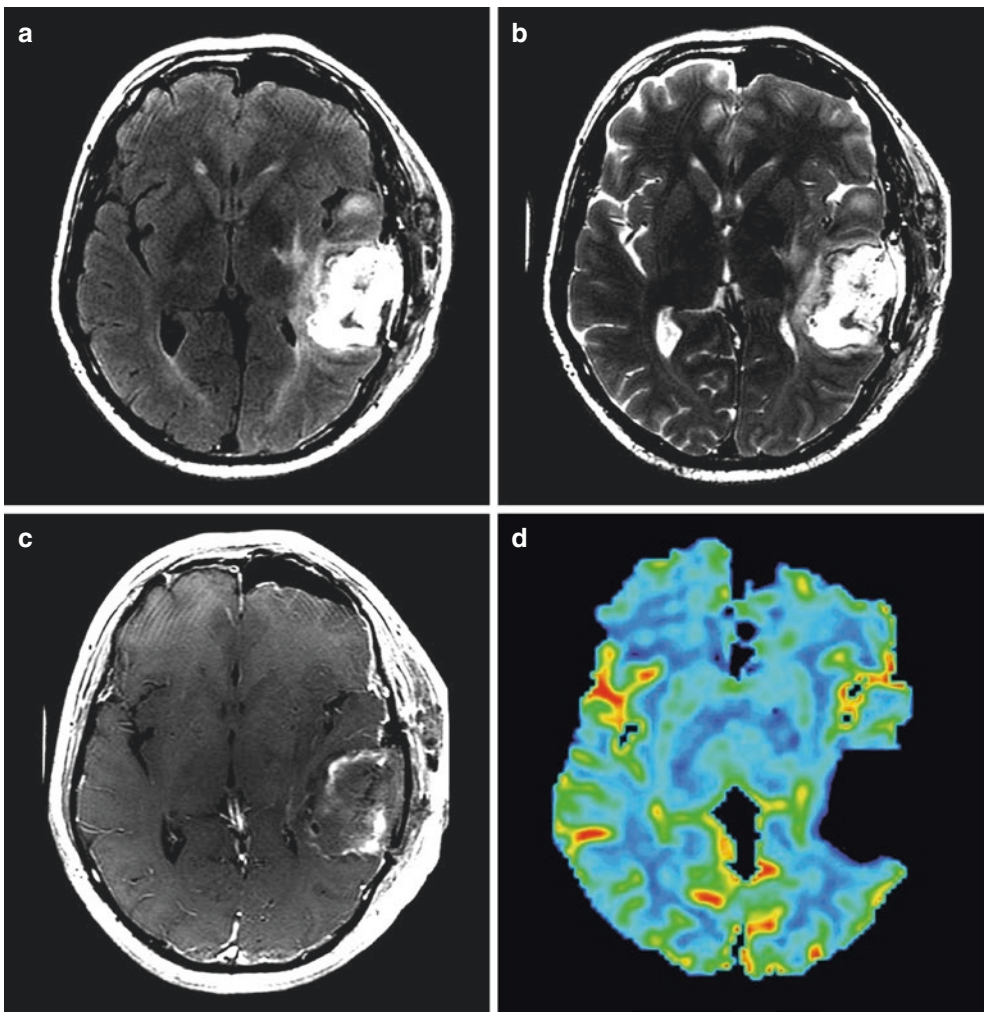

Fig. 35.3 MR FLAIR (**a**), FSE T2-weighted (**b**) and contrast-enhanced SE T1-weighted (**c**) sequences visualize the left temporal-parietal craniotomy and partial removal of the expansive/infiltrative lesion previously documented. Some air bubbles and blood can be seen within the surgical cavity. At the edge of the cavity signs of injured BBB and traces of blood in the anterior region can be appreciated. A reduction in perilesional edema, persistent signs of lesion expansion as visualized in the preoperative images, the appearance of a layer of air in the frontal-polar region, and moderate diastasis of the repositioned bone flap can also be appreciated. (**d**) MR perfusion study shows no appreciable signs of high perfusion at the margins of the surgical cavity

Follow-Up Performed at 4 Months After Surgery, Radiotherapy, and Concomitant Chemotherapy

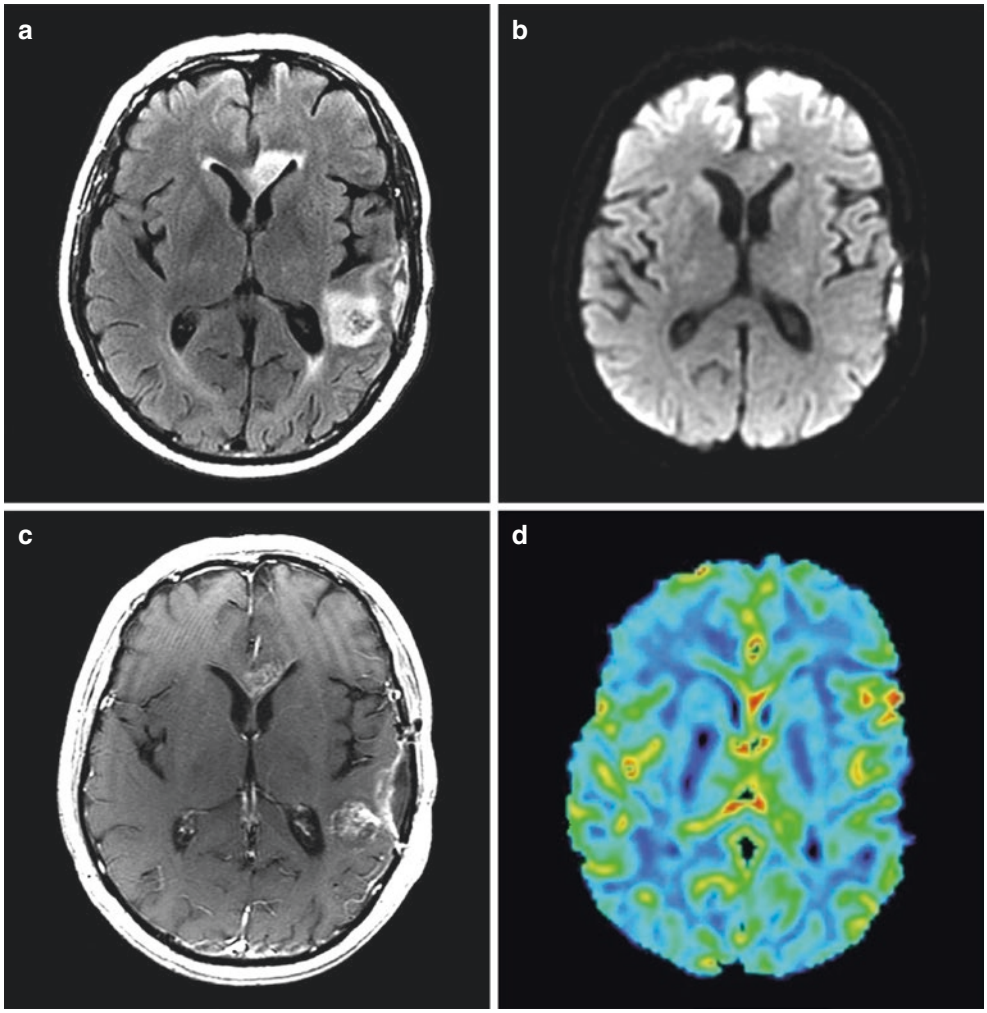

Fig. 35.4 MR FLAIR (**a**) and diffusion-weighted (**b**) sequences show a reduction in size of the surgical cavity, with air and blood no longer appreciable. The air layer in the frontal-temporal regions and the signs of expansion are also no longer visible. (**c**) Contrast-enhanced MR SE T1-weighted sequence displays an increase in the thickness of the marginal zone with signs of altered BBB, the presence of some tissue with neoplastic appearance extending into the brain parenchyma. Another area with signs of altered BBB not shown in the previous examination can be seen in the genu of the corpus callosum, in the left parasagittal region. (**d**) MR perfusion study shows a slight increase in perfusion indices near the margins of the surgical cavity and at the genu of the corpus callosum

Follow-Up Performed at 7 Months After Surgery and Adjuvant Chemotherapy

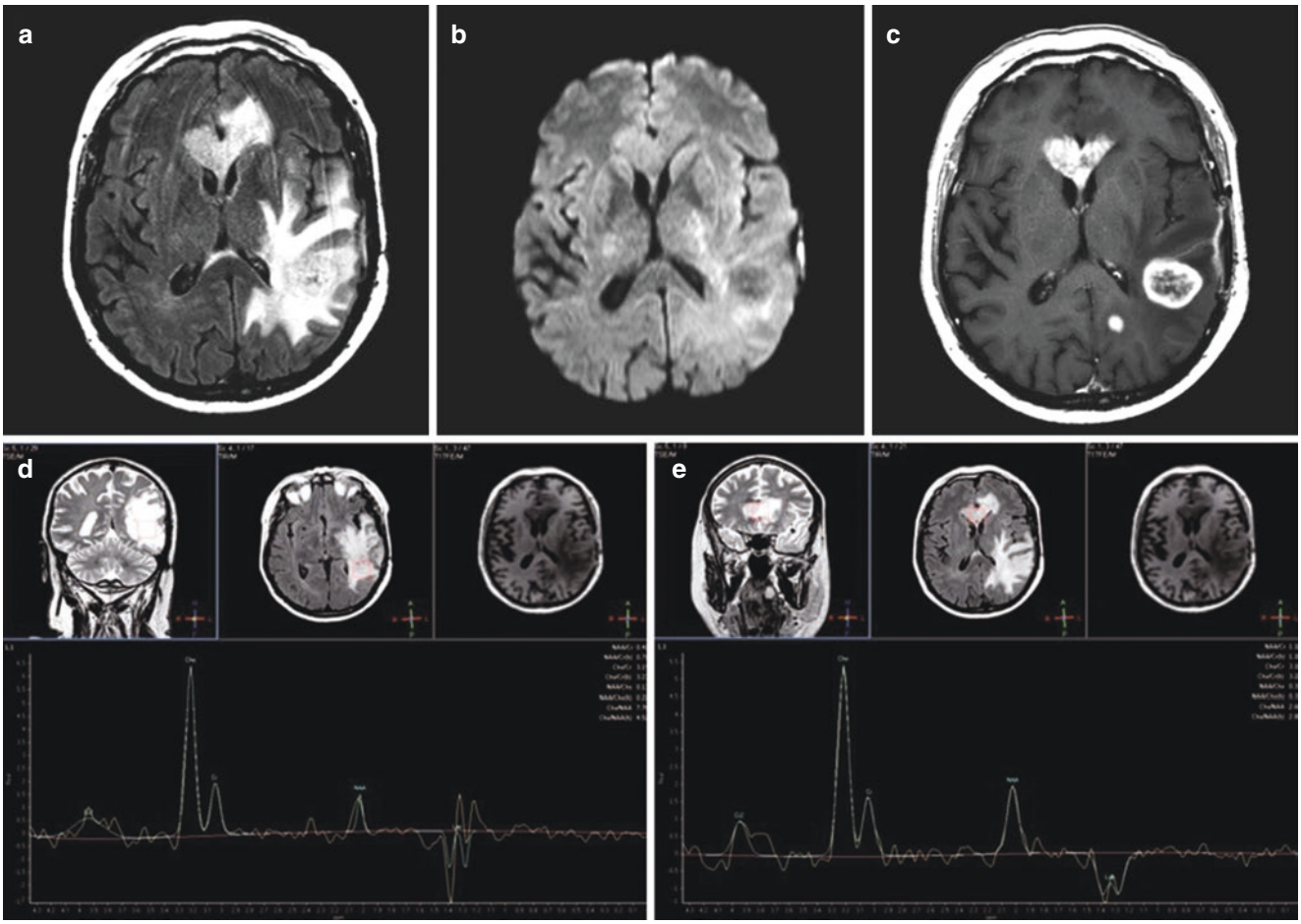

Fig. 35.5 MR FLAIR sequence (**a**) and diffusion-weighted imaging (**b**) show an increase in size of the expansive/infiltrative lesion peripherally in the left parietal-temporal surgical cavity. An increase in signal hyperintensity can also be seen indicating edema-infiltration peripheral to the lesion extending anteriorly in the left temporal-polar region, posteriorly in the retroparatrigonal area and deep to involve the capsules/nuclei. Signs of expansion are associated, with a reduction in the visualization of the CSF spaces and compression/shift of the left lateral ventricle. (**c**) Contrast-enhanced MR SE T1-weighted sequence shows an increase in the size of the lesion located at the genu of the corpus callosum, the appearance of another small area of disease in the left retrotrigonal region, and an increase in nodular enhancement at the surgery site. MR spectroscopy performed at the surgical margins (**d**) and at the genu of the corpus callosum (**e**) shows strong signs of tumor proliferation (high Cho/Cr and Cho/NAA ratios), and intense replacement/infiltration of the parenchyma from high-grade recurrence/progression (low ratio of NAA/Cr) primitive brain tumor

Follow-Up Performed at 9 Months After Surgery and Further Cycles of Adjuvant Chemotherapy

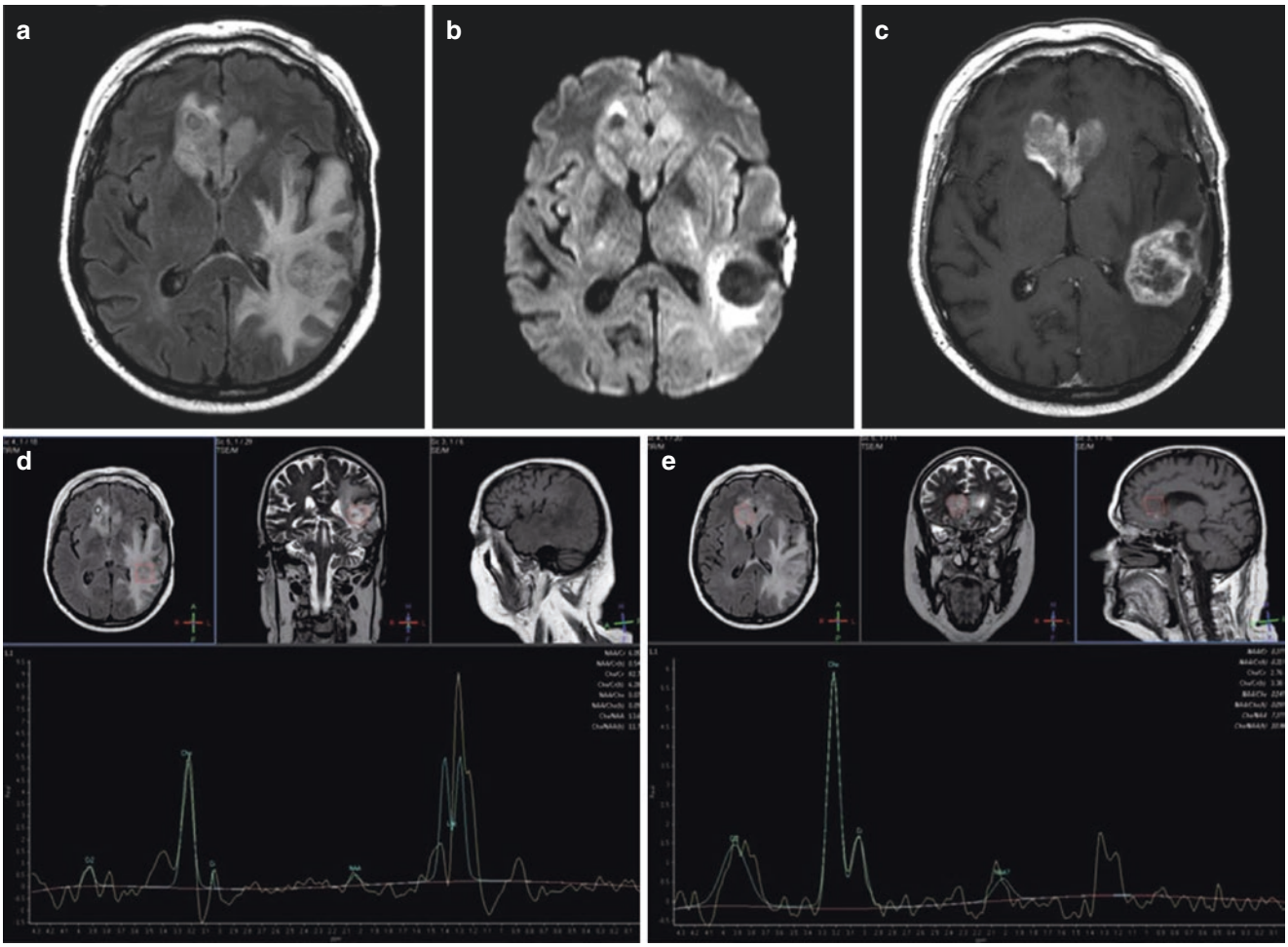

Fig. 35.6 MR FLAIR sequence (**a**), diffusion-weighted imaging (**b**), and contrast-enhanced SE T1-weighted sequence (**c**) show further increased size of the expansive/infiltrative lesions located in left temporal-parietal region and at the genu of the corpus callosum, the latter having extended to the right hemisphere. MR spectroscopy at the surgical margins (**d**) and at the corpus callosum (**e**) shows a further decrease in the NAA/Cr peak and increase in lipid peak indicative of tumor necrosis

Glioblastoma Multiforme: Lesion Related to Treatment at 2 Years from Surgery and Tumor Recurrence at 3 Years Retreated with Surgery

Case 36

Francesco Fabbiano, Jacopo Scaggiante, Andrea Wlderk, Giuseppe Cannavale, Michela Celestre, Claudio Colonnese, and Marcello Bartolo

- 19-year-old man, a professional athlete.
- Episode of tonic-clonic seizure while doing sport activity.
- Glioblastoma multiforme.

F. Fabbiano (✉)
Department of Neuroradiology, I.R.C.C.S. INM Neuromed, Pozzilli, Isernia, Italy

Department of Diagnostic Imaging, Valmontone Hospital, Rome, Italy

Department of Radiology and Neuroradiology, Villa Benedetta, Rome, Italy

J. Scaggiante
Department of Diagnostic and Interventional Radiology, University of Rome Tor Vergata, Rome, Italy

A. Wlderk
Department of Radiology and Neuroradiology, Villa Benedetta, Rome, Italy

Department of Diagnostic and Interventional Radiology, University of Rome Tor Vergata, Rome, Italy

G. Cannavale
Department of Radiological, Oncological and Anatomo-Pathological Sciences, University La Sapienza, Rome, Italy

M. Celestre
Department of Diagnostic Imaging, Valmontone Hospital, Rome, Italy

C. Colonnese
Department of Diagnostic and Therapeutic Neuroradiology, I.R.C.C.S. INM Neuromed, Pozzilli, Isernia, Italy

Department of Human Neurological Sciences, University La Sapienza, Rome, Italy

M. Bartolo
Department of Diagnostic and Therapeutic Neuroradiology, I.R.C.C.S. INM Neuromed, Pozzilli, Isernia, Italy

T. Scarabino, S. Pollice (eds.), *Imaging Gliomas After Treatment*, https://doi.org/10.1007/978-3-030-31210-7_46

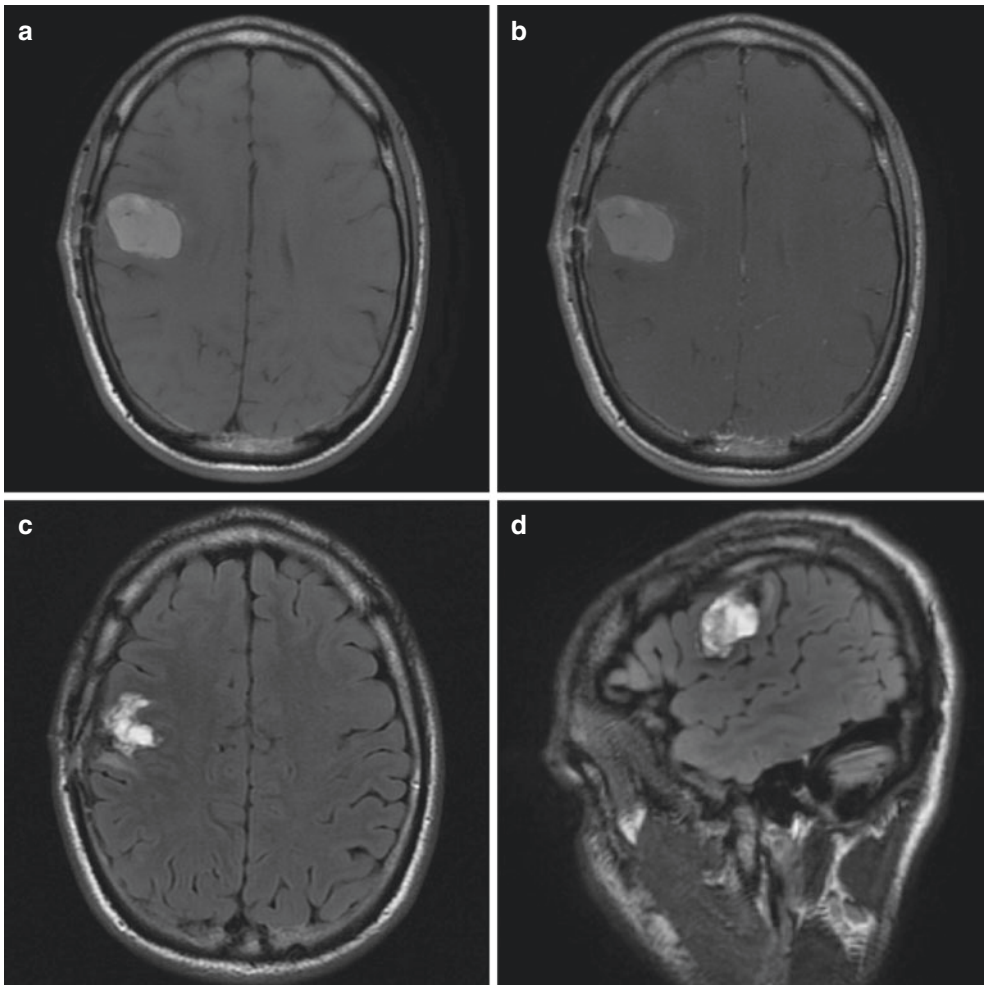

Fig. 36.1 (**a–d**) First postoperative MRI. (**a**) The surgical cavity is homogeneously hyperintense due to surgical apposition material, without any significant blood reported with CT scans during postoperative follow-up. (**b**) Contrast-enhanced T1-weighted MRI shows no parenchymal contrast enhancement close to the surgical cavity. There is only a thin and uniform dural thickening close to the surgical access, likely reactive. (**c**, **d**) Imaging reports a weak hyperintensity on T2 FLAIR MRI, without junctional blurring, likely due to reactive gliosis

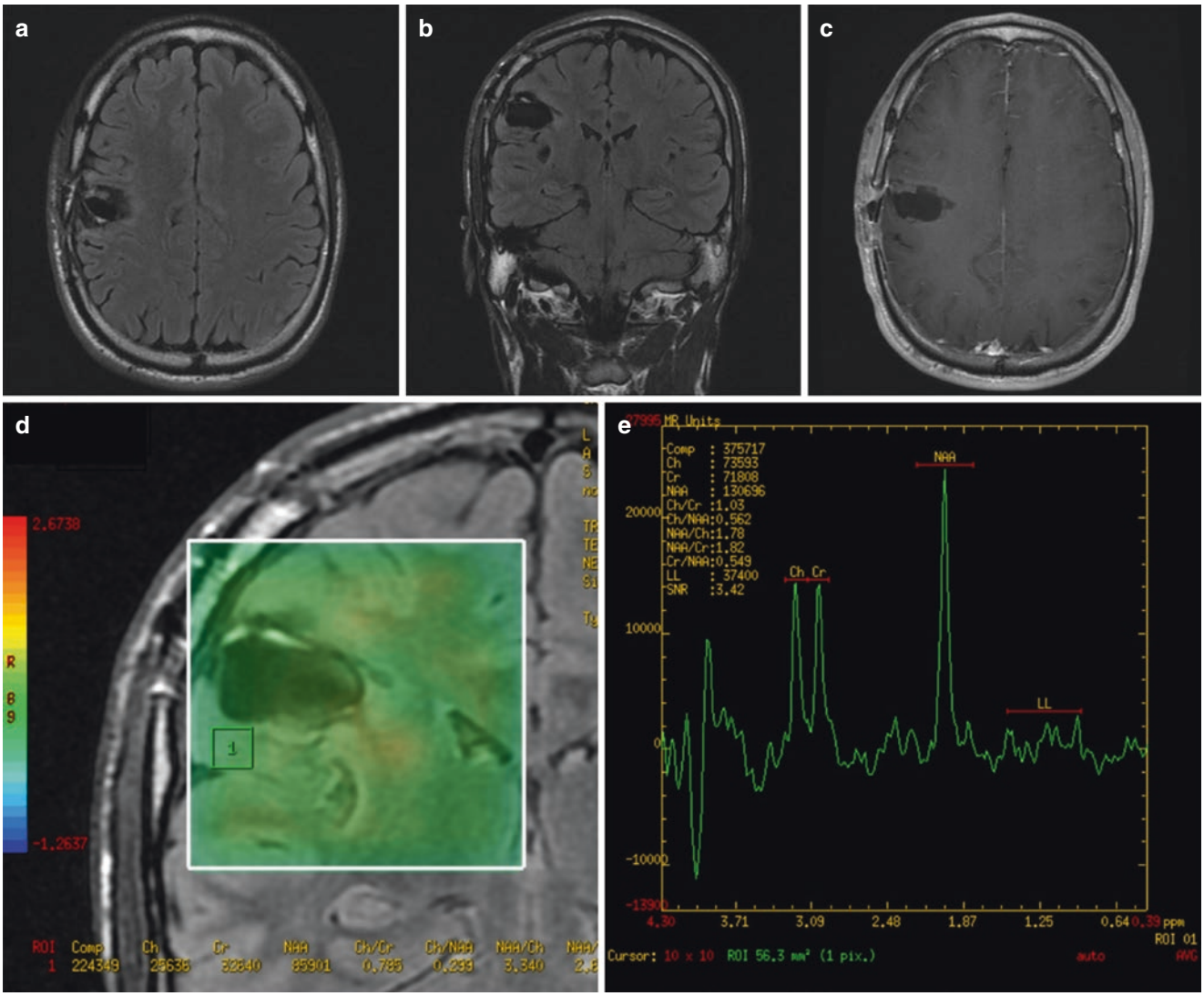

Fig. 36.2 (**a–e**) 3-month follow-up while doing radiotherapy. (**a–c**) The surgical cavity is reduced in size and presents a signal intensity similar to cerebrospinal fluid. There is a weak increase in the T2 FLAIR hyperintensity on the antero-medial aspect of the surgical cavity. (**d**, **e**) There are no increased values of CBV in perfusion MRI with normal ratio of choline to creatine (Ch/Cr) and choline to N-acetylaspartate (Cho/NAA) on multivoxel long TE MR spectroscopy

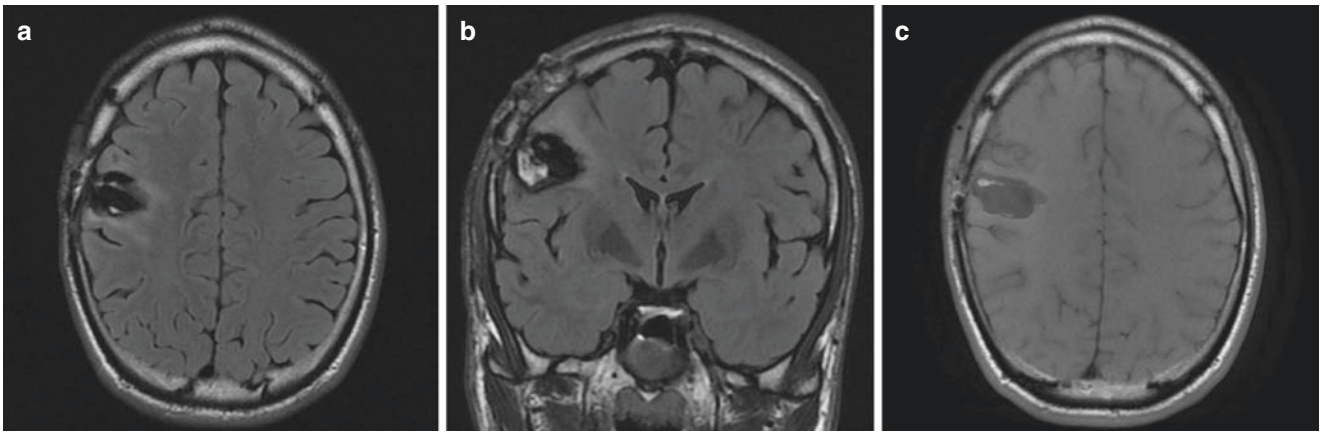

Fig. 36.3 (**a–c**) 6-month follow-up. (**a**, **b**) A further decrease in size and increase in T2 FLAIR hyperintensity on the antero-medial aspect of the surgical cavity. (**c**) Imaging confirms the absence of contrast enhancement of the parenchyma adjacent to the surgical cavity and the dural thickening at the surgical access, of likely reactive significance

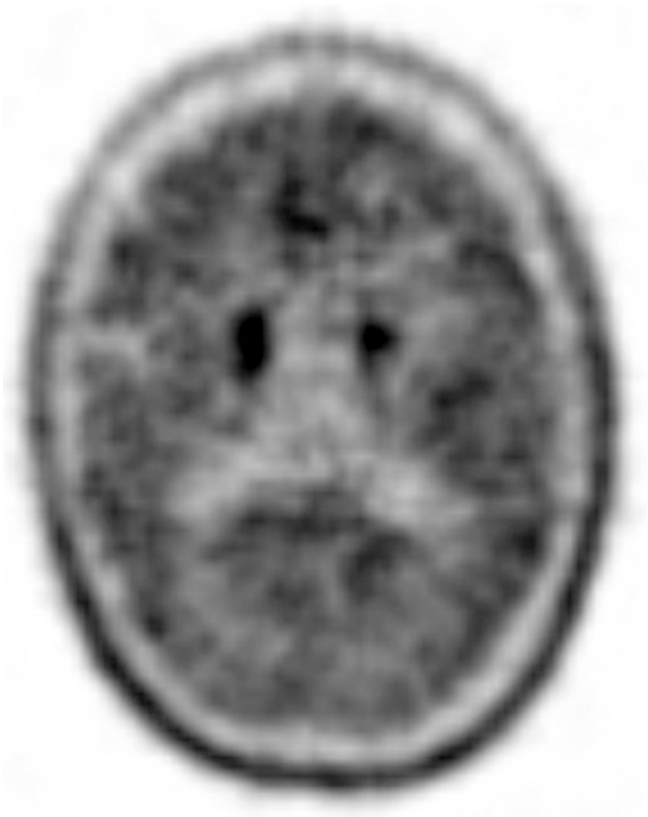

Fig. 36.4 F-DOPA pet scan. Absence of significant areas of pathological hyperaccumulation of the ^{18}F-DOPA

Interval: For 2 years there are no morphological changes with perfusion and spectroscopic stability at 3-month-period follow-up.

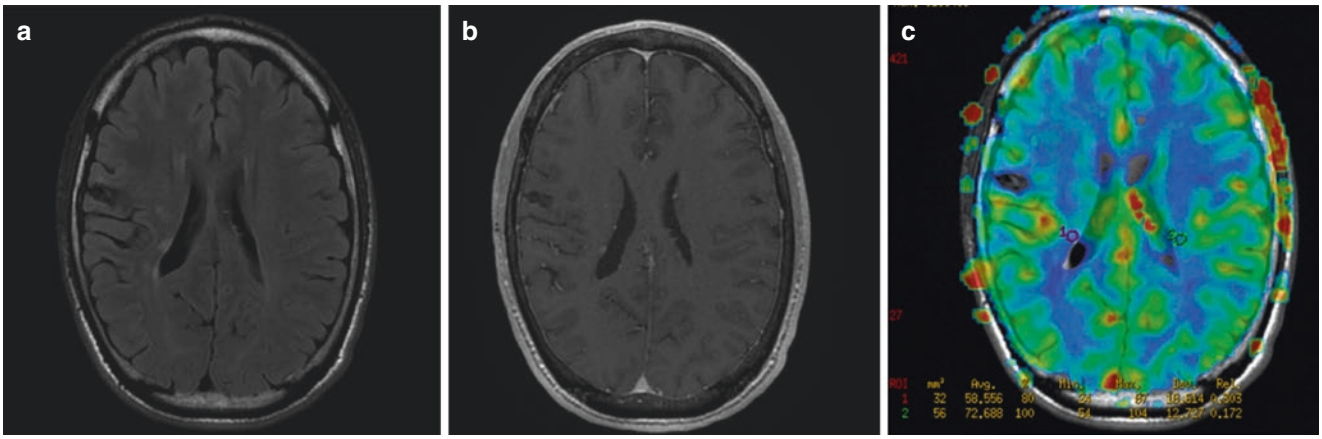

Fig. 36.5 (**a–c**) MRI at 2 years from surgery. Imaging shows a right, circumscribed, periventricular subependymal area of high T2-weighted signal intensity (maximal axial diameter: 7.5 mm) with homogeneous enhancement. Perfusion-weighted imaging (PWI) reports a normal Cerebral Blood Volume ratio (rCBV) as compared with the contralateral side

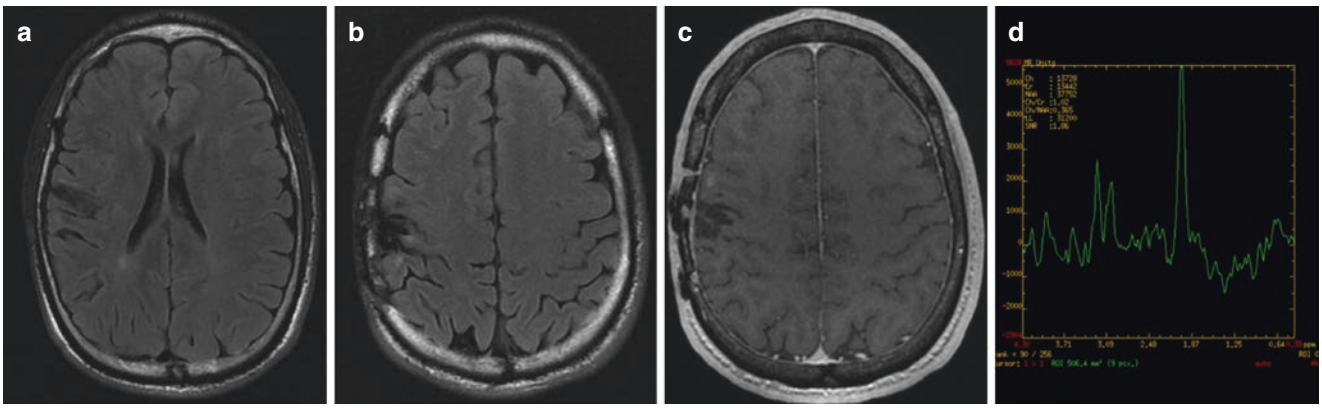

Fig. 36.6 (**a–d**) 27-month follow-up. (**a**, **b**) Imaging reports the disappearance of the T2-FLAIR hyperintensity of the right periventricular subependimal area, and there is no more pathological parenchymal enhancement (**c**). Therefore, the area was a lesion related with the treatment. (**c**, **d**) There is a little circumscribed-enhancing area, with increased signal intensity on T2-weighted FLAIR imaging, without pathologic CBV values elevation as compared with the contralateral side and normal ratio of choline to creatine (Ch/Cr) and choline to N-acetylaspartate (Cho/NAA) on multivoxel long TE MR spectroscopy (**d**)

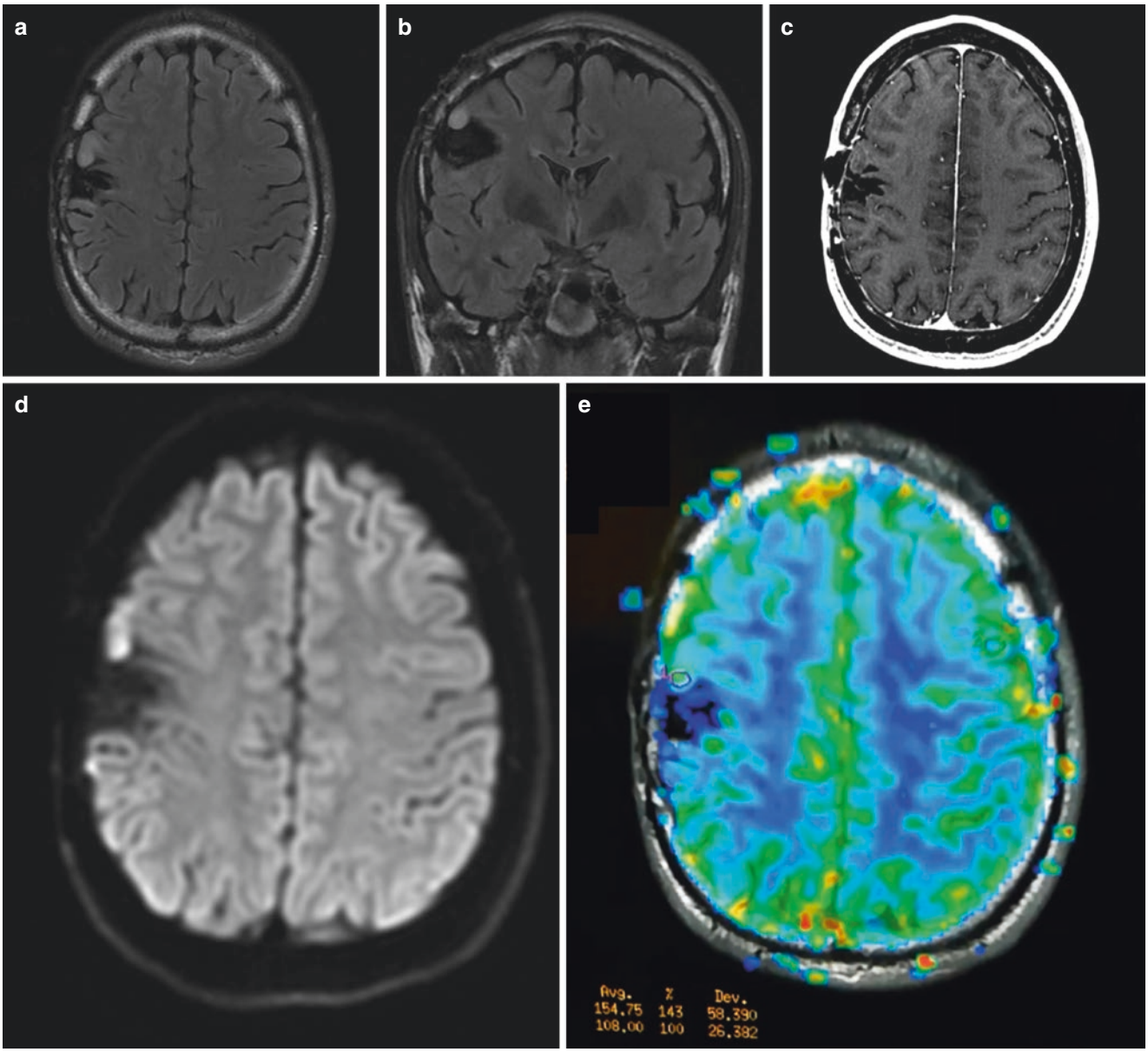

Fig. 36.7 (**a–e**) MRI at 3 years from surgery. (**a**, **b**) Imaging shows a cortical-subcortical increased T2-weighted signal intensity with junctional blurring on the superior aspect of the surgical cavity. (**c**) There is a weak contrast enhancement. (**d**) The area is hyperintense on diffusion-weighted imaging (DWI) with a moderate reduction in ADC values. Moreover, there is a moderate increase in the Cerebral Blood Volume ratio (rCBV) as compared with the contralateral side. (**e**) Multivoxel long TE MR spectroscopy reports increased ratio of choline to creatine (Ch/Cr) and choline to N-acetylaspartate (Cho/NAA). The neuroimaging is related with tumor recurrence

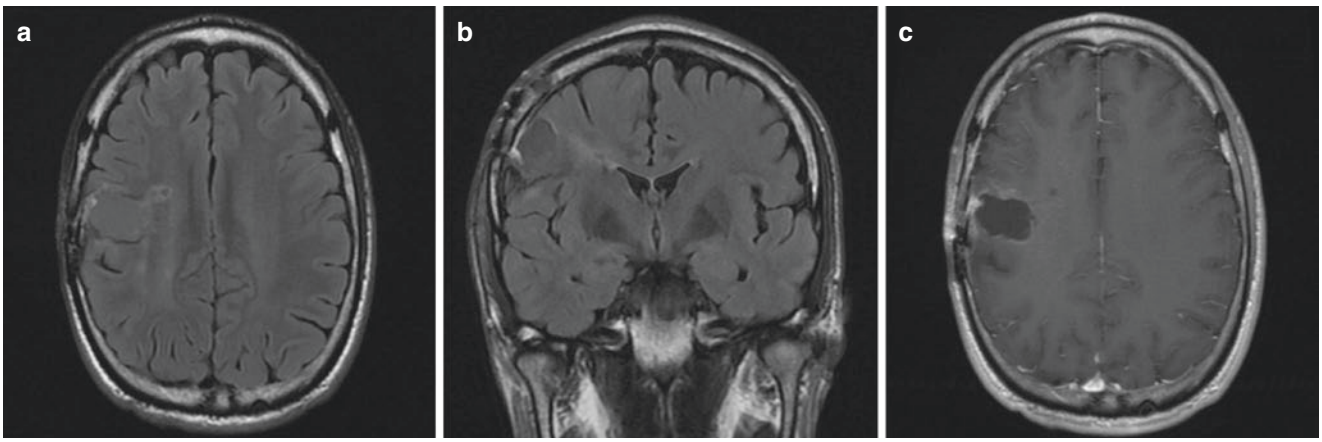

Fig. 36.8 (**a–c**) Follow-up after surgery for tumor recurrence. (**a**, **b**) Complete surgical resection of tumor recurrence; the previous T2-FLAIR hyperintensity of the right periventricular subependimal area is still not evident. (**c**) Imaging reports a weak enhancement close to the surgical margins due to blood–brain barrier damage and further dural enhancement, likely reactive

Radionecrosis: MR Follow-Up in Metastasis from Breast Cancer

Case 37

Mario Muto and Fabio Zeccolini

- 14-year-old patient with a history of meningeal spread of leukemia treated with whole brain radiation therapy.
- Follow-up MR morphologic study without and with contrast medium administration performed after whole brain radiation therapy.

Follow-Up at 15 Months

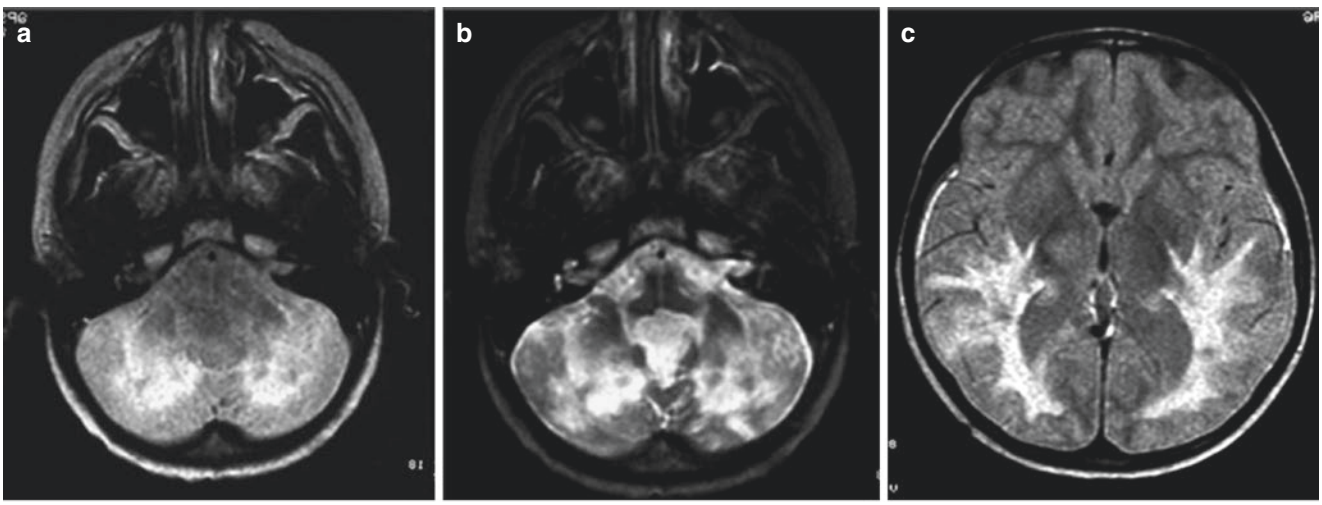

Fig. 37.1 MR performed with SE-DP (**a**, **c**, **e**), FSE (**b**, **d**, **f**), and contrast-enhanced SE T1-weighted (**g**, **h**, **i**) sequences. The images depict widespread signal alteration (hyperintensity in T2) in the white matter (acute leukoencephalopathy) with enhancement after contrast medium administration in the periventricular white matter (radionecrosis)

M. Muto (✉) · F. Zeccolini
Department of Neuroradiology, "Cardarelli" Hospital,
Naples, Italy

T. Scarabino, S. Pollice (eds.), *Imaging Gliomas After Treatment*, https://doi.org/10.1007/978-3-030-31210-7_47

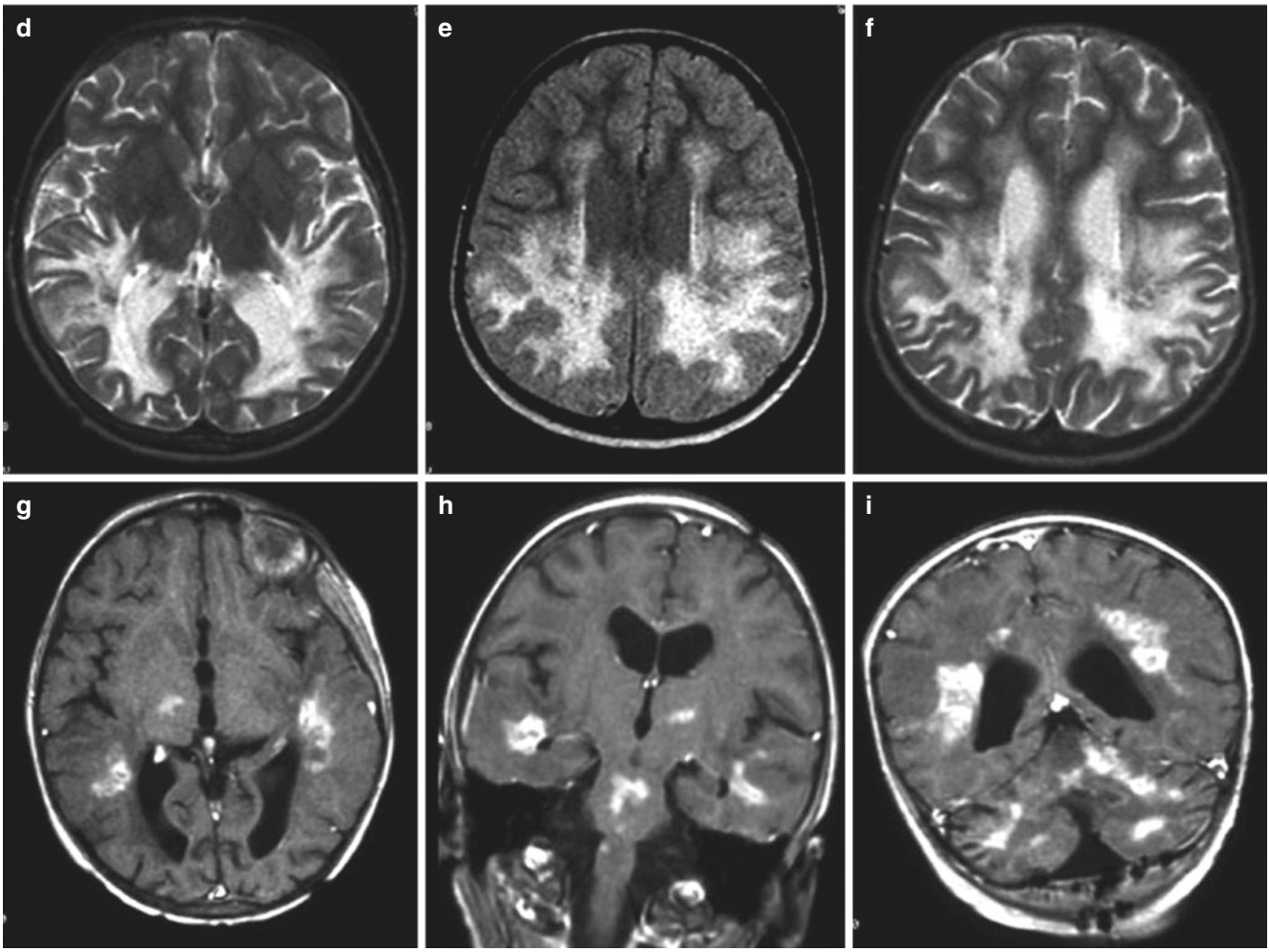

Fig. 37.1 (continued)

Radionecrosis: Morphofunctional MR Follow-Up in Metastasis from Breast Cancer

Case 38

Teresa Popolizio, Nicola Sforza, and Roberto Izzo

- 48-year-old patient with breast lesion secondary to previous breast cancer.
- Morphofunctional MR follow-up performed with morphologic imaging, diffusion, and spectroscopy at 1 year from stereotactic therapy of metastasis from breast cancer.

Follow-Up 1 at Year From Surgery of Breast Cancer in Symptomatic Patient

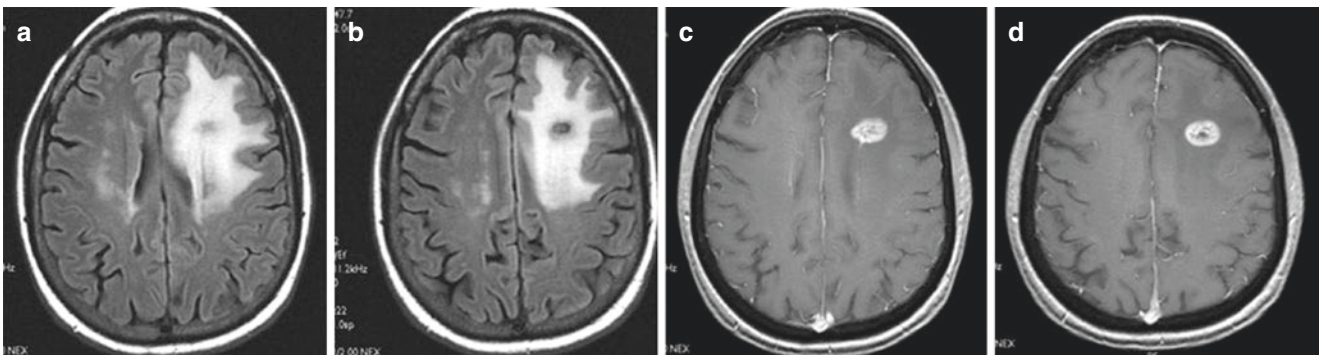

Fig. 38.1 MR FLAIR (**a**, **b**) and contrast-enhanced SE T1-weighted (**c**, **d**) sequences show a nodular lesion surrounded by edema in the left frontal region with iso-hypointensity in FLAIR and thick enhancing ring in the contrast-enhanced images

T. Popolizio (✉) · N. Sforza · R. Izzo
Department of Neuroradiology, Fondazione IRCCS "Casa Sollievo della Sofferenza", San Giovanni Rotondo, FG, Italy

T. Scarabino, S. Pollice (eds.), *Imaging Gliomas After Treatment*, https://doi.org/10.1007/978-3-030-31210-7_48

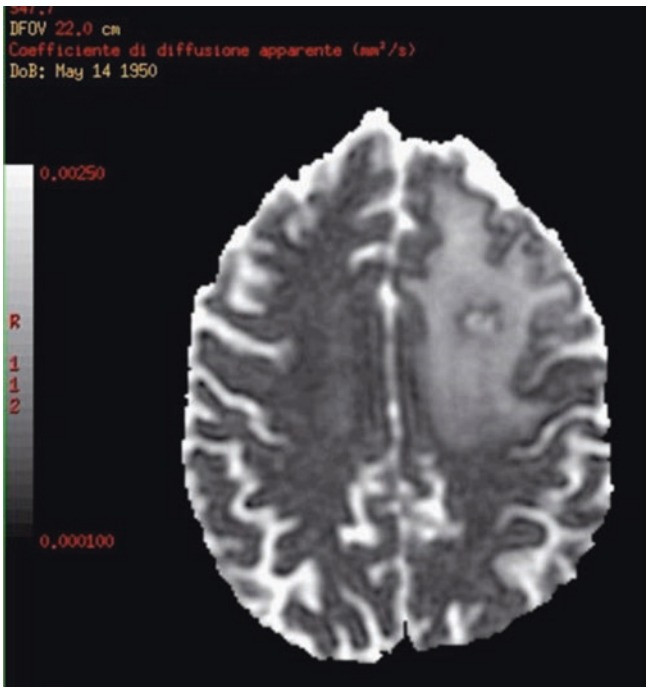

Fig. 38.2 MR diffusion-weighted image with ADC map shows high restriction of diffusion within the lesion

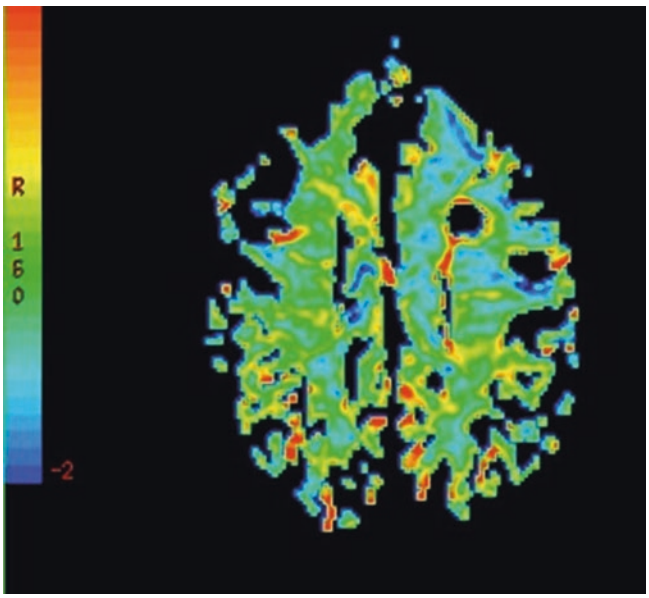

Fig. 38.3 MR perfusion study with CBV map shows the lesion devoid of perfusion

Radionecrosis: MR Follow-Up in Astrocytoma

Case 39

Alessandro Stecco, Alessio Paschè, Laura Masini, Marco Krengli, and Alessandro Carriero

- 47-year-old patient treated with surgery for a grade III astrocytoma of the left temporal lobe.
- Morphofunctional MR follow-up performed with morphologic imaging, diffusion-weighted imaging, and spectroscopy 12 months after surgery and radiation therapy.

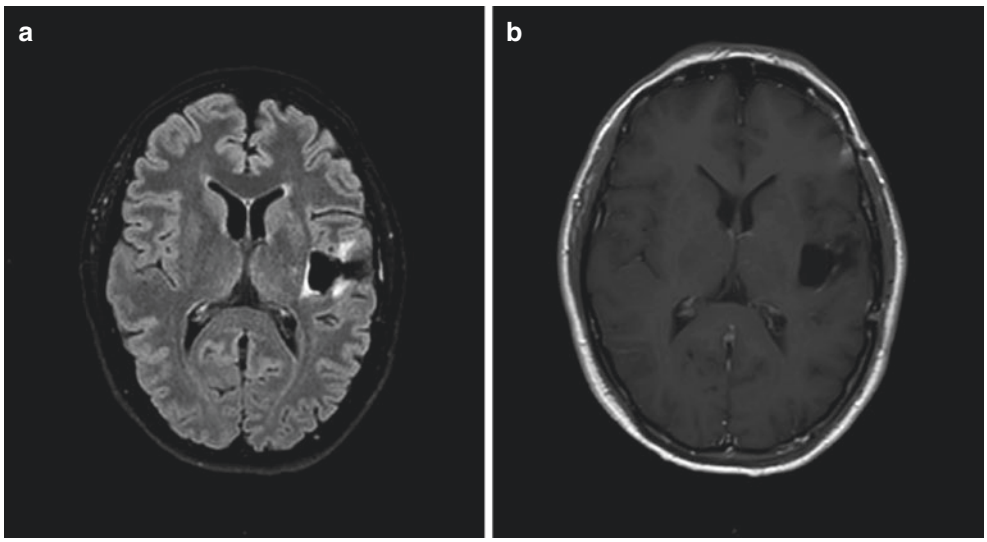

Fig. 39.1 (**a**, **b**) Follow-up at 12 months after surgery and radiation therapy. *MR FLAIR-weighted and contrast-enhanced SE T1-weighted sequences.* A left temporal lobe lesion with moderate edema and very low enhancement due to the presence of a necrotic component can be seen

A. Stecco (✉)
Neuroradiology Unit, AOU "Maggiore della Carità", DIMET, Università del Piemonte Orientale, Novara, Italy
e-mail: alessandro.stecco@uniupo.it

A. Paschè · A. Carriero
Department of Radiology, AOU "Maggiore della Carità", DIMET, Università del Piemonte Orientale, Novara, Italy

L. Masini · M. Krengli
Department of Radiation Oncology, AOU "Maggiore della Carità", DIMET, Università del Piemonte Orientale, Novara, Italy

T. Scarabino, S. Pollice (eds.), *Imaging Gliomas After Treatment*, https://doi.org/10.1007/978-3-030-31210-7_49

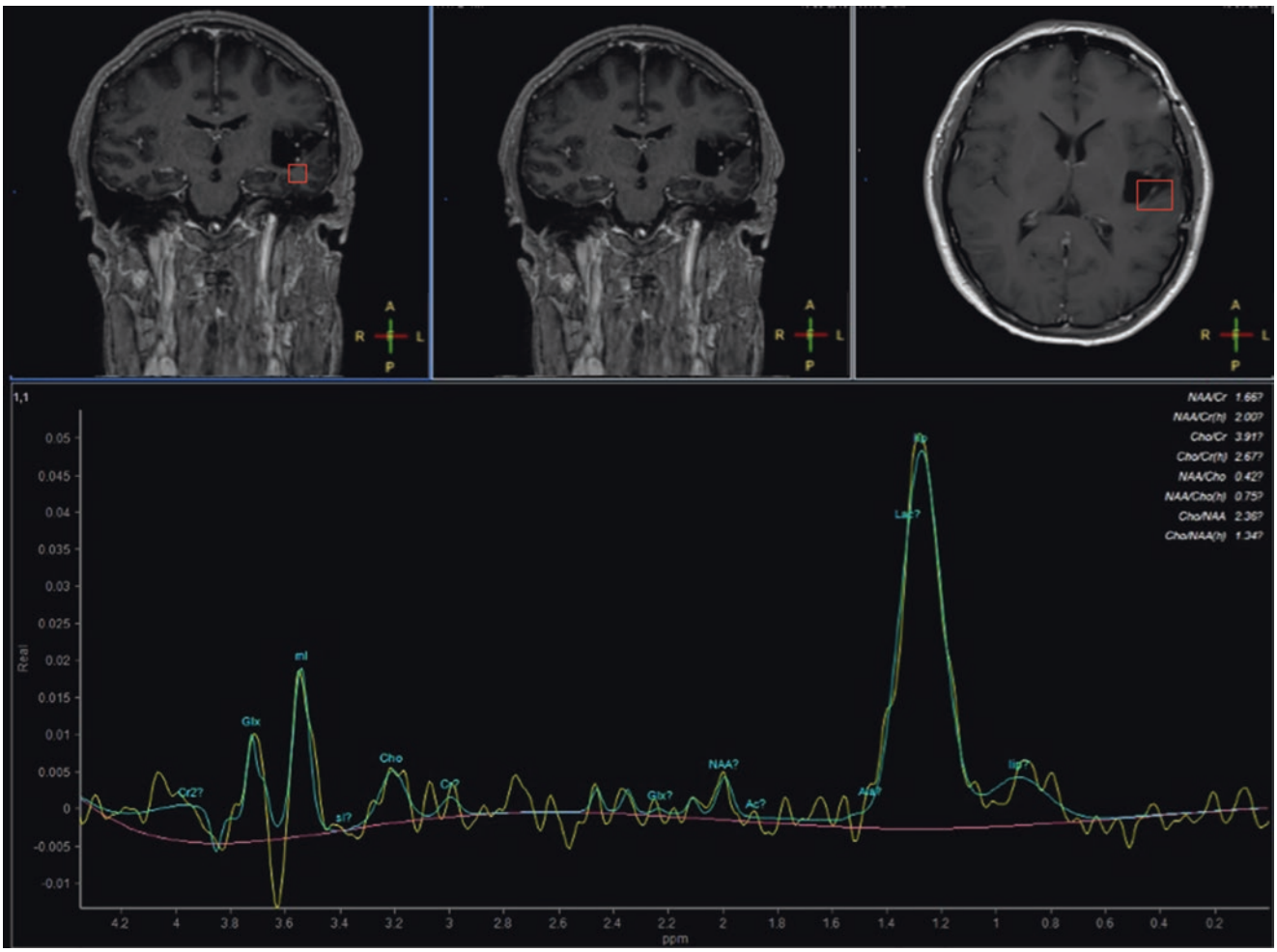

Fig. 39.2 *MR single-voxel spectroscopy.* In this sequence, the ROI placed in the lesion shows a high Lac/Lip peak indicating necrosis and a low component of NAA and Cho

Radionecrosis: Morphofunctional MR Follow-Up in Glioblastoma

Case 40

Teresa Popolizio, Nicola Sforza, and Daniela Grasso

- 53-year-old patient with glioblastoma.
- Morphofunctional MR follow-up performed with morphologic imaging, diffusion-weighted imaging, and spectroscopy 9 months after surgery and radiation therapy in a patient with glioblastoma.

Follow-Up at 9 Months After Surgery and Radiation Therapy

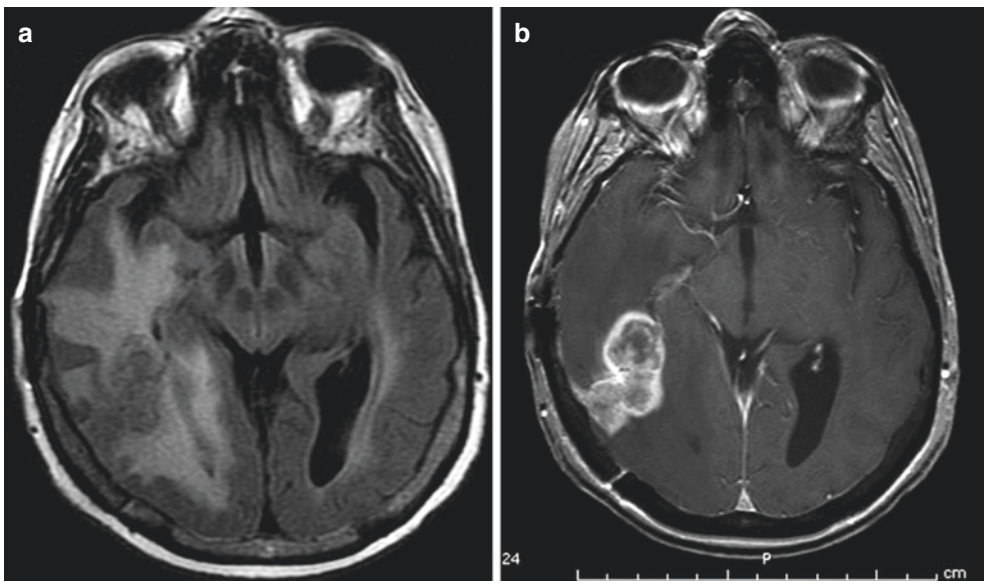

Fig. 40.1 MR FSE T2-weighted (**a**) and contrast-enhanced SE T1-weighted (**b**) sequences. A right temporal-occipital lesion with moderate edema and patchy enhancement due to the presence of a necrotic component can be seen. There is also a significant mass effect on the adjacent midline structures, particularly with obliteration of the ventricular junction

T. Popolizio (✉) · N. Sforza · D. Grasso
Department of Neuroradiology, Fondazione IRCCS "Casa Sollievo della Sofferenza", San Giovanni Rotondo, FG, Italy

T. Scarabino, S. Pollice (eds.), *Imaging Gliomas After Treatment*, https://doi.org/10.1007/978-3-030-31210-7_50

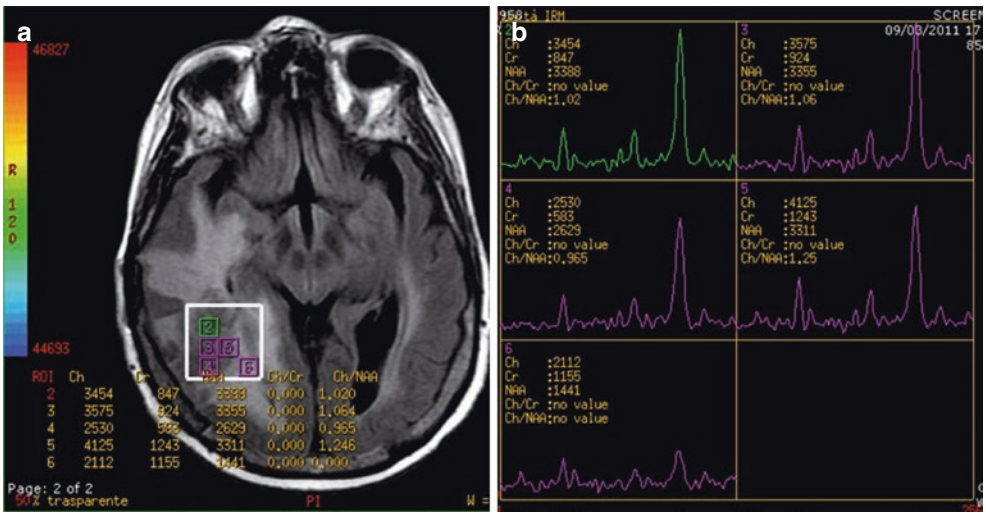

Fig. 40.2 (**a**, **b**) MR single-voxel spectroscopy with ROI placed in the lesion shows a high Lac/Lip peak indicating necrosis and a low component of NAA and Cho

Late Radionecrosis: CT/MR Performed in Nasopharyngeal Carcinoma

Case 41

Tommaso Scarabino, Saverio Pollice, Gilda Morlino, Michela Capuano, Angela Lorusso, and Alberto Maggialetti

- 60-year-old patient with previous radiation therapy in undifferentiated nasopharyngeal carcinoma.
- CT/MR follow-up performed at 3 and 4 years after radiation therapy.

Follow-Up Performed at 3 Years After Radiation Treatment

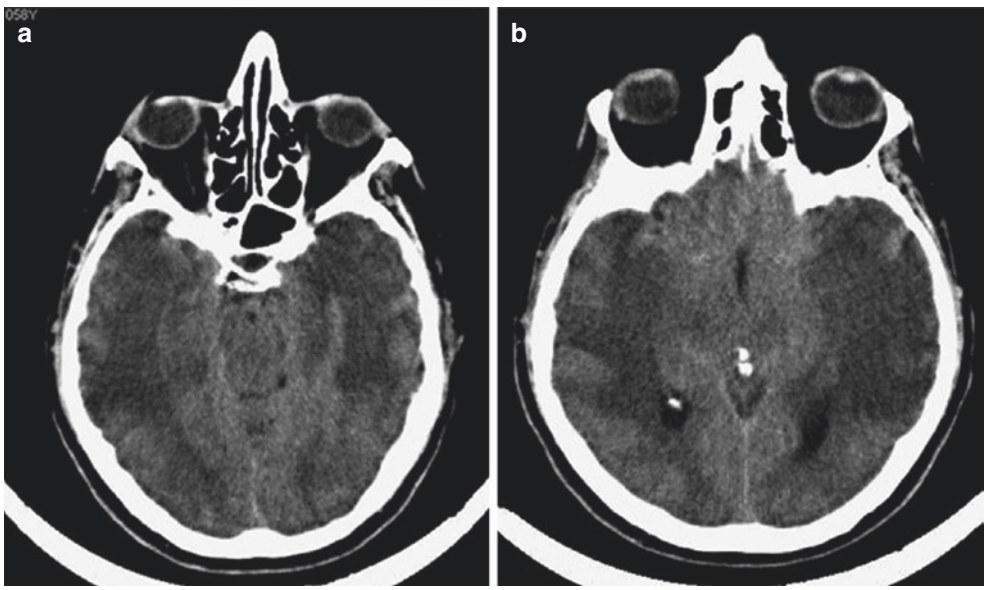

Fig. 41.1 (**a**, **b**) Emergent morphologic CT scan shows an ill-defined cortical-subcortical hypodensity in the bilateral temporal area extending cranially and involving the frontal and parietal lobes

T. Scarabino (✉) · S. Pollice · M. Capuano A. Lorusso
Department of Radiology, "L. Bonomo" Hospital, Andria, BT, Italy

G. Morlino
Department of Radiology, "Di Venere" Hospital, Bari, BA, Italy

A. Maggialetti
Ricerche Radiologiche Center, Molfetta, BA, Italy

T. Scarabino, S. Pollice (eds.), *Imaging Gliomas After Treatment*, https://doi.org/10.1007/978-3-030-31210-7_51

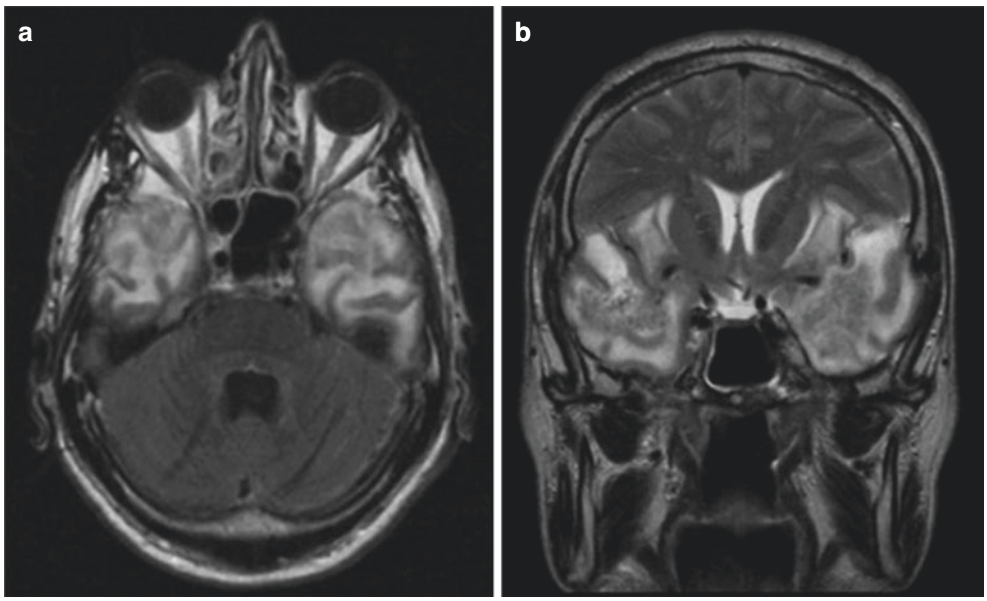

Fig. 41.2 Axial (**a**) and sagittal (**b**) MR FLAIR sequences show bilateral temporal-polar cortical-subcortical heterogeneous hyper-intensity extending cranially into the parietal lobe. Coexisting atrophy of the nasopharyngeal mucosa can also be appreciated

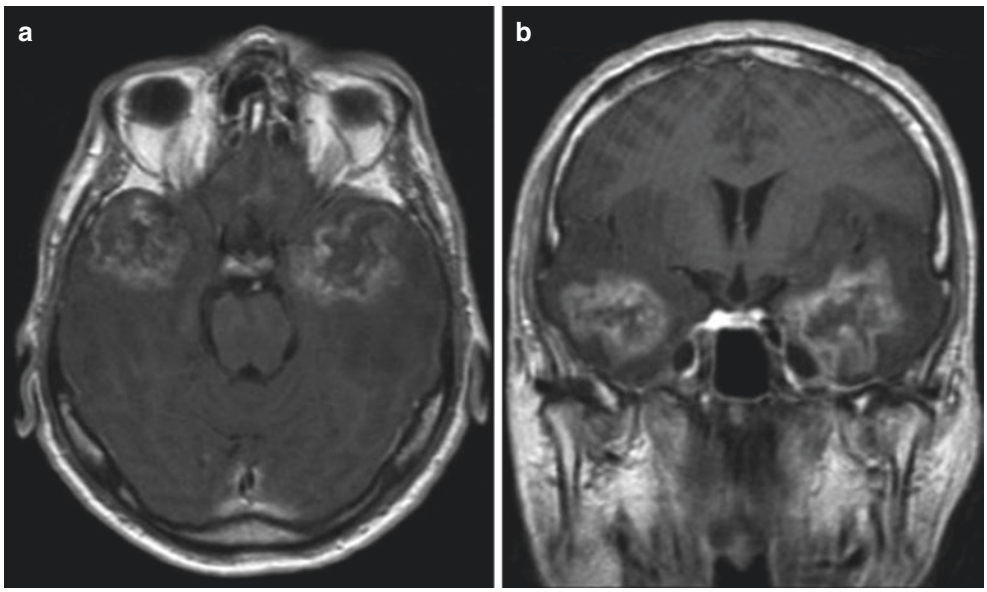

Fig. 41.3 Contrast-enhanced axial (**a**) and coronal (**b**) MR SE T1 sequences show thick and irregular enhancement of the margins of the lesion described above with central hypointensity attributable to necrosis, surrounded by a wide area of hypointensity indicating perilesional edema

Follow-Up Performed at 4 Years

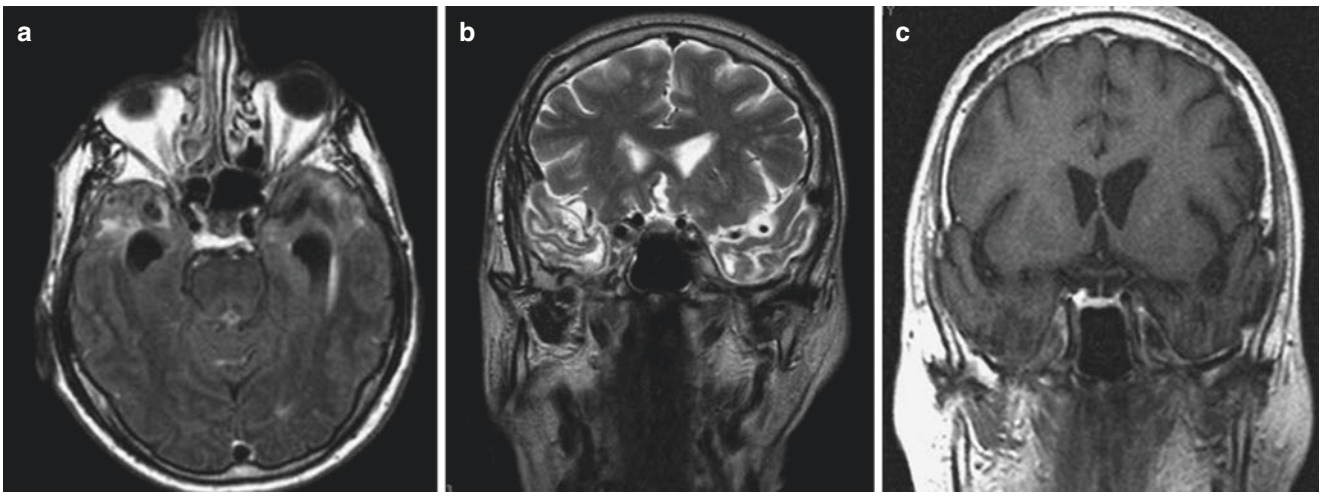

Fig. 41.4 MR FLAIR (**a**), FSE T2-weighted (**b**), and contrast-enhanced SE T1-weighted (**c**) sequences show moderate and irregular residual alteration of the cortical-subcortical signal in the temporal-polar region bilaterally, slight edema, and no significant pathologic enhancement. Mild traction dilatation of the adjacent ventricular temporal horns can also be appreciated

Late Radionecrosis: CT/MR Follow-Up in Nasopharyngeal Carcinoma

Case 42

Teresa Popolizio, Nicola Sforza,
and Rosario Francesco Balzano

- 54-year-old patient with previous radiation therapy in nasopharyngeal carcinoma.
- MR and CT follow-up performed with morphologic imaging, diffusion, and spectroscopy 2 years after radiation treatment in nasopharyngeal carcinoma.

Follow-Up at 2 Years After Radiation Therapy

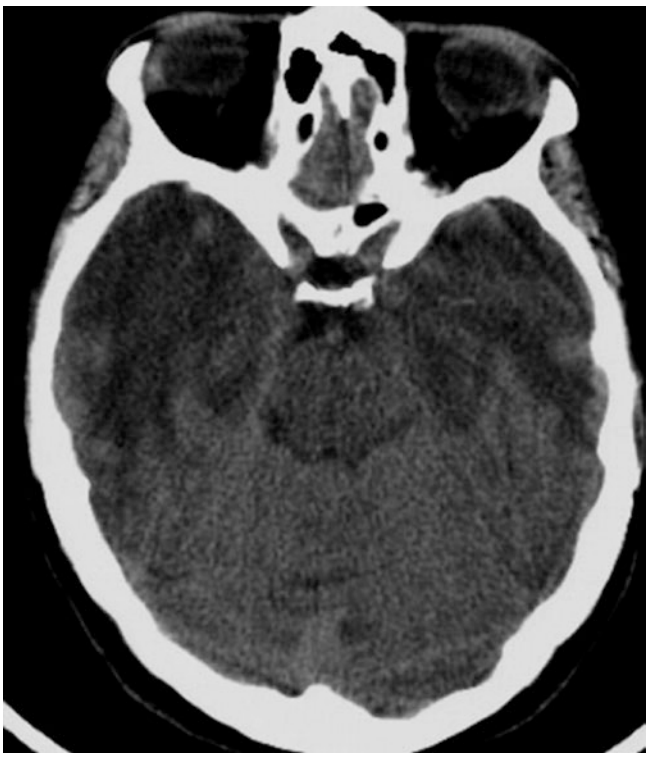

Fig. 42.1 CT scan in emergency shows a slight cortical-subcortical hypodensity in the temporal region bilaterally

T. Popolizio (✉) · N. Sforza
Department of Neuroradiology, Fondazione IRCCS "Casa Sollievo della Sofferenza", San Giovanni Rotondo, FG, Italy

R. F. Balzano
Department of Radiology, Universityof Foggia, Foggia, FG, Italy

T. Scarabino, S. Pollice (eds.), *Imaging Gliomas After Treatment*, https://doi.org/10.1007/978-3-030-31210-7_52

Preoperative Imaging

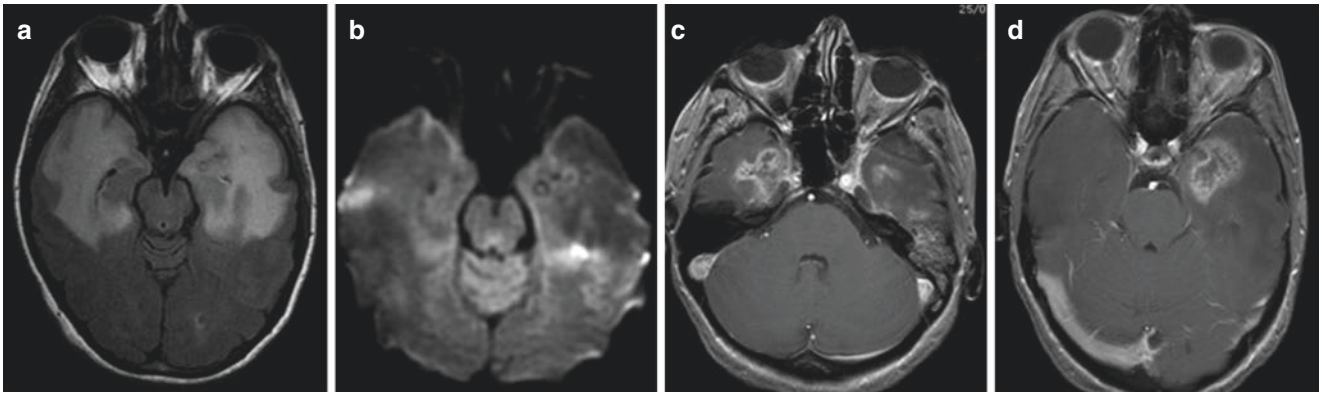

Fig. 42.2 MR FLAIR (**a**), diffusion-weighted (**b**), and contrast-enhanced SE T1-weighted (**c**, **d**) sequences. Patchy hyperintensity can be seen in the cortical-subcortical temporal-polar region bilaterally (**a**, **b**). After administration of contrast medium, thick and irregular enhancement of the margins of the lesions is visualized with central hypointensity attributable to necrosis, surrounded by a large area of hypointensity indicating perilesional edema (**c**, **d**)

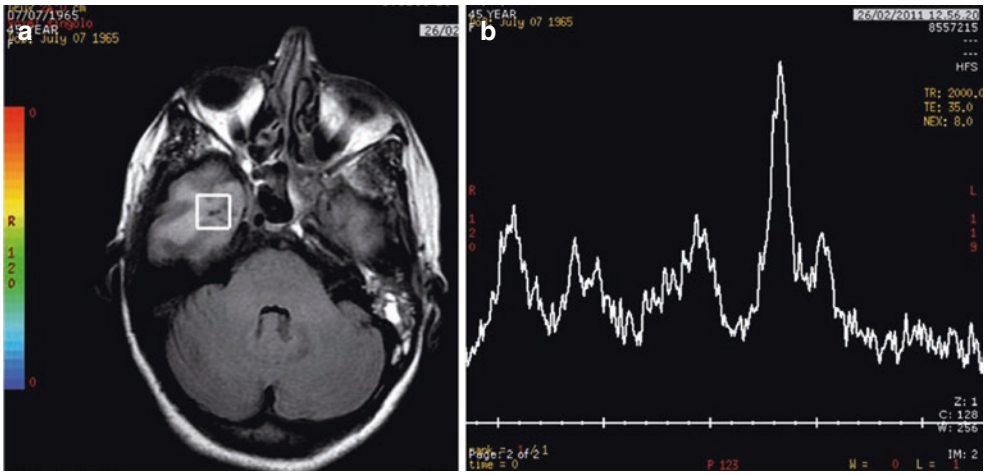

Fig. 42.3 (**a**, **b**) MR single-voxel spectroscopy with ROI placed on right temporal lesion shows a high peak of the Lac/Lip ratio indicating necrosis and a low component of NAA and Cho

Late Radionecrosis: Postoperative and Postradiation Therapy Follow-Up in Meningioma

Case 43

Ferdinando Caranci and Sossio Cirillo

- Patients with previous surgery of a right frontal meningioma subsequently irradiated.
- Postoperative and postradiation therapy follow-up performed late (3 and 4 years) with MR morphologic and perfusion sequences.

Postoperative and Postradiation Therapy Follow-Up at 3 Years

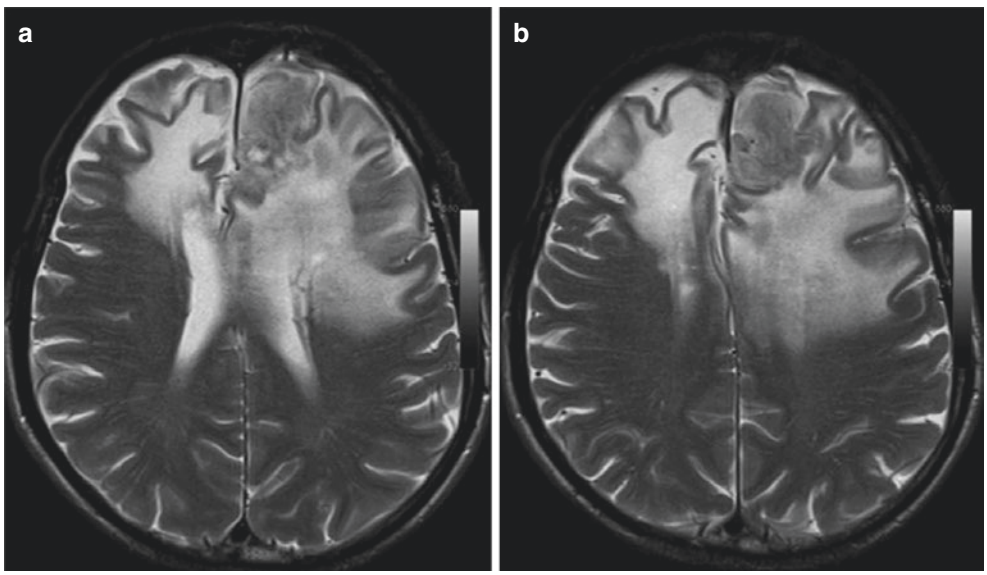

Fig. 43.1 (**a**, **b**) MR FSE T2-weighted sequence. An extended halo of high signal in the bilateral frontal region and extending more on the left indicates vasogenic edema. At that level in the parasagittal area some relatively hypointense tissue with irregular margins can be seen

F. Caranci (✉)
Department of Precision Medicine, School of Medicine, University of Campania "Luigi Vanvitelli", Naples, Italy

S. Cirillo
Department of Medicine and Health Sciences "V. Tiberio", University of Molise, Campobasso, Italy

T. Scarabino, S. Pollice (eds.), *Imaging Gliomas After Treatment*, https://doi.org/10.1007/978-3-030-31210-7_53

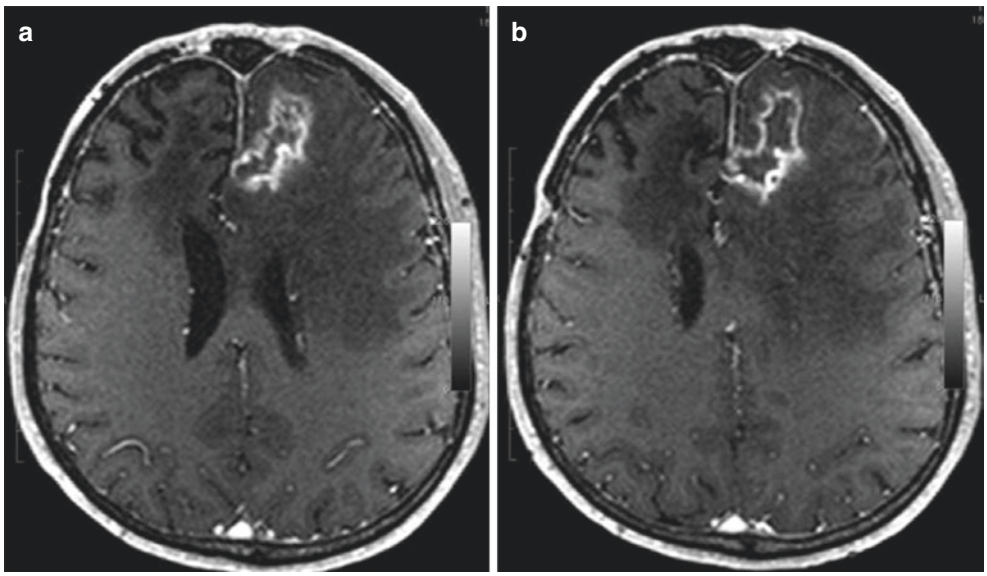

Fig. 43.2 (**a**, **b**) Contrast-enhanced MR SE T1-weighted images. The tissue in the left frontal area shows necrotic component and peripheral enhancement

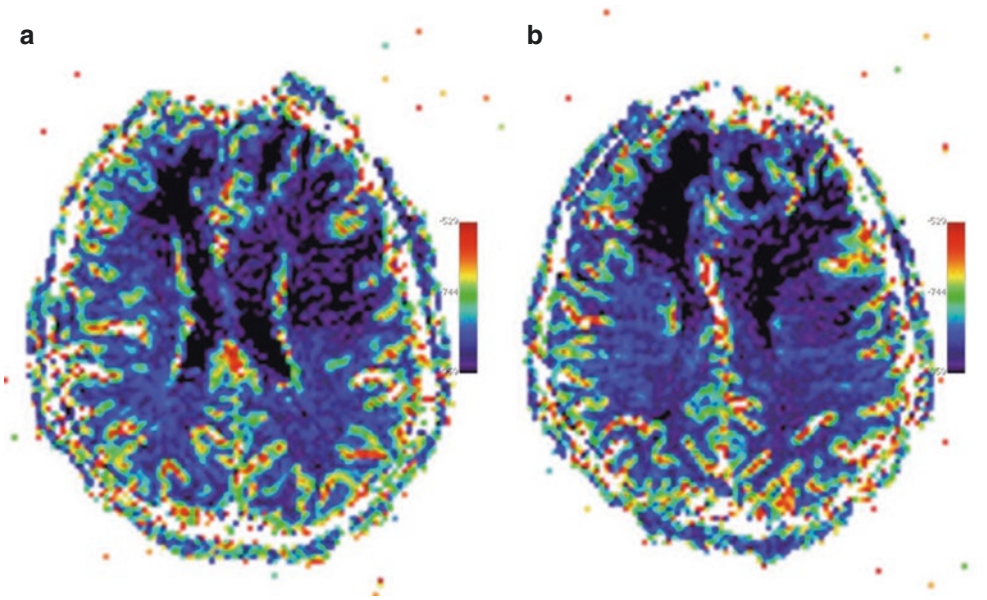

Fig. 43.3 (**a**, **b**) MR perfusion with CBV map. The lesion shows a clear reduction in cerebral blood volume values (CBV)

Postoperative and Postradiation Therapy Follow-Up at 4 Years

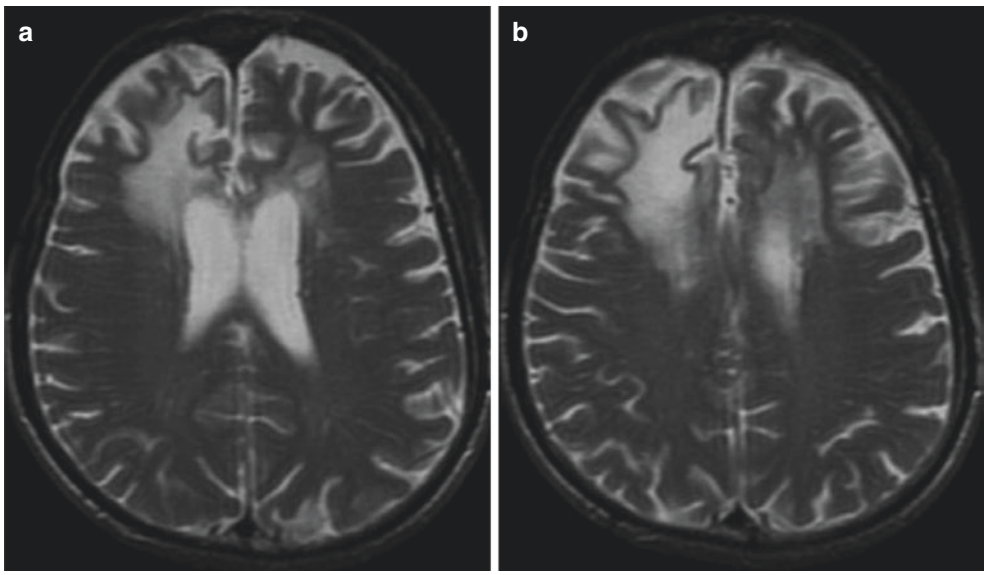

Fig. 43.4 (**a**, **b**) MR FSE T2-weighted sequence. Subtotal disappearance of the vasogenic edema can be appreciated, along with the remaining right-sided gliotic changes resulting from the previous surgery

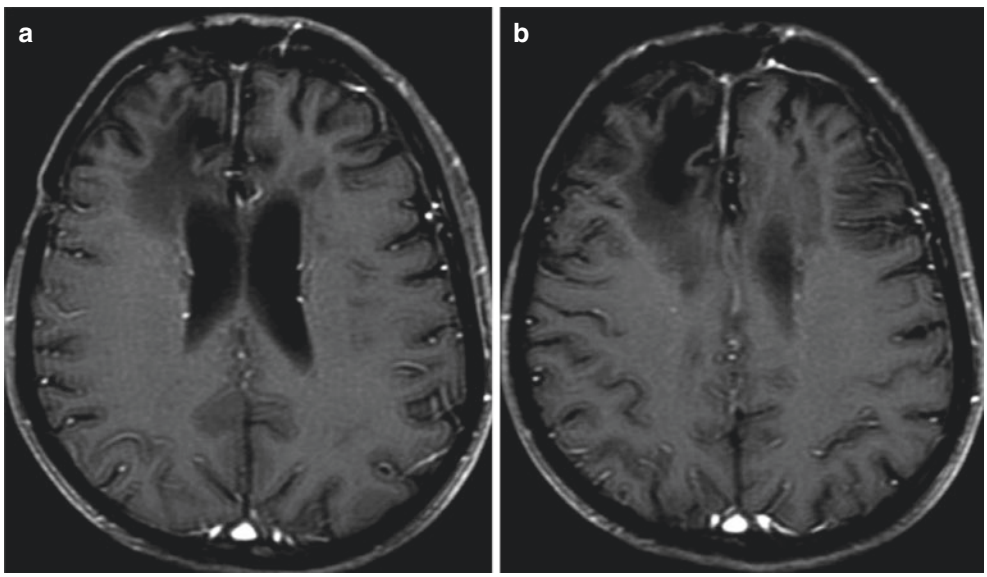

Fig. 43.5 (**a**, **b**) Contrast-enhanced MR SE T1-weighted images. The images show the disappearance of radiation necrosis changes described in the left frontal region

Radionecrosis: 3T Multimodal MR Follow-Up in Anaplastic Astrocytoma

Case 44

Tommaso Scarabino, Teresa Popolizio, Saverio Pollice, Vincenzo D'Angelo, and Alfonso Di Costanzo

- 46-year-old patient with left frontal-opercular anaplastic astrocytoma and subsequent anaplastic transformation treated with surgery and partial excision and combined radiation therapy–chemotherapy and subsequent adjuvant second-level chemotherapy.
- 3T multimodal MR follow-up performed with morphologic sequences, diffusion, and perfusion imaging and spectroscopy preoperatively and at 6 and 12 months after surgery and combined radiation therapy–chemotherapy.

Preoperative Imaging

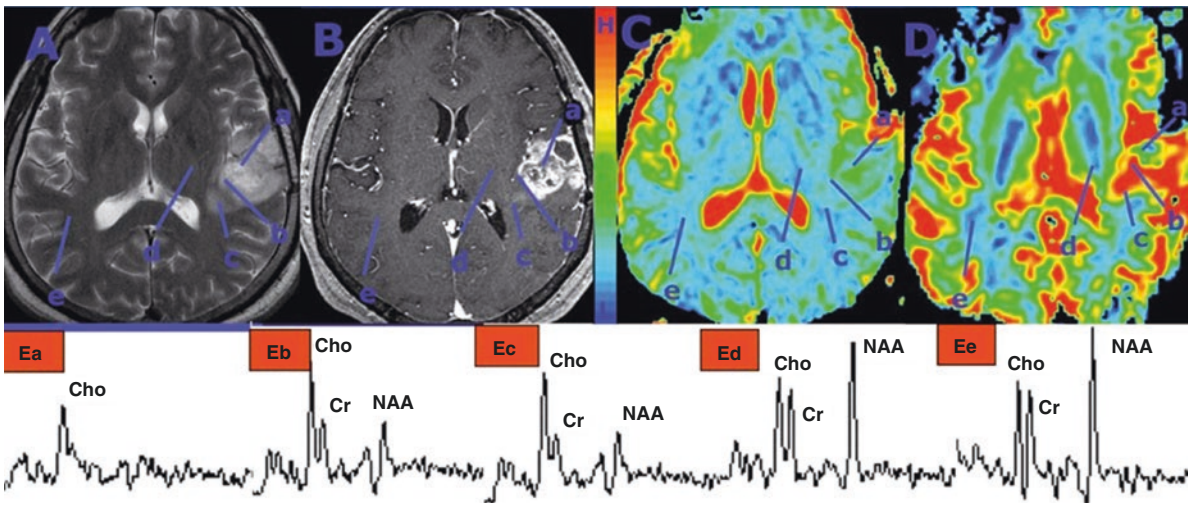

Fig. 44.1 MR FSE T2-weighted (**a**) and contrast-enhanced SE T1-weighted (**b**) sequences show an almost completely solid lesion with heterogeneous enhancement, moderate edema, and with a slight mass effect on midline structures. Multimodal MR with diffusion-weighted imaging and ADC map (**c**), perfusion study with CBV map (**d**), and single-voxel spectroscopy with multiple ROIs (**e**). The spectra placed over and immediately behind the almost completely solid enhancing lesion have the typical tumor pattern, with high Cho peak and inversion of the Cho/NAA ratio. In these ROIs, the ADC is decreased and the CBV is increased. The spectra in the apparently edematous area beyond the enhancing margins have overall reduced levels of all metabolites but with a pattern indicating tumor infiltrated edema. In these areas ADC is decreased and CBV is increased. Moving away from the lesion, the metabolic pattern along with the ADC and CBV values returns to normal as in the contralateral hemisphere

T. Scarabino (✉) · S. Pollice
Department of Radiology, "L. Bonomo" Hospital, Andria, BT, Italy

T. Popolizio · V. D'Angelo
Department of Neuroradiology, Scientific Institute "Casa Sollievo della Sofferenza", San Giovanni Rotondo, FG, Italy

A. Di Costanzo
Department of Neurology, University of Molise, Campobasso, Italy

T. Scarabino, S. Pollice (eds.), *Imaging Gliomas After Treatment*, https://doi.org/10.1007/978-3-030-31210-7_54

Follow-Up Performed at 6 Months After Surgery and Combined Radiation Therapy–Chemotherapy

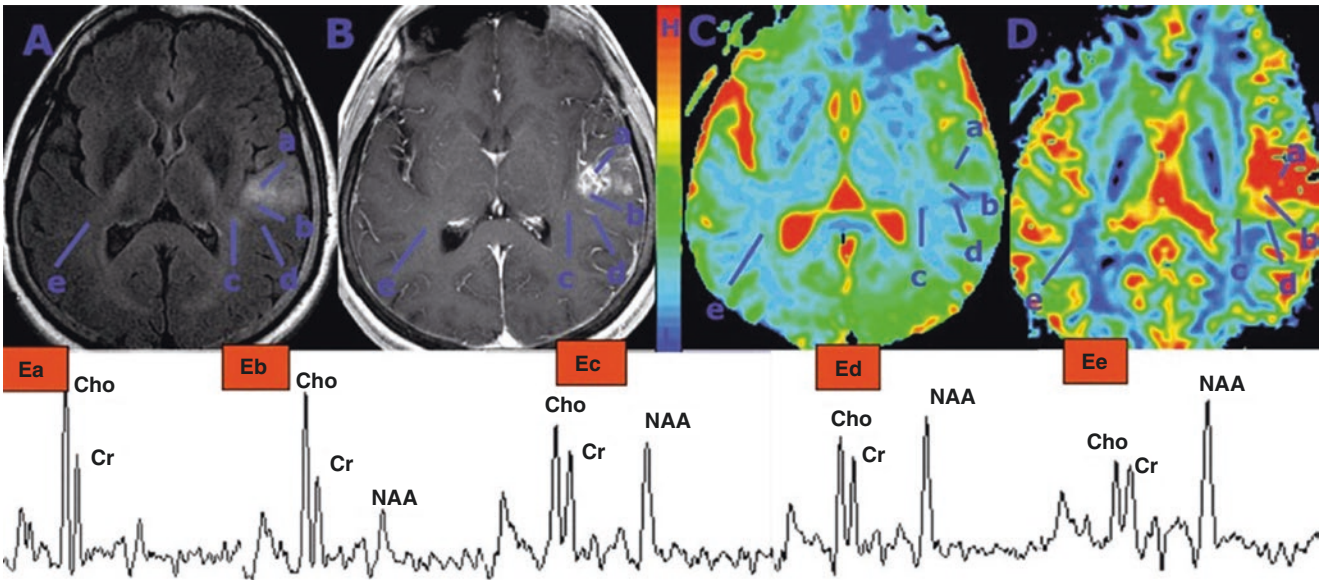

Fig. 44.2 (**a**, **b**) MR FSE T2-weighted and contrast-enhanced SE T1-weighted sequences. The appearance of the lesions suggests a worsening, with progression toward a probable glioblastoma multiforme. The lesion appears larger, with heterogeneous enhancement due to central necrotic components and increased surrounding edema and little mass effect on the midline structures. Multimodal MR with diffusion-weighted imaging and ADC map (**c**), perfusion study with CBV map (**d**), and single-voxel spectroscopy with multiple ROIs (**e**). The treatment performed has led to the appearance of a necrotic component characterized by increased ADC and decreased CBV. These indicators instead retain the tumor pattern in the enhancing areas and immediately adjacent to the lesion

Follow-Up Performed at 12 Months After Surgery and Combined Radiation

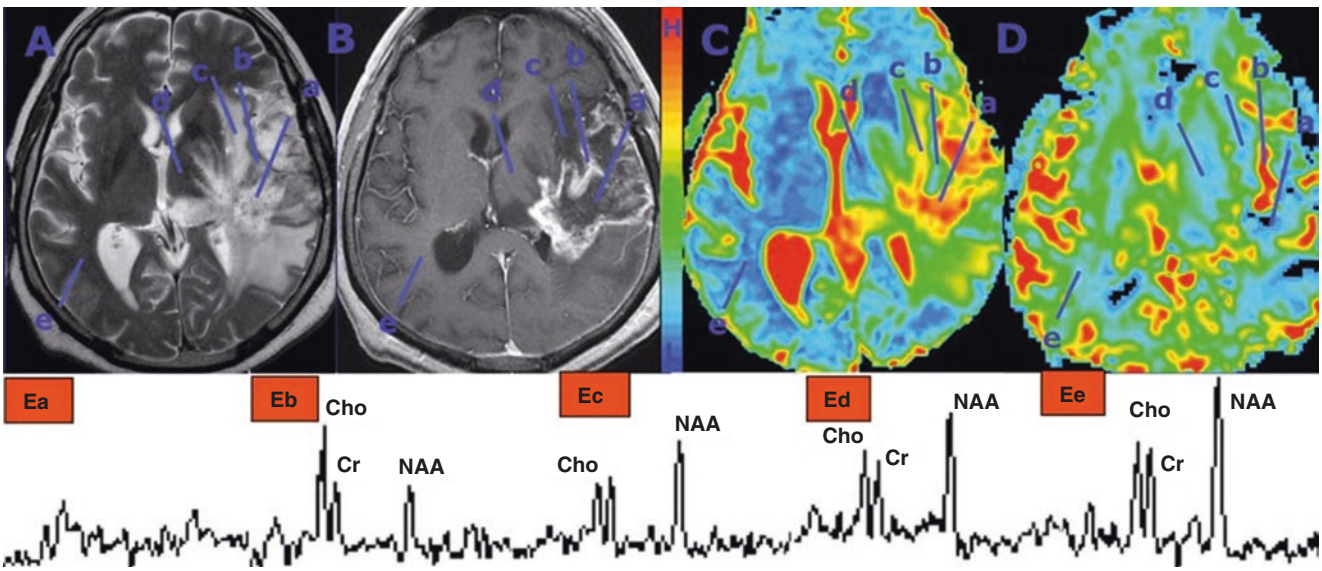

Fig. 44.3 Morphofunctional MR with FSE T2-weighted (**a**), contrast-enhanced SE T1-weighted (**b**) sequences, diffusion-weighted imaging with ADC map (**c**), perfusion study with CBV map (**d**), and multivoxel spectroscopy with multiple ROIs (**e**). The results obtained by radiation therapy and chemotherapy show a further significant increase in the size of the tumor surrounded by abundant edema and moderate mass effect on the midline structures. The lesion displays an almost complete radio-induced necrotic transformation with irregular peripheral enhancement. Consequently the spectra show a reduction in the levels of all metabolites, with a corresponding increase in ADC and decrease in CBV. These indices are inverted in the areas of healthy tissue and in the surrounding tissue adjacent to the lesion

Radiation-Induced Leukoencephalopathy: MR Follow-Up After Whole Brain Radiation Therapy

Case 45

Mario Muto and Alessandra D'Amico

- 56-year-old patient with secondary lesion from previous breast cancer.
- MR follow-up at 1, 3, and 6 years after stereotactic radiation therapy for metastatic brain lesion from breast cancer.

Follow-Up at 1 Year After Breast Cancer Surgery in Symptomatic Patient

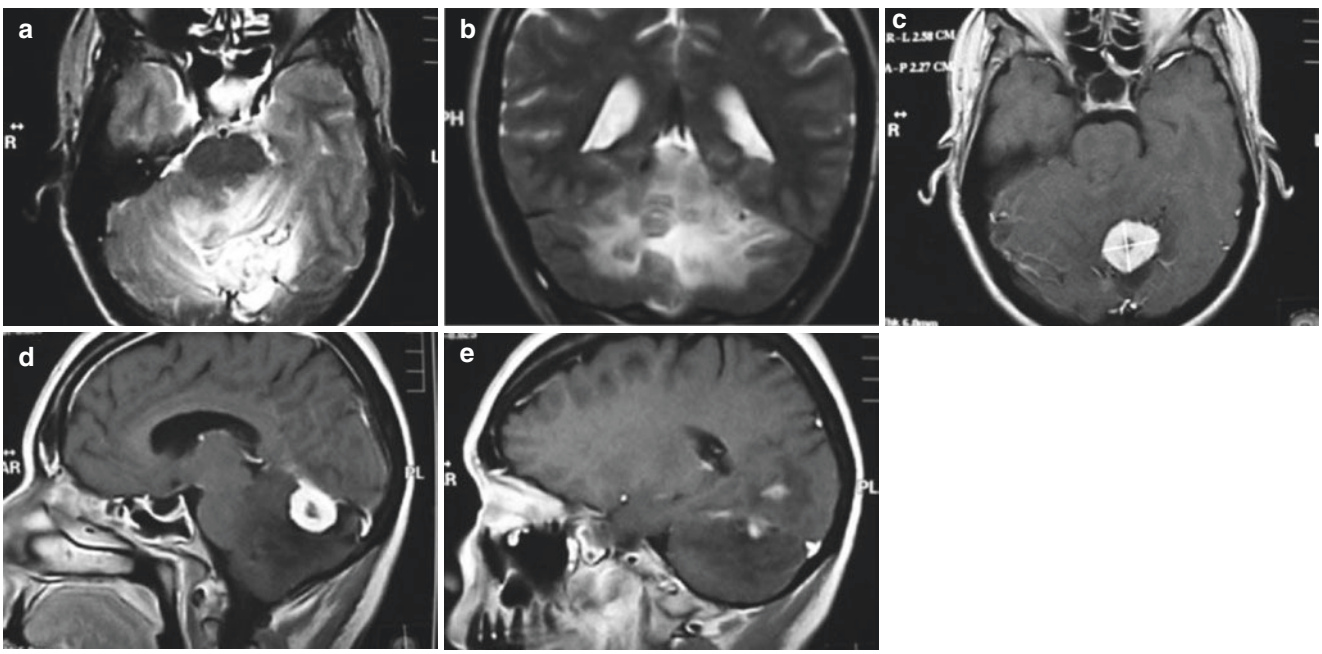

Fig. 45.1 MR FSE T2-weighted (**a**, **b**) and contrast-enhanced SE T1-weighted (**c**–**e**) sequences. The images show a secondary nodular lesion in the right occipital region, with the accessory finding of a small meningioma adhering to the tentorium

M. Muto (✉) · A. D'Amico
Department of Neuroradiology, "Cardarelli" Hospital,
Naples, Italy

T. Scarabino, S. Pollice (eds.), *Imaging Gliomas After Treatment*, https://doi.org/10.1007/978-3-030-31210-7_55

Follow-Up at 1 Year After Stereotactic Radiation Therapy for Metastasis

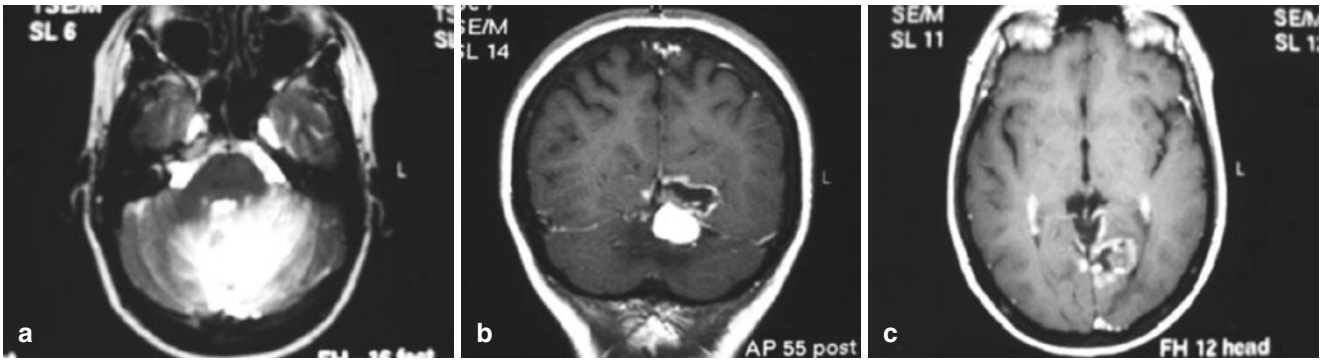

Fig. 45.2 MR FSE T2-weighted (**a**) and contrast-enhanced SE T1-weighted (**b**, **c**) sequences. Signal alteration and enhancement typical of radionecrosis can be appreciated in the left occipital region, with persistence of the tentorial meningioma, which appears unchanged in size with abundant surrounding edema

Follow-Up at 3 Years

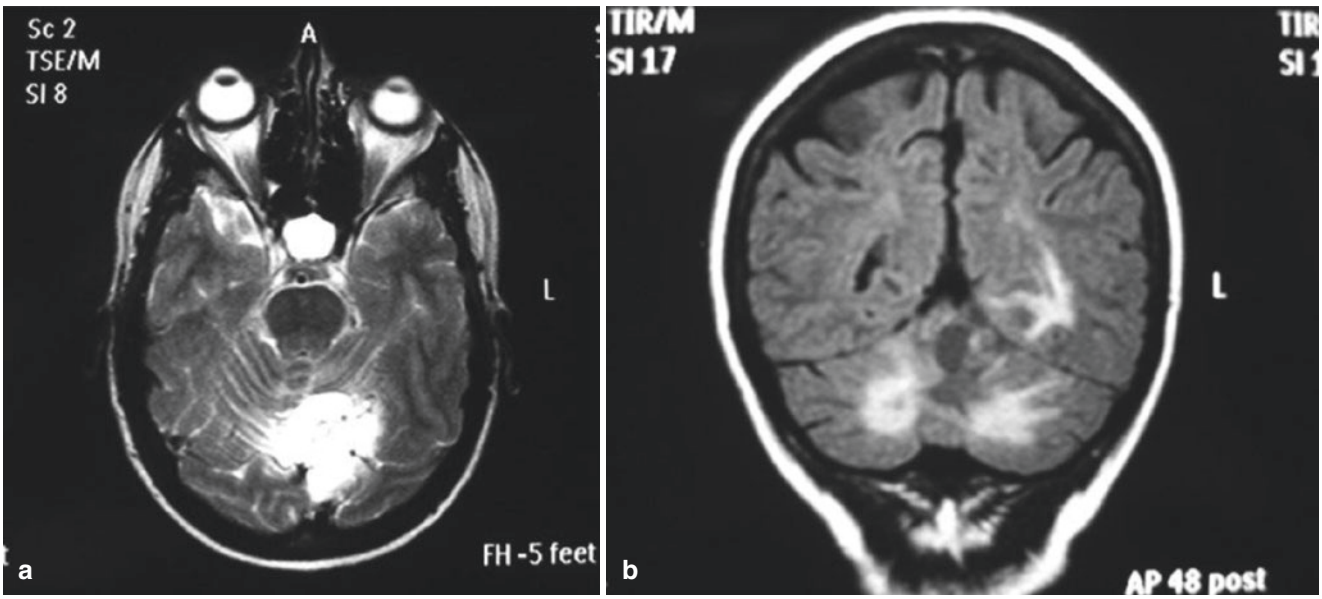

Fig. 45.3 MR FSE T2-weighted (**a**) and FLAIR (**b**) sequences. A modest reduction in the size of the tentorial lesion and the appearance of an area of softening with postirradiation atrophy both in the cerebellar and occipital region are shown. A related allergic diathesis hindered the completion of the study with contrast agents

Follow-Up at 6 Years

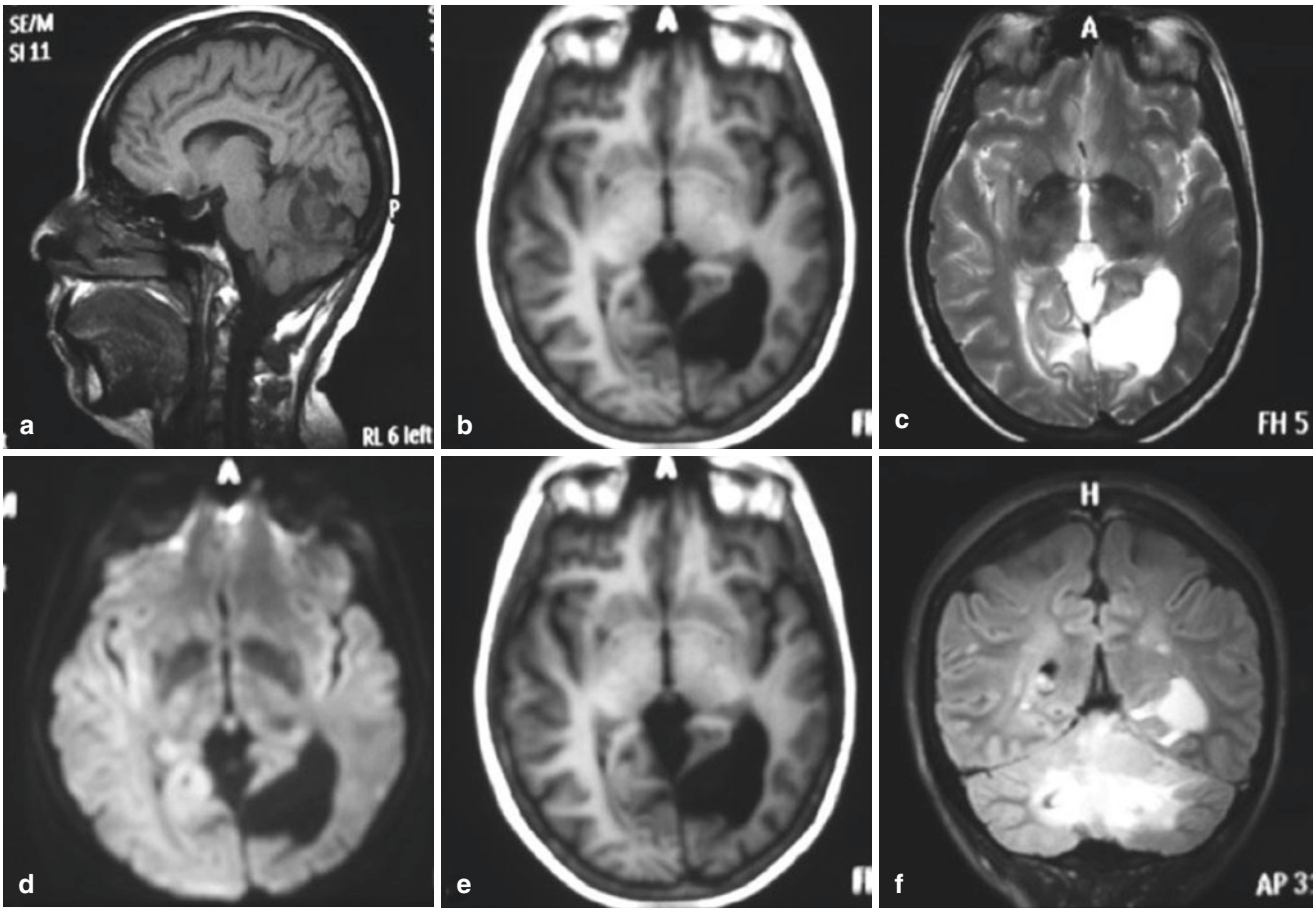

Fig. 45.4 MR SE T1-weighted (**a**, **b**), FSE T2-weighted (**c**), SE DP (**d**), and FLAIR (**e**) sequences. The images show softening with further extension of the left occipital and cerebellar atrophy and reduction in the size of the tentorial lesion

Late Sequelae: Postoperative MR Follow-Up After Radiation Therapy in Diffuse Intrinsic Pontine Glioma

Case 46

Domenico Cicala, Ferdinando Caranci, Anna Nastro, Carmela Russo, Maria De Liso, and Sossio Cirillo

- 4-year-old patient with diffuse intrinsic pontine glioma treated by radiation therapy.
- Postoperative MR follow-up performed with MR morphologic sequences.

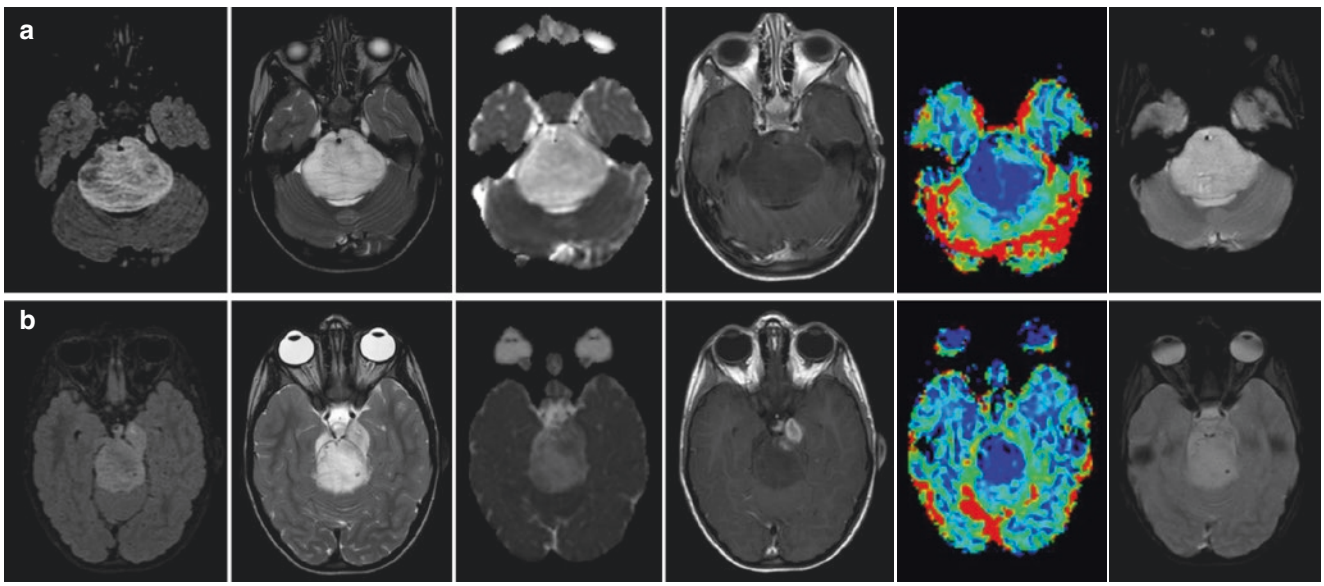

Fig. 46.1 Preoperative imaging. *Axial FLAIR image, T2-weighted image, ADC map, contrast-enhanced SE T1-weighted image, CBV map, and T2*-weighted image at the level of the transverse pontine section* (**a**) *and of the upper section extended toward the midbrain* (**b**). Diffuse intrinsic pontine glioma (DIPG). Massive infiltrative enlargement of the pons compressing the fourth ventricle with effacement of the sulci and the cerebello-pontine cistern. The lesion extends superiorly to the midbrain, with an exophytic component in the left para-pontine cistern which fills the Meckel's cave (**b**); this component shows higher values of perfusion on CBV maps, partially restricted diffusion with lower intensity on ADC maps; it also shows inhomogeneous structure, with irregular areas of rim enhancement on contrast-enhanced SE T1 sequence, suggestive of necrotic-cystic nature and higher-grade lesion's portion. Small microangiopathic foci of hypointensity in T2∗ images are observed within the lesion

D. Cicala · A. Nastro · C. Russo · M. De Liso
Department of Neurosciences, "Santobono-Pausilipon" Pediatric Hospital, Naples, Italy

F. Caranci (✉)
Department of Medicine and Health Sciences "V. Tiberio", University of Molise, Campobasso, Italy

S. Cirillo
Department of Precision Medicine, School of Medicine, University of Campania "Luigi Vanvitelli", Naples, Italy

T. Scarabino, S. Pollice (eds.), *Imaging Gliomas After Treatment*, https://doi.org/10.1007/978-3-030-31210-7_56

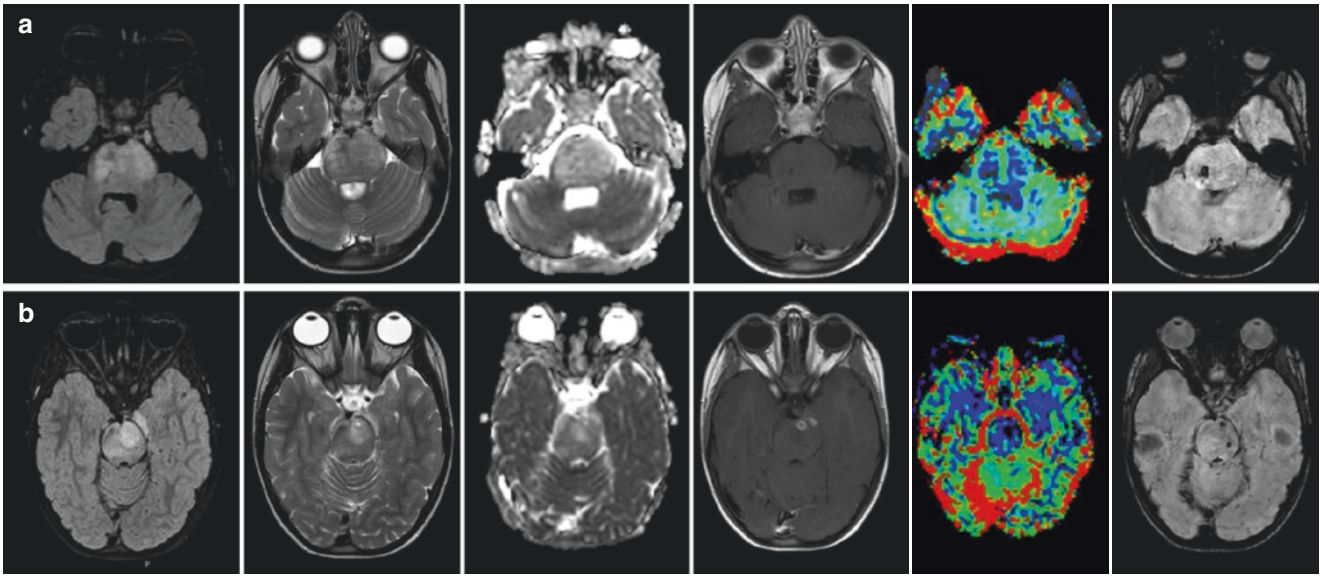

Fig. 46.2 Follow-up at 8 months after radiation therapy. *Axial FLAIR image, T2-weighted image, ADC map, contrast-enhanced SE T1-weighted image, CBV map, and T2*-weighted image at the level of the transverse pontine section* (**a**) *and of the upper section extended toward the midbrain* (**b**). Considerable reduction in brain stem enlargement as well as in exophytic amount of the lesion, and a volumetric decrease of the nodules with irregular impregnation. Hypointense area caused by hemosiderin depositions in the right part of pons (**a**), as a result of a previous needle biopsy, is also shown in T2∗ images

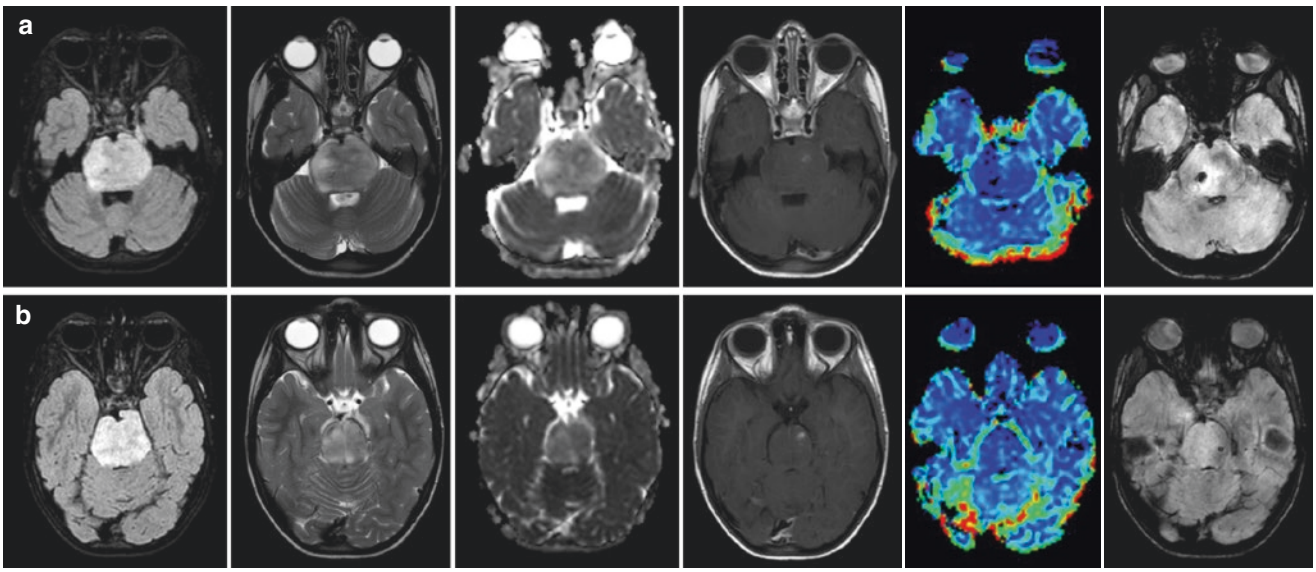

Fig. 46.3 Follow-up at 11 months after radiation therapy. *Axial FLAIR image, T2-weighted image, ADC map, contrast-enhanced SE T1-weighted image, CBV map, and T2*-weighted image at the level of the transverse pontine section* (**a**) *and of the upper section extended toward the midbrain* (**b**). MR study performed during a subacute onset worsening of the clinical status reveals moderate pontine swelling, probably related to radiation-induced effects; it shows inhomogeneous structure, due to the appearance of a pseudo-nodular area in the left part of the pons (**a**) with slight enhancement on contrast-enhanced SE T1 sequences and thin rim of relative restricted diffusion on ADC map; no foci of increased perfusion is observed within the newly emerged area on CBV map, but only a slight increased signal is shown at the neighboring pontine tissue; further reduction of midbrain areas of nodular enhancement (**b**)

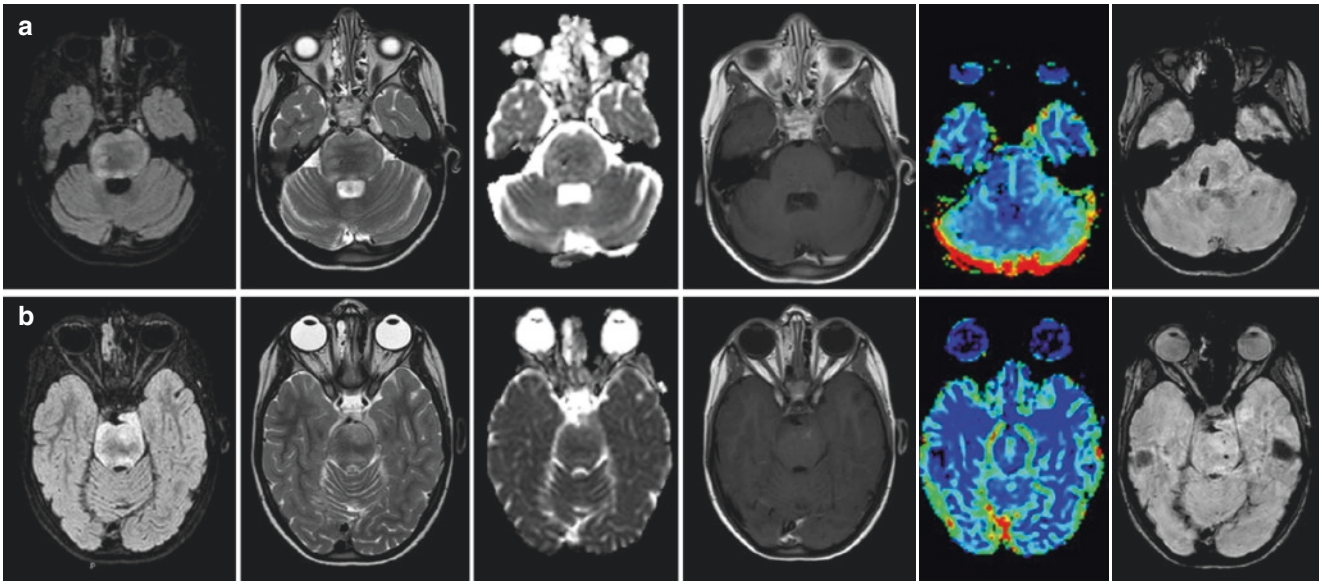

Fig. 46.4 Follow-up at 18 months after radiation therapy. *Axial FLAIR image, T2-weighted image, ADC map, contrast-enhanced SE T1-weighted image, CBV map, and T2*-weighted image at the level of the transverse pontine section* (**a**) *and of the upper section extended toward the midbrain* (**b**). Disappearance of the brain stem enlargement as well as of the pontine area of nodular enhancement. Further reduction of the upper and exophytic components is observed. No area of increased perfusion or diffusion is observed within the lesion. Small new foci of hypointensity in T2∗ images are observed in the deep white matter of left middle cerebellar peduncle (**a**), due to radiation-induced microangiopathy

Radiation Therapy-Induced Tumor Pseudoprogression: MR Follow-Up in Pilocytic Astrocytoma

Case 47

Teresa Popolizio, Nicola Sforza, and Roberto Izzo

- 18-year-old patient with pilocytic astrocytoma.
- MR follow-up at 1, 4, and 7 months after surgery and radiotherapy.

Preoperative Imaging

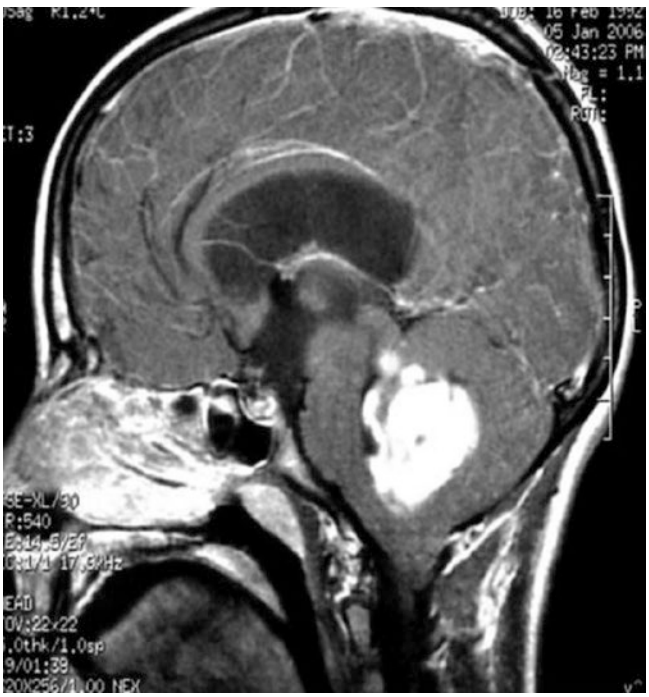

Fig. 47.1 Contrast-enhanced MR SE T1-weighted sequence shows a voluminous vermian mass obliterating the IV ventricle with intense and homogeneous enhancement

T. Popolizio (✉) · N. Sforza · R. Izzo
Department of Neuroradiology, Fondazione IRCCS "Casa Sollievo della Sofferenza", San Giovanni Rotondo, FG, Italy

T. Scarabino, S. Pollice (eds.), *Imaging Gliomas After Treatment*, https://doi.org/10.1007/978-3-030-31210-7_57

Early Postoperative Imaging

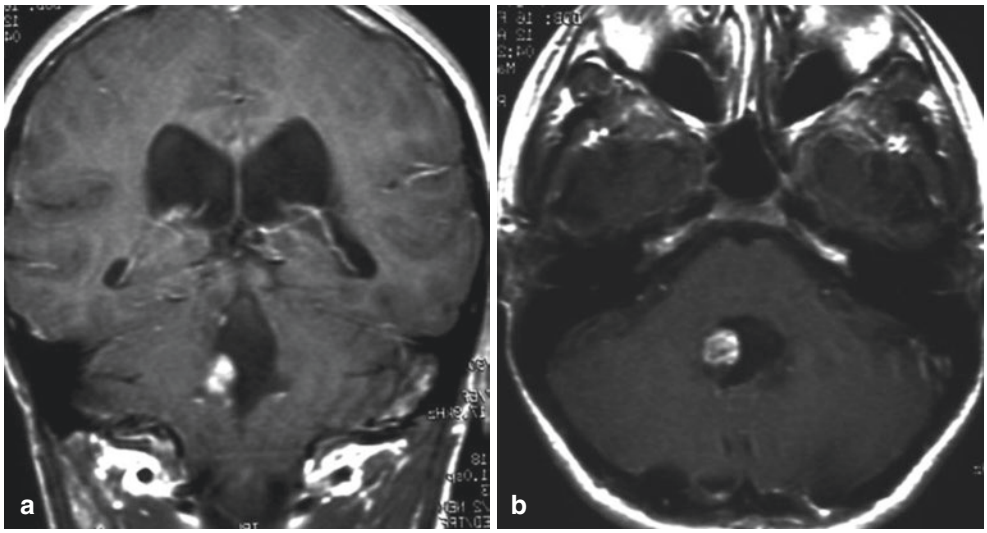

Fig. 47.2 (**a**, **b**) MR contrast-enhanced SE T1-weighted sequences show residual neoplastic tissue occupying the right portion of the IV ventricle

Imaging at 1 Month After Surgery and Radiation Therapy

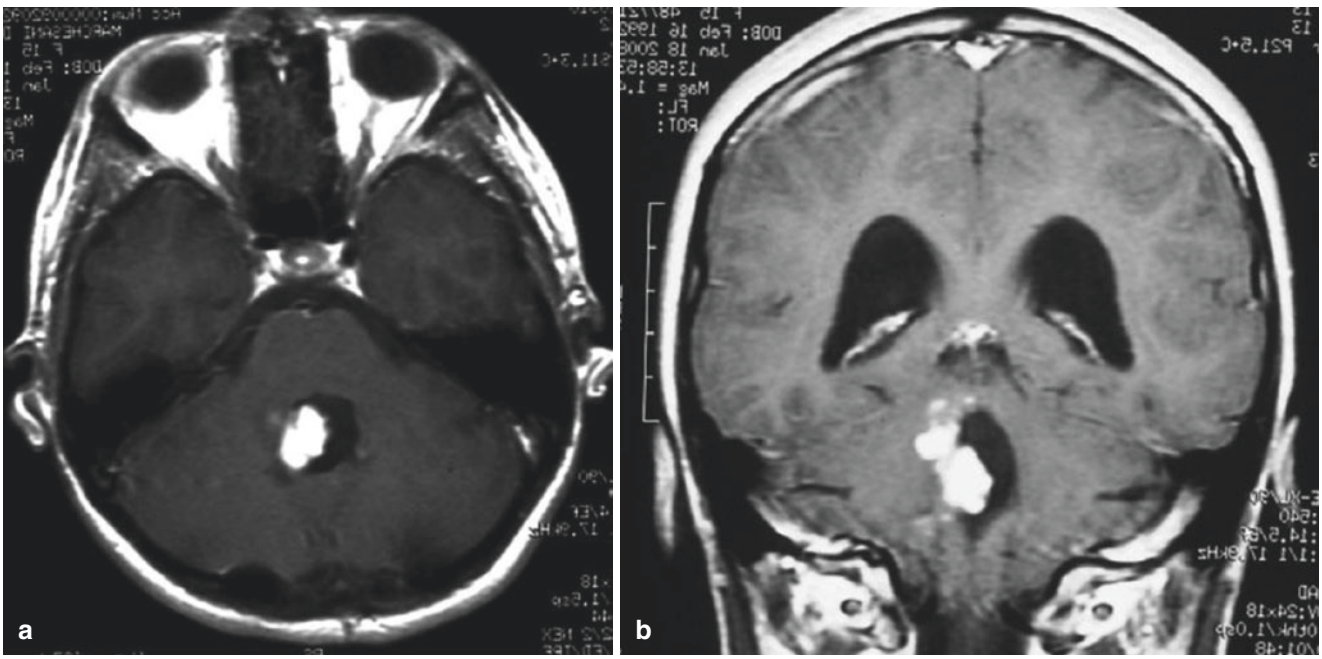

Fig. 47.3 (**a**, **b**) Contrast-enhanced MR SE T1-weighted sequences show an increase in the volume of the residual cancer

Imaging at 4 Months

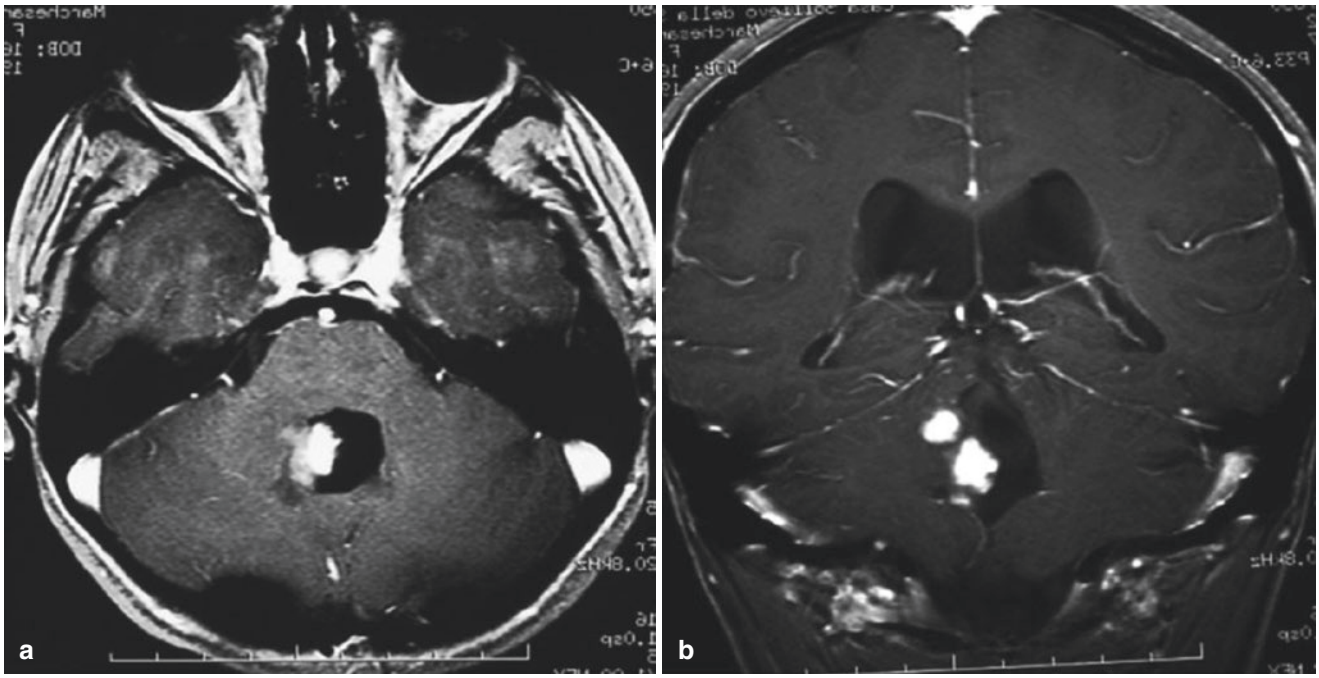

Fig. 47.4 (**a**, **b**) Contrast-enhanced MR SE T1-weighted sequences. There has been a moderate reduction in the volume of the residual cancer

Imaging at 7 Months

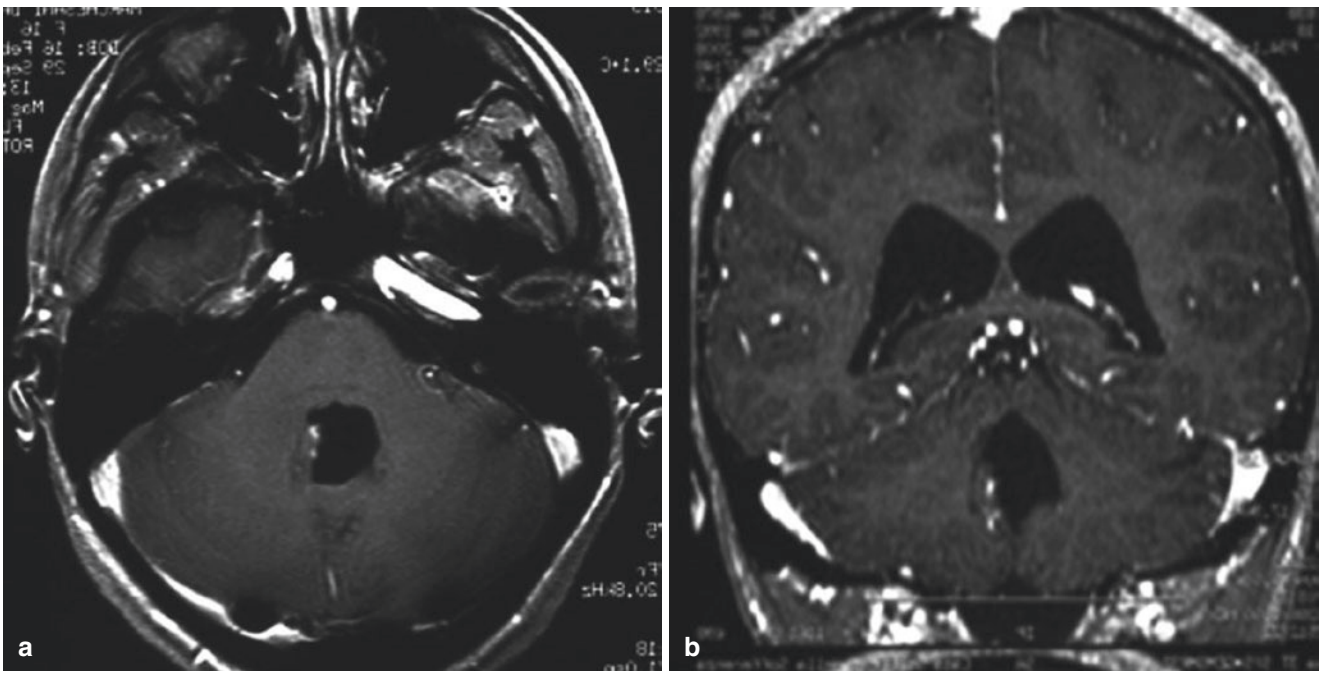

Fig. 47.5 (**a**, **b**) Contrast-enhanced MR SE T1-weighted sequence. There has been a significant reduction in the volume of residual cancer

Chemotherapy-Induced Tumor Pseudoprogression: 3T MR Follow-Up in Glioblastoma

Case 48

Teresa Popolizio, Nicola Sforza, and Anna Maria Pennelli

- 73-year-old patient with right temporal glioblastoma treated with partial surgical excision and combined radiation therapy–chemotherapy.
- 3T MR follow-up performed at 1, 3, 9, and 12 months after surgery and combined radiation therapy–chemotherapy.

Preoperative Imaging

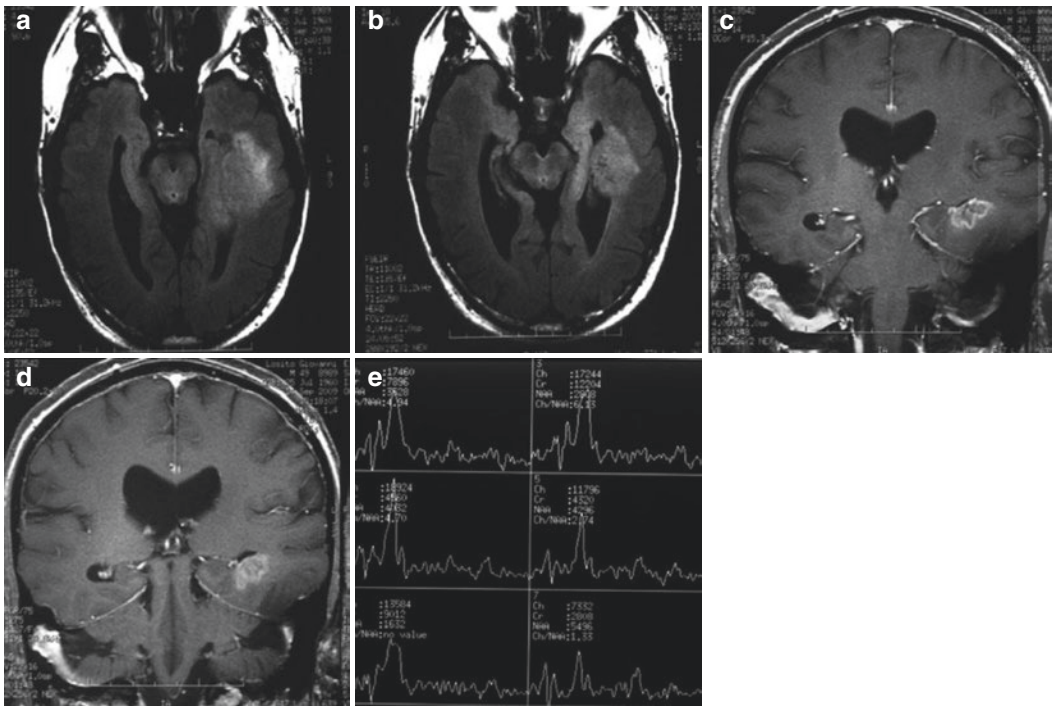

Fig. 48.1 MR FLAIR (**a**, **b**), contrast-enhanced SE T1-weighted (**c**, **d**) sequences, and spectroscopy (**e**). A large mass with limited edema is visualized compressing the adjacent temporal horn of the right lateral ventricle. The oval-shaped mass with ill-defined and lobulated margins appears hyperintense in FLAIR (**a**, **b**), and inhomogeneously enhanced after contrast medium administration (**c**, **d**). The spectroscopy study (**e**) reveals a high Cho peak indicating aggressive biological behavior

T. Popolizio (✉) · N. Sforza · A. M. Pennelli
Department of Neuroradiology, Fondazione IRCCS "Casa Sollievo della Sofferenza", San Giovanni Rotondo, FG, Italy

T. Scarabino, S. Pollice (eds.), *Imaging Gliomas After Treatment*, https://doi.org/10.1007/978-3-030-31210-7_58

Follow-Up at 1 Month After Surgery

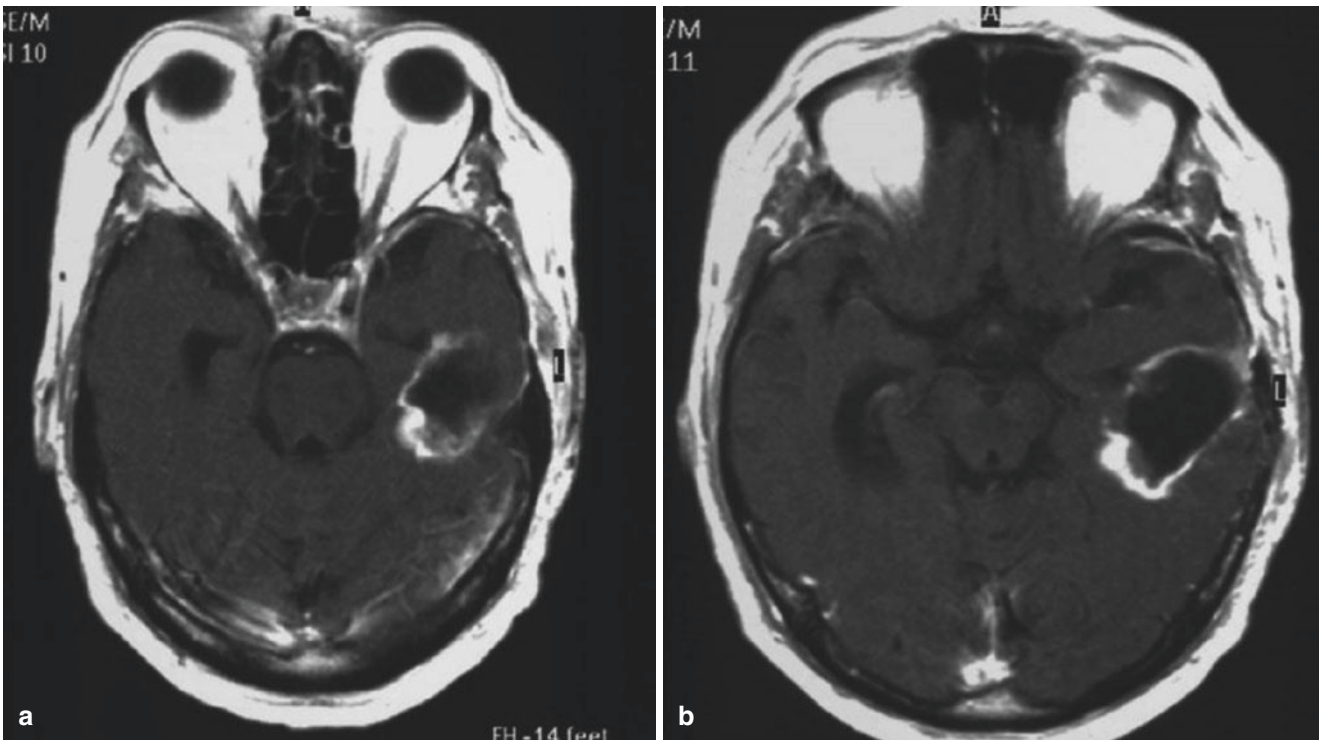

Fig. 48.2 (**a**, **b**) Contrast-enhanced MR SE T1-weighted sequences show the postsurgical appearance of a large cystic-like lesion with thick and irregular rim enhancement

Follow-Up at 3 Months After Surgery and Adjuvant Tomotherapy–Chemotherapy

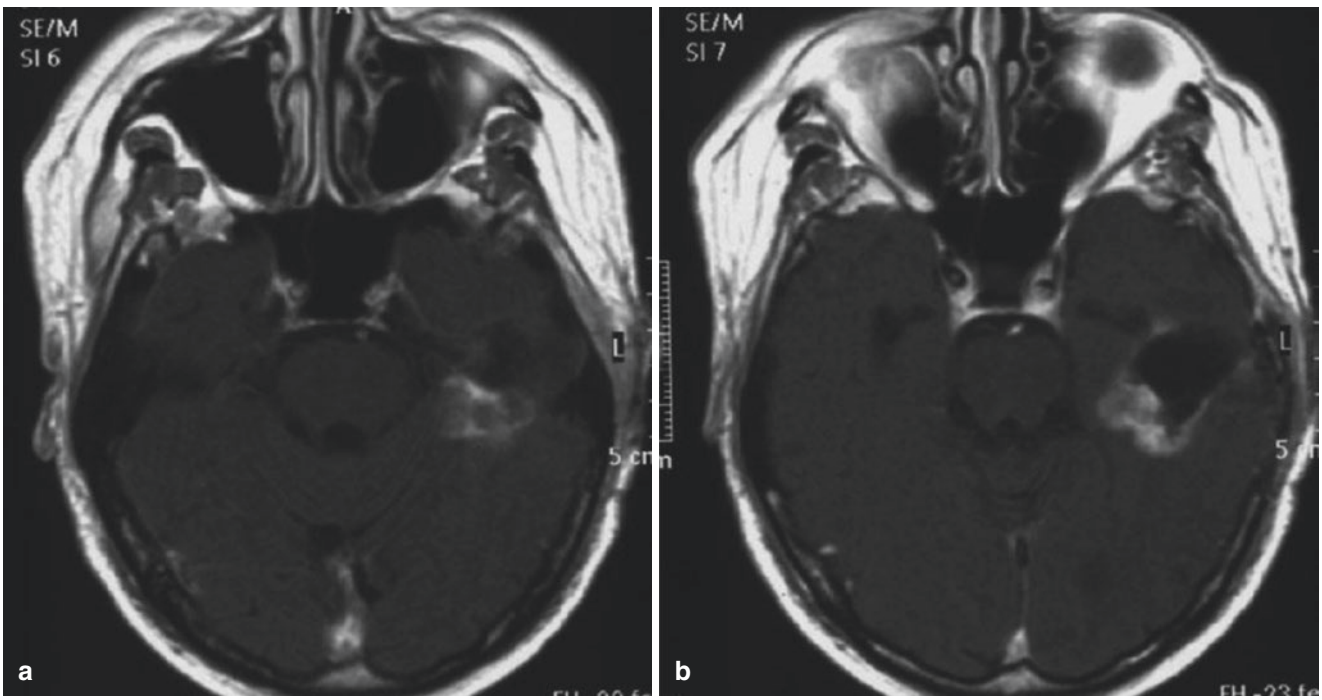

Fig. 48.3 (**a**, **b**) Contrast-enhanced MR SE T1-weighted sequences show an increase in the peripherally enhancing solid component

Follow-Up at 9 Months

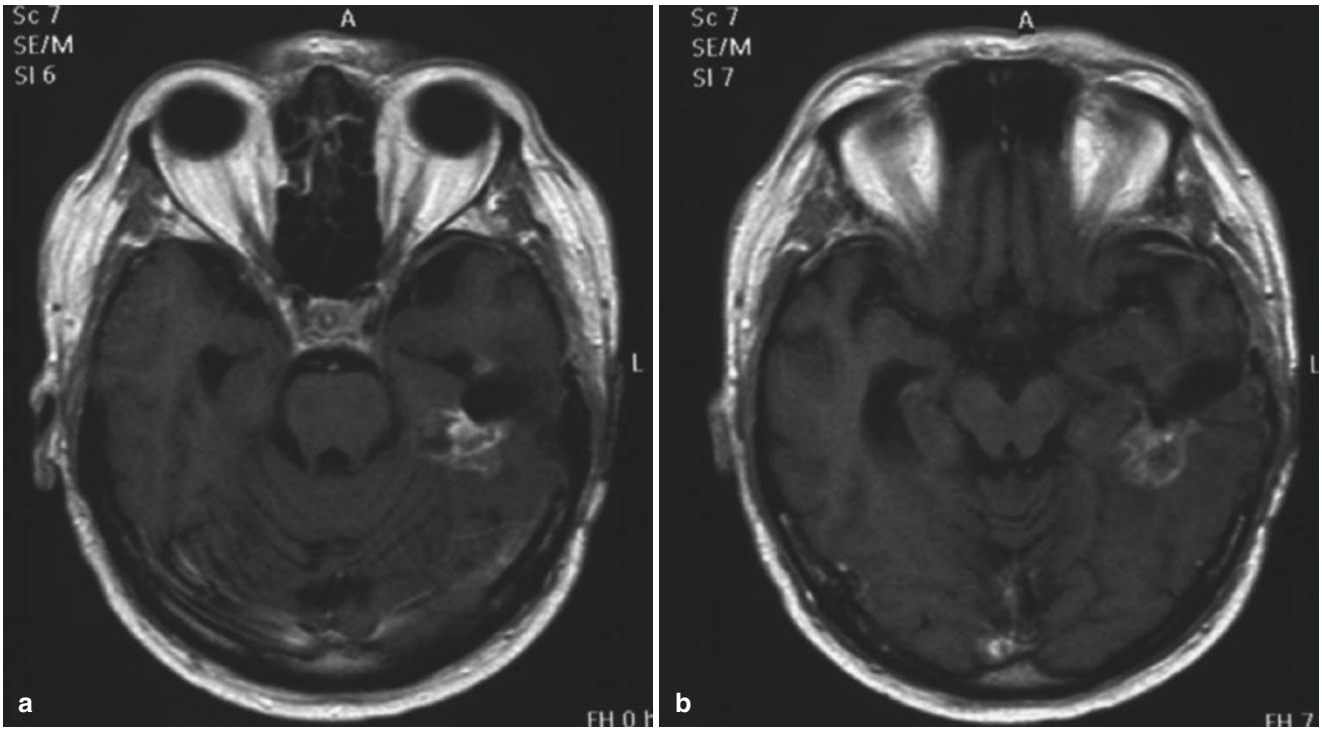

Fig. 48.4 (**a**, **b**) Contrast-enhanced MR SE T1-weighted sequence. A reduction in volume can be seen of both the cystic and solid portions with a substantial necrotic component

Follow-Up at 12 Months

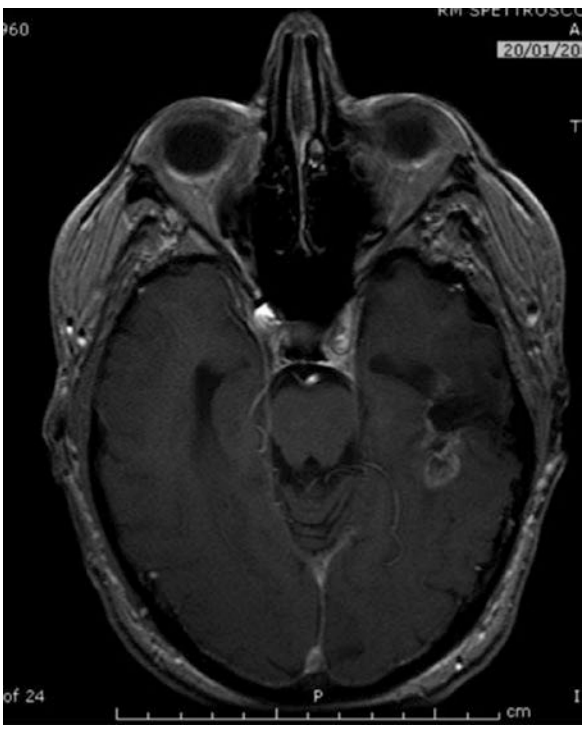

Fig. 48.5 Contrast-enhanced MR SE T1 sequence shows a further reduction in volume of the lesion

Pseudoprogression with Disease Progression: 3T Morphofunctional MR Follow-Up in Anaplastic Astrocytoma

Case 49

Massimo Caulo, Chiara Briganti, Valentina Panara, Simone Salice, Domenico Tortora, and Armando Tartaro

- 59-year-old patient with right frontal anaplastic astrocytoma treated with partial surgery and combined radiation therapy–chemotherapy.
- 3T morphofunctional MR follow-up performed with morphologic imaging, diffusion-weighted imaging, perfusion study, and spectroscopy at 7, 15, and 28 months after surgery and combined radiation therapy–chemotherapy.

Follow-Up Performed at 7 Months After Surgery and Combined Radiation Therapy–Chemotherapy

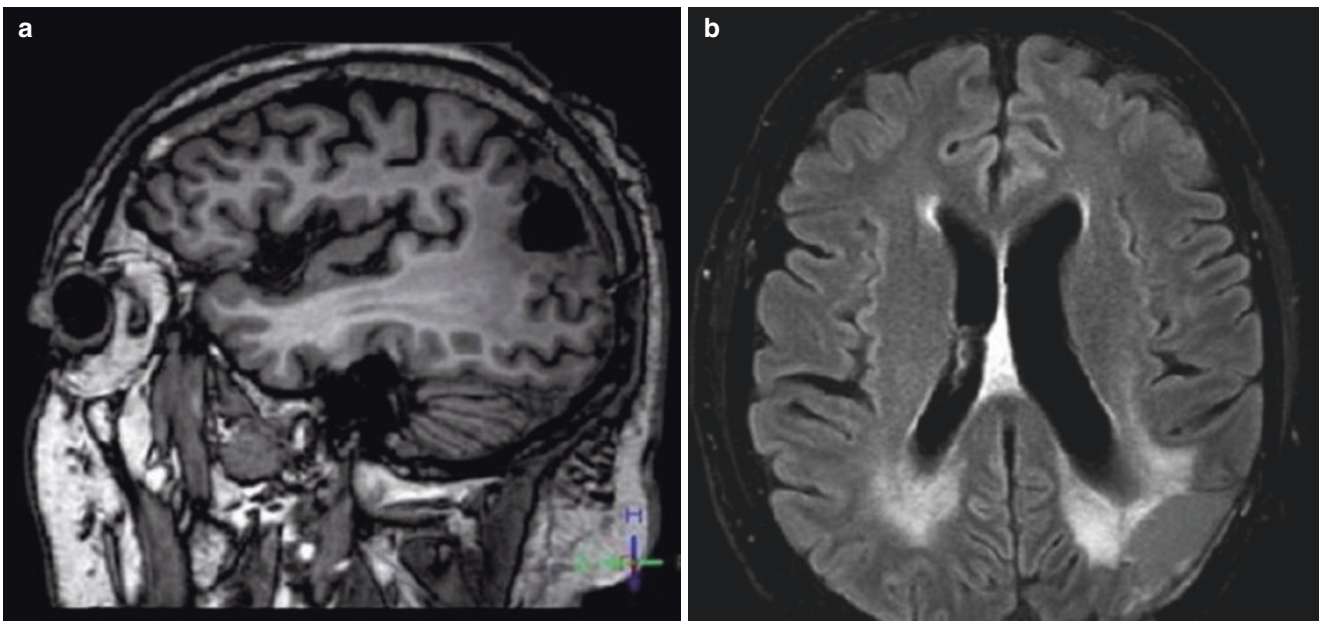

Fig. 49.1 Contrast-enhanced MR SE T1-weighted (**a**) and FLAIR (**b**) sequences show the postsurgical site in the left parietal lobe

M. Caulo · C. Briganti · V. Panara · S. Salice · D. Tortora
A. Tartaro (✉)
Department of Neurosciences and Imaging, Institute of Advanced Biomedical Technologies, "G. d'Annunzio" University, Chieti-Pescara, Italy
e-mail: tartaro@unich.it

T. Scarabino, S. Pollice (eds.), *Imaging Gliomas After Treatment*, https://doi.org/10.1007/978-3-030-31210-7_59

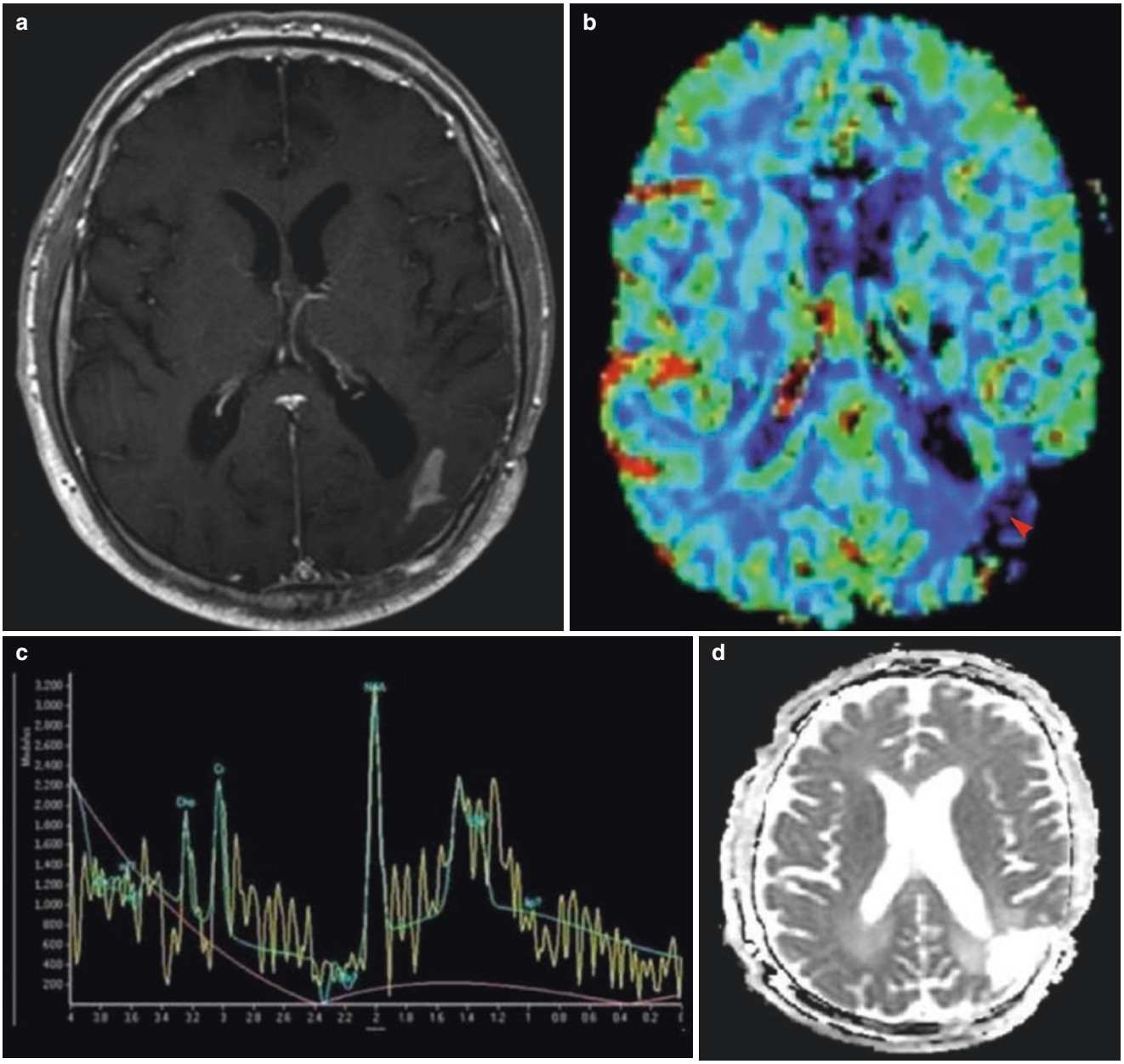

Fig. 49.2 (**a**) Contrast-enhanced MR SE T1-weighted sequence shows 3 mm nodular contrast enhancement at the anterior-medial portion of the surgical cavity. (**b**) MR perfusion study with CBV map. The value of rCBV [CBV lesion/contralateral white matter CBV = 2.2] has not increased at the nodular area of contrast enhancement (*red arrow*). (**c**) MR single/multivoxel spectroscopy. The Cho/Cr (1.2) and Cho/NAA (1.4) ratios are not indicative of high cell turnover, and the presence of the Lac peak confirms the presence of necrosis. (**d**) MR diffusion-weighted image with ADC map shows increased ADC values (1.323 ± 0.336 mm^2/s) within the area of contrast enhancement

Follow-Up Performed at 15 Months

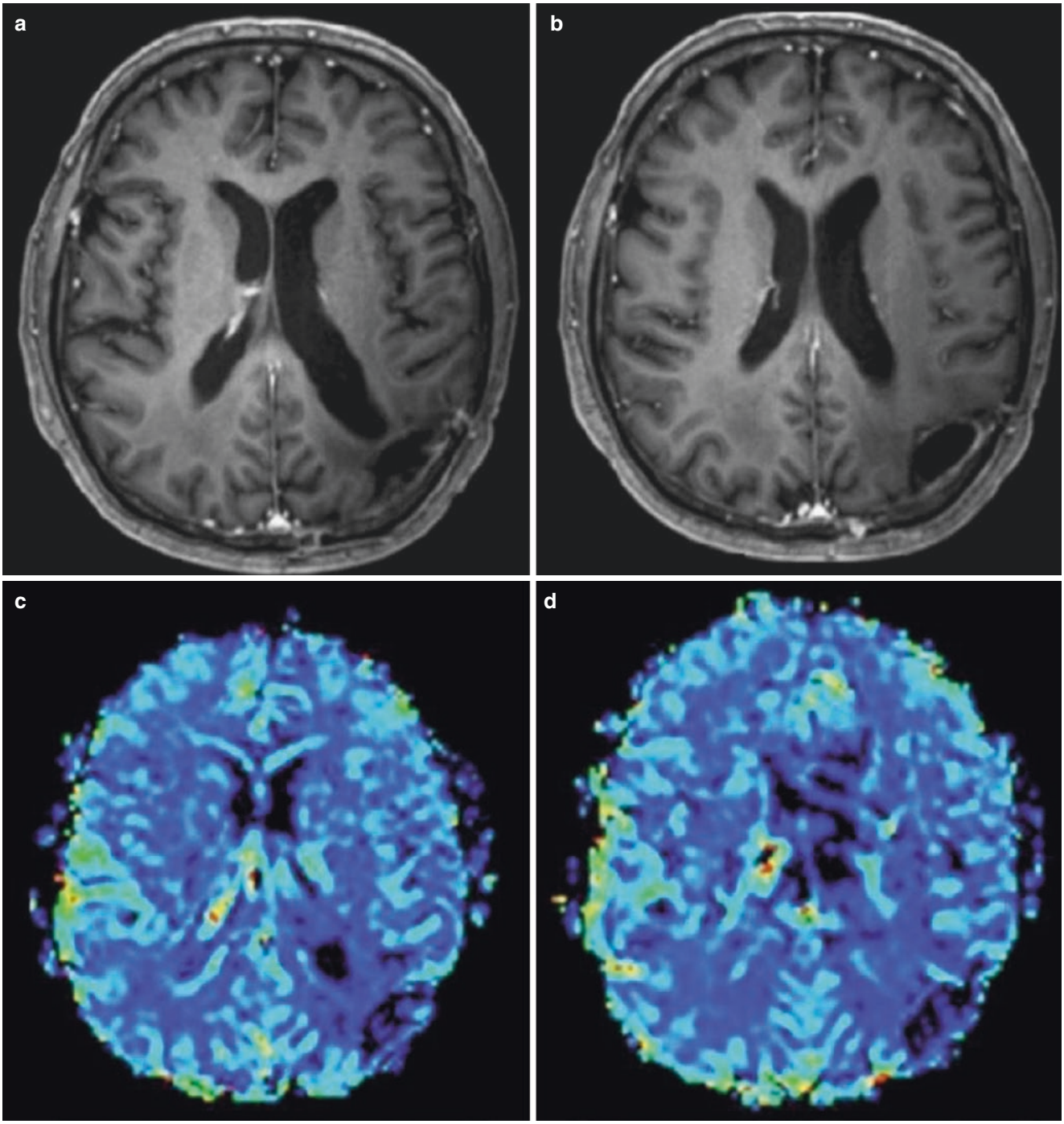

Fig. 49.3 Contrast-enhanced MR SE T1-weighted sequences and perfusion study show complete absence of contrast enhancement (**a**, **b**) associated with zero values of CBV (**c**, **d**), both indicative of the absence of disease progression

Follow-Up Performed at 28 Months

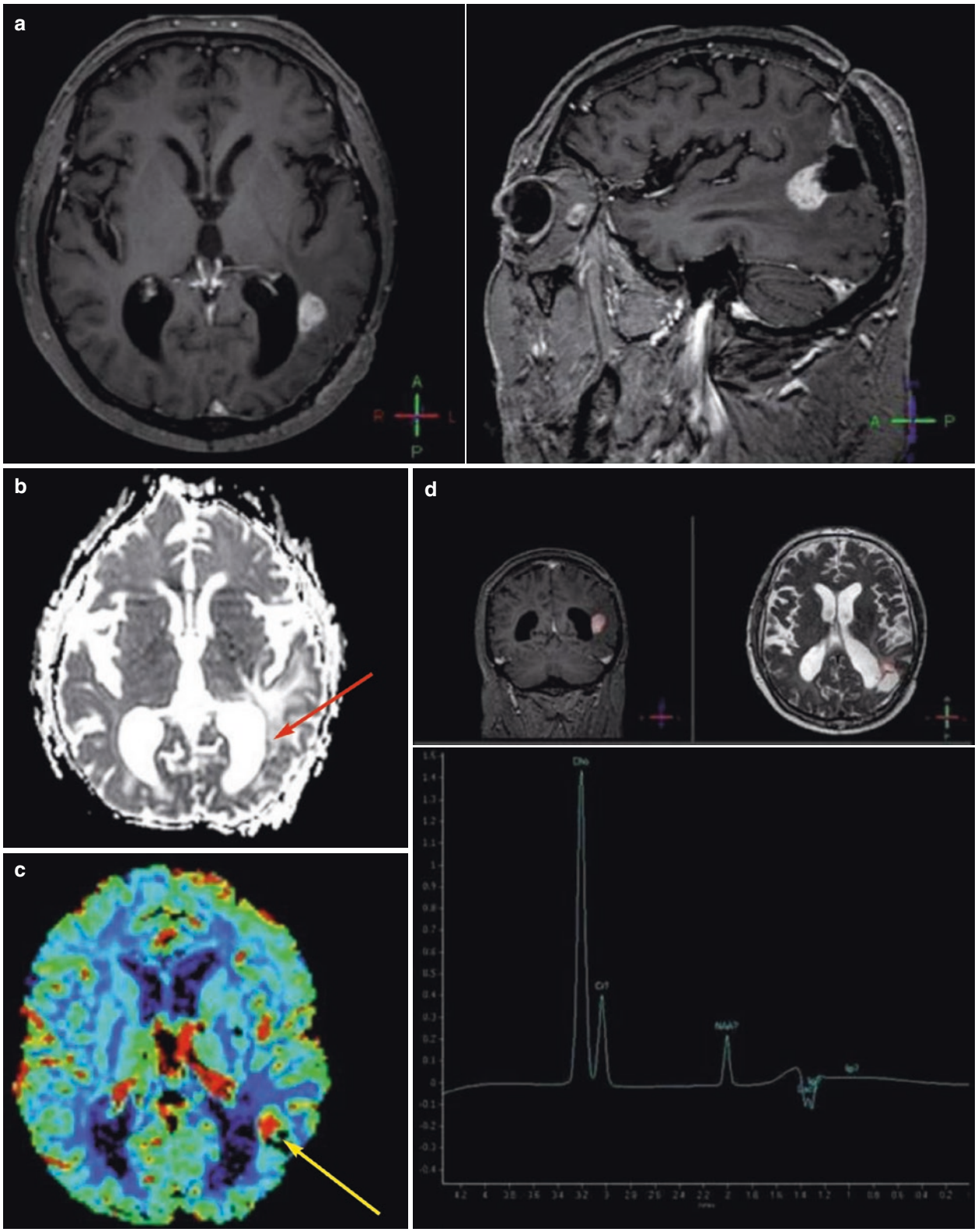

Fig. 49.4 (**a**) Contrast-enhanced MR SE T1-weighted sequence visualizes ependymal contrast enhancement on the surface of the lateral wall of the ventricular trigone and a nodule of contrast enhancement indicating tumor recurrence. (**b**) MR diffusion-weighted image with ADC map confirms the morphologic data with reduced ADC values (0.823 ± 0.116 mm^2/s) at the nodule indicating increased cellularity (*red arrow*). (**c**) MR perfusion study with CBV map confirms the morphologic data of recurrence with significantly increased values of rCBV (5.2) [CBV lesion/contralateral white matter CBV] corresponding to the area of contrast enhancement close to the surgical cavity (*yellow arrow*). (**d**) MR single voxel spectroscopy shows a reversal of the Cho/Cr (3.8) and Cho/NAA (4.1) peaks at the area of disease progression. The presence of a lipids peak indicates necrosis

Drug-Induced Leukoencephalopathy: MR Follow-Up After Corticosteroid Therapy

Case 50

Teresa Popolizio, Nicola Sforza, and Rosario Francesco Balzano

- 42-year-old patient with Crohn's disease.
- Early MR follow-up after steroid therapy.

Early Follow-Up After Steroid Therapy

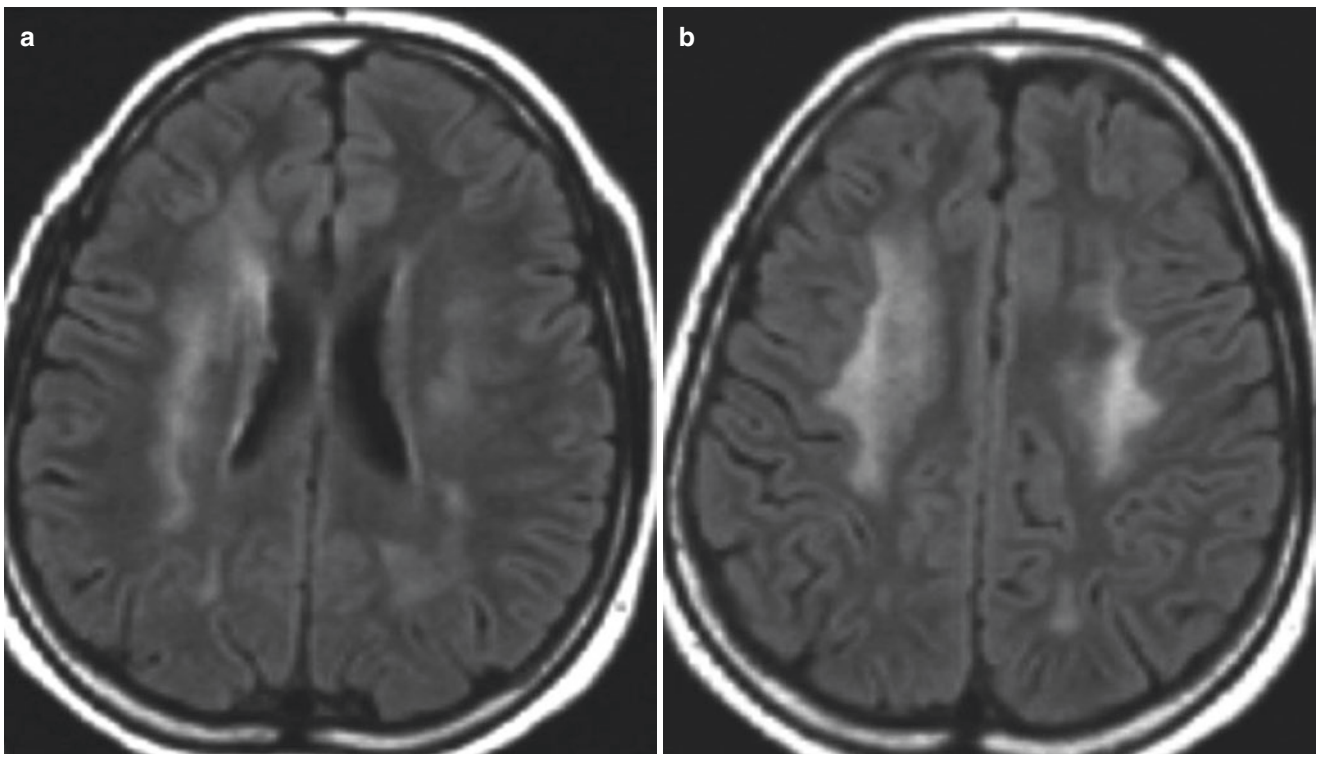

Fig. 50.1 (**a**, **b**) MR FLAIR sequences show diffuse bilateral hyperintensity of the periventricular white matter

T. Popolizio (✉) · N. Sforza
Department of Neuroradiology, Fondazione IRCCS "Casa Sollievo della Sofferenza", San Giovanni Rotondo, FG, Italy

R. F. Balzano
Department of Radiology, University of Foggia, Foggia, FG, Italy

T. Scarabino, S. Pollice (eds.), *Imaging Gliomas After Treatment*, https://doi.org/10.1007/978-3-030-31210-7_60

Drug-Induced Leukoencephalopathy: MR Follow-Up After Methotrexate Therapy

Case 51

Teresa Popolizio, Nicola Sforza, and Anna Maria Pennelli

- 52-year-old patient with Non-Hodgkin lymphoma.
- MR follow-up in chronic phase after treatment with methotrexate.

Late Follow-Up After Chemotherapy

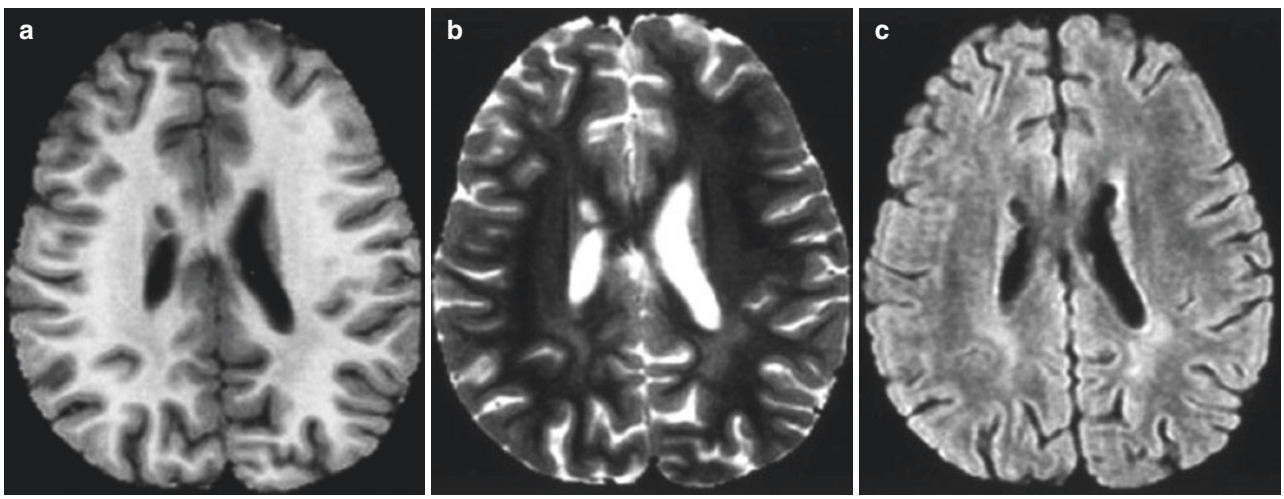

Fig. 51.1 MR SE T1-weighted (**a**), FSE T2-weighted (**b**), and FLAIR (**c**) sequences. Slight and circumscribed signal alteration (hypointensity in T1 and T2, hyperintensity in FLAIR) can be appreciated in the posterior periventricular white matter bilaterally

T. Popolizio (✉) · N. Sforza
Department of Neuroradiology, Fondazione IRCCS "Casa Sollievo della Sofferenza", San Giovanni Rotondo, FG, Italy

A. M. Pennelli
Department of Radiology, Fondazione IRCCS "Casa Sollievo della Sofferenza", San Giovanni Rotondo, FG, Italy

T. Scarabino, S. Pollice (eds.), *Imaging Gliomas After Treatment*, https://doi.org/10.1007/978-3-030-31210-7_61

Drug-Induced Thrombosis: MR Follow-Up After L-Asparaginase Therapy

Case 52

Teresa Popolizio, Nicola Sforza, and Daniela Grasso

- 8-year-old patient with acute lymphoblastic leukemia.
- Early MR follow-up after L-asparaginase treatment.

Early Imaging After Chemotherapy

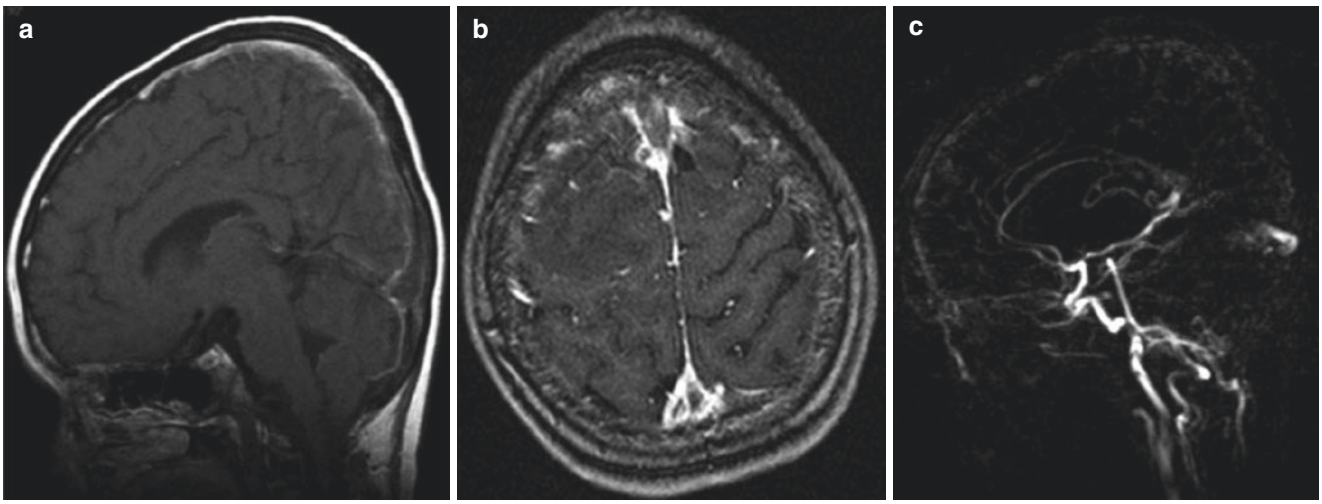

Fig. 52.1 MR SE T1-weighted sequence (**a**) and MR angiography (3D TOF) in (**b**), 2D PC MIP in (**c**). Note the T1 hyperintensity from acute thrombosis with consequent "delta gap" sign in the single partition and no flow signal in the superior sagittal sinus in the MIP image

T. Popolizio (✉) · N. Sforza
Department of Neuroradiology, Fondazione IRCCS "Casa Sollievo della Sofferenza", San Giovanni Rotondo, FG, Italy

D. Grasso
Department of Radiology, Fondazione IRCCS "Casa Sollievo della Sofferenza", San Giovanni Rotondo, FG, Italy

T. Scarabino, S. Pollice (eds.), *Imaging Gliomas After Treatment*, https://doi.org/10.1007/978-3-030-31210-7_62

PRES (Posterior Reversible Encephalopathy Syndrome): MR Follow-Up After Cyclosporine Therapy

Case 53

Teresa Popolizio, Nicola Sforza, and Anna Maria Pennelli

- 35-year-old patient with severe atopic dermatitis.
- MR follow-up after treatment with cyclosporine.

Imaging After Chemotherapy

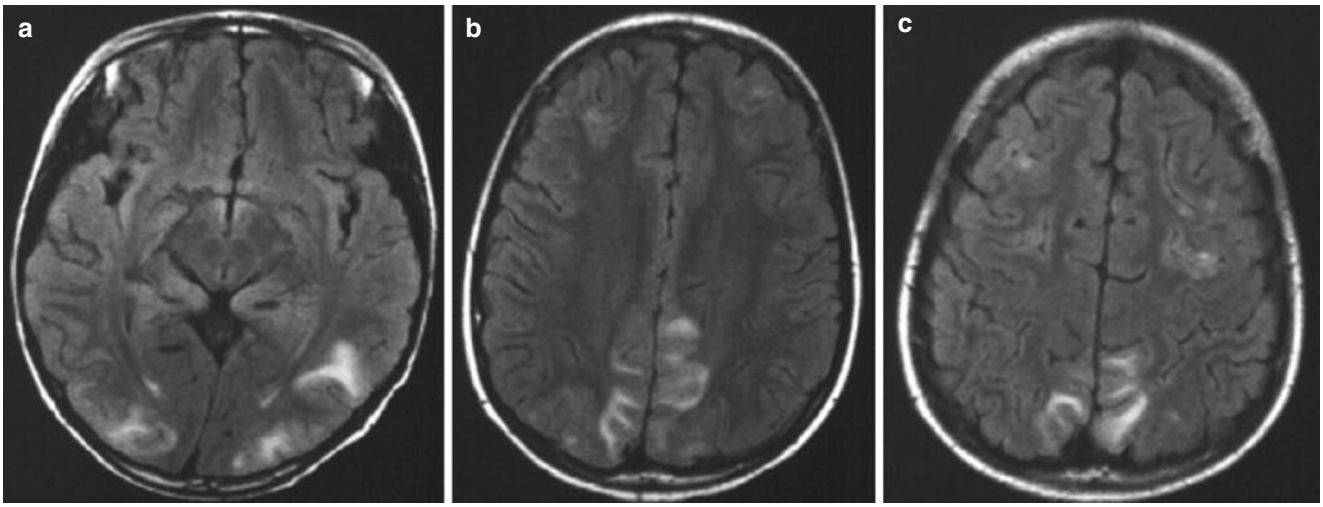

Fig. 53.1 (**a**–**c**) MR FLAIR sequences show symmetric and bilateral cortical-subcortical hyperintensity particularly in the parietal and occipital lobes and also in the frontal lobes attributable to vasogenic edema

T. Popolizio (✉) · N. Sforza
Department of Neuroradiology, Fondazione IRCCS "Casa Sollievo della Sofferenza", San Giovanni Rotondo, FG, Italy

A. M. Pennelli
Department of Radiology, Fondazione IRCCS "Casa Sollievo della Sofferenza", San Giovanni Rotondo, FG, Italy

T. Scarabino, S. Pollice (eds.), *Imaging Gliomas After Treatment*, https://doi.org/10.1007/978-3-030-31210-7_63

PRES (Posterior Reversible Encephalopathy Syndrome): MR Follow-Up After Cisplatin Therapy

Case 54

Teresa Popolizio, Nicola Sforza, and Anna Maria Pennelli

- 75-year-old patient with lung cancer.
- MR follow-up after treatment with cisplatin.

Imaging After Chemotherapy

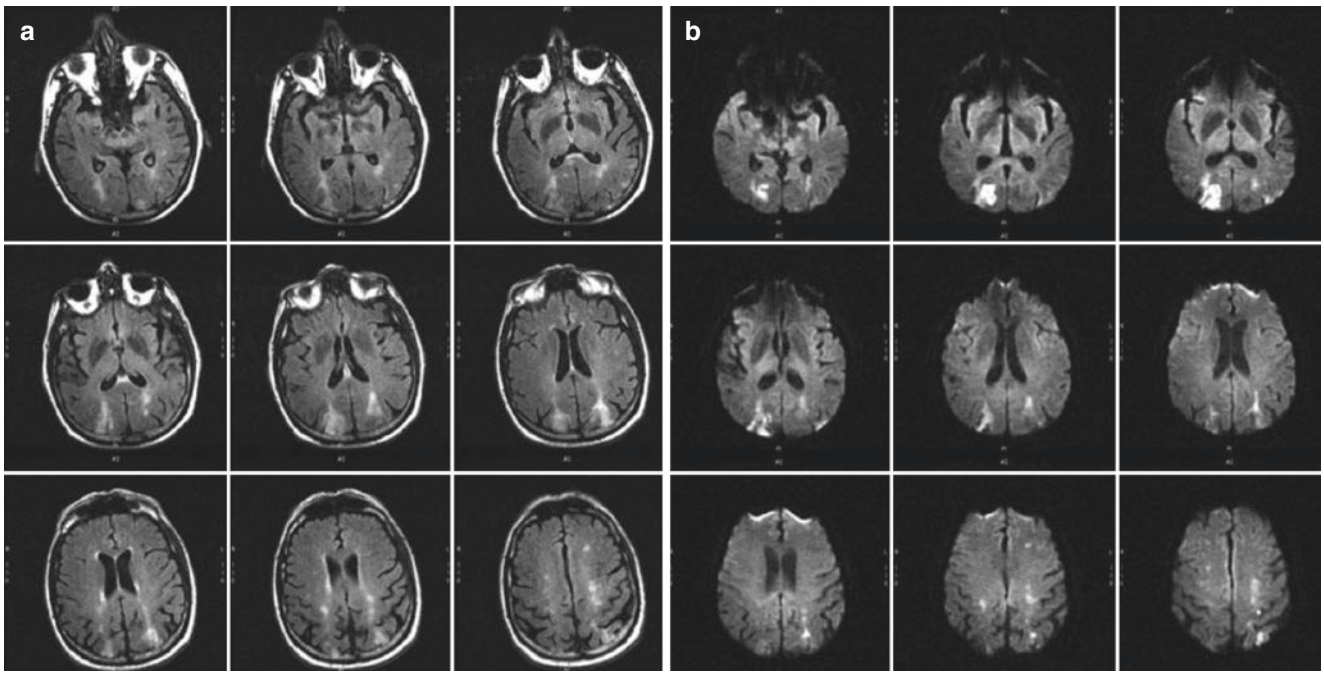

Fig. 54.1 MR FLAIR (**a**), diffusion-weighted (**b**), SE T1-weighted (**c**), and contrast-enhanced SE T1-weighted (**d**) sequences. The symmetrical and bilateral cortical-subcortical hyperintensity (**a**, **b**) involving the parietal and occipital lobes suggest vasogenic edema. The isointense lesions in T1 (**c**) display moderate enhancement (**d**)

T. Popolizio (✉) · N. Sforza
Department of Neuroradiology, Fondazione IRCCS "Casa Sollievo della Sofferenza", San Giovanni Rotondo, FG, Italy

A. M. Pennelli
Department of Radiology, Fondazione IRCCS "Casa Sollievo della Sofferenza", San Giovanni Rotondo, FG, Italy

T. Scarabino, S. Pollice (eds.), *Imaging Gliomas After Treatment*, https://doi.org/10.1007/978-3-030-31210-7_64

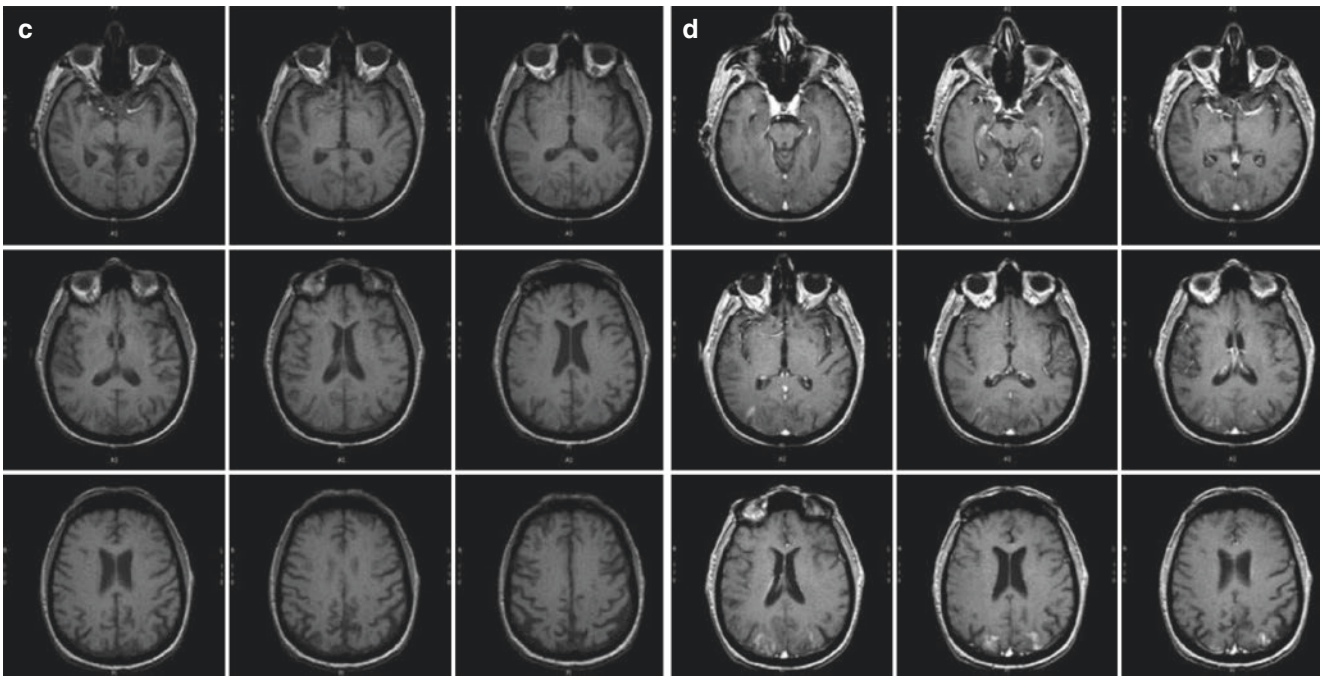

Fig. 54.1 (continued)

Morphofunctional MR in the Diagnosis and Follow-Up of Cerebral Gliomas

Case 55

Tommaso Scarabino, Alberto Maggialetti, Saverio Pollice, Angela Lorusso, Gilda Morlino, Michela Capuano, and Teresa Popolizio

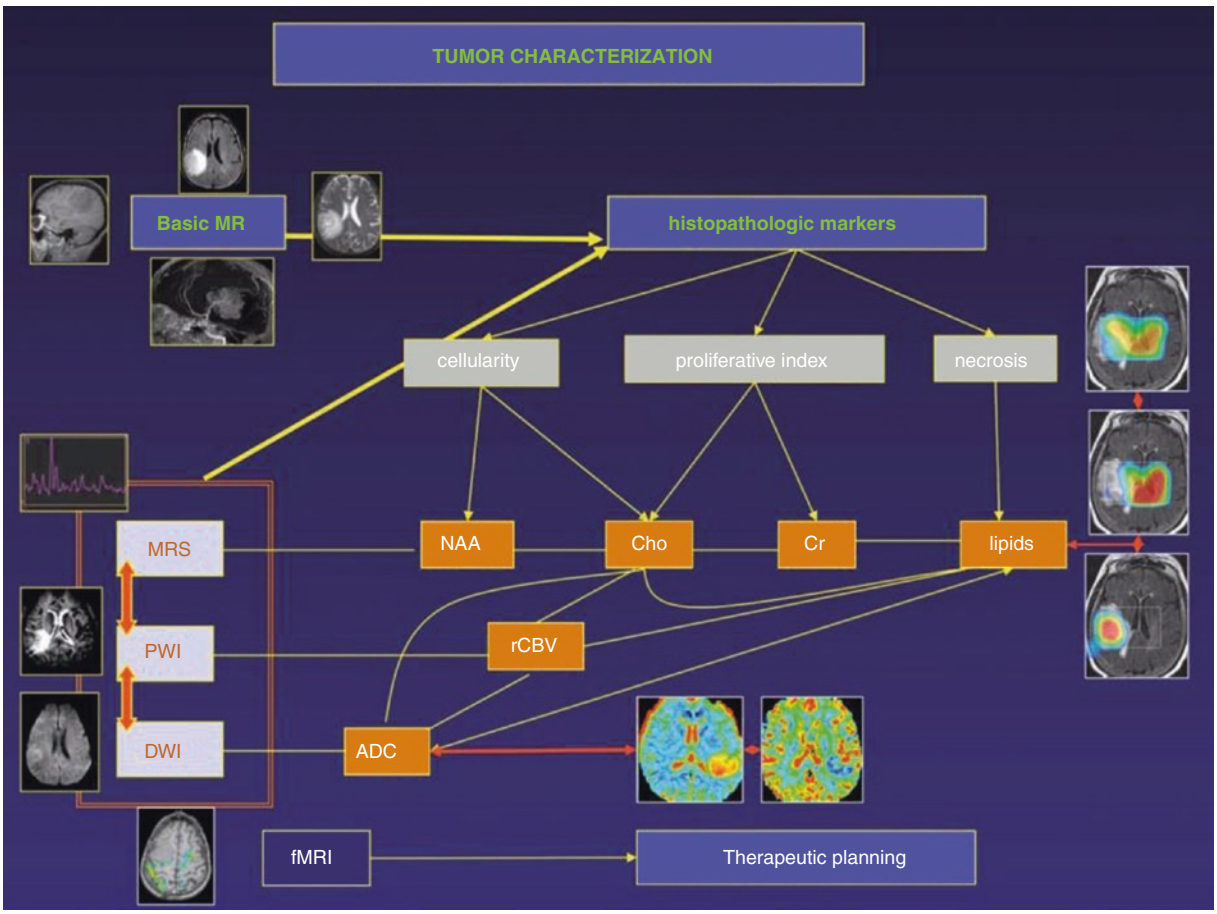

Fig. 55.1 Morphologic MR imaging without and with contrast medium is the examination of choice for the characterization of tumors in both diagnosis and follow-up. A thorough analysis of the radiologic signs, the comparison with the patient's clinical information, and the therapy performed can lead to a correct diagnosis. However, some cases are difficult to diagnose because of the extreme tissue heterogeneity and the frequent coexistence of different pathologic patterns. The morphologic examination therefore may require the addition of advanced MR techniques, i.e., functional MR (spectroscopy, diffusion, perfusion, cortical activation), which enable a neuropathologic study in vivo. The functional and physiologic data on cell metabolism, as well as hemodynamic and diffusion parameters, provide a biologic interpretation of the heterogeneity and complexity typical of these tumors, thus improving the diagnostic accuracy, sensitivity, and specificity of MR and enabling a more precise and comprehensive diagnosis for the surgeon

T. Scarabino (✉) · S. Pollice · A. Lorusso · M. Capuano
Department of Radiology, "L. Bonomo" Hospital, Andria, BT, Italy

A. Maggialetti
Ricerche Radiologiche Center, Molfetta (Ba), Italy

G. Morlino
Department of Radiology, "Di Venere" Hospital, Bari, Italy

T. Popolizio
Department of Neuroradiology, Scientific Institute "Casa Sollievo della Sofferenza", San Giovanni Rotondo (Fg), Italy

T. Scarabino, S. Pollice (eds.), *Imaging Gliomas After Treatment*, https://doi.org/10.1007/978-3-030-31210-7_65

Correction to: Chemotherapy and Future Developments

Ileana De Roma, Lucia Lombardi, and Gennaro Gadaleta-Caldarola

Correction to: T. Scarabino, S. Pollice (eds.), *Imaging Gliomas After Treatment*, https://doi.org/10.1007/978-3-030-31210-7_4

The original version of the chapter title "Chemotherapy Chemotherapy and Future Developments" was revised and has been corrected to "Chemotherapy and Future Developments".

The updated online version of this chapter can be found at https://doi.org/10.1007/978-3-030-31210-7_4

T. Scarabino, S. Pollice (eds.), *Imaging Gliomas After Treatment*, https://doi.org/10.1007/978-3-030-31210-7_66